RESIDUAL STRENGTH OF CLAY AND CLAY-SHALES BY ROTATION SHEAR TESTS

Daniel P. LaGatta

Harvard University

Prepared for:

Army Corps of Engineers

June 1970

Unclassified

Security Classification

DOCUMENT CONTROL DATA - R & D

(Security classification of title, body of abstract and indexing annotation must be entered when the overall report is classified)

1. ORIGINATING ACTIVITY (Corporate author) Harvard University Cambridge, Massachusetts	2a. REPORT SECURITY CLASSIFICATION Unclassified 2b. GROUP

3. REPORT TITLE

RESIDUAL STRENGTH OF CLAY AND CLAY-SHALES BY ROTATION SHEAR TESTS

4. DESCRIPTIVE NOTES (Type of report and inclusive dates)
Final report

5. AUTHOR(S) (First name, middle initial, last name)
Daniel P. LaGatta

6. REPORT DATE	7a. TOTAL NO. OF PAGES	7b. NO. OF REFS
June 1970	220	36

8a. CONTRACT OR GRANT NO. DACW39-69-C-0028 and DACW39-67-C-0024 b. PROJECT NO. c. d.	9a. ORIGINATOR'S REPORT NUMBER(S) Soil Mechanics Series No. 86 9b. OTHER REPORT NO(S) (Any other numbers that may be assigned this report) U. S. Army Engineer Waterways Experiment Station Contract Report S-70-5

10. DISTRIBUTION STATEMENT

This document has been approved for public release and sale; its distribution is unlimited.

11. SUPPLEMENTARY NOTES	12. SPONSORING MILITARY ACTIVITY
Prepared under contract for U. S. Army Engineer Waterways Experiment Station, CE, Vicksburg, Mississippi	Office, Chief of Engineers, U. S. Army Washington, D. C.

13. ABSTRACT

The objectives of this investigation were to (a) develop a rotation shear machine to measure the residual shear strength (constant shearing resistance at which material undergoes continuous deformation under a constant state of effective stress) of clays and clay-shales; (b) investigate testing errors; and (c) measure residual shear strengths of representative types of highly plastic clays and clay-shales. In the rotation shear test, torque is applied to the bottom of the specimen and two force transducers measure the couple necessary to maintain the upper half of the specimen stationary. Disc-shaped or annular specimens with thicknesses from 0.1 to 2.5 cm and outside diameters of 7.11 cm can be tested. The inside diameter of annular specimens is 5.08 cm. Vertical stresses up to 200 kg per cm^2 on annular specimens are applied by a lever system. Rates of rotation can be varied from one revolution in 40 minutes to one revolution in 28 days. It was found that soil extrusion from the peripheral boundaries of the specimen introduce error by causing redistribution of the vertical stress on the specimen, with the error increasing as the ratio of inner radius to outer radius of the annular specimen decreases and as the rate of soil extrusion increases. Other errors evaluated were those resulting from inaccuracies in the lever system, side friction of confining rings, and errors in moment due to the electronic measuring system and due to friction between the center disc and the inner periphery of annular specimens. Remolded specimens of three materials (Pepper shale, Cucuracha shale, and London clay) tested under an effective normal stress of 8 kg per cm^2 had residual friction angles varying from 7.3 to 8.4 deg. Variations in residual shear strength were investigated for normally consolidated versus overconsolidated specimens, for specimens sheared at different rates of peripheral displacement, and for specimens prepared by several different remolding procedures.

DD FORM 1 NOV 1473 REPLACES DD FORM 1473, 1 JAN 64, WHICH IS OBSOLETE FOR ARMY USE.

Unclassified

Security Classification

14 KEY WORDS	LINK A		LINK B		LINK C	
	ROLE	WT	ROLE	WT	ROLE	WT
Clay-shales						
Clays						
Residual strength						
Shear strength						
Shear tests						

Contract Report S-70-5

Report

on

RESIDUAL STRENGTH OF CLAY AND CLAY-SHALES BY ROTATION SHEAR TESTS

by

Daniel P. La Gatta

to

U. S. ARMY CORPS OF ENGINEERS

WATERWAYS EXPERIMENT STATION

as fulfillment of

Contract No. DACW39-69-C-0028

and partial fulfillment of

Contract No. DACW39-67-C-0024

Soil Mechanics Series No. 86

Harvard University

Cambridge, Massachusetts

June 1970

223

FOREWORD

The work described in this report was initiated in connection with Contract DACW39-67-C-0024, "Use of Atterberg Limits in Applied Soil Mechanics," but the majority of the work was performed under Contract DACW39-69-C-0028, "Research Study on Residual Shear Strength of Soils," both contracts being between the U. S. Army Engineer Waterways Experiment Station (WES) and Harvard University. The contracts were sponsored by the Office, Chief of Engineers (OCE), under ES-535, "Use of Atterberg Limits in Applied Soil Mechanics," and ES-545, "Residual Shear Strength of Soils."

The general objective of this research, which was initiated in 1967, was to develop a rotation shear machine for the purpose of measuring residual shear strengths of clays and clay-shales, to investigate testing errors in the rotation shear tests, and to measure the residual shear strengths of selected highly plastic clays and clay-shales. The work was performed and the report prepared by Mr. Daniel P. LaGatta at Harvard University.

The contract was monitored by Mr. B. N. MacIver, Chief, Laboratory Research Section, Embankment and Foundation Branch, under the general supervision of Messrs. A. A. Maxwell, Assistant Chief, and J. P. Sale, Chief, Soils Division, WES.

Contracting officers were COL Levi A. Brown, CE, and COL Ernest D. Peixotto, CE, successive Directors of the Waterways Experiment Station during the conduct of this study and the preparation and publication of this report. Technical Directors were Messrs. J. B. Tiffany and F. R. Brown.

PREFACE

Professor Arthur Casagrande's lectures on Soil Mechanics have provided the stimulation for the author's initiation of this research. Professor Casagrande suggested that a rotation shear machine would be best suited for this investigation and a machine designed by the author was completed in November 1967.

Special acknowledgment is given to Professor Steve Poulos, who directed this research. His numerous discussions with the author have aided in all phases of the investigation.

The author is grateful to Professor Ronald Hirschfeld, Associate Professor of Civil Engineering at the Massachusetts Institute of Technology, for his constructive criticism of the first draft of this report.

Grateful acknowledgment is given to Mr. Fay Welch, research machinist, who built the rotation shear machine used in the research.

Mr. Charles E. Osgood, technical associate in the Harvard Soil Mechanics Laboratory, assisted in the preparation of the figures.

The author wishes to express his appreciation to the U.S. Army Corps of Engineers, who sponsored this investigation.

TABLE OF CONTENTS

TABLE OF CONTENTS (continued)

TABLE OF CONTENTS (concluded)

LIST OF TABLES

LIST OF TABLES (concluded)

LIST OF FIGURES

LIST OF FIGURES (continued)

LIST OF FIGURES (continued)

LIST OF FIGURES (continued)

LIST OF FIGURES (concluded)

NOTATIONS AND DEFINITIONS

B specimen thickness

B_c specimen thickness after being consolidated to a given effective stress

ΔB change in specimen thickness

e void ratio

e_o void ratio of specimen as prepared and before application of load

e_{cr} critical void ratio = void ratio at which the shearing resistance is independent of continuous deformation under a constant state of stress

L_w liquid limit

M moment measured in a rotation shear test

NC normally consolidated

OCR overconsolidation ratio = ratio of maximum past vertical stress to the vertical stress at which a specimen is sheared

P_w plastic limit

P_i plasticity index = $L_w - P_w$

R_1 outer radius of rotation shear specimen

R_2 inner radius of rotation shear specimen

S strength shear strength of a specimen which has been consolidated to the desired effective stress and then sheared so slowly that the induced pore pressures are negligible

δ displacement of the outer periphery of a rotation shear specimen

$\dot{\delta}$ rate of displacement of outer periphery of a rotation shear specimen

δ_p displacement required to reach peak strength

δ_r displacement required to reach residual strength

$\bar{\sigma}_v$ effective vertical stress applied to the top of a specimen

τ_a weighted average shear stress computed from the moment measured during a rotation shear test by assuming the shear stress is uniform

τ_p peak strength measured in a rotation shear test

τ_r residual strength = the constant shearing resistance at which a material undergoes continuous deformation under a constant state of effective stress

ϕ_r residual friction angle = $\tan^{-1} \tau_r / \bar{\sigma}_v$

SYNOPSIS

The purpose and scope of this investigation was: (1) develop a rotation shear machine specifically for the purpose of measuring the residual shear strength of clays and clay-shales; (2) investigation of test errors; (3) measurement of the residual strength of several representative types of highly plastic clays and clay-shales for which the residual shear strength is of great practical importance.

The residual strength is defined as the constant shearing resistance at which a material undergoes continuous deformation at a constant state of effective stress.

A review of past research revealed that the residual strength had not been reached in many cases because the tests were not carried to sufficient displacement. This error may be detected by plotting the displacement on a logarithmic scale, which accentuates the slope of the shear stress versus displacement curve at large displacements.

In the rotation shear machine that was designed and built for this investigation, torque is applied to the bottom of the specimen and two force transducers measure the couple necessary to maintain the upper half of the specimen stationary. This machine permits:

1. Testing of disc-shaped or annular specimens with an outer diameter of 7.11 cm. An inner diameter of 5.08 cm was used for the annular specimens.
2. Testing of specimens with thicknesses from 0.1 cm to 2.5 cm.
3. Application of vertical stresses (by a lever system) of 100 kg/sq cm on a disc-shaped specimen and 200 kg/sq cm on an annular specimen.
4. Ten rates of rotation from 1 rev/40 min to 1 rev/28 days, corresponding to rates of peripheral displacement of 5.6×10^{-1} cm/min to 5.6×10^{-4} cm/min.
5. Use of a horizontally split confining ring with a clearance between 0 and 0.002 inch, or a solid confining ring.
6. Measurement of forces with an accuracy of $\pm 0.3\%$ over a range of shearing resistance of 0.1 to 15 kg/sq cm.

An investigation of the test errors in the rotation shear test indicated that soil extrusion from the peripheral boundaries of the specimen may introduce an error by causing a redistribution of the vertical stress on the specimen. At the residual state, the vertical stress may reach a constant (but nonuniform) distribution and hence result in a constant resistance. It is believed that extrusion causes the effective vertical stress, $\bar{\sigma}_v$, to be lower at the periphery (where the extrusion occurs) than at the center of the specimen as shown in the sketch.

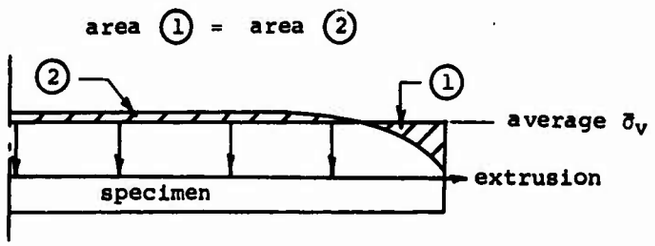

Because the moment arm for area 1 is larger than the moment arm for area 2, the measured moment is lower than it would be if $\bar{\sigma}_v$ were uniform. Thus the residual strength computed from the measured moment by assuming a uniform distribution of $\bar{\sigma}_v$ is too low. Test results indicate that the error caused by soil extrusion increases as:

1. The ratio of the inner radius to the outer radius of the specimen, R_2/R_1, decreases.
2. The rate of soil extrusion increases.

For a test on a disc-shaped specimen in which unlimited extrusion was permitted, the measured residual strength was about 40% lower than for an identical test in which extrusion was minimized by using a solid confining ring. For annular specimens from which unlimited extrusion was permitted, the error ranged between 2% and 15%. Test results indicate that this error is virtually eliminated by using annular specimens with $R_2/R_1 = 0.70$ confined by a solid ring to minimize extrusion.

Other errors and their estimated effect on the residual strength when using an annular specimen are:

1. Inaccuracies in the lever system, ± 0.1 to $\pm 0.25\%$.
2. Reduction in $\bar{\sigma}_v$ due to side friction, -0.5%.
3. Error in moment due to the electronic measuring system, $\pm 0.3\%$.
4. Error in measured moment caused by friction between the center disc and the inner periphery of an annular specimen, $+1.4\%$.

When a solid confining ring is used, failure occurs near a porous disc. The measured residual strength was found to be the same whether failure occurred in the center of the specimen or near a porous disc. This result led to the use of 2-mm-thick specimens, permitting faster consolidation and more rapid shearing rates than have been common in the past.

Principal results on three remolded materials used in the investigation are summarized below:

Material	Liquid Limit L_w	Plastic Limit P_w	Residual Friction Angle for $\bar{\sigma}_v$ = 8.0 kg/sq cm
Pepper Shale	71	22	7.4°
Cucaracha "Shale"	156	42	7.3°
London Clay	72	22	8.4°

Tests on 2-mm-thick specimens of the three highly plastic clays indicated that a rate of peripheral displacement ranging from 5.6×10^{-3} cm/min to 5.6×10^{-1} cm/min had a negligible effect on the residual strength.

The effect of the overconsolidation ratio on the residual strength was investigated by performing tests on specimens of remolded Pepper Shale and remolded Cucaracha "Shale" with overconsolidation ratios from 1 to 100. The difference in residual strength for normally consolidated and overconsolidated specimens was between 0% and 20% (the largest difference in the residual friction angle was 1.4°).

Tests on annular specimens of London Clay indicate the relationship between τ_r and $\bar{\sigma}_v$ is a straight line through the origin inclined at 9.3° for the undisturbed specimens tested and 8.3° for remolded specimens of the same sample. These values are considerably lower than previously published. The author believes that the main reason for the difference between these results and previously published results may be due to not carrying the previous tests to sufficient displacement.

The effect of the degree of remolding on the residual strength was investigated by remolding a sample of Cucaracha "Shale" by two methods:

1. Air-drying and slaking four times ($L_w = 49$, $P_w = 21$).
2. Air-drying and slaking four times, air-drying a fifth time and crushing in a disc mill ($L_w = 156$, $P_w = 42$).

The residual strength of both remolded samples was practically identical. However, ten times more displacement was required to reach the residual strength in tests using the less plastic material. This result suggests that the technique of preparing remolded materials may have a negligible effect on the measured residual strength.

CHAPTER 1

INTRODUCTION

1.1 PURPOSE

The investigations described in this report were concerned with the measurement of the residual S strength of clays. The residual S strength* is the shearing resistance measured in an S test, at which a material undergoes continuous deformation under a constant state of effective stress. The purposes of this investigation were (1) design a rotation shear machine, (2) develop an efficient test procedure for accurate measurement of the residual strength and (3) determine to what extent the residual S strength is affected by specimen shape, type of radial confinement, overconsolidation ratio and rate of deformation. The following materials were used in the investigation: (1) ground Muscovite, (2) remolded Warm Springs Shale, (3) remolded and undisturbed Pepper Shale, (4) remolded Cucaracha "Shale" and (5) remolded and undisturbed London Clay.

1.2 RESIDUAL S STRENGTH – A WORKING HYPOTHESIS

The stress-strain curve obtained in a conventional direct shear S test on a heavily overconsolidated clay is characterized by a sharp peak as shown in Fig. 1-1. The peak shear strength occurs at relatively small displacements and the shearing resistance decreases as displacement continues until it finally reaches a constant value.

It is hypothesized that the large displacements required to achieve the residual S strength presumably cause the soil to reach a critical void ratio (Casagrande, 1936), i.e., when the soil reaches the residual S strength, it undergoes no further volume changes in the failure zone and the soil is in the "critical" or residual state (Poulos, 1969). The concept of residual S strength will be discussed with the aid of the hypothetical curves shown in Fig. 1-2.

Figure 1-2a is a plot of void ratio versus effective vertical stress, $\bar{\sigma}_v$ on a horizontal plane in a direct shear S test on clay. The upper curve, A-B, represents the virgin compression curve for this clay. If a direct shear S test is performed on a specimen with an initial void ratio designated by point 1, application of shear stresses will cause a decrease in void ratio. This decrease in void ratio, plotted as a function of displacement, is shown by the dashed line in Fig. 1-2b. The dashed line in Fig. 1-2c shows that the shear stress increases with displacement until a maximum shear stress (peak strength) is reached. The void ratio at this peak strength is represented by point 2 in Fig. 1-2a. If tests with different values of $\bar{\sigma}_v$ were performed, the relationship between void ratio at peak strength and $\bar{\sigma}_v$ would be given by the heavy dashed line, a-b in Fig. 1-2a.

Continued displacement beyond that required to develop the peak strength results in a decrease in shearing resistance until at very large displacements it becomes constant which, by definition, is the residual strength. The void ratio continues to decrease as displacement continues beyond the peak strength until it also becomes constant. This void ratio, designated as e_{cr} in Figs. 1-2a and 1-2b, is the critical void ratio. The relationship between critical void ratio and $\bar{\sigma}_v$ would be that shown by the line e_{cr} in Fig. 1-2a (Casagrande, 1938; Roscoe, 1958).

---

*The S strength is measured in a specimen which has been consolidated to the desired effective stress and then sheared slowly enough to insure that the induced pore pressures are negligible. Such a test is called an S test or a consolidated-drained (CD) test.

The line C-D in Fig. 1-2a represents a portion of a swelling curve for the clay under discussion. If a direct shear test is performed at the same $\bar{\sigma}_v$ (overconsolidation ratio, OCR > 10) used in the test on the normally consolidated soil, the initial void ratio would be represented by the point 1'. The shear stresses in this case may cause a very slight decrease in void ratio at first, depending on $\bar{\sigma}_1/\bar{\sigma}_3$ after swelling. As displacement continues, the void ratio increases until at the peak shear strength, the void ratio has increased to point 2'. Similar tests at different values of $\bar{\sigma}_v$ would result in a relationship between the void ratio at peak strength and $\bar{\sigma}_v$ such as that shown by the line c-d in Fig. 1-2a. Continued displacement causes a substantial reduction in strength until at very large displacements, the strength becomes independent of displacement as shown in Fig. 1-2c.

The reduction in resistance beyond the peak strength in normally consolidated clays is mainly a result of destroying bonding between clay particles and orienting them in the direction of movement. For overconsolidated clays, the reduction in strength is due to the increase in void ratio as well as the destruction of bonding and the orientation of clay particles.

In the hypothetical curves of Fig. 1-2, the residual strength and e_{cr} are assumed to be independent of OCR. Intuitively, it would seem that the large displacement required to achieve the residual S strength would cause sufficient remolding on the failure plane to destroy the effects of overconsolidation.

Figure 1-2d is a plot of the shear stress and normal stress in the plane of shear for the case of a heavily overconsolidated clay. The usual assumptions concerning the stresses in a direct shear test are made: (1) failure occurs on a horizontal plane, and (2) $\tau/\bar{\sigma}_v = \tan\phi$.

Most data available concerning the residual strength of clays indicate the tests have not been carried to sufficiently large displacements to accurately define the residual S strength (Section 2.3). Volume change measurements have not been adequate to substantiate the uniqueness of the critical void ratio e_{cr} because (1) it is difficult to accurately measure the overall volume changes at large strains and (2) the critical void ratio generally exists only in a thin zone of soil adjacent to the failure plane.

1.3 SCOPE

The scope of this investigation is as follows:

(1) Review the development and the concept of residual S strength in the field of soil mechanics.

(2) Review past investigations concerning the measurement of residual shear strength.

(3) Design a strain control rotation shear machine permitting:
   (a) Application of vertical stresses up to 100 kg/cm^2.
   (b) Measurement of shear stresses with an accuracy and precision of approximately 0.3%.
   (c) Both disc-shaped and annular specimens to be tested.
   (d) Specimen thicknesses from 1 mm to 25 mm.
   (e) Peripheral confinement by either horizontally split or solid confining rings.
   (f) Variation in rate of specimen deformation by a smooth, vibration-free transmission system.

(4) Develop a procedure for testing undisturbed and remolded clays.

(5) Perform laboratory tests to determine to what extent the residual S strength is affected by:
   (a) Specimen shape and radial confinement.
   (b) Overconsolidation ratio(OCR).
   (c) Rate of displacement.

CHAPTER 2

REVIEW OF PAST RESEARCH ON RESIDUAL STRENGTH OF CLAYS

2.1 INTRODUCTION

The purpose of this chapter is to outline the early development of the concept of residual strength and to discuss results of several more recent investigations on this subject. The number of papers written on residual strength during the past five years might lead one to believe that this area of research is relatively new in soil mechanics. In fact, some of the earliest research on the shear strength of soil was performed to study the loss of strength of clays subjected to large deformations.

In Section 2.2 emphasis is placed on presenting those papers which appear to be milestones in the early development.

More recent papers are discussed in Section 2.3 to focus attention on aspects of this topic believed to require further research.

2.2 EARLY DEVELOPMENT

In 1846, Alexander Collin, in his important book, Experimental Research on Landslides in Clay Strata, stated that the object of his research was the "study of mechanics as applied to equilibrium of clay soils." From a study of the location and shape of the slip plane in about 15 slides, Collin concluded that these slides were caused by inadequate shear strength of the soil. Much of Collin's work was in stiff fissured clay. He recognized that cut slopes in these soils, stable during construction, might fail at a later time. He concluded that this time effect was a result of softening due to entry of water into the slope. To support this conclusion, Collin performed undrained shear strength tests* on remolded clays and found that the strength was greatly influenced by the water content. Times to failure were thirty seconds or less in these tests and Collin stated:

> Knowledge of the absolute instantaneous resistance is of no use in construction practice . . . A permanent resistance is therefore the only one which it is necessary to know . . . What length of time, in effect, must elapse until a body subjected to a pressure can be considered capable of resisting it indefinitely? Is it a day, a year, or a century . . .

Much research has been directed toward answering this question. The work presented in this report reflects the present interest in finding the "permanent resistance" of a clay under S conditions.

The amount of shear testing performed between 1846 and the 1920's was meager, and little light was shed on the stress-deformation properties of soils. In the 1920's, activity in this area of soil mechanics increased significantly with the development of the direct shear device in Europe (Krey, 1926).

In the early 1930's, Tiedemann began studying the stress-deformation characteristics of clays using a rotation shear machine (Hvorslev, 1969). Shortly afterward, Hvorslev (1936) and Haefeli (1938) used rotation shear machines to investigate the strength of clay. Both Tiedemann and

---

*Collin, of course, did not refer to his tests as undrained, nor did he discuss the importance of drainage conditions during the tests. The tests consisted of failing a clay prism in double-shear by adding a weight to a central, unsupported length of prism.

Hvorslev were specifically interested in investigating the shear strength of clays at large displacements.

Hvorslev (1936) published results that showed a reduction in shearing resistance after the peak strength had been passed. Tests on remolded Little Belt clay (L_w = 126, P_w = 36) indicated a drop in resistance to about 40% of the peak strength after a displacement of 9 cm. Hvorslev concluded that his investigations demonstrated "the shear resistance after failure depends, to a large extent, on the displacement after failure . . ." Considering that the specimen thickness was 2 cm, and total duration of the test was between 15 and 22 hours, it is likely that these tests were not S-tests.

In 1937 Tiedemann published the results of rotation shear tests on remolded and undisturbed clay. He found that at very large displacements the shear strength was a fraction of the peak strength and that it approached a constant value. Tiedemann referred to this approximately constant reduced strength as "Reinen Gleitwiderstand" (pure sliding resistance). In general, deformations were of the order of 10 to 25 cm before "pure sliding resistance" was reached. It is probable that Tiedemann's tests on remolded clays were S-tests, with tests lasting up to four weeks in some cases.

Haefeli (1938) called the last point of the stress deformation curve obtained from rotation shear tests "Restscherspannung" (remaining shear strength). It is clear from the shape of the stress-displacement curve that "Restscherspannung" does not refer to a shear strength which is independent of displacement. In a paper in English, Haefeli (1951) used the term residual strength as a translation for Restscherspannung. However, the tests reported by Haefeli were creep tests and they were not carried to sufficient displacement to achieve a constant shearing resistance.

Hvorslev (1938, 1939) introduced the term "ultimate minimum shear strength" to describe the approximately constant strength measured at large deformations.

Renewed construction activity on the existing Panama Canal in the 1940's and interest in the construction of a sea level canal, gave impetus to re-evaluation of slides on the slopes along the existing canal. The amount of interest this work generated may be gauged by the number of papers and discussions presented during a 1949 symposium on the Panama Canal sponsored by the American Society of Civil Engineers. In one of these papers, Binger and Thompson (1949) describe a direct shear test performed on a sample of undisturbed Cucaracha "shale" in which the two mating surfaces of the test specimens were polished to simulate slickensides. The slope of a strength envelope obtained from a series of such tests was 10 degrees and this slope was used for analyzing cuts in the Cucaracha formation in order to develop a relationship between depth of excavation and required slopes. This study appears to be the first use of a strength smaller than peak strength for stability analysis for slopes in slickensided clay-shale.

In his discussion of the paper by Binger and Thompson, Casagrande (1949) commented as follows:

> Many of the observed slides have moved slowly, showing only a small reduction in the effective shear strength before and after each movement. This condition is particularly significant when compared to the large differences between the maximum and residual* (after failure) strength values obtained in all laboratory tests on Cucaracha, because it makes it appear probable that the resistance of the banks to sliding had already the character of residual strength when the cuts were made.

Thus, Casagrande recognized that the stability of a cut slope may be governed by a strength that would be measured in the laboratory only after passing the peak strength.

---

*To the author's knowledge, this is the first time the word "residual," in connection with the shear strength of a soil, has been used in an English publication.

The proposed sea level canal also stimulated the U. S. Corps of Engineers Waterways Experiment Station to study the strength characteristics of Atlantic Muck, "in particular, the decrease in the ultimate residual values of the shearing resistance after initial failure of the material . . ." (Waterways Experiment Station, 1951). A rotation shear machine was built at the Waterways Experiment Station under the supervision of Dr. M. J. Hvorslev (Hvorslev and Kaufman, 1952) and a number of tests performed on Atlantic Muck. The tests were intended to be constant water content tests but it was recognized that drainage could not be completely prevented.

In discussing results of their torsion shear tests on Atlantic Muck, Hvorslev and Kaufman (1951) state the following with regard to the slickensided failure surface:

> The changes in soil structure and composition in the immediate vicinity of such surfaces, and the influences of such changes on the residual shearing resistances are not yet known.

In discussing these data later, Hvorslev (1960) writes:

> It is probable that shear strains promote orientation of the clay particles in a direction parallel to that of the principle strain . . . If the strains are very large, they cause formation of slickensided failure surfaces . . .

This was the first time that the reduction in strength after the peak strength and the formation of slickensides were linked to reorientation of clay particles in the failure zone.

2.3 RECENT DEVELOPMENTS

The renewed interest in the shear strength of soils at large strain in the past five years is chiefly due to the Fourth Rankine lecture presented by Professor Skempton (1964). In this paper, Skempton re-analyzed a number of slides and showed that the shear strength at failure may be close to the drained residual strength. He determined the residual strength by repeatedly shearing a specimen in a direct shear machine. After completing the first shear, with a displacement of about 0.3 in., the upper half of the shear machine was pushed back to its original position and then pulled forward again, this process being repeated until "the strength of the clay had dropped to a steady (residual) value." In the few stress versus displacement curves Skempton presents, the author noticed that the displacements at which the tests reached the residual strength were smaller than displacements which had previously been reported (Hvorslev, 1936; Tiedemann, 1937) and also smaller than those measured in tests performed early in this research.

The large displacements necessary to achieve residual strength led the author to plot the stress versus the logarithm of the displacement. This technique accentuates the slope of the stress-displacement curve at large displacements, allowing the residual strength to be defined with less ambiguity. The ambiguity that can result from plotting the displacement on an arithmetic scale is illustrated in Figs. 2-1 and 2-2. Figure 2-1 has been reproduced from Skempton (1964). It appears that the residual strength has been defined at a displacement of 1.5 inches. Replotting this curve on a semi-log plot in Fig. 2-2 shows that the test has been stopped before the residual strength has been clearly defined. The data could be extrapolated within the wide ranges shown. The last point on the curve may be due to random test error which caused it to lie above the true curve. If this one test may be taken as typical of the data used by Skempton, it appears that his conclusions concerning the relationship between the shear strength calculated from the analysis of failed slopes and the residual strength measured in the laboratory (the "residual factor") may be significantly in error.

The results of two major research programs concerning residual strength were published in 1966. The first was carried out at Imperial College by Petley (1966). This study was performed on several undisturbed clays and Kaolinite, using repeatedly reversed direct shear tests. In discussing his laboratory testing technique, Petley states:

> In view of the need for a relatively simple method of obtaining the residual parameters of a soil, attention was focused on developing techniques of testing in which the residual strength could be measured with reasonable accuracy in the types of apparatus available in a normal laboratory, i.e., shear box and triaxial compression.

He also comments, "For research purposes, of course, the torsion shear apparatus is essential ..."

The direct shear tests used in Petley's research were performed on specimens that were 6 cm square and 2.5 cm thick. The lower half of the direct shear box was pushed forward mechanically at a constant rate. After completing the first traverse, with a displacement of about 0.3 in., the direction was reversed and the lower shear box was returned to its initial position rapidly. The reversal technique was continued until a steady shear stress was recorded. The forward shear stages were carried out slowly enough to ensure S conditions. It was not possible to measure the shear load during the reversal part of the test. Tests performed in this manner typically lasted 19 days, with total displacement in the forward direction of 1 to 3 inches. The data obtained are plotted as a series of stress versus displacement curves, one for each forward traverse of the shear box. In many cases, a constant residual strength was not reached in the repeatedly reversed direct shear test. Figures 2-3 and 2-4 show some typical data obtained by Petley, replotted on a semi-log plot. The last point of each traverse of the shear box has been plotted against the total displacement. It can be seen that in some cases, the tests were terminated prematurely. In other tests, the residual strength has been defined satisfactorily.

Petley concluded from his tests that the residual strength is not dependent on stress history or the rate of shearing displacement. Since a number of Petley's tests did not reach the residual condition, it is felt that further study of the effects of stress history and rate of displacement are required before their influence on the residual strength can be established.

Figure 2-5, taken from Petley's thesis, shows a general relationship between clay fraction and ϕ_r (slope of residual strength envelope) for London clay and several other clays in England. Although the residual strength may not have been accurately defined in some tests, Fig. 2-5 does show that ϕ_r decreases as the clay fraction increases.

The second major research program on the residual strength of soils was performed at the Massachusetts Institute of Technology (Herrmann and Wolfskill, 1966). Their tests were predominantly repeatedly reversed direct shear tests on 2-inch-square test specimens. A few tests were performed at the Massachusetts Institute of Technology on the Waterways Experiment Station rotation shear machine (Hvorslev and Kaufman, 1952). The soils tested were resedimented samples of Culebra clay shale and Cucaracha clay shale from the Panama Canal Zone and the Pierre shale from Missouri. A study of the stress versus displacement curves led the author to the conclusion that some of the tests had not reached the residual strength as defined in Chapter 1. In a number of tests, a minimum resistance was reached for a given traverse after which continued displacement caused an increase in the shear stress, as illustrated in Fig. 2-6. The minimum resistance measured in each traverse was tabulated and the smallest of these values was defined as the residual strength. It was also found that, as a test continued, the minimum stress measured in any single traverse would increase as the traverses were continued beyond a certain number. Figure 2-7 shows the minimum $(\phi/\bar{\sigma}_v)$ from the individual pulls, versus the log of the total displacement. The residual strength was defined by the minimum shearing resistance measured in such a test.* Herrmann and Wolfskill state:

---

*Herrmann and Wolfskill present the results of their tests in tabular form and do not plot the entire shear stress versus displacement curve for a test.

> It is characteristic for the residual shear strength of various individual shears to increase slightly after the true residual has been reached. The residual is determined in this manner (i.e., local minimum) because the residual has been defined as the lowest drained strength exhibited by a sample.

This definition, which eliminates reference to the deformation, is completely unsatisfactory since the "lowest drained strength exhibited by a sample" occurs upon initial straining on the way up to the peak strength.

The tendency for the shear stress versus deformation curve to increase after an apparent minimum has been reached is attributed by the investigators to:

> . . . a more undulated failure surface which is formed as the initial flat one is slowly disturbed and remade by continued cycles of forward and reverse shears. For this reason, it is necessary to measure the residual soon after it is reached in each test if the same type of residual is to be determined from each test.

It is difficult to imagine how an initially flat failure plane that requires a minimum amount of work to produce shear displacement will be transformed to some other shape that requires more work. As will be shown later, no test performed with the Harvard rotation shear machine exhibited this phenomenon of increased resistance once a minimum had been reached. This tendency for the residual strength to increase beyond a certain point appears to be peculiar to the repeated direct shear test and may be due to some uninvestigated test error.

One test error investigated by Herrmann and Wolfskill was the friction between the two Teflon-coated halves of the shear box. Tests were performed to evaluate the friction coefficient of Teflon on Teflon. Figure 2-8 shows the results of these tests. The shearing resistance versus displacement curve displays the typical "saddle" shape that many of the direct shear tests on soils exhibited. This shape has never been found in numerous tests on Teflon performed on the Harvard rotation shear machine. In addition, the upper limit of the coefficient of friction for Teflon measured in the M.I.T. investigation was much higher than the values obtained with the Harvard rotation shear machine (Section 3.9).

Herrmann and Wolfskill state that their first objective was to discover the most expedient means for determining the residual strength of a soil. And they conclude:

> The rotation shear machine ultimately gave correct results, but by far the most expedient method is the repeated direct shear test. It is more expedient in terms of time involved as well as in terms of being a much less involved test to run.

In light of the discussion above concerning the stress versus displacement curves obtained from repeatedly reversed direct shear tests, this conclusion hardly seems justified. Furthermore, repeated direct shear tests typically lasted 20 to 40 days. As will be shown in subsequent chapters, the residual strength of soil at a vertical stress of 16 kg/sq cm can be satisfactorily determined with the machine designed for this investigation (Harvard rotation shear machine) in 5 to 6 days, including the time required to consolidate the specimen to the test pressure. The process of shearing a soil continuously in one direction is certainly more efficient at obtaining the residual state than the back and forth motion used in repeatedly reversed direct shear tests.

Placement of a remolded specimen in the Harvard rotation shear machine is no more involved than placing a remolded specimen in a direct shear machine. Preparation of an undisturbed annular specimen is undoubtedly more difficult than placing an undisturbed specimen for a direct shear box. The technique for trimming annular specimens for the Harvard rotation shear machine (Section 4.5) worked very well on the London clay and should work equally well on any homogeneous stiff-to-hard clays. The trimming of an undisturbed disc-shaped specimen to fit the Harvard rotation shear machine is easier than trimming a square undisturbed specimen to fit a direct shear box.

Herrmann and Wolfskill also investigated the use of triaxial tests which were continued to large strains and of triaxial tests on specimens which had a pre-cut, inclined plane. They concluded that the residual strength could not be determined with either of these two types of triaxial tests.

A somewhat different repeatedly reversed direct shear test has been used by Kenney (1967) to measure residual strengths. Kenney's tests were performed on remolded soil which was placed between two circular porous discs. The specimen had a diameter of 8 cm and an initial thickness of about 3mm. It was placed at a moisture content exceeding the liquid limit and was confined with a ring during consolidation. When consolidation was complete, the confining ring was removed and the sample was sheared forward and backward over a distance of 2 mm each side of center. The tests were performed slowly enough to assure S-conditions.

Figure 2-9 shows the only stress versus displacement curve presented by Kenney, replotted on a semi-log plot. The shape of this curve gives a reasonably well-defined residual strength. It is interesting to note that the residual shear strength appears to have been reached at a total displacement of only 1.4 cm.

As a result of his investigations, Kenney concluded that:

> The residual strength of a natural soil is dependent upon mineral composition and, to a lesser extent, on system chemistry and magnitude of $\bar{\sigma}_v$. It is not related to plasticity or grain size of the soil, nor is it significantly influenced by strain rate.

Details of the test procedures used for determining the Atterberg limits and grain size distribution are not given. Hence, Kenney's conclusions concerning the usefulness of these two parameters cannot be adequately evaluated. Furthermore, the usefulness of the conclusion that the residual strength is a function of mineral composition should be questioned because of the difficulties encountered in using X-ray diffraction tests to obtain a quantitative clay mineral analysis. Five techniques of calculating amounts of clay minerals were applied by Pierce and Siegel (1969) to the same sets of diffractograms and significantly different results were obtained. The authors conclude:

> No uniformity is apparent in the results except for the dominance of montmorillonite which could be inferred from the physical aspects of the samples.

Results of rotation shear tests used to determine the residual strength of the Boom clay have been reported by de Beer (1967). These tests were performed on annular specimens with an internal diameter of 4 cm, an external diameter of 8 cm, and a height of 1.8 cm. De Beer presents a typical result of such a test which has been replotted on a semi-log plot in Fig. 2-10. It is clear that this test has been terminated prematurely. It is interesting to compare these data with Tiedemann's (1937) data, which are shown on a semi-log plot in Fig. 2-11. Tiedemann's tests define the residual strength reasonably well although further displacement would be desirable.

2.4 SUMMARY

The concept of residual shear strength or the "permanent resistance" of a soil may be traced back to the work of Collin (1846). Hvorslev (1937) made a significant contribution to the knowledge of the stress versus displacement characteristics of clays at large displacements. An important practical step was made by Casagrande (1949) when he realized that a heavily overconsolidated, slickensided soil may have an in situ shear strength approximating the residual strength. Hvorslev (1960) pointed out that the large displacements attained in the rotation shear machine cause orientation of the clay particles which results in slickensides.

Skempton (1964) gave new impetus to the study of residual strength, resulting in several

major research programs on this subject. Unfortunately, in many cases the residual S strength has not been accurately determined in previous investigations because tests were stopped before the residual strength was attained.

This review indicates that a testing machine and an efficient test procedure needed to be developed which would allow the large displacements necessary to unambiguously define the residual S strength of clays in order to investigate factors which may influence this strength.

CHAPTER 3

DESIGN OF THE ROTATION SHEAR MACHINE

3.1 INTRODUCTION

The first rotation shear machine used in soil mechanics was reported in 1916 (U.S. Bureau of Standards, 1916). It was not until the early 1930's, however, that the rotation shear machine became a significant research tool (Hvorslev, 1936, 1939; Tiedemann, 1937; Haefeli, 1938). The early rotation shear machines were stress-control devices. The shape of the stress-deformation curve beyond the peak strength was obtained by adjusting the shear load until a uniform rate of deformation was achieved. These early rotation shear machines have been discussed by Hvorslev (1939).

In 1947, Hvorslev designed and built a sophisticated rotation shear machine capable of both stress-control and strain-control loading (Hvorslev and Kaufman, 1952). Most contemporary rotation shear machines are closely patterned after his basic design.

In 1965 a strain-control rotation shear machine was built at Harvard to study the residual shear strength of soils (Sembenelli and Ramirez, 1965). It consisted of a shearing unit in which a disc-shaped specimen was placed between a stationary lower porous disc and a rotating upper porous disc. Torque was applied to the upper porous disc by the cable and pulley arrangement shown in Fig. 3-1. Load was applied by the hydraulic jack, and the rate of piston travel (and thus the rate of rotation of the porous disc) was controlled by means of a micrometer flow valve in the hydraulic fluid system of the jack. The resistance offered by the specimen was measured with a proving ring. Normal loads were applied to the specimen by means of a lever system. A photograph of this machine is shown in Fig. 3-2.

A re-evaluation of this design, in 1967 when the present research program was initiated, led to the conclusion that a new rotation shear machine should be built.

3.2 GENERAL DESCRIPTION

The new rotation shear machine is comprised of four basic units:

1. The shearing unit – The specimen is placed into the shearing unit for consolidation and shearing. The machine is designed to test disc-shaped specimens with a diameter of 7.11 cm or annular specimens with an O.D. of 7.11 cm and an I.D. of 5.08 cm. The specimen thickness may vary from 0.1 cm to 2.5 cm. Specimens can be undisturbed or remolded.

2. Vertical loading system – A dead weight loading system allows a maximum vertical stress $\bar{\sigma}_v$, of 100 kg/sq cm to be applied to the disc-shaped specimen and 200 kg/sq cm to the annular specimen.*

3. Torque application – Torque is applied to the specimen by a mechanical transmission system which provides ten speeds of rotation varying from one revolution in 43 min. to one revolution in 28 days (rates of peripheral displacement of 5.6×10^{-1} cm/min to 5.6×10^{-4} cm/min).

*A second machine has been built which allows a maximum vertical stress of 25 kg/sq cm to be applied on a disc-shaped specimen and 50 kg/sq cm on an annular specimen.

4. Moment measuring system – Two force transducers located in the shearing unit measure a force couple from which the shear stresses are computed.

The design of each of these basic units is described under separate headings.

3.3 SHEARING UNIT

Figure 3-3 is a cross section of the shearing unit with all major parts numbered. The parts list is shown in Fig. 3-4. A photograph showing an exploded view of the shearing unit is shown in Fig. 3-5 and a photograph of the assembled unit is shown in Fig. 3-6.

The shearing unit consists mainly of a turntable (14),* two loading platens (8) containing porous stainless steel discs (9) which allow drainage, a vertical spacer (7), a moment transfer plate (6) and a top plate (1). The soil specimen which is radially confined by a ring (10) is placed between the loading platens. The specimen is sheared by rotating the lower platen which is fixed to the turntable (14). The upper platen, vertical spacer and moment transfer plate form a rigid unit containing a thrust bearing (20) which permits the unit to rotate enough to activate two force transducers (2) whose tips contact the wings of the moment transfer plate (see top view in Fig. 3-3). The transducers are held in transducer clamps (2) which are screwed into the top plate. The top plate is prevented from rotating by two adjustable horizontal restraining arms (4). Contact between the restraining arms and the top plate is made through precision ball bearings which allow the top plate to move vertically as the soil specimen consolidates or swells.

Vertical loads are transmitted through a 0.5-inch-diameter, hardened stainless steel ball and loading platen to the top plate.

The top plate, and the cyclindrical part of the moment transfer plate are made of aluminum to reduce weight. All other parts of the shearing unit are Type 316 stainless steel.

The turntable is provided with a Lucite reservoir (13) sealed by an O-ring (see Figs. 3-3 and 3-6). The flexible wall of the reservoir is split vertically at one location, and each edge of the split ring is reinforced with a Lucite block. The blocks have been drilled, and one of them tapped for two screws, which allow the ring to be clamped to form a continuous unit (see Fig. 3-6). This permits removal and installation of the reservoir while a test is in progress.

Three miniature extensometers (0.01 mm/div) may be attached to the top plate to measure any tilting of this plate during consolidation or shear. One such tilt dial (18) is shown in Fig. 3-3. The dial has a vertical stem which slides into the top plate and is locked into position by means of a nylon-tipped screw. The top of the vertical stem is threaded so that the dial may be easily "zeroed" by turning the wingnut at the top of the stem.

The shearing unit has been designed to allow the radial confining ring to be fixed to the turntable (fixed ring configuration) or to be completely independent of the turntable (floating ring configuration). The fixed ring configuration is achieved by supporting the confining rings on three vertical pins (11). Each of the three pins is, in turn, supported on the inclined plane of a horizontal support pin (12). An enlarged detail of this support system is shown in Fig. 3-7. Insertion or extraction of the horizontal pin results in vertical movement of the vertical support pin. When the pins are in the "up" position and the turntable is rotated, the pins contact the sides of holes bored in the bottom of the confining ring, causing it to rotate with the turntable. If shearing has been started with the confining ring in the floating configuration (vertical pins down), one must allow sufficient rotation of the turntable to align the vertical support pins with the holes in the confining ring before raising the pins to fix the confining ring to the turntable.

---

*Numbers in parentheses refer to numbered parts on Fig. 3-3 and in parts list, Fig. 3-4.

3.4 APPLICATION OF VERTICAL STRESS

The vertical stress is applied to the specimen by means of a loading yoke and a counterbalanced lever system. A lever system was chosen because of its simplicity and reliability.

Two machines have been built; Machine No. 1 utilizes a double lever system, and Machine No. 2 a single lever system. The upper lever of the double lever system has a ratio of 10 to 1 and the lower lever, with two weight hangers, gives the system overall ratios of 20 to 1 and 40 to 1 (see Fig. 3-8). The upper lever (10 to 1) has a vertically movable fulcrum which allows it to be kept in a horizontal position regardless of changes in specimen thickness, preventing large vertical movements of the weight hangers when testing very compressible soils. Provision for keeping the upper lever level improves the precision of the lever by minimizing the effects of changing friction at the fulcrum as a result of rotation of the knife edge on their bearing blocks. (The lower lever of the double lever system does rotate on its fulcrum but the forces on the knife edge are smaller than those on the upper lever and hence friction is not as important.) The lever system is connected to the lower beam of a loading yoke.

The maximum vertical stress that may be applied with the double lever system on a 7.11-cm-diameter, disc-shaped specimen is 100 kg/sq cm (200 kg/sq cm on an annular specimen).

The single lever system also utilizes a vertically adjustable fulcrum which allows the lever to be leveled during a test (see Fig. 3-9). The maximum loads that may be applied with the single lever system are 25 kg/sq cm and 50 kg/sq cm on a disc and annular specimen, respectively.

Both lever systems are fabricated of 2024-T4 aluminum where stress will allow, to minimize weight.* The knife edges and bearing blocks used in the lever system are case-hardened, cold-rolled steel. Figure 3-10 shows a typical knife edge and bearing block. In Machine No. 1 the heavy loads imposed by the knife edge on the lower yoke link (see Fig. 3-8) required the link to be fitted with an insert of oil-tempered Ketos tool steel.

The loading yokes of both machines are entirely 2024-T4 aluminum to minimize weight. The loading yoke is not counterbalanced, and when in position on the loading ball the stress applied to an annular specimen is 0.36 kg/sq cm for Machine No. 1 and 0.30 kg/sq cm in the case of Machine No. 2. When consolidating soils from near the liquid limit, the first load increment is achieved by the weight of the upper half of the shearing unit and upper beam of the loading yoke only, which places a stress of 0.19 kg/sq cm on an annular specimen in Machine No. 1 and 0.15 kg/sq cm in Machine No. 2.

The shearing unit is placed in the machine by removing the upper beam of the loading yoke. The remainder of the yoke is held in position by two adjustable clamps on the vertical rods of the yoke. The clamps rest on guides attached to the base plate of the shearing unit when they support the weight of the loading yoke. Figure 3-11 shows a guide and a clamp when not supporting the yoke. The guide holes have a diameter 1.5 times the diameter of the yoke rods and allow the yoke to be completely unimpeded during the application of vertical load.

The lever system was tested with a series of high tensile steel proving rings and the accuracy was found to be approximately 0.1% of any given load (Appendix A). The actual lever ratios are given in the table below.

---

*Stresses in the upper lever of the double lever system require this lever to be fabricated from cold-rolled steel.

Machine Number	Design Ratio	Measured Ratio
1	20:1	19.92:1
1	40:1	39.85:1
2	5:1	4.99:1
2	10:1	9.98:1

Both lever systems are counterbalanced by means of a second lever as shown in Figs. 3-8 and 3-9.

3.5 TORQUE APPLICATION

The turntable of the shearing unit is rotated by means of a mechanical transmission train shown schematically in Fig. 3-12 and equipment manufacturers are listed in Fig. 3-13. The synchronous gear motor which has a shaft speed of 15 rpm and an output torque of 3.1 in.-lb is coupled to the input shaft of a ten-position, adjustable ratio gear reducer giving the turntable speeds shown in Fig. 3-12. The adjustable gear box is coupled to a fixed-ratio (30:1) speed reducer which is coupled to the worm rotating the turntable. Maximum reduction from the motor speed of 1200 rpm to the slowest turntable speed is 48×10^6 to 1. The maximum torque available at the shearing unit is 1700 in.-lb (equivalent to a maximum shear stress of 28 kg/sq cm on an annular specimen). Figure 3-14 is a photograph of the assembled transmission system.

One of the requirements of the transmission train was that it be as vibration free as possible. To reduce the amount of vibration at its source, several gear motors were tested to determine which produced the least vibration. The Globe Industries gear motor was found to produce much less vibration than motors manufactured by Bodine, Inc. and Holtzer-Cabot Company.

To reduce vibrations at the soil specimen, the motor and adjustable gear box are mounted on a different structural frame from that on which the turntable is mounted.

In order to achieve smooth rotation of the turntable (i.e., free from stick-slip), final gear reduction is achieved by two double-throated worm gear speed reducers. Double-throated worm gearing results in large area contact on all gear teeth in mesh as opposed to essentially a thin band contact on standard single-throated worm gears. The number of teeth in mesh is also increased from one tooth, as in the standard single-throated worm gears, to 1/8 of all teeth on the gear for double-throated gears. This results in a larger sliding surface, lower sliding pressure, and smoother operation of the gears.

To check for smoothness of rotation, the speed reducers used in the transmission system were tested by attaching a precision pulley to their output shaft and hanging a weight from the periphery of the pulley by means of a thin piano wire. Movement of the weight was observed with a 0.0001-inch dial gage.* Any erratic movement of the shaft would be clearly reflected by the needle of the dial gage. In this manner, it was determined that common cylindrical, single-throated worm gears were unsatisfactory because of a stick-slip type movement at low speeds of rotation.

*This test also led to an evaluation of the uniformity of movement of various dial gages. Dial gages made by Federal Products, Inc., Ames Company, Soiltest, Inc., British Indicators, and Mercer Company (Great Britain) were used. Dial gages made by Federal Products, Inc. were found to be the most satisfactory.

Final tests for precision and smoothness of operation were performed after the transmission system was assembled. A precision pulley was attached to the worm shaft (see Fig. 3-12) and the transmission operated at all speeds and under varying load conditions. The system was found to be very smooth and the rate of rotation so precise that measurements of actual peripheral displacement were judged unnecessary. Displacements are determined by multiplying elapsed time by the rate of turntable rotation.

3.6 MOMENT MEASURING SYSTEM

Shear stresses are computed from the geometry of the test specimen and the moment acting on the specimen. The forces of the couple which prevent rotation of the upper platen are measured by two Dynisco force transducers located in the top plate (as shown in Figs. 3-3 and 3-15). The moment is computed by multiplying the average of the two measured forces by the fixed distance between the transducers.

Ideally, the two force transducers should measure identical forces. This is not always the case, because the compressibility of the transducers is not identical.

When the two transducers are not measuring identical forces, the transducer clamp may be screwed into or out of the top plate until the forces are equal. Numerous tests have been performed where the initial unequal forces were recorded and then the forces balanced by adjusting the transducer clamps. The moment measured in both cases is practically identical.

Transducers with maximum force ranges of 5, 10, 25, 50, 100 and 300 lb with repeatibility of 0.1% of full scale output are available. Judicious selection of transducers for a given test will allow measurement of the forces at the residual state with an accuracy of approximately 0.1% to 0.3% over a range of residual shear strengths of 0.1 to 15.0 kg/sq cm. The transducers may be changed during a test to improve precision as the residual strength is reached and the forces decrease.

The force transducers have a sensitivity of approximately 3.5 millivolts per volt of excitation and are excited by a precision power supply at 6 volts D.C. The output voltage of the force transducers is displayed by digital millivoltmeters with an accuracy of 0.05 millivolts and a reading resolution of 0.005 millivolts. (For a clay with a shear resistance of 6 degrees, at $\bar{\sigma}_v$ = 1.0 kg/sq cm the output voltage of a 10 lb transducer would be approximately 3 millivolts.)

Initially, transducer outputs were passed through a four-position switching box which allowed one millivoltmeter to measure the output of four transducers. Use of a second millivoltmeter allows the two transducers of a single test to be observed simultaneously. The switching box is designed to energize all four transducers continuously. A schematic diagram and parts list of the voltage measuring system is shown in Fig. 3-16. A photograph of the system is shown in Fig. 3-17.

The force transducers were calibrated by application of lead weights* to a loading yoke suspended from the transducer tip. Several loading-unloading cycles were performed over a period of several days on each transducer. The output voltage versus load curve for any given transducer was found to have essentially constant shape but the curves would be displaced along the voltage axis because of zero drift in the transducers. The repeatibility of the voltage versus load curves for a given transducer was determined to be 0.1% of full scale output or less when the transducer's zero load reading was subtracted from the readings obtained at any load. The linearity of the calibration curves was also determined to be 0.1% of full scale output or less. Details of a typical transducer calibration are given in Appendix B.

*The lead weights used for calibration were weighed on a Mettler balance to assure their accuracy.

During a rotation shear test, after the transducer readings have been recorded, each transducer clamp is screwed out of the top plate far enough to break contact between the transducer tip and the moment transfer plate allowing the zero load reading to be recorded. This allows a check on the operation of the transducer as well as permitting greater accuracy in determining the force measured by each transducer.

3.7 SPECIMEN CONFINEMENT

The horizontal boundaries of a test specimen are formed by the rotating lower porous disc and the stationary upper porous disc. The outer periphery of both the annular and disc-shaped specimens is confined by a ring. The inner periphery of the annular specimen is confined by a plastic disc which slides into appropriate recesses in the upper and lower loading platens (see Fig. 3-20).

Initially, loading platens were made of 0.5-inch-thick Alundum discs. These discs proved unsatisfactory because they were broken under the combined vertical and shear stresses applied during a test.

The Alundum discs were replaced with porous, Type 316 stainless steel discs manufactured by Mott Metallurgical Corporation, Hartford, Connecticut. The porous stainless steel discs have a permeability of 2×10^{-2} cm/sec and a maximum pore size of 40 microns. Each 0.25-inch-thick disc was epoxied to a solid stainless steel disc and the periphery of each porous disc was tapered to prevent binding in the confining ring due to tilting. A radial clearance of 0.001 inch was desired between the leading edge of the porous disc and the inside diameter of the confining ring. Due to difficulty in machining the porous stainless steel, satisfactory tolerances in the radial clearance could not be achieved.

The disc-shaped loading platen which has finally been adopted is shown in Fig. 3-18. The porous stainless steel disc is inset in the stainless steel loading platen. This allows the periphery of the loading platen to be coated with a 0.001-inch-thick layer of Teflon-S. The Teflon on the leading edge of the platen is then machined to a diameter 0.001 inch smaller than the confining rings. The periphery of the porous stainless steel disc must still be machined but the radial tolerances are not critical. To prevent extrusion of the specimen into any annular space which may exist between the porous disc and the loading platen, kaolin with a water content slightly above the plastic limit is forced into any annular voids.

Machining the periphery of the porous stainless steel disc results in a smear zone which reduces the horizontal permeability of the disc. To assure sufficient permeability, the discs were pickled in a solution of 65 gm ferric chloride, 195 cc of 35% hydrochloric acid, and 5 cc of nitric acid. Ten minutes of pickling at room temperature was sufficient to dissolve enough of the smear to assure adequate horizontal drainage. After pickling, the porous disc was rinsed in distilled water and passivated in a 35% solution of nitric acid at room temperature.

Figure 3-19 shows the loading platen used for annular specimens. It is similar to the disc-shaped platen except that the center has been bored out to receive a Teflon spacer disc which forms the inner peripheral boundary of the annular specimen (see Fig. 3-20). The spacer disc has a diameter of 0.002 inch smaller than the inner periphery of the loading platens. Three sliding Teflon legs are fitted into the bottom of the disc. The height of the spacer disc is adjusted by turning three screws which push the Teflon legs out of the disc. When the disc is in position and extends the desired distance above the lower porous disc, the remolded clay may be placed in the annular space provided by the disc and the confining ring (see Fig. 3-21). When the specimen has been completed, the three screws are removed. Adhesion between the disc and the clay holds the disc in place (the three Teflon legs barely support the weight of the disc itself). The spacer is free to move vertically

as the soil consolidates while supporting almost no vertical load.

The outer periphery of the test specimen is confined by radial rings. To force failure in the center of the specimen, confining rings were previously split horizontally to allow one half of the ring to rotate while the other half remains stationary, forcing failure in the plane of the horizontal separation. Sembenelli and Ramirez (1965) designed the confining rings with a 0.005-inch clearance between them, maintained by steel ball bearings. In addition to establishing the 0.005-inch clearance, the ball bearings reduce the friction between the rotating upper ring and the stationary lower ring. Experience with this confining ring showed that a 0.005-inch clearance allowed excessive soil extrusion for tests carried to large deformations.

To minimize soil extrusion and to simplify the design of the confining rings, it was decided to use split confining rings with zero clearance between them. Zero clearance between the two halves of the confining rings introduces two related problems. First, friction between the soil specimen and the confining ring reduces $\bar{\sigma}_v$ on the failure plane. Secondly, the load placed into the upper half of the confining ring by side friction is transmitted between the mating surfaces of the two halves. When the lower ring rotates, the friction on the mating surfaces causes an increase in the measured moment. While these two errors tend to cancel each other, their exact effect is difficult to determine analytically. The absolute value of both errors may be reduced by (1) using a thin test specimen, and (2) reducing the coefficient of friction between the specimen and the confining ring. The standard specimen thickness for tests using split confining rings was chosen as 6 mm. For most tests, about 2 mm of the specimen will extend into the upper half of the confining ring. Friction between the soil specimen and confining ring was minimized by using Teflon confining rings.

A detailed analysis of the error in $\bar{\sigma}_v$ and the measured moment due to side friction is presented in Appendix A. Results of this analysis are shown below for an annular specimen with $\tau_r/\bar{\sigma}_v = 0.10$ (τ_r = residual shear strength, $\bar{\sigma}_v$ = applied vertical stress) and a coefficient of friction between soil and Teflon μ_{ST} of 0.10.

$$\bar{\sigma}'_v/\bar{\sigma}_v = 0.98$$

$$M_c/M_r = 0.02$$

$\bar{\sigma}_v$ = vertical stress applied to the top of the specimen

$\bar{\sigma}'_v$ = vertical stress on failure plane

M_r = moment due to shear stress on failure plane ($\bar{\sigma}'_v = 0.98\ \bar{\sigma}_v$)

M_c = moment due to friction between confining rings

Friction between the two halves of the confining ring may be eliminated by temporarily separating the two halves of the ring during the test (Section 4.8). The transducer readings are recorded before and after separation, giving an indication of the moment due to friction between the rings.

During early tests at vertical stresses of 4.0 kg/sq cm and above, soil extruded between the rings, forcing them apart. To minimize this problem, small removable Lucite clamps were built to fit on the circumference of the confining rings, limiting their separation to 0.001 to 0.002 inch.

To prevent soil extrusion between the Lucite clamp locations, the confining rings are fabricated from Type 316 stainless steel with a 0.003-inch-thick coating of Teflon-S bonded onto all their surfaces.*

*Initially, Teflon rings were used but they were not rigid enough to prevent soil extrusion between the clamps.

As previously mentioned, the split confining ring is intended to permit failure in the center of the specimen. It was found that if the specimen was not pre-weakened in the center by insertion of a thin blade, failure would not occur in the center of the specimen but near one of the porous discs. Early tests indicated no significant difference in the residual strength measured in tests with failure planes in the center of the specimen or within 0.5 to 1.00 mm of a porous disc.

It was concluded that split confining rings may not be necessary and that an unsplit confining ring could be used. Substitution of an unsplit confining ring would greatly simplify the test procedure.

To evaluate the difference between the two types of rings, an unsplit confining ring (subsequently called solid ring) was made. The solid ring has exactly the same radial dimensions as the split confining ring and is 7.5 mm thick and made of Teflon. When a 7.5-mm-thick solid confining ring is used, the thickness of the test specimen may be varied by controlling the height of the vertical support pins. Specimens 2mm, 3mm, and 6mm thick have been used.

The test errors introduced by the boundary conditions of a solid confining ring are also related to side friction between the specimen and the ring. An analysis of this error is presented in Appendix A and indicates the error in $\bar{\sigma}_v$ is lower when solid rings are used because the failure plane is closer to the upper platen. The error due to friction between the two halves of the split confining ring is eliminated, but an error due to friction between the rotating confining ring and the stationary portion of the soil specimen is introduced. This error is much smaller than the error due to friction between the two halves of the split ring (Section A.4 and Section A.5). It may be eliminated by temporarily raising or lowering the ring during a test.

Both the solid and split confining rings are designed to extend below the top of the lower platen when a 6-mm-thick specimen is used (see Fig. 3-7). This permits easy centering of the confining ring in spite of the 0.0005-inch radial clearance. The upper platen is centered on the soil specimen by means of a 0.125-inch-diameter centering pin when a disc-shaped specimen is used as shown in Fig. 3-3. When an annular specimen is used, the center spacer initially centers the upper platen on the specimen.

3.8 MEASUREMENT OF VERTICAL DEFORMATION

Measurement of vertical deformation during consolidation and shear may be made with four dial gages. A central dial, graduated in units of 0.0001 inch, displays movements of the loading yoke directly above the center of the specimen (see Fig. 3-22). Three tilt dials, graduated in units of 0.01 mm, may be positioned near the periphery of the top plate as shown in Fig. 3-3. These three dials measure the change in distance between the top plate and the turntable and are intended to allow a better evaluation of volume changes. In general, these tilt dials are not used for the following reasons:

1. Soil extrusion was usually not completely prevented; therefore, accurate volume change measurements are not possible.
2. The tilt dials prevent removal of the Lucite reservoir during shear and hence obviate the possibility of separating the split confining rings or raising the solid confining ring.

The central dial measures the compressibility of the entire shearing unit as well as the compressibility of the soil. Load versus apparatus compressibility curves for Machines No. 1 and No. 2 are given in Appendix B.

3.9 EVALUATION OF ROTATION SHEAR MACHINE

To periodically check the overall performance of each rotation shear machine, including electronic components, and to compare the two machines, a "standard specimen" of Teflon is used. This standard specimen consists of two rings each 3 mm thick, with an O. D. of 7.11 cm and an I. D. of 5.08 cm. The two rings are placed in the shearing unit between the annular loading platens. The lower Teflon ring is rotated at a speed of 1 rev/40 min and the force couple required to prevent rotation of the upper Teflon ring is measured.

A check test is performed at a single vertical stress for a given set of transducers. The test is continued until one complete revolution of the lower Teflon ring is achieved. Usually, six pairs of transducer readings are taken during this single revolution.

Figure 3-23 is a plot of τ_a (average shear stress) versus $\bar{\sigma}_v$ obtained with the Teflon rings in Machine No. 1 and in Machine No. 2. These tests were performed using transducers with a maximum allowable force of 10 lbs. The data show no significant difference between the two machines. These results indicate that $\tau_a/\bar{\sigma}_v$ decreased from 0.049 to 0.037 as $\bar{\sigma}_v$ increased from 1.0 to 12.0 kg/sq cm. The mating surfaces of the air-dried Teflon rings used in these tests were not polished or cleaned chemically but simply wiped off before placing the rings for each test. The ambient relative humidity was approximately 70% and the temperature was 26 degrees C ± 0.5 degree.

Results of using the Teflon rings to determine $\tau_a/\bar{\sigma}_v$ at a vertical stress of 12.0 kg/sq cm with different sets of transducers are shown below:

	Maximum Transducer Load - lbs	
	10	25
$\tau_a/\bar{\sigma}_v$	0.037	0.038

CHAPTER 4

TEST PROCEDURE

4.1 SOIL PREPARATION

The manner in which each of the soils used in this research was remolded is related to its undisturbed condition. Therefore, the details of each remolding procedure are presented together with the soil description in the chapters containing the data for that soil.

In all cases, the materials were remolded with distilled water to the liquid limit and then air-dried to a water content which allowed them to be easily placed into the confining ring. For the soils used in this investigation, a placement water content equivalent to a liquidity index from 0.6 to 0.9 has been satisfactory.

No advance preparation is required when testing undisturbed materials other than obtaining a sufficiently large, intact sample to be trimmed to fit the confining ring.

4.2 APPARATUS PREPARATION

When the rotation shear machine is initially assembled, the shearing unit is in place to permit proper vertical positioning of the loading yoke. Subsequently, the loading yoke is held in position by the yoke clamps. To prepare for a test, proceed as follows:

1. Remove the upper beam from the loading yoke (see Fig. 4-1).
2. Install the annular or disc-shaped loading platens on the turntable and spacer.
3. Insert the turntable in the worm gear hub.
4. Place a dummy specimen on the lower loading platen and assemble the remainder of the shearing unit, excluding transducers. In order to permit the top of the confining ring to extend above the top of the soil specimen during a test, it is recommended that the specimen thickness does not exceed 5 mm when using 7.5-mm-thick confining rings.
5. Place the upper beam of the loading yoke on the load transfer ball and tighten the upper nuts on the yoke rods to secure the upper beam. Release the yoke clamps.
6. Level the loading lever by adjusting the screw jack of the movable fulcrum (refer to Fig. 3-8). The counterbalance lever should be approximately horizontal when the loading lever has been leveled, which is achieved by turning the turnbuckle which connects the two levers. If the previous test was performed on a specimen of the same thickness as that for the test being planned, steps 4 to 6 can be omitted.
7. Align the top plate so that the restraining arm bearing surfaces are perpendicular to the restraining arms. Adjust the restraining arms until the ball bearing tips just contact the bearing surfaces.
8. Lock the yoke clamps, remove the upper beam of the loading yoke and remove the shearing unit.
9. Set the ratio on the adjustable gear box to obtain the desired rate of peripheral displacement. Start the motor and allow it to operate for a short time to remove any slack in the transmission system.

10. Place the desired confining ring on the three vertical support pins (the heads of the screws which hold the two halves of the split confining ring together must be on top) and adjust the height of the pins to obtain the desired specimen thickness. A depth gauge such as shown in Fig. 4-2 works very well for this purpose.
11. If an annular specimen is to be used, the Teflon center spacer should be placed in the lower loading platen and the three elevation screws adjusted until the top surface of the spacer is level and extends about 2 mm above the confining ring. A centering pin is placed after the elevation of the disc has been set.
12. Coat the lower 1/4 inch of the inner periphery of the Lucite reservoir with stopcock grease.
13. Take the turntable, with the confining ring in position, to a humid room to place the specimen. The porous discs of the loading platens should be kept dry.

4.3 SPECIMEN PLACEMENT – REMOLDED

1. The remolded soil is placed in the confining ring in small amounts with a flexible steel spatula until the surface of the porous disc is completely covered with a layer of soil about 1 mm thick. A 4-inch flexible spatula is bowed with 3 mm to 6 mm of its tip against the soil as shown in Fig. 4-3. (A 1.8-cm-wide spatula is used with disc-shaped specimens, and a spatula with a 0.8-cm width is used with annular specimens.) The spatula is pulled across the soil surface while the blade is repeatedly flexed vertically. This action helps to obtain a uniform, air-free specimen. The process is repeated until the confining ring is completely filled. Special care must be taken to assure that no voids exist along the periphery of the confining ring or near the centering pin (or the center spacer if annular specimens are being prepared).
2. The top surface of the specimen is leveled by slowly pulling a stiff-backed straight edge across the surface, using the top of the confining ring as a guide as shown in Fig. 4-4. If an annular specimen is being formed, the periphery of the center spacer may be cleaned with a sharp pointed knife held vertically and pulled around the spacer periphery as shown in Fig. 4-5. After the periphery of the center spacer is cleaned, the centering pin and the elevating screws are removed.
3. If a split confining ring is being used, three or more Lucite C-clamps should be placed around the periphery of the rings and then the screws holding the ring together should be removed.
4. Place the reservoir in position and snap it over the O-ring in the turntable. The specimen is now ready to be placed in the machine for consolidation.

4.4 SPECIMEN PLACEMENT – UNDISTURBED DISC

The apparatus preparation for performing tests on undisturbed specimens is as described in Section 4.2 with one additional step. After the height of the support pins has been set (Step 9 of Apparatus Preparation), the confining ring is lifted off the pins.

Tests in this investigation were generally performed on 2-mm-thick undisturbed specimens.

Trimming a heavily overconsolidated clay which is brittle and may have weak zones is a very tedious job. To minimize error due to fatigue, the first two steps of the test procedure presented below are usually performed one day before the final trimming.

1. A disc of soil about twice the desired specimen thickness and with a diameter of 1 cm larger* than the specimen is carefully trimmed from the undisturbed block. A specimen may also be trimmed from a sample taken with a 3-inch sampling tube in which case the diameter of the sample is only slightly larger than the diameter of the specimen. In either case, the top and bottom surfaces of the soil disc must be trimmed flat and practically parallel.
2. After the soil disc is trimmed flat, the diameter of the disc should be carefully trimmed until it is about 2 mm larger than the specimen. This is accomplished by placing the disc of soil on a glass plate and placing a plastic plate with a diameter 2 mm larger than the specimen on top of the disc as a guide. The diameter of the soil disc is reduced by carefully shaving small amounts of soil from its periphery with a sharp knife. It is helpful to apply a slight pressure to the top surface of the specimen by pressing down on the plastic disc. The disc also helps minimize the loss of moisture during this phase of trimming.
3. Place the confining ring upside down in a soil lathe and center the soil disc on the ring. Carefully reduce the diameter of the disc with a trimming tool. The confining ring, in position on the lathe, and the trimming tool are shown in Fig. 4-6. The trimming tool is designed to trim the soil disc to a radius 0.002 inch larger than the inside diameter of the ring.
4. When the diameter of the soil disc just above the confining ring has been trimmed to the proper size, place the plastic disc on top of the soil and press down gently to force the specimen into the ring, being careful not to tilt the specimen.
5. Continue trimming until the specimen protrudes below the bottom of the confining ring. Observe the stratification and inhomogeneities that become apparent during trimming and record them.
6. Determine the water content of those trimmings from the periphery of the sample which are representative of the soil in the confining ring.
7. Carefully cut away the excess soil above the specimen. It is usually preferable to maintain a greater thickness of soil over the center of the specimen by starting at the periphery and working toward the center. Using a sharp, stiff straight-edge, trim the specimen exactly flush with the ring.
8. Place a glass plate on top of the specimen and look through the plate to be sure that the surface of the specimen is exactly flat and flush with the top of the ring.
9. Remove the confining ring and soil from the lathe, invert the ring and place the trimmed surface of the specimen on the lower loading platen. Carefully center the specimen until the confining ring may be pushed down away from the top of the specimen, into position on the three vertical support pins (the height of the pins has been previously established during the apparatus preparation).
10. Trim the top of the specimen extending above the confining ring as described in Step 7 above.
11. Repeat Step 8 to check the top surface. Figure 4-7 shows the completely trimmed disc.
12. Place the reservoir in position and snap it over the O-ring in the turntable.

*The diameter of the disc is initially 1 cm larger than the specimen to allow for any broken edges which may occur while trimming the top and bottom surfaces flat.

4.5 SPECIMEN PLACEMENT – UNDISTURBED ANNULUS

The following procedure has only been used to trim undisturbed annular specimens from the London clay which is a very easy soil to trim. The procedure may require modification if other clays are tested. The annular specimens trimmed for this research were 2 mm and 3 mm thick. Proceed as follows.

1-8. Identical with Steps 1 through 8 as described in Section 4.4.

9. Remove the confining ring and soil from the lathe, invert the ring, and place the trimmed surface of the specimen on a glass plate.

10. Trim the top of the specimen extending above the confining ring as described in Step 7 above.

11. Repeat Step 8 to check the top surface.

12. Place the confining ring and specimen between the brass trimming clamp as shown in Fig. 4-8 and tighten the clamping screws.

13. Begin trimming the unsupported portion of the soil disc by boring a hole in the center with a sharp pointed knife. Continue the trimming of the soil by working from the center of the disc to the inner periphery of the brass rings.

14. Remove the clamping screws and separate the brass rings by sliding them off the confining ring. Figure 4-9 shows a soil specimen at this stage of the procedure.

15. Place the specimen on the lower loading platen, carefully centering the specimen. Push the confining ring down away from the top of the specimen into position on the three vertical support pins (the height of the pins has been previously established during the apparatus preparation).*

16. Insert the Teflon center spacer into position. The top of the spacer should protrude about 1 mm above the top of the soil annulus.

17. Carefully trim the top of the specimen extending above the confining ring, maintaining a greater thickness of soil at the center spacer. When the top surface of the soil annulus is nearly flush with the confining ring, remove the center spacer.

18. Using a sharp, stiff straight-edge, trim the specimen exactly flush with the confining ring. The straight-edge should be placed at the center of the specimen and pulled to the outer periphery.

19. Insert the center spacer into position. It may be necessary to trim the inner circumference of the soil annulus by guiding the point of a knife around the bore of the lower platen.

20. Remove the centering pin and the elevating screws from the center spacer.

21. Place the reservoir in position and snap it over the O-ring in the turntable.

The specimen is now ready to be placed in the machine for consolidation.

---

*When a 5-mm-thick specimen is to be used, the specimen will protrude 1 mm above the confining ring.

4.6 CONSOLIDATION

1. Place the turntable with the soil specimen in the worm gear hub.

2. The upper platen and the moment transfer plate, as a unit, should be placed on the surface of the specimen, aligning the "wings" of the moment transfer plate parallel to the horizontal restraining arms (visual alignment is sufficient). See Fig. 4-10.

3. Raise the confining ring by pushing the horizontal support pins all the way in. This centers the upper loading platen on the specimen as well as confining the entire specimen within the ring.

4. Insert a 6-inch-long centering pin into the bushing of the moment transfer plate and use it as a guide to slide the top plate into position as shown in Fig. 4-11. The top plate will also be aligned by the ball bearing tips of the horizontal restraining arms. When the top plate is seated on the thrust bearing of the moment transfer plate, remove the 6-inch-long centering pin and position the load transfer ball and the upper beam of the loading yoke.

5. The beam which supports the central vertical dial should be placed on the vertical posts and the dial zeroed by adjusting the nuts on which the support beam rests. Placing the upper half of the shearing unit in position should be accomplished as quickly as possible, since zero time for the load increment added by the weight of these parts must be taken as the time the vertical dial is in position and zeroed. (This operation takes about one minute.) When testing remolded specimens, the reservoir should be filled with distilled water as soon after zero time as possible. When testing undisturbed soils, only enough water is added to the reservoir to bring the water surface just below the drain holes in the lower platen. The annular space between the top of the reservoir wall and the upper platen should be covered with plastic to minimize loss of moisture from the soil.

6. When the time curve for the initial load on the remolded specimens has developed a well-defined secondary branch, the weight of the loading yoke is placed on the specimen by releasing the yoke clamps. To apply the load uniformly, one yoke clamp is released but the yoke rod is held in position manually until the second clamp is released.

7. Due to the consolidation which takes place under the initial load increments, the load transfer link between the loading yoke and the lever system will have moved away from the knife edge (Fig. 3-8). Before subsequent loads are applied by adding weight to the hangers, the movable fulcrum should be lowered until the knife edge just contacts the load transfer link.

8. If the test is to be performed with "floating" confining rings, the vertical pins which support the ring should be lowered by extracting the horizontal pin in the turntable.

9. Increase $\bar{\sigma}_v$ to 0.5 kg/sq cm by placing the necessary lead weight on the hanger. The remaining load increments are applied using $\Delta \bar{\sigma}_v / \bar{\sigma}_v = 1$ when possible. Each load increment is left on until the time curve has developed a well-defined secondary branch.

10. When testing undisturbed soils, the load increments should be placed on the specimen rapidly (approximately 10-minute intervals) until the load at which the test is to be performed or the known preconsolidation load is reached. The reservoir should then be filled and changes in specimen thickness recorded until a well-defined secondary branch is recorded.

4.7 PRECUTTING THE SOIL SPECIMEN

If failure is desired in the middle of the specimen, it is necessary to precut the specimen on a horizontal plane passing between the two halves of the split confining ring. This is accomplished after the specimen has been consolidated to the effective stress at which the test is to be performed. The details of the procedure are as follows:

1. Remove the water from the reservoir by means of a syringe or syphon; then remove the Lucite reservoir wall by unscrewing the two clamping screws and spreading the flexible reservoir until it can be slid off the turntable. Record the vertical dial reading.
2. Remove the C-clamps and separate the two halves of the confining ring slightly by inserting the edge of a razor blade between them. A 0.003-inch-thick steel blade is then inserted between the rings into the soil specimen; a 0.003-inch-thick feeler gage has also been used successfully to precut the specimen (see Fig. 4-12).
3. When the blade has been inserted around the entire periphery of the specimen, the upper confining ring is lowered to contact the lower confining ring. The upper ring is rotated as it is lowered by inserting the small brass tools shown in Fig. 4-13 into the holes provided in the top surface of the upper confining ring and applying a horizontal couple as well as a vertical force.
4. Install the Lucite C-clamp on the periphery of the split confining rings. Replace the reservoir and refill it with distilled water.
5. Vertical dial readings should be recorded until they indicate only secondary compression is occurring.

4.8 SHEARING THE SPECIMEN

At some stage during the secondary compression branch of the time curve of the final load increment (and after precutting, if this has been done), the transducers must be screwed into the top plate. The transducers should be installed at least one-half hour before the start of shearing to allow sufficient warm-up time for the electronic equipment.

1. Screw one transducer into the top plate just far enough to contact the wing of the moment transfer plate. It may be necessary to back the horizontal restraining arms away from the top plate so the top plate will move slightly when the first transducer has just contacted the moment transfer plate. Connect the transducer cable to the switching box and turn on the digital millivoltmeter. Contact between the transducer probe and the moment transfer plate will now be indicated by the millivoltmeter.
2. Install the second transducer until it just contacts the moment transfer plate. Connect this transducer cable to the switching box and turn on the second millivoltmeter.
3. Adjust the horizontal restraining arms until they just touch their respective bearing surfaces in the top plate. By very small adjustments of the transducers and horizontal restraining arms, one can quickly have all four of these units barely touching their respective bearing surfaces. When the system has been properly adjusted, slight finger pressure applied to the top of either vertical post supporting the horizontal restraining arms will be immediately reflected by both transducers.

4. Just before shearing is started, the zero load readings for each transducer should be obtained by temporarily backing each force transducer out of the top plate just far enough to break contact between the transducer tip and the moment transfer plate.

5. Level the lever system if necessary and record the vertical dial reading. Check that the adjustable gear box has been set for the desired ratio of peripheral displacement.

6. Start the motor to begin shear; at the first sign of increased voltage on the millivoltmeters, note the starting time. Readings of both transducers should be recorded at intervals which clearly define the shape of the average shear stress versus log displacement curve. Readings of the central vertical dial should be recorded at elapsed time of 0.1, 0.25, and 0.5 minutes and immediately after the transducer readings are recorded.

7. During those phases of the test when volume changes are large the lever must be releveled by adjusting the movable fulcrum.

When the split confining rings are being used, the Lucite C-clamps are not removed until the shear stress versus displacement curve is horizontal. At that time, transducer readings with and without the C-clamps are recorded in the following manner.

8. Remove the water from the reservoir and then the reservoir wall. Record the transducer readings and the central vertical dial with the C-clamps in position. Remove the C-clamps and separate the split confining rings by inserting the edge of a razor blade between them. Record the transducer readings at suitable intervals until the force couple begins to decrease. Then lower the upper half of the confining ring and rotate it to seat it completely (forcing most of the soil out from between the rings). Replace the C-clamps and reinstall and fill the reservoir. The central vertical dial reading should be recorded during separation of the rings along with the transducer readings, and after the reservoir has been reinstalled.

When the solid confining ring is used, it is left in position until the shear stress versus displacement curve is horizontal. The confining ring may then be lifted off the vertical support pins to eliminate any friction caused by the ring.

8a. Remove the water from the reservoir and then the reservoir wall. Record the transducer readings and the vertical dial reading. Raise the confining ring above the specimen and let it rest on the top platen just above the specimen. Record the transducer readings and central vertical dial at suitable intervals until the force couple begins to decrease. The force couple generally begins to decrease in 2 to 4 minutes, and there is a sufficient film of water on the periphery of the specimen to prevent it from drying. If the ring is to be left off the specimen for a longer period of time, the periphery of the specimen can be kept moist by placing water on the confining ring and allowing it to fall between the ring and the platen over the periphery of the specimen. When the moment begins to decrease, lower the confining ring back into position and replace the reservoir.

In addition to eliminating friction due to the confining ring, the techniques described in Steps 8 and 8a introduce an error due to stress changes at the specimen boundary. A complete discussion of these effects on the measured residual strength is presented in Appendix A.

In many cases, it is desirable to determine the shear strength of a single test specimen at several different vertical stresses. When the residual strength has been clearly defined at a given vertical stress, the vertical stress is increased by adding the necessary weight to a hanger and the test continued until the residual strength is defined at this new vertical stress.

4.9 DATA ACQUISITION

To improve the accuracy of the transducer output, it is necessary to subtract the "no load" voltage output from the output at any given load. The "no load" output for each transducer is obtained just before the start of a test (Section 4.8, Step 4). These no load readings are assumed to apply during the early stages of the test when the transducer outputs (hence the shear stresses) are changing rapidly. As the shear stress versus displacement curve approaches a horizontal asymptote, new "no load" readings should be taken immediately after each set of transducer readings is recorded, by unscrewing each transducer clamp just enough to break contact between the transducer probe and the moment transfer plate.

Peripheral displacement is obtained by multiplying elapsed time from the start of shear by the appropriate constant determined by the circumference of the test specimen and the speed of the turntable.

It is important that the data be reduced and plotted immediately after readings are taken. Comments regarding any steps taken during the test such as separating or raising confining rings, as well as any observations which might influence test results such as soil extrusion, are recorded directly on the data sheet.

4.10 REMOVING THE SPECIMEN FROM THE MACHINE

1. At the conclusion of the test, with the motor operating, remove the central vertical dial support beam.
2. Tighten the yoke clamps.
3. Remove the transducers from the top plate.
4. Remove the water from the reservoir and unload the specimen. During the unloading phase, the lever system should be leveled at each decrement.
5. Remove the upper beam of the yoke.
6. Stop the motor.
7. Lift the top plate and the moment transfer plate off the specimen.
8. Remove the turntable from the worm gear and place it in the humid room.
9. Separate the upper and lower platens by inserting a knife or other tool between them and wedging the top platen upward. This will separate the specimen on the failure plane most of the time.
10. Study the failure zone in detail and describe it with the aid of sketches or photographs.
11. Water contents should be taken from the failure zone if the specimen thickness is great enough to permit it and if the specimen separates on a failure plane. If the specimen does not separate on a failure plane, a water content of the entire specimen thickness may be taken. In this case, the portion of the moisture content specimen next to the porous discs should be scraped off to minimize the effect of swelling during unloading.

Unloading and dismantling must be done quickly to minimize absorption of water from the porous disc.

CHAPTER 5

REDUCTION AND PRESENTATION OF DATA

5.1 DETERMINATION OF SHEAR STRESS

The data necessary to compute the shear stress and displacement consist of two transducer readings and the time elapsed from the start of the test. Each transducer reading is corrected for zero drift by subtracting its "no load" from its loaded reading. This difference is multiplied by the appropriate calibration constant (Appendix B) to obtain the force measured by each transducer. The average force measured by the two transducers is multiplied by the distance between them to obtain the moment required to prevent the upper platen from rotating. The magnitude of the moment transmitted through the specimen depends on the shear stress versus displacement characteristics of the soil.

In a rotation shear specimen, the tangential deformation in a horizontal plane varies with the radius. The horizontal shear stress will therefore be a function of the radius and the shape of the stress-displacement curve.

When the stress-displacement curve is horizontal, the shear stress distribution on the failure plane will be uniform (assuming the vertical stress is uniform) and may be computed from the following equation:

$$\tau_a = \frac{3M}{2\pi\left(R_1^3 - R_2^3\right)} \tag{5.1}$$

where: M = moment

R_1 and R_2 = outer and inner radii of the specimen, respectively

Equation 5.1 gives the weighted average shear stress at any time during a test. The use of Eq. 5.1 for plotting the stress-displacement curve is illustrated in Fig. 5-1. The solid line in Fig. 5-1a represents the true stress versus displacement curve of the soil. At a time in the test when the displacement on the outer and inner peripheries of the specimen is δ_1 and δ_2, respectively, the corresponding shear stresses will be τ_1 and τ_2 (Fig. 5-1a). The distribution of shear stress at this time is shown in Fig. 5-1b, and the shear stress computed from Eq. 5.1 will be $\tau_{a,1}$. The effect of using Eq. 5.1 at other stages of the test is illustrated in Figs. 5-1c through 5-1e. As a matter of convenience, τ_a is plotted at a displacement equal to the displacement of the outer periphery. This plotting technique shifts the shear stress versus displacement curve to the right (dotted curve in Fig. 5-1a). When the shear stress at the inner periphery of the specimen has decreased to the residual strength, the two curves become horizontal and Eq. 5.1 will give an accurate determination of the residual strength.*

*Hvorslev (1937) has shown mathematically (assuming that stress versus displacement curve is linear to the peak) and experimentally that the maximum τ_a computed from Eq. 5.1 is very close to the peak strength measured in direct shear tests when an annular specimen with $R_2/R_1 = 0.5$ was used.

5.2 PLOTTING DATA

The technique of plotting the peripheral displacement on a logarithmic scale was introduced in Section 2.3. This technique accentuates the slope of the stress displacement curve at large deformations relative to the slope at small deformations, allowing the horizontal portion of the curve to be defined with less ambiguity. All plots of shear stress versus displacement used in this work are semi-log plots of "average" shear stress, τ_a versus outer peripheral displacement.

Typical plots used to present the test data are shown in Fig. 5-2. The "title block" of each figure gives the type of soil used and the test number in the first line. The state of the soil is shown in the second line (undisturbed or remolded). The overconsolidation ratio (OCR) for specimens of remolded soil will also be shown on the second line of the title block. Normally consolidated specimens will be designated by NC.

The third line of a title block describes the thickness at the start of consolidation and the shape of the test specimen. Other constant parameters in the test, such as the rate of peripheral displacement $\dot{\delta}$, are shown in the fourth line of the title block.

The lower portion of Fig. 5-2 is the curve of τ_a versus δ, and the upper portion shows the change in specimen thickness, ΔB versus δ. The specimen thickness at the start of shear, B_c, is shown on the ΔB versus δ plot of each test.

Many tests performed in this research consist of a single specimen tested at more than one vertical stress and, in some cases, at several rates of peripheral displacement. To present the data more clearly, changes in either $\bar{\sigma}_v$ or rate of peripheral displacement are plotted from a translated peripheral displacement axis. An example of this technique is shown in the lower half of Fig. 5-3. The first phase of this test was performed at $\bar{\sigma}_v$ = 1.0 kg/sq cm and the results are shown by the open circles. The specimen was initially sheared at a rate of peripheral displacement of 5.6×10^{-2} cm/min (dashed line). After about 10 cm of displacement at this velocity, $\dot{\delta}$ was decreased to 5.6×10^{-3} cm/min. To clearly show the stress versus displacement curve at this second velocity, the data are plotted assuming the displacement was zero at the instant the velocity was decreased (open circles, solid line). This same plotting technique is used when the vertical stress is increased during a test. In this test $\bar{\sigma}_v$ was increased from 1.0 kg/sq cm (open circles) to 2.0 kg/sq cm (black dots).

The peripheral displacement axis for curves of ΔB versus δ are translated to correspond with the stress-displacement curves.

It was pointed out in Section 3.7 that the boundary conditions in the rotation shear test do not prevent soil extrusion during a test. For this reason, the change in specimen thickness does not represent a change in void ratio only. These curves do not become horizontal when the shear stress versus peripheral displacement curves are horizontal because of soil extrusion.

A typical residual strength line obtained from a series of tests is shown in Fig. 5-4. The residual shear stress axis has been enlarged to exaggerate the slope of the strength line. In some cases, a line representing the peak strength τ_p will be plotted along with the residual strength line.

CHAPTER 6

INVESTIGATION OF TEST ERRORS

6.1 PURPOSE AND SCOPE

The purpose of this phase of the investigation was to investigate the test errors associated with measuring the residual strength of clays in the Harvard rotation shear machine.

One source of error, believed to be common to all rotation shear machines, is due to soil extrusion from the peripheral boundaries of the specimen. Soil extrusion prevents accurate volume change measurements and, more important, it is believed to cause a nonuniform distribution of vertical stress on the failure plane, which invalidates the computation of residual strength which is based on the assumption that the distribution is uniform.

The magnitude of the error due to soil extrusion is influenced by the type of radial confinement, which controls the amount of extrusion, and the specimen shape, which affects the degree of nonuniformity of vertical stress. Thus residual strength tests were performed using (1) horizontally split confining rings and solid confining rings to determine the effect of different rates of extrusion; and (2) disc-shaped and annular specimens because the effect of redistribution of vertical stress was expected to be smaller for annular specimens. Errors in vertical stress and the measured moment due to side friction between the specimen and the confining ring are summarized in this chapter and discussed in detail in Appendix A.

6.2 ERROR IN RESIDUAL STRENGTH DUE TO THE SPECIMEN EXTRUDING FROM THE CONFINING RING

6.2.1 DESCRIPTION OF MATERIALS USED IN THIS PHASE OF THE INVESTIGATION

Two materials were used in this study. One was a commercially available ground muscovite powder (Fisher Scientific, mica powder, Catalogue No. M-231). This material was ground finer by means of a ball mill to the gradation shown in Fig. 6-1. The ground muscovite had a liquid limit of 52 and was nonplastic.

The other material used was remolded Warm Springs Shale. The Atterberg limits of the undried material are tabulated below and plotted on the Plasticity Chart in Fig. 6-2. The grain size distribution is shown in Fig. 6-1.

Soil	L_w	P_w	P_i
Warm Springs Shale	39	17	22

At the plastic limit, the material was medium tough. When a pat of soil was air-dried from slightly below the liquid limit, it had medium to high dry strength.

6.2.2 TEST PROCEDURE

The test procedure is described in detail in CHAPTER 4. TEST 1 on the ground muscovite was performed on a 12-mm-thick specimen; all other tests reported in this chapter were performed on 6-mm-thick specimens. Tests which were confined by a split confining ring were precut by

inserting a 0.003-inch-thick blade between the two halves of the confining ring as described in Section 4.7. When the residual state was reached, the two halves of the ring were temporarily separated to eliminate friction between them (Section 4.8). In tests using a solid confining ring, the ring was not raised as suggested in Section 4.8 so that extrusion with this ring would be minimal.

6.2.3 COMPARISON OF SPLIT VERSUS SOLID CONFINING RINGS USING DISC-SHAPED SPECIMENS

The first series of tests was performed on ground muscovite. Duplicate tests were performed at vertical stresses of 1 and 2 kg/sq cm for both types of confinement. The shear stress versus displacement curves for these tests are shown in Figs. 6-3 to 6-6. The dashed line in these figures shows the results of the initial phase of each test, during which the rate of peripheral displacement was 0.056 cm/min. When the residual state had been reached at this velocity, the rate of peripheral displacement was reduced to 0.0056 cm/min. In this chapter, only the results obtained at 0.0056 cm/min will be compared (the effects of rate of displacement are discussed in CHAPTER 10). The triangles in Figs. 6-3 and 6-4 represent the shear strength measured when the split confining ring was separated to eliminate friction.

Figures 6-3 to 6-6 indicate that the average shear stress was essentially constant over a large range of peripheral displacement for all tests. Table 6-1 is a summary of the results of these four tests on disc-shaped specimens and shows that the tests with split confining rings gave lower residual strengths than tests using solid confining rings.

Changes in specimen thickness (ΔB) which took place during each test are shown in the upper part of Figs. 6-3 to 6-6. The change in specimen thickness during shear is a reflection of both change in void ratio and soil extrusion. The shapes of these curves suggest that the change in thickness is mainly due to reduction in void ratio during the early stages of the test because they are straight lines on a semi-log plot. In the final stages of the test, the slope on the semi-log plot, of the ΔB versus δ curves increases, indicating that the decrease in specimen thickness is due mainly to soil extrusion which became visible during the latter stage of the tests. Figures 6-7 and 6-8, which are arithmetic curves of ΔB versus δ for $\bar{\sigma}_v$ = 1.0 kg/sq cm (Fig. 6-7) and $\bar{\sigma}_v$ = 2.0 kg/sq cm, show that extrusion was greater in tests using split rings. The difference between the curves for a split confining ring and a solid confining ring can only be due to extrusion. These curves also show that the rate of soil extrusion increases considerably in tests using a split confining ring when $\bar{\sigma}_v$ is increased from 1.0 to 2.0 kg/sq cm. The final slope of the curve of change in thickness versus peripheral displacement, which is an index of soil extrusion, is shown in Table 6-1 under the heading "rate of soil extrusion."

Table 6-1 summarizes results from these tests and shows that tests using a solid confining ring gave consistently higher residual strengths than tests using a split confining ring. The magnitude of this difference is greater than any error which can be attributed to friction caused by the solid confining ring (see Section 6.4.3).

6.2.4 RESULTS OF CONTROLLED SOIL EXTRUSION TESTS ON DISC-SHAPED SPECIMENS

Additional study of the effect of soil extrusion on residual strength was made by performing a test on a disc-shaped specimen of remolded Warm Springs Shale in which the rate of soil extrusion could be changed during the test by installing or removing the plastic C-clamps from the outer periphery of the split confining ring (Sections 3.4 and 4.7). A second test on a disc-shaped specimen was performed using a solid confining ring.

The stress-displacement curve for the test using the split confining ring is shown in Fig. 6-9.

The average shear stress increases to a pronounced peak of approximately 0.48 kg/sq cm at a peripheral displacement of 3 cm and then begins to decrease. At approximately 10 cm of displacement, the rate of vertical displacement begins to increase slightly on the semi-log plot, indicating soil extrusion was becoming more important than secondary time effects. At a peripheral displacement of 23 cm (Point 1), the C-clamps were installed to restrict the clearance between the confining rings.

Installation of the C-clamps increased the average shear stress because of friction between the mating surfaces of the ring and because of the decreased rate of extrusion. After approximately 80 cm of displacement, the C-clamps were removed. The remainder of the τ_a and ΔB versus δ curves are shown more clearly in Fig. 6-10 in which the displacement subsequent to Point 2 is plotted. τ_a immediately dropped from a value of 0.5 kg/sq cm to approximately 0.45 kg/sq cm (Point 2 to Point 3). The shear stress and the thickness remained constant for an additional displacement of 2 cm (Point 3 to Point 4). Then the shear stress dropped from 0.45 to 0.26 kg/sq cm and the thickness decreased substantially as the specimen extruded between the split confining ring.

Due to the large amount of soil extruded during this test, the upper loading platen tilted slightly and moved downward into the lower half of the confining ring. The radial clearance between the upper platen and the lower ring was insufficient to allow free rotation of the lower confining ring. The retarded rate of decrease of τ_a just before Point 5 and the abrupt increase in τ_a at Point 5 probably occurred as the platen entered the lower ring.

A second test was performed on the remolded Warm Springs Shale using a solid confining ring. Figure 6-11 shows the results of this test. Comparison of Figs. 6-11 and 6-9 indicates a striking difference between the shape of the two τ_a versus δ curves. The pronounced peak obtained in the test using a split confining ring (Fig. 6-9) is absent in the test using a solid confining ring. Figure 6-11 also shows that at large displacements the rate of soil extrusion has been greatly reduced by using the solid confining ring.*

In Fig. 6-9 a dashed line has been drawn from the point of maximum τ_a which is believed to be relatively unaffected by the influence of soil extrusion, to Points 3 and 4 which are believed to represent the residual strength for this test. The shape of this dashed curve is very similar to the shape of the τ_a versus δ curve obtained in the test using the solid confining ring. Thus, the pronounced peak in Fig. 6-9 is an artifact of the large amount of extrusion that occurred before the C-clamps were installed.

Results of these tests on disc-shaped specimens of Warm Springs Shale are shown in Table 6-3. For the test with a split ring, the residual strength recorded is the one measured immediately after removing the C-clamps (Points 3 to 4, Fig. 6-10) because it is believed that this value has not been greatly influenced by soil extrusion. The results of these tests show that the residual strength measured in the test using a solid ring is lower than τ_r measured in the test using a split ring, in spite of the higher rate of extrusion with the split ring. The shape of the τ_a versus δ curve after 10 cm of displacement in the test using a solid ring indicates that τ_r for this test may be low, possibly as a result of extrusion. The magnitude of this possible error would not, however, explain the anomaly of these data.

At the completion of each of these tests, water contents were obtained from each specimen. Figure 6-12a shows the results of water content determinations taken from the test using a split confining ring.** The water content samples included the entire specimen thickness. The moisture

---

*The specimen confined by the split confining ring was precut before it was sheared, which accounts for the small change in thickness during the early part of this test.

**The C-clamps were removed and extrusion allowed for about 30 cm of displacement in the test using a split confining ring before the test was stopped and the water content samples taken.

content at the periphery of the disc was significantly higher than the moisture content at the center of the disc, indicating that $\bar{\sigma}_v$ was lower at the periphery than at the center of the disc. On the other hand, the moisture content distribution for the test using the solid confining ring (Fig. 6-12b) showed a much smaller increase in water content with increasing radius, indicating the $\bar{\sigma}_v$ was more uniform than in WSS TEST 1.

It is suggested that the difference between the measured residual strength using disc-shaped specimens confined by a solid confining ring or a split confining ring is related to the amount of soil which extrudes from the peripheral boundaries of each specimen.

If no extrusion occurs and the specimen is contractive, the increase in tangential displacement with increasing radius causes a corresponding tendency for the void ratio to decrease with increasing radius. Since the loading platens are rigid, there can be no actual difference in void ratio. The vertical stress will be redistributed accordingly, decreasing at the maximum radius and increasing at the minimum radius with the average $\bar{\sigma}_v$ remaining constant (Hvorslev, 1937). For a dilative specimen, the tendency for the void ratio to increase as the radius increases will cause $\bar{\sigma}_v$ to increase at the maximum radius and decrease at the minimum radius. When the residual state is reached on the entire failure plane, there will no longer be a tendency for a change in void ratio and the vertical stress will become uniform.

However, if soil is permitted to extrude from the failure plane, $\bar{\sigma}_v$ will not become uniform even at the residual state. Instead, $\bar{\sigma}_v$ will be lower than average at the location where extrusion is occurring, and soil will be "pumped" from a zone where $\bar{\sigma}_v$ is higher than average. A steady state condition will be achieved with the distribution of $\bar{\sigma}_v$ becoming constant but not uniform. Since $\bar{\sigma}_v$ will be lower at the periphery than at the center of the specimen for any given average $\bar{\sigma}_v$, the measured moment will be smaller than if $\bar{\sigma}_v$ were uniform; hence, τ_r computed from Eq. 5.1 will be smaller than the true residual strength.

One would expect that tests using annular specimens would be less affected by redistribution of $\bar{\sigma}_v$ for a given rate of soil extrusion. To determine if this is the case, a series of tests was performed on the ground muscovite powder and remolded Warm Springs Shale which duplicated the first series except that they were performed on annular specimens.

6.2.5 COMPARISON OF SPLIT VERSUS SOLID CONFINING RINGS USING ANNULAR SPECIMENS

Stress versus displacement and ΔB versus displacement curves for tests on ground muscovite using annular specimens are shown in Figs. 6-12 to 6-16. These tests were performed in a manner identical to that of the tests on disc-shaped specimens (Section 6.2.3) with the exception that Ground Muscovite Test 7 was initially sheared with $\bar{\sigma}_v$ equal to 0.5 kg/sq cm and $\bar{\sigma}_v$ was subsequently increased to 1.0 and 2.0 kg/sq cm which were the values used for other tests.

Table 6-2 summarizes the results of these four tests and shows that the residual strength is not significantly affected by the type of confining ring, even though the rate of extrusion is higher in the case of split confining rings.*

Arithmetic plots of ΔB versus δ for these tests are shown in Figs. 6-17 and 6-18. These curves are very similar to the ΔB versus δ curves obtained in tests using disc-shaped specimens (Figs. 6-7 and 6-8). The rates of soil extrusion for both series of tests are summarized in Tables 6-1 and 6-2 and show that for comparable types of confinement the rate of soil extrusion is essentially independent of specimen shape.

---

* $\tau_r/\bar{\sigma}_v$ for the muscovite used in this investigation varies between 0.278 and 0.282. Horn and Deere (1962) report the coefficient of kinematic friction for cleaved muscovite crystals to be between 0.22 and 0.26. The normal stress at which their tests were performed is not given.

The residual strength results summarized in Tables 6-1 and 6-2 show that tests on disc-shaped specimens give slightly lower residual strengths than tests on annular specimens when radial confinement is by a solid ring. These data suggest that disc-shaped specimens are potentially useful for determining the residual strength of a soil so long as soil extrusion is minimized (in this case, by using a solid confining ring). Their use may be restricted to tests at relatively low vertical stress when testing soils in a contractive state, since the tests performed on ground muscovite indicate a substantial increase in soil extrusion as the vertical stress is increased from 1.0 to 2.0 kg/sq cm.

6.2.6 RESULTS OF CONTROLLED SOIL EXTRUSION TESTS USING ANNULAR SPECIMENS

Additional confirmation of the importance of soil extrusion in a rotation shear test was obtained by a set of tests performed on the remolded Warm Springs Shale using annular specimens. Results of the tests using a split confining ring are shown in Figs. 6-19 and 6-20. Comparing Fig. 6-19 with Fig. 6-9 (duplicate test using disc-shaped specimen), the following observations may be made:

1. The maximum τ_a is larger in the test using an annular specimen due to the smaller effect of progressive failure.
2. The initial shape of the τ_a versus δ curve (C-clamps not installed) has a less pronounced peak for the annular than for the disc-shaped specimen.
3. Removal of the C-clamps at Point 2 resulted in a drop in τ_a of about 0.10 kg/sq cm which is approximately twice the drop in τ_a observed with the disc-shaped specimen. There are two reasons which might explain this observation. First, the stress exerted by the C-clamps could not be controlled accurately, although differences should be small. Second and more important, if the additional moment due to friction between the confining rings were identical in both tests, the computed τ_a would be larger for the annular specimen, since the equation used to compute τ_a for annular specimens ($\tau_a = KM$, where K is a function of geometry only) has a larger constant multiplier than does the equation used to compute τ_a when disc-shaped specimens are used.
4. The τ_a versus δ curve from Point 2 until the test was stopped has been replotted in Fig. 6-20. τ_a remains unchanged for slightly more displacement in this test than in the test on a disc even though the ΔB versus δ curves are very similar (Fig. 6-10). This result might be expected since the measured moment is less sensitive to the effects of redistribution of $\bar{\sigma}_v$ for the annulus.
5. The value of τ_a immediately after removal of the C-clamps is slightly larger for the annular specimen than for the disc-shaped specimen (0.477 versus 0.455 kg/sq cm). As explained previously, the C-clamps do not prevent soil extrusion entirely and it is likely that $\bar{\sigma}_v$ would be slightly nonuniform even while the C-clamps were in place.
6. After about 3 cm of peripheral displacement subsequent to removal of the C-clamps in the test using an annular specimen, τ_a begins to decrease, probably due to the redistribution of $\bar{\sigma}_v$. Eventually, τ_a becomes constant again due to a constant but <u>nonuniform</u> distribution of $\bar{\sigma}_v$.
7. This new constant value of τ_r (with extrusion) is much larger for the case of the annular specimen than for the disc-shaped specimen (0.405 versus 0.206 kg/sq cm). This indicates the reduction in τ_a as a result of soil extrusion is smaller for the annular specimen than for the disc, as would be expected.

A second test was performed on an annular specimen of Warm Springs Shale using a solid confining ring. The results of this test are shown in Fig. 6-21. Comparing the shape of the τ_a versus δ curve for this test with results obtained from the annular specimen using a split confining ring (Fig. 6-19), one finds that the two curves are similar until the C-clamps were installed in the test using a split confining ring.

The results of these tests on annular specimens of Warm Springs Shale are shown in Table 6-4. For the test with a split confining ring, the residual strength recorded is the one measured immediately after removing the C-clamps (Points 3 and 4, Fig. 6-20).

The results of tests on remolded Warm Springs Shale, summarized in Tables 6-3 and 6-4, show a pattern similar to the one observed for tests on ground muscovite. Namely, the disc-shaped specimens give lower residual shear strengths than the annular specimens. This result is attributed to the greater influence of the redistribution of $\bar{\sigma}_v$ in tests on disc-shaped specimens.

One other result of these tests, not shown by the tests on ground muscovite, is that if soil extrudes during a test on an annular specimen, the measured strength may be low. Figure 6-20 shows that the residual strength of remolded Warm Springs Shale dropped 15% when extrusion was permitted.

Factors which will determine the importance of redistribution of $\bar{\sigma}_v$ in a rotation shear test are:

1. Ratio of inside to the outside radius of the specimen. As this ratio increases, the effect of redistribution will decrease. In the Harvard rotation shear machine, this ratio is 0.70; other existing rotation shear machines have radius ratios from 0.51 to 0.66.
2. The amount of soil extrusion: In the tests on ground muscovite, the amount of soil extrusion is considered very small. The largest rate of extrusion (Section 6.2.5) measured in these tests was 8×10^{-4} in./cm. No direct comparison between the rate of extrusion experienced with the Harvard rotation shear machine and other designs is available.

6.3 ERROR CAUSED BY FAILURE OCCURRING NEAR A LOADING PLATEN

The possibility of failure taking place at the interface between the soil specimen and the porous disc seems remote when one contrasts the size of the clay particles (minus 0.002 mm) with the height of the asperities on a porous disc such as is used in the Harvard rotation shear machine (on the order of 0.1 to 0.2 mm).

Results of the tests on annular specimens of ground muscovite (Table 6-2) and remolded Warm Springs Shale (Table 6-4) indicate that the maximum difference in residual strength between tests where failure occurred at the midplane of the specimen and those where failure occurred about 0.5 mm from the top porous disc, was 3%. This difference includes all other sources of error as well as the one due to location of the failure plane.

In tests with more plastic materials (CHAPTERS 7, 8 and 9), failure never took place at the porous disc, although in some tests, only a thin slickensided film of clay adhered to the disc when the test was dismantled. No significant difference in residual strength was measured in tests where only a slickensided film remained on a disc as compared to those tests in which the slickenside was farther from the disc.

It is concluded from these data that forcing failure to occur near a porous disc does not introduce any significant error in the residual strength.

6.4 ERRORS IN VERTICAL STRESS

6.4.1 ERROR CAUSED BY LEVER SYSTEM

The precision of the lever system was determined by a series of load-unload cycles performed with proving rings in place of the shearing unit. The precision was found to be as good as the proving rings themselves, i.e., 0.1% to 0.25%.*

Errors in the residual strength caused by the lever system are estimated to be not greater than plus or minus 0.1% to 0.25% of any given value.

6.4.2 ERROR CAUSED BY SIDE FRICTION

Load applied to the top surface of a specimen confined in a ring is diminished with depth due to side friction. Equations are derived in Section A.2 for the ratio of the vertical stress on the failure plane, $\bar{\sigma}_v'$, to the vertical stress on the top of the specimen, $\bar{\sigma}_v$.

In tests using a split confining ring (6-mm-thick specimens), failure generally occurs 0.2 cm below the top of the specimen. In this case, $\bar{\sigma}_v'$ will be about 2% lower than $\bar{\sigma}_v$ for annular specimens and 1% lower than $\bar{\sigma}_v$ for disc-shaped specimens.

In tests using a solid confining ring, failure generally occurs about 0.05 cm below the top of the specimen, and $\bar{\sigma}_v'$ will be about 0.5% lower than $\bar{\sigma}_v$ for annular specimens and 0.2% lower than $\bar{\sigma}_v$ for disc-shaped specimens.

6.5 ERRORS IN THE MEASURED MOMENT

6.5.1 ERRORS CAUSED BY MEASURING SYSTEM

The force transducers used have an accuracy of about plus or minus 0.1% for the upper 80% of their range and about plus or minus 0.3% for the lower 20% of their range. The transducer power supply and the digital millivoltmeter have an accuracy of plus or minus 0.1%.

Hence, with the proper selection of transducers, the maximum error in the measured moment due to the electronic measuring system would be plus or minus 0.3%. The technique for ensuring that the electronic components are functioning properly is explained in Section A.3.

6.5.2 ERROR CAUSED BY FRICTION IN THE SPLIT CONFINING RING

The detailed analysis of this error is made in Section A.4. It shows that if failure occurs at the same elevation as the split in the ring and $\tau_r/\bar{\sigma}_v$ for the soil being tested is 0.10, the measured shear stress will be about 2.5% high due to friction between the two halves of the ring. As $\tau_r/\bar{\sigma}_v$ increases, the percent error decreases.

This error may be eliminated by temporarily separating the two halves of the confining ring when measuring the moment (Section 4.8).

6.5.3 ERROR CAUSED BY FRICTION BETWEEN THE SOLID CONFINING RING, THE STATIONARY PLATEN AND THE STATIONARY PART OF THE SPECIMEN

Results of measuring moments with the solid confining ring in position and with it removed are reported in Section A.5. These data indicate that the additional shear stress due to ring friction is independent of $\bar{\sigma}_v$ and the overconsolidated ratio, and is about 0.020 kg/sq cm for tests

---

*The lead weights placed on the hangers were within 0.05% of their rated weight.

using Pepper Shale and Cucaracha "Shale" and is about 0.030 kg/sq cm for London Clay.

A more complete discussion of the effect of removing the confining ring during a test is presented in Section A.5 where it is concluded that removing the confining ring for a few minutes during a test eliminates the error due to friction without introducing any other significant error.

6.5.4 ERROR CAUSED BY FRICTION BETWEEN ROTATING CENTER DISC AND THE STATIONARY PART OF THE SPECIMEN

Observations made of test specimens at the end of a test showed that a slickenside was developed on the inner periphery of the stationary part of the specimen, indicating the center disc rotates during the test (see Fig. 3-20). If it is assumed that the coefficient of friction between the Teflon center disc and the slickensided surface of soil is one-half $\tau_r/\bar{\sigma}_v$, the computed residual strength will be about 1.4% high due to this friction.

6.6 CONCLUSIONS

The investigations described in Section 6.2 have indicated that an error in the measured moment will result if soil is permitted to extrude from the confining ring. This error is not associated with friction between the elements used to confine the specimen, but with a redistribution of the vertical stress on the failure plane. Extrusion from between a split confining ring will cause the vertical stress to decrease at this specimen boundary. Since the vertical load is constant, $\bar{\sigma}_v$ will increase at the inner periphery of the specimen. At the residual state the vertical stress will achieve a constant (but nonuniform) distribution and hence a constant moment will be measured. Because $\bar{\sigma}_v$ is reduced at the outer periphery of the specimen, the moment will be smaller than if $\bar{\sigma}_v$ were uniform; hence, the computed τ_r will be too small.

The most important factors influencing the magnitude of this error due to vertical stress distribution are:

1. The ratio of the minimum specimen radius R_2 to its maximum radius R_1. As this ratio decreases, the effect of redistribution of $\bar{\sigma}_v$ increases.
2. The amount of soil which is extruded from the specimen.
3. The magnitude of the average vertical stress.
4. The residual strength of the soil.

Tests on disc-shaped specimens of ground muscovite summarized in Table 6-1 indicate that if soil is allowed to extrude from between the halves of a split confining ring, τ_r will be about 12% lower than if extrusion is reduced by using a solid confining ring. On the other hand, if the same boundary conditions (hence the same amount of extrusion) are imposed on an annular specimen ($R_2/R_1 = 0.7$), the residual strength is unaffected (Table 6-2).

Comparing the results of tests on disc-shaped specimens with results from annular specimens indicates that disc-shaped specimens may be useful at low effective stresses when a solid confining ring is used.

The clearance between the halves of the split ring used in the tests on ground muscovite was 0.002 inch and the amount of soil extruded during a test was small. To determine the maximum error that could result from allowing soil to extrude during a test on an annular specimen, tests were performed with a solid confining ring which was removed from the specimen after the residual state was reached.

When the confining ring is removed, the moment drops to a new value which is independent of displacement, as shown in the sketch below. This new "residual state" is due to a constant but nonuniform distribution of $\bar{\sigma}_v$.

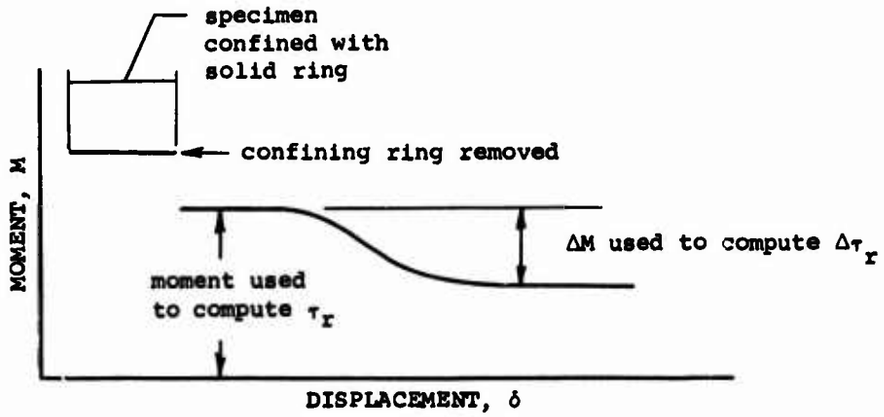

The results of these tests, shown in Table 6-5, give an indication of the maximum error that can occur due to soil extrusion from a specimen with $R_2/R_1 = 0.70$. Further investigations are needed before the error due to soil extrusion can be completely evaluated. These investigations can be made using annular specimens confined with a split ring designed to allow the clearance between the halves of the ring to be varied. The rings should also be designed to permit them to be temporarily separated to eliminate friction caused by the soil extruding into the gap between them.

It is believed that using annular specimens ($R_2/R_1 = 0.70$) with a solid confining ring reduces the error due to soil extrusion (redistribution of $\bar{\sigma}_v$) to a tolerable value.

Other sources of error in τ_r and their estimated maximum magnitude are summarized below.

Source of Error	Probable Magnitude of Error in τ_r When Using Annular Specimens
$\bar{\sigma}_v$ due to lever system	± 0.1% to ± 0.25%
$\bar{\sigma}_v$ due to side friction	- 0.5%
Moment measuring system	± 0.3%
Friction between center disc and specimen	+ 1.4%

The sum of these errors is always positive (+ 0.4% to + 1.4%) while the small error (when using an annular specimen and a solid confining ring) due to soil extrusion will always be negative.

CHAPTER 7

PEPPER SHALE

7.1 PURPOSE AND SCOPE

To determine whether the residual S strength was independent of overconsolidation ratio (OCR), the Pepper Shale was used in the following testing program:

State and Condition	Specimen Shape	Confinement
Remolded, normally consolidated	Annulus	Solid ring
Remolded, overconsolidated	Annulus	Solid ring
Undisturbed	Disc	Solid ring

As further evidence of the effect of soil extrusion on determining the residual strength in a rotation shear test, two tests were performed on remolded disc-shaped specimens. One was radially confined with a solid ring and the other had no radial confinement.

7.2 SOIL DESCRIPTION

The soil used in this investigation was obtained by the U.S. Army Corps of Engineers during exploration for Waco Dam, Texas. All specimens were obtained from a 6-inch-long section of Denison sample 29 taken at a depth of between 82.5 to 83.4 ft. in Hole No. 8A6C-351.

The undisturbed soil was a black, heavily overconsolidated clay, which was hard and brittle. The sample was homogeneous in color and consistency. It had a soapy feel when rubbed with the fingers and could be shaved with a sharp knife into very thin, translucent shavings which had a slight yellowish tint. At its natural water content of about 21%, it could be shined with the thumbnail to a very high gloss.

When immersed in distilled water at its natural water content, the soil disintegrated into flat, flake-shaped pieces between about 0.5 and 4 mm thick. After swelling for 48 hours, these flakes could be completely remolded between the fingers to a smooth paste with moderate effort.

The air-dried soil disintegrated rapidly to fine sand-sized particles when slaked in distilled water. After 48 hours of immersion, the particles could be very easily remolded to a smooth paste between the fingers.

There was no reaction to HCL in this sample, although samples above and below it have calcareous zones. No slickensides were observed in the sample. The specific gravity of the solids is 2.76.

The soil to be used for remolded specimens was obtained by air-drying thin shavings of the undisturbed soil. The air-dried shavings were ground into a fine powder, using a mortar and pestle, and then added to distilled water and dried to the desired water content. Soil prepared in an identical manner was used to determine the Atterberg limits, which are tabulated below and shown on the Plasticity Chart in Fig. 7-1.

Treatment	L_w	P_w	P_i
Air-dried	70.5	21.5	49.0
Oven-dried	75.5	23.0	52.5

At the plastic limit, the soil was tough. When a pat of soil was air-dried from near the liquid limit, it had a very high dry strength. Results of a hydrometer analysis performed on the air-dried soil are shown in Fig. 7-2. A 0.01 N solution of sodium metaphosphate was used as the suspending fluid.

7.3 TEST RESULTS

7.3.1 REMOLDED – NORMALLY CONSOLIDATED SPECIMENS

Shear stress versus displacement curves for the four tests in this phase of the investigation are shown in Figs. 7-3 to 7-6. The maximum average shear stress occurs at displacements of 0.06 to 0.09 cm. There is an abrupt decrease in strength beyond the peak, and the residual strength is reached at about 1 to 2 cm of displacement. The value of $\bar{\sigma}_v$ has little or no effect on the displacement required to reach τ_r.

Measurements of change in thickness during shear for these tests show that very little soil extrusion occurred during TESTS 1, 2 and 3; slightly more extrusion occurred in TEST 4, which was performed at the highest vertical stress (12.0 and 20.0 kg/sq cm).

Table 7-1 summarizes the results of these tests. The residual strength line obtained from the tests (Fig. 7-7) is a straight line through the origin with a slope of 7.5 degrees. The peak strength (τ_p) line, also shown in Fig. 7-7, has a slope of 11.7 degrees and a cohesion intercept of 0.04 kg/sq cm. The confining ring was not removed at the peak strength; hence τ_p includes the friction due to the confining ring which is estimated to be equivalent to a shear stress between 0.01 and 0.03 kg/sq cm.

Table 7-2 summarizes observations of the failure plane at the end of these tests and shows that all the failure planes were very shiny and essentially flat with shallow circular striations.

TEST 5 was performed on a disc-shaped specimen to determine if the residual strength would be the same as that obtained with an annular specimen when soil extrusion was minimized by confining the disc with a solid ring. Figure 7-8 shows the results of this test, which are summarized in Table 7-3 along with TEST 1, the companion test on an annular specimen. The residual strengths measured at the three vertical stresses used are slightly lower than the strengths measured in the test on the annular specimen. This result may be due to a small redistribution of $\bar{\sigma}_v$ on the disc. However, the differences are so small that this cannot be given as a definite conclusion. The ΔB versus δ curves are practically identical for both tests (compare Figs. 7-3 and 7-8).

Results from TESTS 1 and 5 at $\bar{\sigma}_v$ = 1.0 kg/sq cm have been plotted together in Fig. 7-9. The τ_a versus δ curve for the disc-shaped specimen lies to the right of the curve for the annular specimen. This shift is a result of the technique of computing τ_a (Section 5.1) which gives a weighted average of the true shear stress distribution. The maximum τ_a measured with the disc-shaped specimen is slightly lower than that measured with the annular specimen (0.22 versus 0.26 kg/sq cm). Since the disc is the extreme case in which τ_a (the weighted average shear stress) would deviate from the true peak strength, it would seem unlikely that the difference between the true peak strength and τ_p measured in the test using an annular specimen (R_2/R_1 = 0.70) would be larger than 0.04 kg/sq cm.

In CHAPTER 6 it was suggested that soil extrusion caused a redistribution of $\bar{\sigma}_v$ on the failure plane. One way of demonstrating that $\bar{\sigma}_v$ was not uniform when there was extrusion would be to show that radial stresses existed on the failure plane. If the radial stresses did exist, the author suspected that they would affect the topography of the slickenside obtained in a test. To ascertain whether this was the case, a test was performed on a radially unconfined, disc-shaped specimen of remolded Pepper Shale. The results of this test are shown in Fig. 7-10. The τ_a versus δ curve showed no sign of achieving a horizontal asymptote when the test was stopped at a displacement of 1.8 cm. The result from an identical test (TEST 5) with radial confinement is shown by the dashed line in Fig. 7-10.

Photographs of the slickensides from the unconfined test in Fig. 7-11 show that the striations on the failure plane spiral out from the center.* Striations on the slickensides of a confined specimen have a concentric circular pattern. The spiral striations must be the result of combined tangential and radial displacement (hence radial stress) on the failure plane.

7.3.2 REMOLDED – OVERCONSOLIDATED SPECIMENS

According to the working hypothesis discussed in CHAPTER 1, the residual strength should be independent of the OCR. This aspect of the hypothesis was examined by performing a series of tests on remolded Pepper Shale in which specimens were consolidated to 10 kg/sq cm and then unloaded to a stress of 1.0, 2.0 or 4.0 kg/sq cm.

Shear stress versus deformation curves for these tests are shown in Figs. 7-12 to 7-15. The results are summarized in Table 7-4. The residual strength line shown in Fig. 7-18 lies slightly above the strength line obtained from the tests on normally consolidated specimens.

The summary plot of the shear stress versus displacement curves shown in Fig. 7-16 shows:

1. The ratio $\tau_p/\bar{\sigma}_v$ and the rate of dilation at the peak increase with increasing OCR.
2. Displacement at the peak (δ_p) decreases from 0.060 cm to 0.023 cm as the OCR increases from 2.5 to 10.
3. The displacement required to reach the residual strength (δ_r) decreases from 6.0 cm to 2.0 cm as the OCR increases from 2.5 to 10. (At OCR = 1, the displacement required to reach τ_r is 3.0 cm.)

The ΔB versus δ curves for all these tests indicate the soil was dilative at the start of the test. In TESTS 7 and 8, the specimen thickness, B, becomes essentially constant at a displacement of about 1 cm when the residual strength has been reached. In TESTS 9 and 10, B begins to decrease at a displacement of about 2 cm due to a slight amount of extrusion which could be observed in these tests.

After the residual strength had been measured at $\dot{\delta} = 5.6 \times 10^{-3}$ cm/min in TEST 7, $\dot{\delta}$ was reduced to 5.6×10^{-4} cm/min. The residual strength measured at $\dot{\delta} = 5.6 \times 10^{-4}$ cm/min, shown in the inset in Fig. 7-12, indicates there is no difference in τ_r measured at these two velocities.

The residual strength line from these tests (Fig. 7-18) shows that the difference between it and the strength line from normally consolidated specimens increases as the OCR increases. To investigate the effect of overconsolidation further, a test was performed on the remolded Pepper Shale at $\bar{\sigma}_v = 1.0$ and with an overconsolidation ratio of 100.

---

*Spiral striations were not observed on the failure planes of tests on ground Muscovite or Warm Springs Shale confined with a split ring, reported in Chapter 6, because soil extrusion was not unlimited, and the slickensides were not as well-defined as with the Pepper Shale.

The results of TEST 11, performed at $\bar{\sigma}_v$ = 1.0 kg/sq cm and at an overconsolidation ratio of 100, are shown in Fig. 7-17 along with the τ_a versus δ curve from TEST 7 ($\bar{\sigma}_v$ = 1.0, OCR = 10). The results of TEST 11 are also included in Table 7-4. When the OCR increased from 10 to 100, the peak strength increased and the displacement required to achieve peak strength decreased. The displacement required to achieve the residual strength is somewhat larger for TEST 11 than for the tests with an overconsolidation ratio of 10. The ΔB versus δ curve for TEST 11 shows the specimen was strongly dilative and reaches a constant thickness at about the same displacement the residual strength is reached. The residual strength of 0.122 falls between the results of the tests with overconsolidation ratios of 1 and 10 (see Table 7-4).* Table 7-5 summarizes observations made of the failure planes for the tests on overconsolidated specimens. They were very shiny, with no observable difference in shine between these failure planes and those observed in normally consolidated specimens. The topography of the failure planes in the overconsolidated specimens had shallow radial and tangential undulations which were absent from the failure planes of the normally consolidated specimens.

7.3.3 UNDISTURBED SPECIMENS

Comparison of the residual strengths of remolded and undisturbed specimens would provide additional data concerning the effect of the OCR, and a series of tests on undisturbed disc-shaped specimens was performed.

The τ_a versus δ curves of the five tests in this series (TESTS 12 to 16) are shown in Figs. 7-19 to 7-23 and the results are summarized in Table 7-6. Figure 7-24 is a summary of the τ_a versus δ curves for the tests on undisturbed specimens and shows:

1. The ratio $\tau_p/\bar{\sigma}_v$ ranges between 0.25 and 0.31 with no correlation with $\bar{\sigma}_v$.
2. ΔB versus δ for TEST 12 shows B is increasing during this test; in all other tests it was decreasing (including TEST 13 which was a duplicate of TEST 12).
3. The displacement required to achieve peak (δ_p) decreases from 0.07 cm to 0.03 cm as $\bar{\sigma}_v$ increases from 1.0 to 4.0 kg/sq cm.
4. The displacement required to achieve the residual strength (δ_r) ranges between 20 cm and 35 cm with no relationship between δ_r and $\bar{\sigma}_v$.

In general, the shapes of the shear stress versus displacement curves for these tests are more irregular than the curves for tests on overconsolidated specimens (compare Figs. 7-16 and 7-24).

Results of change in thickness measurements for this series of tests indicate the specimens may not be truly undisturbed. It is difficult to handle and trim a specimen for any laboratory test without causing some disturbance, b the problem is particularly acute in trimming thin specimens for the rotation shear machine. Both top and bottom surfaces of the disc are trimmed flush with the confining ring with a stiff knife, causing some disturbance to the surfaces. To minimize soil extrusion, a solid confining ring was used in these tests, forcing failure to occur near the top of the disc, where the disturbance was greatest.

While the specimens used in this series of tests are not truly undisturbed, it is likely that their structure (even near the top or bottom of the disc) was significantly different from that of the completely remolded specimens. Evidence for this conclusion is twofold:

---

*All tests were performed on specimens from the same batch of remolded soil prepared at the start of the investigation.

1. The peak strengths measured with undisturbed specimens are, in most cases, higher than the peak strengths of the remolded specimens (Tables 7-1 and 7-6).
2. Displacements to peak are smaller for undisturbed specimens than for remolded specimens (Tables 7-1 and 7-6).

These results were obtained in spite of the fact that the undisturbed specimens were discs, which would cause the peak strength to be lower and the deformation to peak to be larger than for a duplicate test on an annular specimen (see Fig. 7-9).

A residual strength line from the undisturbed specimens is shown in Fig. 7-25, along with the residual strength line obtained from the remolded, normally consolidated specimens. Between 1 and 2 kg/sq cm, the two strength lines are practically identical. At $\bar{\sigma}_v$ = 4.0 kg/sq cm, the strength of the undisturbed specimens is significantly lower than the strength from the remolded specimens.

At the completion of the two tests on undisturbed specimens with $\bar{\sigma}_v$ = 4.0 kg/sq cm, samples were taken to determine the water content distribution (nearly the entire specimen thickness was used). Results of these water content determinations, presented in Fig. 7-26, show that there has been a significant increase in water content at the periphery of the discs. This water content distribution indicates that $\bar{\sigma}_v$ was lower at the periphery than at the center of the disc.*

Results of these five tests on undisturbed specimens are difficult to evaluate for the following reasons:

1. Probable disturbance due to specimen preparation.
2. Nonuniform moisture contents in two tests, indicating redistribution of $\bar{\sigma}_v$ on the failure plane.
3. Unexplained irregularities in four of the τ_a versus δ curves.

The fact that the residual strengths from undisturbed specimens are practically the same as those from remolded specimens at $\bar{\sigma}_v$ of 2.0 kg/sq cm and less may be fortuitous. The measured strengths from the undisturbed specimens may be below the true residual strength due to a minor redistribution of $\bar{\sigma}_v$. At $\bar{\sigma}_v$ = 4.0 kg/sq cm, the existence of a nonuniform distribution of vertical stress is verified by water content determinations made at the completion of the tests.

7.4 CONCLUSIONS

7.4.1 REMOLDED – NORMALLY CONSOLIDATED SPECIMENS

Results of tests on normally consolidated, annular specimens indicate the residual strength line of remolded Pepper Shale is a straight line through the origin, at a slope of 7.5 degrees for a vertical stress range of 1.0 to 20 kg/sq cm (Fig. 7-7). The peak strength line for a vertical stress range of 1.0 to 12.0 kg/sq cm is represented by a straight line with a slope of 11.7 degrees and a cohesion intercept of 0.04 kg/sq cm, but this intercept may be partly due to friction between the upper platen and the rotating confining ring which was not removed at the peak strength.

Displacements to the peak strength range from 0.060 cm at $\bar{\sigma}_v$ = 1.0 kg/sq cm to 0.090 at 12.0 kg/sq cm. The amount of displacement required to achieve the residual strength decreases from 3 cm at $\bar{\sigma}_v$ = 1.0 kg/sq cm to 1.5 cm at $\bar{\sigma}_v$ = 12.0 kg/sq cm with the test at $\bar{\sigma}_v$ = 4.0, not fitting the general pattern and requiring 7 cm of displacement to achieve τ_r.

*These specimens showed a decrease in thickness in spite of an increase in water content because of trimming disturbance near the failure zone and soil extrusion. The failure zone was removed when the tops of the discs were scraped to minimize the effect on the water content determinations of water adsorbed from the porous discs.

A test performed on a disc-shaped specimen of remolded Pepper Shale at three vertical stresses gave slightly lower strengths than a similar test on an annular specimen. These results may be due to a small redistribution of $\bar{\sigma}_v$ on the disc-shaped specimen.

Striations on the failure plane of an unconfined disc-shaped specimen spiral out from the center of the specimen (Fig. 7-11). It is hypothesized that the spiral striations are a result of combined tangential and radial displacements on the failure plane which would be associated with a nonuniform distribution of $\bar{\sigma}_v$.

7.4.2 REMOLDED – OVERCONSOLIDATED SPECIMENS

The results of tests on remolded, annular specimens with overconsolidation ratios ranging from 1 to 100 and $\bar{\sigma}_v$ ranging from 1 to 4 kg/sq cm indicate the residual strength of these specimens is higher than the residual strengths of normally consolidated specimens (Fig. 7-18).

The magnitude of the differences is small and the number of tests limited, making conclusions concerning the effect of the OCR difficult. The number of tests would have to be increased to obtain statistically significant results before definite conclusions could be reached.

The τ_a versus δ curves for these tests are summarized in Fig. 7-16, which shows that the deformation necessary to reach the peak strength decreases from 0.06 cm to 0.02 cm as the OCR increases from 1 to 100.

Deformations required to reach the residual strength are not easily correlated with the overconsolidation ratio. There seems to be no definite trend established between the displacement required to reach the residual strength and the OCR. However, test results show that a displacement of 0.2 cm results in a shearing resistance of 81% to 55% of the peak strength as the OCR increases from 1 to 10.

7.4.3 UNDISTURBED SPECIMENS

Tests on undisturbed disc-shaped specimens were performed to help establish the effects of the overconsolidation ratio on the residual strength. The results of these tests are believed to be inconclusive due to a redistribution of $\bar{\sigma}_v$. In two tests ($\bar{\sigma}_v$ = 4.0 kg/sq cm), water content determinations at the end of the tests showed that the water content was greater at the periphery than at the center of the disc, indicating $\bar{\sigma}_v$ was not uniform. It is inferred from these water content measurements that $\bar{\sigma}_v$ may not have been uniform at the lower effective stresses used in these tests, causing the measured strength to be low.

CHAPTER 8

CUCARACHA "SHALE"*

8.1 PURPOSE AND SCOPE

The purpose of this phase of the investigation was to test specimens of remolded material from the Cucaracha formation of the Panama Canal Zone to determine:

1. The residual strength line for vertical stresses between 1 and 20 kg/sq cm.
2. The effect of overconsolidation on the residual strength of the remolded material.
3. Whether there was a difference in residual strength between material which had been remolded by slaking in distilled water or by air-drying and crushing in a disc mill.

All tests were performed on annular specimens with solid confining rings. No undisturbed specimen could be trimmed from the intensely slickensided sample available.

8.2 SOIL DESCRIPTION

The material used in this investigation was obtained by the U. S. Corps of Engineers during explorations of a slide area at Hodges Hill, Panama Canal Zone. The material tested was from Denison sample 13, taken at a depth of between 57.5 to 58.5 feet in Hole No. CRW-15. The sample was air-dried when received and was reddish purple, hard, and highly slickensided. The sample breaks easily into irregular, bulky-shaped pieces having a volume between a few cubic centimeters and about 100 cc. The pieces are generally bounded on at least two sides (which may be parallel or perpendicular) by very glossy slickensides which are generally dark reddish purple. The remaining sides of a broken piece are irregular and lighter colored and may also have relatively minor slickensides which are less shiny than the major slickenside surfaces.

In general, the slickenside surfaces have wide shallow undulations perpendicular to the axis of movement. These wide undulations dip into the surface of the slickenside parallel to the axis of movement so that they are not continuous along the slickenside. Most, but not all of the slickensides have closely spaced striations superimposed on their surface (see Fig. 8-1). Occasionally, the slickensides contain light gray spots and streaks which are as shiny as the rest of the surface. The cross section of a slickensided surface examined with a stereoscopic microscope (100X) has the appearance of molten glass. The air-dried soil can be shaved with a sharp knife into thin shavings. A shaved surface can be shined to a high gloss with the thumbnail and has a smooth, soapy feel. The ability to be shaved into thin shavings, as well as the appearance of the slickensides, indicates the sample contains a negligible amount of sand. There is no reaction to HCL. The air-dried material slakes very quickly into silt and fine sand-sized particles in distilled water. When the slaked material was immersed in water and viewed under a microscope, the particles were bulky and opaque. All of the fine sand-sized particles could be easily broken on a microscope slide with the point of a pin.

---

*The formation and diagenesis of the Cucaracha formation has not been unequivocally defined and some geologists question whether the term shale is correct.

A representative piece of the sample was air-dried and slaked four times. The liquid limit was 49 and the plastic limit 28. The material had low toughness at the plastic limit. When air-dried from near the liquid limit, the material was easily crushed into fine sand-sized particles between the fingers. At a moisture content below the plastic limit, the soil achieved a high gloss when rubbed against the fingernail. The liquid and plastic limits did not appear consistent with the glossy slickensides that were observed in the sample.

The author assumed that the silt-sized and sand-sized particles remaining after slaking were actually slightly bonded clusters of clay particles. To disaggregate these clusters, the material was air-dried a fifth time and crushed for six minutes in a disc mill (Angstrom Model No. T250). (This mill is designed to operate with a zero clearance between the grinding surfaces when there is no soil in the mill.) The material was ground to a fine powder which was added to distilled water. At the liquid limit the crushed material was very smooth and creamy, had the consistency of a very light grease, and felt soapy between the fingers. The crushed material was also very thixotropic at the liquid limit. When a pat of the crushed material was air-dried from near the liquid limit, it had an extremely high dry strength. Results of the Atterberg limits on samples prepared by both types of treatment are shown below and on the Plasticity Chart in Fig. 8-2.

Treatment	L_w	P_w	P_i	Activity
Slaked four times	49	28	21	0.5
Slaked four times and crushed	156	42	114	1.1

Results of the hydrometer tests on samples prepared by both treatments are shown in Fig. 8-3. The hydrometer tests were performed using a 0.01 N solution of sodium metaphosphate. The specific gravity of the crushed material is 2.85. The specific gravity of the uncrushed material was not determined.

8.3 TEST RESULTS

8.3.1 SLAKED AND CRUSHED CUCARACHA: NORMALLY CONSOLIDATED

The τ_a versus δ and ΔB versus δ curves for the seven tests performed in this phase of the investigation are shown in Figs. 8-4 to 8-10. The residual strength line obtained from the tests shown in Fig. 8-12 is a straight line between effective vertical stresses of 2 and 20 kg/sq cm with a slope of 6.4 degrees and a cohesion intercept of 0.1 kg/sq cm. Results of tests at $\bar{\sigma}_v$ = 1.0 kg/sq cm indicate the strength line is curved below 2.0 kg/sq cm and the actual cohesion intercept is very near zero (Fig. 8-13). The results of all tests are summarized in Table 8-1.

To study the reproducibility of results, three duplicate tests were performed at $\bar{\sigma}_v$ = 1.0 kg/sq cm. The τ_a versus δ curves for these tests (TESTS 1, 2 and 3) are shown in Figs. 8-4, 8-5 and 8-6. The results of TESTS 1 and 2, plotted in Fig. 8-6, along with τ_a versus δ curve for TEST 3 show:

1. The peak strength (τ_p) ranges between 0.410 and 0.420 kg/sq cm.
2. The displacements to peak (δ_p) vary between 0.020 and 0.037 cm.
3. The residual strength for TESTS 1 and 2 are practically identical (0.195 versus

0.190 kg/sq cm). The residual strength for TEST 3 is 0.151 kg/sq cm.

4. The displacement required to achieve the residual strength (δ_r) varies between 0.7 and 10 cm.
5. The ΔB versus δ curves for TESTS 1 and 2 are practically identical and show B decreased more in these tests than in TEST 3.

The shapes of the τ_a versus δ curve for TESTS 1 and 2 are similar with the exception that about four times more displacement is required to reach τ_r in TEST 2 than in TEST 1. The τ_a versus δ curve for TEST 3 has a more pronounced peak than TESTS 1 and 2, due to a more abrupt reduction in τ_a beyond the peak (τ_p is practically identical in all three tests). The possibility that redistribution of $\bar{\sigma}_v$ is responsible for the low residual shear strength and more peaked τ_a versus δ curve of TEST 3 seems remote since an annular specimen and a solid confining ring were used in this test. In fact, the ΔB versus δ curves (Fig. 8-6) indicate less soil extrusion occurred (hypothesized to be necessary for redistribution of $\bar{\sigma}_v$ at the residual state) in TEST 3 than in TESTS 1 and 2.

Indirect evidence that the results obtained in TEST 3 are not influenced by redistribution of $\bar{\sigma}_v$ may be seen in Fig. 8-4. After 9 cm of displacement in TEST 1, with the residual strength well-defined, the confining ring was removed. Substantial extrusion occurred as demonstrated by the ΔB versus δ curve in the upper part of Fig. 8-4. The τ_a versus δ curve in the lower part of Fig. 8-4 shows that this unrestricted extrusion had a small effect on the measured residual strength. The results of TEST 3 cannot be explained by any known test error and may represent the range of scatter to be expected in repeat tests on this material under identical conditions.

TESTS 4, 5 and 6 (Figs. 8-7 to 8-9) were multiple load tests, each performed at two values of $\bar{\sigma}_v$. The τ_a versus δ curve for the first phase (lowest $\bar{\sigma}_v$) of each test has a well-defined horizontal section. During the second phase of TESTS 4 and 5 (higher $\bar{\sigma}_v$), τ_a decreases after an initial constant shearing resistance has been reached. In TEST 4 this reduction is small and gradual. In TEST 5, however, the reduction is more abrupt and the magnitude of reduction is about twice the magnitude measured in TEST 4. Once the reduction has occurred, the shear strength remains nearly constant for a large amount of displacement (in both cases, for more than one complete revolution, equal to 22.3 cm of displacement). Enough data have been collected to demonstrate that this phenomenon is not due to normal scatter.

The reason for the unusual shape of the τ_a versus δ curve during the second stress level in TESTS 4 and 5 has not been established. The residual strengths measured at the end of these tests (with confining ring removed) have been corroborated by the results of TESTS 5 and 7 (see Table 8-1).

To determine the effect of rate of displacement on this material, the residual strength was determined at $\dot{\delta} = 5.6 \times 10^{-2}$, 5.6×10^{-3} and 5.6×10^{-4} cm/min. The negligible effect of these rates of displacement on the residual strength may be seen in Fig. 8-10 and Table 8-3.

For all practical purposes, it is concluded that changing the rate of displacement by a factor of 100 did not influence the residual strength, once the residual strength was reached.

To establish the most efficient test procedure for determining the residual strength of a soil, it would be of interest to perform tests having very high rates of displacement during the early stages of the test. After a constant shearing resistance was reached, the rate of displacement would be reduced to determine the strength at a slower rate of displacement. The results of such a test would be compared with results of a test which was performed at the slow rate of displacement throughout the entire test.

A description of the failure plane at the end of each test is included in Table 8-2. In general, the failure planes were very shiny and at vertical stresses of 8 kg/sq cm and above they were nearly as glossy as the natural slickensides observed in this sample.

8.3.2 SLAKED AND CRUSHED CUCARACHA: OVERCONSOLIDATED

The results of the two tests performed at $\bar{\sigma}_v$ = 1.0 kg/sq cm and with an overconsolidation ratio (OCR) of 10 and 100, respectively, are shown in Figs. 8-14 and 8-15 and are summarized in Table 8-4. The results of TEST 8 (OCR = 10) have been plotted in Fig. 8-15 along with the results of TEST 9. When these results are compared with the results obtained for the normally consolidated specimens (Table 8-4), the following observations can be made:

1. The peak strength increases with increasing OCR.
2. There is no definite trend in the displacement required to reach the peak.
3. The residual strength from the overconsolidated specimens falls within the range of the results from normally consolidated specimens.
4. No trend can be observed between the OCR and the amount of displacement required to achieve the residual strength.

The larger peak strength in the overconsolidated specimens is due to the smaller void ratio at the start of shear and in TEST 8 may have been influenced by negative pore pressures which were unable to dissipate in the early stages of the test. The more rapid reduction in strength beyond the peak for the overconsolidated specimens may also be influenced by the dissipation of induced pore pressure.

To reduce the possibility that the pore pressure dissipation would influence the shape of the τ_a versus δ curve during the first part of a test, the first stage of TEST 9 with OCR = 100 was performed at $\dot{\delta} = 5.6 \times 10^{-4}$ cm/min (Fig. 8-15). This lower rate of displacement permitted collecting more data during the early stages of the test, and these additional data have been plotted arithmetically in Fig. 8-16. The reversal of curvature in the stress versus displacement curve at δ = 0.1 mm suggests that even at this rate of displacement the test was not completely drained in the early stages. This reversal of curvature is typical of a saturated soil in a dilative state when drainage is not permitted (Hirschfeld, 1958). In addition, the measurement of ΔB indicates that almost no volume change was taking place during the early stages of this test. As the tests progress, however, the pore pressure dissipates and the ΔB versus δ curve for both tests becomes essentially horizontal as shown in Figs. 8-14 and 8-15. The residual strength from these two tests is shown in Table 8-4 along with the strength measured in the normally consolidated specimens. The difference between the normally consolidated specimens and the overconsolidated specimens is small, and the results of the latter fall within the range of results obtained from the normally consolidated tests.

8.3.3 SLAKED, UNCRUSHED CUCARACHA: NORMALLY CONSOLIDATED

The large difference in plasticity characteristics between the crushed and uncrushed material from the Cucaracha formation afforded an excellent opportunity to determine the residual strength of the two clays of identical mineralogical composition but very different plasticity characteristics. It is believed that the difference in plasticity characteristics was mainly a result of disaggregating clusters of clay particles.* Slaking and manual remolding were insufficient to break up the clusters to obtain the true clay size fraction.

*Some breakage of grains could occur during grinding, but it is believed that it was of minor importance in affecting the large change in plasticity.

Results of two tests performed on the slaked material are shown in Figs. 8-17 and 8-18. The τ_a versus δ curve obtained from a test on the crushed material at the same vertical stress is shown by a dashed line on each figure. There is a striking difference in the τ_a versus δ curves obtained from the same material treated in the two different manners. At $\bar{\sigma}_v$ = 1.0 kg/sq cm, the peak strengths of the two specimens are very similar (0.43 versus 0.42 kg/sq cm). At $\bar{\sigma}_v$ = 4.0 kg/sq cm, the peak strength of the slaked material is 30% higher than the peak strength for the crushed material. One might expect that the difference between the peak strengths would decrease as $\bar{\sigma}_v$ increases for two materials with such differences in grain size distribution and plasticity. In addition to differences in grain size and plasticity, the crushed material was very thixotropic while the slaked material exhibited no noticeable thixotropy.

It is hypothesized that the anomalies of the measured peak strength may be caused by the difference in thixotropy. The thixotropic gain in strength is likely to contribute a larger part of the peak strength at low vertical stresses, resulting in a peak strength nearly equal to the peak strength of the slaked material. Indirect evidence of the importance of thixotropy on the peak strength of the crushed material may be seen in Fig. 8-12 which indicates the peak strength line may have a cohesion intercept as large as 0.15 kg/sq cm which, in part, may be due to thixotropy.

Figure 8-17 shows that the test performed on the slaked material at $\bar{\sigma}_v$ = 1.0 kg/sq cm required more than ten times as much displacement as the test on the crushed material to define τ_r satisfactorily.* The same phenomenon may be observed in Fig. 8-18 for the tests at $\bar{\sigma}_v$ = 4.0 kg/sq cm.

Eventually, the residual strength of the slaked material achieves essentially the same value as the residual strength of the crushed material (Table 8-5 and Fig. 8-19). Although the residual strength of the slaked material was the same as that of the crushed material, the slickensides obtained in tests on the slaked material were not as shiny as the slickensides obtained in tests on the crushed material.

8.4 CONCLUSIONS

8.4.1 SLAKED AND CRUSHED CUCARACHA

The shape of the τ_a versus δ curves for all the tests in this series are essentially the same, with the maximum τ_a occurring at displacements ranging between 0.02 and 0.03 cm. The residual strength has generally been reached by 2 cm of displacement. The amount of displacement necessary to reach the residual strength appears to be independent of the vertical stress over a range of $\bar{\sigma}_v$ from 1.0 to 12.0 kg/sq cm.

The residual strength line shown in Fig. 8-12 is a straight line between $\bar{\sigma}_v$ = 2.0 and 20.0 kg/sq cm. Below $\bar{\sigma}_v$ = 2.0 kg/sq cm, the strength line has been drawn as a smooth curve extrapolated through the origin. That portion of the strength line below $\bar{\sigma}_v$ = 8.0 kg/sq cm has been redrawn in Fig. 8-13 to a larger scale to emphasize the curvature of the strength line between 0 and 2 kg/sq cm.

The results of a limited number of tests (OCR = 10 and 100) on the crushed Cucaracha indicate that the effect of overconsolidation on the residual strength of the remolded "shale" is small (see Table 8-4). Results of all tests performed on normally consolidated specimens of crushed Cucaracha are shown in Fig. 8-11 and the results are summarized in Table 8-1.

---

*In TEST 10 it became obvious at about 9 cm of displacement that a very large amount of displacement would be required to define τ_r. To expedite the test, δ was increased from 5.6×10^{-3} to 28×10^{-3} cm/min. When sufficient displacement had accumulated to define τ_r at this faster velocity, δ was decreased to 5.6×10^{-3} cm/min.

The stress versus displacement curves for the tests on the overconsolidated material, shown in Figs. 8-14 and 8-15, have a much more pronounced peak than the tests on the normally consolidated material. The sharp peak may be influenced by negative pore pressures which were unable to dissipate during the early stages of the tests.

8.4.2 SLAKED, UNCRUSHED CUCARACHA

Duplicate tests on the uncrushed and crushed material, which had widely different plasticity characteristics, gave essentially identical residual strengths (see Fig. 8-19). Comparison of the stress versus displacement curves for these tests (Figs. 8-17 and 8-18) shows that at least ten times more displacement is necessary to reach the residual state in tests using the uncrushed material. Observation and manipulation of the uncrushed material at the completion of a test indicated that the plasticity of the material had been increased significantly. This increase in plasticity is mainly due to breaking down the silt and fine sand-size grains which are conglomerated grains of clay. When the uncrushed material is tested at higher vertical stress, the larger shear stresses are more efficient at crushing the material and less deformation is required to achieve the residual strength, as demonstrated by comparing Figs. 8-17 and 8-18.

Finding that the residual strength of the uncrushed and crushed Cucaracha are identical suggests that the technique of preparing remolded materials may not be too important when measuring the residual strength. If confirmed by tests on other materials, this result can save considerable effort when testing highly overconsolidated clays which usually are difficult to remold. Although large displacements may be needed if remolding is incomplete, most of the displacement can be obtained at a rapid rate which can be reduced when the residual strength is measured.

The results of duplicate tests on the uncrushed and crushed Cucaracha also emphasize the difficulties of obtaining a simple relationship between residual strength and plasticity or grain-size distribution. While the Atterberg limits of a clay are affected by the degree of remolding, the residual strength may not be influenced because of the remolding that takes place during the test.

CHAPTER 9

LONDON CLAY

9.1 PURPOSE AND SCOPE

Attempts to measure the residual strength of undisturbed Pepper Shale were inconclusive due to redistribution of $\bar{\sigma}_v$ on the disc-shaped specimens (Section 7.3.3). The consistency and homogeneity of the London Clay permitted trimming undisturbed annular specimens, thus minimizing errors due to redistribution of $\bar{\sigma}_v$.

To determine whether there was any difference between the residual strength of remolded and undisturbed specimens, the following tests were performed:

State	Specimen Shape	Confinement	Range of $\bar{\sigma}_v$ kg/cm^2
Undisturbed	Annulus	Solid ring	1 to 8
Remolded	Annulus	Solid ring	1 to 8

The large amount of test data reported in the literature (Skempton et al., 1969) concerning the residual S strength of London Clay obtained from repeatedly reversed direct shear tests provided an excellent opportunity to compare the results of these tests with results obtained from rotation shear tests.

9.2 SOIL DESCRIPTION

The London Clay was obtained from Professor A. W. Bishop of Imperial College, London, and comes from a reservoir site at Wraysbury, South Buckinghamshire. The sample was a five-inch-long section from a four-inch-diameter undisturbed sample taken at a depth of about 40 feet.

The clay as received was stiff, brown and had a water content of about 28%.* It was easily trimmed with a knife and could be remolded with moderate effort, having the consistency of a medium to highly plastic clay. The sample appeared to be essentially homogeneous at first inspection, with a few small (1 to 2 cc) pockets and lenses (less than 0.5 mm thick) of fine sand. When trimming the undisturbed test specimens, it became clear that there was silt or fine sand scattered throughout the sample. There were several zones which felt more "gritty" (when trimmed with a knife) than the bulk of the sample. No slickensides or fissures were observed in the sample.

Pieces of undisturbed soil immersed in distilled water swelled without disintegration. After swelling for 48 hours, the soil could be easily remolded to a smooth paste.

Air-dried chunks of the undisturbed soil slaked to discrete pieces ranging in size from 3 mm down to being barely distinguishable to the unaided eye. The larger pieces had a well-defined laminar structure but had a basically bulky shape. After being submerged for 30 minutes, the air-dried soil was very easily remolded to a smooth paste between the fingers.

---

*In the letter of transmittal, the soil is referred to as the Blue London Clay.

This sample of the London Clay (undisturbed state) effervesced strongly when treated with hydrochloric acid.

The liquid and plastic limits of the soil remolded from its natural water content were 71.5 and 22.4, respectively. These results are plotted on the Plasticity Chart in Fig. 9-1. At the plastic limit, the soil was tough. At a water content below the plastic limit, it acquired a medium shine when rubbed on the thumbnail. The remolded, air-dried soil had a high dry strength. The specific gravity of the solids was 2.72.

The results of two hydrometer tests using a 0.01 N solution of sodium metaphosphate are shown in Fig. 9-2. The upper one inch of the sample was remolded from the natural water content to a water content of about 65% and used for tests to determine the residual strength from remolded specimens. A second hydrometer test was performed on a representative section of the sample used for undisturbed specimens because this section of the sample was thought to have more silt than the upper one inch of the sample. The results from these tests are practically identical. The expectation that the portion of the sample used for the undisturbed specimens was more silty than the portion used for remolded specimens is probably due to the "gritty" feel experienced when trimming the specimen with a knife. The remolded soil, placed with a spatula, did not feel gritty.

9.3 TEST RESULTS

9.3.1 REMOLDED NORMALLY CONSOLIDATED SPECIMENS

The stress versus displacement curves for these tests are shown in Figs. 9-3 to 9-5 and the results are summarized in Table 9-1. The residual strength line shown in Fig. 9-7 is drawn as a straight line, through the origin at a slope of 8.3 degrees. Figure 9-6 is a summary plot of the shear stress versus displacement curves and shows:

1. The ratio $\tau_p/\bar{\sigma}_v$ decreases from 0.362 to 0.273 as $\bar{\sigma}_v$ increases from 1 to 8 kg/sq cm.
2. The displacement to the peak strength (δ_p) is independent of $\bar{\sigma}_v$ and equal to about 0.10 cm.
3. The displacement required to achieve the residual strength (δ_r) ranges from about 10 cm for tests at $\bar{\sigma}_v$ = 1.0 and 2.0 kg/sq cm to 4 cm for the test at $\bar{\sigma}_v$ = 8.0 kg/sq cm.

Figure 9-6 indicates that the rate of soil extrusion was much larger in TEST 3 than in the other tests in this series. The last point plotted on the ΔB versus δ curve (Fig. 9-5) for TEST 3 appears suspicious, and may be in error. The rate of extrusion for each specimen of remolded London Clay is shown in Table 9-5. Two rates of extrusion are shown for TEST 3; the first value was computed using the slope of the ΔB versus δ curve at the final plotted point (Fig. 9-5), and the second value uses the slope at the penultimate point. This second value fits the pattern established by the other tests and supports the suspicion that the final point on the ΔB versus δ curve of TEST 3 may be in error.

The large values of $\Delta B/B_c$ at the end of the tests (Table 9-5) are due to both soil extrusion and the very large shear strains in the tests.

Table 9-5 shows that the extrusion which occurred in TEST 3 has not affected the measured residual strength.

Table 9-1 shows that $\tau_r/\bar{\sigma}_v$ for TEST 1 ($\bar{\sigma}_v$ = 1.0 kg/sq cm) is slightly higher than $\tau_r/\bar{\sigma}_v$ for the other tests. This tendency was also observed in the results from tests on the crushed Cucaracha "Shale" but not for remolded Pepper Shale. It seems reasonable to assume that in some soils the soil particles cannot be as effectively arranged at low stresses as at higher stresses, causing the strength line to curve slightly at low stresses. Sufficient data have not been collected

at very low vertical stresses to substantiate this hypothesis.

Descriptions of the failure planes at the end of these tests are summarized in Table 9-2. All the failure planes had a medium shine which was significantly less reflective than the failure planes obtained with the Pepper Shale or the crushed Cucaracha material.

9.3.2 UNDISTURBED ANNULAR SPECIMENS

Stress versus displacement curves for the four tests in this series are shown in Figs. 9-8 to 9-11 and the results are summarized in Table 9-3. The residual strength line shown in Fig. 9-13 is a straight line through the origin at a slope of 9.3 degrees. Figure 9-12 is a summary plot of the shear stress versus displacement curves from these tests and shows:

1. The ratio $\tau_p/\bar{\sigma}_v$ decreases from 0.342 to 0.320 as $\bar{\sigma}_v$ increases from 2.0 to 8.0 kg/sq cm. TEST 4 ($\bar{\sigma}_v$ = 1.0) deviates from the pattern and the ratio $\tau_p/\bar{\sigma}_v$ for this test is 0.315.
2. The displacement required to reach the peak (δ_p) is essentially independent of $\bar{\sigma}_v$ and equal to about 0.08 cm.
3. The displacement required to reach the residual strength (δ_r) is about 40 cm for the tests at $\bar{\sigma}_v$ = 1 and 2 kg/sq cm, about 3 cm at $\bar{\sigma}_v$ = 4 kg/sq cm, and 10 cm for $\bar{\sigma}_v$ = 8 kg/sq cm.

The ΔB versus δ curves for the tests on undisturbed specimens are very similar to the ΔB versus δ curves for the remolded specimens (compare Figs. 9-6 and 9-12). For each type of specimen, more soil extruded for the test at $\bar{\sigma}_v$ = 8.0 kg/sq cm than for tests at the lower vertical stresses, but the results of these tests fall on the straight strength lines formed by the other tests in each series.

The peak strength lines obtained from the tests on undisturbed specimens and remolded specimens are shown in Fig. 9-14. The peak strengths from undisturbed and remolded specimens are surprisingly similar, and the small difference between the peak strengths of the remolded and the undisturbed soils may indicate the specimens were not truly undisturbed.* Another indication that the specimens were disturbed are the ΔB versus δ curves for these tests which show the undisturbed soil is in a contractive state during shear, even at $\bar{\sigma}_v$ = 1 kg/sq cm. The disturbance may be from sampling or due to trimming the specimens as discussed in Section 7.3.3.

Results of direct shear tests on specimens cut from an undisturbed block sample of London Clay from Wraysbury, with similar Atterberg limits and grain size distribution, have been published by Skempton et al., (1969). The peak strength line from these tests, plotted in Fig. 9-14, has a cohesion intercept of 0.32 kg/sq cm. The data reported by Skempton have considerable scatter, with the ratio $\tau_p/\bar{\sigma}_v$ ranging between 0.82 and 0.43 as $\bar{\sigma}_v$ increases from 0.6 to 4.2 kg/sq cm. The peak strength line from the annular rotation shear tests may be low because of possible disturbance as discussed above.

9.4 CONCLUSIONS

Residual shear strength lines from tests on remolded and undisturbed annular specimens are shown in Fig. 9-7 and Fig. 9-13, respectively. Both strength lines have been drawn as straight lines through the origin. The strength line from undisturbed specimens is inclined at 9.3 degrees while the one from the remolded soil is inclined at 8.3 degrees. The reason for this difference is not clear but may be related to different ion concentrations in the pore fluid due to remolding the

*The standard procedure for obtaining 4-inch-diameter samples in England is to drive a thin-wall tube that has a cutting shoe at the bottom into the clay.

soil with distilled water (Kenney, 1967). The influence of changes in ion concentration in pore fluids has not been adequately investigated.

In Fig. 9-15 the residual strength of the London Clay from Wraysbury is compared with results published by Skempton et al. (1969) on samples of London Clay from the same site and with similar Atterberg limits and grain size distribution. The residual strength reported by Skempton is much greater than the residual strengths obtained using rotation shear tests. This difference may be due to not reaching the residual state in the direct shear tests (Section 2.3).

The consequences of this large difference in residual strength are most important when attempting to evaluate experience with slope failures in overconsolidated clays. Before guidelines can be established to estimate the design strengths to be used in such soils, it is important to accurately measure the peak and residual strengths.

CHAPTER 10

SUMMARY AND CONCLUSIONS

10.1 DEFINITION OF RESIDUAL S STRENGTH

The residual S strength is the shearing resistance measured in an S test, at which a material undergoes continuous deformation under a constant state of effective stress and at a constant void ratio. This unique condition of constant stress and constant void ratio during continuous deformation is called the residual state which Poulos (1969) has suggested is identical to the critical state defined by Casagrande (1936) for sands.

10.2 REVIEW OF PAST RESEARCH ON RESIDUAL STRENGTH OF CLAYS

A review of past research revealed that in many cases the residual S strength had not been reached because of insufficient displacement. As a result, many of the values of residual strength reported in the literature are too high. The main reason for this error is believed to be due to the difficulty in recognizing when the shearing resistance becomes independent of deformation if the shear stress versus displacement curve is plotted with arithmetic scales. In this investigation, displacements in rotation shear tests used to measure residual strength were plotted on a logarithmic scale. This plotting technique accentuates the slope of the stress-displacement curve at large displacements, permitting the point at which the shear stress becomes independent of displacement (i.e., the residual strength) to be chosen more precisely. The ambiguity that can result from plotting the displacement on an arithmetic scale is illustrated in Figs. 2-1 and 2-2.

10.3 DESIGN OF THE ROTATION SHEAR MACHINE

Casagrande (1965) emphasized the advantages of using a rotation shear machine to study the residual strength of clay because it allows large unidirectional displacement to be applied to a specimen. The rotation shear machine that the author designed and built for this investigation, referred to as the Harvard rotation shear machine, permits:

1. Testing disc-shaped specimens with a diameter of 7.11 cm or annular specimens with an outside diameter of 7.11 cm and an inside diameter of 5.08 cm.
2. The specimen thickness to be between 1 mm and 25 mm.
3. Application of a vertical stress of 100 kg/sq cm on a disc-shaped specimen and 200 kg/sq cm on an annular specimen.*
4. The rate of rotation to be varied in 10 increments from 1 rev/40 min to 1 rev/28 days (rate of peripheral displacement of 5.6×10^{-1} cm/min to 5.6×10^{-4} cm/min).
5. The torque to be applied with a smooth vibration-free transmission system.
6. The use of (i) a horizontally split confining ring with clearances between 0 and about 0.002 inch, or (ii) a solid confining ring.

---

*A second machine has been built which allows a maximum vertical stress of 25 kg/sq cm on a disc-shaped specimen and 50 kg/sq cm on an annular specimen.

Torque is applied to the bottom of the specimen by the transmission system. Two force transducers measure the force couple necessary to keep the upper half of the specimen stationary. The design permits exchanging the transducers at any time during a test, which allows more sensitive transducers to be installed as the shearing resistance decreases to the residual strength.

In general, a specimen thickness of 6 mm was adopted for use with a split confining ring and 2 mm for use with a solid ring.

When a solid confining ring is used, failure occurs near a porous disc. When a split confining ring is used, the specimen may be precut, forcing failure to occur in the center of the specimen. The measured residual strength was found to be the same whether failure occurred in the center of the specimen or near a porous disc.

10.4 INVESTIGATION OF TEST ERRORS

An investigation of test errors presented in CHAPTER 6 suggests that soil extruding from the boundaries of the specimen in a rotation shear test may cause a redistribution of the vertical stress on the failure plane. At the residual state the measured moment is constant and the distribution of effective vertical stress, $\bar{\sigma}_v$, must also be constant. Nevertheless, the vertical stress may not be uniform. Extrusion causes $\bar{\sigma}_v$ to be lower at the periphery than at the center of the specimen and the measured moment at the residual state will be smaller than if $\bar{\sigma}_v$ were uniform; hence, the residual strength computed by assuming a uniform distribution of $\bar{\sigma}_v$ will be too low.

Disc-shaped specimens had lower residual strengths than annular specimens when extrusion was similar for both shapes. These results suggest that the effect of extrusion (hence redistribution of $\bar{\sigma}_v$) increases as the ratio R_2/R_1 of the inner specimen radius to the outer specimen radius decreases.

It is reasonable to assume that the error caused by extrusion increases as the rate of soil extrusion increases, where the rate of extrusion is defined as the slope of the curve of change in thickness ΔB, versus displacement δ, at the time the residual strength is measured.

A solid confining ring with a radial clearance between the confining ring and the loading platens of 0.0005 in. was adopted to minimize the amount of extrusion. For annular specimens used in this investigation ($R_2/R_1 = 0.70$), a rate of extrusion of about 3×10^{-4} in./cm did not noticeably influence the residual strength, τ_r. On the other hand, rates of extrusion as small as 0.2×10^{-4} in./cm are believed to have lowered τ_r by 20% (at $\bar{\sigma}_v = 4.0$ kg/sq cm) on tests using disc-shaped specimens (Section 7.3.3).

Friction between the solid confining ring (which rotates) and the specimen and upper platen (which are stationary) is eliminated by removing the ring temporarily while obtaining the transducer readings from which the moment is computed (Section A-5).

Other errors that are inherent in the Harvard rotation shear machine are discussed in CHAPTER 6 and APPENDIX A and show that the residual strength for an annular specimen using a solid confining ring is 0.4% to 1.4% higher than the correct value.

10.5 TEST RESULTS

10.5.1 REMOLDED, NORMALLY CONSOLIDATED SPECIMENS

The results of rotation shear S tests on annular specimens of three remolded, normally consolidated materials are summarized in Table 10-1, and the relationship between residual strength and effective stress for each material is plotted in Fig. 10-1. All specimens were confined by a solid confining ring.

The shear stress versus displacement curves for all these tests reach a peak strength after

which the shearing resistance is reduced as displacement increases. At $\bar{\sigma}_v$ = 1.0 kg/sq cm, the residual strength (τ_r) was about 45% of the peak strength, while at higher stresses τ_r was about 60% of the peak strength.

Table 10-2 is a summary of the displacement required to reach the peak (δ_p) and the residual (δ_r) strengths. The displacement required to reach the residual strength varied considerably for the three materials. In general, the displacement in each test was continued to about ten times the displacement required to reach the residual strength. The results from tests on Pepper Shale indicate that δ_r decreases as $\bar{\sigma}_v$ increases. No such pattern could be definitely established with the other materials.

The displacements required to reach the peak strength in these remolded, normally consolidated specimens correspond to axial strains of about 20% to 50% in the triaxial test.

10.5.2 REMOLDED, OVERCONSOLIDATED SPECIMENS

The effect of overconsolidation on the residual strength was studied by performing tests on annular specimens of remolded Pepper Shale and crushed Cucaracha Shale at overconsolidation ratios (OCR) ranging from 1 to 100. The results for Pepper Shale are summarized in Table 10-3. A series of tests on specimens consolidated to 10 kg/sq cm indicated that as the overconsolidation ratio increased from 2.5 to 10, τ_r was 1.6% to 21% higher than for identical, normally consolidated specimens. A test at $\bar{\sigma}_v$ = 1.0 kg/sq cm with an OCR = 100 did not continue this trend, however, as τ_r in this test was only 3.4% higher than for an identical, normally consolidated specimen. The displacement required to reach the peak strength decreases from 0.06 cm to 0.02 cm as the OCR increases from 1 to 100. There is no definite trend established between the displacement required to reach the residual strength and the OCR.

Table 10-4 is a summary of the results of tests on overconsolidated specimens of crushed Cucaracha "Shale." Three tests on normally consolidated specimens at $\bar{\sigma}_v$ = 1.0 kg/sq cm gave residual strengths of 0.151 to 0.195 kg/sq cm. Tests at $\bar{\sigma}_v$ = 1.0 kg/sq cm and with an OCR of 10 and 100 gave residual strengths of 0.160 and 0.180 kg/sq cm, respectively. No definite conclusion concerning the effect of OCR on the residual strength can be drawn from these limited data.

10.5.3 RESIDUAL STRENGTH OF REMOLDED AND UNDISTURBED SPECIMENS OF LONDON CLAY

The relationship between τ_r and $\bar{\sigma}_v$ from rotation shear S tests on remolded and undisturbed annular specimens of London Clay from Wraysbury are shown in Fig. 10-2. Results of triaxial tests on specimens sheared along a joint or fissure, published by Skempton et al. (1969), on samples of London Clay from the same site and with similar Atterberg limits and grain size distribution are also plotted in Fig. 10-2. The residual strength reported by Skempton is almost twice as large as the strength measured by the author. The reason for this difference is not clear, but may be due to not reaching the residual state in the triaxial shear tests (Section 2.3).

In the triaxial tests reported by Skempton et al. (1969), the relative movement along the failure plane was about 6 mm. If the rotation shear tests on undisturbed specimens of London Clay reported in Section 9.3.2 had been stopped at 6 mm of displacement (Fig. 9-12), the slope of the shearing resistance versus effective stress line would have been about 14 degrees for $\bar{\sigma}_v$ between 0 and 2.0 kg/sq cm and about 11 degrees at $\bar{\sigma}_v$ = 8.0 kg/sq cm.

The residual strength line (τ_r versus $\bar{\sigma}_v$) from rotation shear tests on the undisturbed specimens is inclined at 9.3 degrees and the strength line from remolded specimens is inclined at 8.3 degrees. The reason for this difference is not known, but may be due to decreasing the ion

concentrations in the pore fluid of the remolded specimens due to remolding the soil with distilled water. Kenney (1967) has shown that τ_r increased for both montmorillonite and hydrous mica when the ion concentration of the pore fluid was increased.

10.5.4 RESIDUAL STRENGTH OF CRUSHED AND UNCRUSHED CUCARACHA "SHALE"

The Cucaracha "Shale" was remolded by two methods, which gave widely different liquid and plastic limits. The material referred to as uncrushed Cucaracha "Shale" was remolded by air-drying and slaking four times, resulting in a liquid limit of 49 and a plastic limit of 28. The crushed Cucaracha "Shale" was air-dried a fifth time and ground in a disc mill to a fine powder and remolded with distilled water. The liquid and plastic limits of the crushed soil were 156 and 42.

Duplicate tests on the crushed and uncrushed material gave essentially the same residual strengths. Table 10-5 summarizes the results of these tests and shows that about ten times more displacement was necessary to reach the residual strength in tests using the uncrushed material. Observation and manipulation of the material from the failure zone of the uncrushed Cucaracha specimens indicated that its plasticity had increased significantly when compared to material outside the failure zone. This increase in plasticity is believed to be due to breaking down silt and fine sand-size grains which are really clusters of clay-sized grains. Apparently, the shear strains applied during the test break down these clusters while air-drying and slaking four times does not.

Finding that the residual strength of the uncrushed and crushed Cucaracha are identical suggests that the technique of preparing remolded materials may not be too important when measuring the residual strength. If confirmed by tests on other materials, this result can save considerable effort when testing highly overconsolidated clays because usually they are difficult to remold. Although large displacements may be needed if remolding is incomplete, most of the displacement can be obtained while rotating rapidly at first and then reducing the rate, if necessary, to measure the residual strength.

The results of duplicate tests on the uncrushed and crushed Cucaracha also emphasize the difficulties of obtaining a correlation between residual strength and plasticity or grain size distribution. While the Atterberg limits of a clay are affected by the degree of remolding, the residual strength may not be influenced because of the degree of remolding that takes place during the test itself.

10.5.5 EFFECT OF RATE OF DISPLACEMENT ON RESIDUAL S STRENGTH

Table 10-6 summarizes the results of tests performed to investigate the effect of the rate of peripheral displacement on the residual strength. Each specimen was initially sheared at $\dot{\delta} = 5.6 \times 10^{-3}$ cm/min. When the residual strength was clearly defined, the velocity was reduced to 0.56×10^{-3} cm/min. No significant change in the shearing resistance was measured for any of the three materials. When the shearing resistance was determined at $\dot{\delta} = 0.56 \times 10^{-3}$ cm/min for the crushed Cucaracha Shale, $\dot{\delta}$ was increased to 56×10^{-3} cm/min. This one-hundredfold increase in shearing velocity caused only a 3.5% increase in the measured residual strength.

10.6 SUGGESTIONS FOR FUTURE RESEARCH

(1) Investigation of the effect of soil extrusion on the residual strength measured in a rotation shear test indicate that soil extrusion can be a major source of error. It was suggested (Section 6.2.4) that extrusion causes a redistribution of the vertical stress on the specimen. Further investigation is needed to determine the distribution of the vertical stress at both the peak and residual strengths. These investigations could be carried out using specimens which are confined

by a split ring designed to permit control of the clearance between the halves of the ring, permitting the rate of extrusion to be varied. The rings should also be designed to allow them to be temporarily separated to eliminate friction caused by the soil extruding between them. The following factors should be studied:

1. Effect of the rate of extrusion on the residual strength of specimens with a given ratio of R_2/R_1.
2. Effect of the ratio, R_2/R_1, on the measured residual strength for a given rate of extrusion.

(2) The working hypothesis presented in CHAPTER 1 suggests that void ratio on the failure plane when the residual state is reached is independent of the initial void ratio of the specimen. A special investigation is required to determine whether meaningful measurements of this void ratio can be made.

(3) Further investigation is needed to establish the most efficient and practical procedure for determining the residual strength. This investigation could be based on results from identical specimens tested at various rates of displacements that were constant for the entire test. The rates of displacement used should include several which did not permit full drainage during the early stages of the test, but the tests would be continued until a constant shearing resistance was reached. Results from these tests would be compared with results from specimens sheared slowly enough to insure full drainage during the entire test. Other specimens would initially be sheared at a rapid test rate to obtain large displacements and then the shearing velocity reduced to determine the residual S strength.

(4) It has been suggested that the reduction in shearing resistance beyond the peak strength for normally consolidated specimens is due to orientation of the clay particles in the direction of movement (Hvorslev, 1960). A qualitative relationship between the degree of orientation and the shearing resistance might be obtained by examining, with a scanning electron microscope, the cross section of specimens from tests terminated at various displacements. Variables which should be studied are overconsolidation ratio, grain size distribution and plasticity characteristics.

(5) Tests are necessary to determine the accuracy with which residual strength can be measured by reversing the direction of movement on the failure plane. Tests should be performed in a rotation shear machine which would permit reversing the direction of movement until a constant shearing resistance is reached. The test should then be continued with rotation in one direction to determine the magnitude of the change in shearing resistance.

(6) Since the residual strength of the uncrushed and crushed Cucaracha Shale are similar, the technique of preparing remolded materials apparently is not important when measuring the residual strength of this material. Testing of other materials remolded by various techniques is suggested. If this result applies to other soils, the considerable effort needed to prepare remolded specimens of highly overconsolidated clays would not be required.

(7) Further investigations of the effect of overconsolidation on residual strength are believed to be desirable. The difference in the strength of normally consolidated and overconsolidated specimens tested by the author was found to be small. Other materials should be tested, and a larger number of tests performed to obtain statistically significant results for each comparison.

LIST OF REFERENCES

Beene, R. W., 1967. "Waco Dam Slide," ASCE Journal, Soil Mechanics and Foundations Division, Vol. 93, No. SM4, pp 35-44.

Binger, W. V., Thompson, T. F., 1949. "Excavation Slopes in the Panama Canal," ASCE Transactions, Vol. 114, pp 734-754.

Casagrande, A., 1936. "Characteristics of Cohensionless Soils Affecting the Stability of Slopes and Earth Fills," Journal of the Boston Society of Civil Engineers, Vol. 23, No. 1, pp 13-32.

Casagrande, A., 1938. "The Shearing Resistance of Soils and Its Relation to the Stability of Earth Dams," Proceedings, Soils and Foundation Conference of the U.S. Engineer Department, pp A-1 to A-20.

Casagrande, A., 1949. Discussion of a paper by Binger, W. V. and Thompson, T. F. "Excavation Slopes in the Panama Canal," ASCE Transactions, Vol. 114, pp 870-874.

Casagrande, A., 1965. Personal communication.

Collin, A., 1846. "Recherches Expérimentales sur les Glissements Spontanés des Terrains Argileux," Carilian-Goeury and Dalmont, Paris. (Translation by W. R. Schriever, University of Toronto Press, 1956).

Corso, J. M., 1955. "Notes on Direct Shear Tests on Thin Samples of Remolded Clay," unpublished report on file in Harvard Soil Mechanics Laboratory.

De Beer, E., 1967. "Shear Strength Characteristics of the Boom Clay," Proceedings Geotechnical Conference, Oslo, Norway, Vol. 1, pp 83-88.

Griffith, J. H., 1922. "Progress Report of Tests on Undisturbed Clay," ASCE Proceedings, Vol. 48, pp 557-579.

Haefeli, R., 1938. "Mechanische Eigenschaften von Lockergesteinen," Schweizerische Bauzeitung, Vol. 3, pp 321-325.

Haefeli, R., 1951. "Investigation and Measurement of the Shear Strength of Saturated Cohesive Soils," Geotechnique, Vol. 2, No. 3, pp 186-207.

Hansen, B., 1961. "Shear Box Tests on Sand," Proceedings Fifth ICSMFE, Vol. 1, pp 127-131.

Herrmann, H. G., Wolfskill, L. A., 1966. "Residual Shear Strength of Weak Shales," M.I.T. Soil Mechanics Publication No. 200, 203 pages.

Hirschfeld, R. C., 1958. "Factors Influencing the Constant Volume Strength of Clays," Ph. D. Thesis, Harvard University.

Horn, H. and Deere, D., 1962. "Frictional Characteristics of Minerals," Geotechnique, Vol. 12, No. 4, pp 319-335.

Hvorslev, M. J., 1936. "A Ring Shearing Apparatus for Determination of the Shearing Resistance and Plastic Flow of Soils," Proceedings ICSMFE, Vol. 2, pp 125-129.

Hvorslev, M. J., 1937. "Uber Die Festickeitseigenschaften Gestorter Bindiger Boden," Ingeniørvidenskabelige Skrifter A - No. 45, Danmarks Naturvidenskabelige Samfund, Copenhagen. (Physical Properties of Remolded Cohesive Soils, Translation No. 69-5, U.S. Army Waterways Experiment Station, 1969).

Hvorslev, M. J., 1939. "The Shearing Resistance of Remolded Cohesive Soils," Proceedings of Soils and Foundation Conference of the U.S. Engineer Department, pp E-1 to E-30.

Hvorslev, M. J., 1939. "Torsion Shear Tests and Their Place in the Determination of the Shearing Resistance of Soils," Proceeding American Society for Testing Materials," Vol. 39, pp 999-1022.

Hvorslev, M. J. and Kaufman, R. I., 1951. "Torsion Shear Tests on Atlantic Muck," Waterways Experiment Station Technical Memorandum No. 3-328, 70 pages.

Hvorslev, M. J. and Kaufman, R. I., 1952. "Torsion Shear Apparatus and Testing Procedures," Waterways Experiment Station Bulletin No. 38, 76 pages.

Hvorslev, M. J. 1960. "Physical Components of the Shear Strength of Saturated Clays," ASCE Research Conference on Shear Strength of Cohesive Soils, Boulder, Colorado, pp 615-641.

Hvorslev, M. J., 1969. Personal communication.

Kenney, T. C., 1967. "The Influence of Mineral Composition on the Residual Strength of Natural Soils," Proceedings Geotechnical Conference, Oslo, Norway, Vol. 1, pp 123-129.

Krey, H., 1926. Erddruck, Erdwiderstand und Tragfähigkeit des Baugrundes, 3rd edition, Wilhelm Ernst and Son, Berlin.

Morgenstern, N. R. and Tchalenko, J. S., 1967. "Microscopic Structures in Kaolin Subjected to Direct Shear," Geotechnique, Vol. 17, No. 4, pp 309-328.

Petley, D. J., 1966. "The Shear Strength of Soils at Large Strains," Ph. D. Thesis, University of London.

Poulos, S. J., 1969. Personal communication.

Rosco, K. H., Schofield, A. N. and Wroth, C. P., 1958. "On the Yielding of Soils," Geotechnique, Vol. 8, No. 1, pp 22-53.

Sembenelli, P. and Ramirez de Arellano, L., 1965. "Development of a Torsion Shear Apparatus," unpublished report on file in Harvard Soil Mechanics Department.

Skempton, A. W., 1964. "Long-Term Stability of Clay Slopes," Geotechnique, Vol. 14, No. 2, pp 77-101.

Skempton, A. W., Schuster, R. L., and Petley, D. J., 1969. "Joints and Fissures in the London Clay at Wraysbury and Edgeware," Geotechnique, Vol. 19, No. 2, pp 205-217.

Tiedemann, B., 1937. "Uber die Schubfestigkeit Bindiger Böden," Bautechnik, Vol. 15, pp 433-435.

U. S. Bureau of Standards, 1916. "Sub-Committee Report on Earth Experiments and Apparatus," ASCE Proceedings, Vol. 42, pp 353-367.

Waterways Experiment Station, 1951. "Torsion Shear Tests on Atlantic Muck, The Panama Canal," Technical Memorandum No. 3-328, Vicksburg, Mississippi.

TABLE 6-1

ROTATION SHEAR S TESTS ON GROUND MUSCOVITE – DISC-SHAPED SPECIMENS

Test No.	Type of Confining Ring	Initial Moisture Content	Residual Shear Strength kg/sq cm		Rate of Soil Extrusion 10^{-4} inches/cm		Location of Failure Plane	Fig. No.
			$\bar{\sigma}_v$ = 1.0	$\bar{\sigma}_v$ = 2.0	$\bar{\sigma}_v$ = 1.0	$\bar{\sigma}_v$ = 2.0		
GM-1	Split	60.0	0.232	0.480	1.2	2.2	Center	6-3
GM-2	Split	62.2	0.226	0.465	0.6	8.0	Center	6-4
GM-3	Solid	67.3	0.271	0.558	0.2	0.7	0.5 mm from top	6-5
GM-4	Solid	61.0	0.247	0.520	0.4	1.5	1.0 mm from top	6-6

TABLE 6-2

ROTATION SHEAR S TESTS ON GROUND MUSCOVITE – ANNULAR SPECIMENS

Test No.	Type of Confining Ring	Initial Moisture Content	Residual Shear Strength kg/sq cm			Rate of Soil Extrusion 10^{-4} inches/cm			Location of Failure Plane	Fig. No.
			$\bar{\sigma}_v$=0.5	$\bar{\sigma}_v$=1.0	$\bar{\sigma}_v$=2.0	$\bar{\sigma}_v$=0.5	$\bar{\sigma}_v$=1.0	$\bar{\sigma}_v$=2.0		
GM-5	Split	62.0	---	0.260	0.556	---	1.1	3.8	Center	6-13
GM-6	Split	63.2	---	0.285	0.560	---	3.2	3.0	Center	6-14
GM-7	Solid	64.7	0.156	0.281	0.553	0.4	0.5	1.3	0.5 mm from top	6-15
GM-8	Solid	59.5	---	0.284	0.550	---	0.4	1.9	0.5 mm from top	6-16

TABLE 6-3

ROTATION SHEAR S TESTS ON WARM SPRINGS SHALE

DISC-SHAPED SPECIMENS

Test No.	Type of Confining Ring	Initial Moisture Content	$\bar{\sigma}_v$ kg/cm^2	τ_r kg/cm^2	Location of Failure Plane	Fig. No.
WSS-1	Split	35.5	1.0	0.455	Unable to locate	6-9, 6-10
WSS-2	Solid	36.0	1.0	0.415	0.5 mm from top	6-11

TABLE 6-4

ROTATION SHEAR S TESTS ON WARM SPRINGS SHALE

ANNULAR SPECIMENS

Test No.	Type of Confining Ring	Initial Moisture Content	$\bar{\sigma}_v$ kg/cm^2	τ_r kg/cm^2	Location of Failure Plane	Fig. No.
WSS-3	Split	38.1	1.0	0.477	Center	6-19, 6-20
WSS-4	Solid	36.5	1.0	0.462	0.5 mm from top	6-21

TABLE 6-5

EFFECT OF UNLIMITED SOIL EXTRUSION ON THE RESIDUAL STRENGTH OF ANNULAR SPECIMENS

Soil	$\bar{\sigma}_v$ kg/cm^2	τ_r kg/cm^2	$\tau_r/\bar{\sigma}_v$	$\Delta\tau_r$ When Extrusion Allowed	$\Delta\tau_r/\tau_r$ %
Remolded Warm Springs Shale	1.0	0.477	0.477	- 0.071	- 15
Remolded Cucaracha "Shale"	1.0	0.195	0.195	- 0.005	- 2.5
Remolded Cucaracha "Shale"	8.0	1.020	0.128	- 0.100	- 9.8
Remolded Pepper Shale	12.0	1.529	0.127	- 0.120	- 7.8

TABLE 7-1

ROTATION SHEAR S TESTS ON REMOLDED PEPPER SHALE

NORMALLY CONSOLIDATED ANNULAR SPECIMENS; $\dot{\delta} = 5.6 \times 10^{-3}$ cm/min

Test No.	Initial Water Content %	e_o	$\bar{\sigma}_v$ kg/cm^2	e_c	τ_p kg/cm^2	$\tau_p/\bar{\sigma}_v$	τ_r kg/cm^2	$\tau_r/\bar{\sigma}_v$	τ_r/τ_p	δ_p cm	δ_r cm	Fig. No.
1	61.8	1.71	1	1.25	0.255	0.255	0.118	0.118	0.462	0.060	3.0	7-3
			2				0.250	0.125				
			4				0.515	0.129				
2	61.2	1.69	4	1.09	0.885	0.221	0.500	0.125	0.565	0.088	7.0	7-4
3	60.0	1.66	8	0.415	1.592	0.199	1.040	0.130	0.652	0.088	2.5	7-5
4	69.1	1.91	12	0.485	2.500	0.208	1.529	0.127	0.610	0.090	1.5	7-6
			20				2.680	0.134				

TABLE 7-2

ROTATION SHEAR S TESTS ON REMOLDED PEPPER SHALE

DESCRIPTION OF FAILURE PLANES – NORMALLY CONSOLIDATED ANNULAR SPECIMENS

Test No.	Initial Water Content %	$\bar{\sigma}_v$ kg/cm^2	Description
1	61.8	1 2 4	Very shiny slickensides at several elevations in specimen. Could not separate specimen on continuous failure plane. Slickensides were flat and had shallow circular striations.
2	61.2	4	Very flat, shiny failure plane adjacent to upper porous disc.
3	60.0	8	Very flat, shiny failure plane with shallow circular striations, about 0.3 mm from upper porous disc.
4	69.1	12 20	Very flat and very shiny failure plane located in center of specimen which was about 1 mm thick.

TABLE 7-3

ROTATION SHEAR S TESTS ON REMOLDED PEPPER SHALE

EFFECT OF SPECIMEN SHAPE ON RESIDUAL STRENGTH: $\dot{\delta} = 5.6 \times 10^{-3}$ cm/min

Test No.	Initial Water Content %	e_o	$\bar{\sigma}_v$ kg/cm^2	e_c	τ_p kg/cm^2	$\tau_p/\bar{\sigma}_v$	τ_r kg/cm^2	$\tau_r/\bar{\sigma}_v$	τ_r/τ_p	δ_p cm	δ_r cm	Fig. No.
1	61.8	1.71	1	1.25	0.255	0.255	0.118	0.118	0.462	0.060	3.0	7-3
Annulus			2				0.250	0.125				7-9
			4				0.515	0.129				
5	61.3	1.69	1	1.06	0.218	0.218	0.115	0.115	0.528	0.126	8.0	7-8
Disc			2				0.230	0.115				7-9
			4				0.490	0.122				

TABLE 7-4

ROTATION SHEAR S TESTS ON REMOLDED PEPPER SHALE

EFFECT OF OCR ON RESIDUAL STRENGTH (ANNULAR SPECIMENS): $\dot{\delta} = 5.6 \times 10^{-3}$ cm/min

Test No.	Initial Water Content %	e_o	$\bar{\sigma}_v$ kg/cm^2	OCR	e_c	τ_p kg/cm^2	$\tau_p/\bar{\sigma}_v$	τ_r kg/cm^2	$\tau_r/\bar{\sigma}_v$	τ_r/τ_p	δ_p cm	δ_r cm	Fig. No.
1	61.8	1.71	1	1	0.125	0.255	0.255	0.118	0.118	0.462	0.060	3.0	7-3
7	63.4	1.75	1	10	0.730	0.438	0.438	0.141	0.141	0.322	0.023	2.0	7-12, 7-16
8	62.0	1.71	1	10	0.806	0.432	0.432	0.145	0.145	0.335	0.022	3.0	7-13, 7-16
9	61.5	1.70	2	5	0.457	0.658	0.329	0.265	0.132	0.403	0.033	4.0	7-14, 7-16
10	61.5	1.70	4	2.5	0.569	1.160	0.290	0.508	0.127	0.438	0.054	6.0	7-15, 7-16
11	63.1	1.74	1	100	0.681	0.502	0.502	0.122	0.122	0.243	0.019	7.0	7-17

TABLE 7-5

ROTATION SHEAR S TESTS ON REMOLDED PEPPER SHALE

DESCRIPTION OF FAILURE PLANES – OVERCONSOLIDATED ANNULAR SPECIMENS

Test No.	Initial Water Content %	$\bar{\sigma}_v$ kg/cm^2	O.C.R.	Description
7	63.4	1	10	Very shiny failure plane with shallow radial and tangential undulations and very shallow circular striations. Located about 0.3 mm below upper platen.
8	62.0	1	10	Unable to separate specimen on entire failure plane. Several very shiny slickensides with radial and tangential undulations.
9	61.5	2	5	Very shiny failure plane adjacent to upper porous disc.
10	61.5	4	2.5	Very shiny failure plane, essentially flat but with some shallow radial and tangential undulations. Located about 0.3 mm below upper platen.
11	63.1	1	100	Specimen destroyed during separation of platens.

TABLE 7-6

ROTATION SHEAR S TESTS ON UNDISTURBED PEPPER SHALE

DISC-SHAPED SPECIMENS: $\dot{\delta} = 5.6 \times 10^{-3}$ cm/min

Test No.	Initial Water Content %	e_o	$\bar{\sigma}_v$ kg/cm^2	e_c	τ_p kg/cm^2	$\tau_p/\bar{\sigma}_v$	τ_r kg/cm^2	$\tau_r/\bar{\sigma}_v$	τ_r/τ_p	δ_p cm	δ_r cm	Fig. No.
12	20.3	0.560	1	0.449	0.252	0.252	0.112	0.112	0.445	0.046	30	7-19, 7-24
13	20.0	0.552	1	0.583	0.271	0.271	0.119	0.119	0.439	0.070	20	7-20, 7-24
14	20.8	0.574	2	0.456	0.618	0.309	0.253	0.126	0.410	0.060	18	7-21 7-24
15	21.1	0.583	4	0.406	1.060	0.260	0.400	0.100	0.378	0.037	30	7-22, 7-24
16	20.3	0.560	4	0.398	1.100	0.280	0.400	0.100	0.364	0.032	35	7-23, 7-24

TABLE 7-7

ROTATION SHEAR S TESTS ON UNDISTURBED PEPPER SHALE

DESCRIPTION OF FAILURE PLANES

Test No.	Initial Water Content %	$\bar{\sigma}_v$ kg/cm^2	Description	Figure No.
12	20.3	1	Very shiny, flat failure plane with circular striations located adjacent to upper porous disc.	7-8
13	20.0	1	Same as Test 12.	7-19
14	20.8	2	Very shiny, flat failure plane with circular striations located about 0.3 mm below upper platen.	7-20
15	21.1	4	Very shiny, flat failure plane with shallow circular striations located adjacent to upper porous disc.	7-21
16	20.3	4	Same as Test 15.	7-22

TABLE 8-1

ROTATION SHEAR S TESTS ON SLAKED AND CRUSHED CUCARACHA "SHALE"

NORMALLY CONSOLIDATED ANNULAR SPECIMENS: $\dot{\delta} = 5.6 \times 10^{-3}$ cm/min

Test No.	Initial Water Content %	e_o	$\bar{\sigma}_v$ kg/cm^2	e_c	τ_p kg/cm^2	$\tau_p/\bar{\sigma}_v$	τ_r kg/cm^2	$\tau_r/\bar{\sigma}_v$	τ_r/τ_p	δ_p cm	δ_r cm	Fig. No.
1	129.1	3.682	1.0	2.614	0.410	0.410	0.195	0.195	0.487	0.027	0.70	8-4, 8-6
2	127.5	3.630	1.0	2.339	0.415	0.415	0.190	0.190	0.458	0.037	3.00	8-5, 8-6
3	134.0	3.802	1.0	2.720	0.420	0.420	0.151	0.151	0.360	0.020	10.0	8-6
4	126.4	3.605	2.0 4.0	2.265	0.660	0.330	0.335 0.570	0.168 0.142	0.507	0.020	1.00	8-7
5	133.0	3.788	4.0 8.0	1.663	1.190	0.298	0.570 1.020	0.142 0.128	0.480	0.028	1.30	8-8
6	115.0	3.275	12.0 20	1.163	2.660	0.222	1.490 2.388	0.124 0.118	0.560	0.034	2.00	8-9
7	127.5	3.632	8.0	1.700	1.615	0.202	0.980	0.122	0.597	0.025	1.50	8-10

TABLE 8-2

ROTATION SHEAR S TESTS ON SLAKED AND CRUSHED CUCARACHA "SHALE"

DESCRIPTION OF FAILURE PLANES – NORMALLY CONSOLIDATED ANNULAR SPECIMENS

Test No.	Initial Water Content %	$\bar{\sigma}_v$ kg/cm^2	Description	Fig. No.
1	129.1	1.0	Very shiny slickensides at several elevations throughout specimen. Failure plane was very shiny and flat, located about 0.5 mm above lower platen.	8-4
2	127.5	1.0	Very shiny failure plane about 0.5 mm above lower platen with shallow radial undulations.	8-5
3	134.0	1.0	Very shiny and very flat failure plane about 0.5 mm below top platen.	8-6
4	126.4	2.0 4.0	Very shiny, very flat failure plane adjacent to top platen.	8-7
5	133.0	4.0 8.0	Highly polished failure plane, slightly concave downward. Thickness of specimen at end of test about 0.35 mm.	8-8
6	115.0	12.0 20.0	Highly polished slickensides observed but continuity of failure plane was destroyed during separation of platens.	8-9
7	127.5	8.0	Highly polished, very flat failure plane about 0.3 mm below upper platen. Gloss of failure plane approaching gloss of natural slickensides.	8-10

TABLE 8-3

ROTATION SHEAR S TESTS ON SLAKED AND CRUSHED CUCARACHA "SHALE"

EFFECT OF RATE OF DISPLACEMENT ON RESIDUAL STRENGTH

Test No.	Initial Water Content %	e_o	$\bar{\sigma}_v$ kg/cm^2	e_c	$\dot{\delta}$ 10^{-3} cm/min	τ_r kg/cm^2	Remarks	Figure No.
7	127.5	3.632	8.0	1.700	5.6 0.56 56	0.980 0.980 1.015	Specimen initially sheared at 5.6×10^{-3} cm/min	8-10

TABLE 8-4

ROTATION SHEAR S TESTS ON SLAKED AND CRUSHED CUCARACHA "SHALE"; $\bar{\sigma}_v = 1.0$ kg/sq cm

EFFECT OF OCR ON RESIDUAL STRENGTH (ANNULAR SPECIMENS); $\dot{\delta} = 5.6 \times 10^{-3}$ cm/min

Test No.	Initial Water Content %	e_o	OCR	e_c	τ_p kg/cm^2	τ_r kg/cm^2	τ_r/τ_p	δ_p cm	δ_r cm	Fig. No.
1	129.1	3.682	1	2.614	0.410	0.195	0.487	0.027	0.70	8-4, 8-6
2	127.5	3.630	1	2.334	0.415	0.190	0.458	0.037	3.00	8-5, 8-6
3	134.0	3.820	1	2.720	0.420	0.151	0.360	0.020	10.0	8-6
8	115.7	3.292	10	1.501	0.655	0.160	0.245	0.011	5.0	8-14, 8-15
9	116.7	3.321	100	1.444	0.910	0.180	0.197	0.020	10.0	8-5

TABLE 9-1

ROTATION SHEAR S TESTS ON REMOLDED LONDON CLAY

NORMALLY CONSOLIDATED ANNULAR SPECIMENS: $\dot{\delta} = 5.6 \times 10^{-3}$ cm/min

Test No.	Initial Water Content %	e_o	$\bar{\sigma}_v$ kg/cm^2	e_c	τ_p kg/cm^2	$\tau_p/\bar{\sigma}_v$	τ_r kg/cm^2	$\tau_r/\bar{\sigma}_v$	τ_r/τ_p	δ_p cm	δ_r cm	Fig. No.
1	67.0	1.821	1	1.112	0.362	0.362	0.177	0.177	0.488	0.11	9.0	9-3, 9-6
2	63.4	1.725	2 4	0.859	0.660	0.330	0.293 0.572	0.146 0.143	0.444	0.90	15.0	9-4, 9-6
3	62.1	1.690	8	0.430	2.180	0.273	1.175	0.147	0.536	0.10	4.0	9-5, 9-6

TABLE 9-2

ROTATION SHEAR S TESTS ON REMOLDED LONDON CLAY

DESCRIPTION OF FAILURE PLANES – NORMALLY CONSOLIDATED ANNULAR SPECIMENS

Test No.	Initial Water Content %	$\bar{\sigma}_v$ kg/cm^2	Description	Fig. No.
1	37.0	1	Medium shiny failure plane slightly inclined toward center of rotation. Failure plane had both radial and tangential undulations.	9-3
2	63.4	2 4	Specimen had two failure planes; one adjacent to upper platen and the other in the middle of the specimen. Both planes had a medium shine, were flat, and had shallow striations.	9-4
3	62.1	8	Failure occurred about 0.2 mm from upper platen. The failure plane had a medium shine with radial and tangential undulations.	9-5

TABLE 9-3

ROTATION SHEAR S TESTS ON UNDISTURBED LONDON CLAY

ANNULAR SPECIMENS: $\dot{\delta} = 5.6 \times 10^{-3}$ cm/min

Test No.	Initial Water Content %	e_o	$\bar{\sigma}_v$ kg/cm^2	e_c	τ_p kg/cm^2	$\tau_p/\bar{\sigma}_v$	τ_r kg/cm^2	$\tau_r/\bar{\sigma}_v$	τ_r/τ_p	δ_p cm	δ_r cm	Fig. No.
4	27.7	0.754	1	0.697	0.315	0.315	0.160	0.160	0.508	0.06	40	9-8, 9-12
5	28.0	0.762	2	0.605	0.685	0.342	0.339	0.170	0.495	0.09	35	9-9, 9-12
6	28.5	0.776	4	0.440	1.322	0.331	0.650	0.162	0.442	0.07	3.5	9-10, 9-12
7	25.3	0.689	8	0.275	2.560	0.320	1.320	0.165	0.520	0.09	10	9-11, 9-12

TABLE 9-4

ROTATION SHEAR S TESTS ON UNDISTURBED LONDON CLAY

DESCRIPTION OF FAILURE PLANES – ANNULAR SPECIMENS

Test No.	Initial Water Content %	$\bar{\sigma}_v$ kg/cm^2	Description	Fig. No.
4	27.7	1	Moderately shiny failure plane adjacent to upper platen.	9-8
5	28.0	2	Very flat, medium shiny failure plane about 0.2 mm below upper platen, with shallow striations.	9-9
6	28.5	4	Very flat, medium shiny failure plane adjacent to upper platen.	9-10
7	25.3	8	Very flat, medium shiny failure plane about 0.2 mm below upper platen, very shallow circular striations.	9-11

TABLE 9-5

ROTATION SHEAR S TESTS ON REMOLDED LONDON CLAY

ANNULAR SPECIMENS

RATE OF EXTRUSION WITH A SOLID CONFINING RING

Test No.	$\bar{\sigma}_v$ kg/cm^2	δ_{max} cm	$\Delta B/B_c$ %	Rate of Extrusion 10^{-4} in./cm	$\tau_r/\bar{\sigma}_v$
1	1.0	33	9.7	0.6	0.177
2	2.0	45	13.9	2.5	0.146
	4.0	24	27.0	3.0	0.143
3	8.0	33	47.0	9.4	0.147
3	Using penultimate point on ΔB vs. δ curve		39.0	3.2	

TABLE 10-1

RESIDUAL SHEARING RESISTANCE OF PEPPER SHALE, CUCARACHA "SHALE" AND LONDON CLAY

Rotation Shear S Tests on Remolded Annular Specimens. $\dot{\delta} = 5.6 \times 10^{-3}$ cm/min, solid confining ring

Material	L_w	P_w	% Minus 2 Micron	Range of $\bar{\sigma}_v$ kg/sq cm	$\tau_r/\bar{\sigma}_v$ for $\bar{\sigma}_v$ (kg/sq cm) = 1	8	20	Reference
Pepper Shale: air-dried and remolded with distilled water	70.5	21.5	73	1-20	0.118	0.130	0.134	Figs. 7-1 to 7-7 Tables 7-1, 7-2
Cucaracha "Shale": air-dried and slaked four times, air-dried and crushed in a disc mill, then remolded with distilled water	156	42	100	1-20	0.179	0.128	0.118	Figs. 8-1 to 8-12 Tables 8-1, 8-2
London Clay: remolded with distilled water from the natural water content	71.5	22.5	65	1-8	0.177	0.147	N. A.	Figs. 9-1 to 9-7 Tables 9-1, 9-2

TABLE 10-2

DISPLACEMENT REQUIRED TO REACH PEAK AND RESIDUAL STRENGTHS

Rotation Shear S Tests on Remolded Annular Specimens. $\dot{\delta} = 5.6 \times 10^{-3}$ cm/min, solid confining ring

Material	Range of $\bar{\sigma}_v$ kg/sq cm	Range of τ_r/τ_p	Range of δ_p cm	Range of δ_r cm
Pepper Shale	1.0 to 12.0	0.462 to 0.610	0.060 to 0.090	1.5 to 3.0
Crushed Cucaracha "Shale"	1.0 to 12.0	0.435 to 0.597	0.028 to 0.034	0.7 to 2.0
London Clay	1.0 to 8.0	0.444 to 0.536	0.10 to 0.90	4.0 to 15

TABLE 10-3

EFFECT OF OVERCONSOLIDATION RATIO ON RESIDUAL STRENGTH OF PEPPER SHALE

Rotation Shear S Tests on Remolded Annular Specimens. $\dot{\delta} = 5.6 \times 10^{-3}$ cm/min, solid confining ring

$\bar{\sigma}_v$ kg/cm^2	OCR	τ_p kg/cm^2	τ_r kg/cm^2	τ_r/τ_v	$\tau_r/\bar{\sigma}_p$	δ_p cm	δ_r cm	Figure No.
1	1	0.255	0.118	0.462	0.118	0.060	3.0	7-3
1	10	0.438	0.141	0.322	0.141	0.023	2.0	7-12, 7-16
1	10	0.432	0.145	0.355	0.145	0.022	3.0	7-13, 7-16
1	100	0.502	0.122	0.243	0.122	0.019	7.0	7-17
2*	1	--	0.250	--	0.125	--	--	7-3
2	5	0.658	0.265	0.403	0.132	0.033	4.0	7-14, 7-16
4	1	0.885	0.500	0.565	0.125	0.088	7.0	7-4
4	2.5	1.160	0.508	0.438	0.127	0.054	6.0	7-15, 7-16

* Residual strength at 2.0 kg/sq cm determined from a specimen previously sheared at $\bar{\sigma}_v = 1.0$ kg/sq cm.

TABLE 10-4

EFFECT OF OVERCONSOLIDATION RATIO ON RESIDUAL STRENGTH OF CRUSHED CUCARACHA "SHALE"

Rotation Shear S Test on Remolded Annular Specimens. $\dot{\delta} = 5.6 \times 10^{-3}$ cm/min, solid confining ring

$\bar{\sigma}_v$ kg/cm^2	OCR	τ_p kg/cm^2	τ_r	τ_r/τ_p	δ_p cm	δ_r cm	Figure No.
1	1	0.415	0.195	0.487	0.027	0.70	8-4, 8-6
1	1	0.415	0.190	0.458	0.037	3.0	8-5, 8-6
1	1	0.420	0.151	0.360	0.020	10.0	8-6
1	10	0.655	0.160	0.245	0.011	5.0	8-14, 8-15
1	100	0.910	0.180	0.197	0.020	10.0	8-15

TABLE 10-5

EFFECT OF METHOD OF REMOLDING ON RESIDUAL STRENGTH OF CUCARACHA "SHALE"

Rotation Shear S Tests on Remolded Annular Specimens. $\dot{\delta} = 5.6 \times 10^{-3}$ cm/min, solid confining ring

Treatment	Liquid Limit L_w	Plastic Limit P_w	% Minus 2 Micron	$\bar{\sigma}_v$ kg/cm^2	τ_r kg/cm^2	δ_r cm	Figure No.
Slaked and crushed	156	42	100	1	0.190 to 0.151	0.70 to 10	8-6
				4	0.570	1.30	8-8
Slaked and uncrushed	49	28	45	1	0.140	70	8-17
				4	0.575	20	8-18

TABLE 10-6

EFFECT OF RATE OF DISPLACEMENT ON RESIDUAL STRENGTH

Rotation Shear S Tests on Remolded Annular Specimens. Solid confining ring.

Material	$\bar{\sigma}_v$ kg/cm^2	$\dot{\delta}$ 10^{-3} cm/min	τ_r kg/cm^2
Pepper Shale	1.0	5.6	0.141
		0.56	0.152
Crushed Cucaracha "Shale"	8.0	56	1.015
		5.6	0.980
		0.56	0.980
London Clay	4.0	5.6	0.572
		0.56	0.561

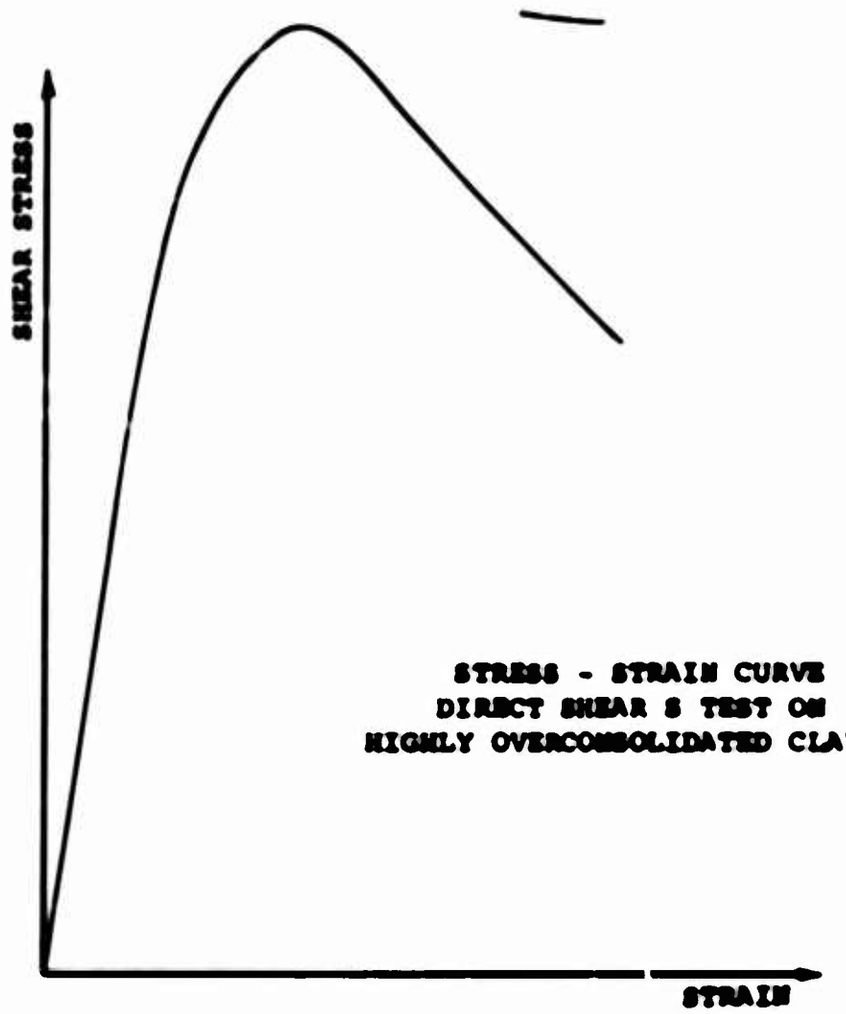

STRESS - STRAIN CURVE
DIRECT SHEAR S TEST ON
HIGHLY OVERCONSOLIDATED CLAY

FIG. 1-1

HYPOTHETICAL RESULTS FROM DIRECT
SHEAR & TESTS ON CLAY
1-2a
1-2b
1-2c
1-2d
VOID RATIO, e
EFFECTIVE VERTICAL STRESS, $\bar{\sigma}_v$
compression
swelling
A
B
C
D
a
b
c
d
1'
2'
3
cr
DISPLACEMENT, δ
SHEAR STRESS
PEAK
RESIDUAL

FIG. 1-2

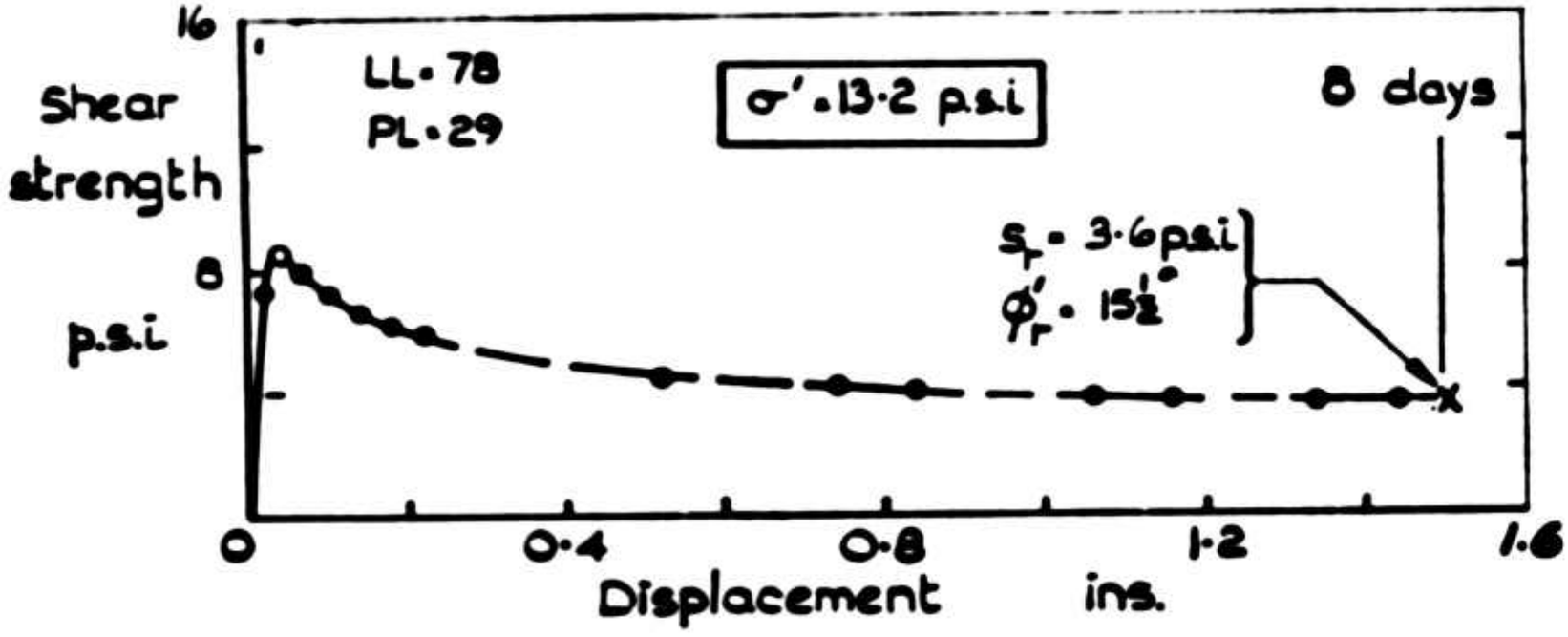

HENDON LARGE STRAIN TEST

REPEATED DIRECT SHEAR TEST
from Skempton, 1964
specimen size:
6 cm sq
2.5 cm thick

FIG. 2-1

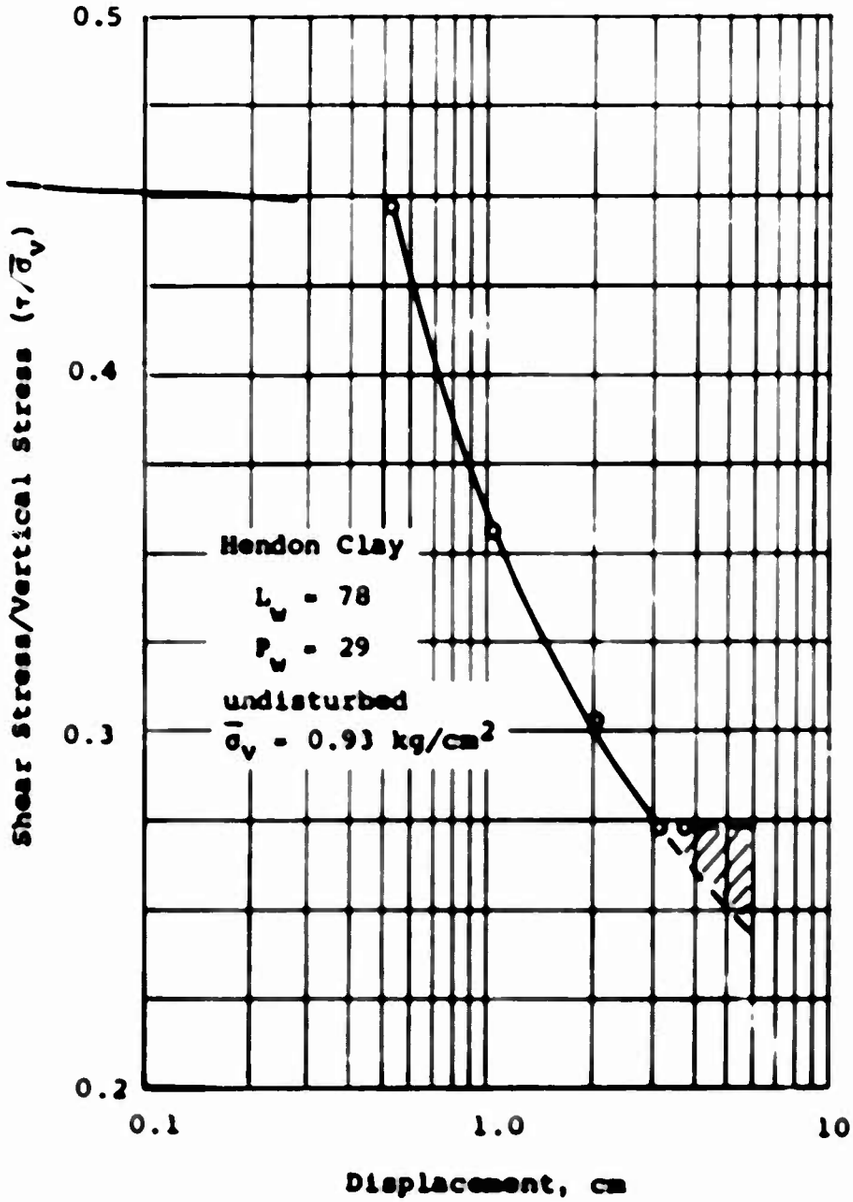

REPEATED DIRECT SHEAR TEST

from: Skempton, 1964
specimen size:
6 cm sq
2.5 cm thick

FIG. 2-2

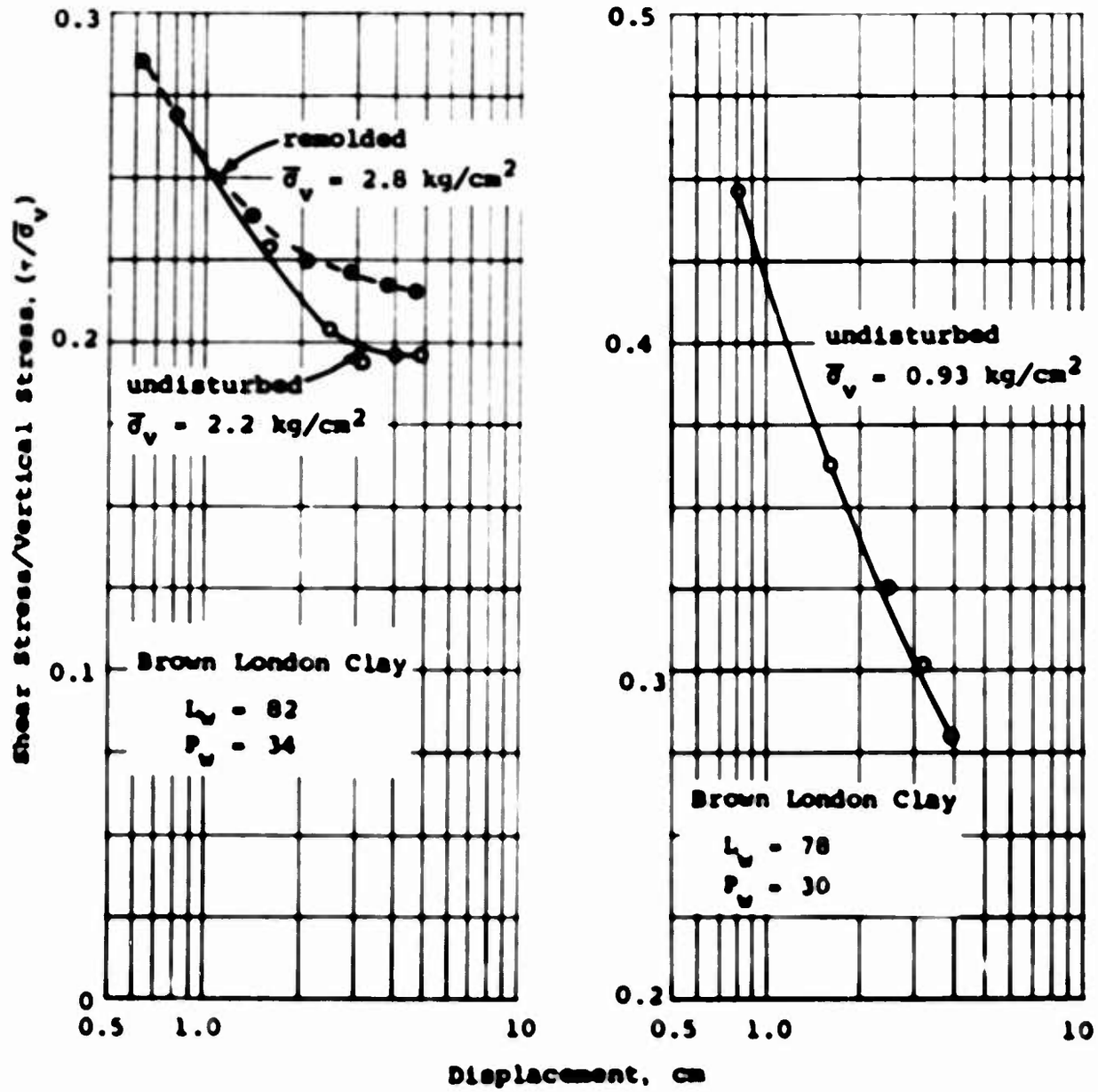

REPEATED DIRECT SHEAR TEST

from: Petley, 1966
specimen size:
6 sq cm
2.5 cm thick

FIG. 2-3

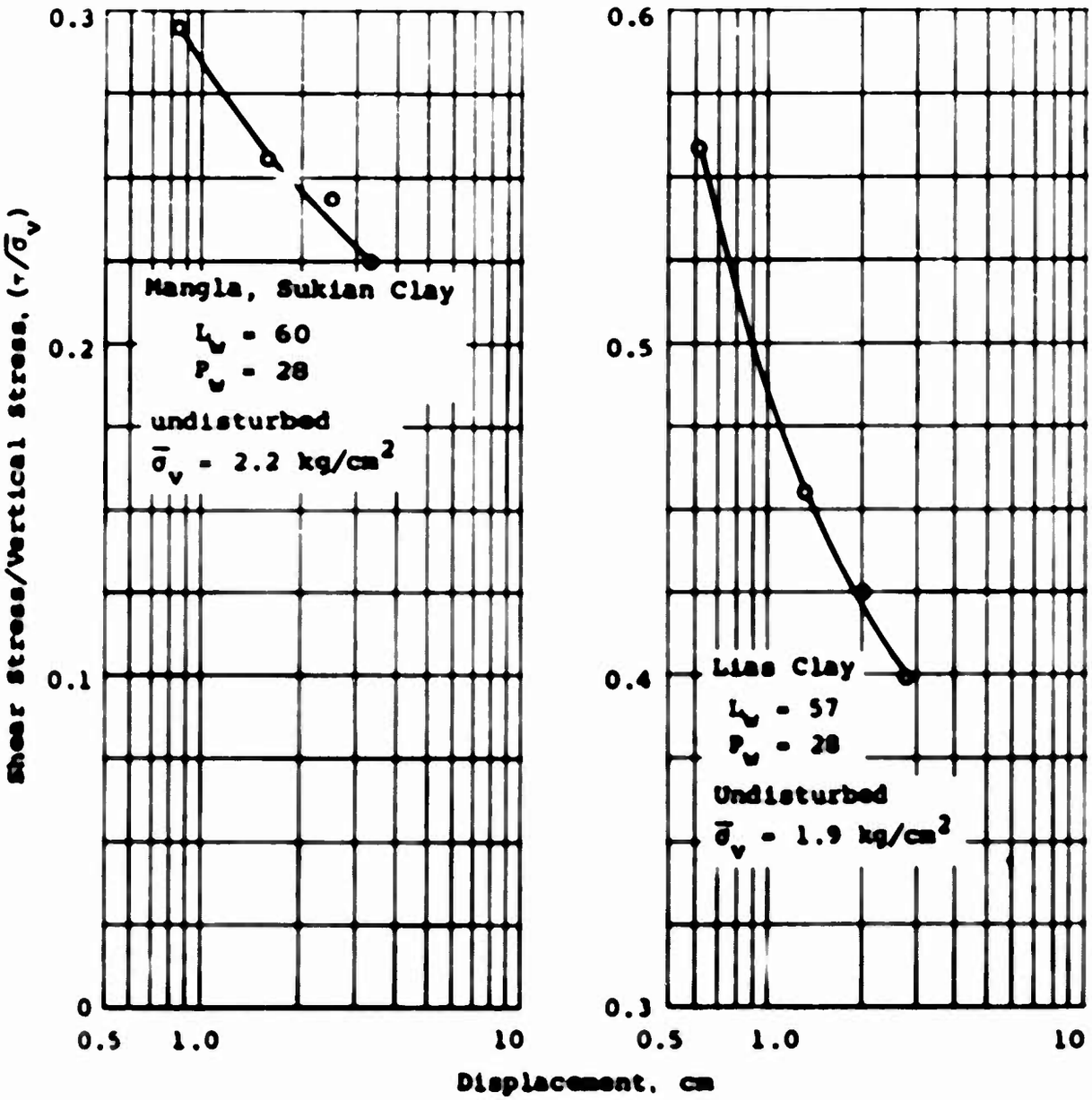

REPEATED DIRECT SHEAR TEST

from: Petley, 1966
specimen size:
6 sq cm
2.5 cm thick

FIG. 2-4

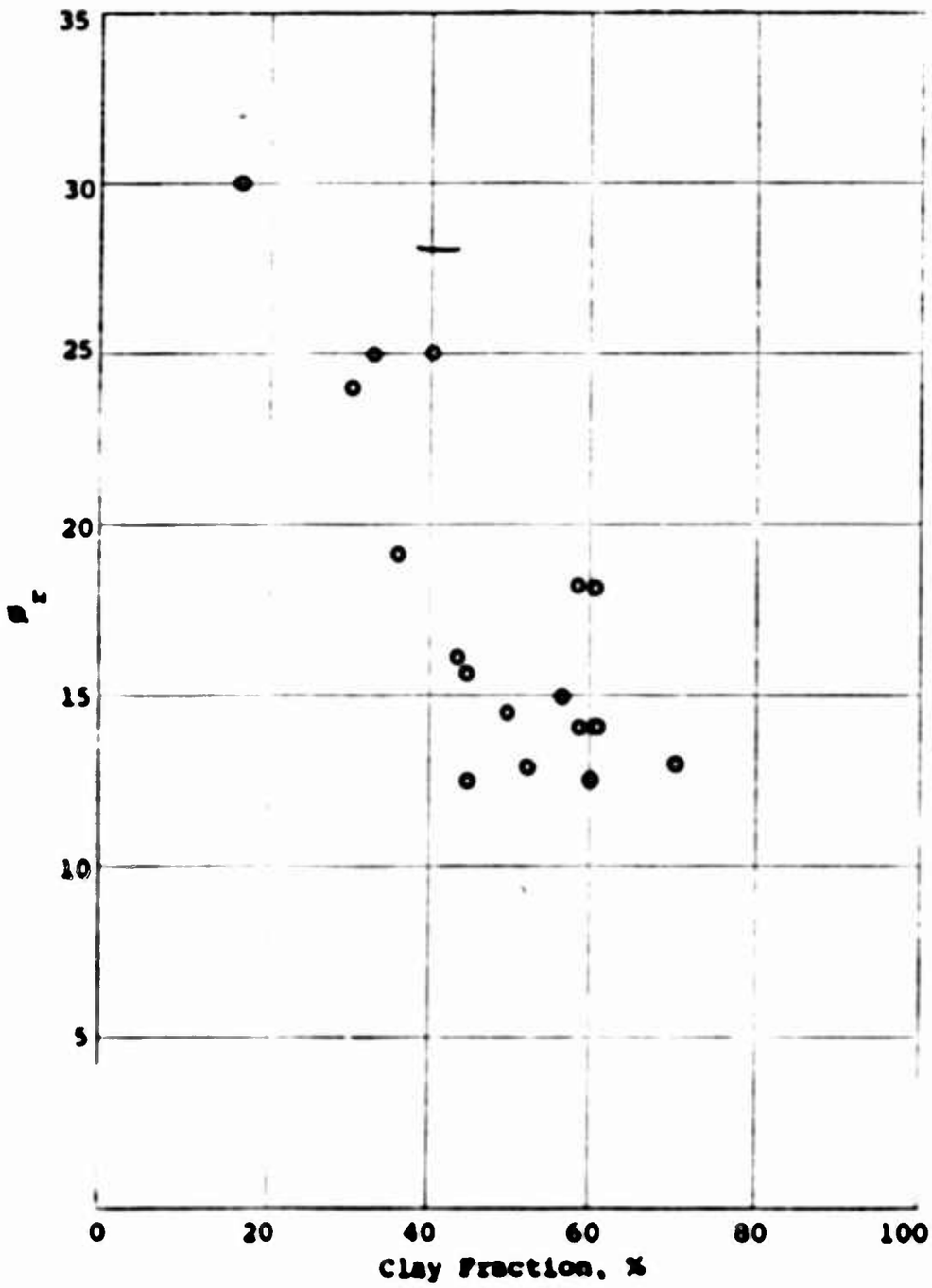

INFLUENCE OF CLAY FRACTION ON ϕ_r

from: Petley, 1966

FIG. 2-5

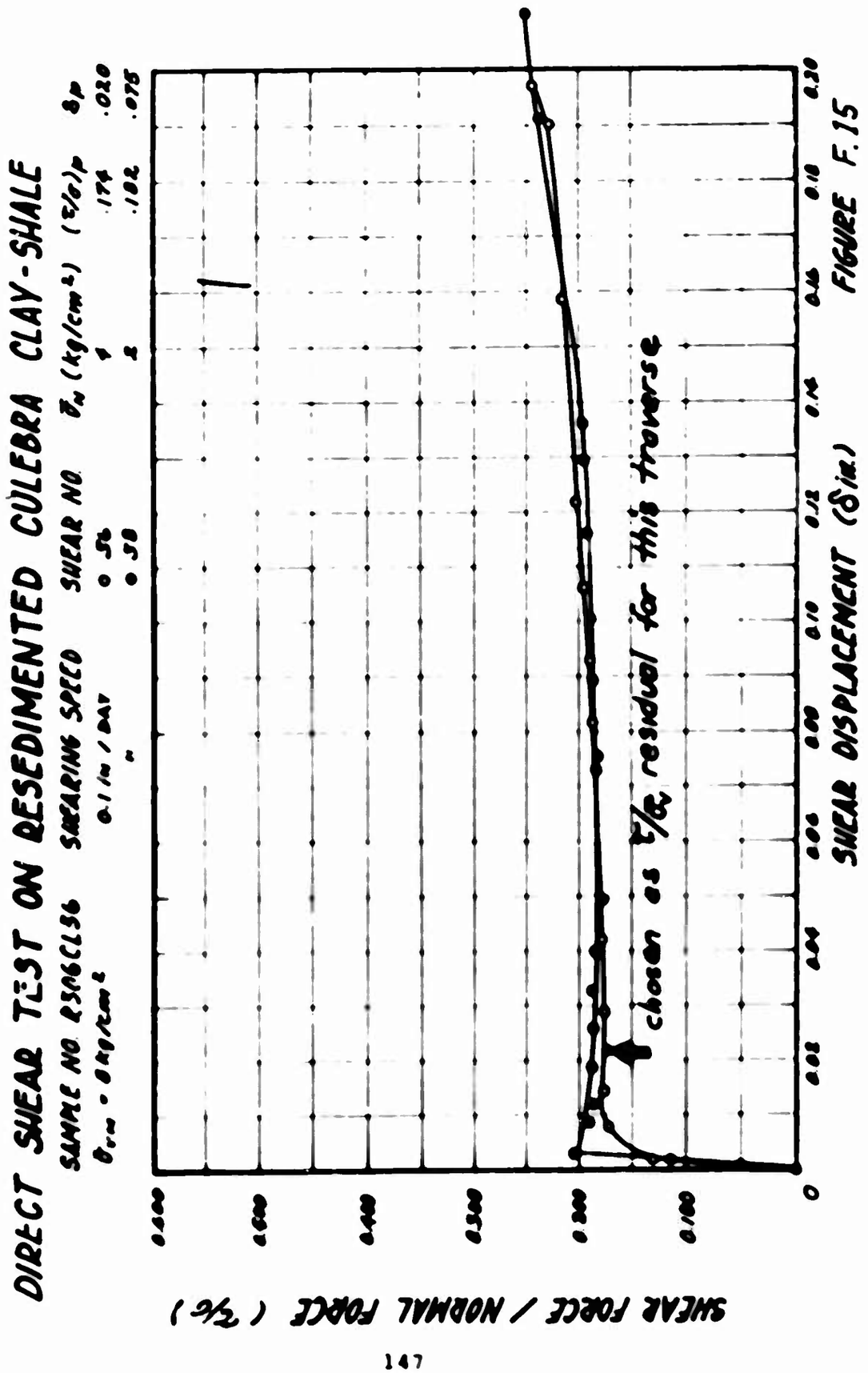
DIRECT SHEAR TEST ON RESEDIMENTED CULEBRA CLAY-SHALE
SHEAR FORCE / NORMAL FORCE (%)
SHEAR DISPLACEMENT (δ in.)
chosen as %c residual for this traverse
reproduced from:
Hermann and Wolfskill, 1966
FIGURE F.15

147

FIG. 2-6

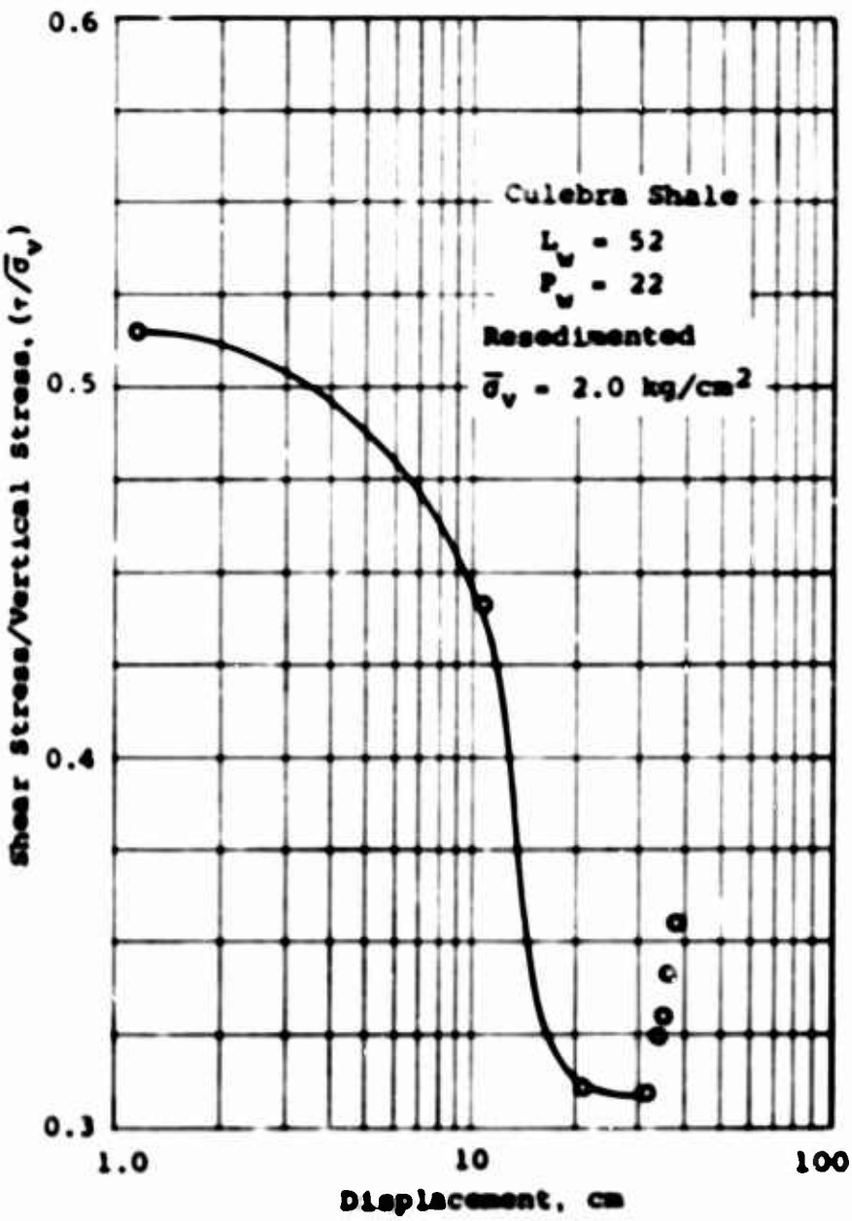

REPEATED DIRECT SHEAR TEST

from: Norman and Wolfskill 1966

specimen size:
5.1 cm sq 0.9 cm thick

FIG. 2-7

FRICTION TEST ON TEFLON COATED SHEAR BOXES

STRAIN RATE EQUALS 01 INCH PER 30 MINUTES

RESULTS:

$\bar{\sigma}_N$ [1] (kg/cm²)	$\bar{\sigma}_N$ [2] (kg/cm²)	$(\tau/\sigma)_{MAX}$	$(\tau/\sigma)_{MIN}$
1 29	2	.219	.068
2.58	4	.092	.064
5.16	8	.091	.051
10 32	16	.103	.053

[1] BASED ON ACTUAL AREA OF CONTACT BETWEEN TWO SHEAR BOX HALVES

[2] EQUIVALENT NORMAL STRESS ON SAMPLE IF PRESENT AND CARRYING ALL LOAD

TYPICAL INDIVIDUAL TEST:

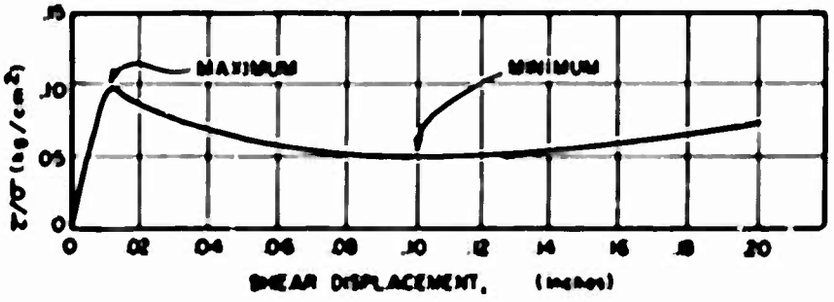

SUMMARY:

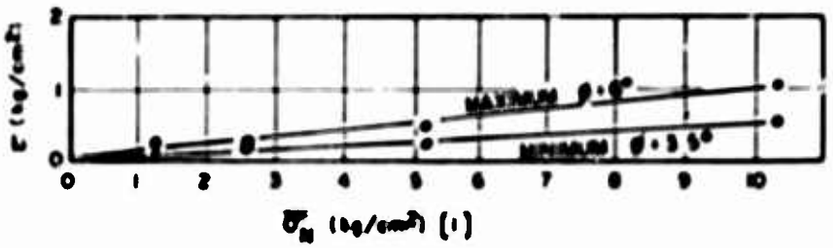

reproduced from:

Herrman and Wolfskill, 1966

73

FIG. 2-8

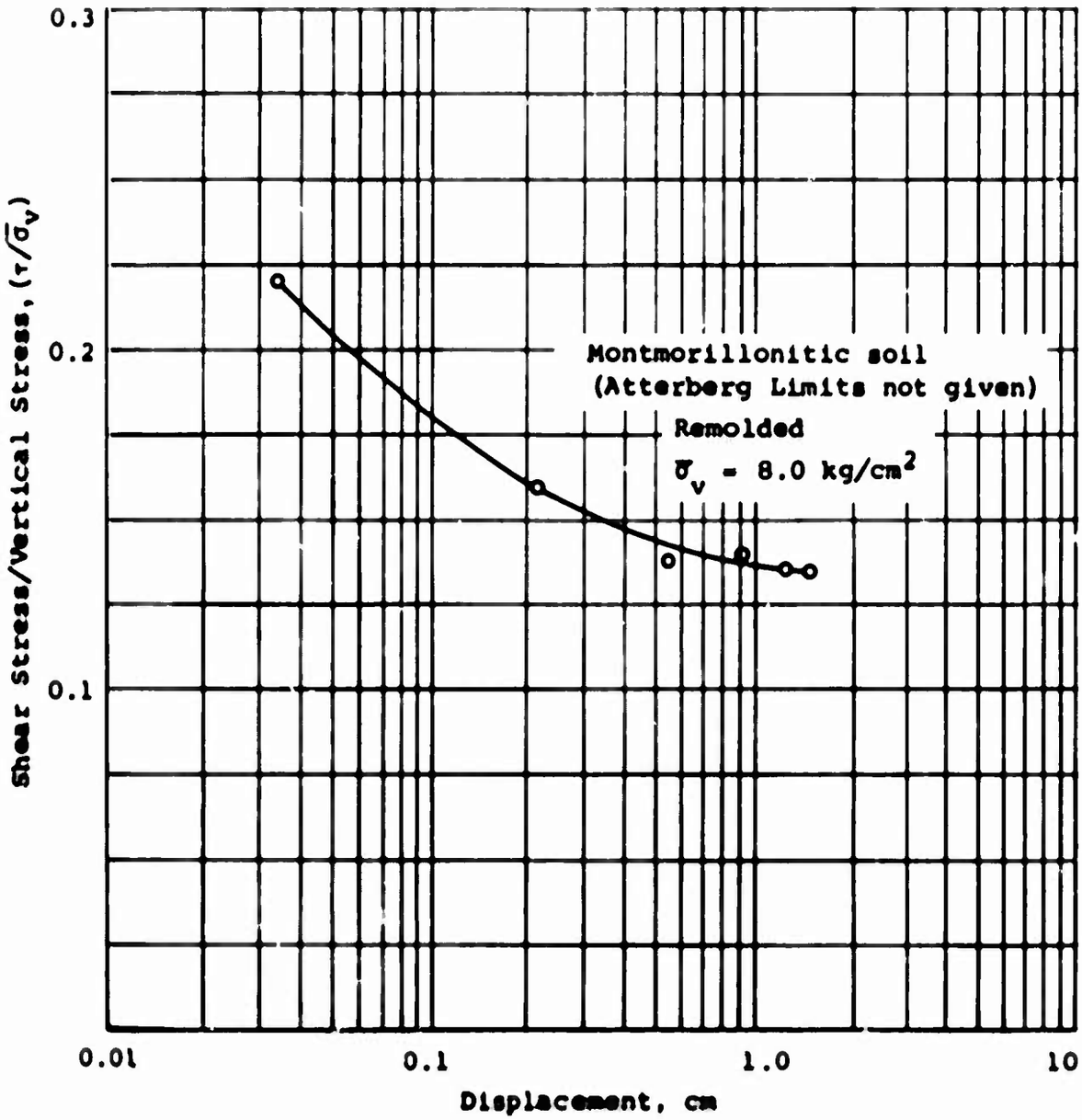

REPEATED DIRECT SHEAR TEST

from: Kenney, 1967
specimen size:
8 cm diameter
0.2 cm thick

FIG. 2-9

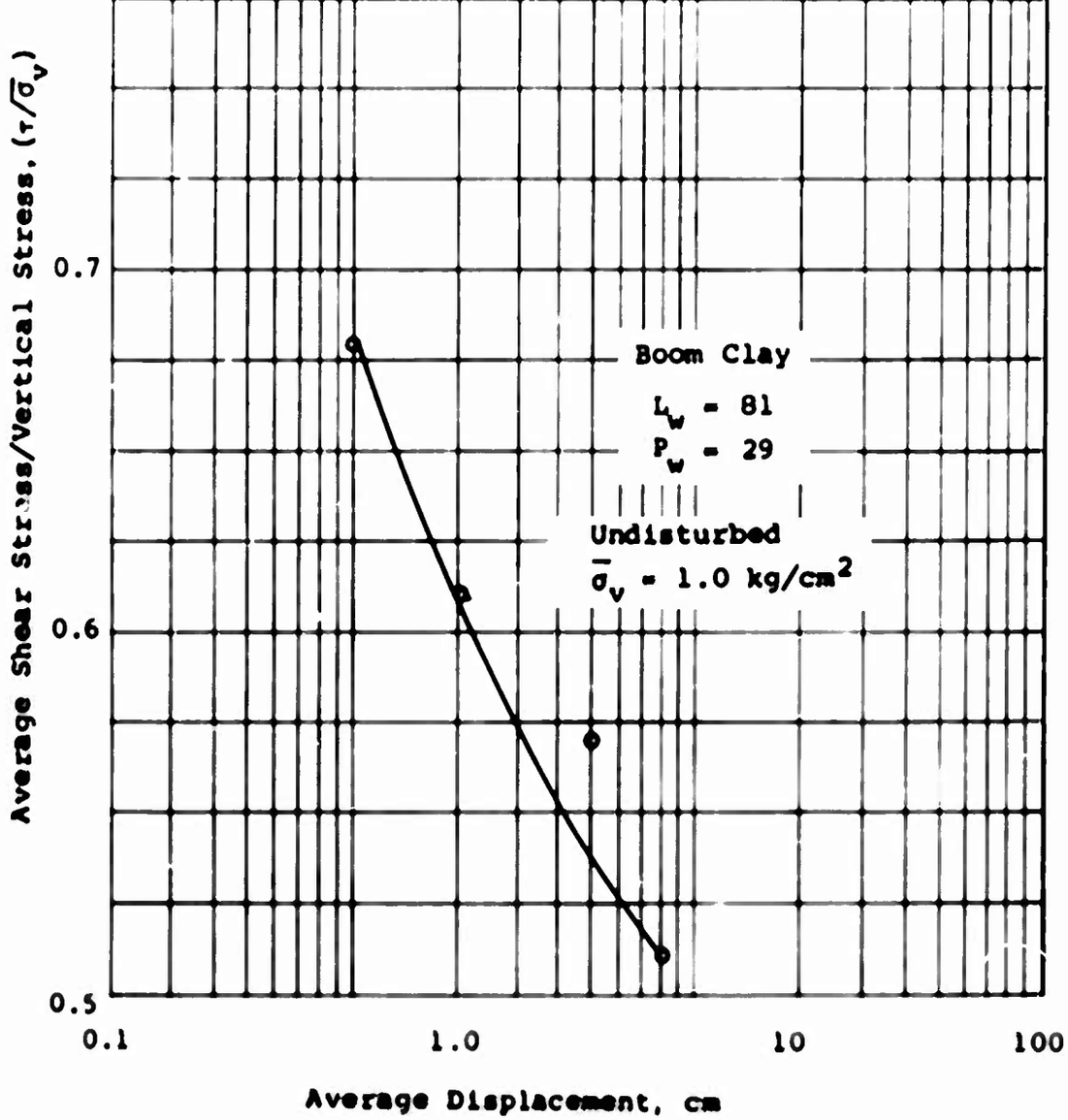

ROTATION SHEAR TEST

from: de Beer, 1967
annular specimen size:
8 cm outside dia
4 cm inside dia
1.8 cm thick

FIG. 2-10

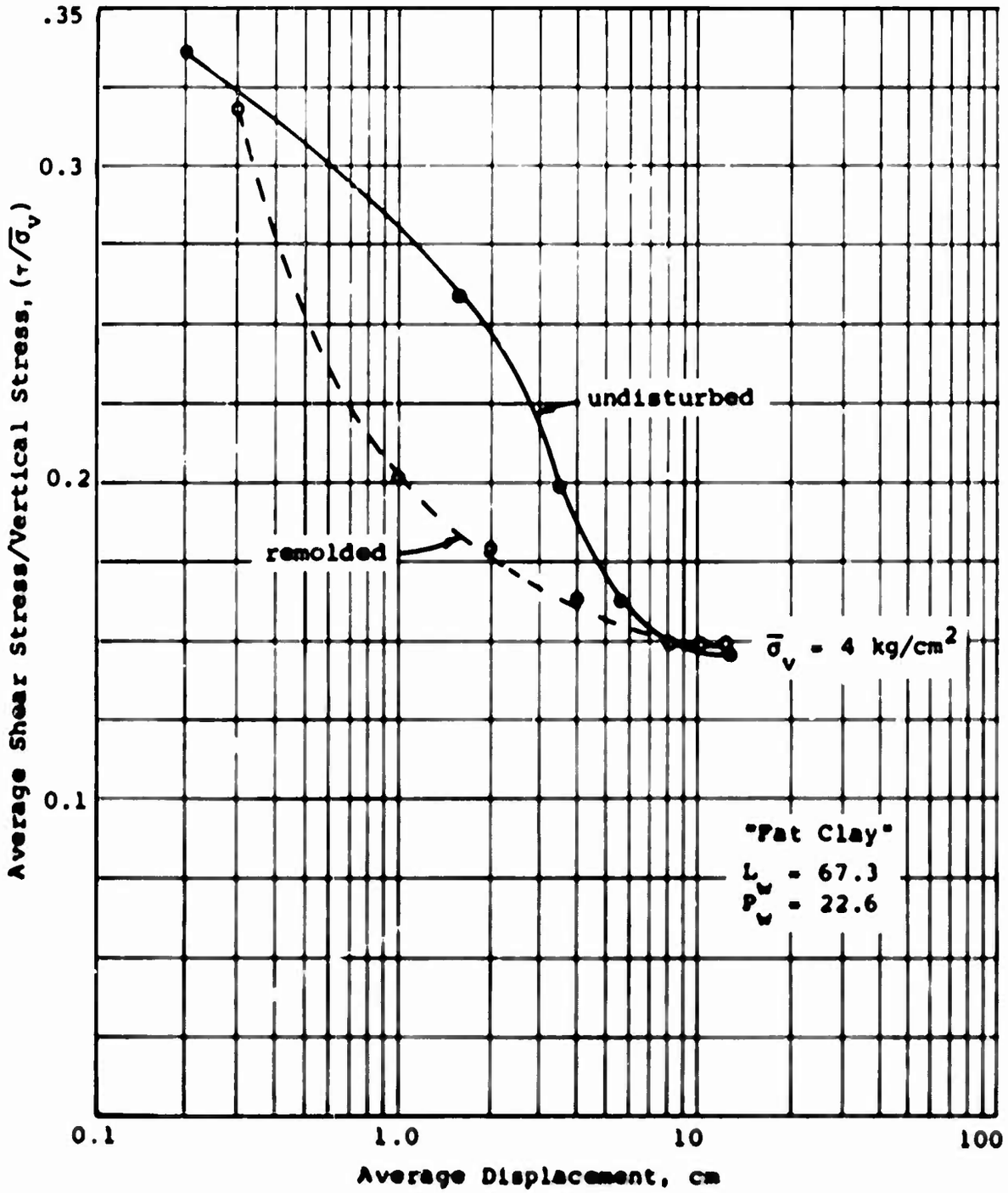

ROTATION SHEAR TEST

from: Tiedemann, 1937
dimensions of specimen
not given

FIG. 2-11

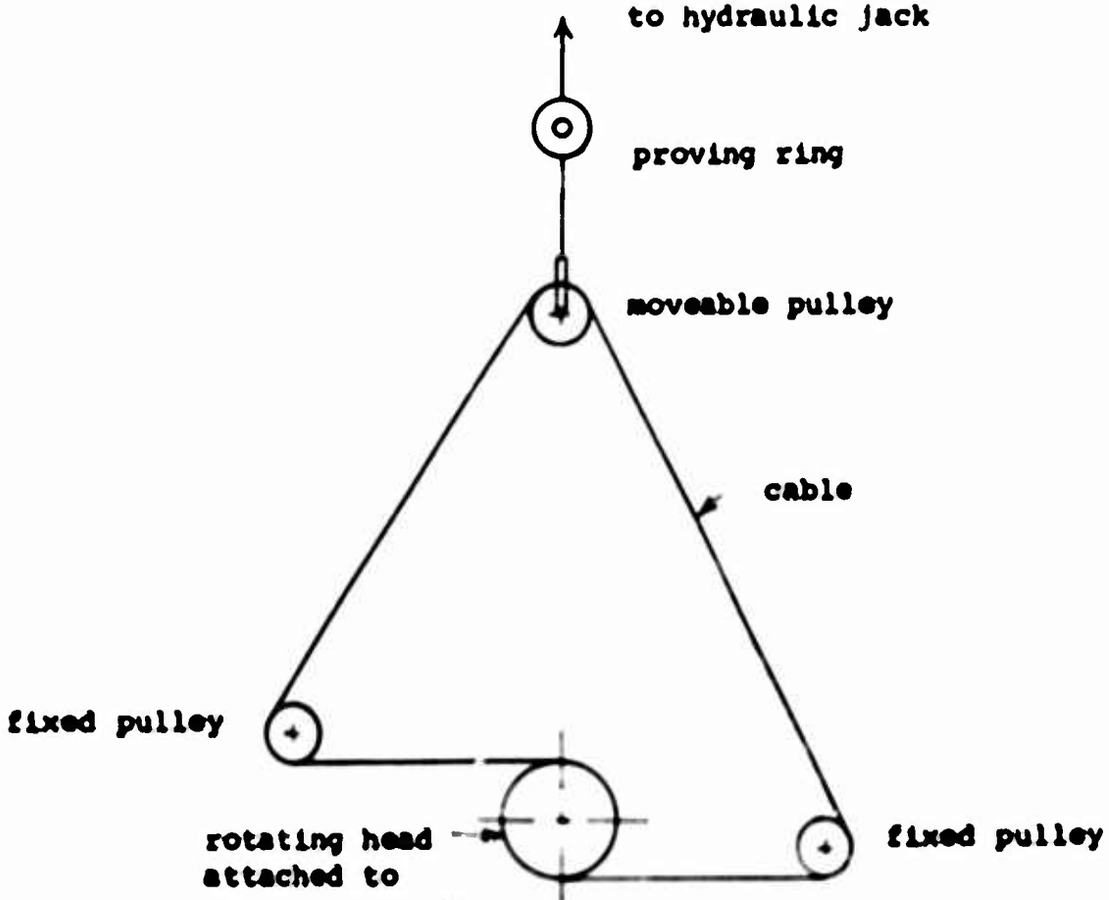

N.T.S.

PULLEY ARRANGEMENT
HYDRAULIC ROTATION
SHEAR MACHINE

FIG. 3-1

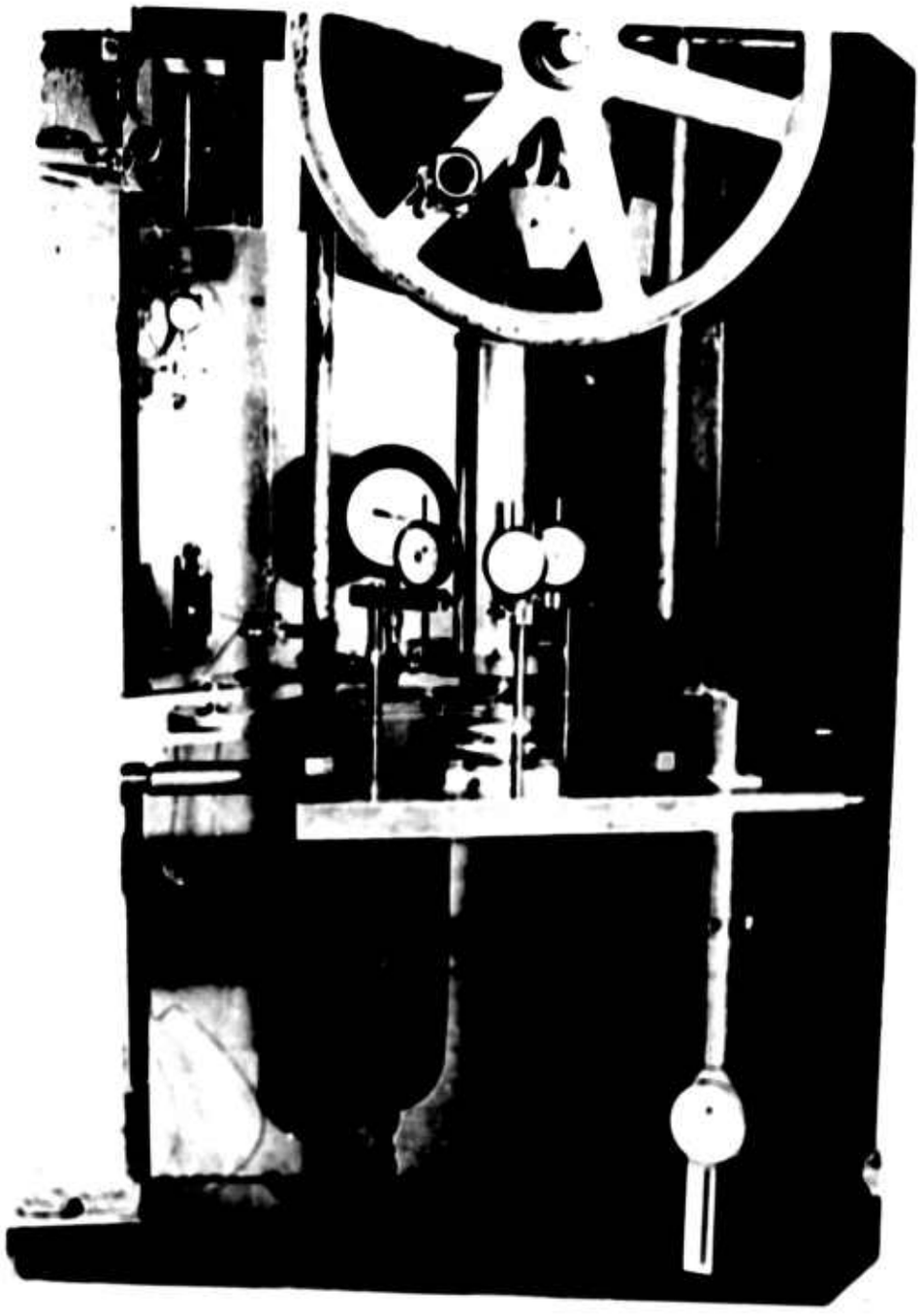

HARVARD

HYDRAULIC ROTATION
SHEAR MACHINE

FIG. 3-2

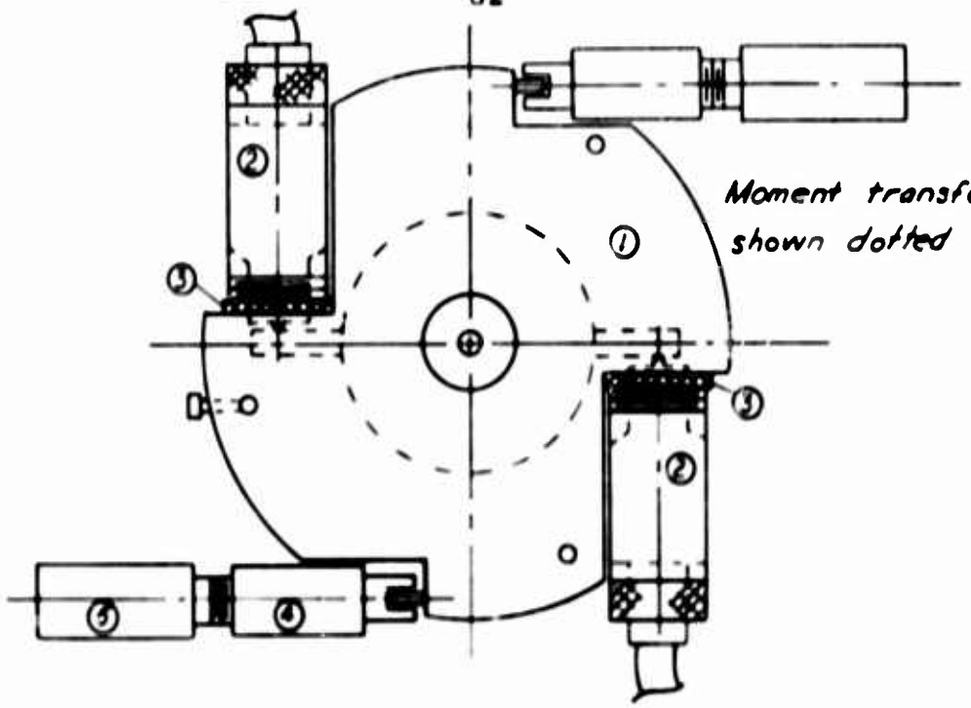

Top View

scale: .5" = 1"

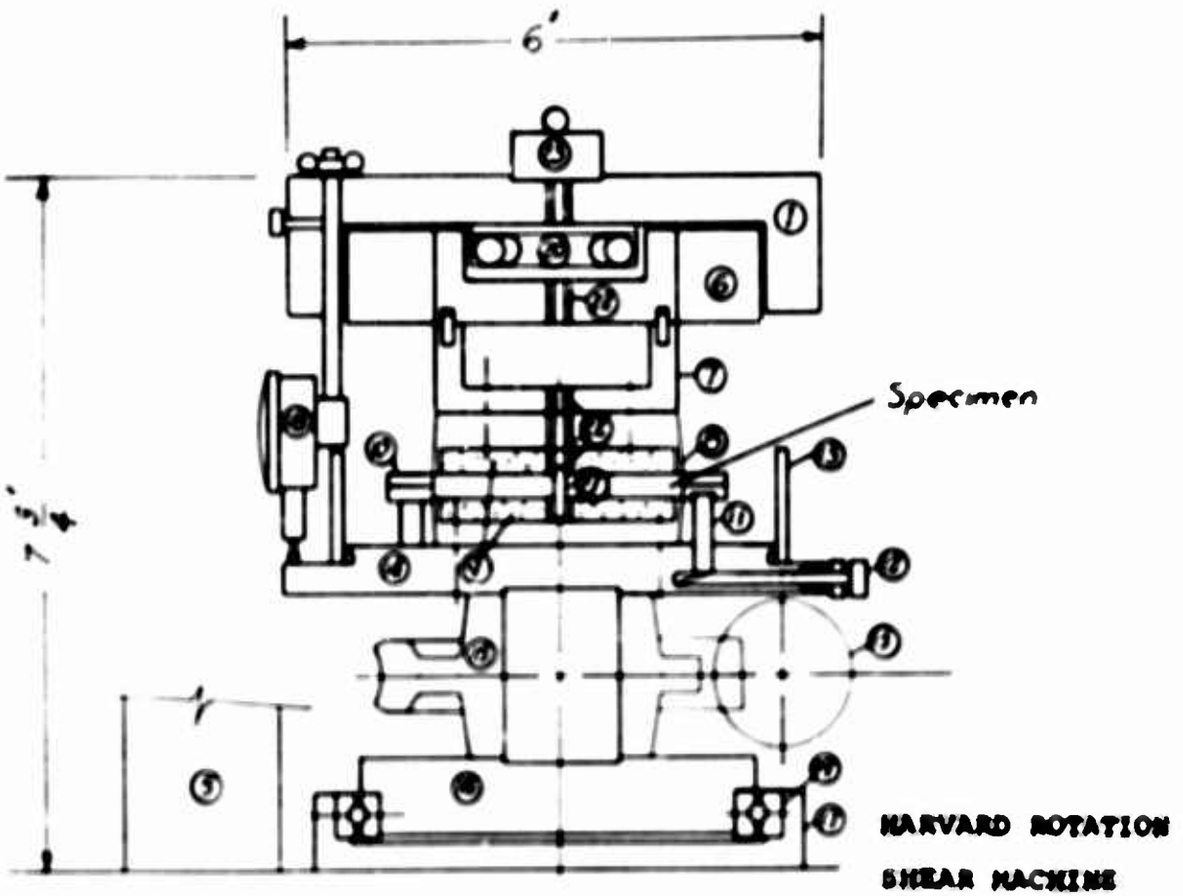

HARVARD ROTATION SHEAR MACHINE

FIG. 3-3

HARVARD

ROTATION SHEAR MACHINE

PARTS LIST

1. Top plate.
2. Adjustable transducer clamp and transducer.
3. Locking nut.
4. Adjustable restraining arm.
5. Vertical post.
6. Moment transfer plate.
7. Hollow spacer.
8. Loading platen.
9. Porous stainless steel discs.
10. Confining ring.
11. Confining ring support pins.
12. Confining ring support pins.
13. Lucite reservoir.
14. Turntable
15. Worm gear.
16. Rotating base.
17. Stationary base.
18. Tilt dial.
19. Four-point contact radial bearing.
20. Thrust bearing.
21. Centering pin.
22. Teflon bushing.
23. Stainless steel loading platen.

FIG. 3-4

SHEARING UNIT
EXPLODED VIEW

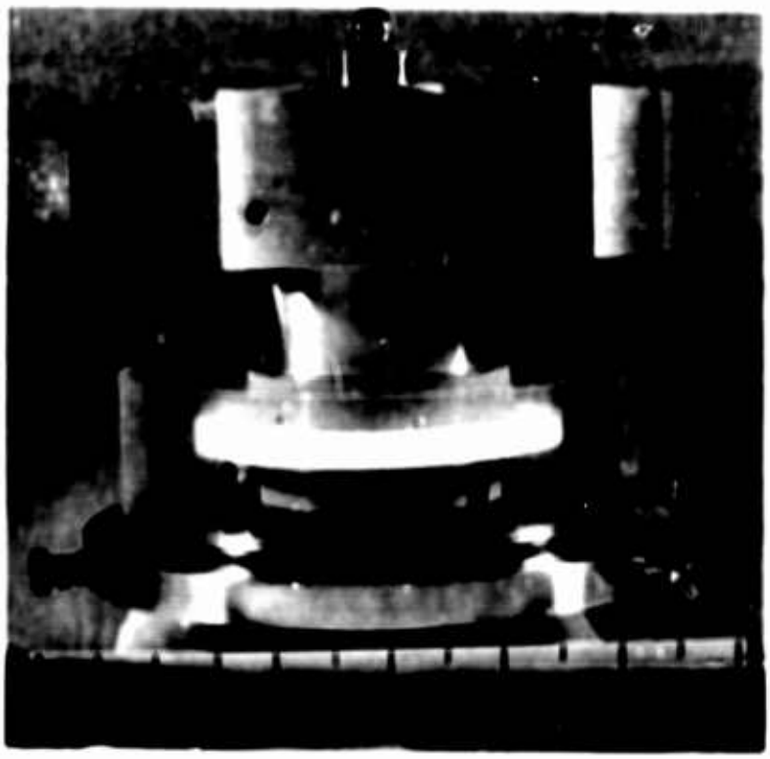

SHEARING UNIT
ASSEMBLED VIEW

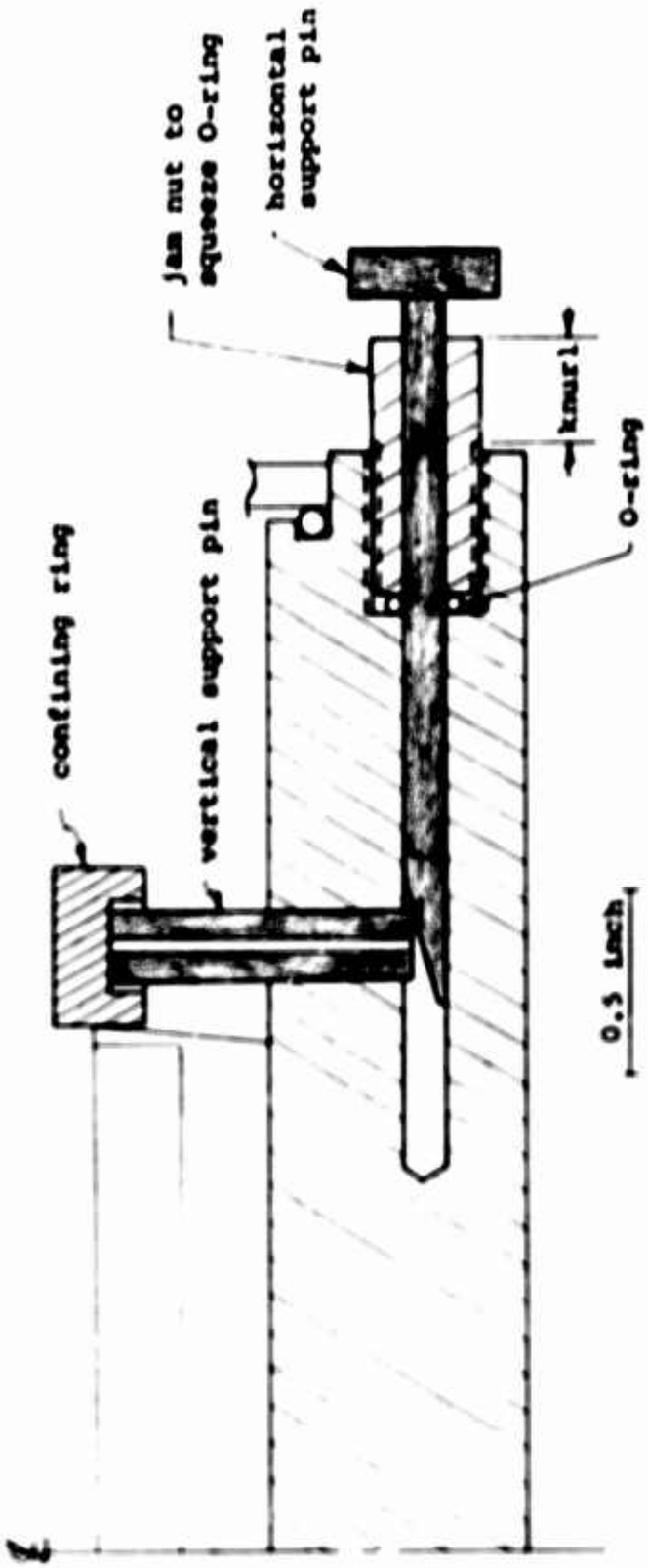

HARVARD
ROTATION SHEAR MACHINE
CONFINING RING SUPPORT PINS

FIG. 3-7

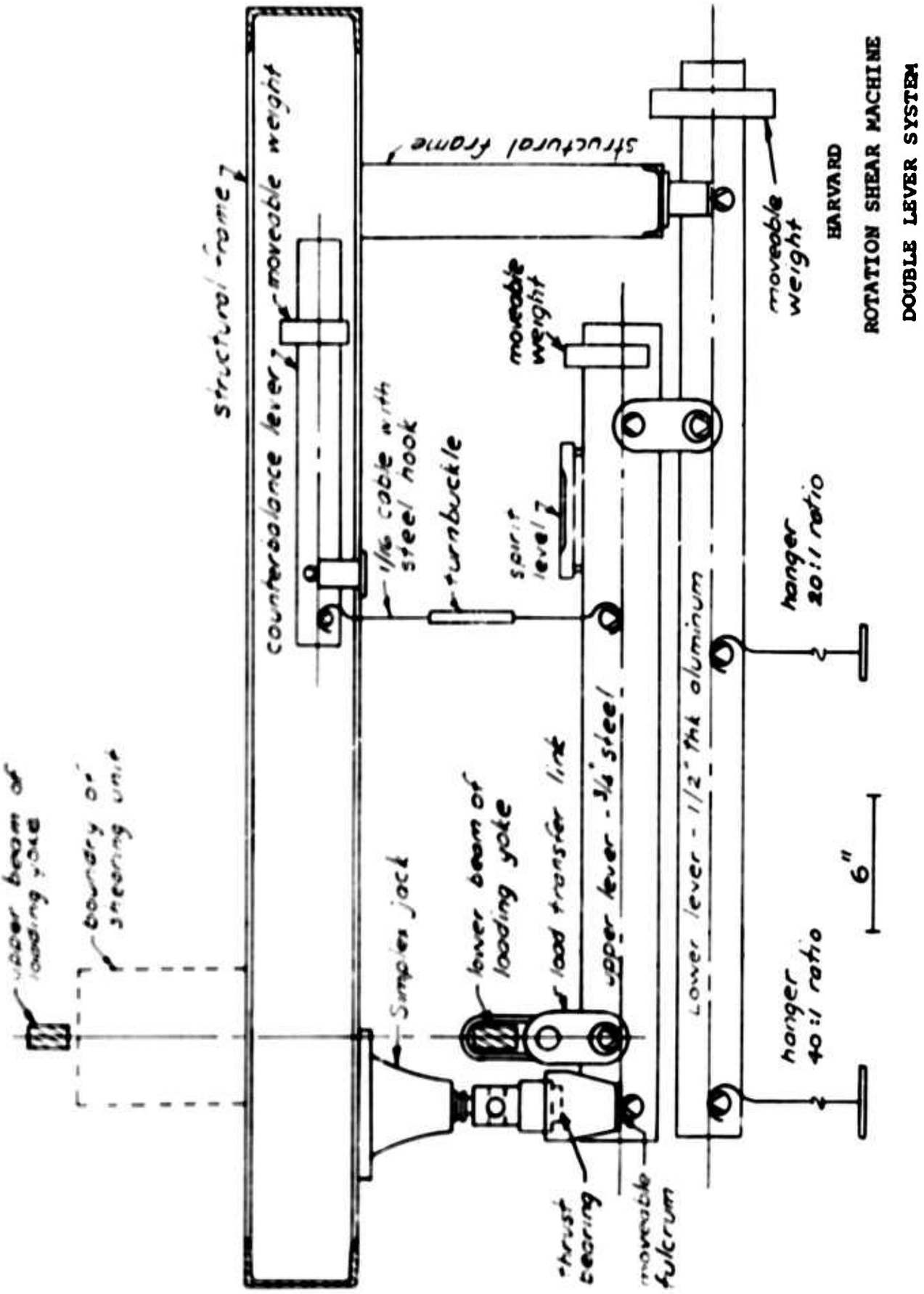
HARVARD
ROTATION SHEAR MACHINE
DOUBLE LEVER SYSTEM
structural frame
counterbalance lever
movable weight
1/8" cable with steel hook
turnbuckle
spring level
movable weight
movable weight
hanger 20:1 ratio
lower lever - 1/2" thk aluminum
upper lever - 3/4" steel
load transfer link
lower beam or loading yoke
specimen jack
thrust bearing
movable fulcrum
hanger 40:1 ratio
6"
upper beam or loading yoke
boundary or shearing unit

FIG. 3-8

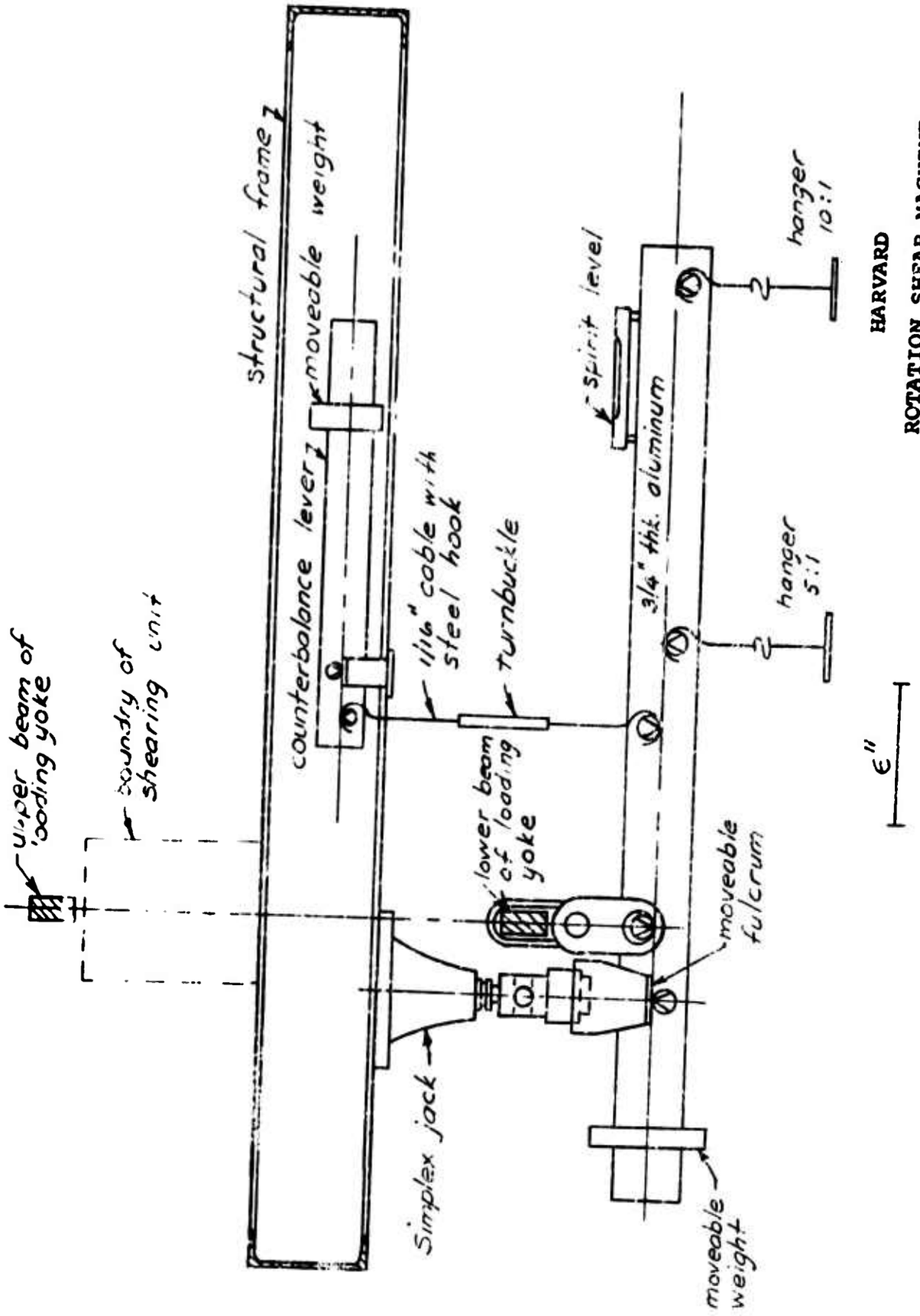
upper beam of loading yoke
boundry of shearing unit
structural frame
moveable weight
counterbalance lever
1/16" cable with steel hook
turnbuckle
lower beam of loading yoke
Simplex jack
moveable fulcrum
moveable weight
3/4" thk. aluminum
spirit level
hanger 10:1
hanger 5:1
ε"
HARVARD
ROTATION SHEAR MACHINE
SINGLE LEVER SYSTEM

FIG. 3-9

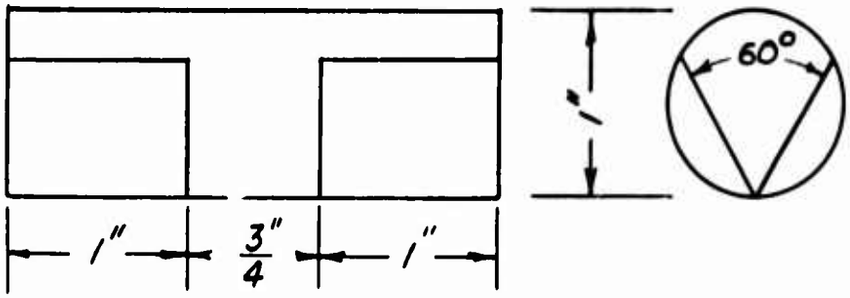

KNIFE EDGE

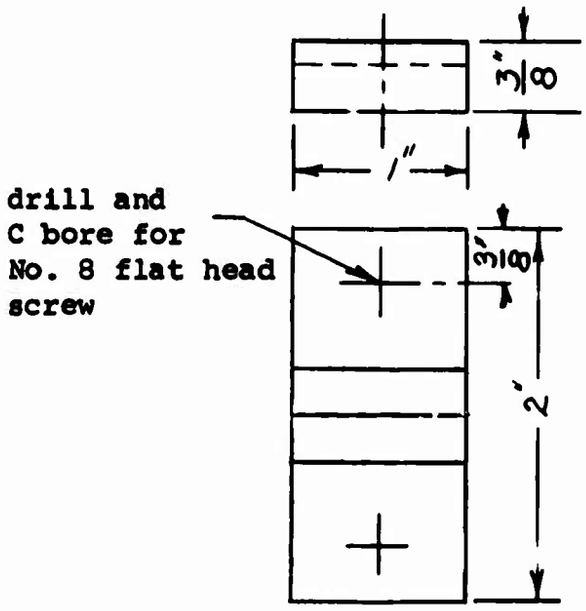

FULCRUM

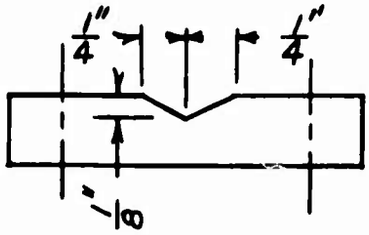

Note
knife edge and fulcrum are fabricated from cold-rolled steel and case hardened

HARVARD

ROTATION SHEAR MACHINE

TYPICAL KNIFE EDGE & FULCRUM

FIG. 3-10

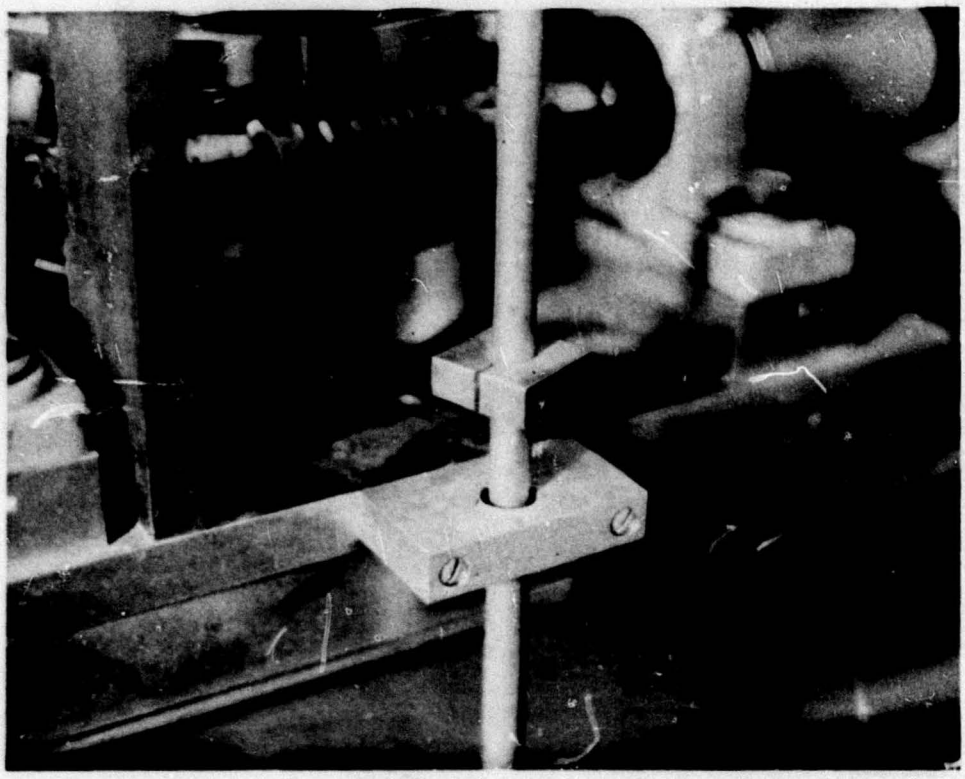

YOKE CLAMP

FIG. 3-11

FIG. 3-12

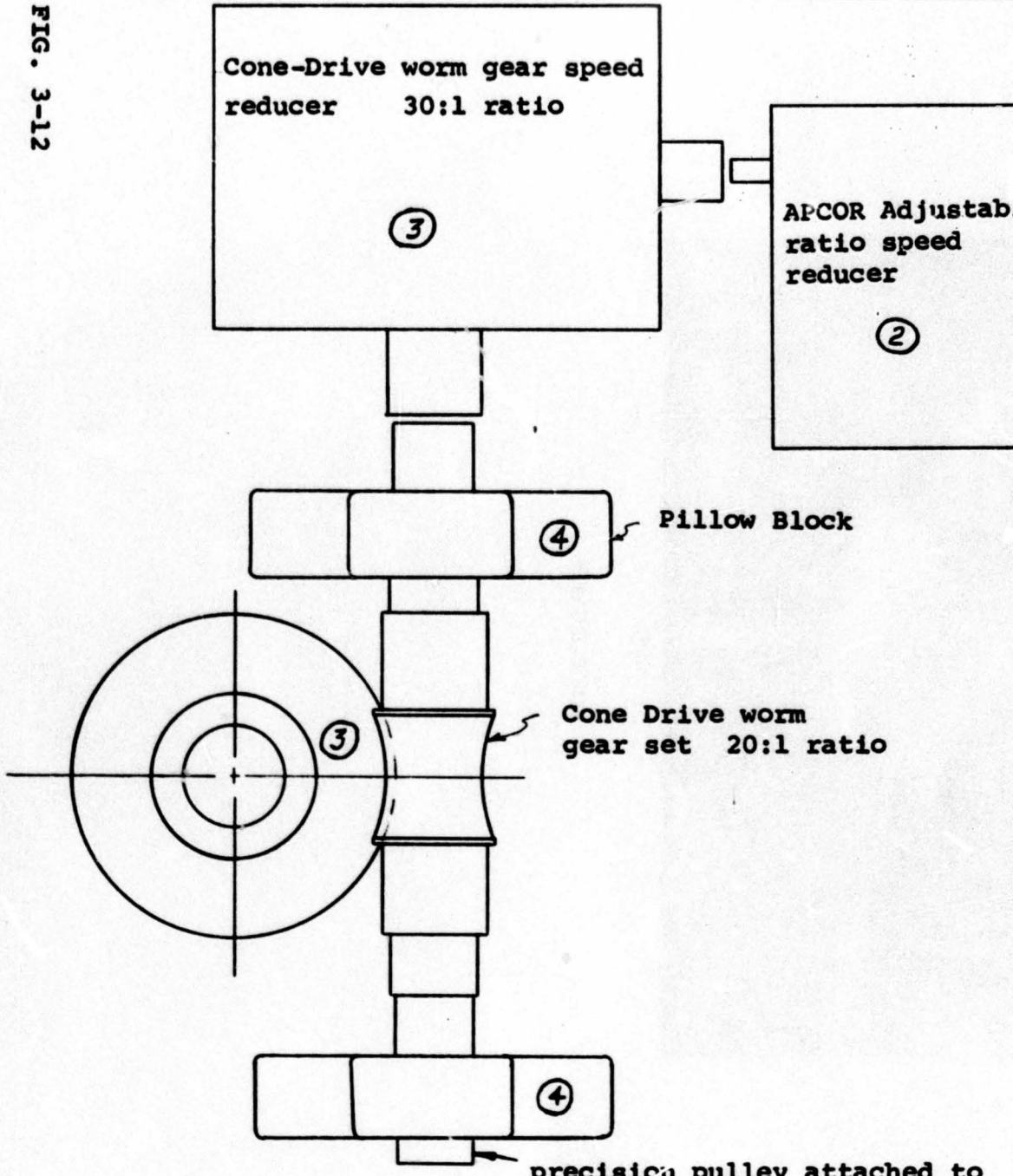

Gear box setting	Rate of peripheral displacement * mm/min.
1:1	5.6
2:1	2.8
5:1	1.12
10:1	5.6×10^{-1}
20:1	2.8×10^{-1}
50:1	1.12×10^{-1}
100:1	5.6×10^{-2}
200:1	2.8×10^{-2}
500:1	1.12×10^{-3}
1000:1	5.6×10^{-3}

*Specimen O.D. = 7.11 mm

HARVARD

ROTATION SHEAR MACHINE

TRANSMISSION SYSTEM

Part No.	Description

1. Globe A.C. hysteresis Syncronous Gear Motor. Output speed is 15 rpm and maximum output torque is 3.1 in-lb. Planetary gear reduction is 80:1.
   Manufactured by: Globe Industries, Inc.
   2275 Stanley Ave.
   Dayton, Ohio 45405
   Approximate cost: $150.

2. APCOR Series 2400 Multiratio Speed Reducer. Maximum output torque is 6 in-lbs. Ten step incremental ratio selector gives ratios shown on Schematic Plan of Transmission Train.
   Manufactured by: Geartronics Corp.
   100 Chelmsford Road
   North Billerica, Mass. 01862
   Approximate cost: $135.

3. Cone-Drive worm gear, fixed ratio speed reducer and Cone-Drive worm gear set.
   Manufactured by: Cone-Drive Gears,
   Div. of Michigan Tool Co.
   7171 E. McNichols
   Detroit, Michigan 48212
   Approximate cost: Speed reducer: $100
   Gear set : $ 70.

4. Precision ball bearing pillow blocks.
   Manufactured by: Boston Gear
   Quincy, Mass.
   Approximate cost: $10 each.

HARVARD

ROTATION SHEAR MACHINE

TRANSMISSION SYSTEM PARTS LIST

FIG. 3-13

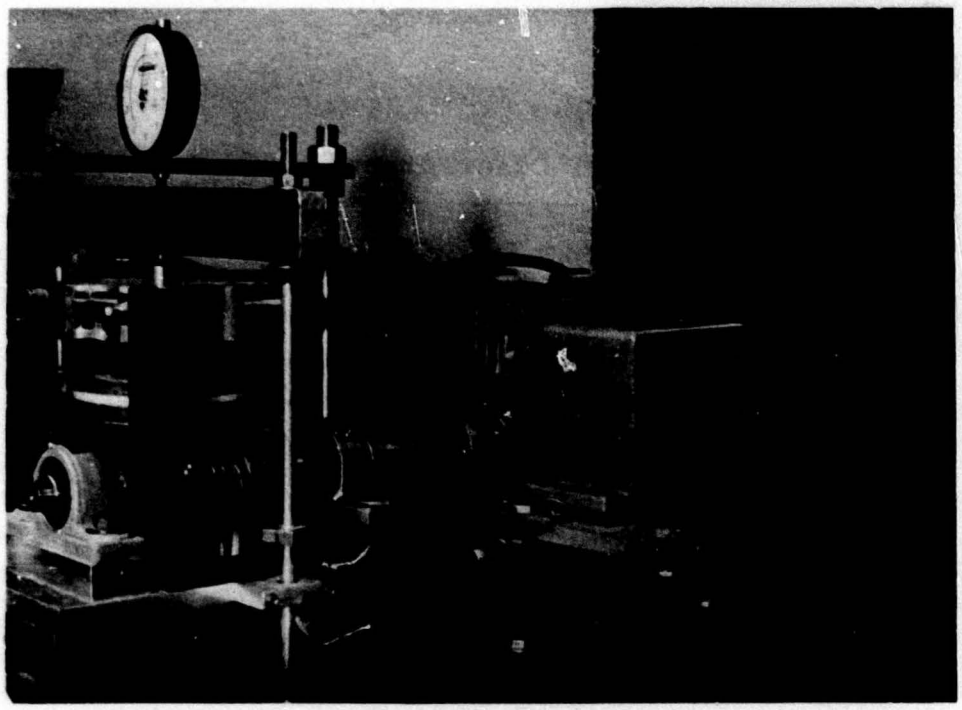

FIG. 3-14 ASSEMBLED TRANSMISSION SYSTEM

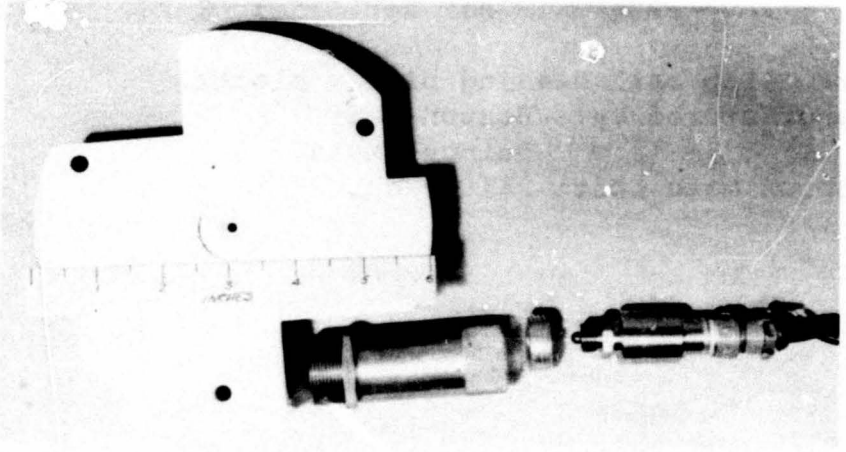

FIG. 3-15 EXPLODED VIEW OF TRANSDUCER ASSEMBLY

FIG. 3-14 and FIG. 3-15

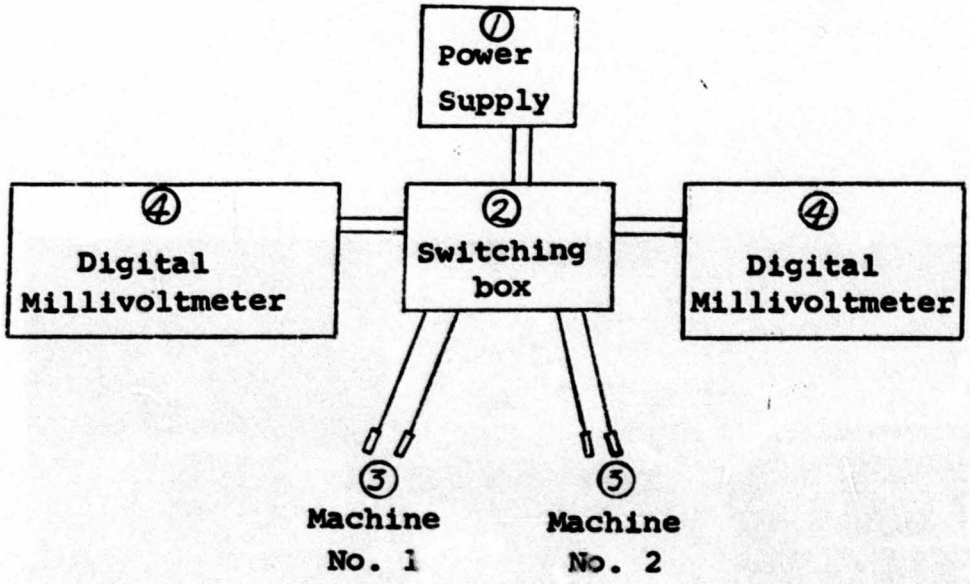

1. Power Supply - Precision DC Power Source 0-20 VDC. Two dual, concentric decade switches provide dial readout to four places with an accuracy of 0.1%.
   Manufactured by: Power Designs Inc.
   1700 Shames Drive
   Westbury, N.Y.
   Approximate cost: $325

2. Switching box - Two position switching box designed to keep all four transducers continuously energized.

3. Transducer - Dynisco Force transducer. Repeatability of 0.1% F.S. Full-scale output 3.5 MV/V. Maximum probe displacement of 0.00035 in.
   Manufactured by: Dynisco, Division of Microdot, Inc.
   20 Southwest Park
   Westwood, Mass. 02090
   Approximate cost: $525

4. Millivoltmeter - Digital millivoltmeter. Full-scale DC range of 40 mv. Accuracy 0.1% F.S. Reading resolution of 5μV.
   Manufactured by: United Systems Corporation
   918 Woodley Road
   Dayton 3, Ohio
   Approximate cost: $445

SCHEMATIC VOLTAGE MEASURING SYSTEM

FIG. 3-16

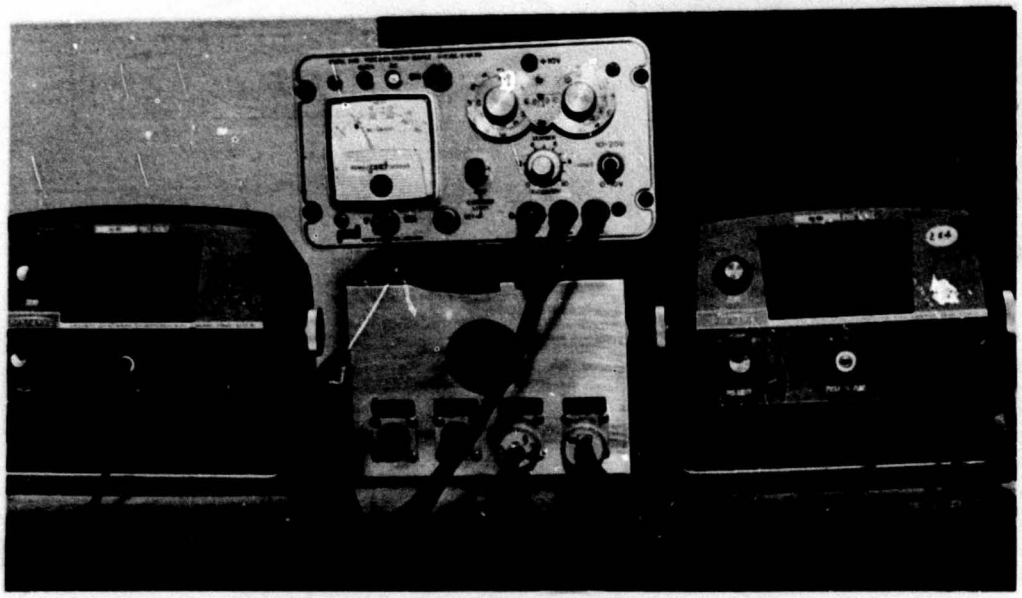

VOLTAGE MEASURING SYSTEM

FIG. 3-17

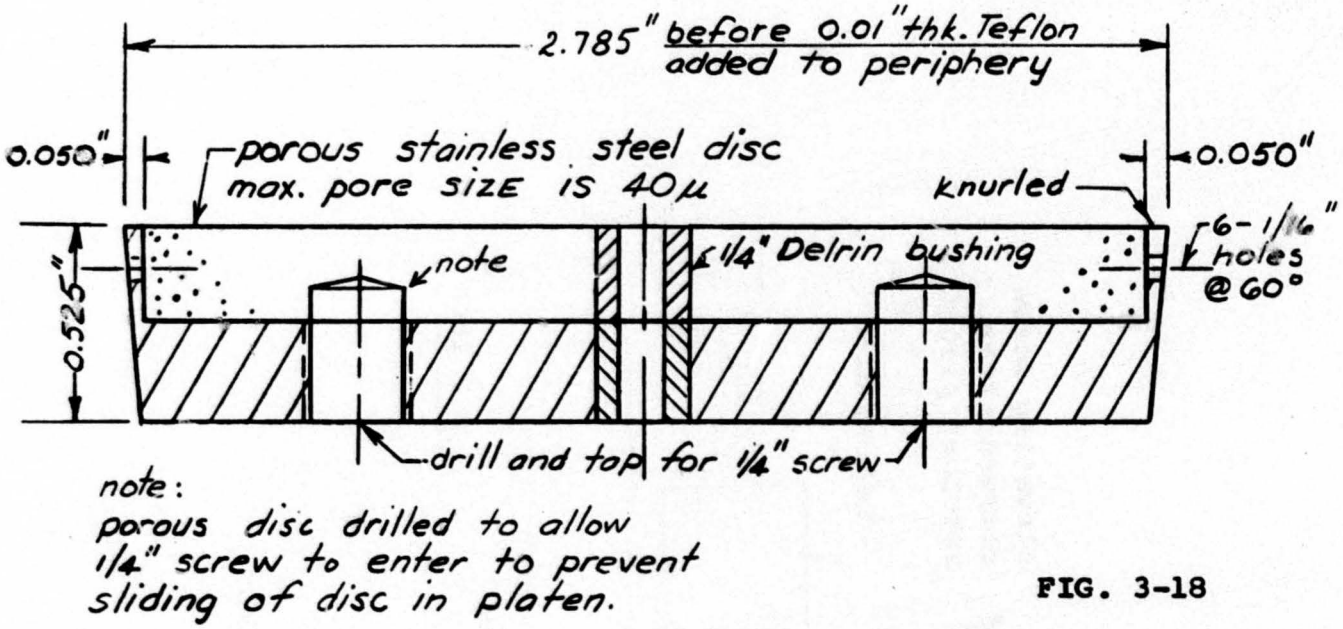

FIG. 3-18

DISC SHAPED LOADING PLATEN

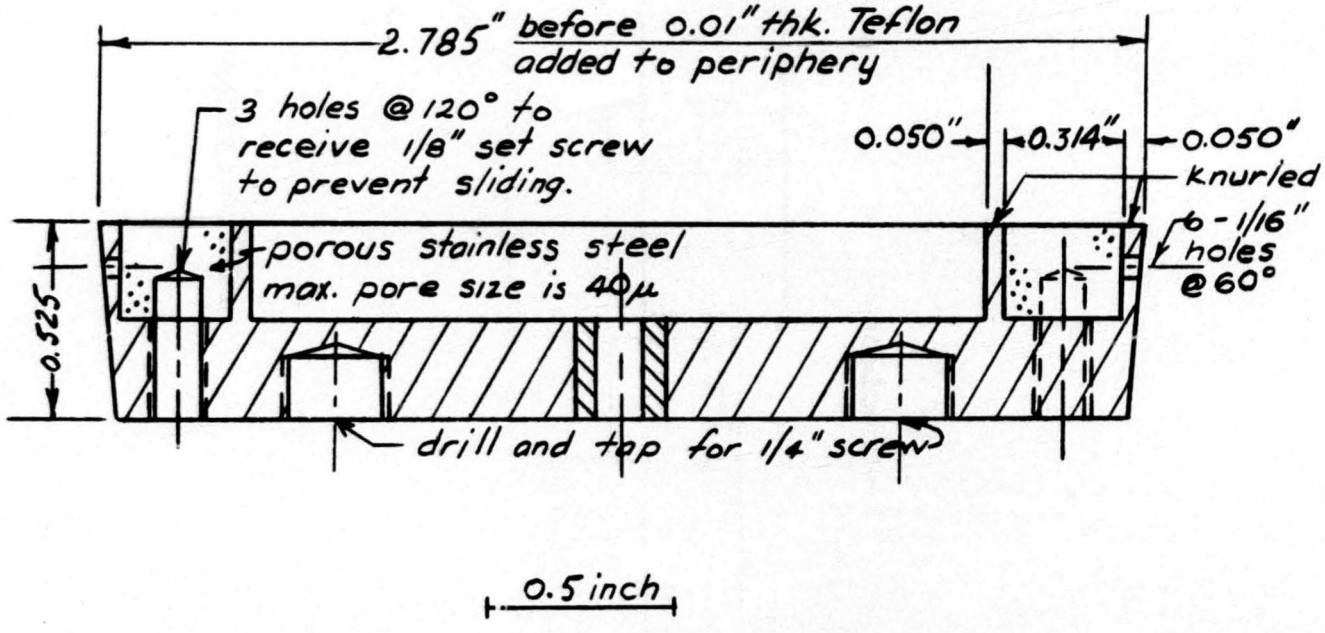

FIG. 3-19

ANNULAR LOADING PLATEN

FIG. 3-18 and FIG. 3-19

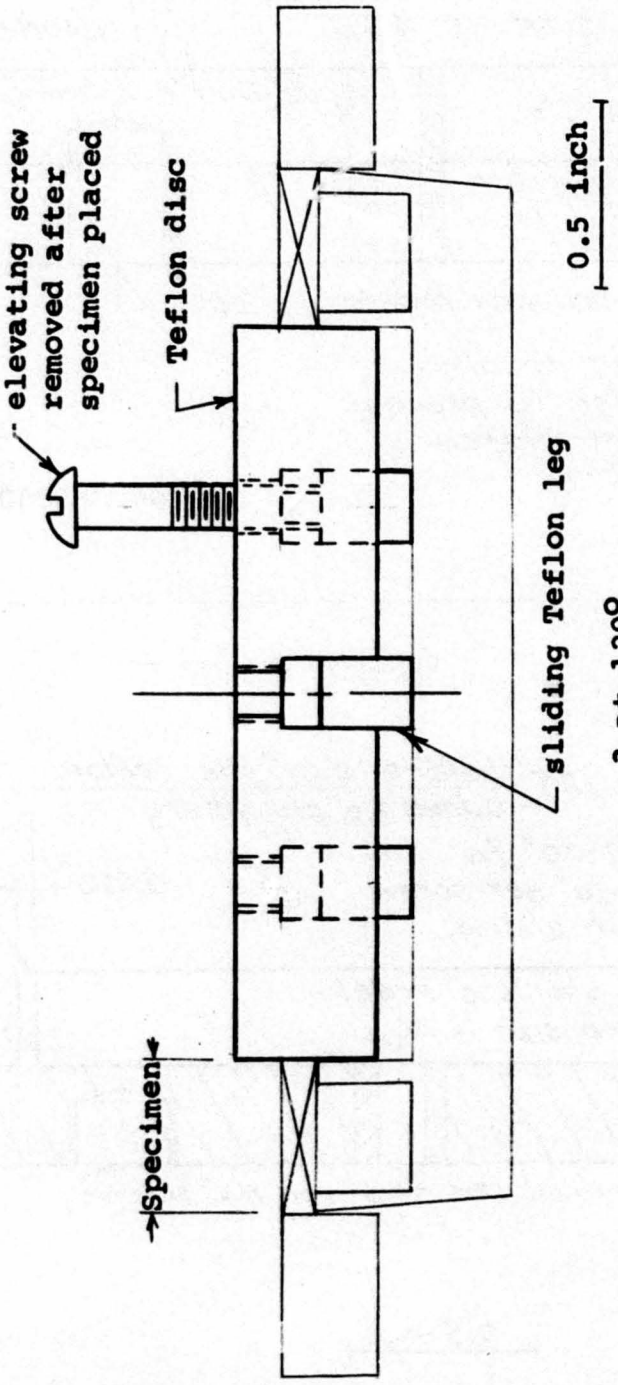

CENTER SPACER FOR ANNULAR SPECIMEN

FIG. 3-20

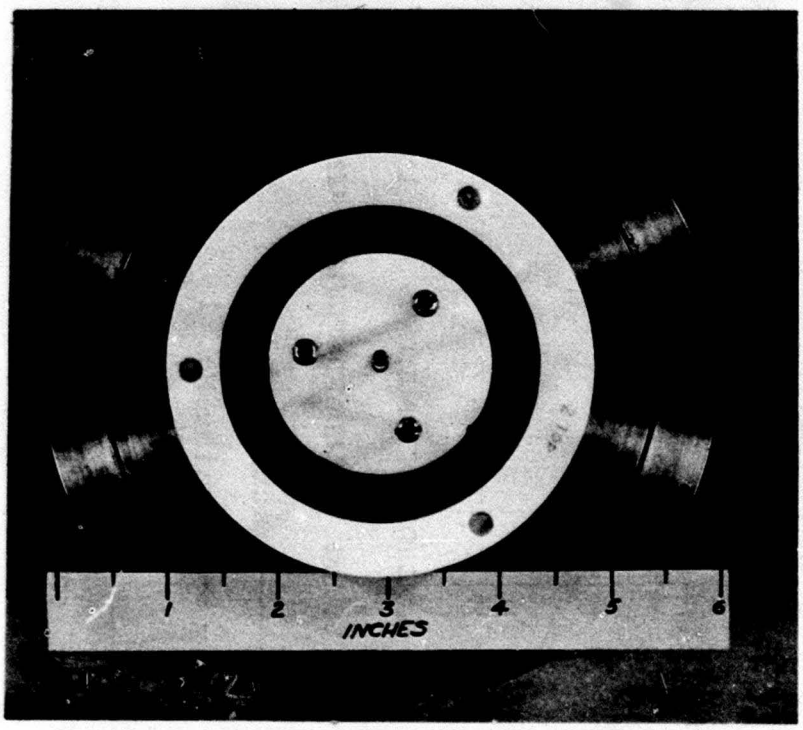

FIG. 3-21

ANNULAR CONFIGURATION

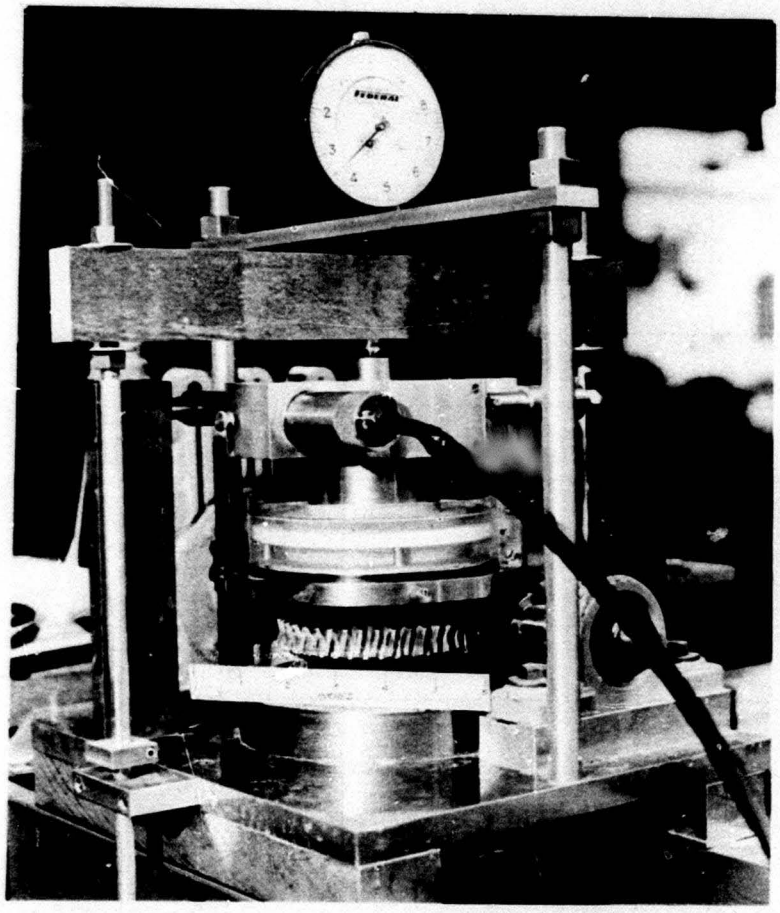

FIG. 3-22

SHEARING UNIT

IN POSITION

FIG. 3-21 and FIG. 3-22

FIG. 3-23

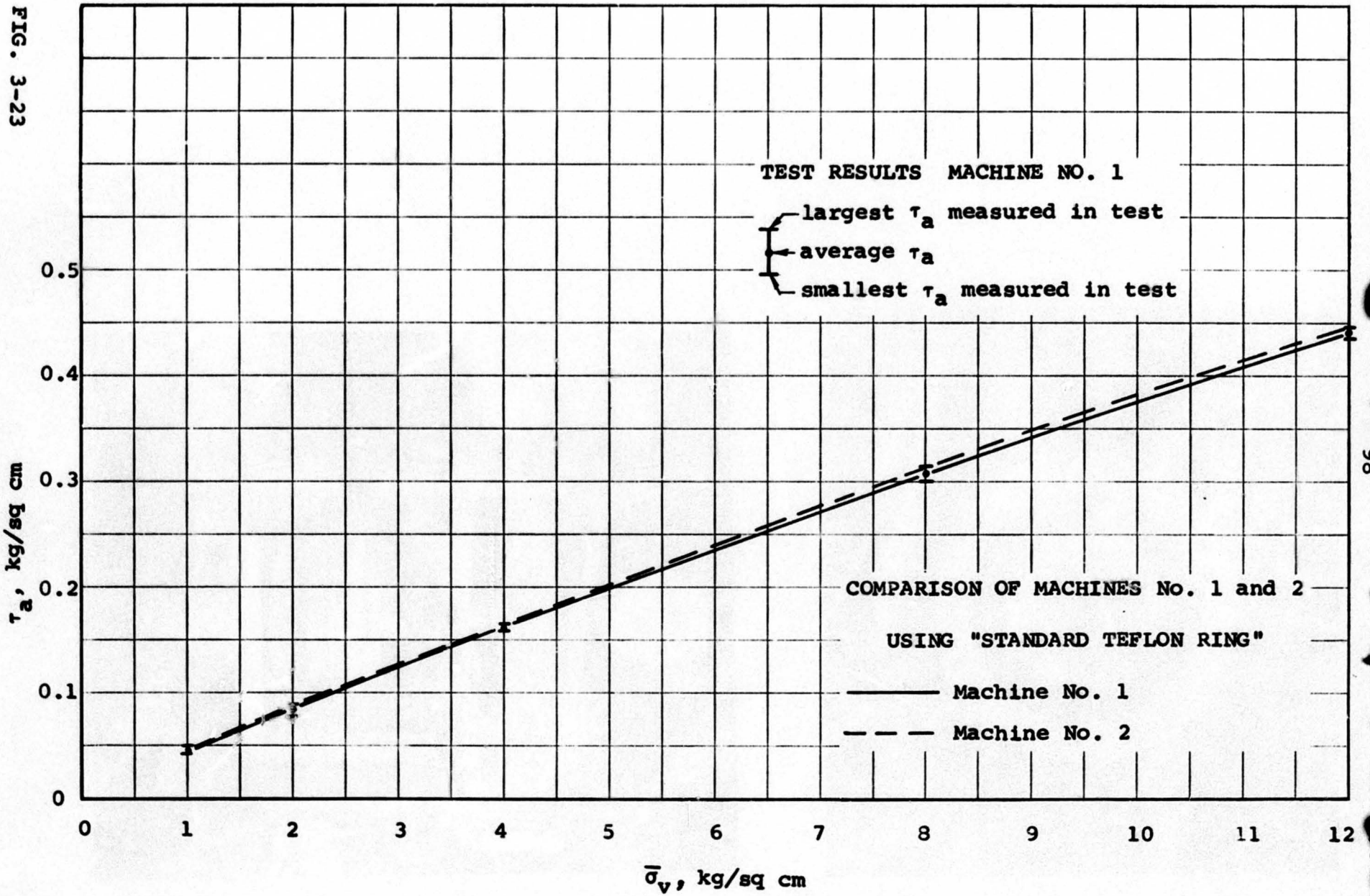
TEST RESULTS MACHINE NO. 1
largest τ_a measured in test
average τ_a
smallest τ_a measured in test
COMPARISON OF MACHINES No. 1 and 2
USING "STANDARD TEFLON RING"
Machine No. 1
Machine No. 2
τ_a, kg/sq cm
$\bar{\sigma}_v$, kg/sq cm
0
0.1
0.2
0.3
0.4
0.5
0
1
2
3
4
5
6
7
8
9
10
11
12

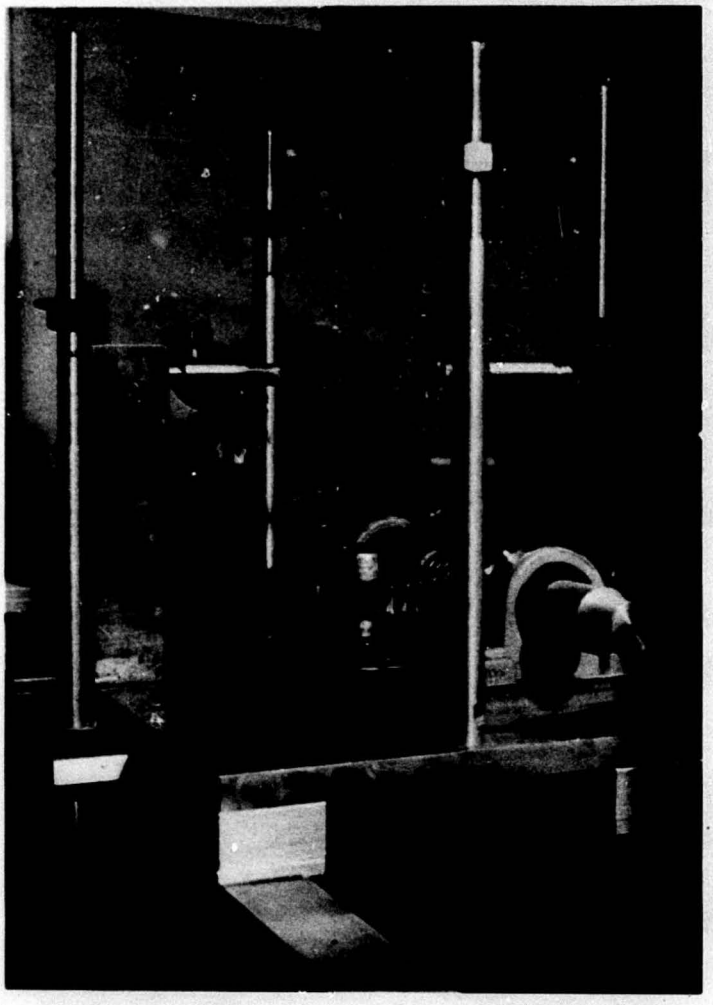

ROTATION SHEAR MACHINE WITH
SHEARING UNIT AND TOP BAR
OF LOADING YOKE REMOVED

FIG. 4-1

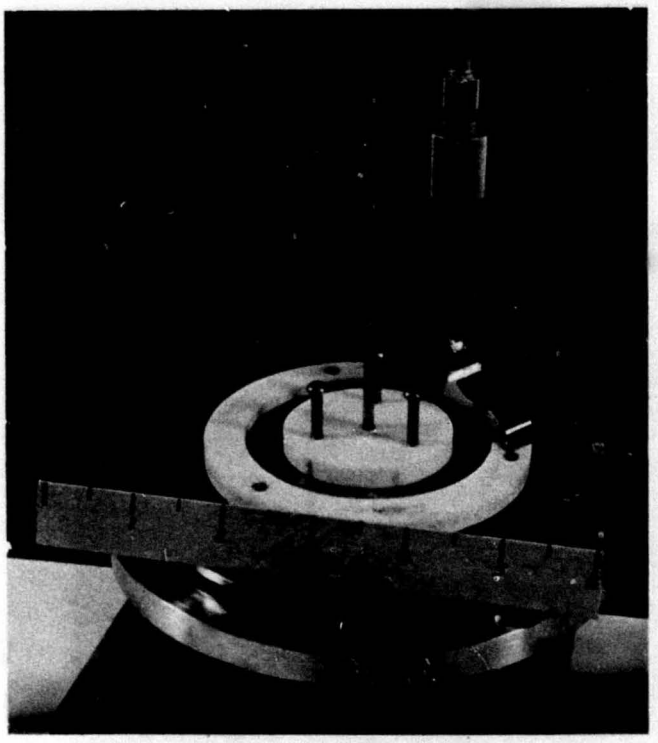

FIG. 4-2 MEASURING SPECIMEN THICKNESS

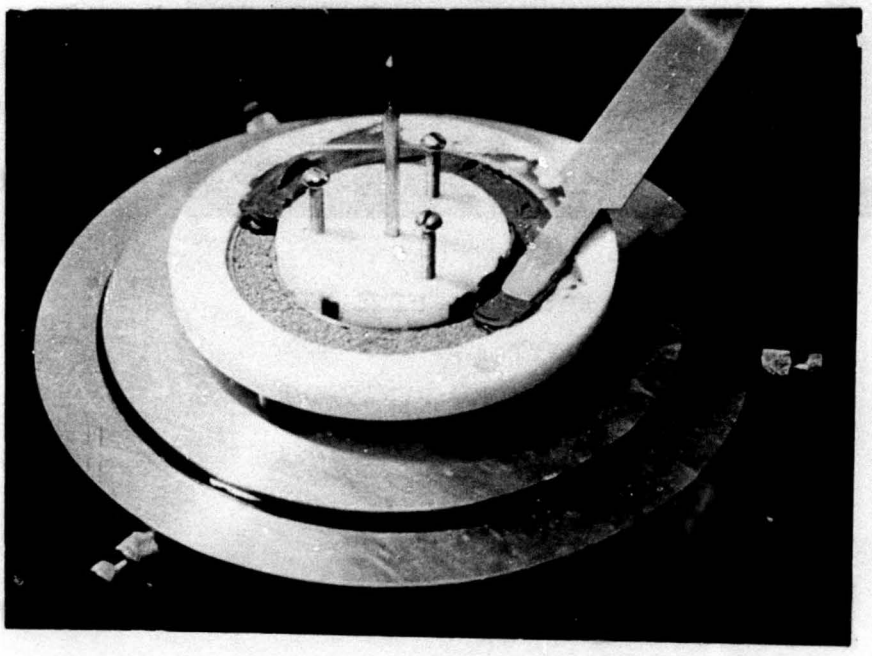

FIG. 4-3 PLACING A REMOLDED SPECIMEN

FIG. 4-2 and FIG. 4-3

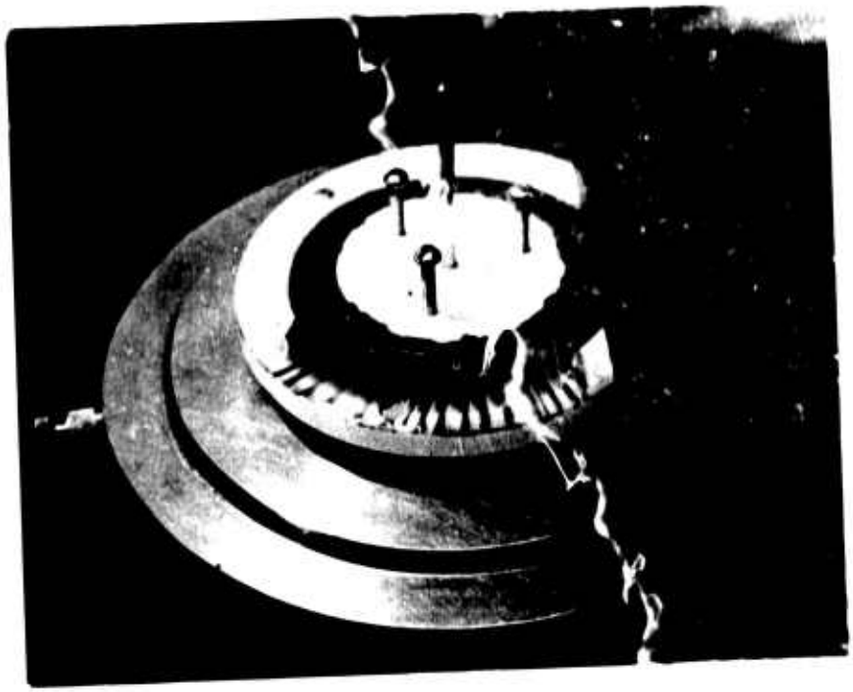

FIG. 4-4 TRIMMING THE TOP OF A REMOLDED SPECIMEN

FIG. 4-5 CLEANING PERIPHERY OF CENTRAL SPACER

FIG. 4-4 and FIG. 4-5

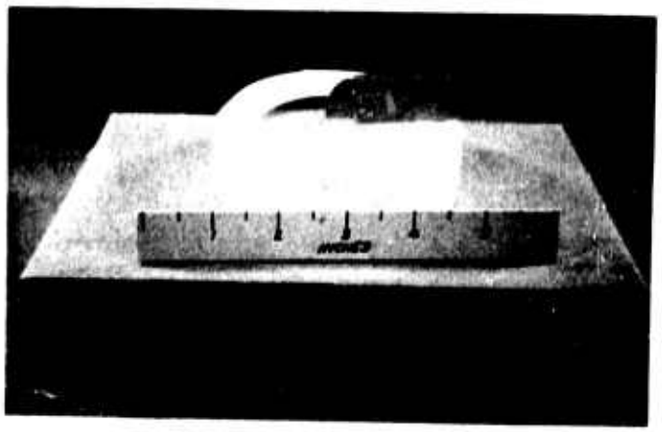

FIG. 4-6 APPARATUS FOR TRIMMING UNDISTURBED SPECIMENS

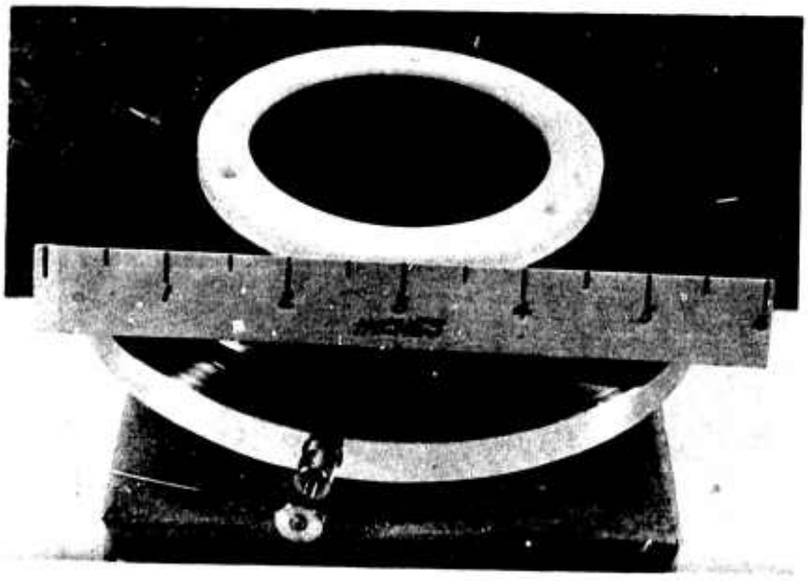

FIG. 4-7 COMPLETED UNDISTURBED DISC

FIG. 4-6 and FIG. 4-7

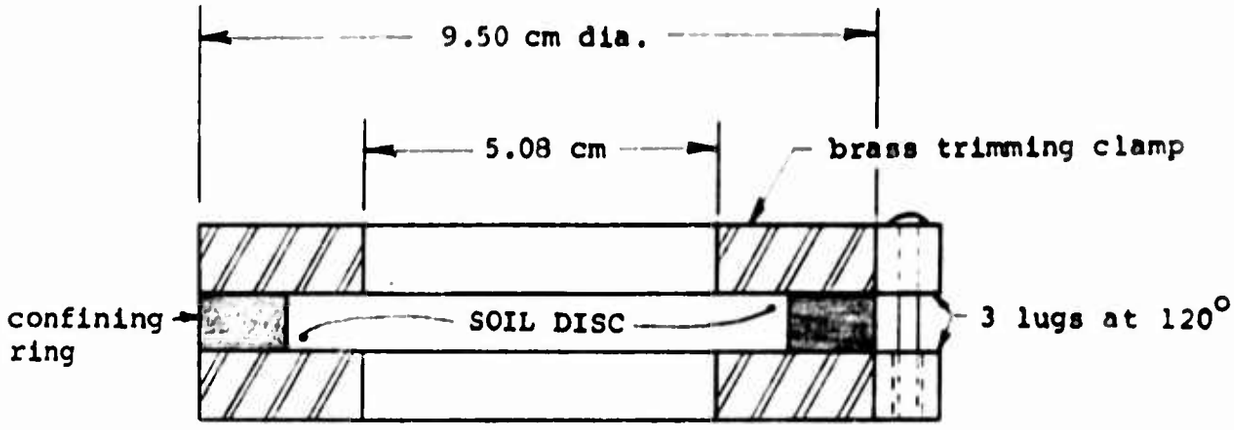

FIG. 4-8 SOIL DISC CLAMPED FOR TRIMMING ANNULAR SPECIMEN

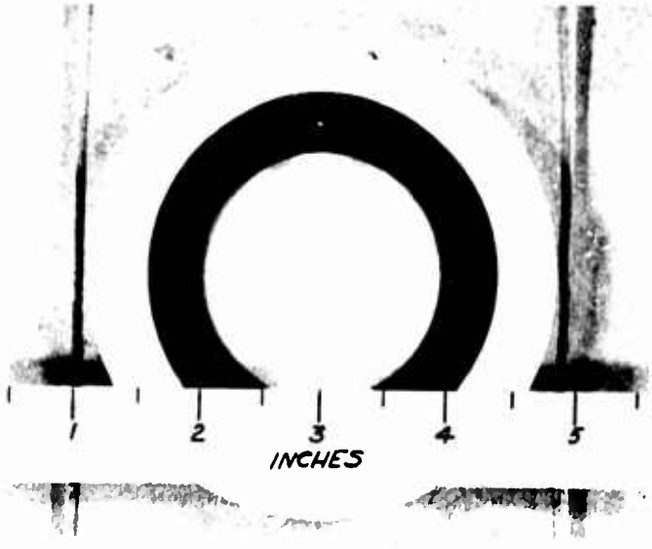

FIG. 4-9 UNDISTURBED ANNULAR SPECIMEN

FIG. 4-8 and FIG. 4-9

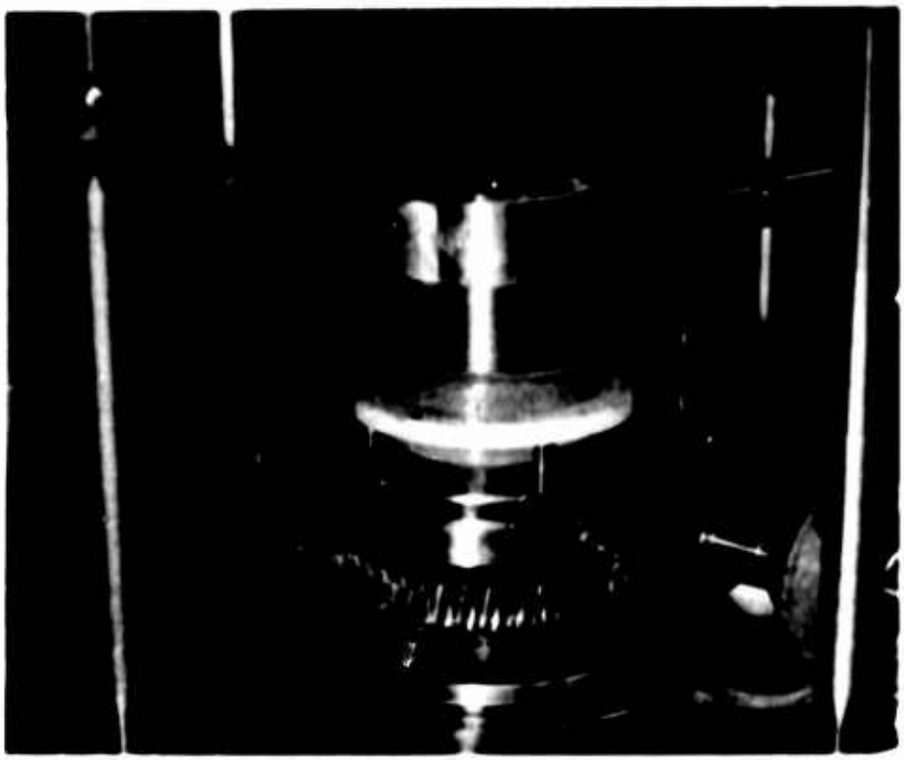

FIG. 4-10 PLACING SPECIMEN IN SHEAR MACHINE

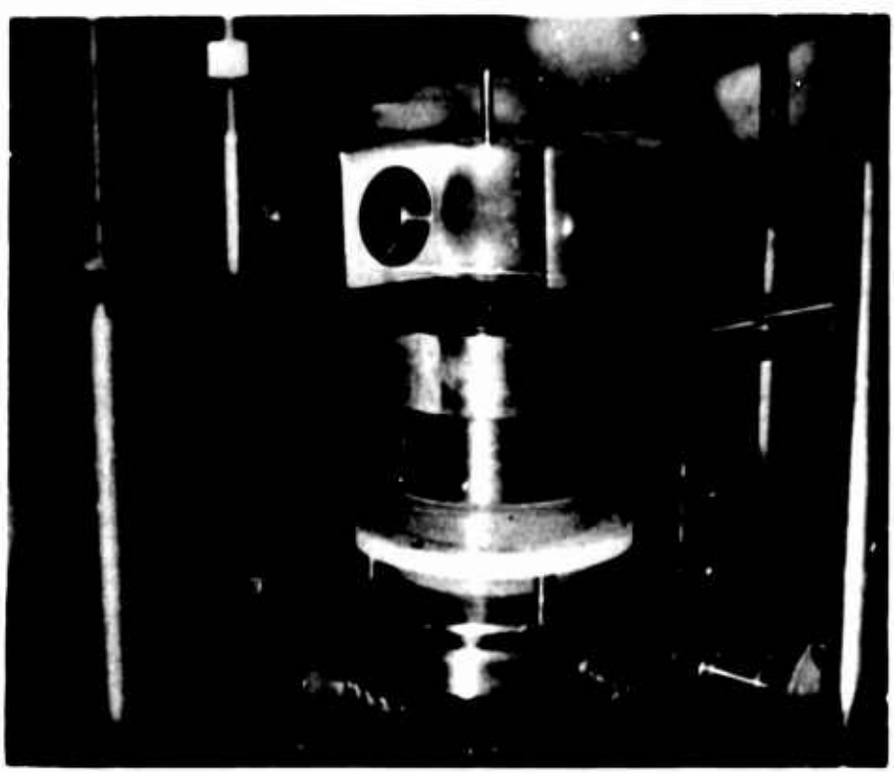

FIG. 4-11 INSTALLING TOP PLATE

FIG. 4-10 and FIG. 4-11

FIG. 4-12 TOOLS FOR PRECUTTING A SPECIMEN

FIG. 4-13 TOOLS FOR ROTATING UPPER CONFINING RING

FIG. 4-12 and FIG. 4-13

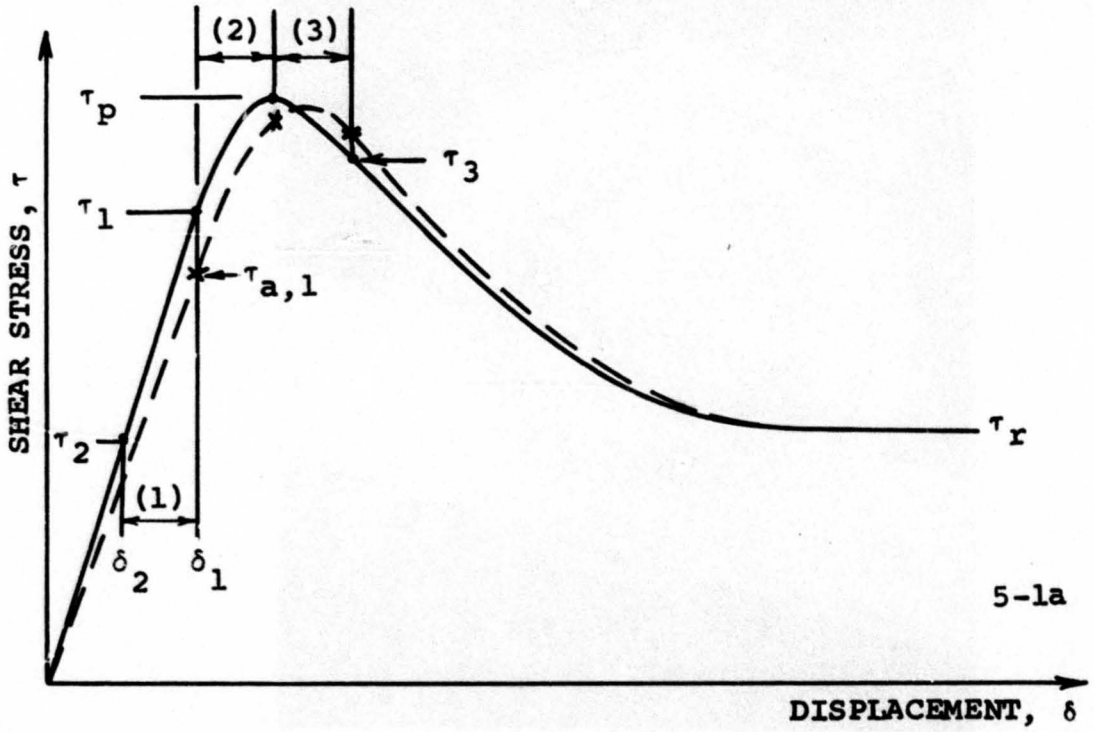

5-1a

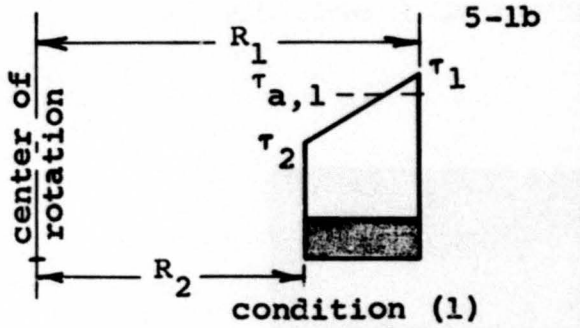

5-1b

condition (1)

5-1c

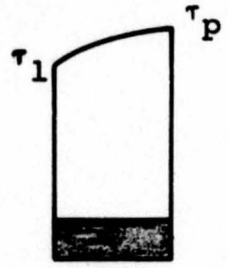

condition (2)

5-1d

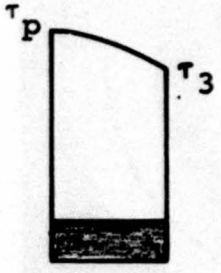

condition (3)

5-1e

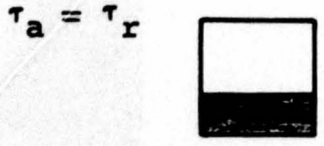

residual condition

EFFECT OF NONUNIFORM SHEAR STRESS ON τ_a versus δ curve

FIG. 5-1

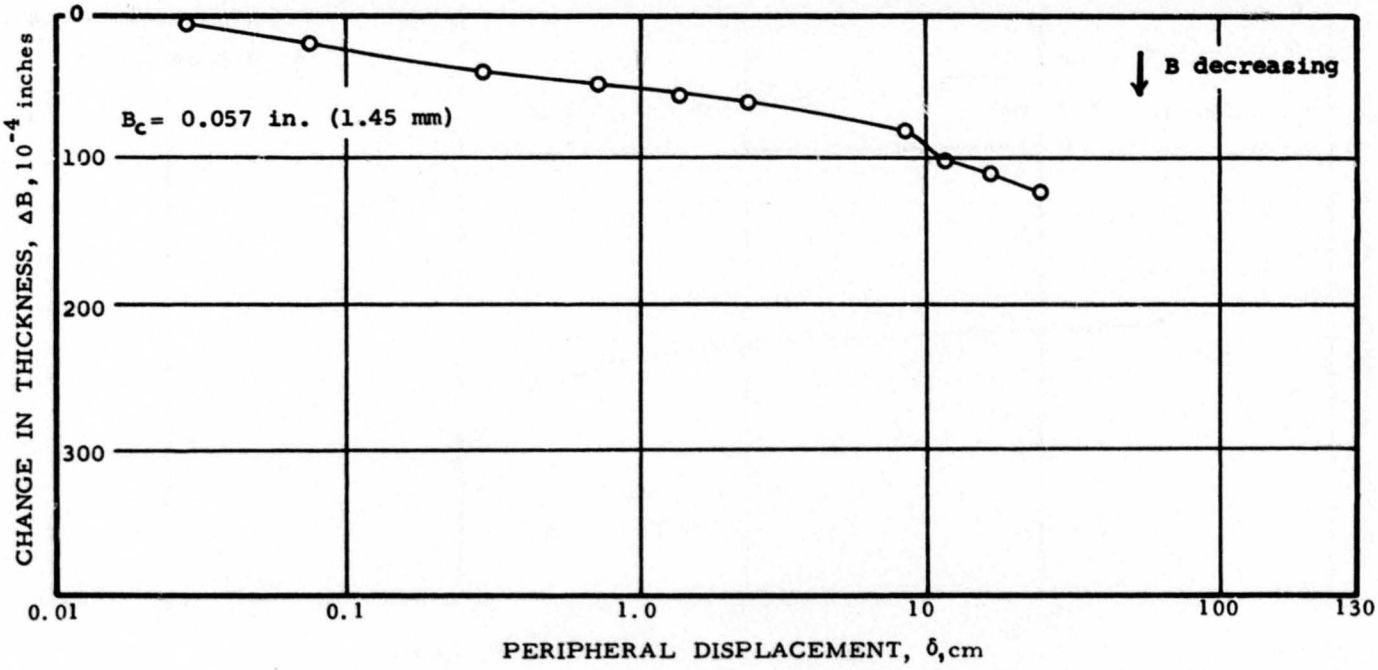
CHANGE IN THICKNESS, ΔB, 10^{-4} inches
0
100
200
300
B_c = 0.057 in. (1.45 mm)
B decreasing
0.01
0.1
1.0
10
100
130
PERIPHERAL DISPLACEMENT, δ, cm

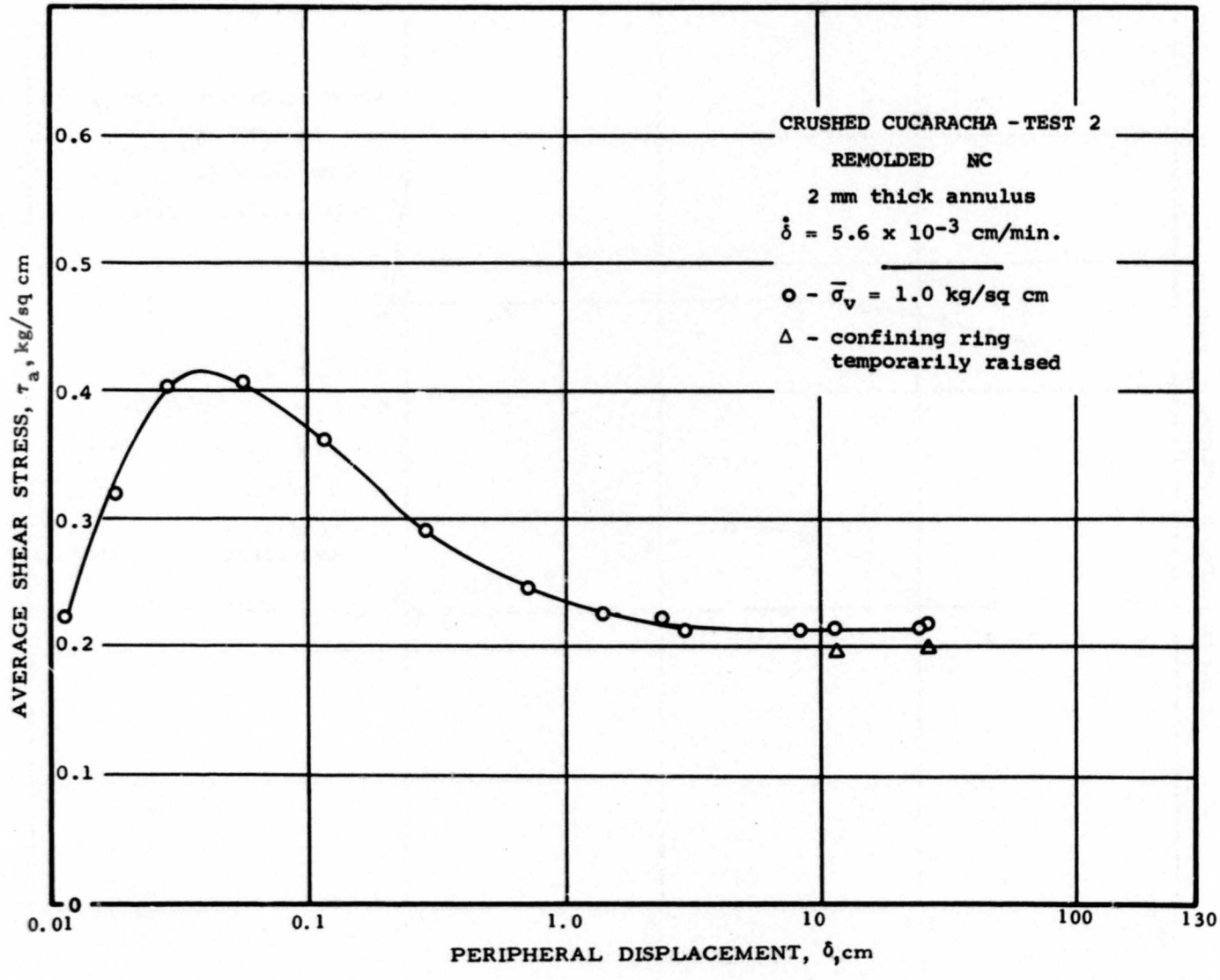
AVERAGE SHEAR STRESS, τ_a, kg/sq cm
0
0.1
0.2
0.3
0.4
0.5
0.6
CRUSHED CUCARACHA - TEST 2
REMOLDED NC
2 mm thick annulus
$\dot{\delta}$ = 5.6 x 10^{-3} cm/min.
o - $\bar{\sigma}_v$ = 1.0 kg/sq cm
Δ - confining ring temporarily raised
0.01
0.1
1.0
10
100
130
PERIPHERAL DISPLACEMENT, δ, cm

FIG. 5-2

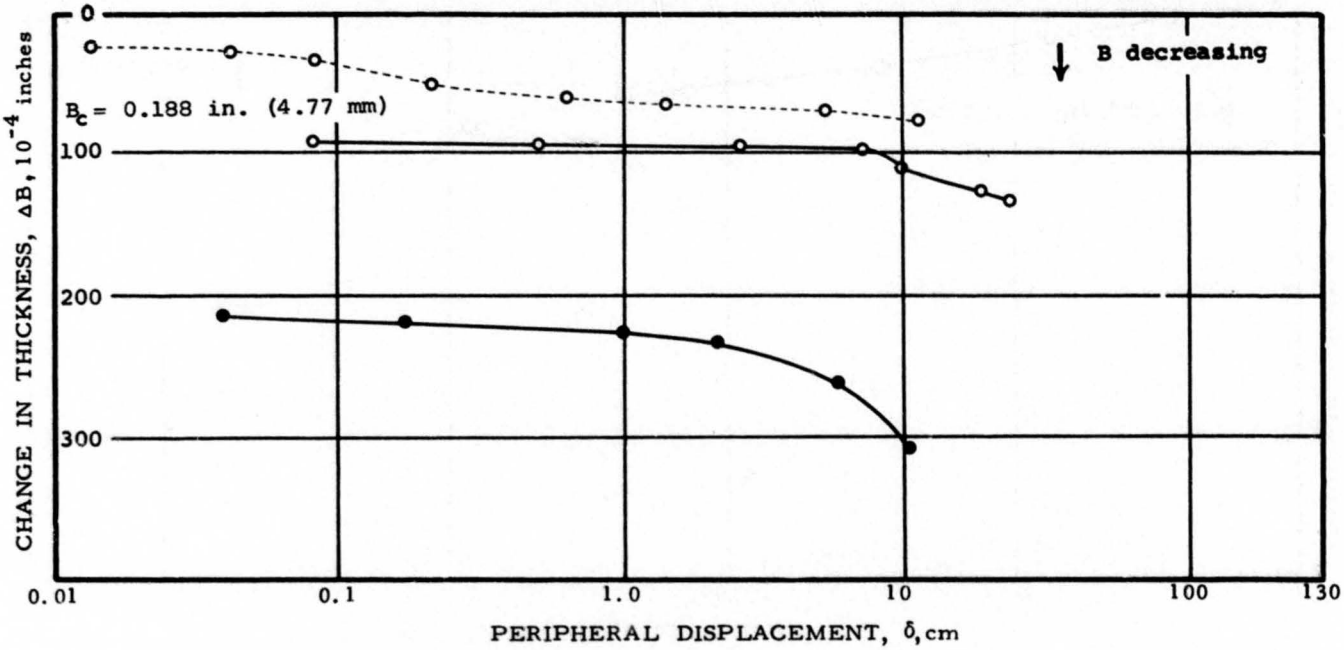
0
100
200
300
B_c = 0.188 in. (4.77 mm)
B decreasing
CHANGE IN THICKNESS, ΔB, 10^{-4} inches
0.01
0.1
1.0
10
100
130
PERIPHERAL DISPLACEMENT, δ, cm

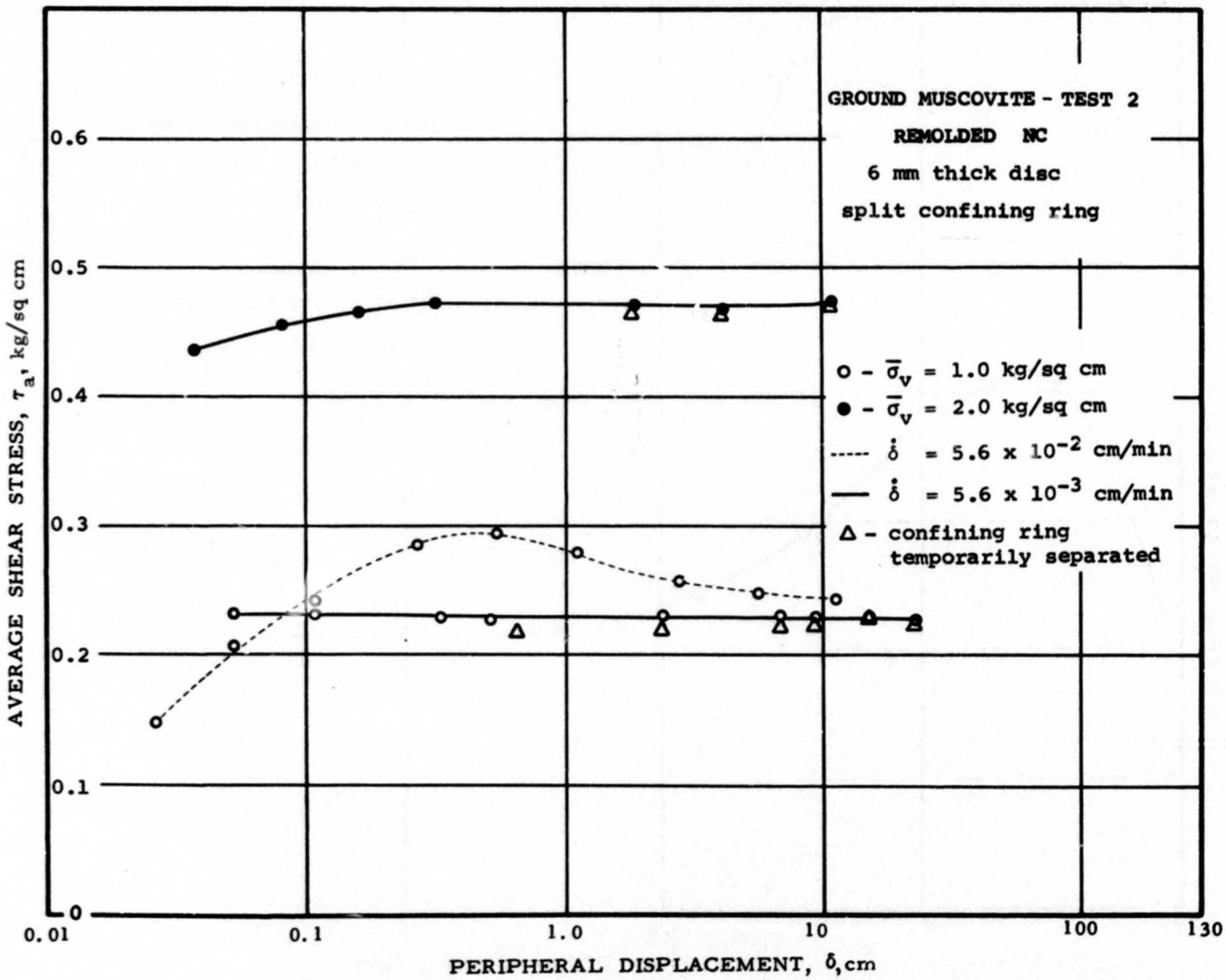
GROUND MUSCOVITE - TEST 2
REMOLDED NC
6 mm thick disc
split confining ring
o - $\bar{\sigma}_v$ = 1.0 kg/sq cm
● - $\bar{\sigma}_v$ = 2.0 kg/sq cm
---- $\dot{\delta}$ = 5.6 x 10^{-2} cm/min
—— $\dot{\delta}$ = 5.6 x 10^{-3} cm/min
Δ - confining ring temporarily separated
0
0.1
0.2
0.3
0.4
0.5
0.6
AVERAGE SHEAR STRESS, τ_a, kg/sq cm
0.01
0.1
1.0
10
100
130
PERIPHERAL DISPLACEMENT, δ, cm

FIG. 5-3

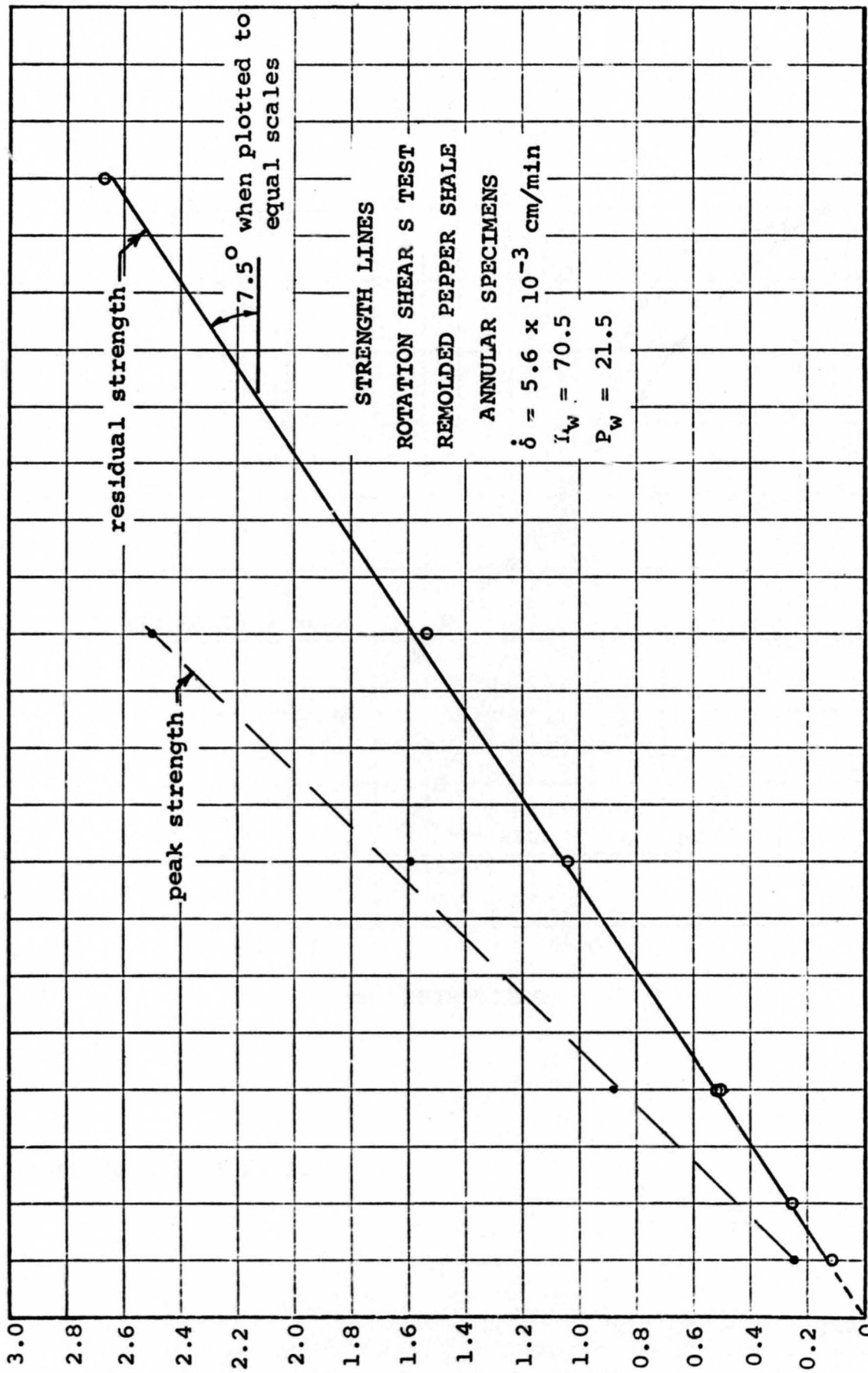
STRENGTH LINES
ROTATION SHEAR S TEST
REMOLDED PEPPER SHALE
ANNULAR SPECIMENS
$\dot{\delta} = 5.6 \times 10^{-3}$ cm/min
$I_w = 70.5$
$P_w = 21.5$
residual strength
peak strength
7.5° when plotted to equal scales
SHEAR STRENGTH, τ_p and τ_r ,kg/sq cm
EFFECTIVE VERTICAL STRESS, $\bar{\sigma}$,kg/sq cm
0
0.2
0.4
0.6
0.8
1.0
1.2
1.4
1.6
1.8
2.0
2.2
2.4
2.6
2.8
3.0
0
1
2
4
8
12
20

FIG. 5-4

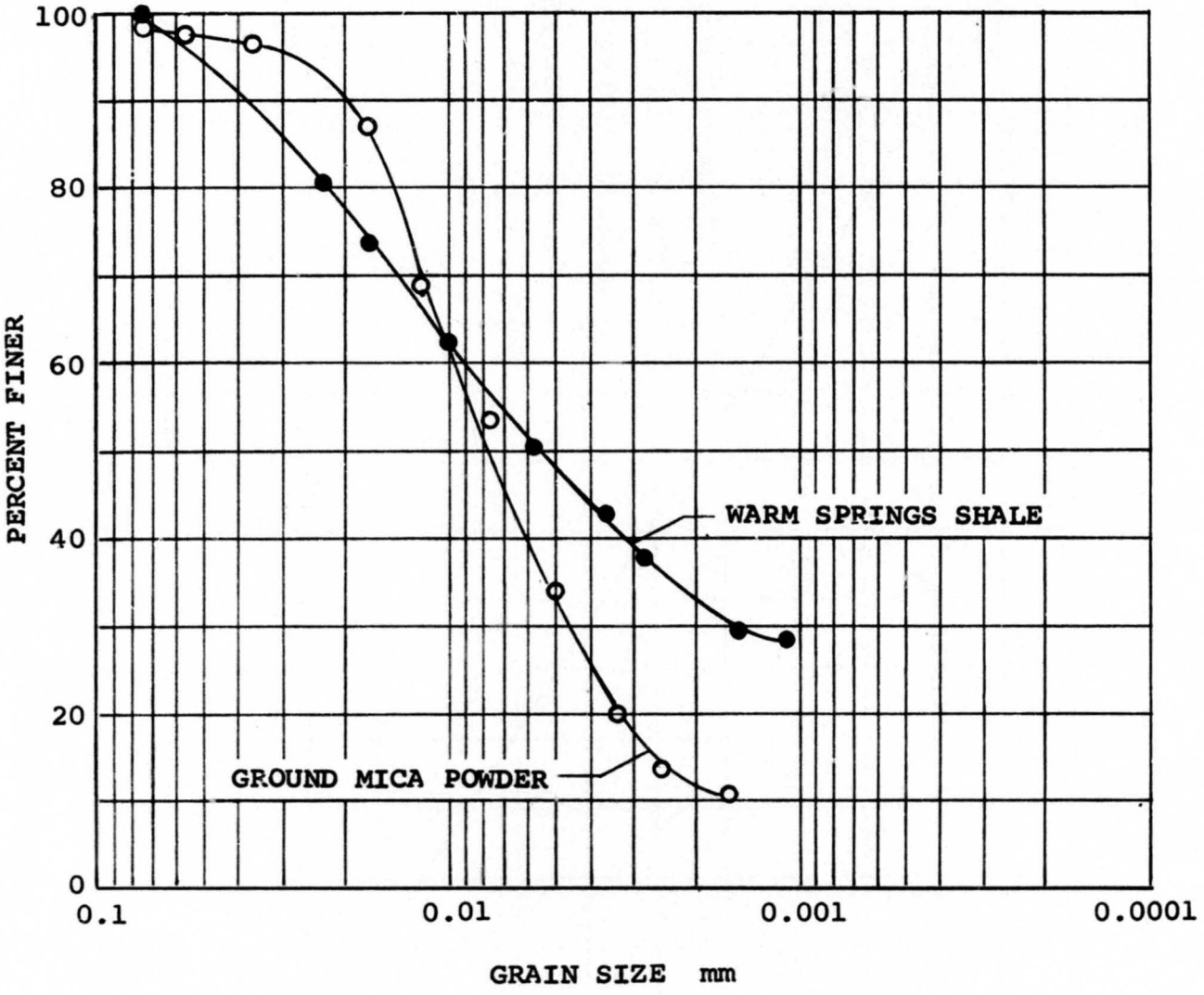

GRAIN SIZE DISTRIBUTION

FIG. 6-1

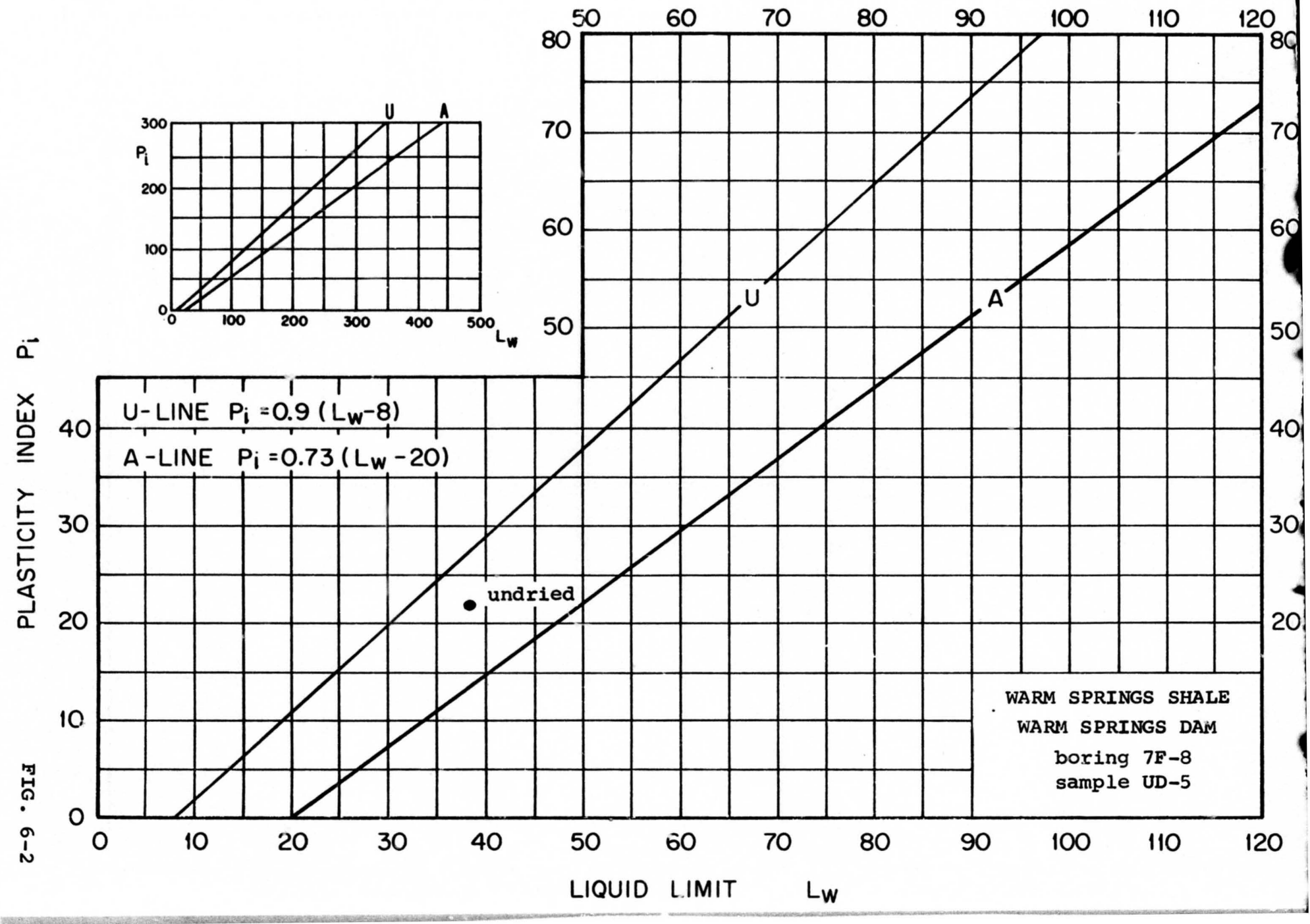
U
A
300
200
100
0
P_i
0
100
200
300
400
500
L_w
U-LINE $P_i = 0.9 (L_w - 8)$
A-LINE $P_i = 0.73 (L_w - 20)$
undried
WARM SPRINGS SHALE
WARM SPRINGS DAM
boring 7F-8
sample UD-5
PLASTICITY INDEX P_i
LIQUID LIMIT L_w
0
10
20
30
40
50
60
70
80
90
100
110
120

FIG. 6-2

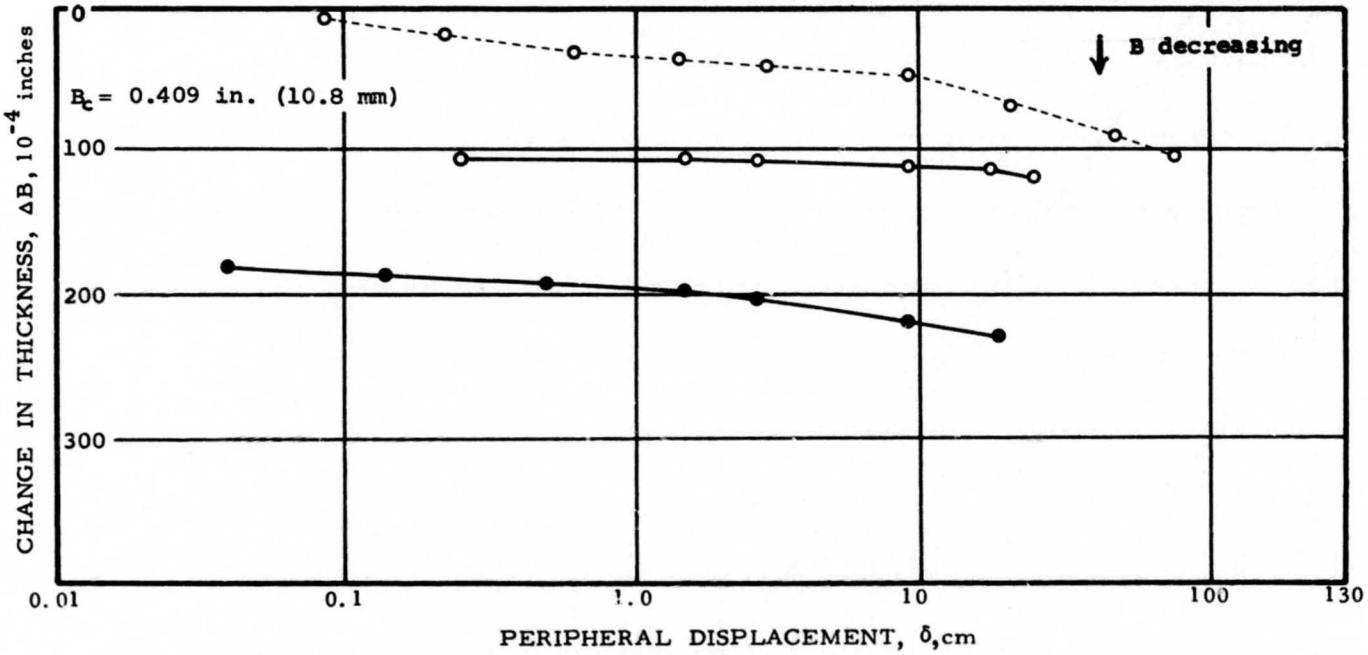
B decreasing
B_c = 0.409 in. (10.8 mm)
CHANGE IN THICKNESS, ΔB, 10^{-4} inches
0
100
200
300
0.01
0.1
1.0
10
100
130
PERIPHERAL DISPLACEMENT, δ, cm

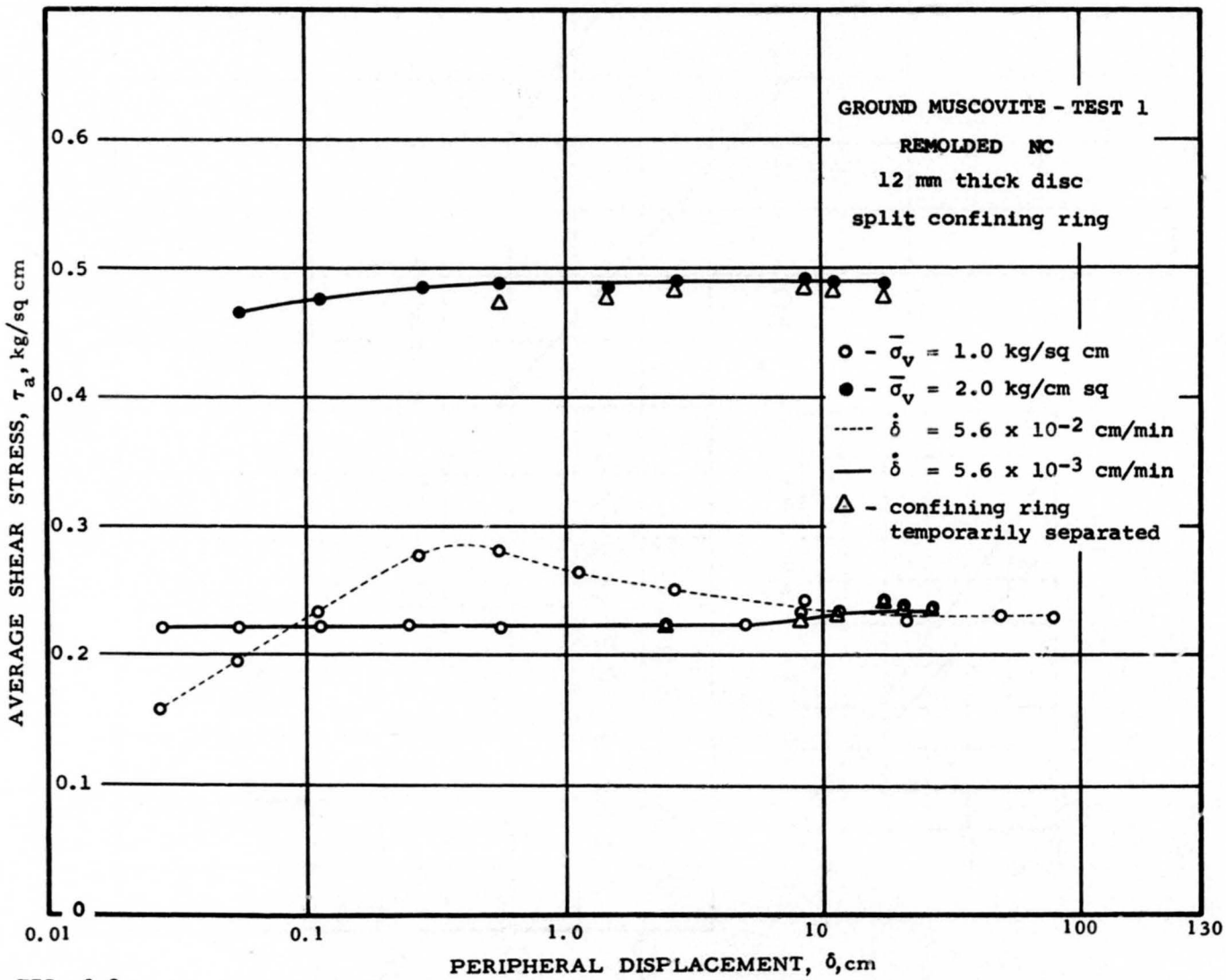
GROUND MUSCOVITE - TEST 1
REMOLDED NC
12 mm thick disc
split confining ring
○ - $\bar{\sigma}_v$ = 1.0 kg/sq cm
● - $\bar{\sigma}_v$ = 2.0 kg/cm sq
---- $\dot{\delta}$ = 5.6 x 10^{-2} cm/min
—— $\dot{\delta}$ = 5.6 x 10^{-3} cm/min
△ - confining ring temporarily separated
AVERAGE SHEAR STRESS, τ_a, kg/sq cm
0
0.1
0.2
0.3
0.4
0.5
0.6
0.01
0.1
1.0
10
100
130
PERIPHERAL DISPLACEMENT, δ, cm

FIG. 6-3

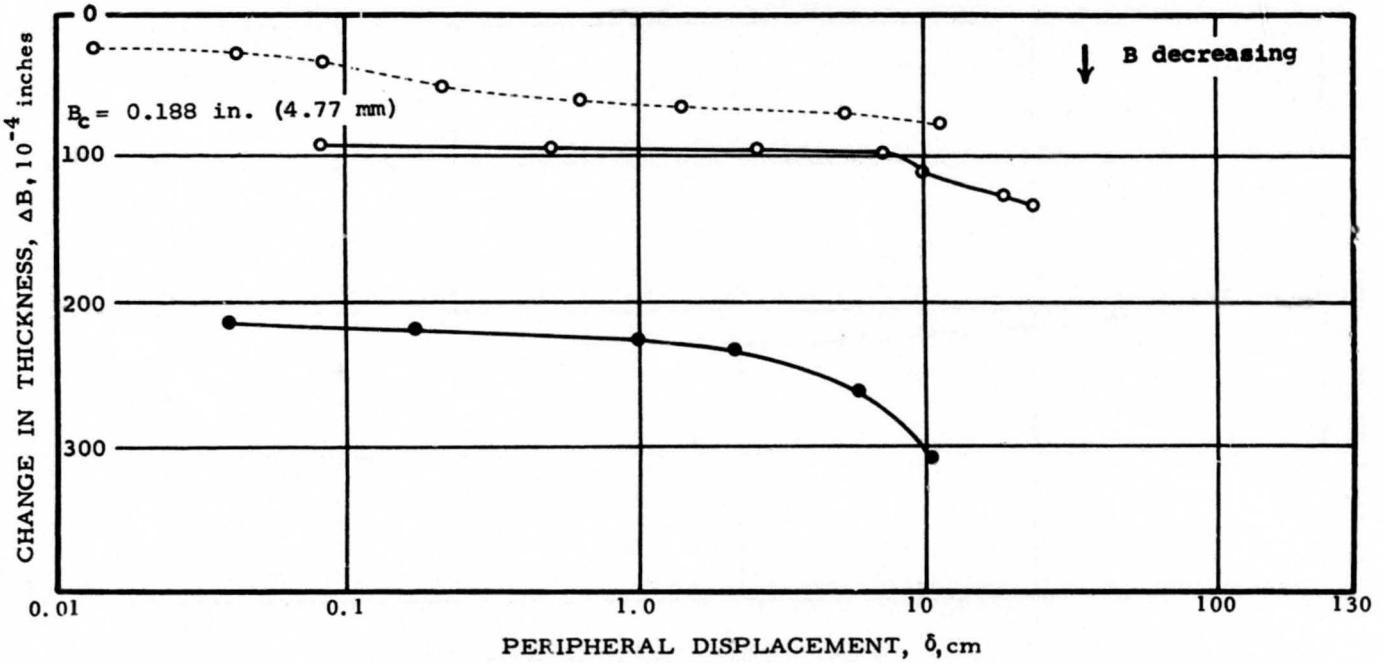
CHANGE IN THICKNESS, ΔB, 10^{-4} inches
0
100
200
300
B_c = 0.188 in. (4.77 mm)
B decreasing
0.01
0.1
1.0
10
100
130
PERIPHERAL DISPLACEMENT, δ, cm

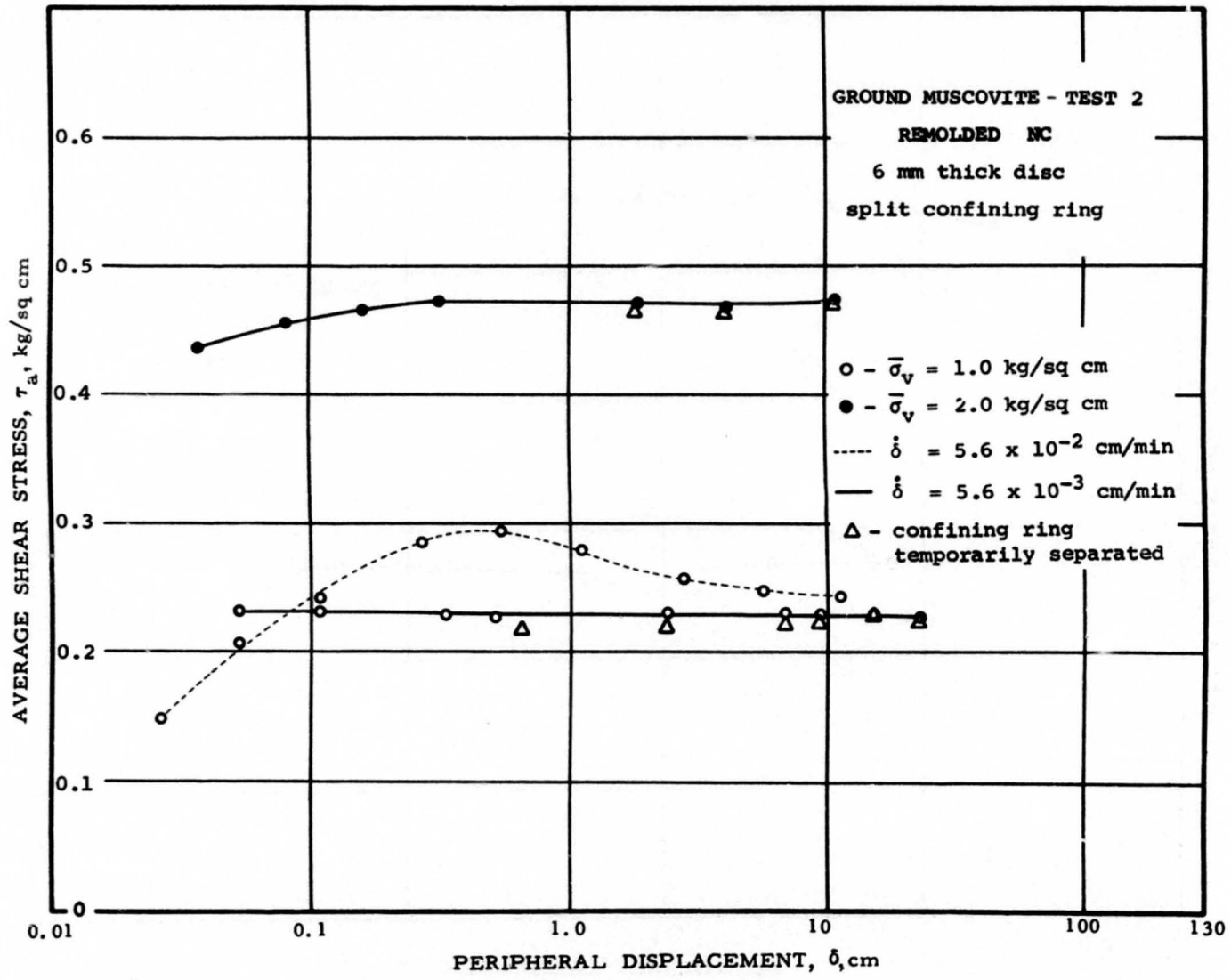
AVERAGE SHEAR STRESS, τ_a, kg/sq cm
0
0.1
0.2
0.3
0.4
0.5
0.6
GROUND MUSCOVITE - TEST 2
REMOLDED NC
6 mm thick disc
split confining ring
o - $\bar{\sigma}_v$ = 1.0 kg/sq cm
● - $\bar{\sigma}_v$ = 2.0 kg/sq cm
---- $\dot{\delta}$ = 5.6 x 10^{-2} cm/min
—— $\dot{\delta}$ = 5.6 x 10^{-3} cm/min
Δ - confining ring temporarily separated
0.01
0.1
1.0
10
100
130
PERIPHERAL DISPLACEMENT, δ, cm

FIG. 6-4

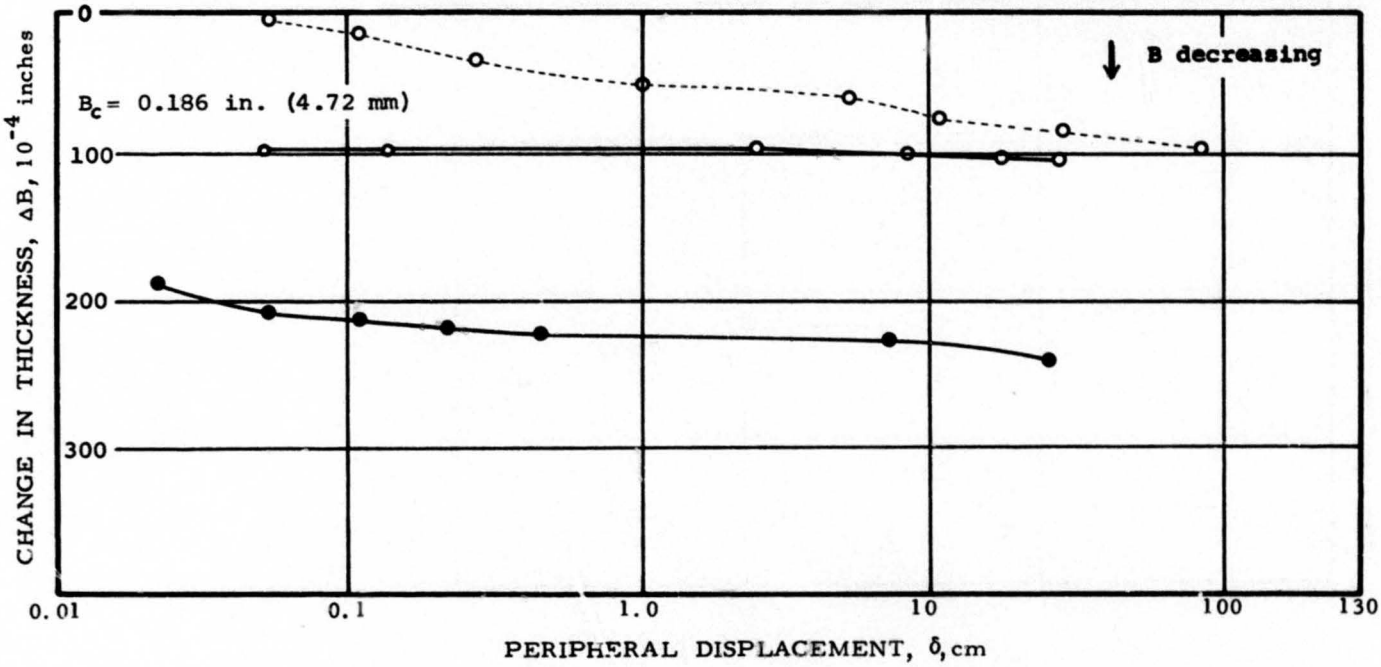
CHANGE IN THICKNESS, ΔB, 10^{-4} inches
0
100
200
300
B_c = 0.186 in. (4.72 mm)
B decreasing
0.01
0.1
1.0
10
100
130
PERIPHERAL DISPLACEMENT, δ, cm

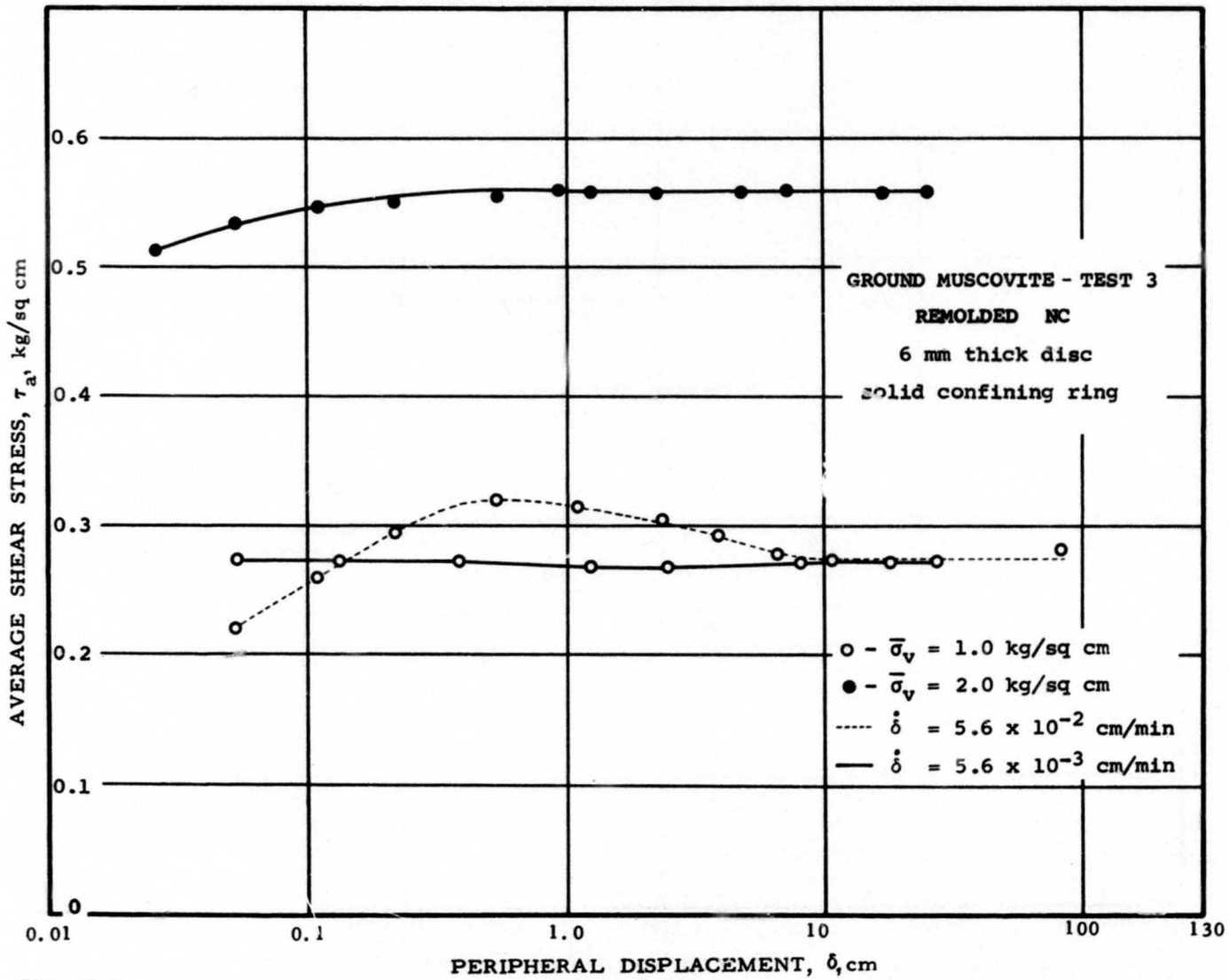
AVERAGE SHEAR STRESS, τ_a, kg/sq cm
0
0.1
0.2
0.3
0.4
0.5
0.6
GROUND MUSCOVITE - TEST 3
REMOLDED NC
6 mm thick disc
solid confining ring
o - $\bar{\sigma}_v$ = 1.0 kg/sq cm
● - $\bar{\sigma}_v$ = 2.0 kg/sq cm
----- $\dot{\delta}$ = 5.6 x 10^{-2} cm/min
—— $\dot{\delta}$ = 5.6 x 10^{-3} cm/min
0.01
0.1
1.0
10
100
130
PERIPHERAL DISPLACEMENT, δ, cm

FIG. 6-5

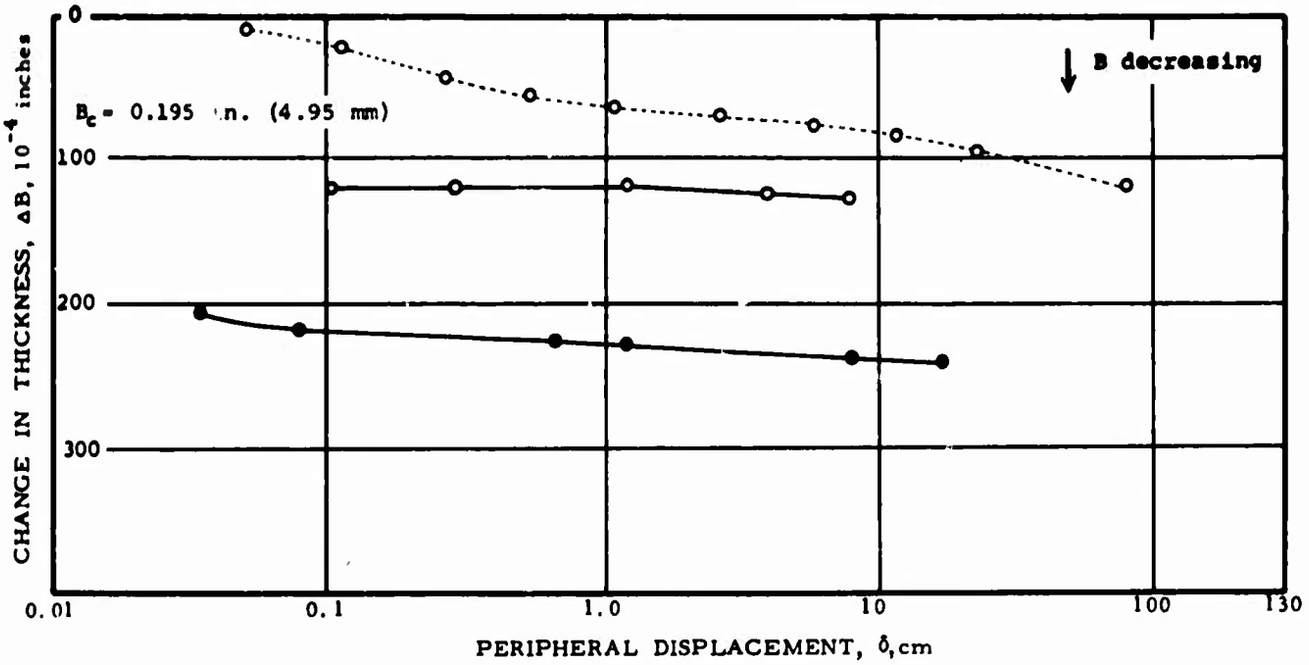
B decreasing
B_c = 0.195 in. (4.95 mm)
CHANGE IN THICKNESS, ΔB, 10^{-4} inches
0
100
200
300
0.01
0.1
1.0
10
100
130
PERIPHERAL DISPLACEMENT, δ, cm

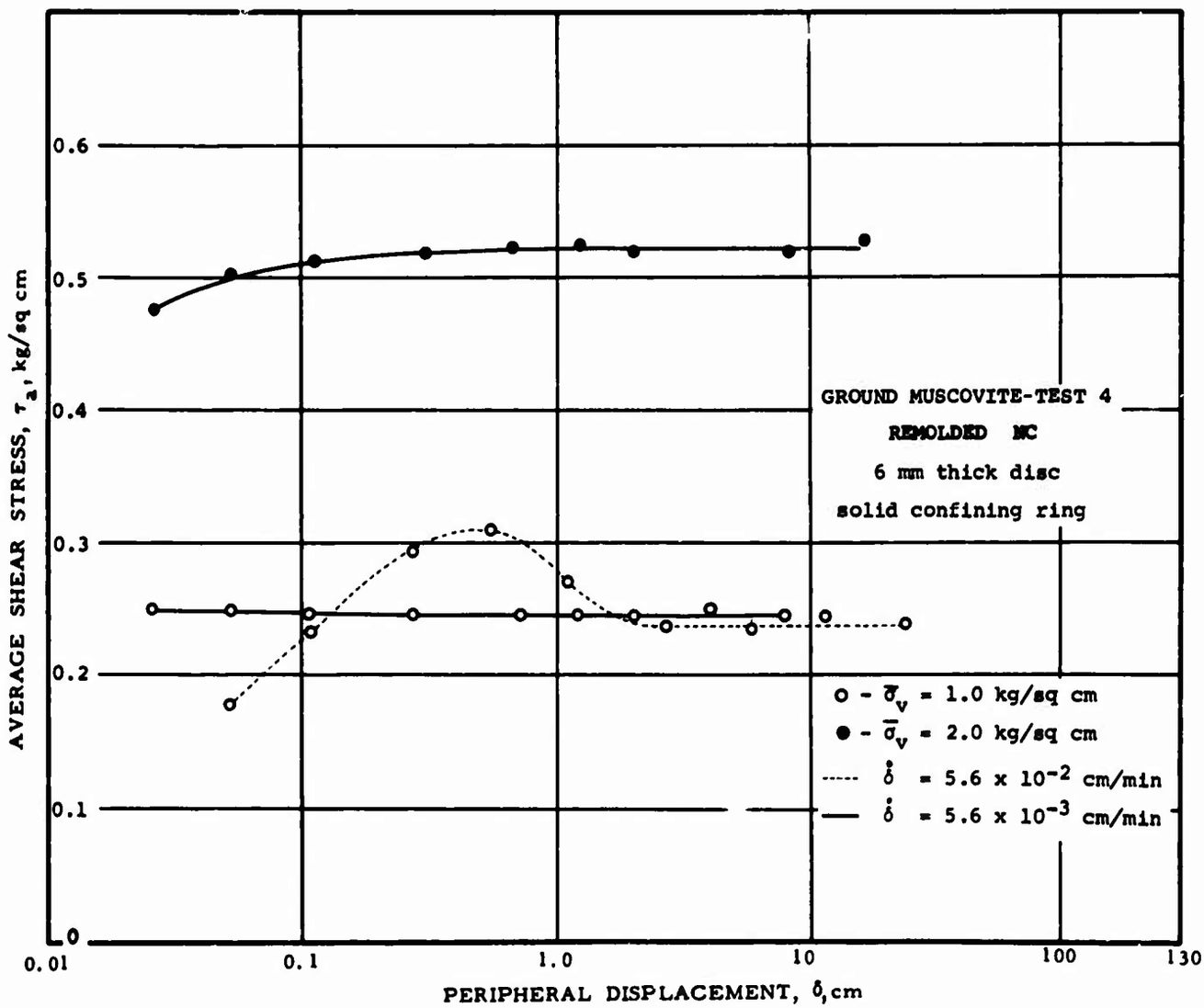
GROUND MUSCOVITE-TEST 4
REMOLDED NC
6 mm thick disc
solid confining ring
○ - $\bar{\sigma}_v$ = 1.0 kg/sq cm
● - $\bar{\sigma}_v$ = 2.0 kg/sq cm
----- $\dot{\delta}$ = 5.6 x 10^{-2} cm/min
—— $\dot{\delta}$ = 5.6 x 10^{-3} cm/min
AVERAGE SHEAR STRESS, τ_a, kg/sq cm
0
0.1
0.2
0.3
0.4
0.5
0.6
0.01
0.1
1.0
10
100
130
PERIPHERAL DISPLACEMENT, δ, cm

FIG. 6-6

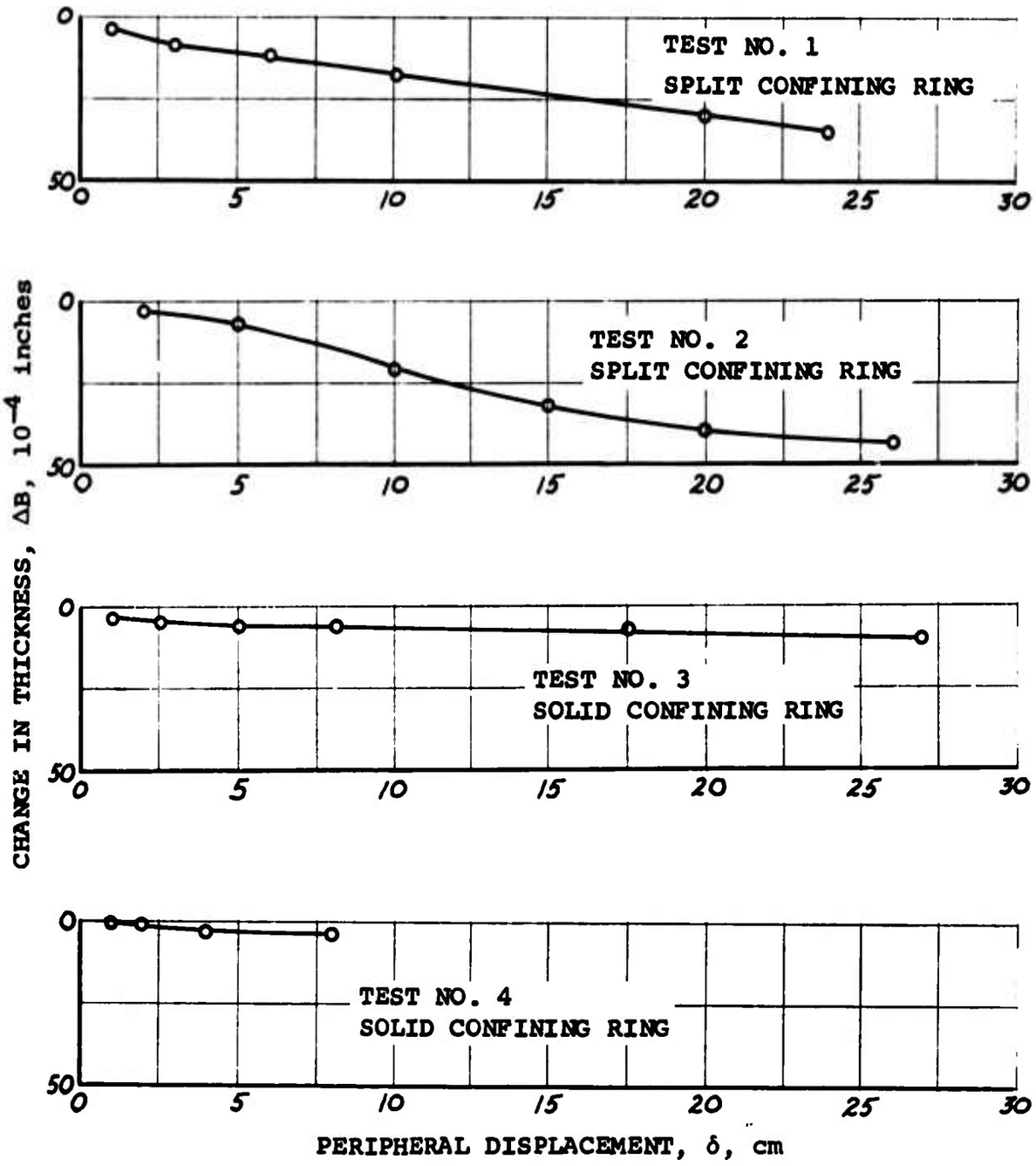

SUMMARY ΔB vs δ
GROUND MUSCOVITE
DISC-SHAPED SPECIMENS
$\bar{\sigma}_v$ = 1.0 kg/sq cm
$\dot{\delta}$ = 5.6 x 10^{-3} cm/min

FIG.6-7

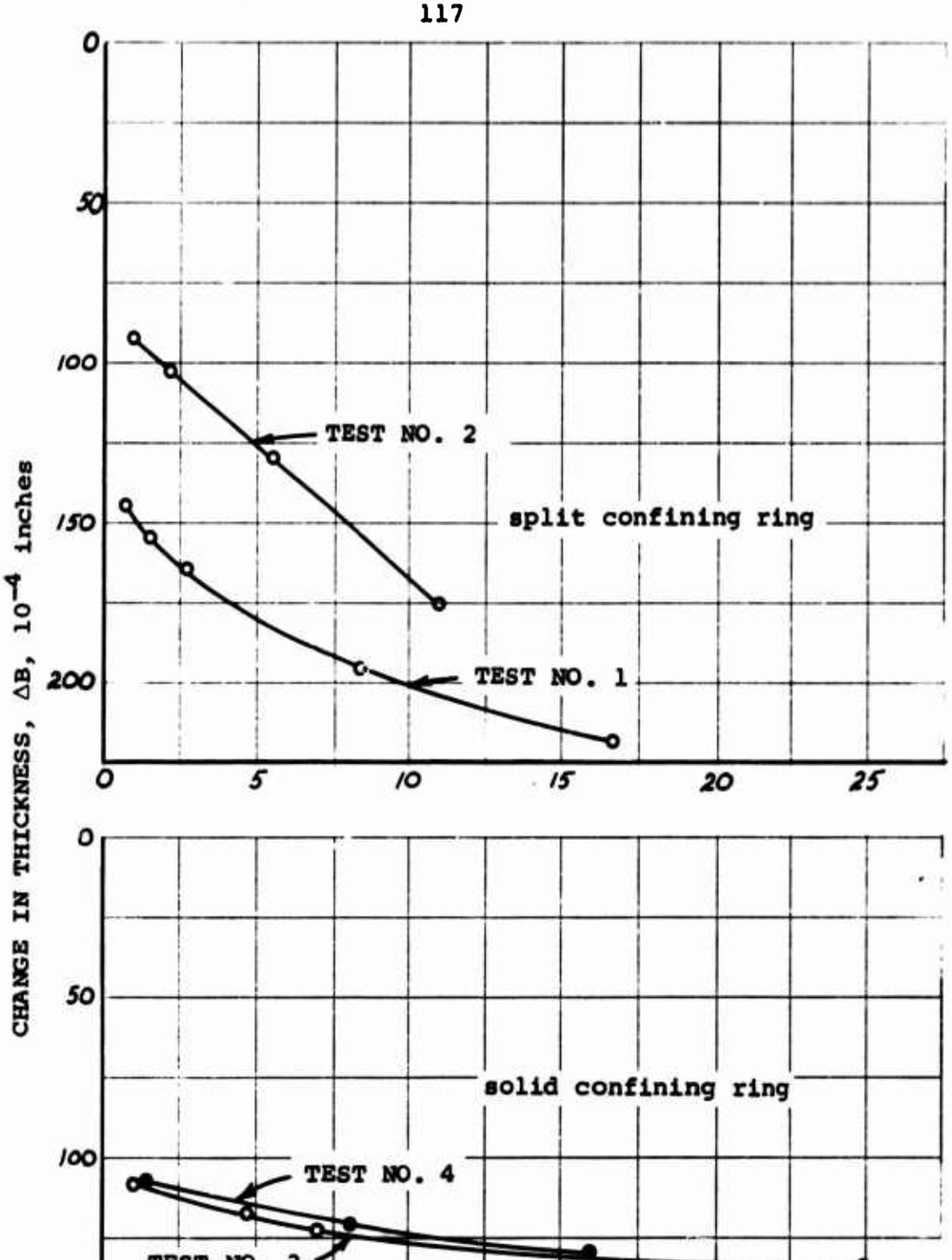

SUMMARY ΔB vs δ
GROUND MUSCOVITE
DISC-SHAPED SPECIMENS
$\bar{\sigma}_v$ = 2.0 kg/sq cm
$\dot{\delta}$ = 5.6 x 10^{-3} cm/min

FIG. 6-8

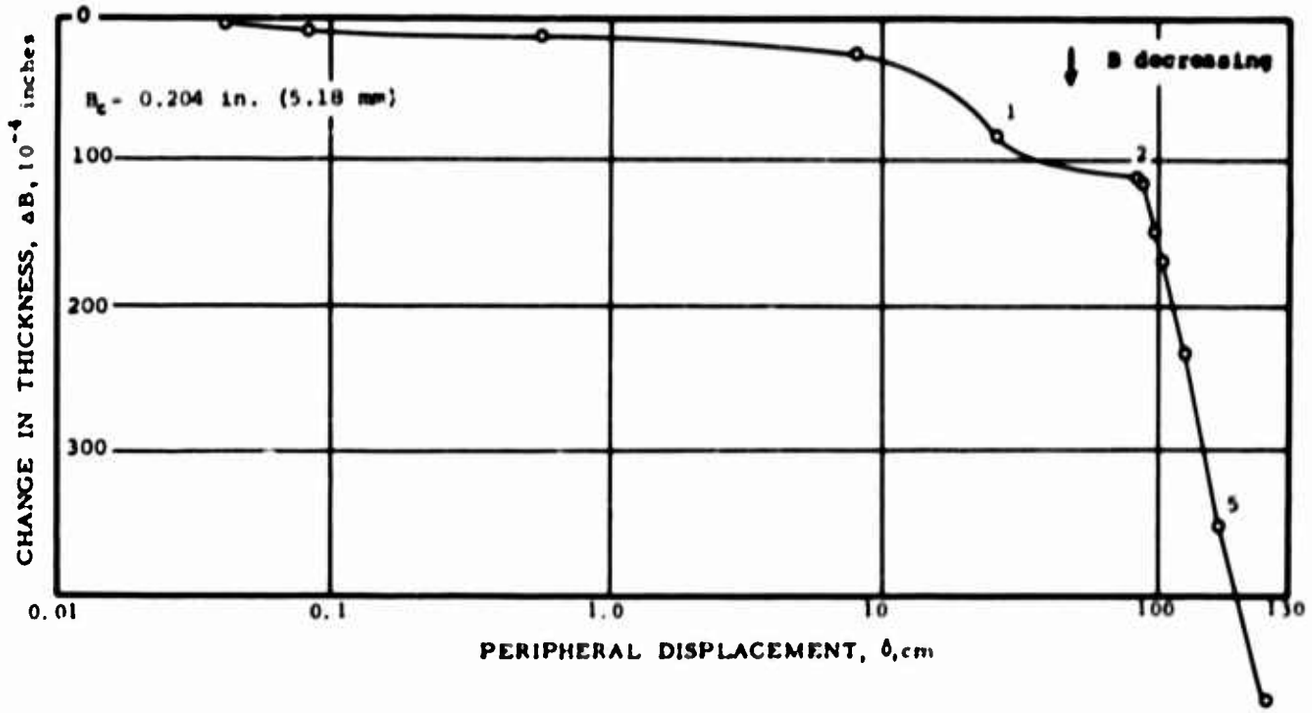
CHANGE IN THICKNESS, ΔB, 10^{-4} inches
B_c = 0.204 in. (5.18 mm)
B decreasing
0
100
200
300
1
2
5
0.01
0.1
1.0
10
100
130
PERIPHERAL DISPLACEMENT, δ, cm

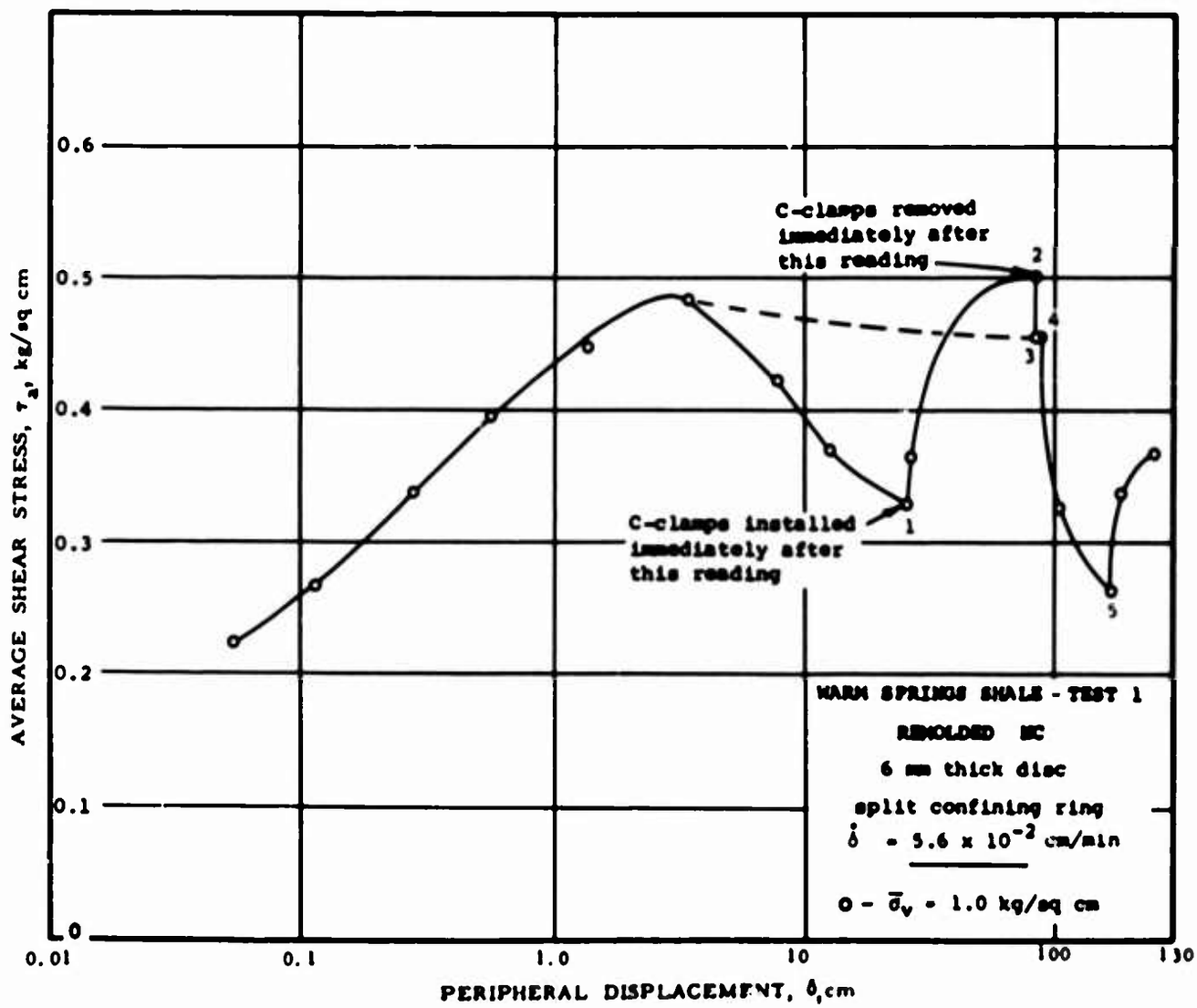
AVERAGE SHEAR STRESS, τ_a, kg/sq cm
0.6
0.5
0.4
0.3
0.2
0.1
0
C-clamps removed immediately after this reading
C-clamps installed immediately after this reading
1
2
3
4
5
WARM SPRINGS SHALE - TEST 1
REMOLDED MC
6 mm thick disc
split confining ring
$\dot{\delta}$ = 5.6 x 10^{-2} cm/min
o - $\bar{\sigma}_v$ = 1.0 kg/sq cm
0.01
0.1
1.0
10
100
130
PERIPHERAL DISPLACEMENT, δ, cm

FIG. 6-9

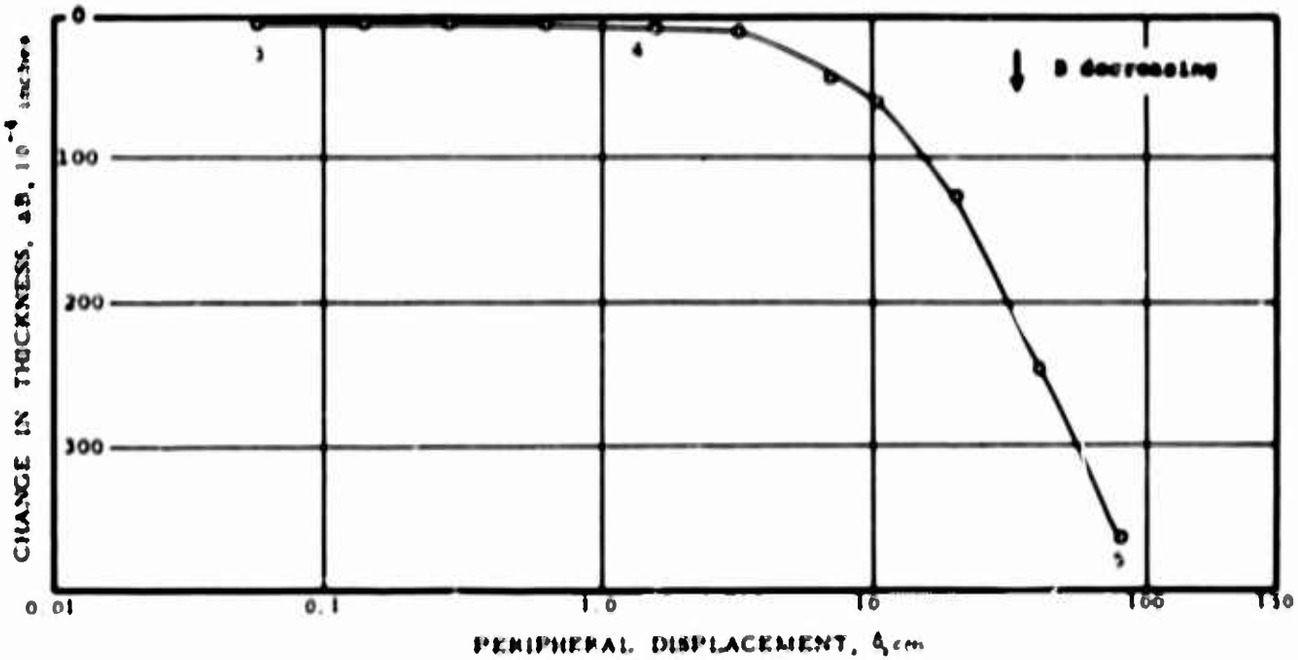
CHANGE IN THICKNESS, Δt, 10⁻⁴ inches
0
100
200
300
0.01
0.1
1.0
10
100
150
PERIPHERAL DISPLACEMENT, δ, cm
δ decreasing
3
4
5

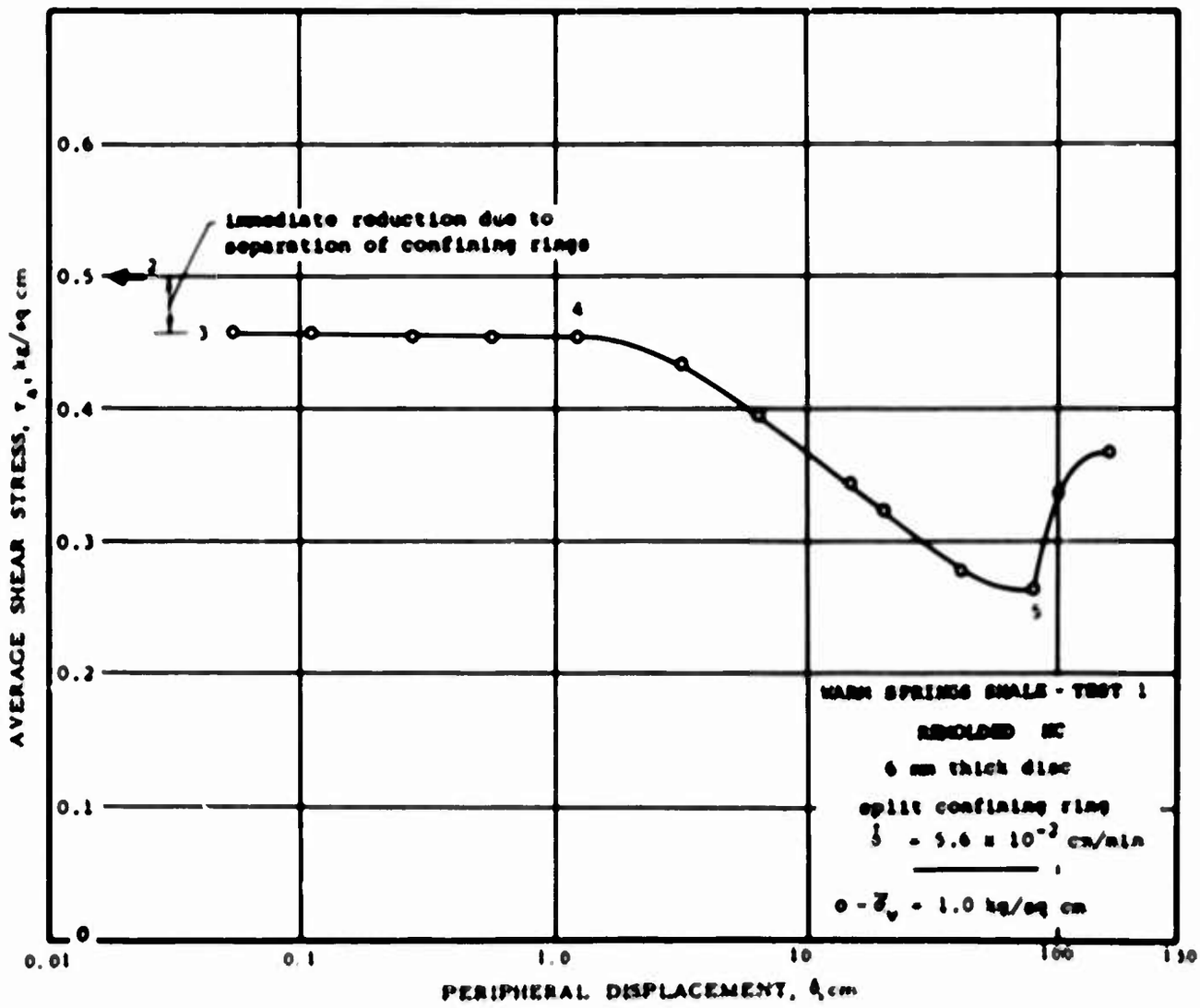
AVERAGE SHEAR STRESS, τ_a, kg/sq cm
0
0.1
0.2
0.3
0.4
0.5
0.6
0.01
0.1
1.0
10
100
150
PERIPHERAL DISPLACEMENT, δ, cm
Immediate reduction due to separation of confining rings
2
3
4
5
WARM SPRINGS SHALE - TEST 1
REMOLDED MC
6 mm thick disc
split confining ring
δ̇ = 5.6 x 10⁻² cm/min
σ - σ_v = 1.0 kg/sq cm

FIG. 6-10

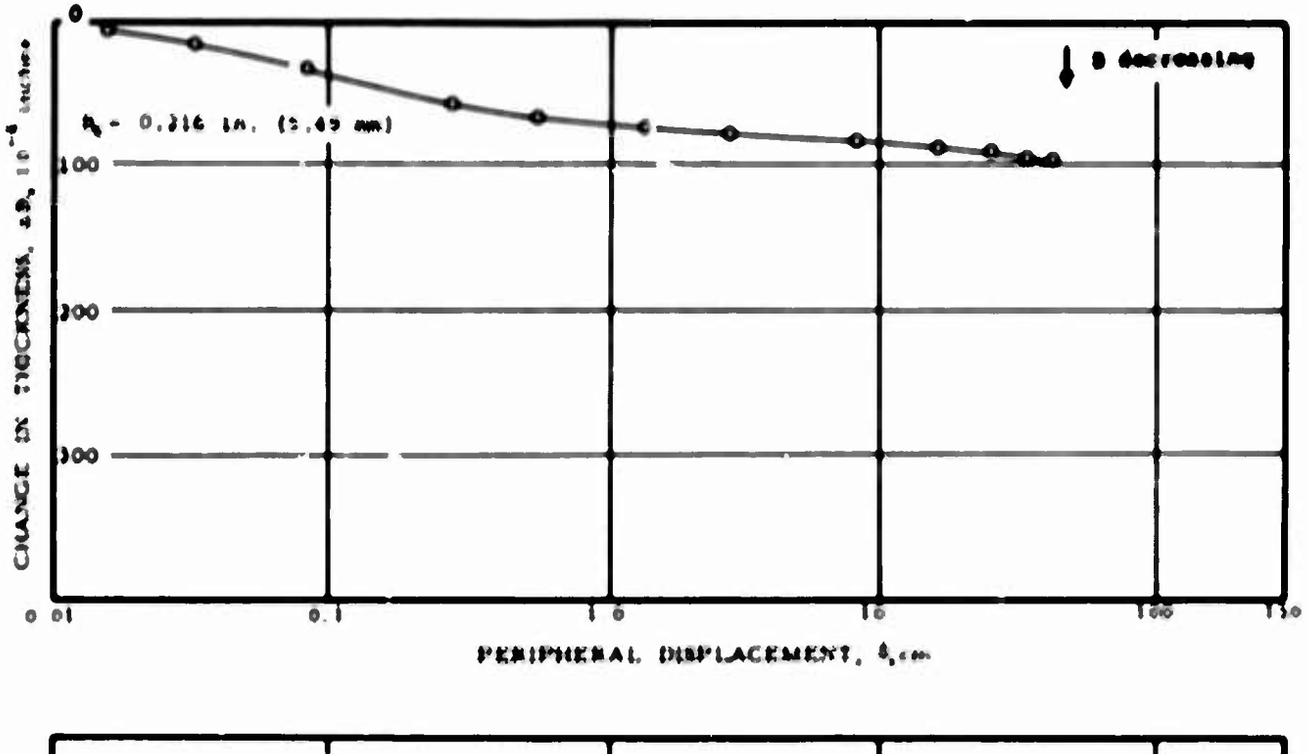
0
100
200
300
0.01
0.1
1.0
10
100
150
δ decreasing
PERIPHERAL DISPLACEMENT, δ, cm

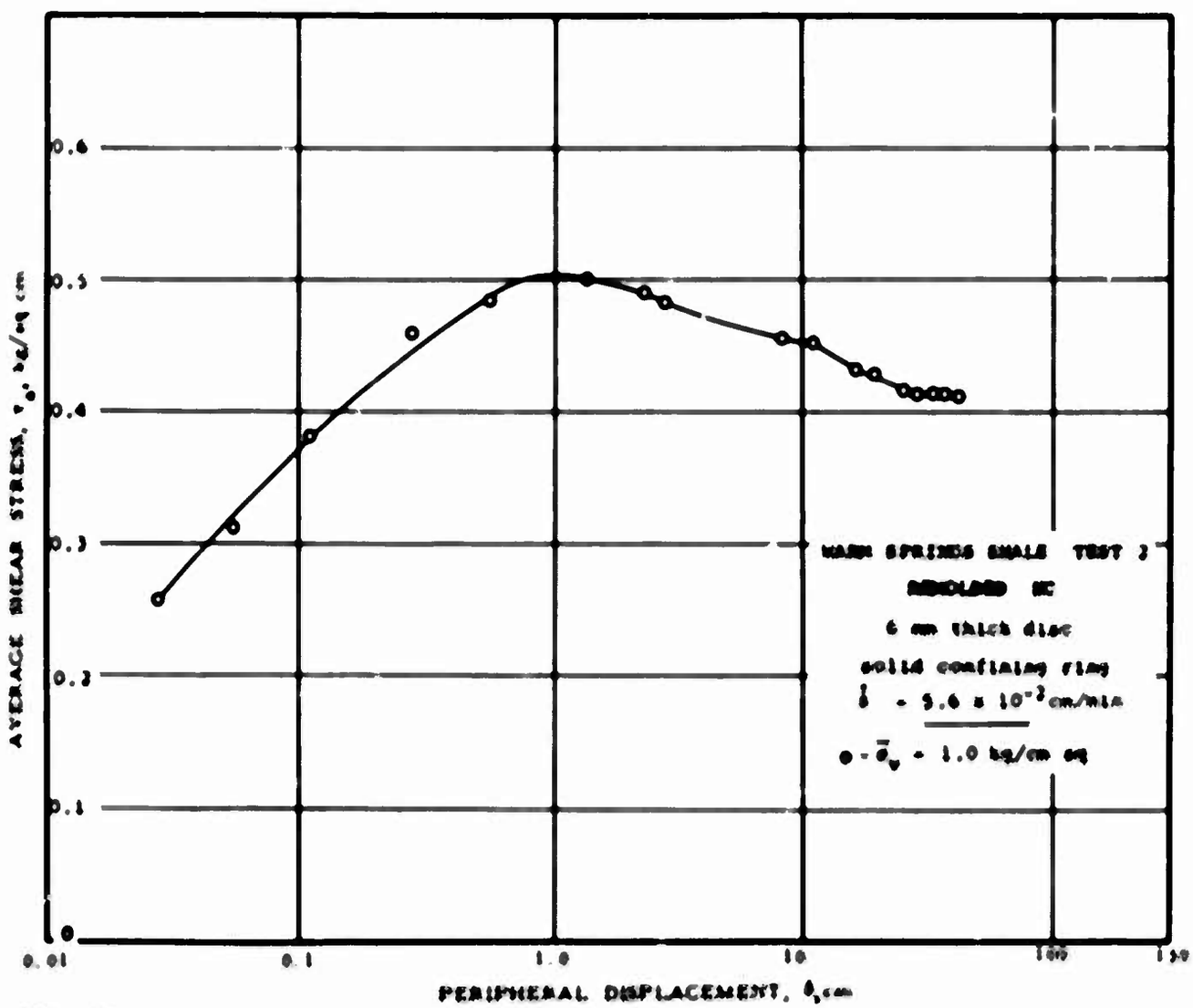
0.6
0.5
0.4
0.3
0.2
0.1
0
0.01
0.1
1.0
10
100
150
MARK SPRINGS SHALE TEST 3
REMOLDED BC
6 mm thick disc
solid confining ring
δ̇ = 5.6 x 10⁻³ cm/min
σ = σ̄v = 1.0 kg/cm sq
PERIPHERAL DISPLACEMENT, δ, cm

FIG. 6-11

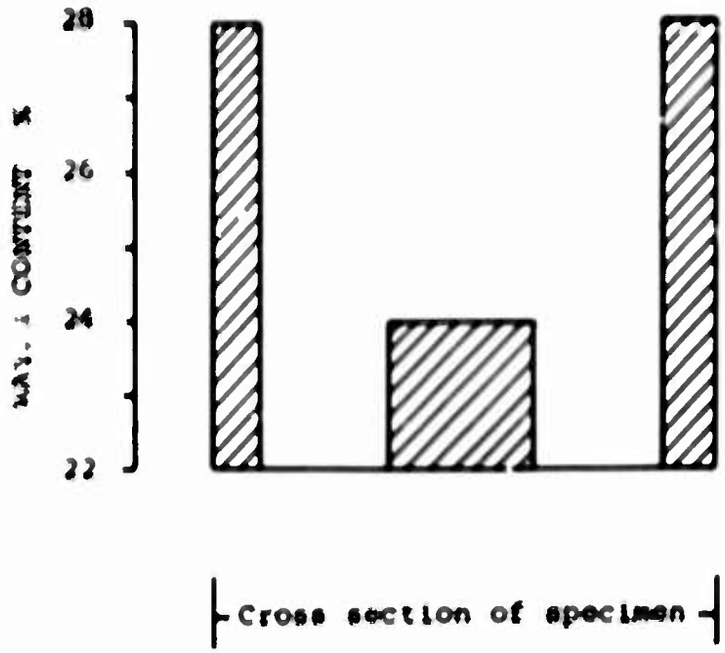

TEST 1

split confining ring

initial water content - 35.5%

REMOLDED MARK SPRINGS SHALE
WATER CONTENT AT END OF TEST

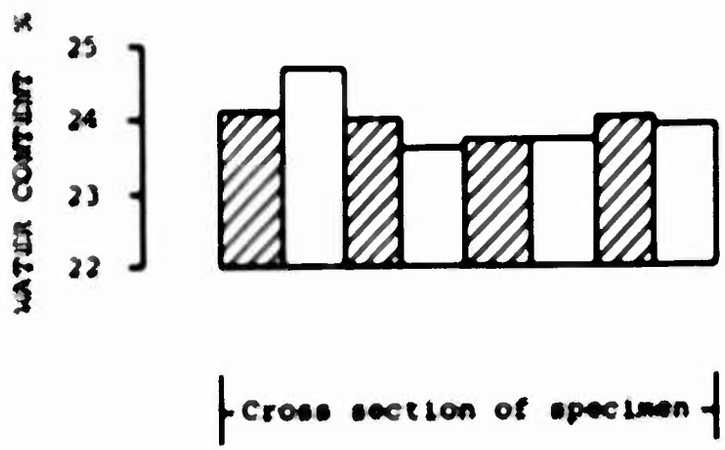

TEST 2

solid confining ring

initial water content - 36.0%

FIG. 6-12

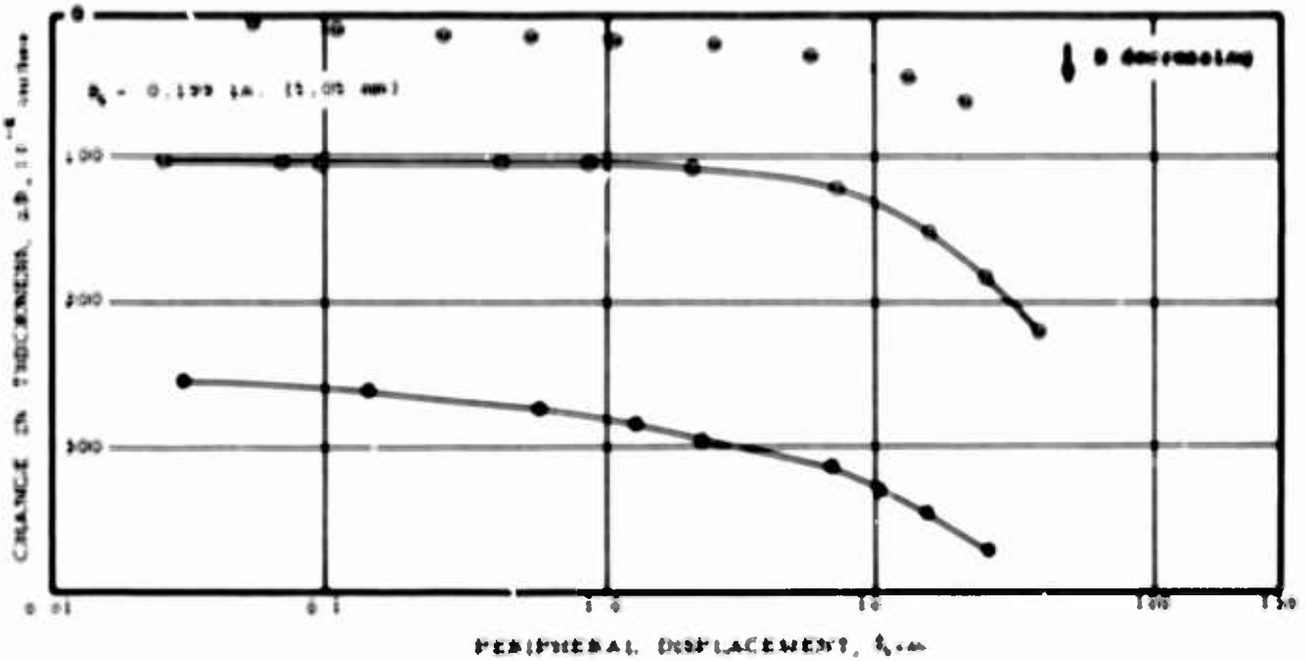
CHANGE IN THICKNESS, Δh, 10⁻⁴ inches
h decreasing
PERIPHERAL DISPLACEMENT, δ, cm

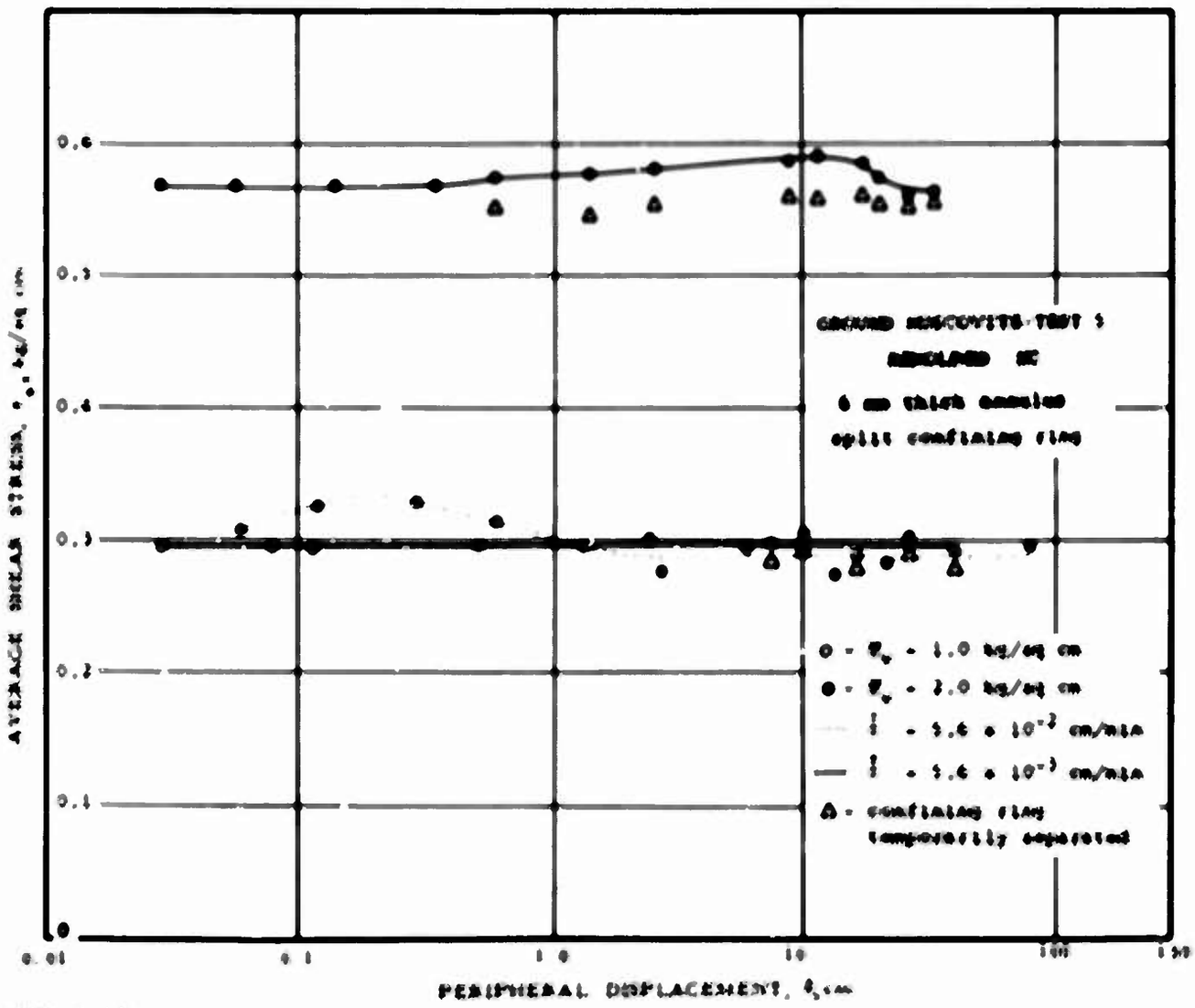
AVERAGE SHEAR STRESS, τ, kg/sq cm
GROUND MUSCOVITE TEST 5
RECLAIMED MC
6 mm thick annular
split confining ring
○ - σv - 1.0 kg/sq cm
● - σv - 2.0 kg/sq cm
— - 5.6 × 10⁻² cm/min
— - 5.6 × 10⁻³ cm/min
Δ - confining ring temporarily separated
PERIPHERAL DISPLACEMENT, δ, cm

FIG. 6-13

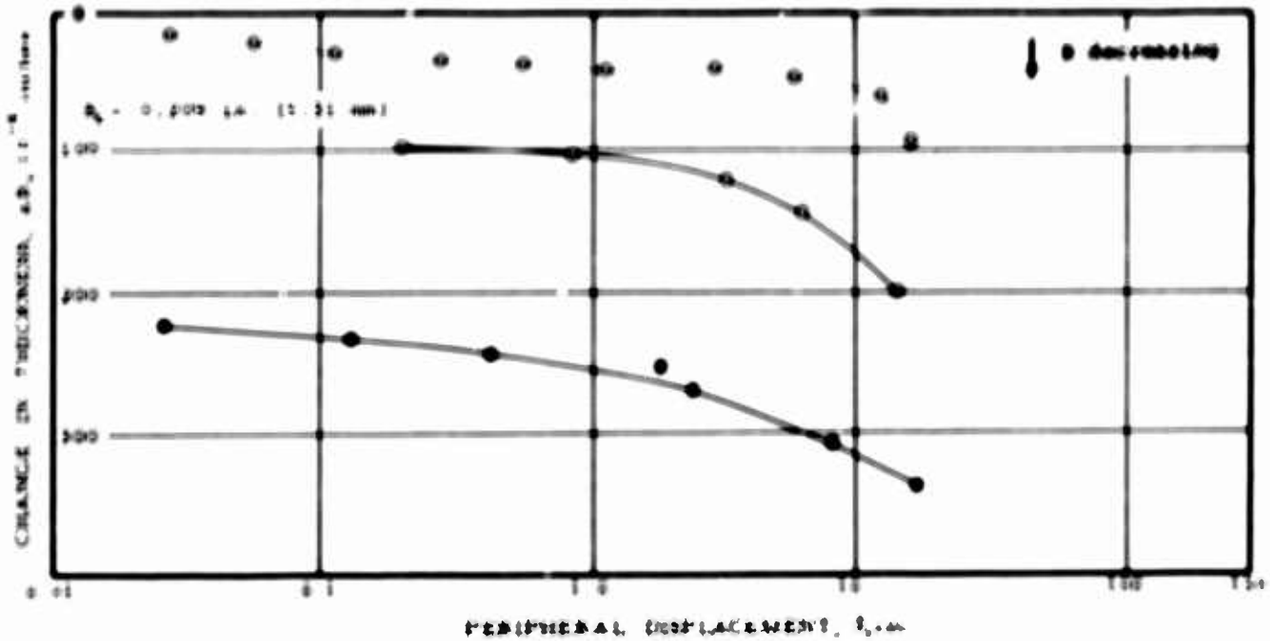
CHANGE IN THICKNESS, Δδ, 10⁻⁴ inches
δ decreasing
δ₀ = 0.009 in. (1.31 mm)
1,000
500
0
0.01
0.1
1.0
10
100
PERIPHERAL DISPLACEMENT, δ, in.

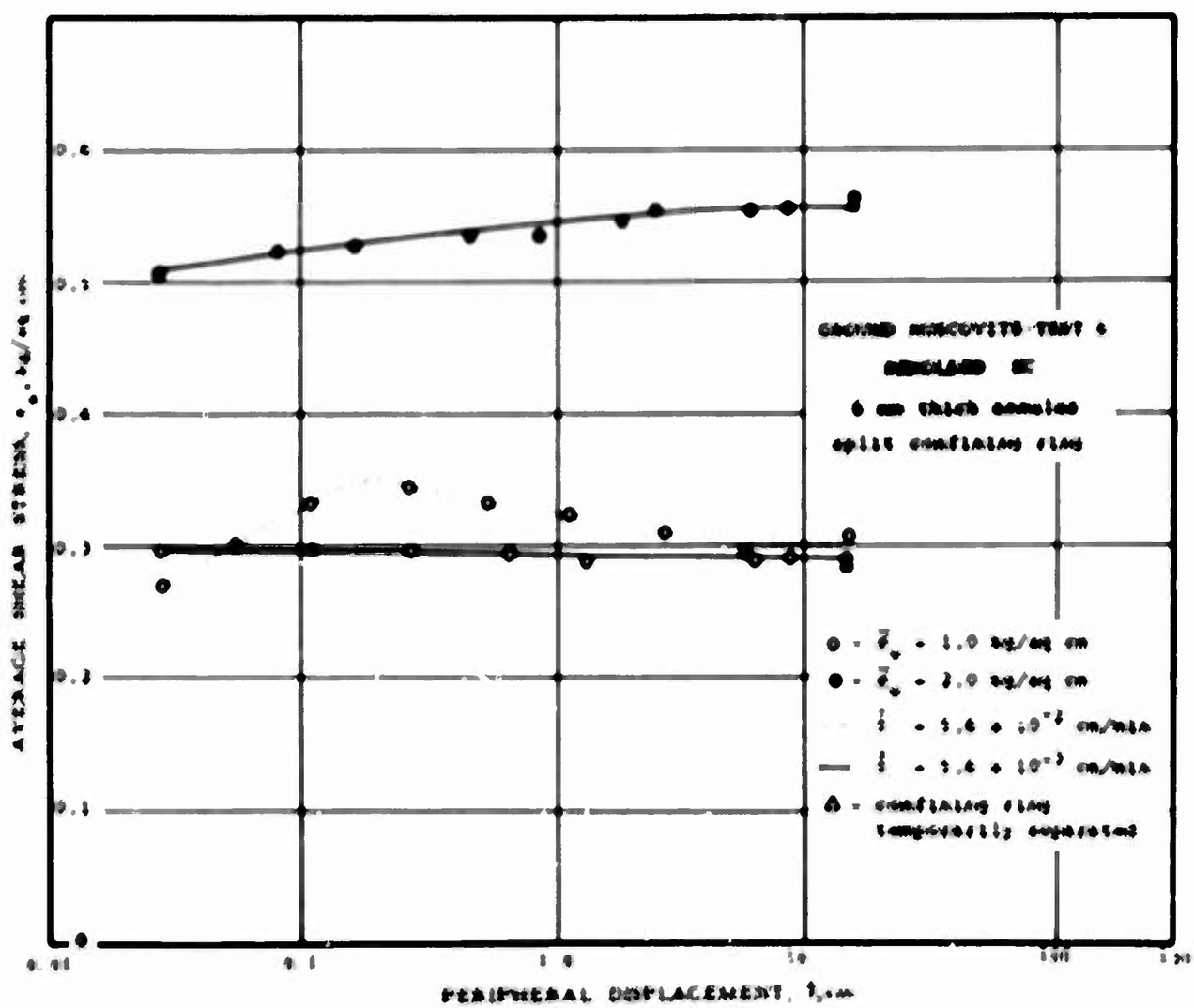
AVERAGE SHEAR STRESS, τ, kg/sq cm
0.6
0.5
0.4
0.3
0.2
0.1
0
0.01
0.1
1.0
10
100
PERIPHERAL DISPLACEMENT, δ, in.
GROUND MUSCOVITE TEST 6
6 cm thick annulus
split confining ring
○ - σ̄v = 1.0 kg/sq cm
● - σ̄v = 2.0 kg/sq cm
δ̇ = 1.6 × 10⁻³ cm/min
δ̇ = 1.6 × 10⁻³ cm/min
Δ - confining ring temporarily separated

FIG. 6-14

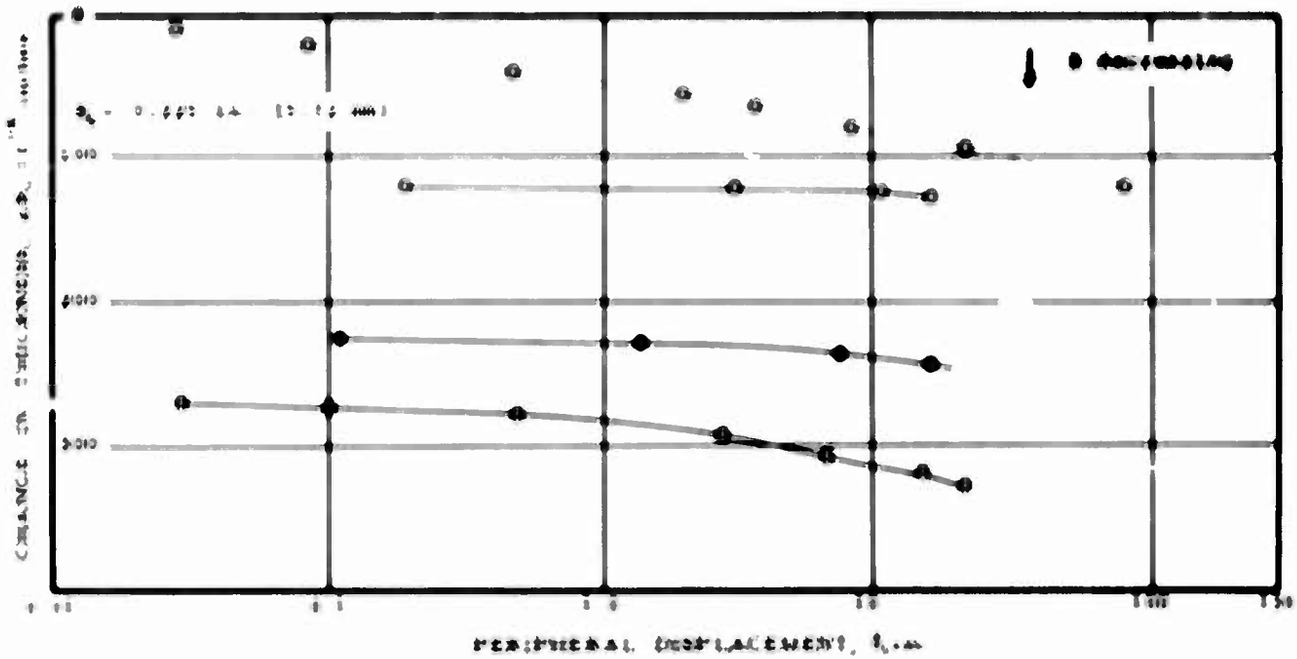

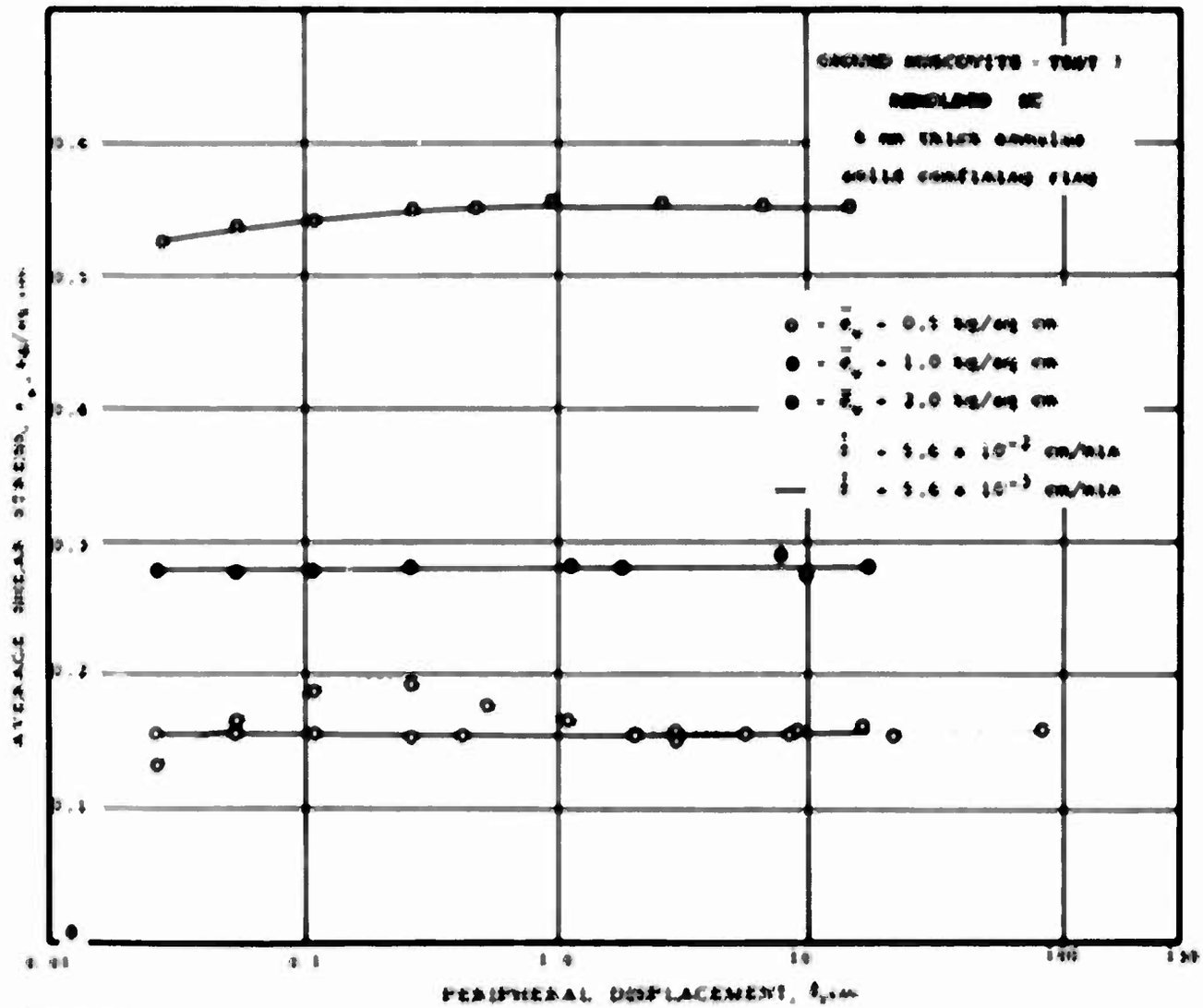
GROUND MUSCOVITE - TEST 1
REMOLDED AT
6 cm thick annulus
with confining ring
o - $\bar{\sigma}_v$ = 0.5 kg/sq cm
● - $\bar{\sigma}_v$ = 1.0 kg/sq cm
● - $\bar{\sigma}_v$ = 2.0 kg/sq cm
$\dot{\delta}$ = 5.6 x 10^{-2} cm/min
$\dot{\delta}$ = 5.6 x 10^{-3} cm/min
PERIPHERAL DISPLACEMENT, δ, cm

FIG. 6-11

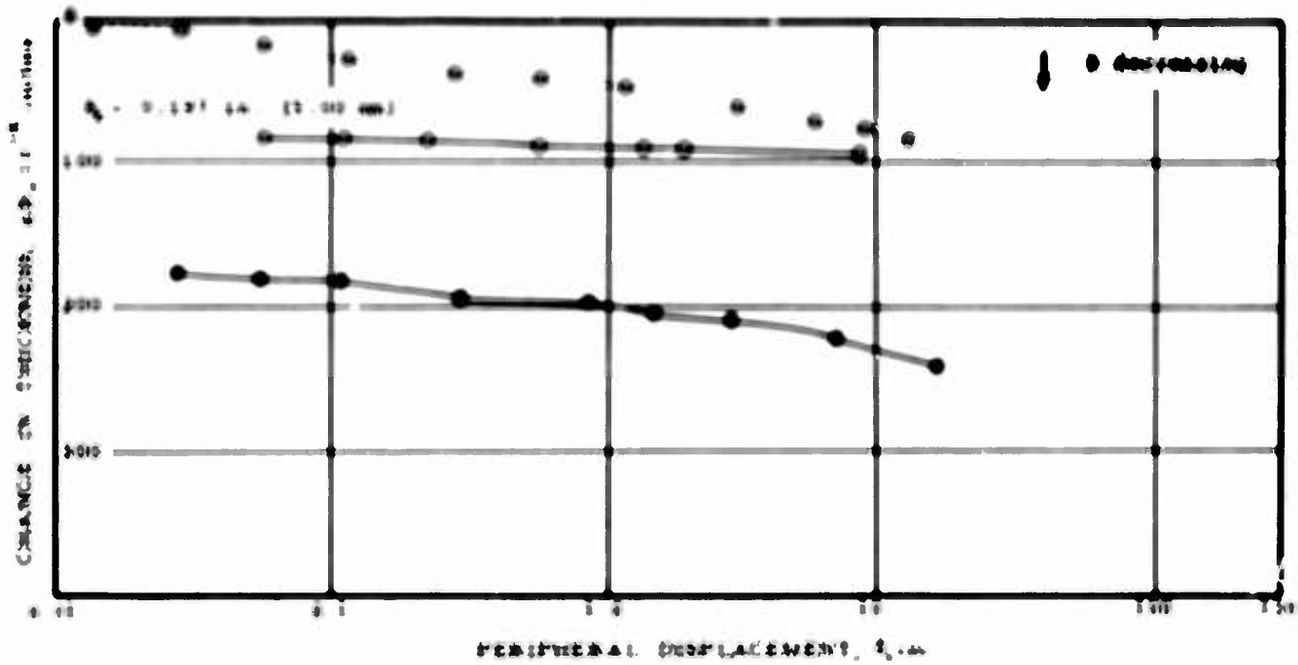
PERIPHERAL DISPLACEMENT, δ, cm

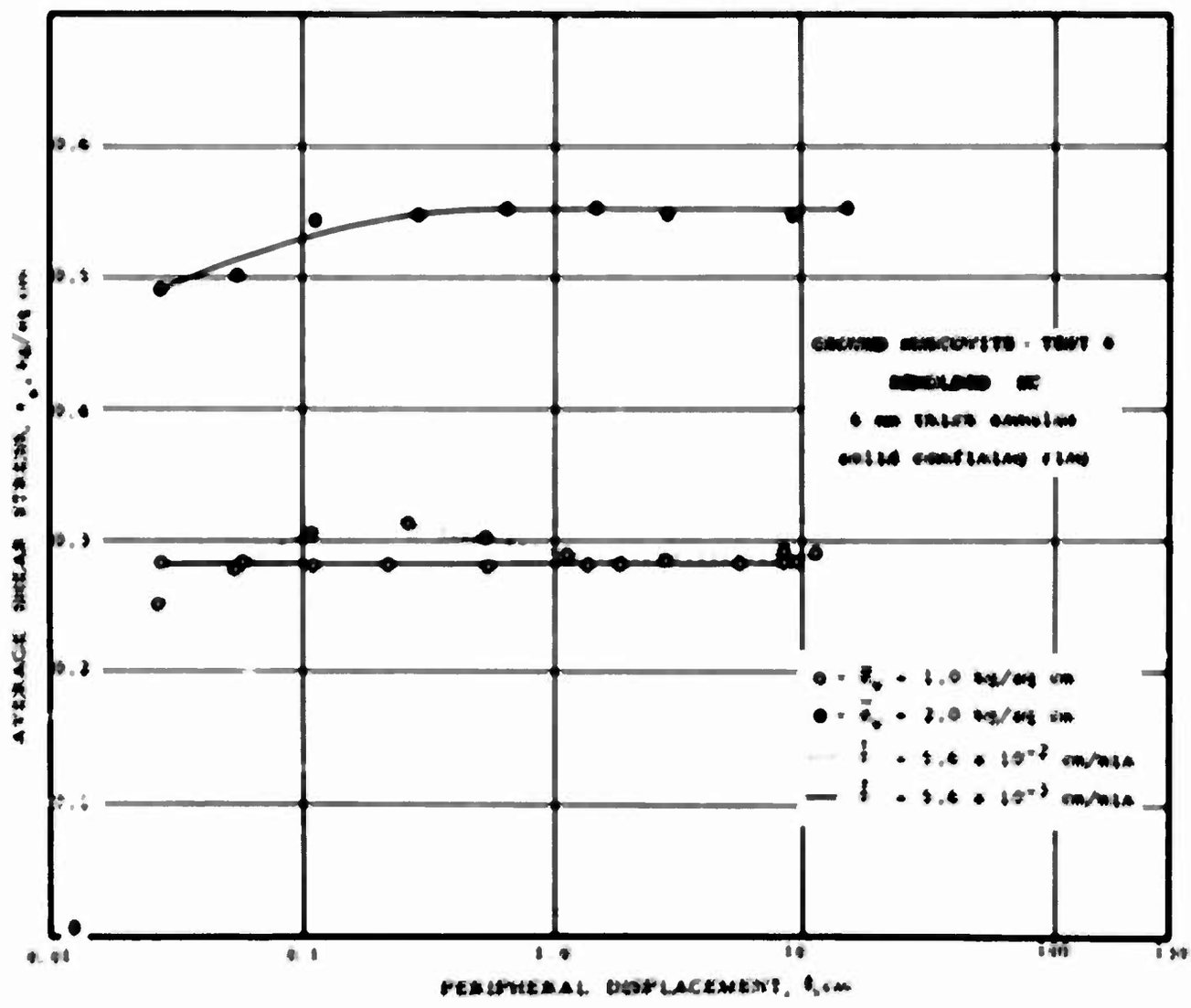
AVERAGE SHEAR STRESS, τ, kg/sq cm
PERIPHERAL DISPLACEMENT, δ, cm

FIG. 6-16

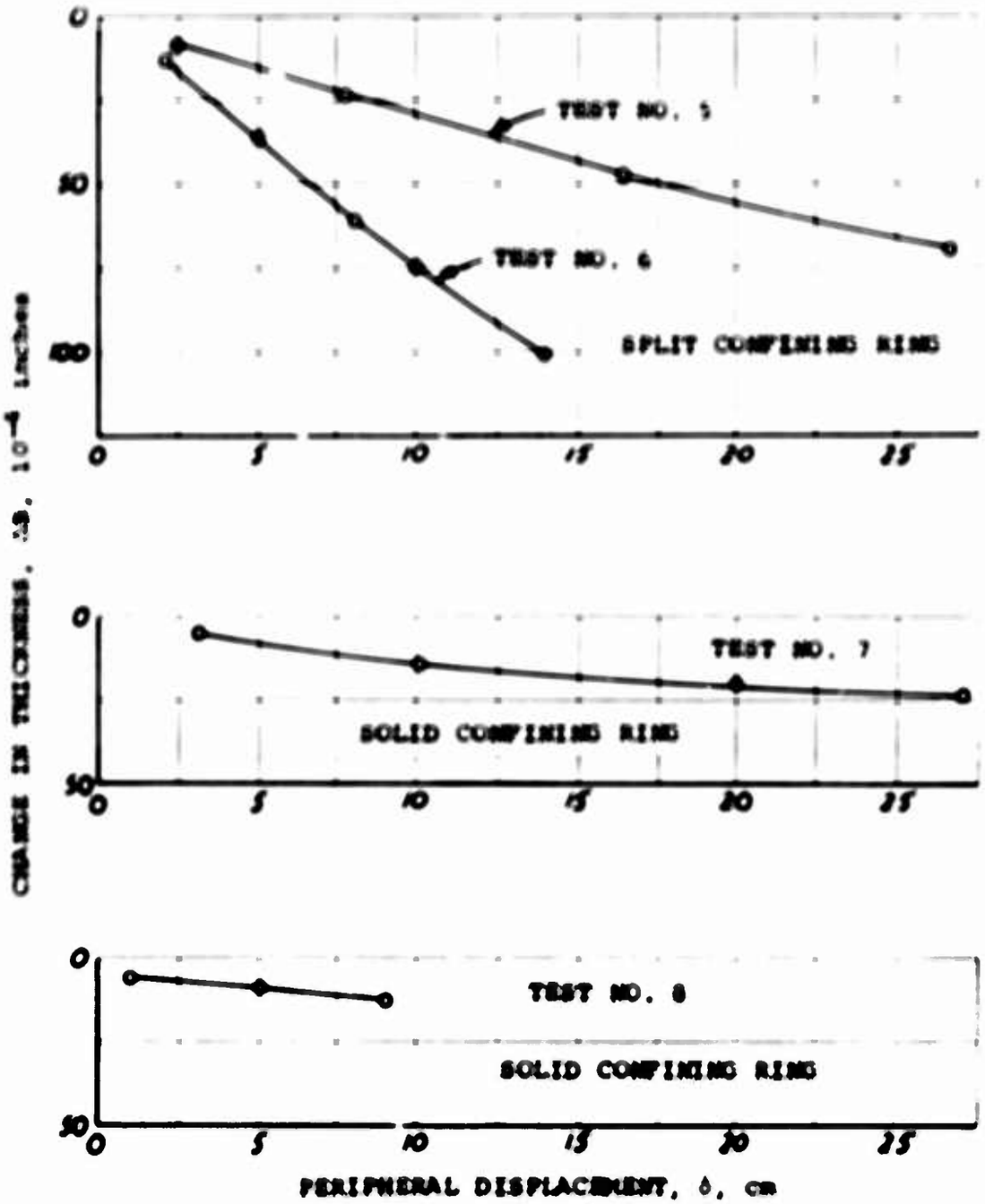

SUMMARY ΔB vs δ
GROUND MUSCOVITE
ANNULAR SPECIMENS
$\bar{\sigma}_v$ = 1.0 kg/sq cm
$\dot{\delta}$ = 5.6 x 10^{-3} cm/min

FIG. 6-17

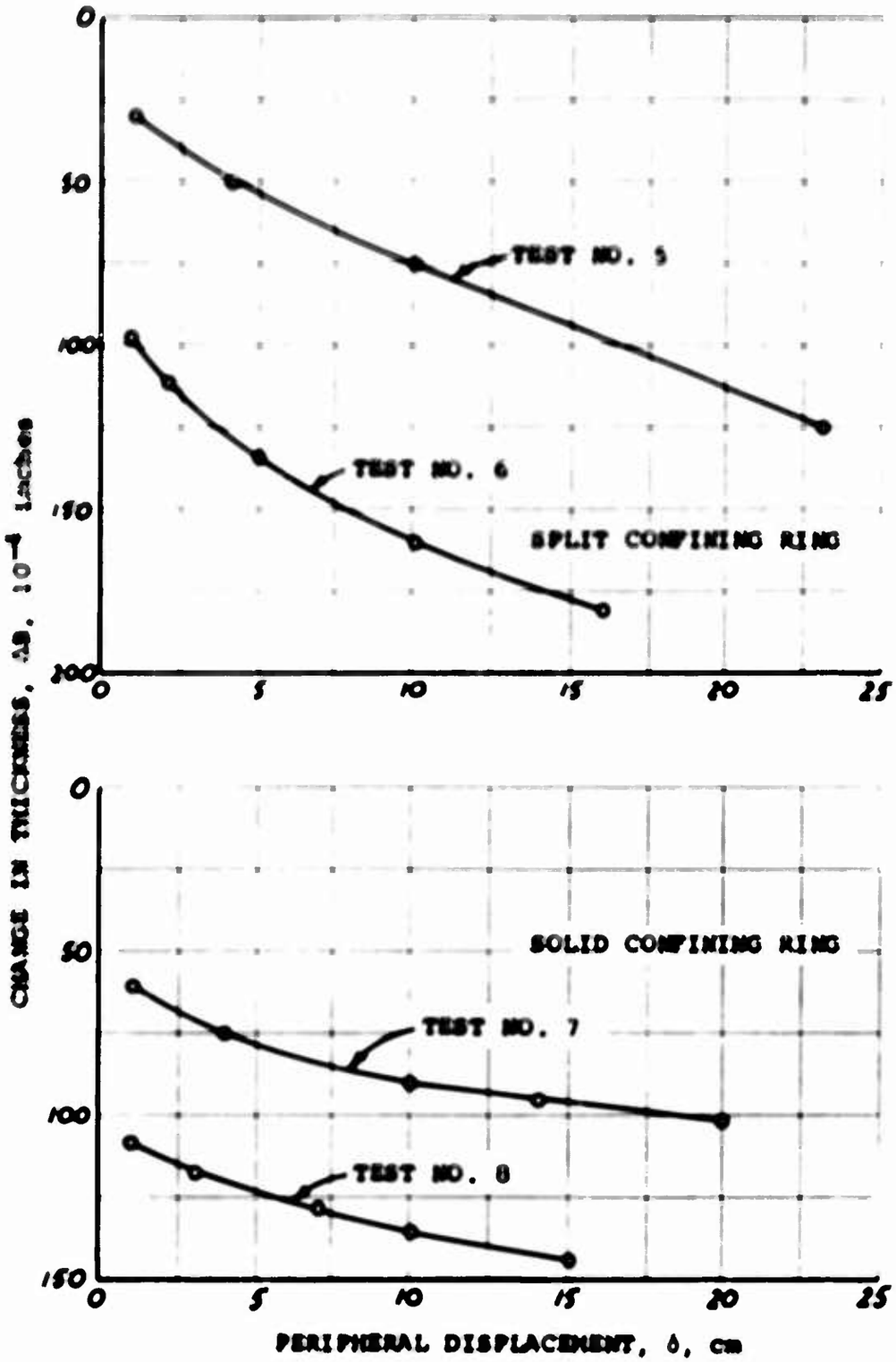

SUMMARY ΔB vs δ
GROUND MUSCOVITE
ANNULAR SPECIMENS
$\bar{\sigma}_v$ = 2.0 kg/sq cm
$\dot{\delta}$ = 5.6 x 10^{-3} cm/min

FIG. 6-18

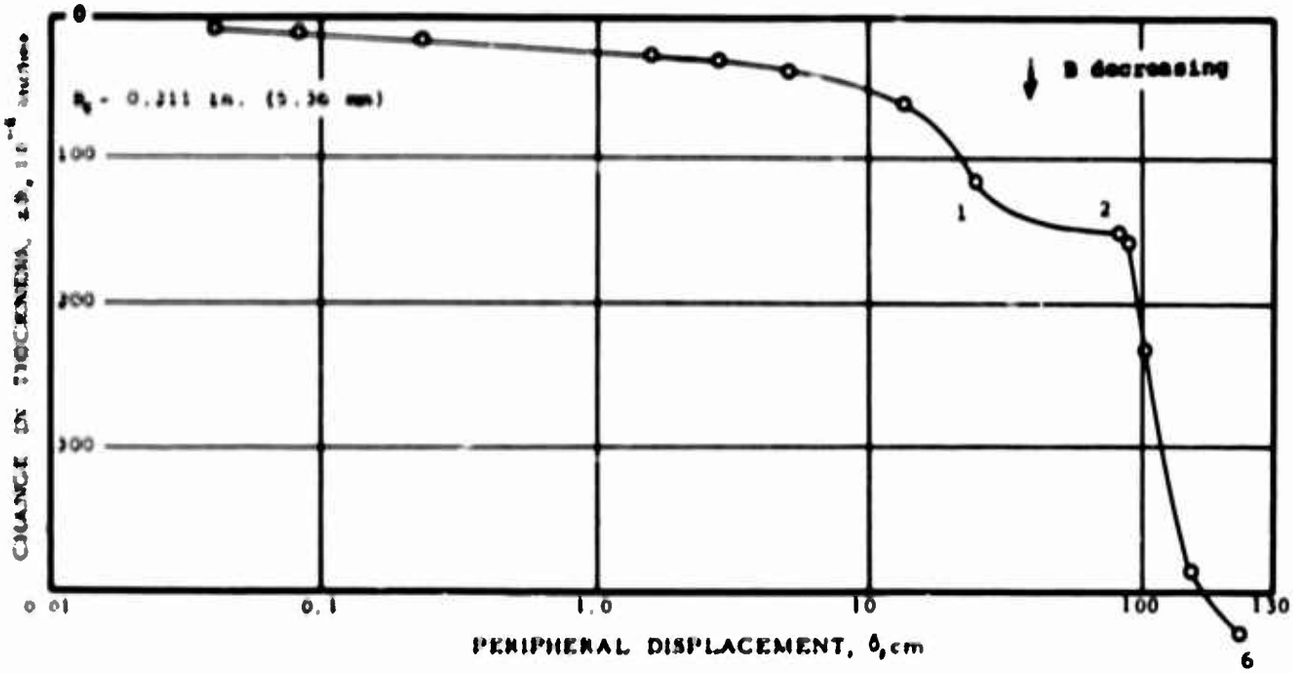
B decreasing
1
2
6
0.01
0.1
1.0
10
100
130
PERIPHERAL DISPLACEMENT, δ, cm

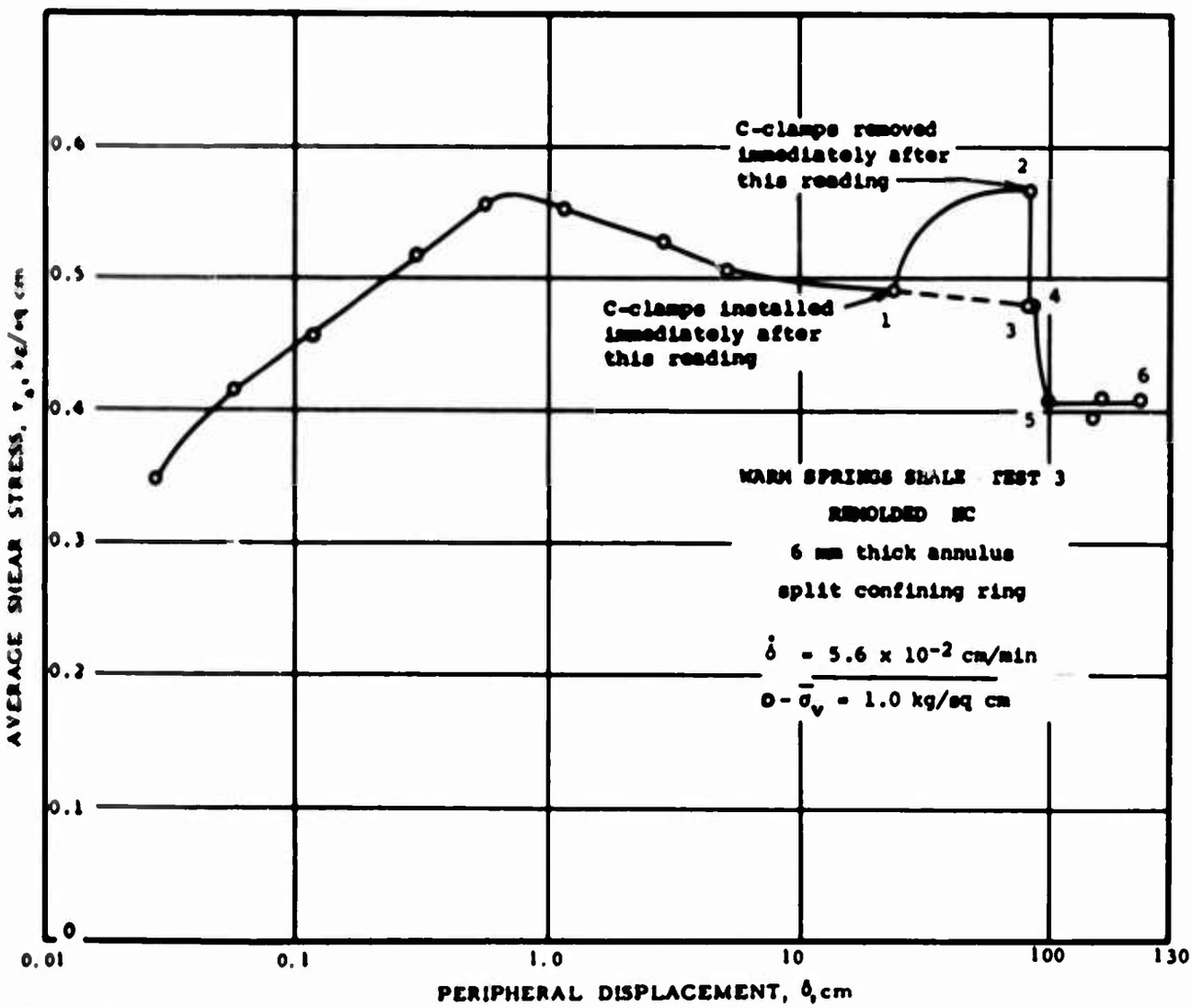
C-clamps removed immediately after this reading
C-clamps installed immediately after this reading
WARM SPRINGS SHALE TEST 3
REMOLDED MC
6 mm thick annulus
split confining ring
δ̇ = 5.6 x 10⁻² cm/min
σ - σ̄v = 1.0 kg/sq cm
AVERAGE SHEAR STRESS, τa, kg/sq cm
0.6
0.5
0.4
0.3
0.2
0.1
0
0.01
0.1
1.0
10
100
130
PERIPHERAL DISPLACEMENT, δ, cm

FIG. 6-19

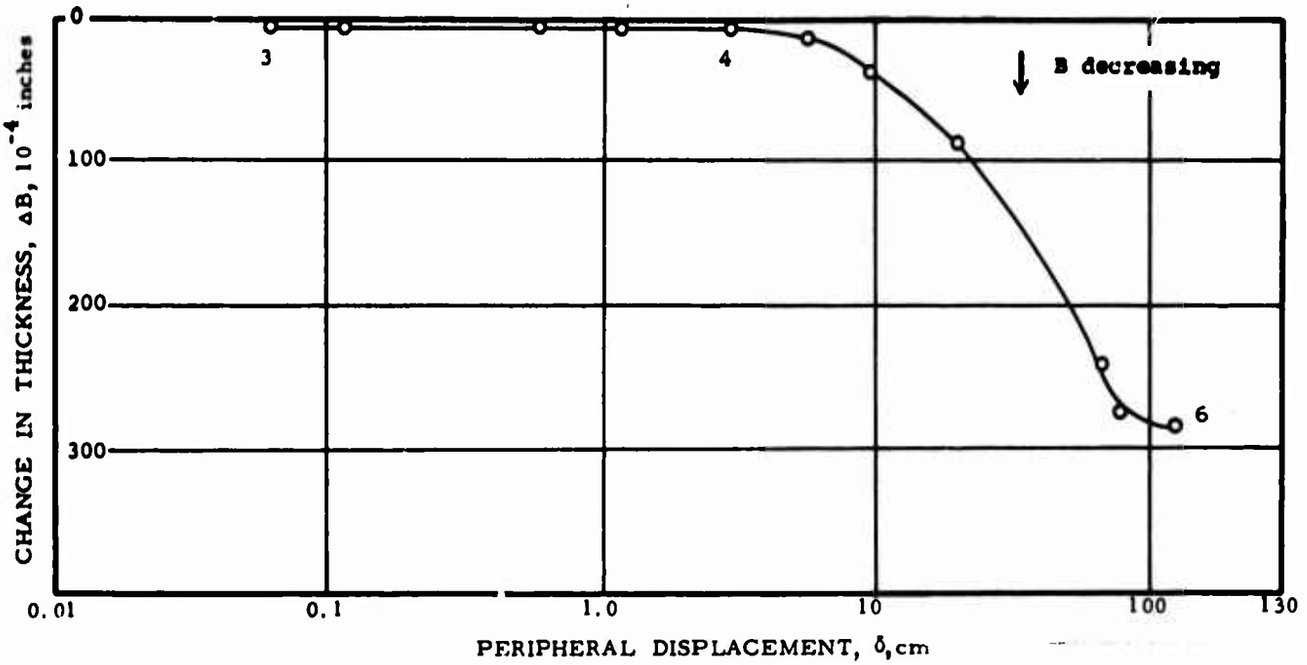
CHANGE IN THICKNESS, ΔB, 10^{-4} inches
0
100
200
300
3
4
6
B decreasing
0.01
0.1
1.0
10
100
130
PERIPHERAL DISPLACEMENT, δ, cm

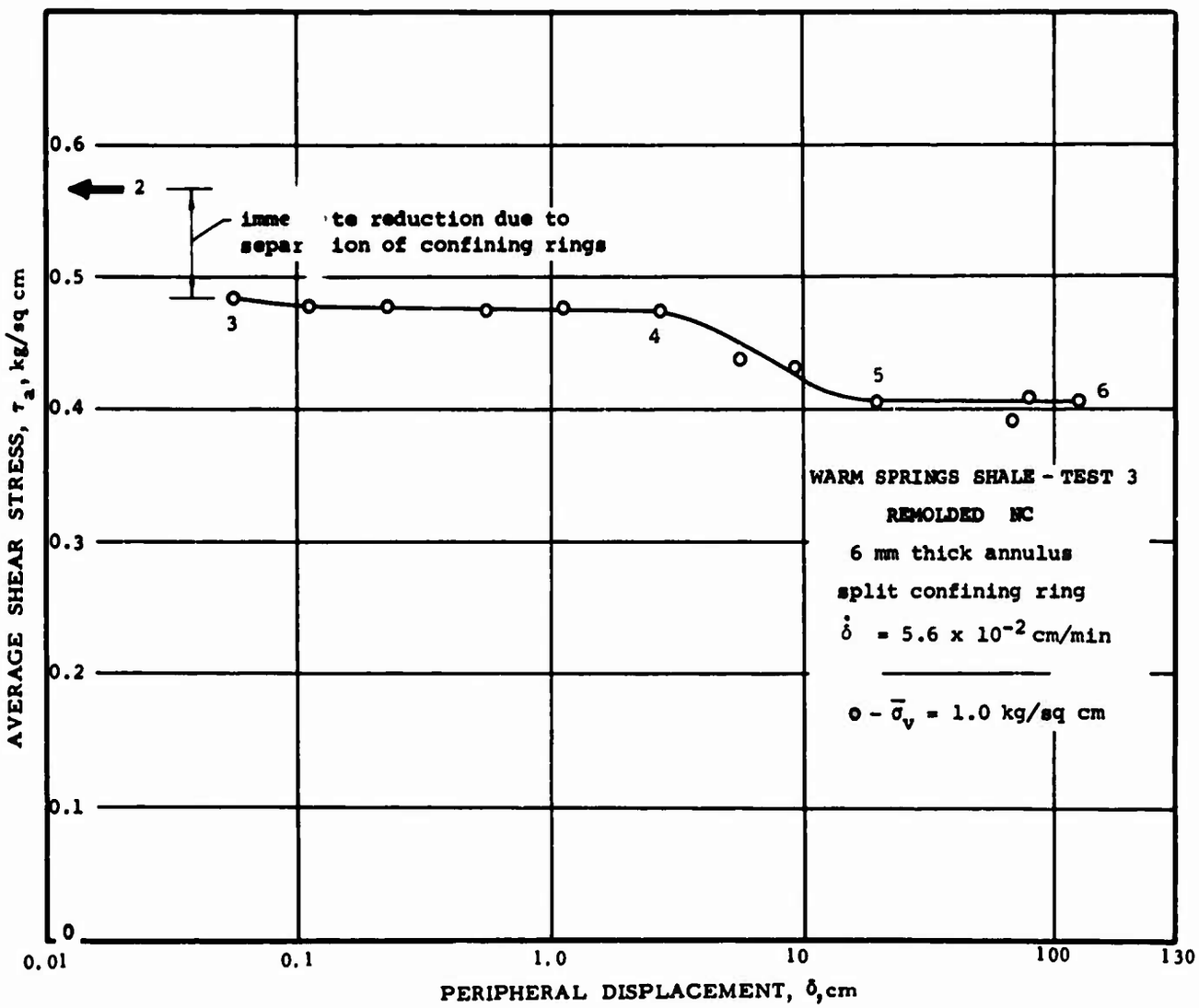
AVERAGE SHEAR STRESS, τ_a, kg/sq cm
0.6
0.5
0.4
0.3
0.2
0.1
0
2
imme te reduction due to
separ ion of confining rings
3
4
5
6
WARM SPRINGS SHALE - TEST 3
REMOLDED NC
6 mm thick annulus
split confining ring
$\dot{\delta}$ = 5.6 x 10^{-2} cm/min
$\sigma - \bar{\sigma}_v$ = 1.0 kg/sq cm
0.01
0.1
1.0
10
100
130
PERIPHERAL DISPLACEMENT, δ, cm

FIG. 6-20

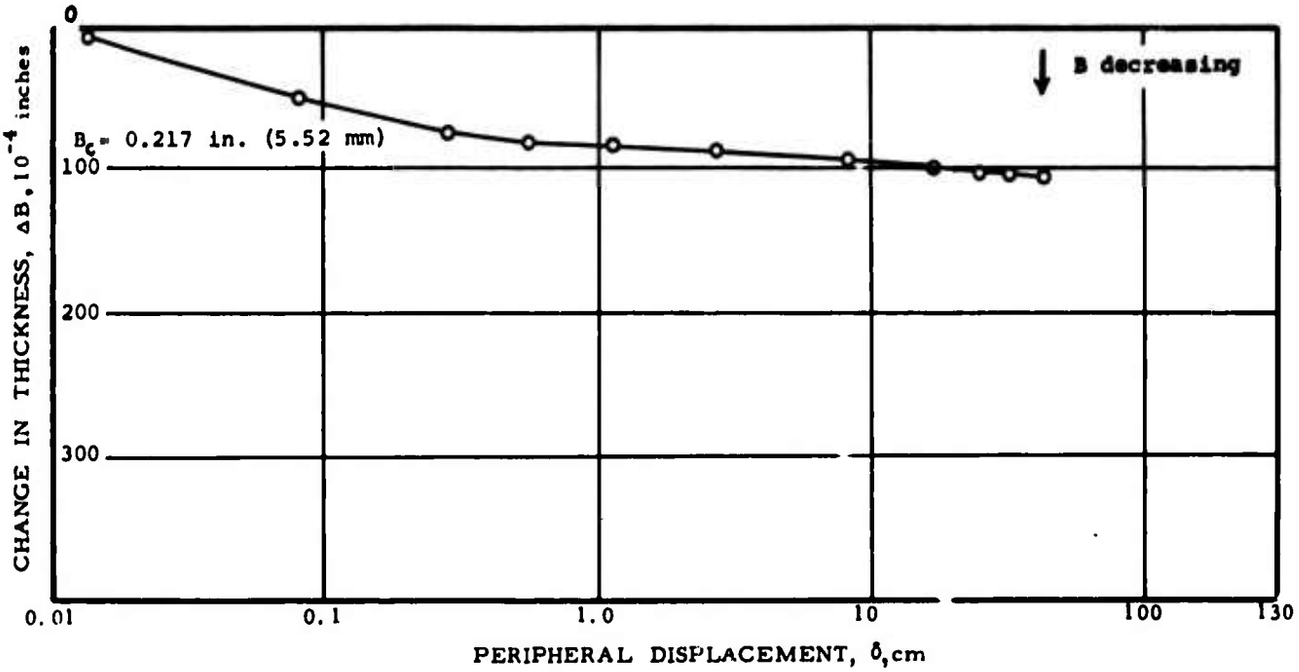
0
100
200
300
B decreasing
B_c = 0.217 in. (5.52 mm)
CHANGE IN THICKNESS, ΔB, 10^{-4} inches
0.01
0.1
1.0
10
100
130
PERIPHERAL DISPLACEMENT, δ, cm

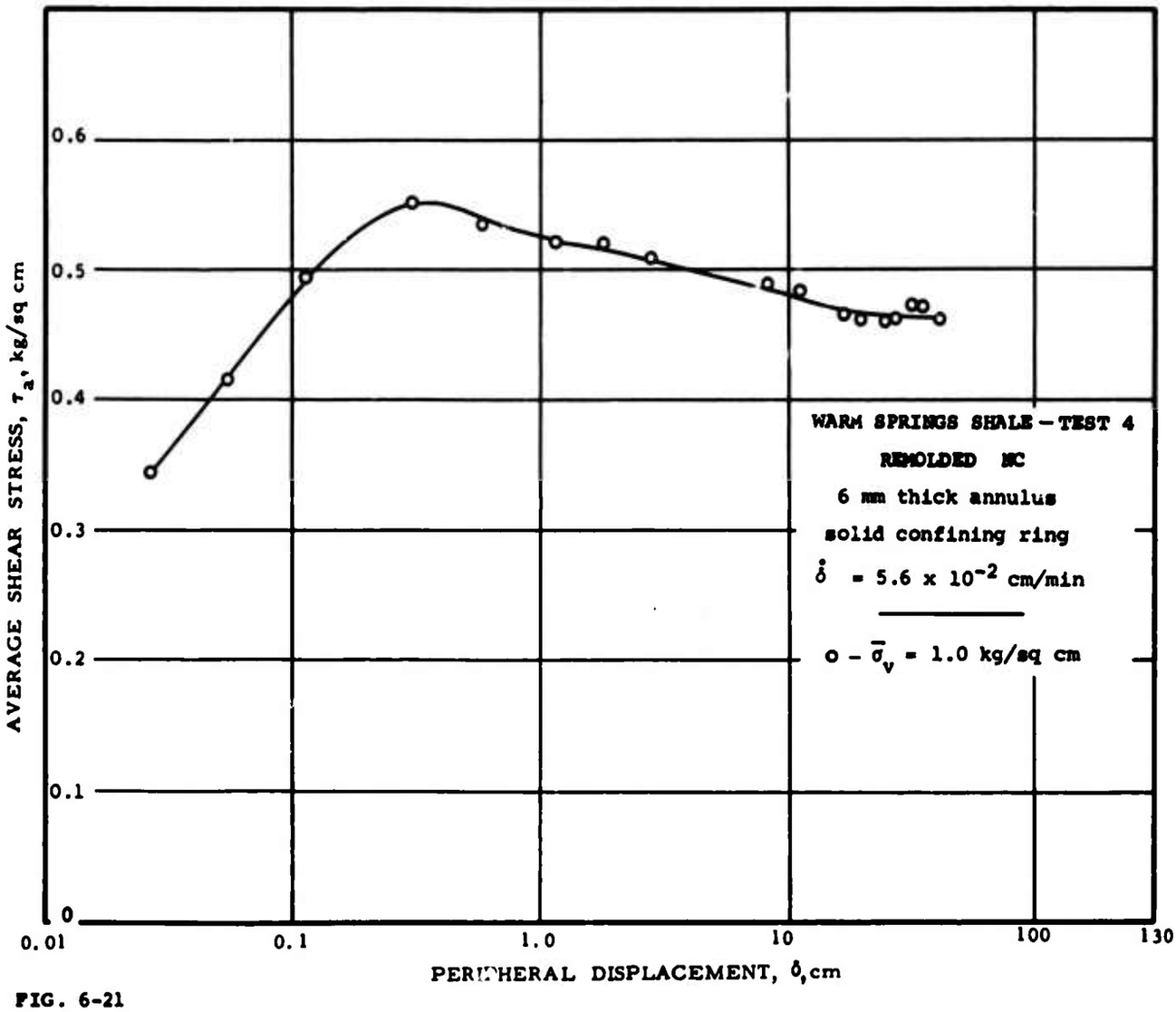
0.6
0.5
0.4
0.3
0.2
0.1
0
AVERAGE SHEAR STRESS, τ_a, kg/sq cm
WARM SPRINGS SHALE – TEST 4
REMOLDED NC
6 mm thick annulus
solid confining ring
$\dot{\delta}$ = 5.6 x 10^{-2} cm/min
o – $\bar{\sigma}_v$ = 1.0 kg/sq cm
0.01
0.1
1.0
10
100
130
PERIPHERAL DISPLACEMENT, δ, cm

FIG. 6-21

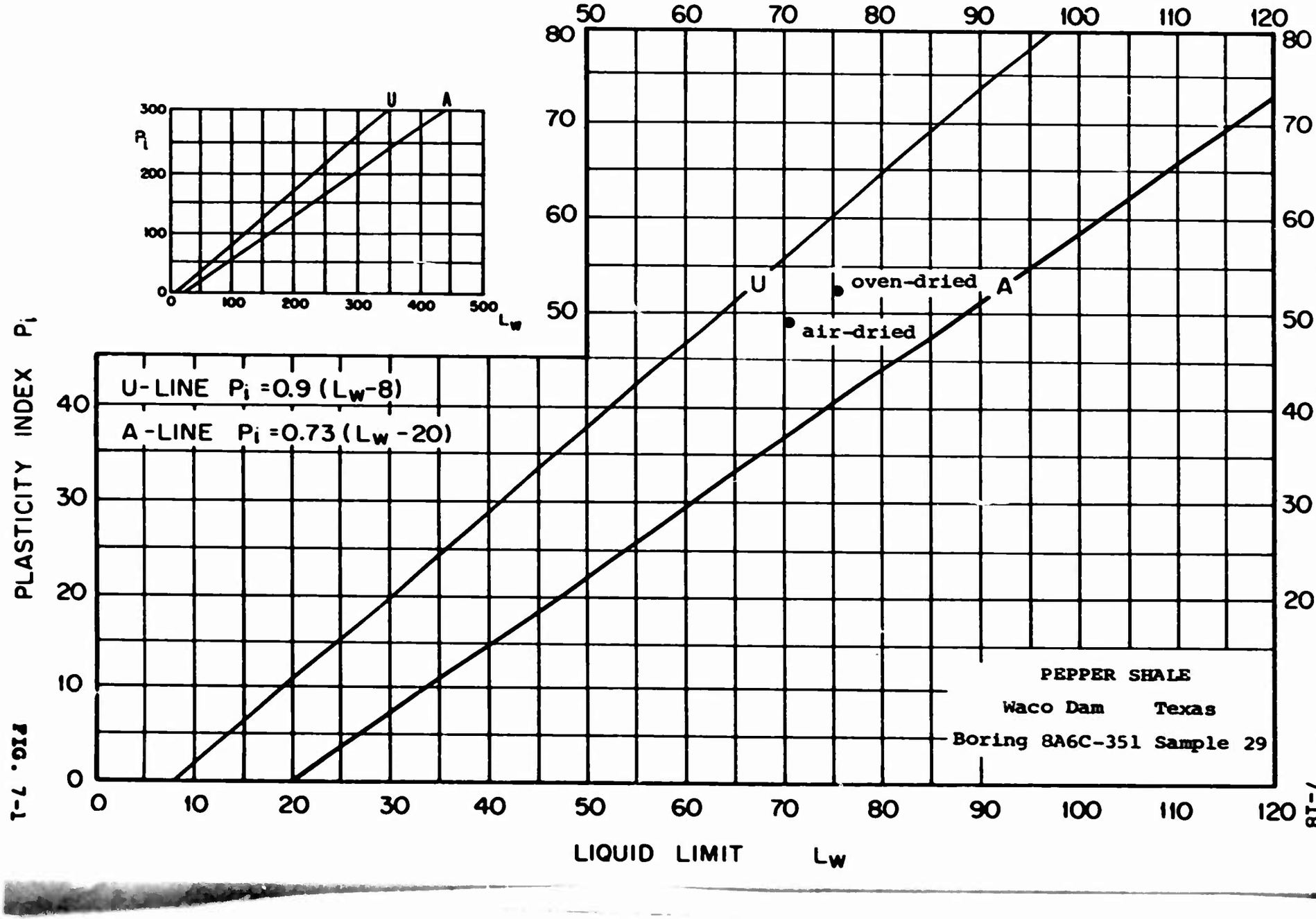
U-LINE $P_i = 0.9 (L_w - 8)$
A-LINE $P_i = 0.73 (L_w - 20)$
U
A
oven-dried
air-dried
PEPPER SHALE
Waco Dam Texas
Boring 8A6C-351 Sample 29
PLASTICITY INDEX P_i
LIQUID LIMIT L_w
0 10 20 30 40 50 60 70 80 90 100 110 120
0 10 20 30 40 50 60 70 80
P_i
0 100 200 300
0 100 200 300 400 500 L_w

FIG. 7-1

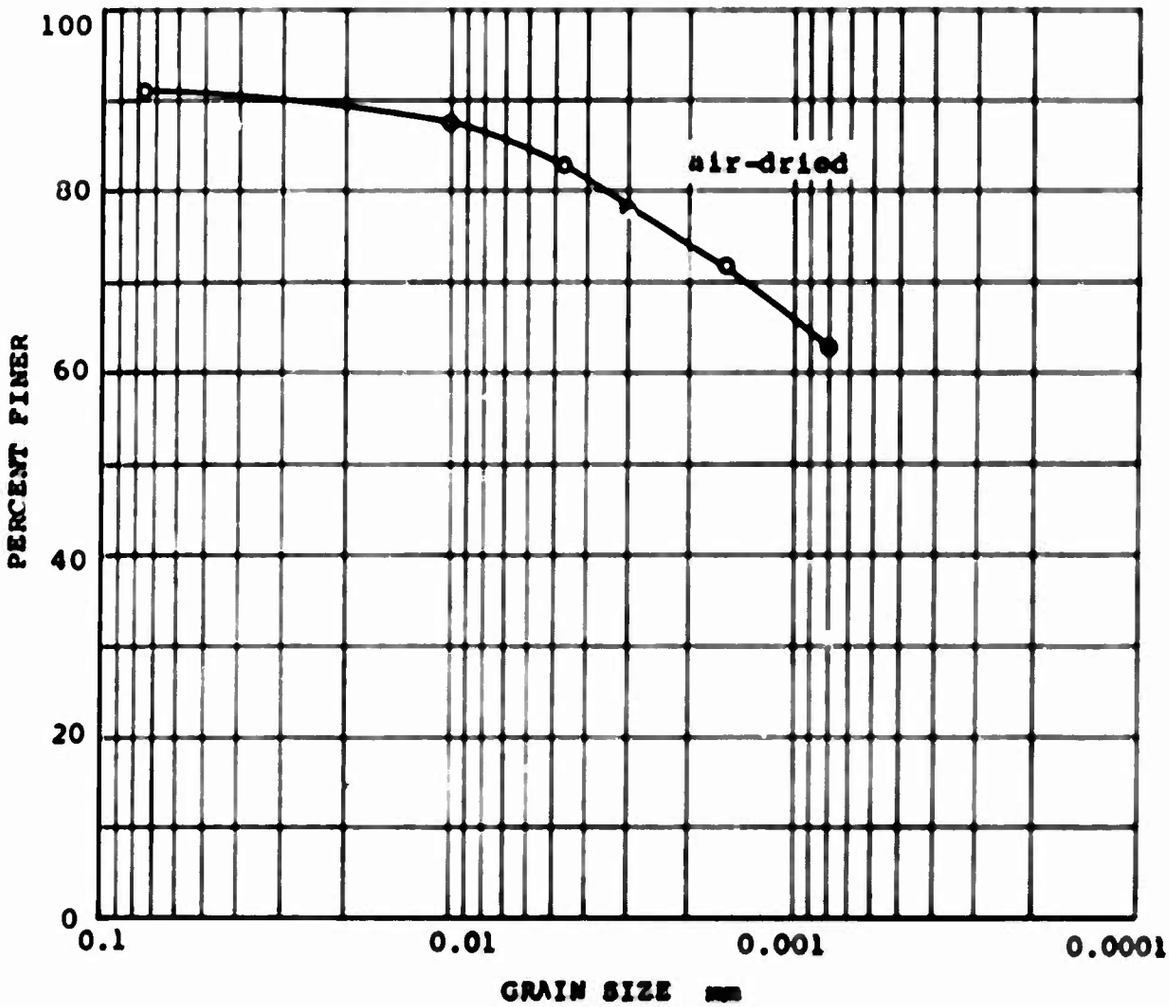

PEPPER SHALE

Waco Dam Texas

Boring BA6C-351 Sample 29

FIG. 7-2

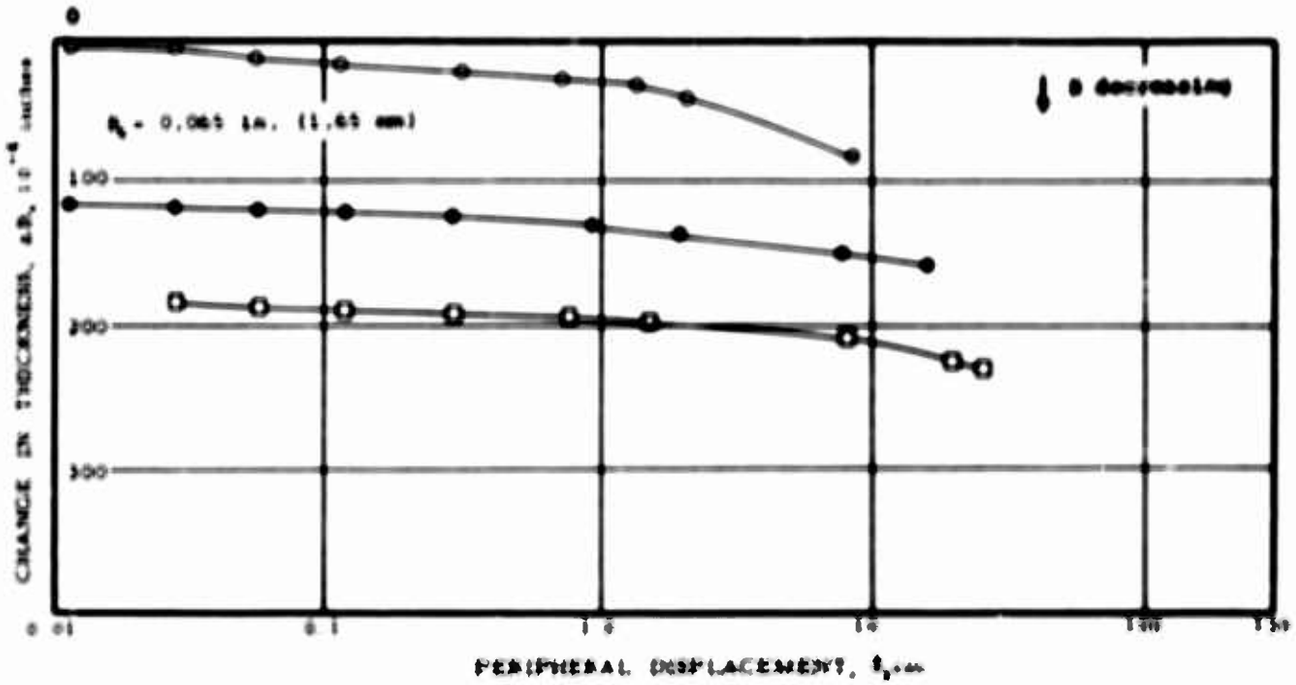
CHANGE IN THICKNESS, Δh, 10^{-4} inches
h_0 = 0.065 in. (1.65 mm)
h decreasing
100
200
300
0.01
0.1
1.0
10
100
PERIPHERAL DISPLACEMENT, δ, cm

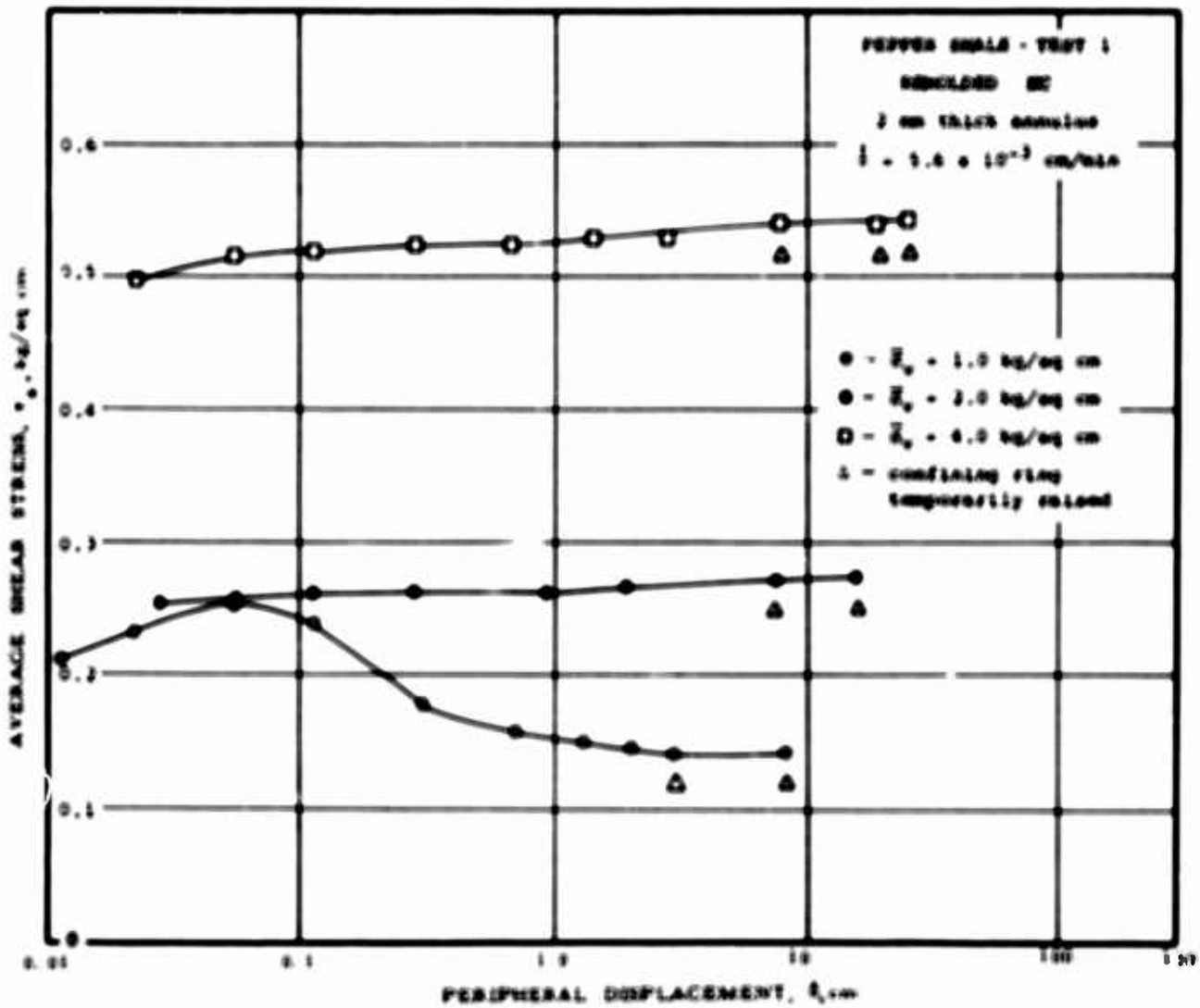
AVERAGE SHEAR STRESS, τ_a, kg/sq cm
PEPPER SHALE - TEST 1
RECOLDED BC
2 cm thick annulus
i = 1.6 x 10^{-3} cm/min
● - $\bar{\sigma}_v$ = 1.0 kg/sq cm
● - $\bar{\sigma}_v$ = 2.0 kg/sq cm
□ - $\bar{\sigma}_v$ = 4.0 kg/sq cm
Δ - confining ring temporarily relaxed
0.6
0.5
0.4
0.3
0.2
0.1
0
0.01
0.1
1.0
10
100
PERIPHERAL DISPLACEMENT, δ, cm

FIG. 7-3

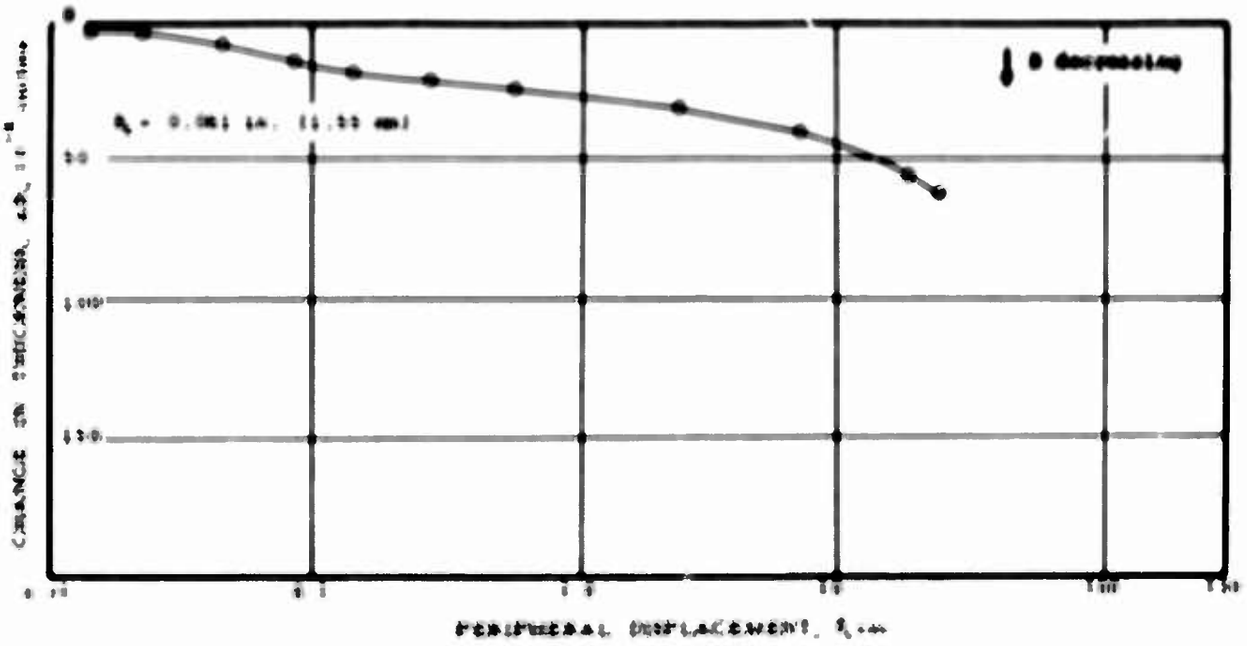

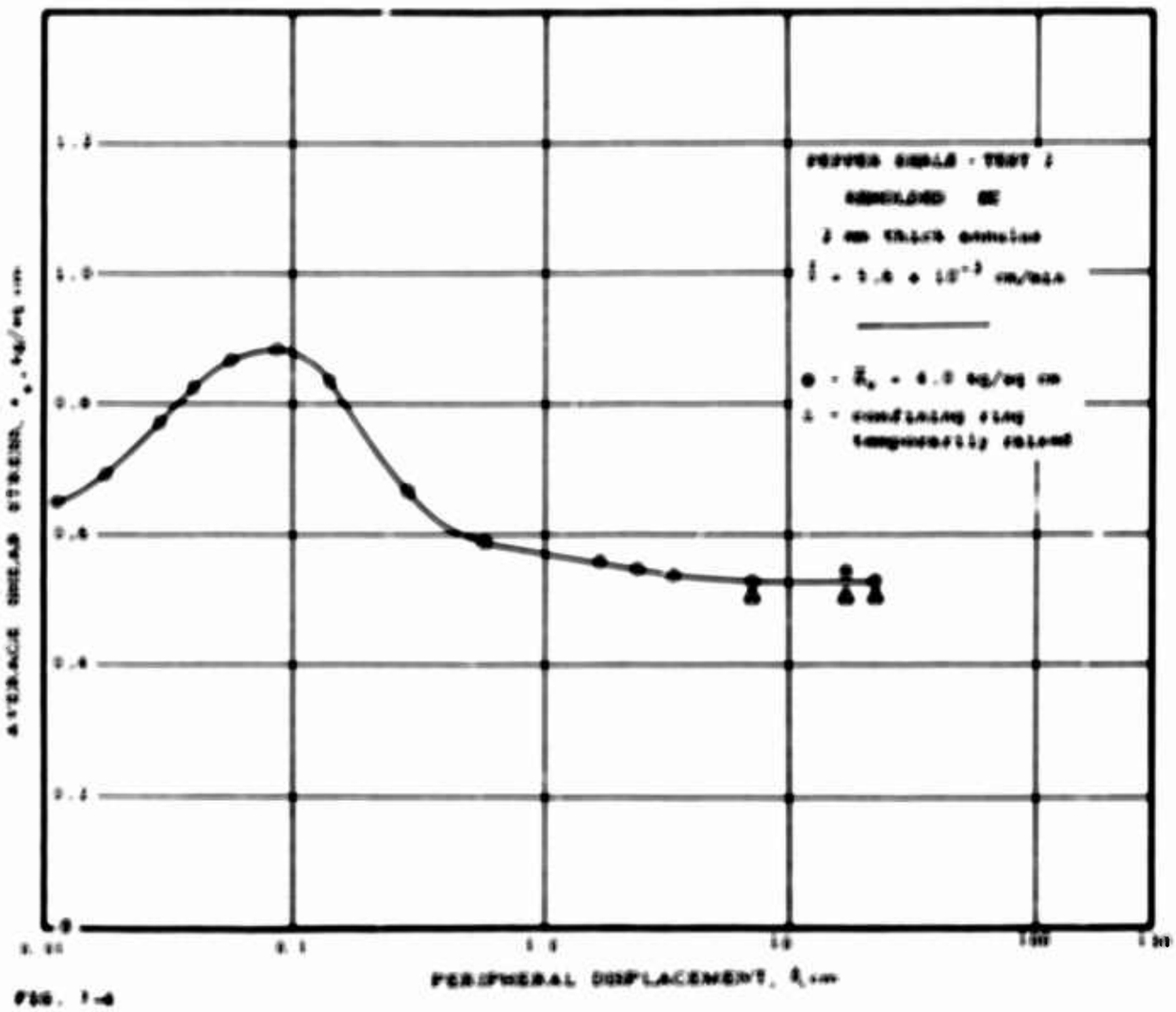

FIG. 7-6

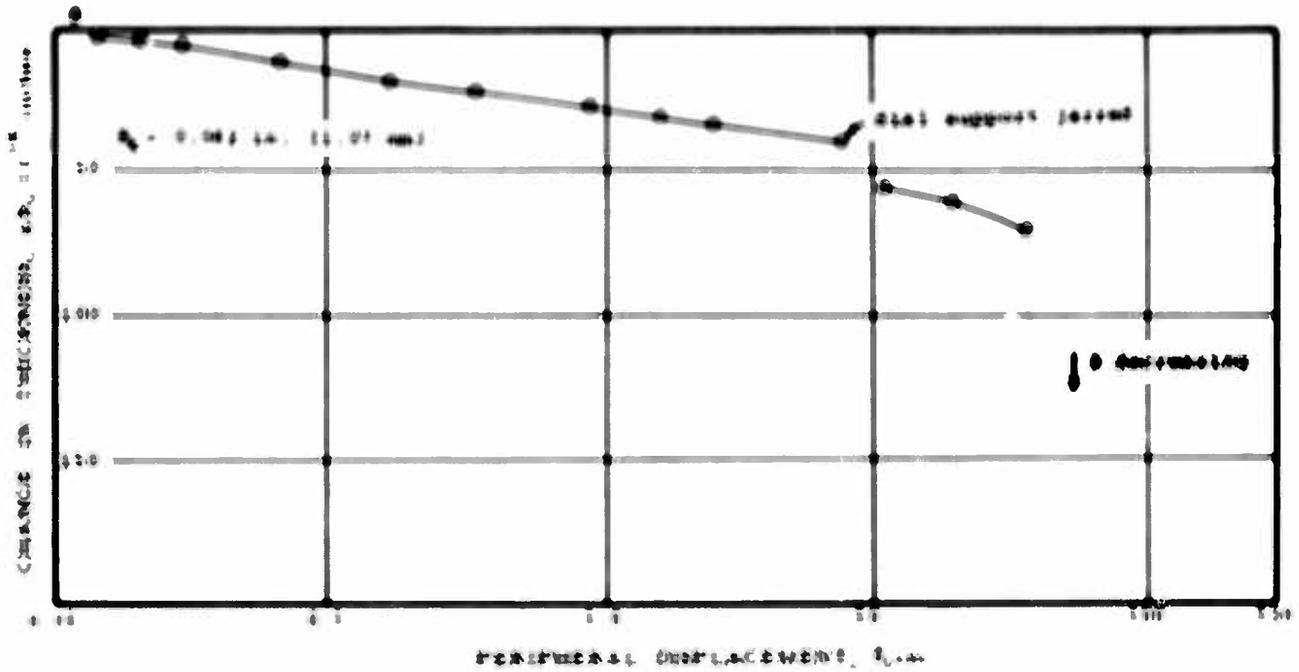

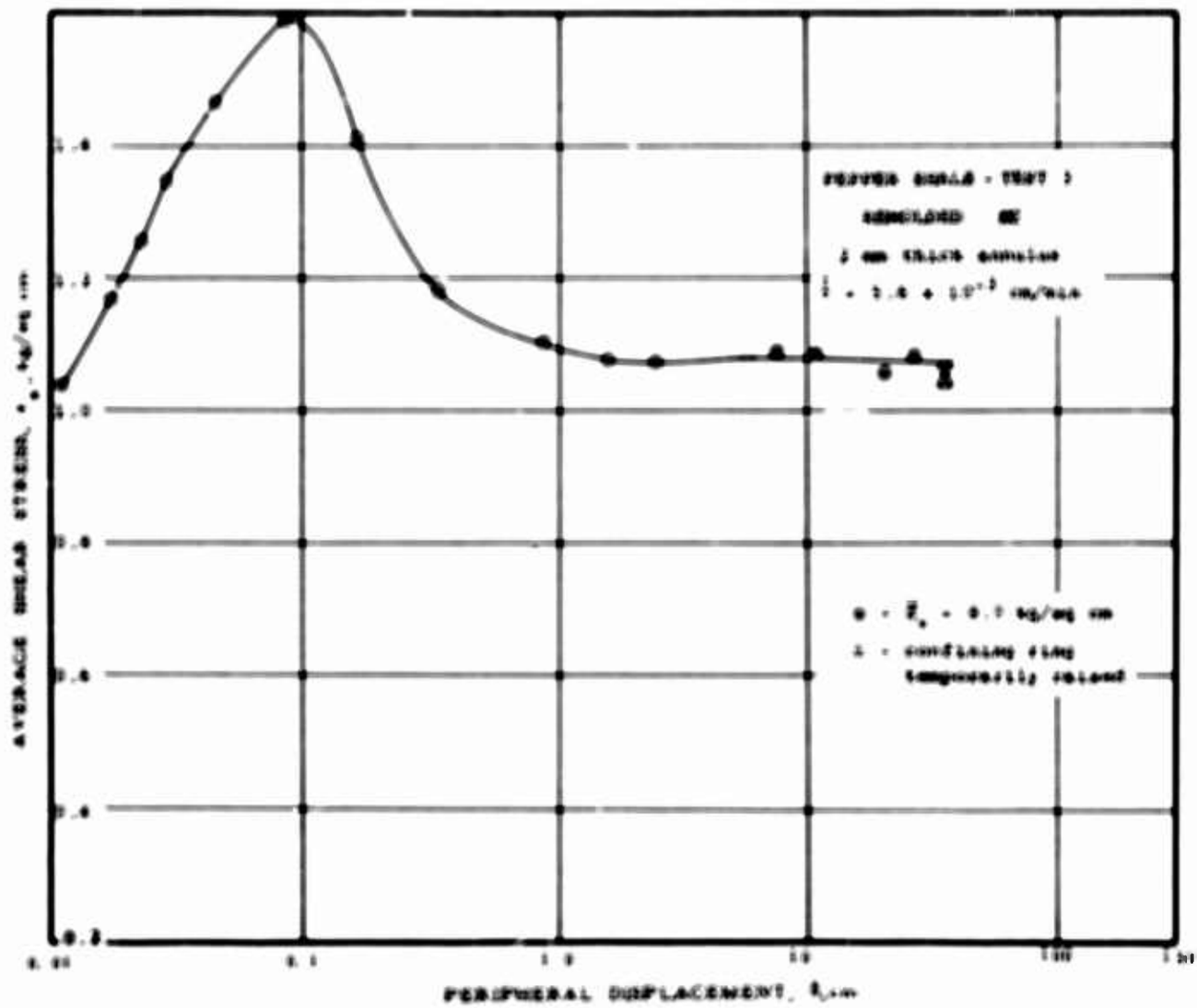

FIG. 1-4

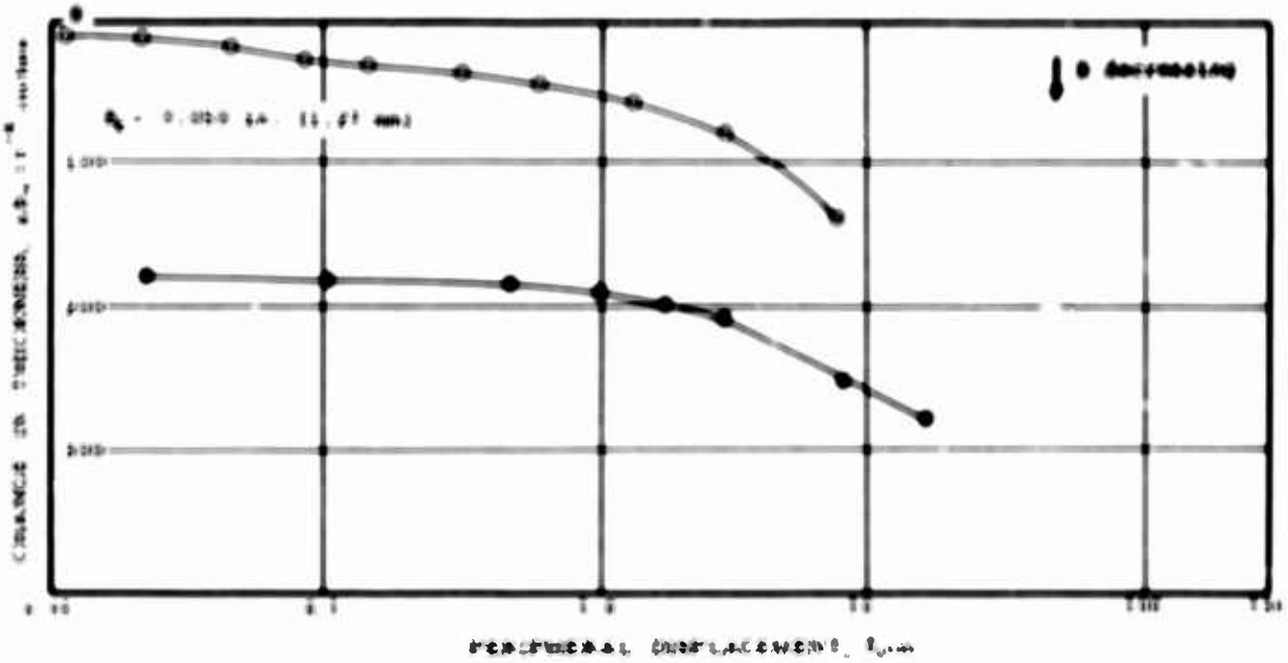

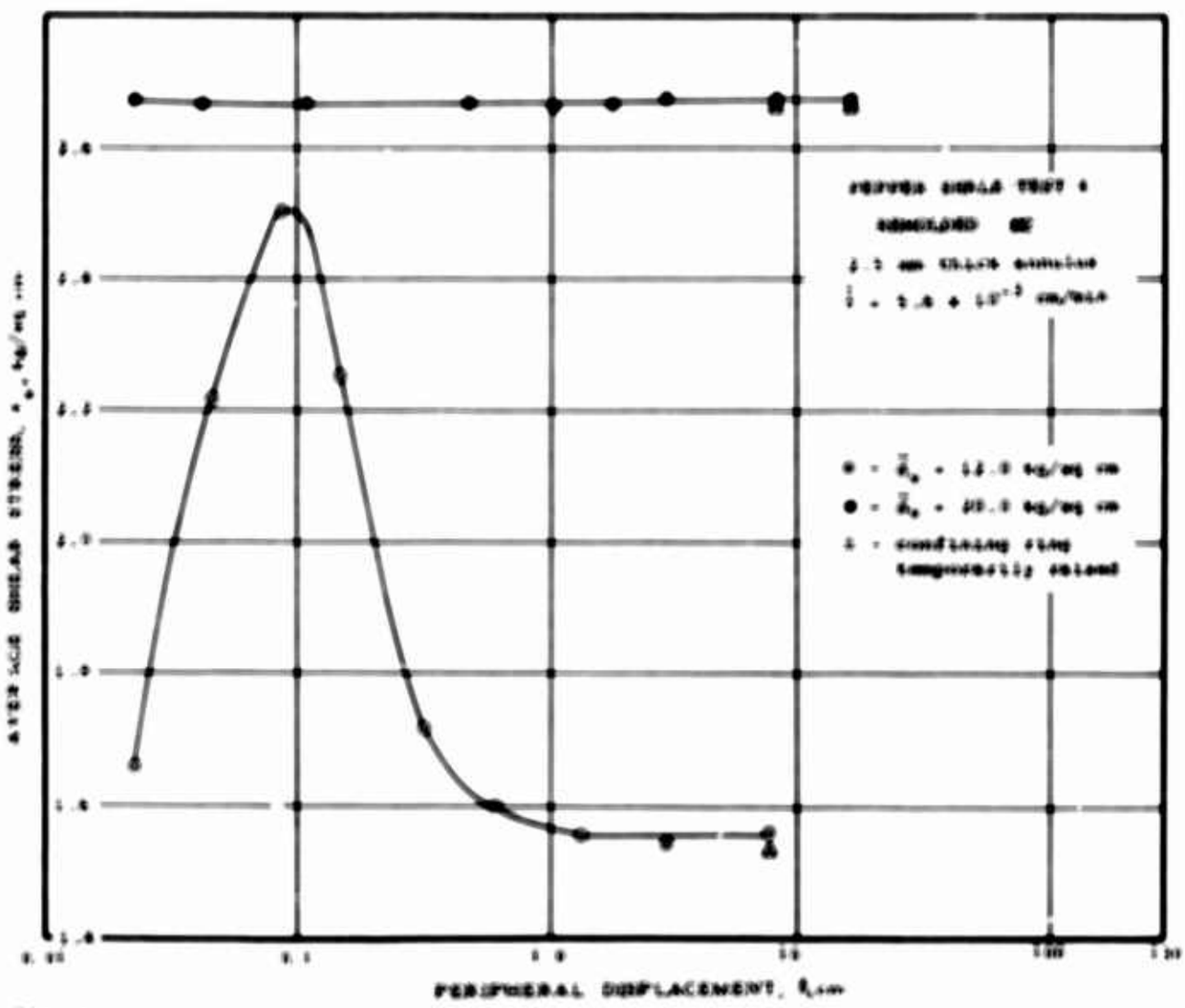

FIG. 1-6

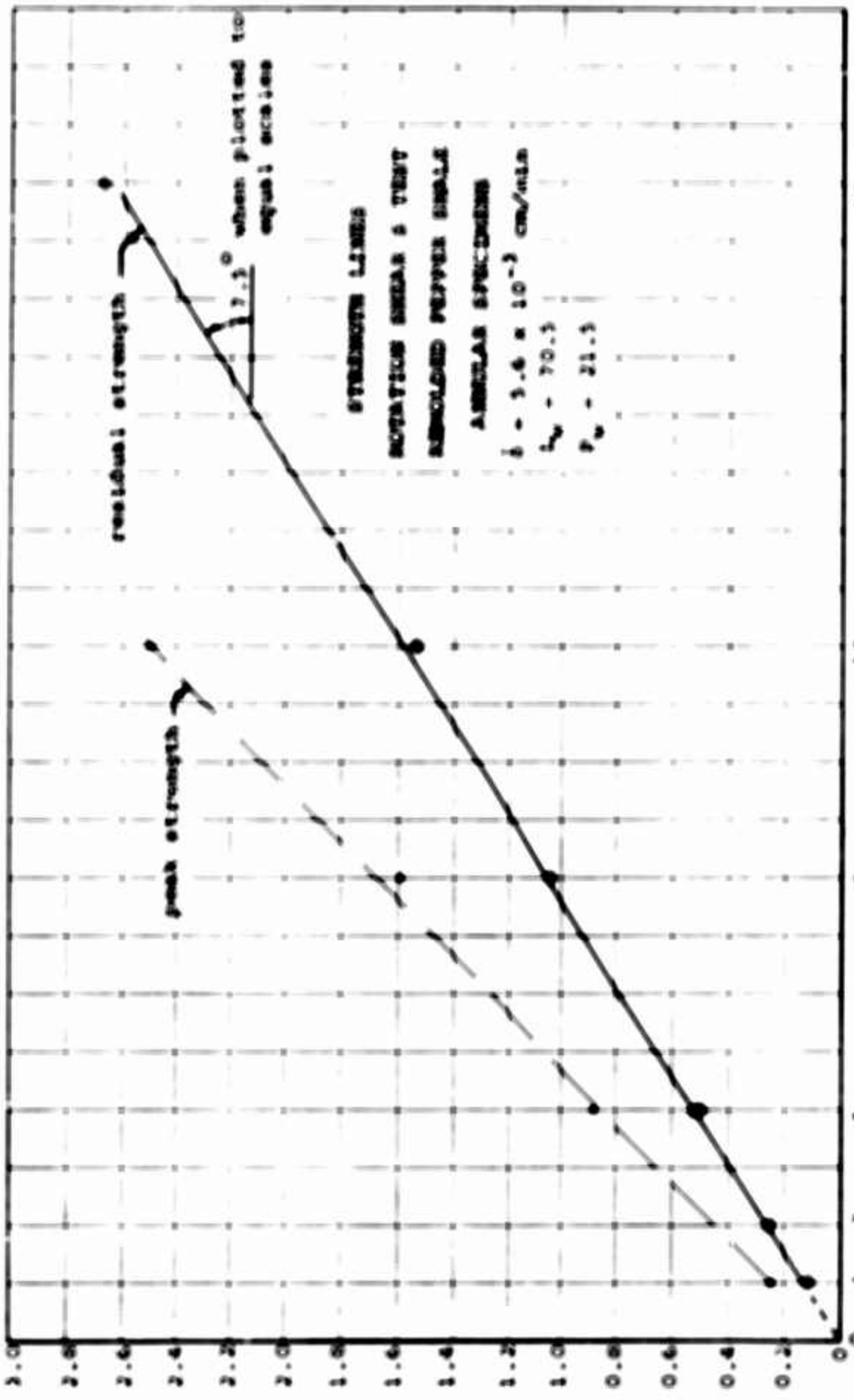
residual strength
peak strength
12.5° when plotted to equal scales
STRAIGHT LINES
REPRESENT SHEAR & TENT
REMOLDED PEPPER SHALE
AMBERLAR SPECIMENS
k = 3.6 x 10⁻² cm/min
h_c = 70.5
P_c = 21.5
0
4
8
12
20
EFFECTIVE VERTICAL STRESS, σ'_v, kg/sq cm
SHEAR STRENGTH, τ_p and τ_r, kg/sq cm

FIG. 7-7

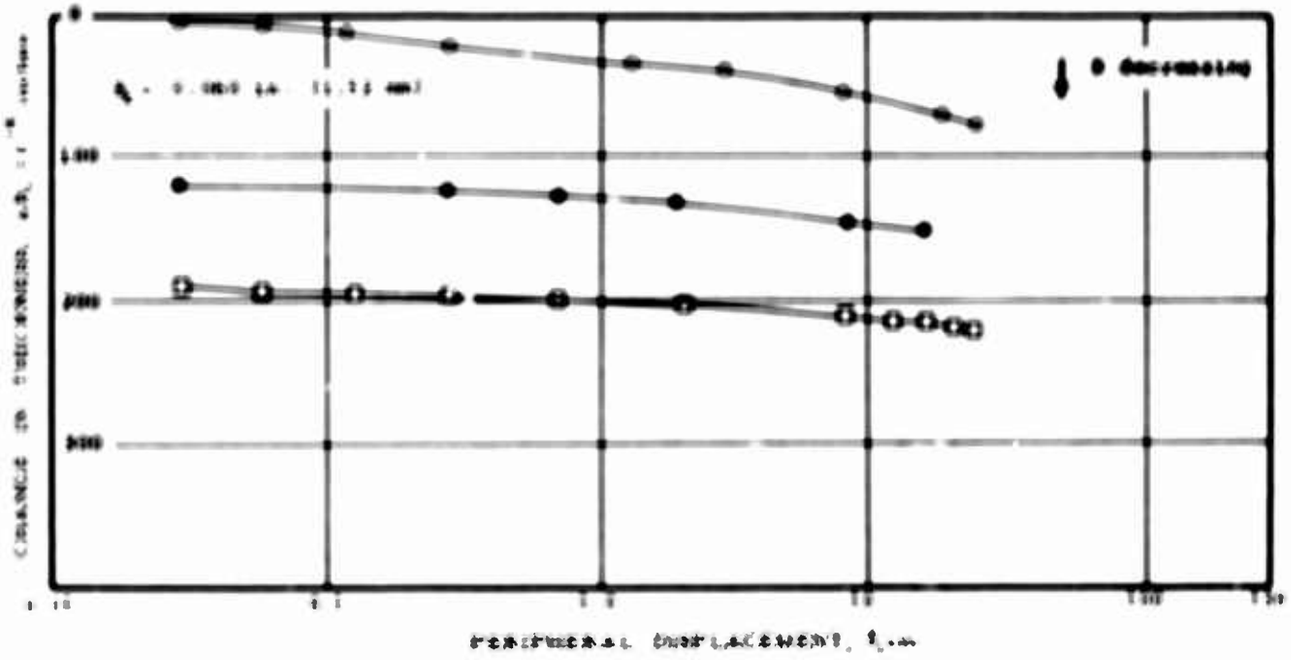

PERIPHERAL DISPLACEMENT, δ_{cm}

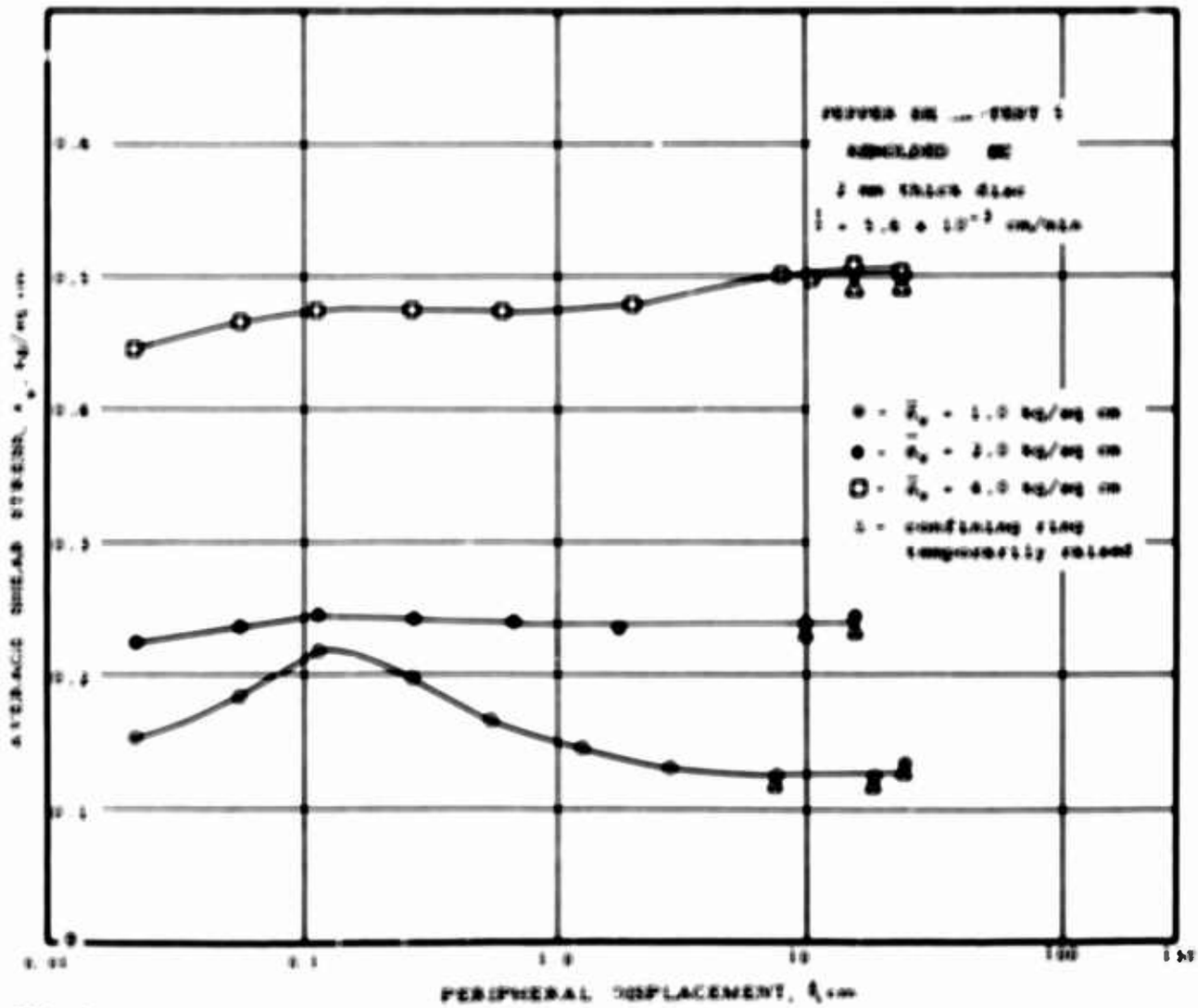

AVERAGE SHEAR STRESS, τ_{av}, kg/sq cm

PERIPHERAL DISPLACEMENT, δ_{cm}

FIG. 7-8

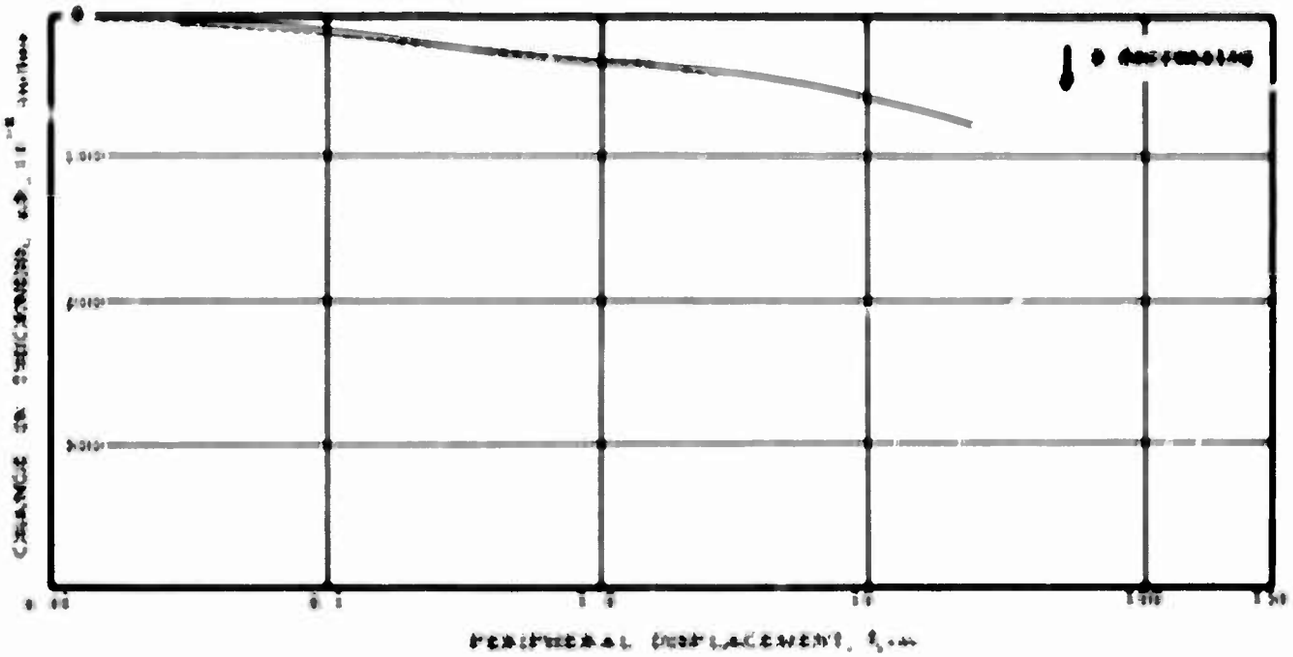

PERIPHERAL DISPLACEMENT, δ, cm

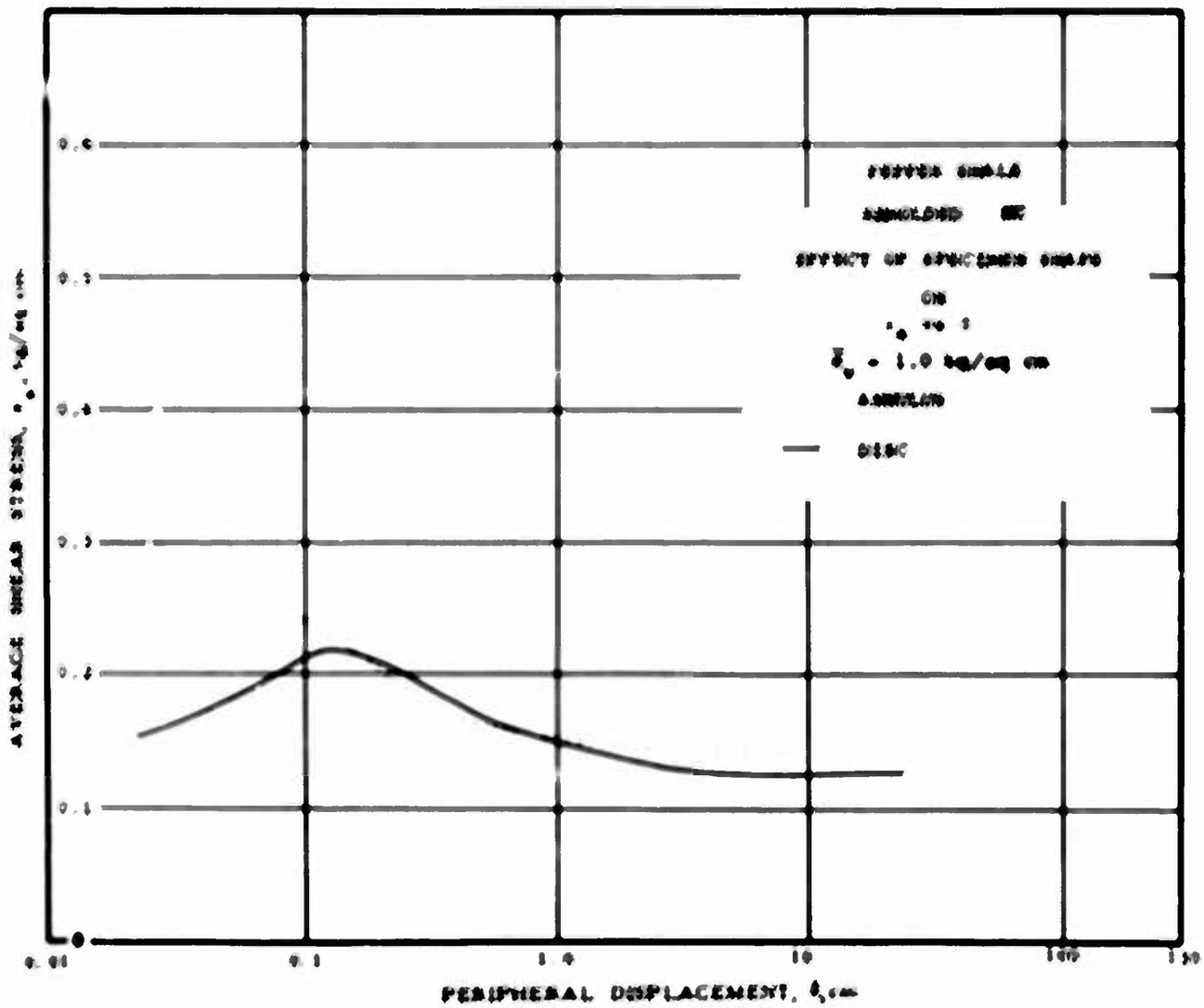

PERIPHERAL DISPLACEMENT, δ, cm

FIG. 7-9

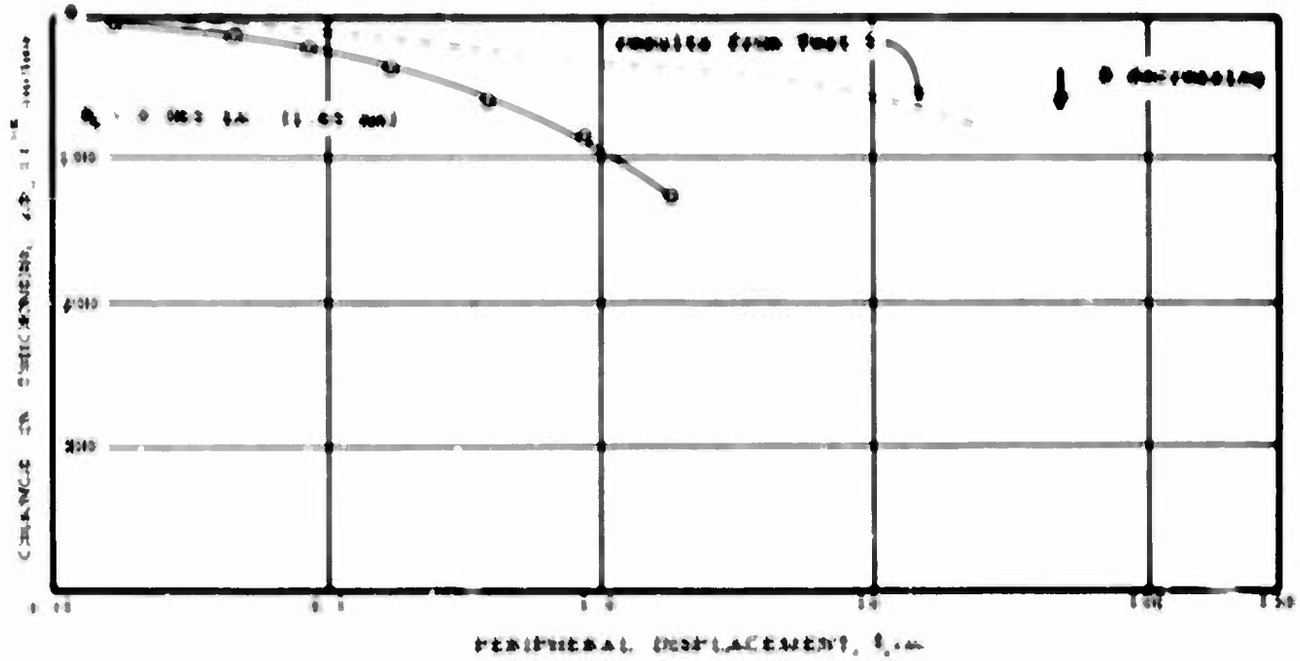
results from Test 5
σ decreasing
PERIPHERAL DISPLACEMENT, δ, cm

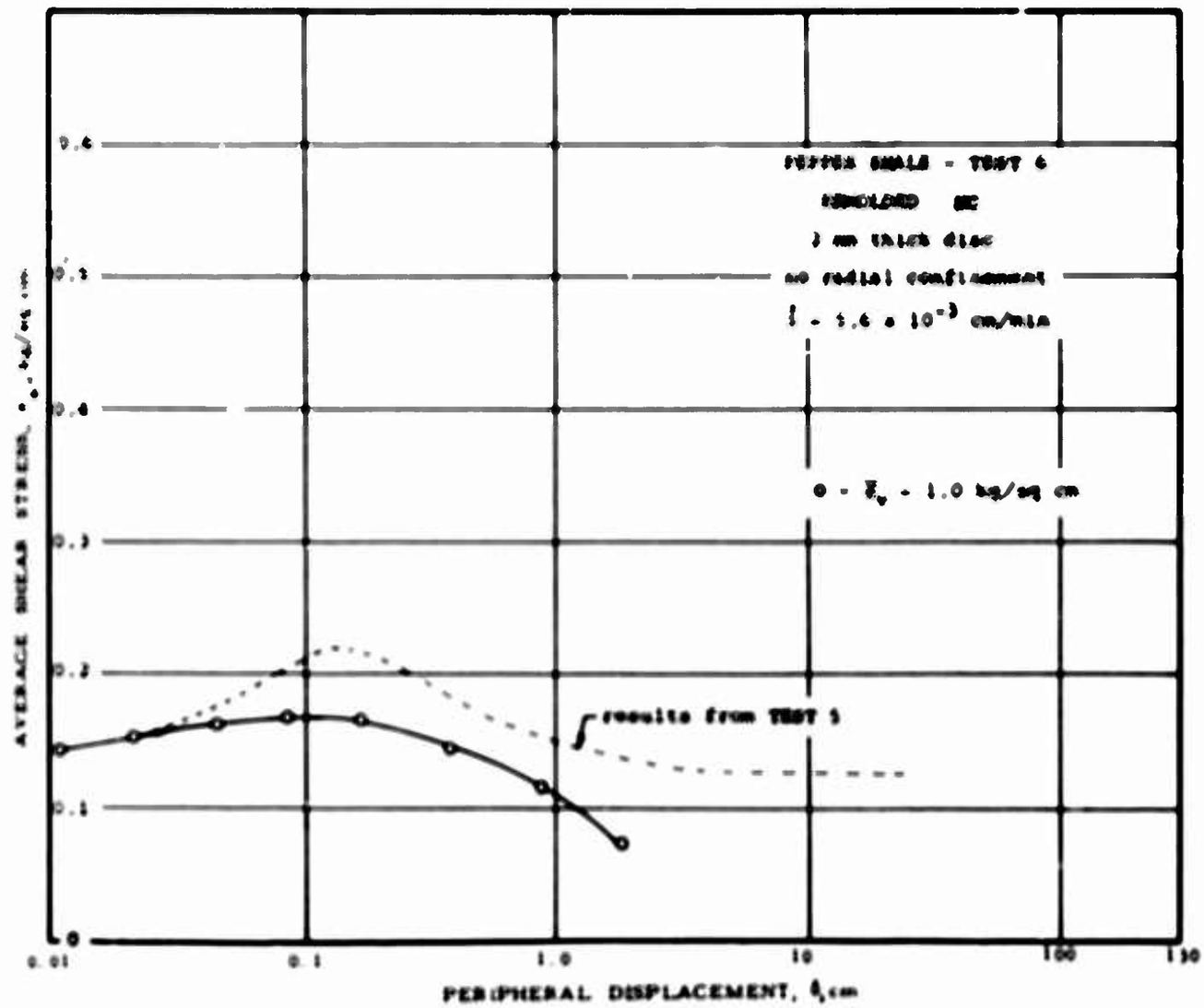
PEPPER SHALE - TEST 6
REMOLDED
3 cm thick disc
no radial confinement
I = 1.6 x 10⁻³ cm/min
0 - σ_v - 1.0 kg/sq cm
results from TEST 5
AVERAGE SHEAR STRESS, τ, kg/sq cm
PERIPHERAL DISPLACEMENT, δ, cm

FIG. 7-10

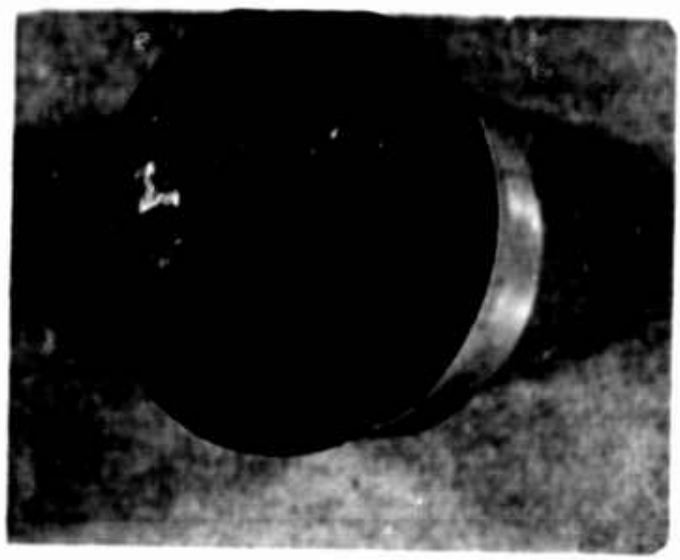

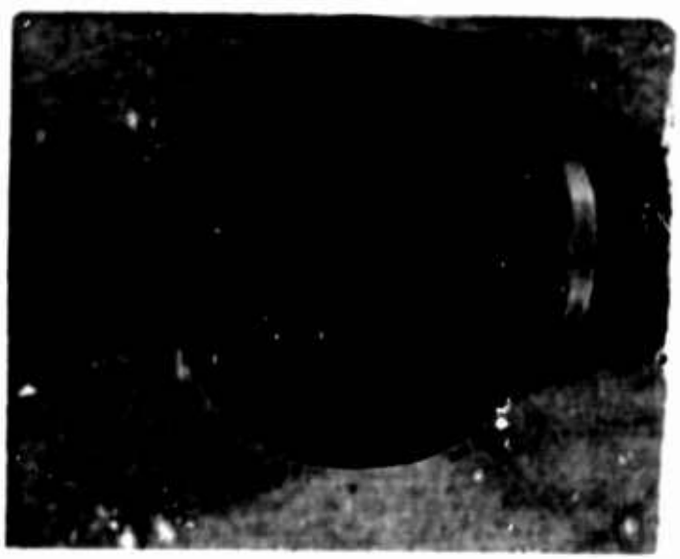

PEPPER SHALE TEST 6

REMOLDED [redacted]

no radial confinement

FIG. 7-11

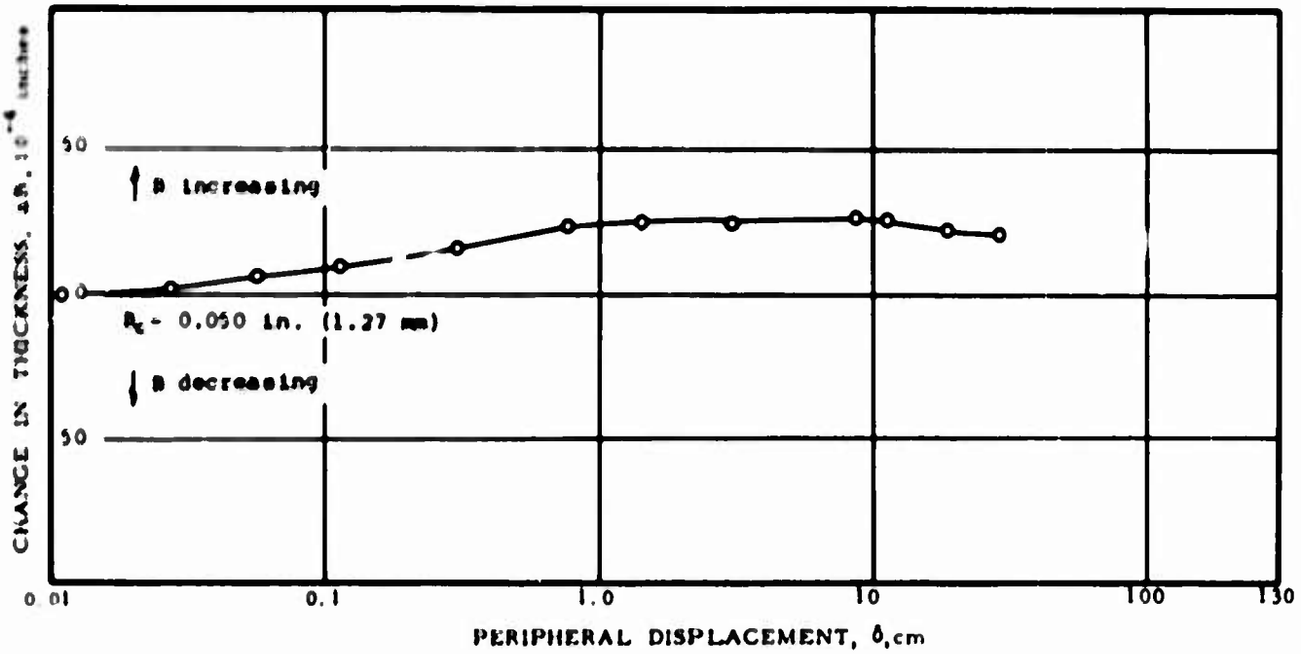
50
δ increasing
0
R_c = 0.050 in. (1.27 mm)
δ decreasing
50
0.01
0.1
1.0
10
100
130
PERIPHERAL DISPLACEMENT, δ,cm

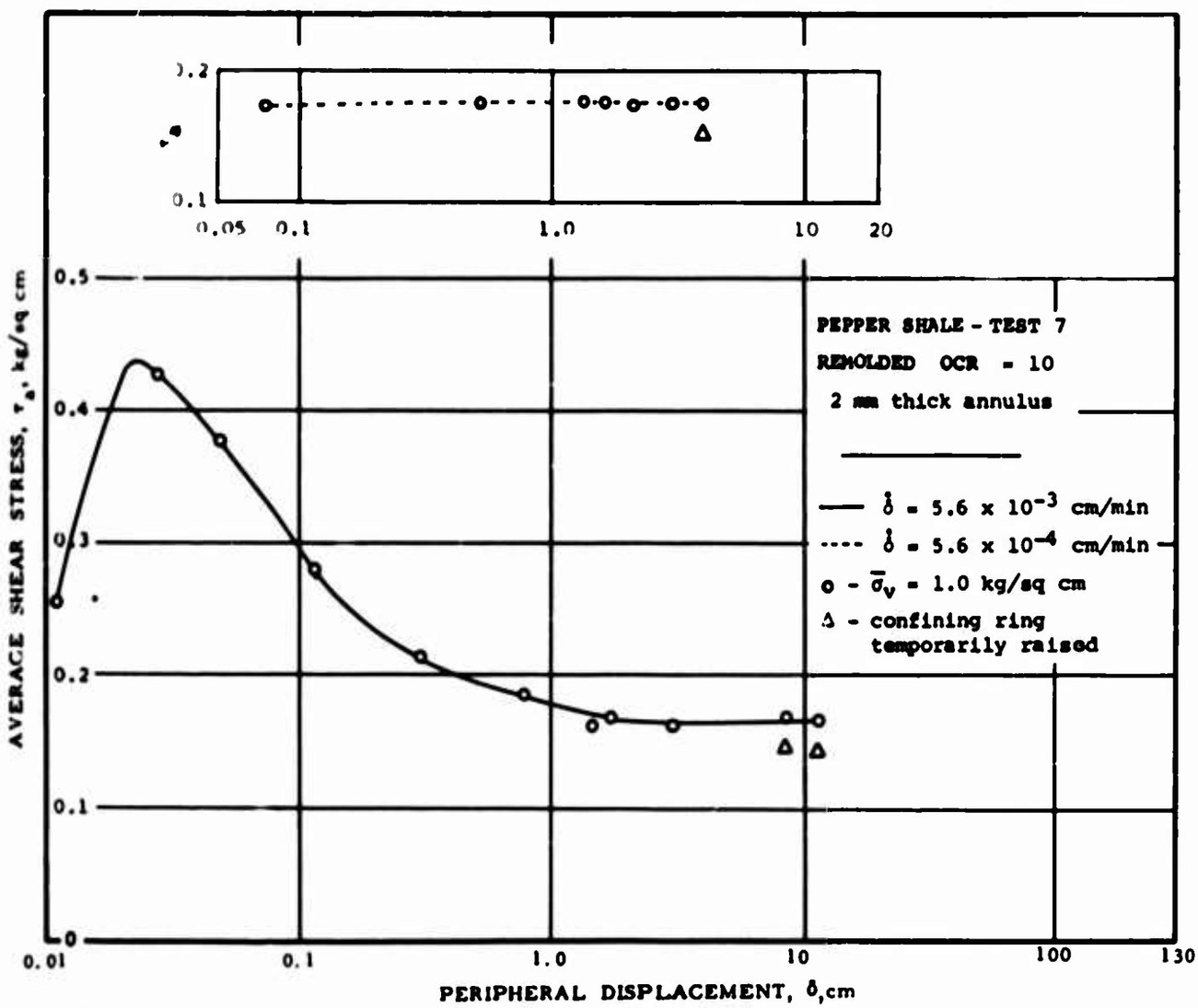
0.2
0.1
0.05
0.1
1.0
10
20
0.5
0.4
0.3
0.2
0.1
0
AVERAGE SHEAR STRESS, τ_a, kg/sq cm
PEPPER SHALE - TEST 7
REMOLDED OCR = 10
2 mm thick annulus
$\dot{\delta}$ = 5.6 x 10^{-3} cm/min
$\dot{\delta}$ = 5.6 x 10^{-4} cm/min
o - $\bar{\sigma}_v$ = 1.0 kg/sq cm
Δ - confining ring temporarily raised
0.01
0.1
1.0
10
100
130
PERIPHERAL DISPLACEMENT, δ,cm

FIG. 7-12

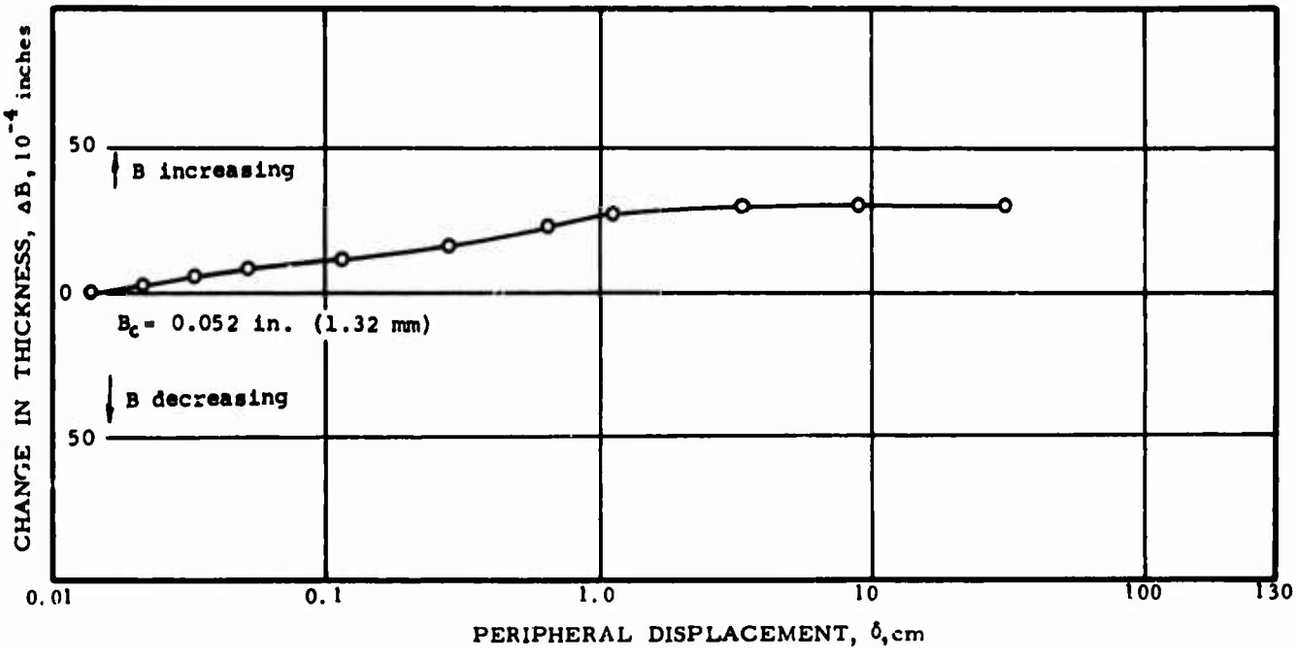
CHANGE IN THICKNESS, ΔB, 10^{-4} inches
50
B increasing
0
B_c = 0.052 in. (1.32 mm)
B decreasing
50
0.01
0.1
1.0
10
100
130
PERIPHERAL DISPLACEMENT, δ, cm

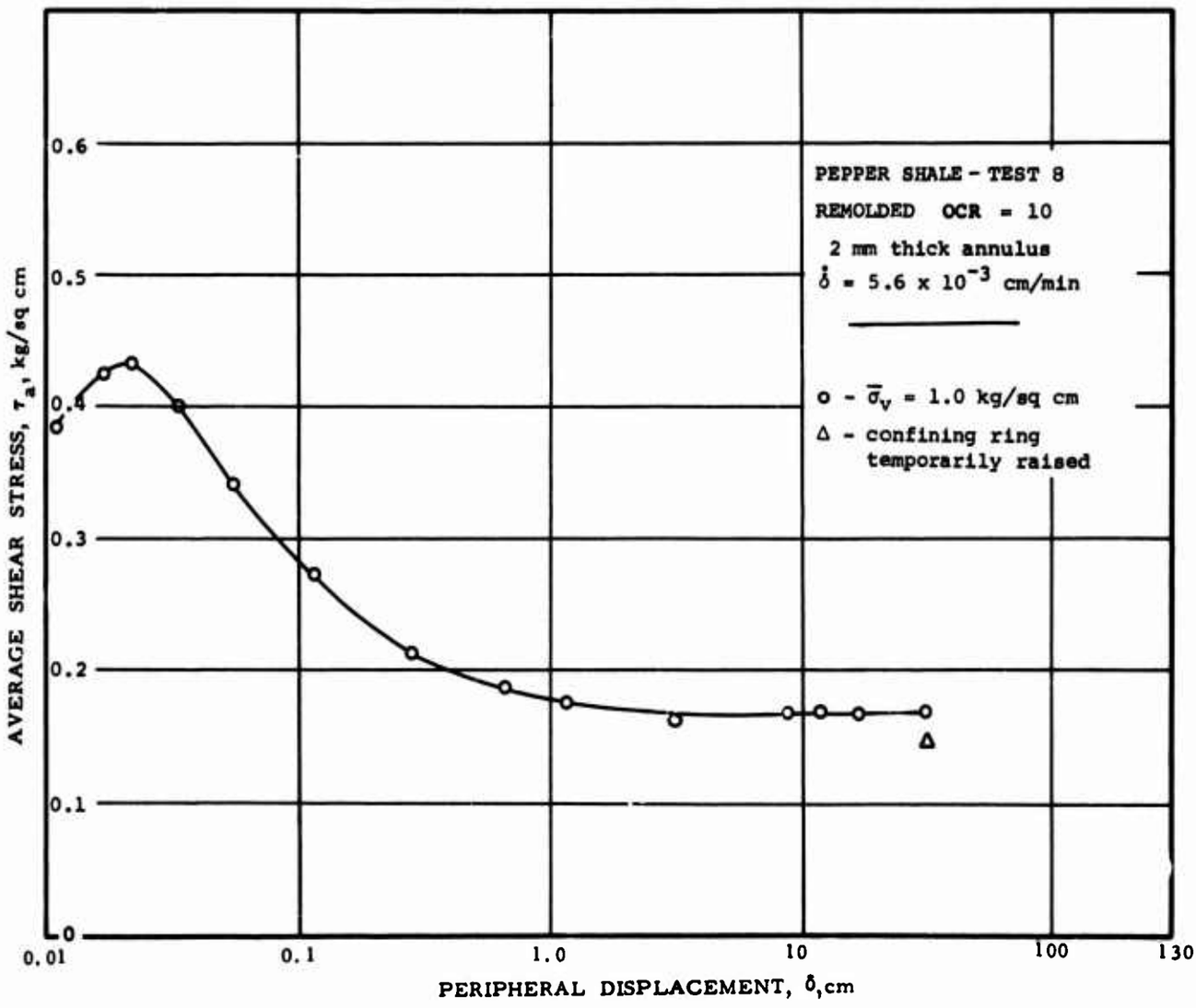
AVERAGE SHEAR STRESS, τ_a, kg/sq cm
0.6
0.5
0.4
0.3
0.2
0.1
0
PEPPER SHALE - TEST 8
REMOLDED OCR = 10
2 mm thick annulus
$\dot{\delta}$ = 5.6 x 10^{-3} cm/min
o - $\bar{\sigma}_v$ = 1.0 kg/sq cm
Δ - confining ring temporarily raised
Δ
0.01
0.1
1.0
10
100
130
PERIPHERAL DISPLACEMENT, δ, cm

FIG. 7-13

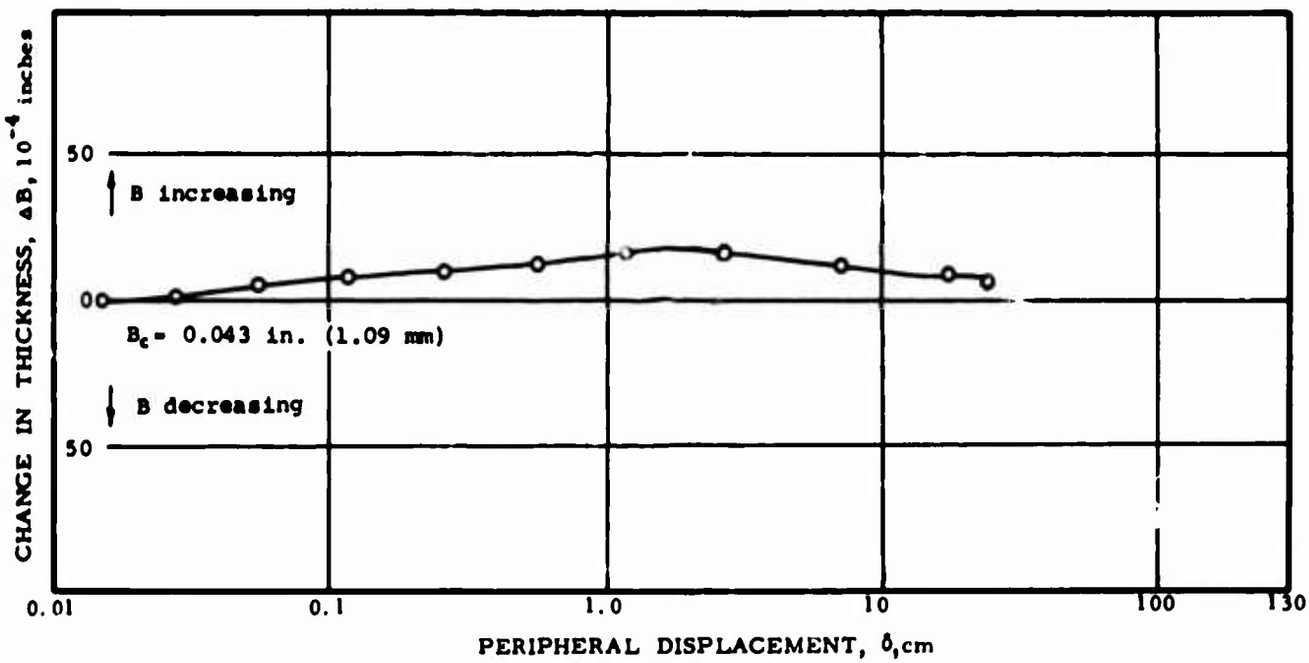
CHANGE IN THICKNESS, ΔB, 10^{-4} inches
50
B increasing
0
B_c = 0.043 in. (1.09 mm)
B decreasing
50
0.01
0.1
1.0
10
100
130
PERIPHERAL DISPLACEMENT, δ, cm

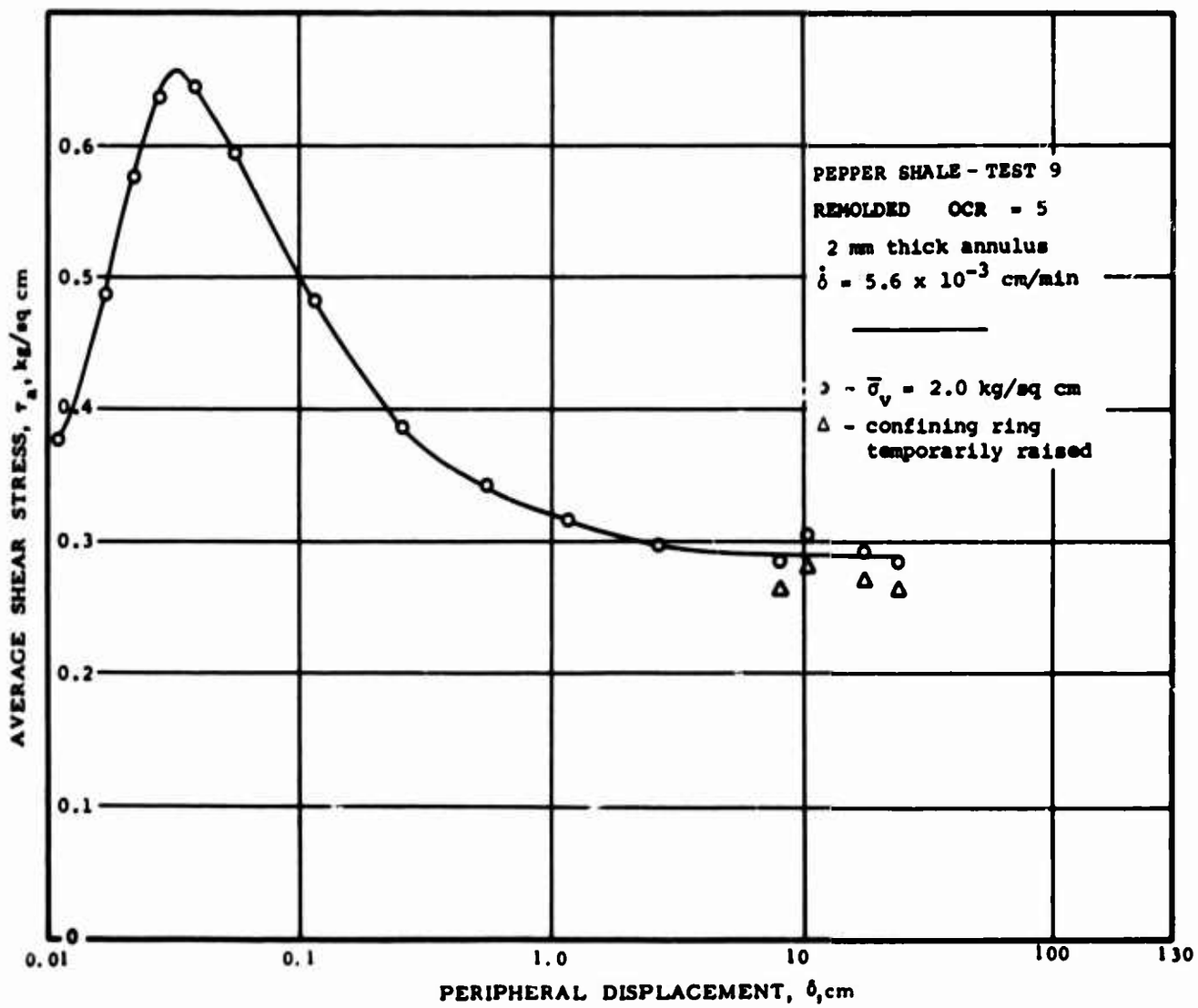
AVERAGE SHEAR STRESS, τ_a, kg/sq cm
0.6
0.5
0.4
0.3
0.2
0.1
0
PEPPER SHALE - TEST 9
REMOLDED OCR = 5
2 mm thick annulus
$\dot{\delta}$ = 5.6 x 10^{-3} cm/min
○ - $\bar{\sigma}_v$ = 2.0 kg/sq cm
Δ - confining ring temporarily raised
0.01
0.1
1.0
10
100
130
PERIPHERAL DISPLACEMENT, δ, cm

FIG., 7-14

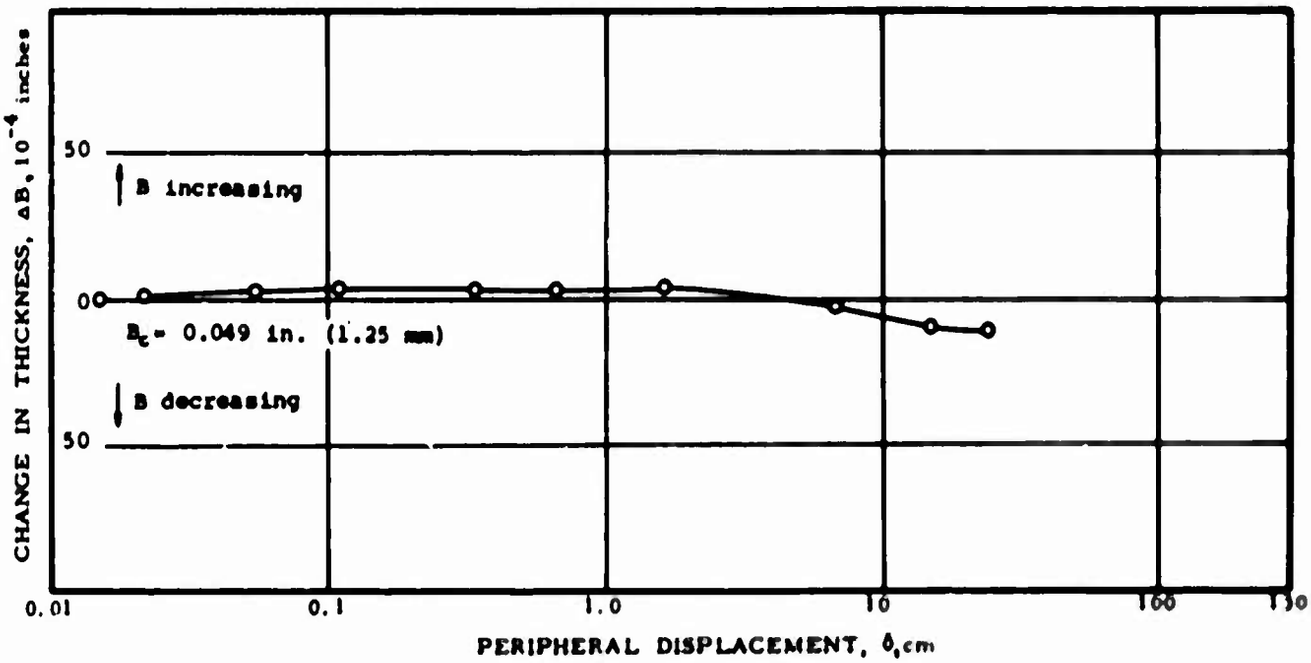
CHANGE IN THICKNESS, ΔB, 10^{-4} inches
50
B increasing
0
B_c = 0.049 in. (1.25 mm)
B decreasing
50
0.01
0.1
1.0
10
100
PERIPHERAL DISPLACEMENT, δ, cm

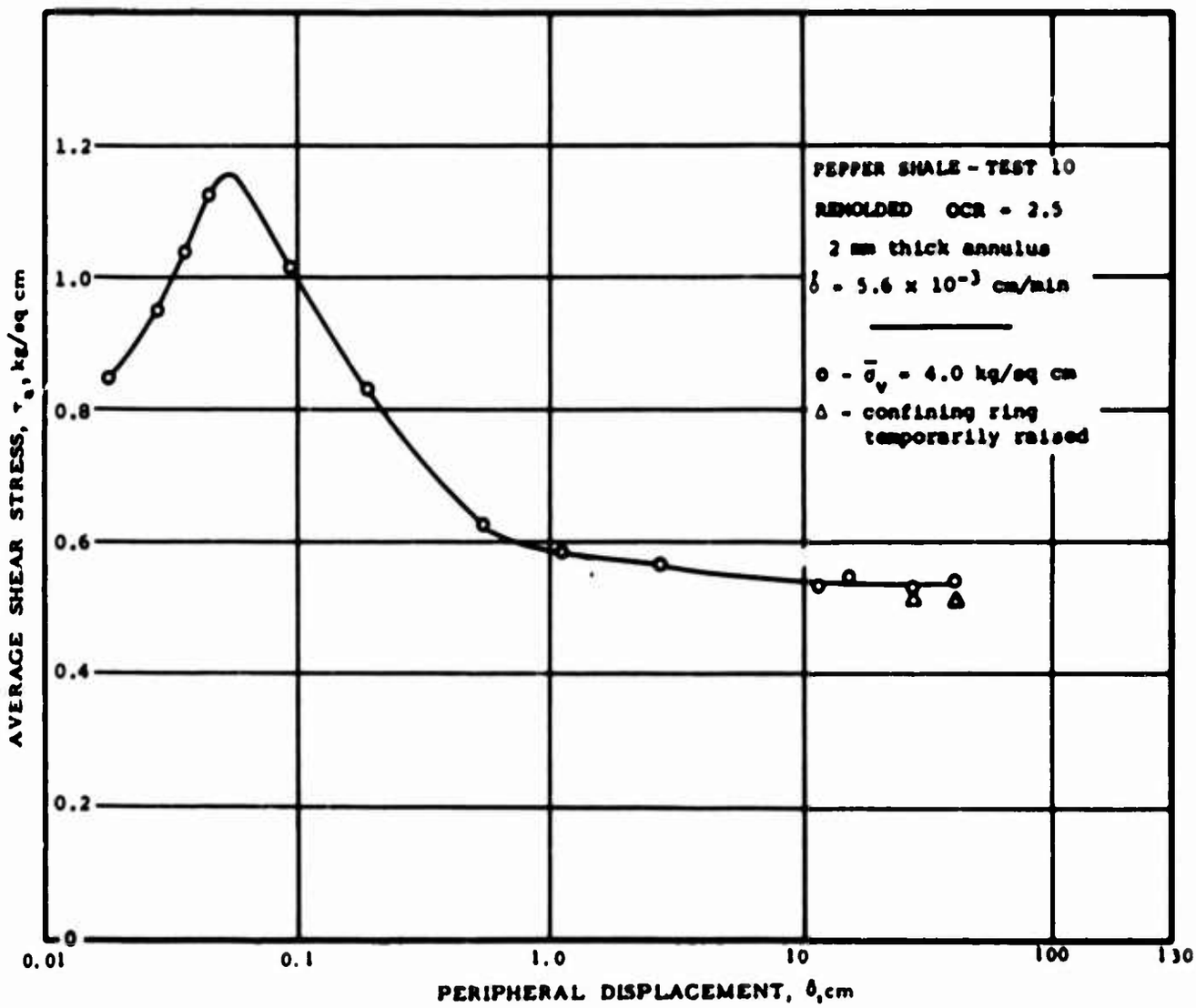
AVERAGE SHEAR STRESS, τ_a, kg/sq cm
1.2
1.0
0.8
0.6
0.4
0.2
0
PEPPER SHALE - TEST 10
REMOLDED OCR = 2.5
2 mm thick annulus
δ̇ = 5.6 x 10^{-3} cm/min
o - $\bar{\sigma}_v$ = 4.0 kg/sq cm
Δ - confining ring temporarily raised
0.01
0.1
1.0
10
100
PERIPHERAL DISPLACEMENT, δ, cm

FIG. 7-15

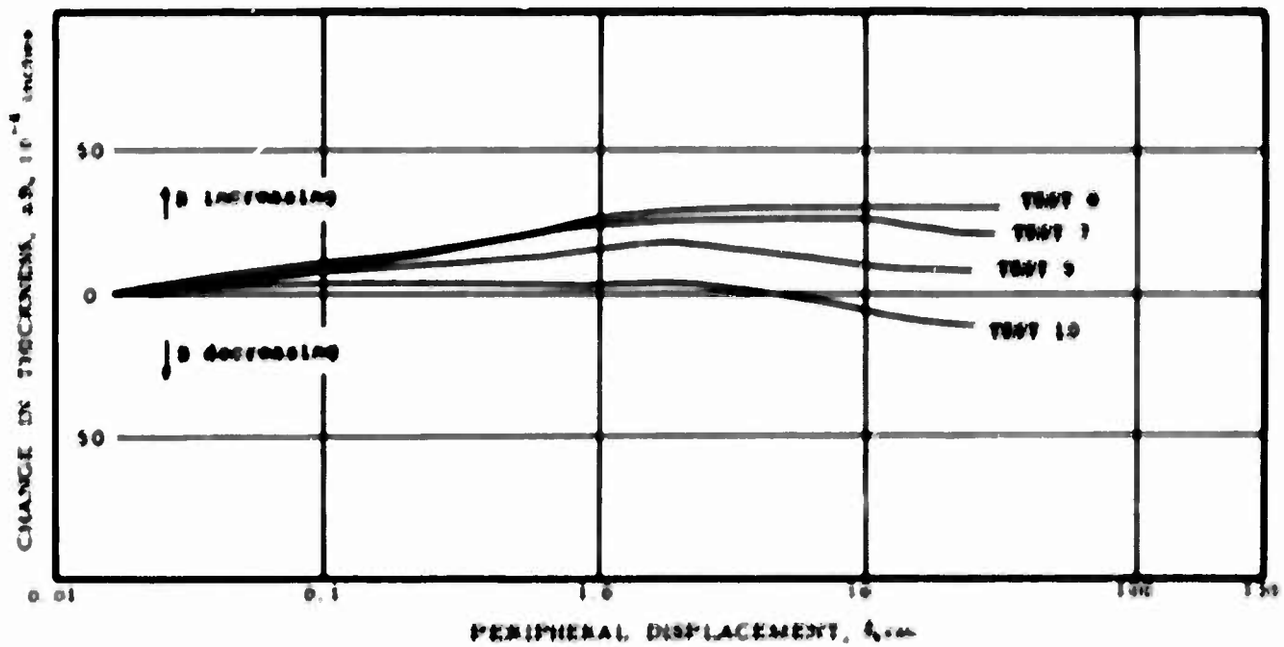
$0
0
$0
↑δ increasing
↓δ decreasing
TEST 8
TEST 7
TEST 9
TEST 10
0.01
0.1
1.0
10
100
PERIPHERAL DISPLACEMENT, δ,cm

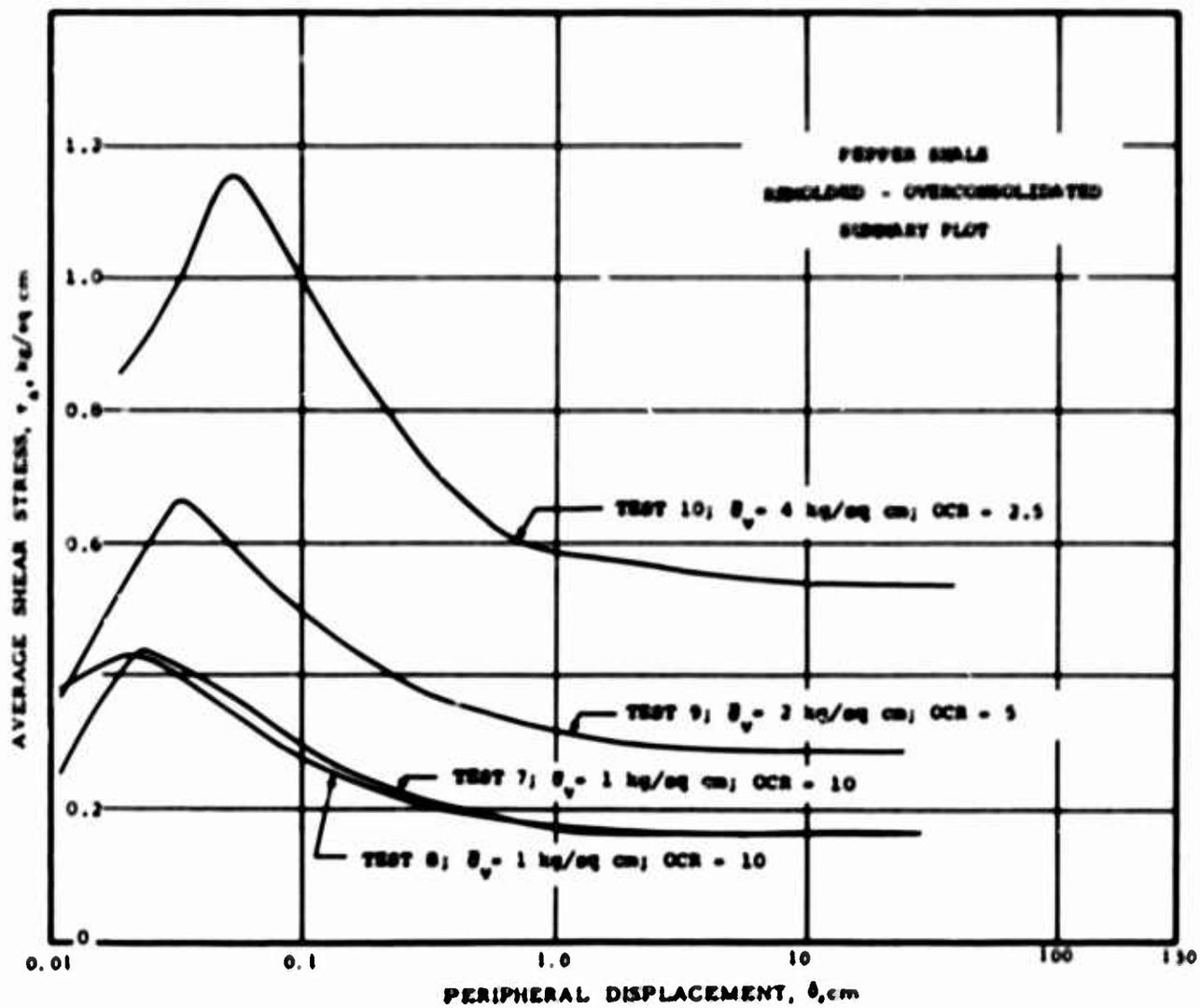
PEPPER SEALS
REMOLDED - OVERCONSOLIDATED
SUBSOIL PLOT
TEST 10; $\bar{\sigma}_v$ = 4 kg/sq cm; OCR = 2.5
TEST 9; $\bar{\sigma}_v$ = 2 kg/sq cm; OCR = 5
TEST 7; $\bar{\sigma}_v$ = 1 kg/sq cm; OCR = 10
TEST 8; $\bar{\sigma}_v$ = 1 kg/sq cm; OCR = 10
AVERAGE SHEAR STRESS, τ_a, kg/sq cm
1.2
1.0
0.8
0.6
0.2
0
0.01
0.1
1.0
10
100
PERIPHERAL DISPLACEMENT, δ,cm

FIG. 7-16

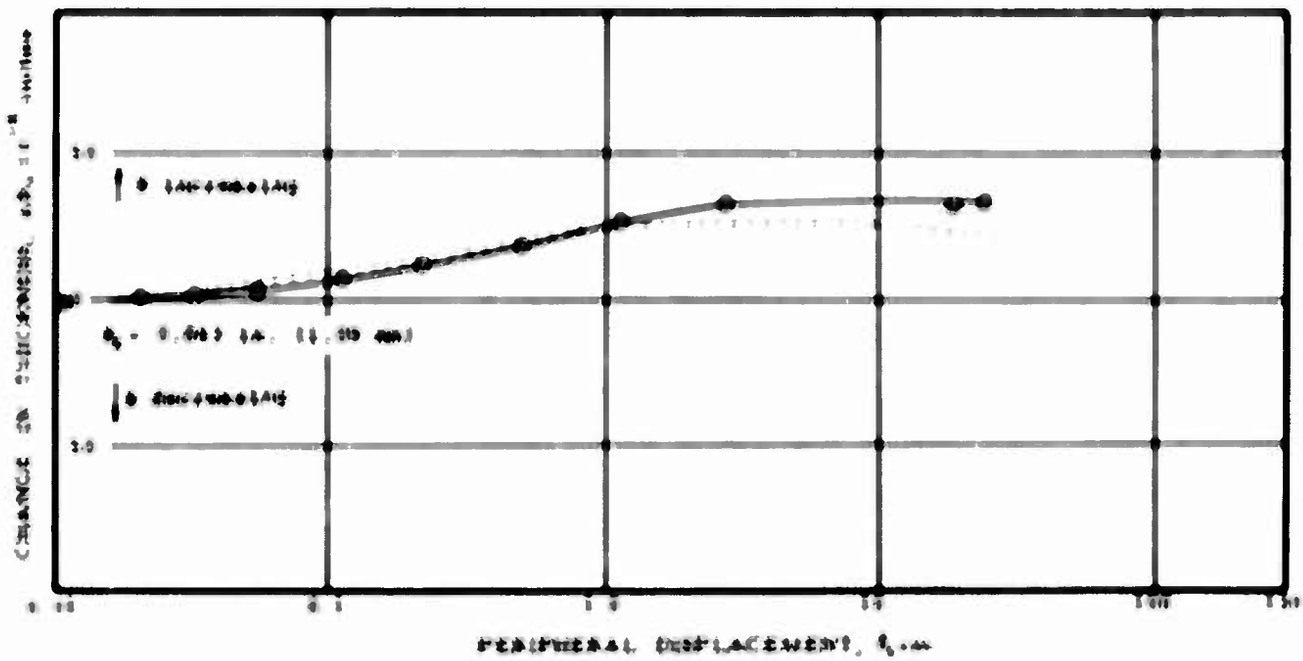

PERIPHERAL DISPLACEMENT, δ, cm

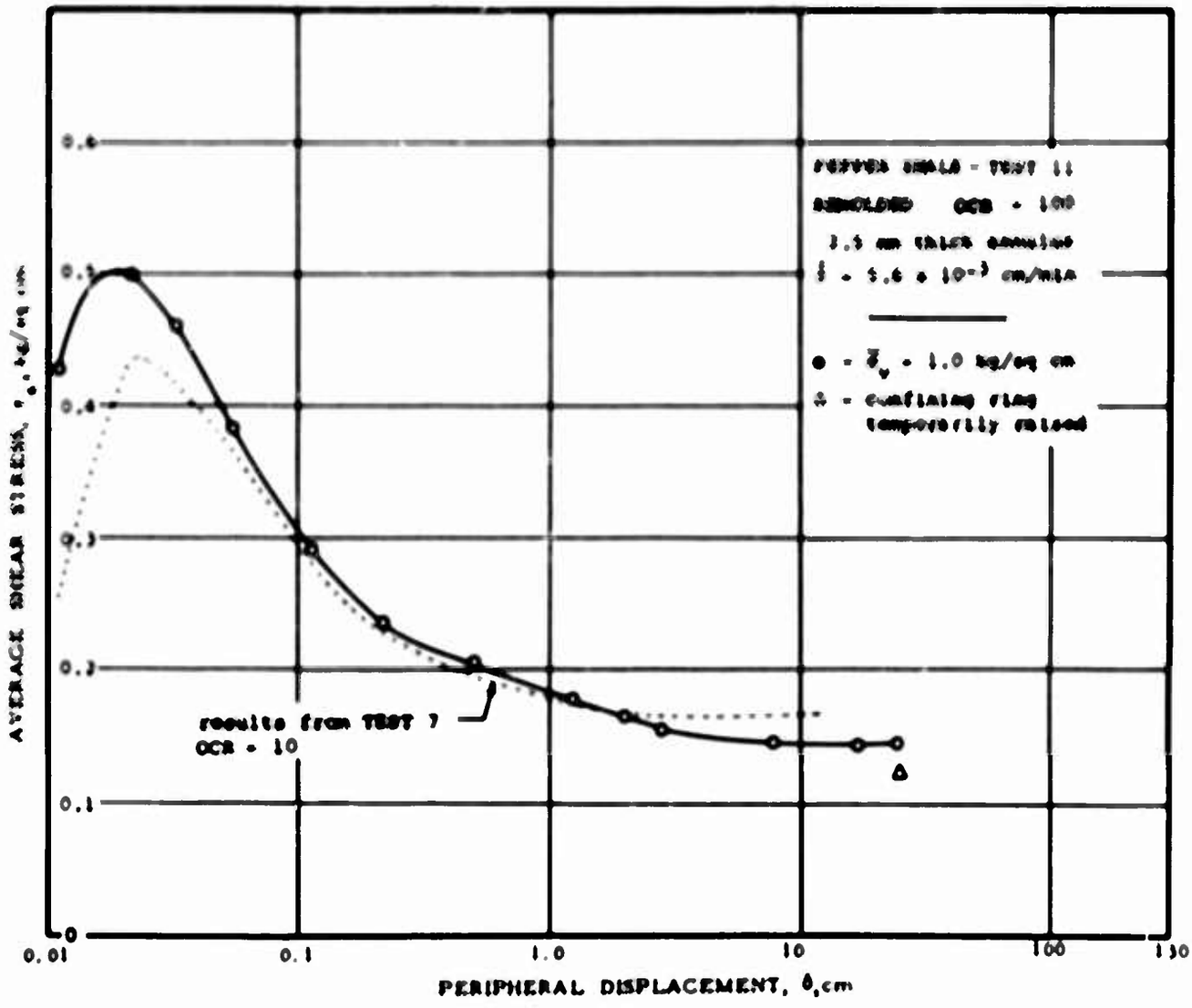

FIG. 7-17

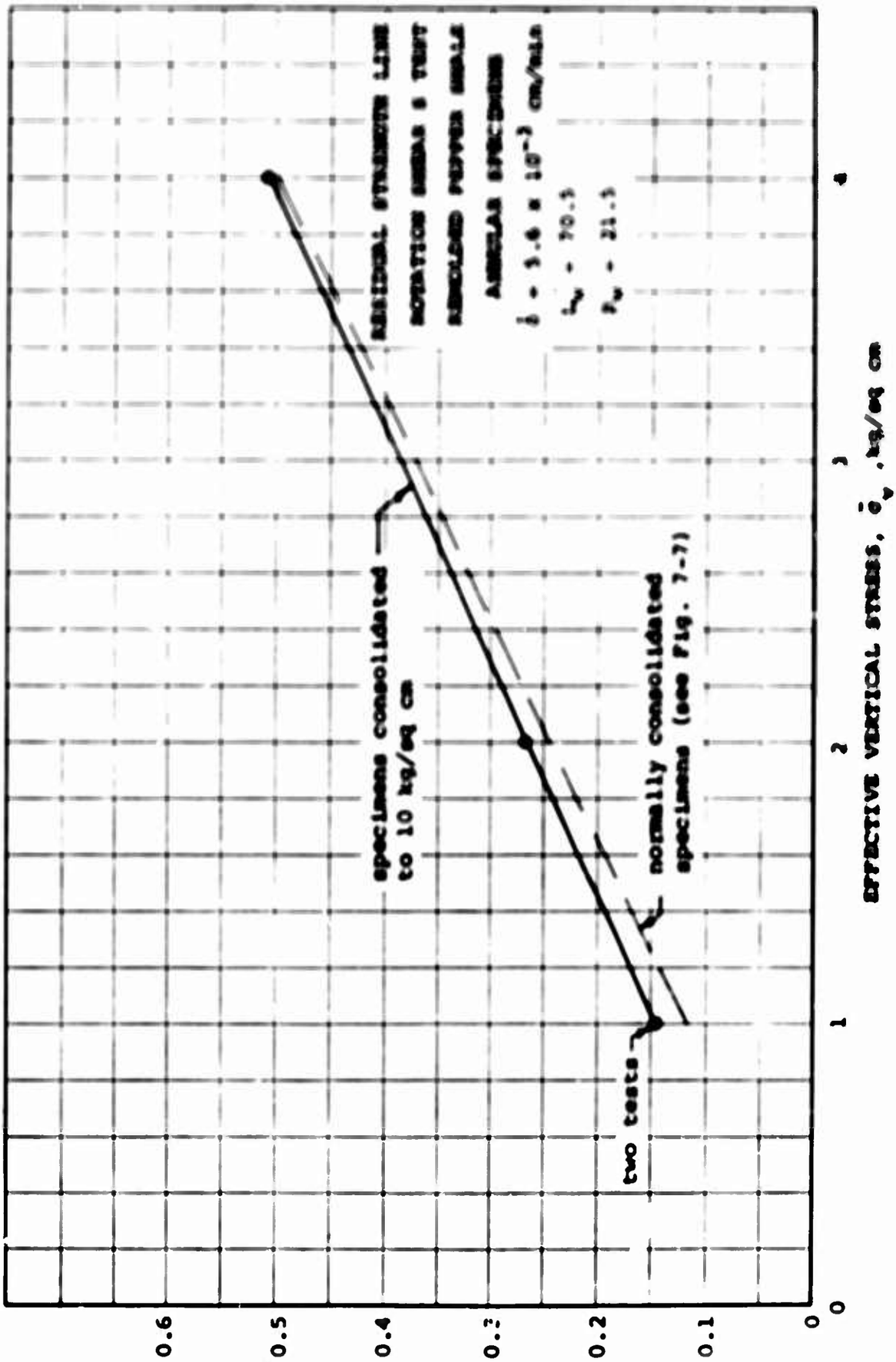
RESIDUAL STRENGTH LINE
ROTATION SHEAR & TEST
REMOLDED PEPPER SHALE
ARKOLAS SPECIMENS
$\dot{\delta}$ = 5.6 x 10^{-3} cm/min
h_o = 20.3
D_o = 21.3
specimens consolidated to 10 kg/sq cm
normally consolidated specimens (see Fig. 7-7)
two tests
RESIDUAL SHEAR STRENGTH, τ_r, kg/sq cm
EFFECTIVE VERTICAL STRESS, $\bar{\sigma}_v$, kg/sq cm
0.6
0.5
0.4
0.3
0.2
0.1
0
1
2
3
4

FIG. 7-18

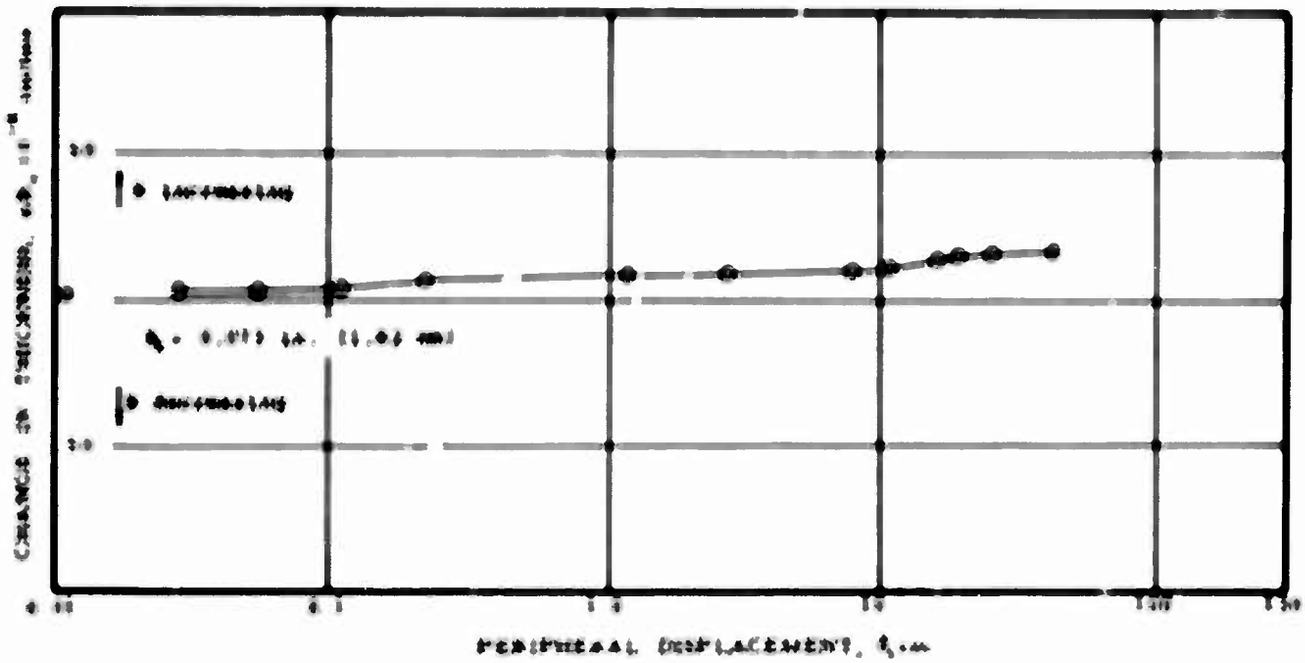

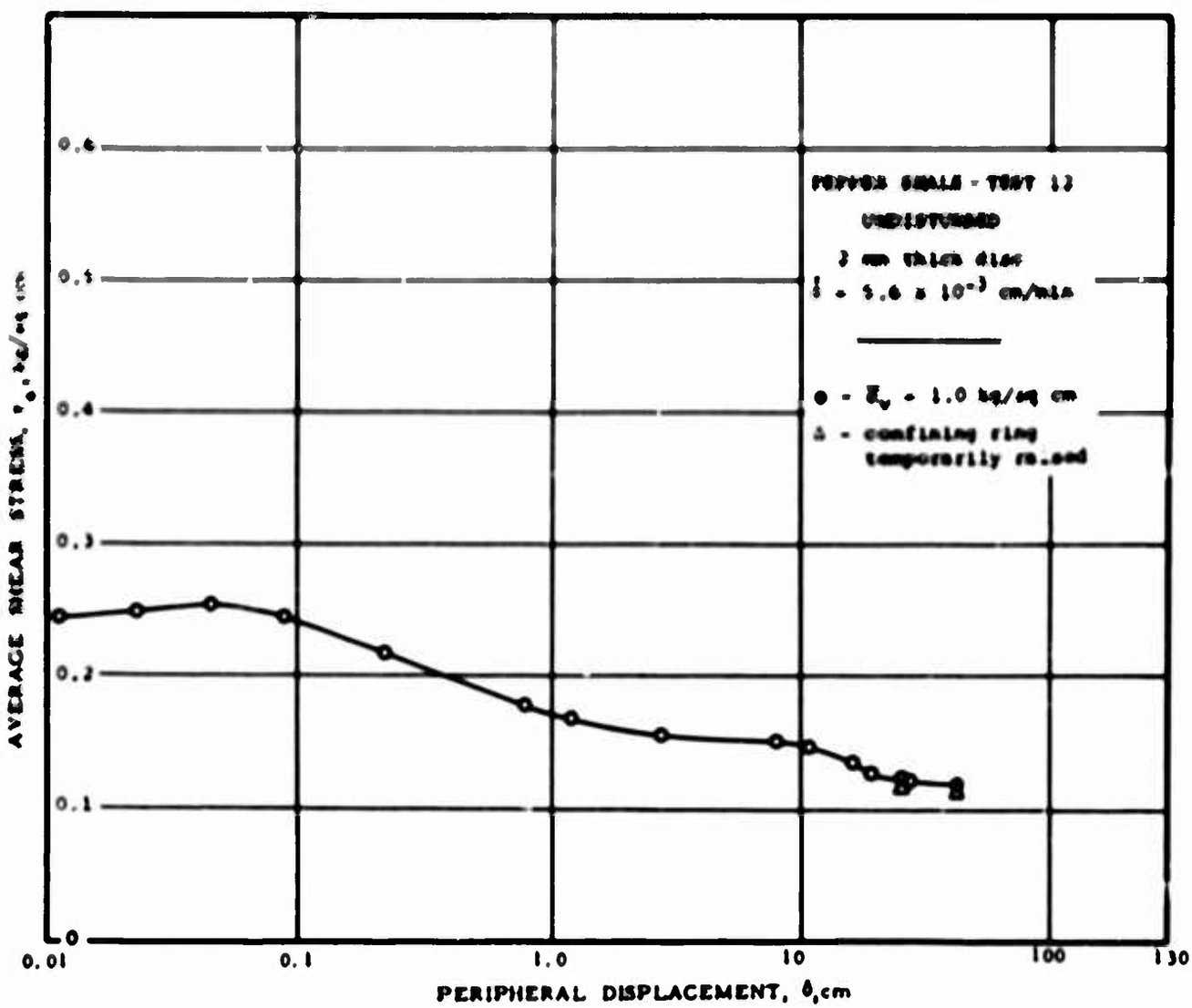
PEPPER SHALE - TEST 12
UNDISTURBED
3 cm THICK DISC
k = 5.6 x 10⁻³ cm/min
● - σ_v = 1.0 kg/sq cm
Δ - confining ring temporarily removed
AVERAGE SHEAR STRESS, τ, kg/sq cm
0.6
0.5
0.4
0.3
0.2
0.1
0
0.01
0.1
1.0
10
100
130
PERIPHERAL DISPLACEMENT, δ, cm

FIG. 7-19

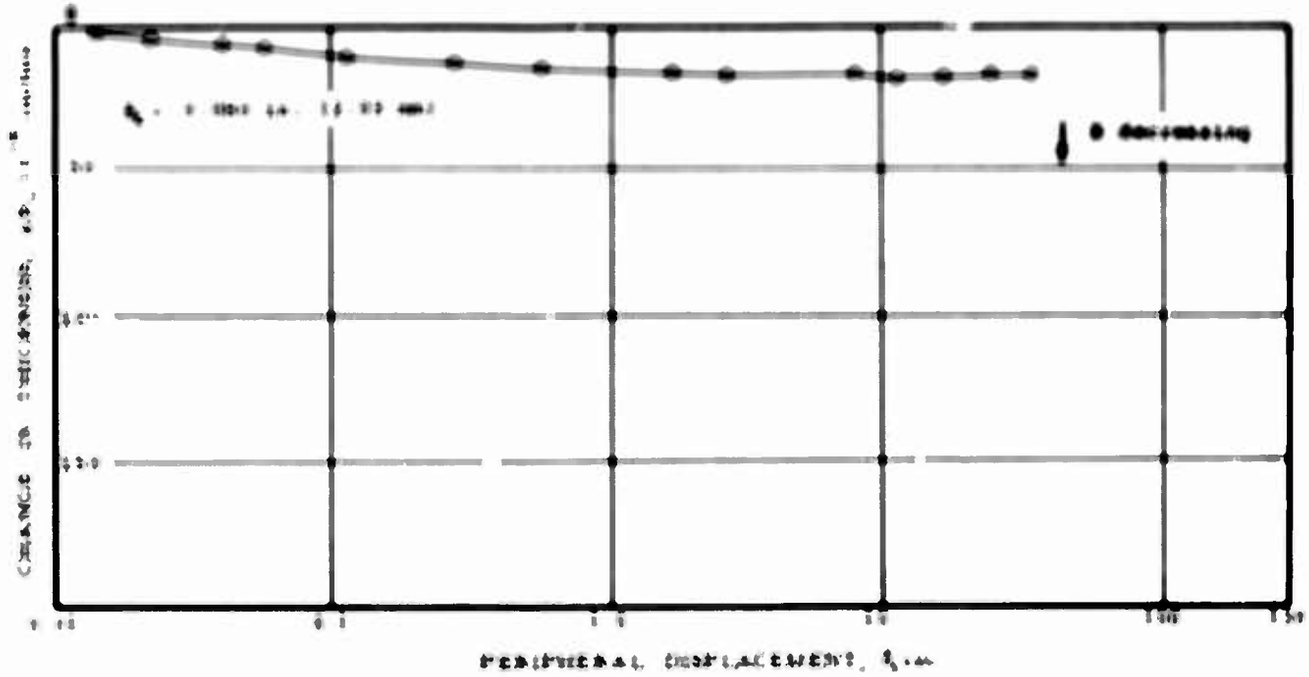

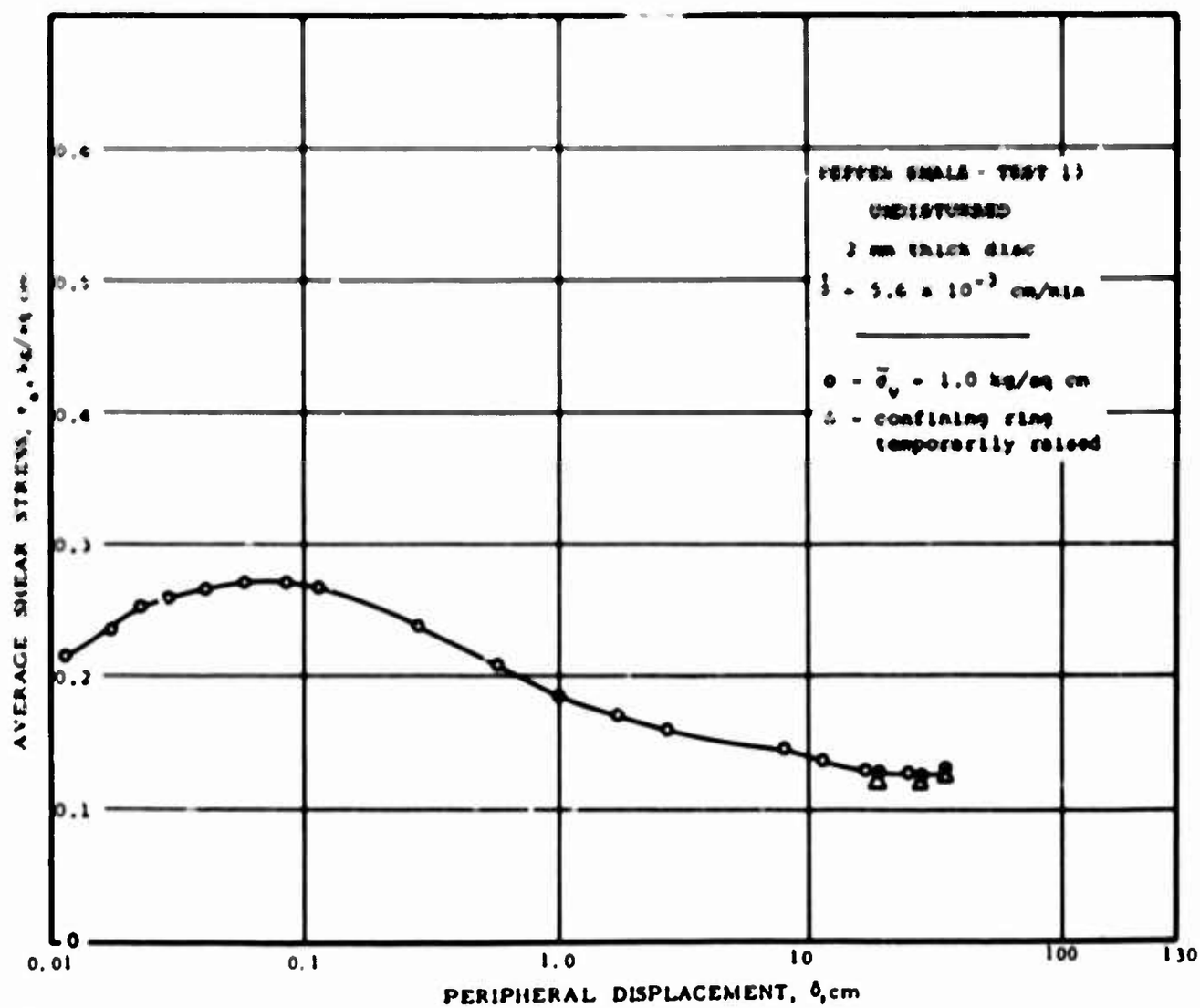
AVERAGE SHEAR STRESS, τ_a, kg/sq cm
0.6
0.5
0.4
0.3
0.2
0.1
0
0.01
0.1
1.0
10
100
130
PERIPHERAL DISPLACEMENT, δ, cm
UNDISTURBED
3 mm thick disc
k = 5.6 x 10^-3 cm/min
σ = σ̄_v = 1.0 kg/sq cm
Δ - confining ring temporarily raised

FIG. 7-20

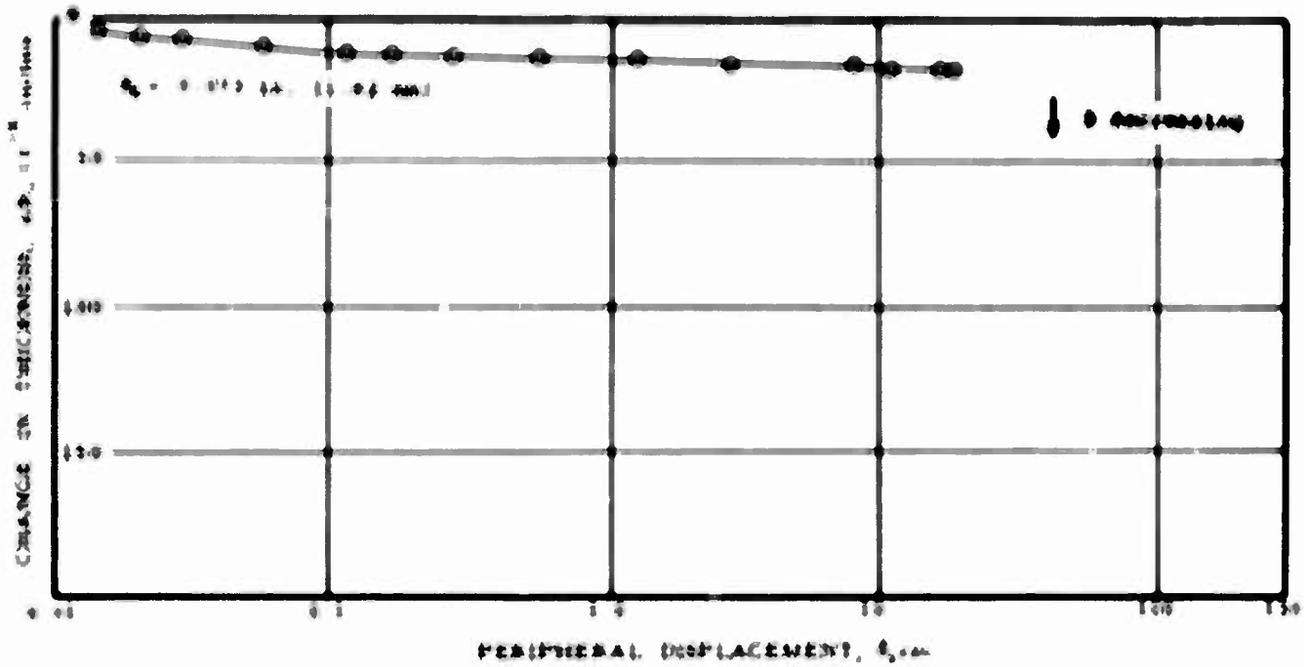

PERIPHERAL DISPLACEMENT, δ, cm

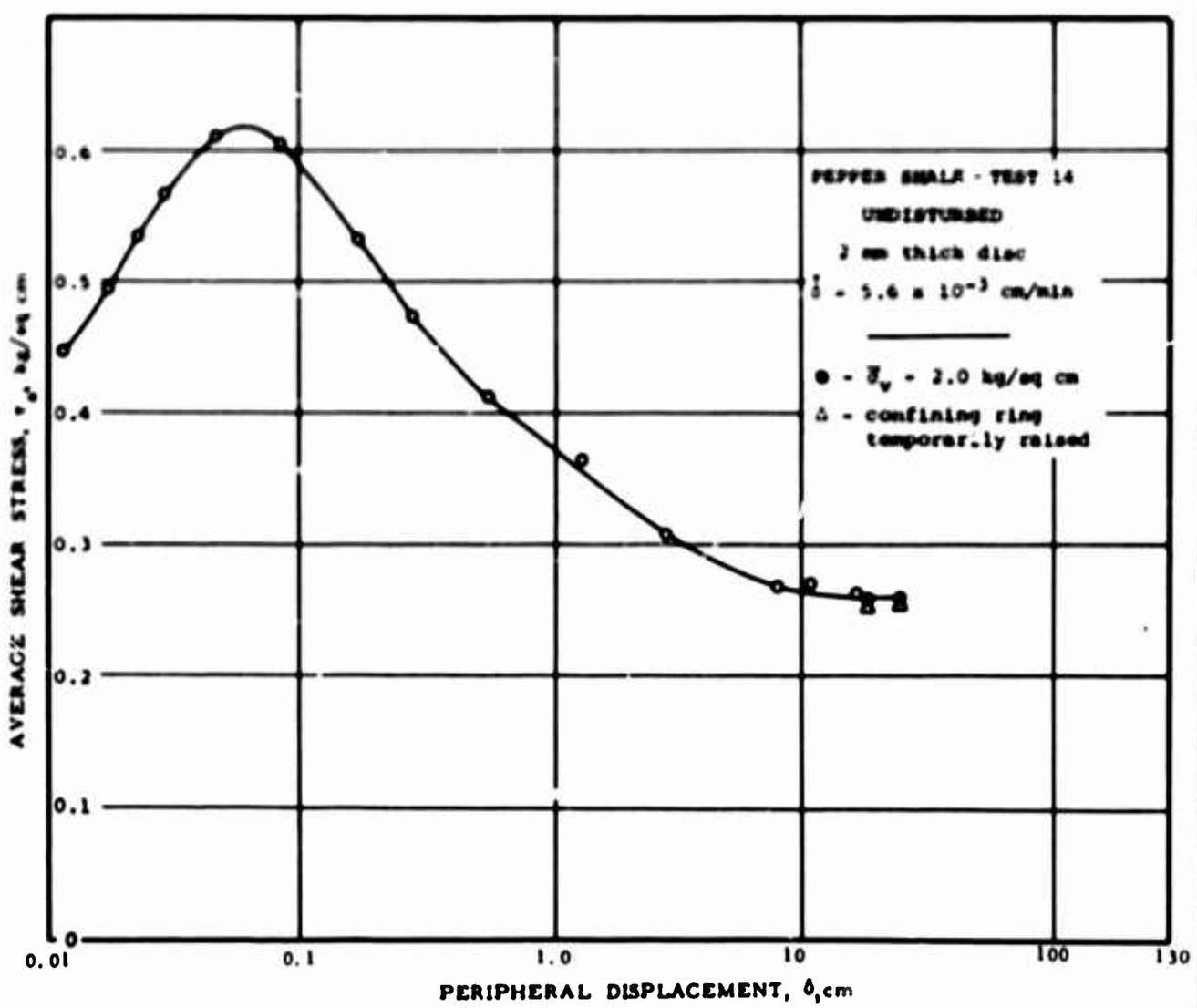

FIG. 7-21

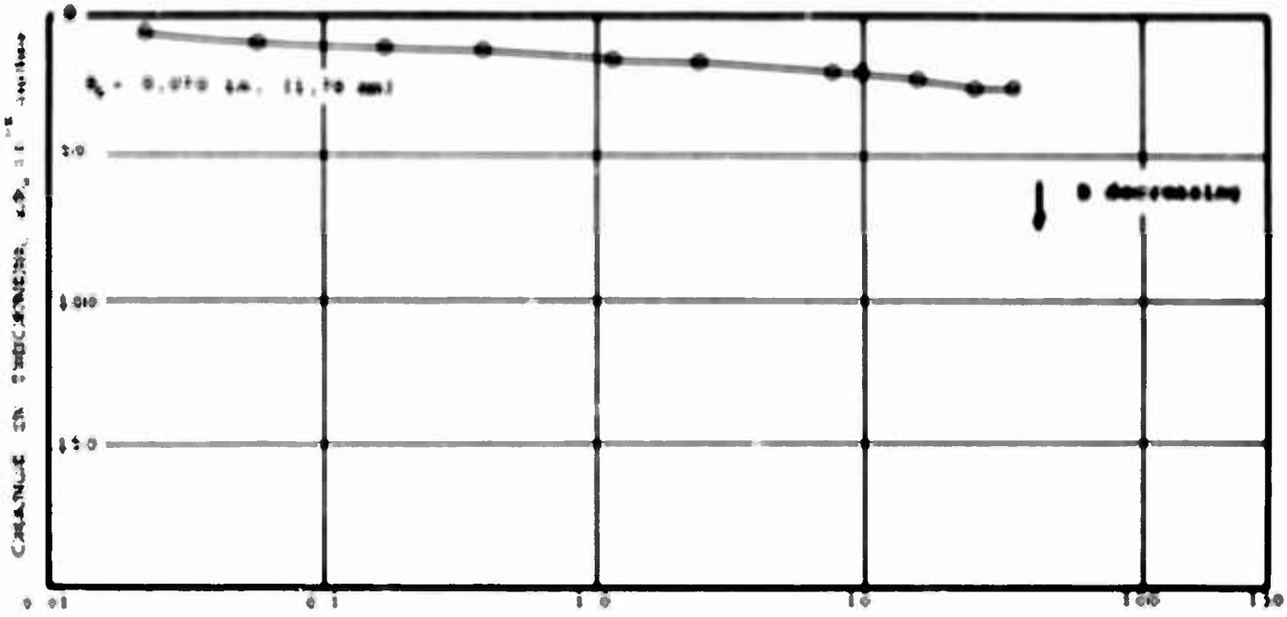
PERIPHERAL DISPLACEMENT, δ, cm

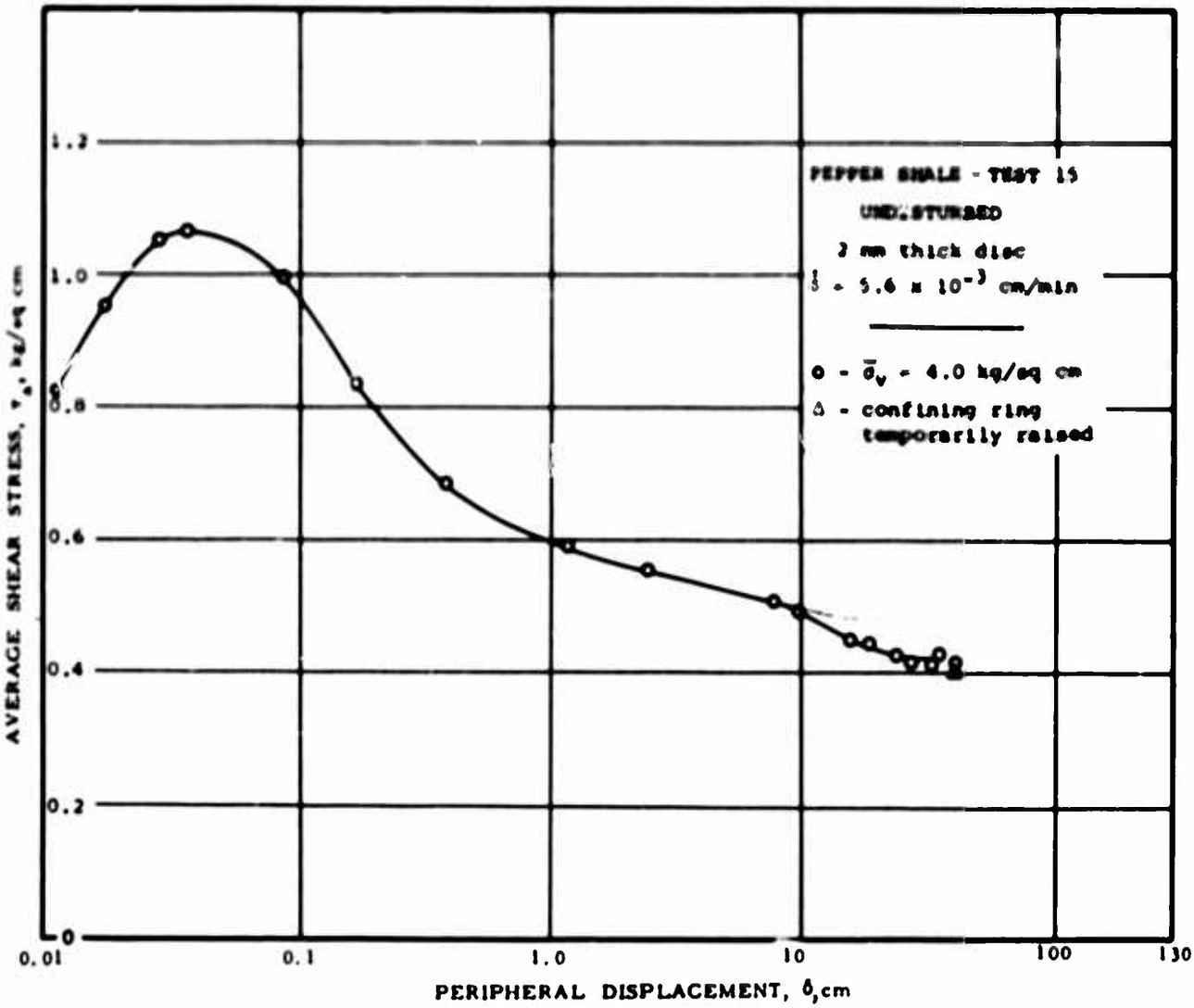
PEPPER SHALE - TEST 15
UNDISTURBED
2 mm thick disc
$\dot{\delta}$ = 5.6 x 10^{-3} cm/min
o - $\bar{\sigma}_v$ = 4.0 kg/sq cm
Δ - confining ring temporarily raised
AVERAGE SHEAR STRESS, τ_a, kg/sq cm
PERIPHERAL DISPLACEMENT, δ, cm

FIG. 7-22

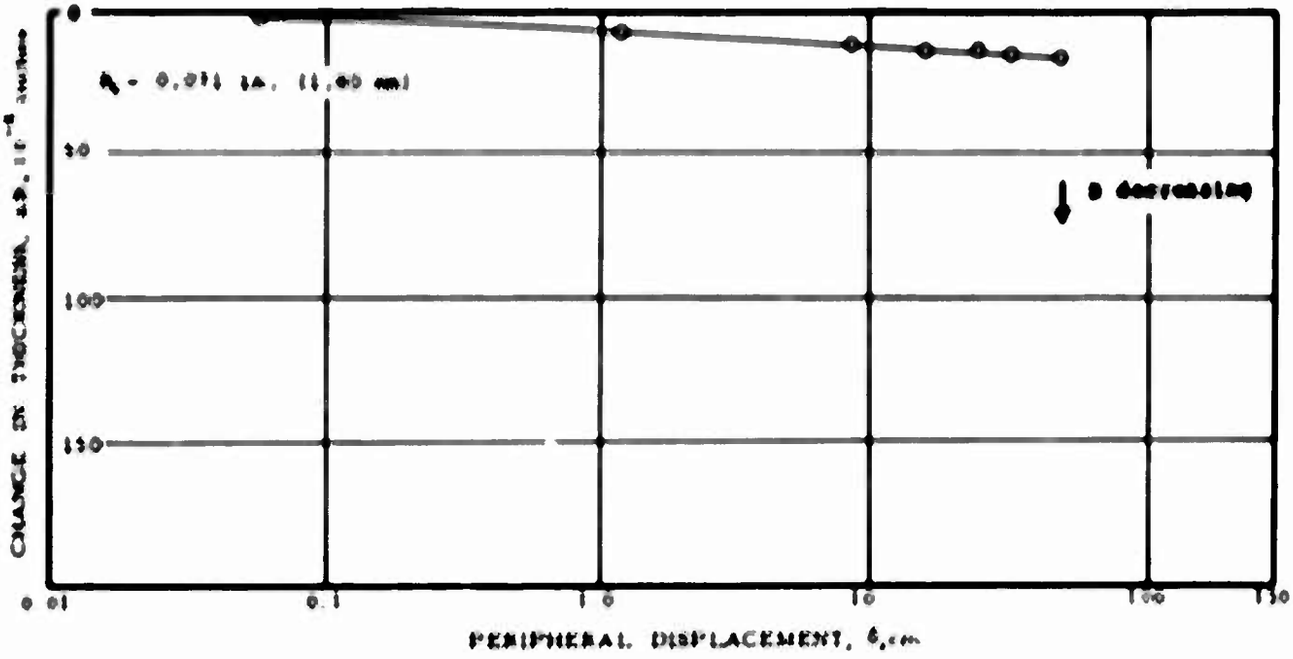
PERIPHERAL DISPLACEMENT, δ, cm

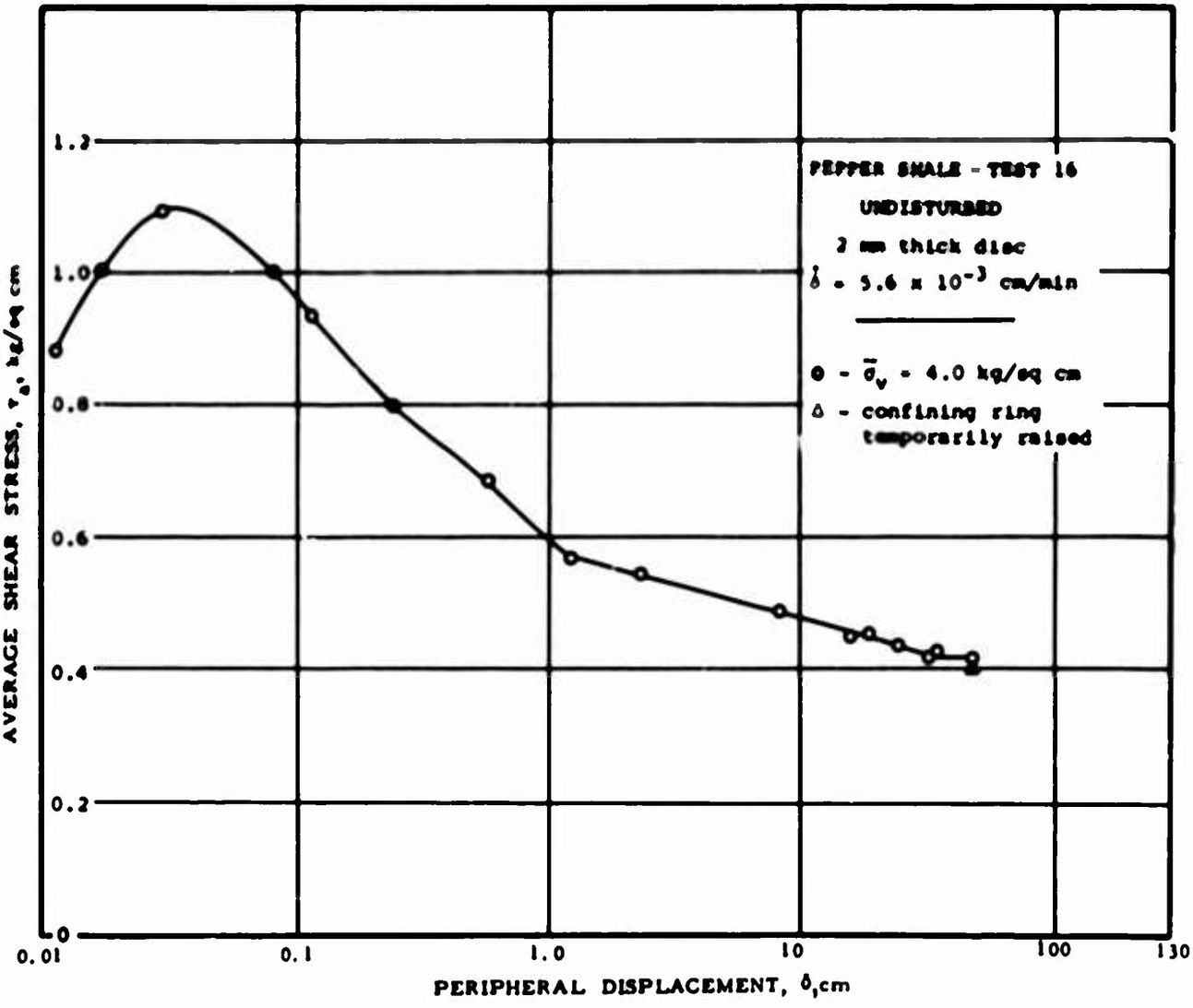
PEPPER SHALE - TEST 16
UNDISTURBED
2 mm thick disc
δ̇ = 5.6 x 10⁻³ cm/min
θ - σ̄v = 4.0 kg/sq cm
Δ - confining ring temporarily raised
AVERAGE SHEAR STRESS, τa, kg/sq cm
PERIPHERAL DISPLACEMENT, δ, cm

FIG. 7-23

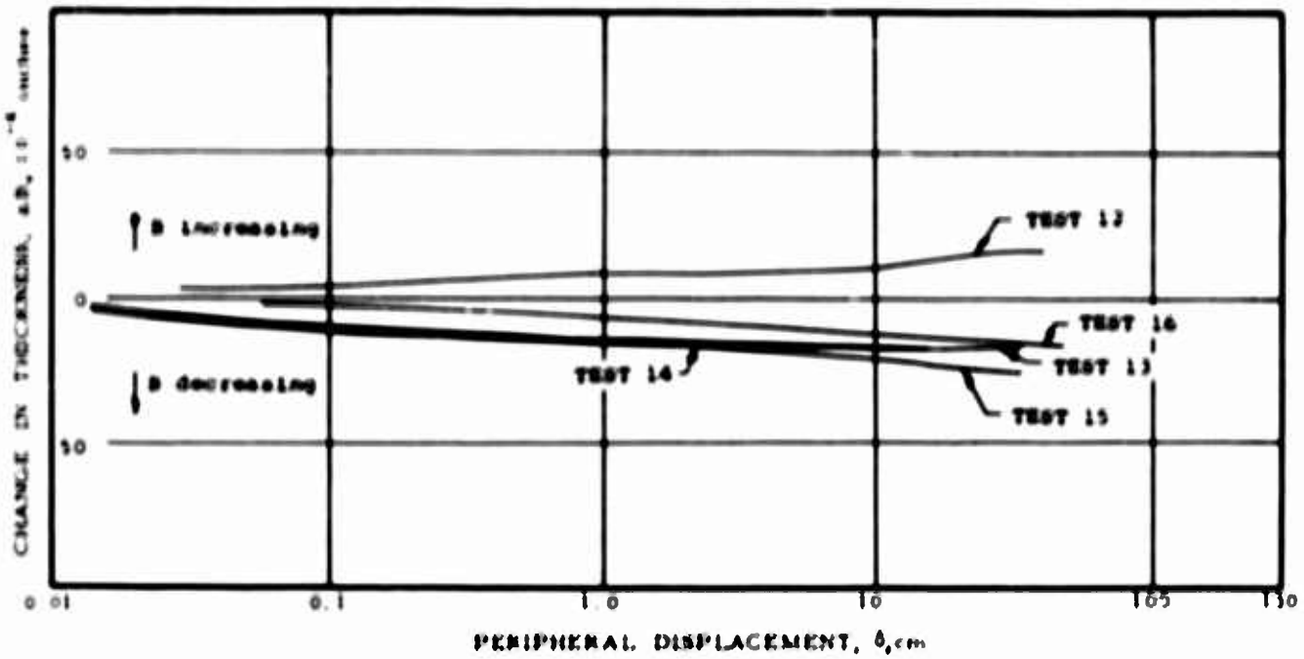
B increasing
B decreasing
TEST 12
TEST 16
TEST 13
TEST 14
TEST 15
0.01
0.1
1.0
10
100
130
PERIPHERAL DISPLACEMENT, δ, cm

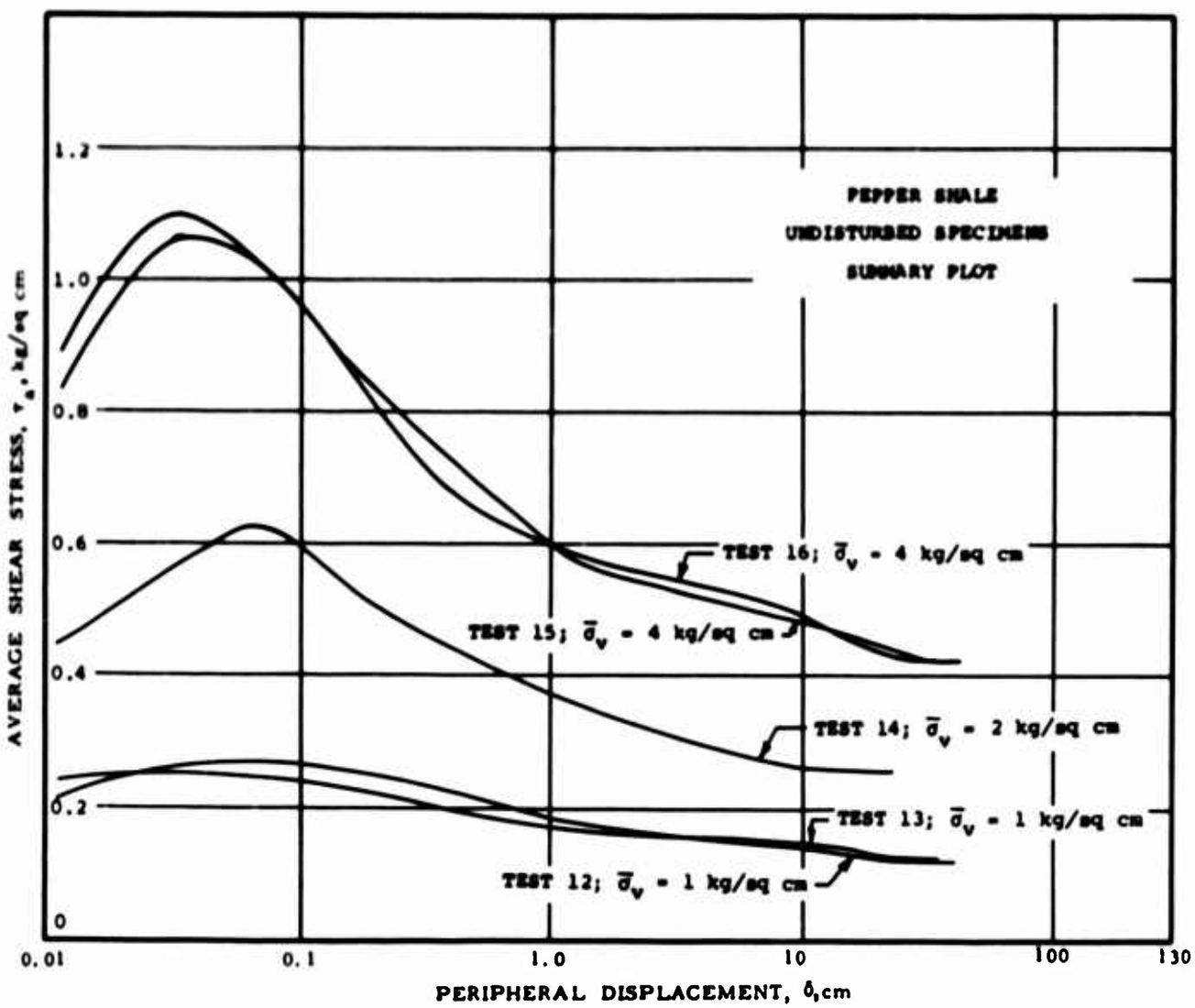
PEPPER SHALE
UNDISTURBED SPECIMENS
SUMMARY PLOT
AVERAGE SHEAR STRESS, τa, kg/sq cm
1.2
1.0
0.8
0.6
0.4
0.2
0
TEST 16; σ̄v = 4 kg/sq cm
TEST 15; σ̄v = 4 kg/sq cm
TEST 14; σ̄v = 2 kg/sq cm
TEST 13; σ̄v = 1 kg/sq cm
TEST 12; σ̄v = 1 kg/sq cm
0.01
0.1
1.0
10
100
130
PERIPHERAL DISPLACEMENT, δ, cm

FIG. 7-24

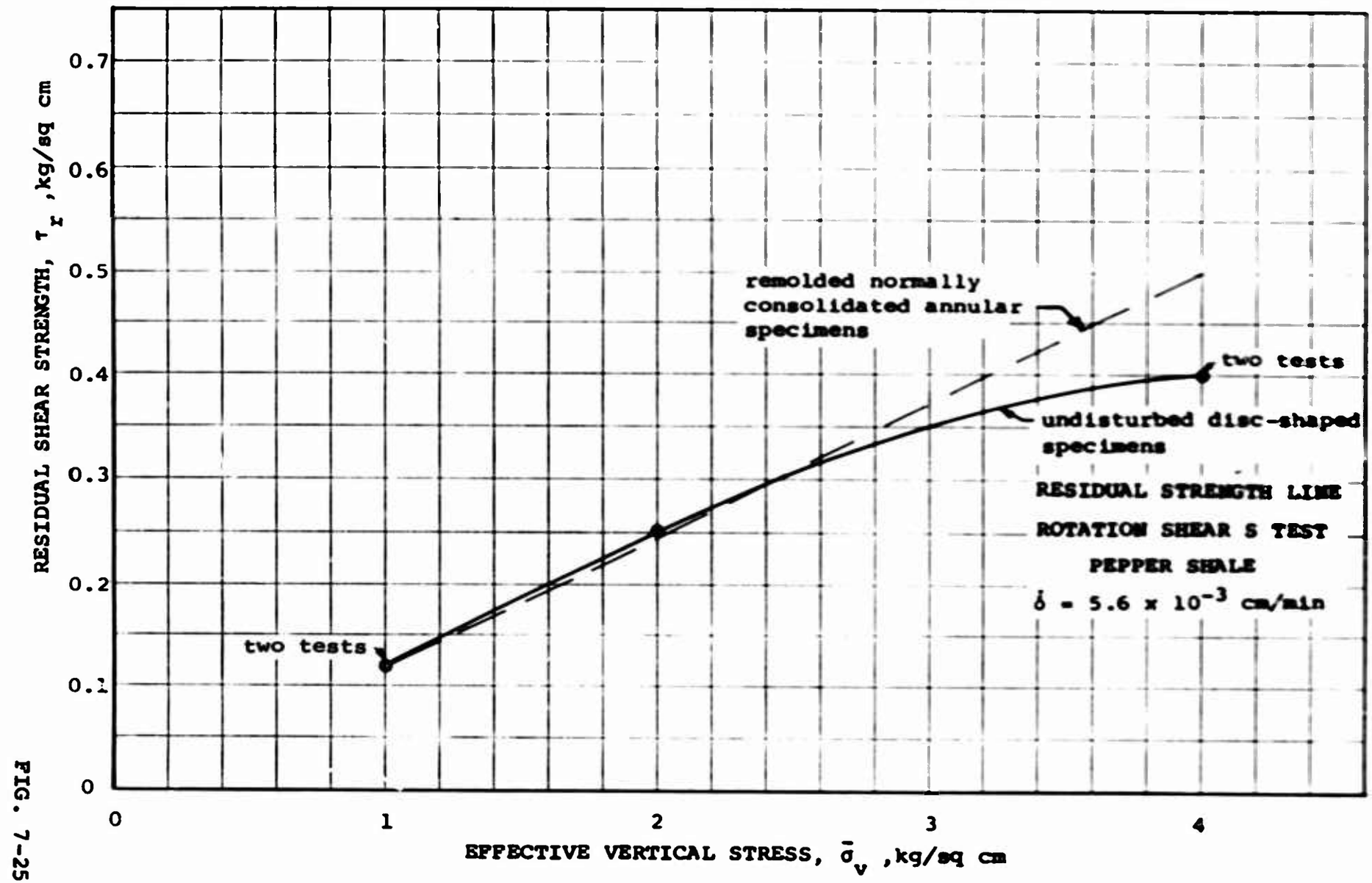
RESIDUAL SHEAR STRENGTH, τ_r ,kg/sq cm
0.7
0.6
0.5
0.4
0.3
0.2
0.1
0
0
1
2
3
4
EFFECTIVE VERTICAL STRESS, $\bar{\sigma}_v$,kg/sq cm
remolded normally consolidated annular specimens
two tests
undisturbed disc-shaped specimens
two tests
RESIDUAL STRENGTH LINE
ROTATION SHEAR S TEST
PEPPER SHALE
$\dot{\delta}$ = 5.6 x 10^{-3} cm/min

FIG. 7-25

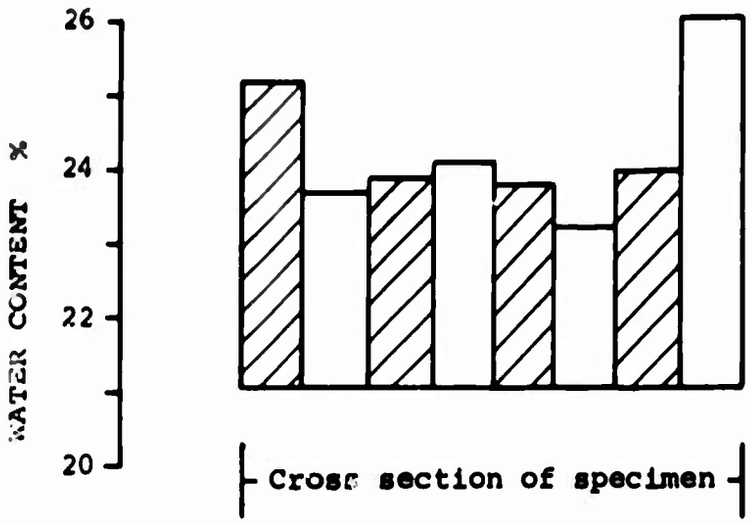

TEST 15

$\bar{\sigma}_v$ = 4.0 kg/sq cm

initial water content 21.1%

UNDISTURBED PEPPER SHALE

WATER CONTENT AT END OF TEST

solid confining ring

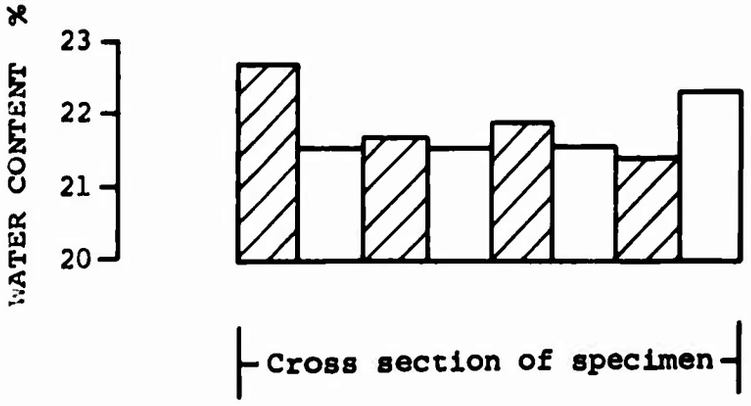

TEST 16

$\bar{\sigma}_v$ = 4.0 kg/sq cm

initial water content = 20.3%

FIG. 7-26

SLICKENSIDE IN CUCARACHA "SHALE"

FIG. 8-1

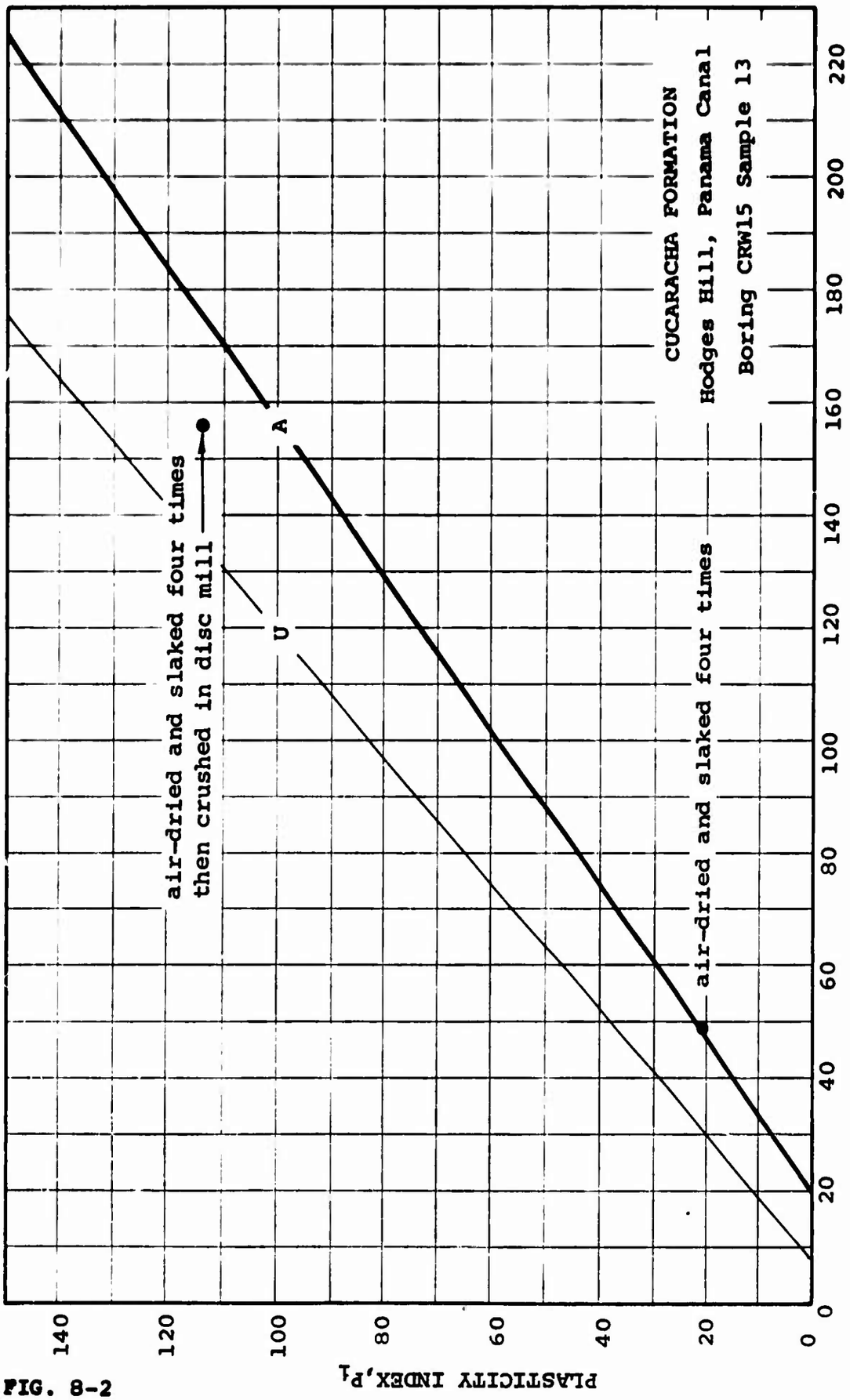
CUCARACHA FORMATION
Hodges Hill, Panama Canal
Boring CRW15 Sample 13
air-dried and slaked four times
air-dried and slaked four times
then crushed in disc mill
A
U
PLASTICITY INDEX, P_I
LIQUID LIMIT, L_w
0
20
40
60
80
100
120
140
160
180
200
220

FIG. 8-2

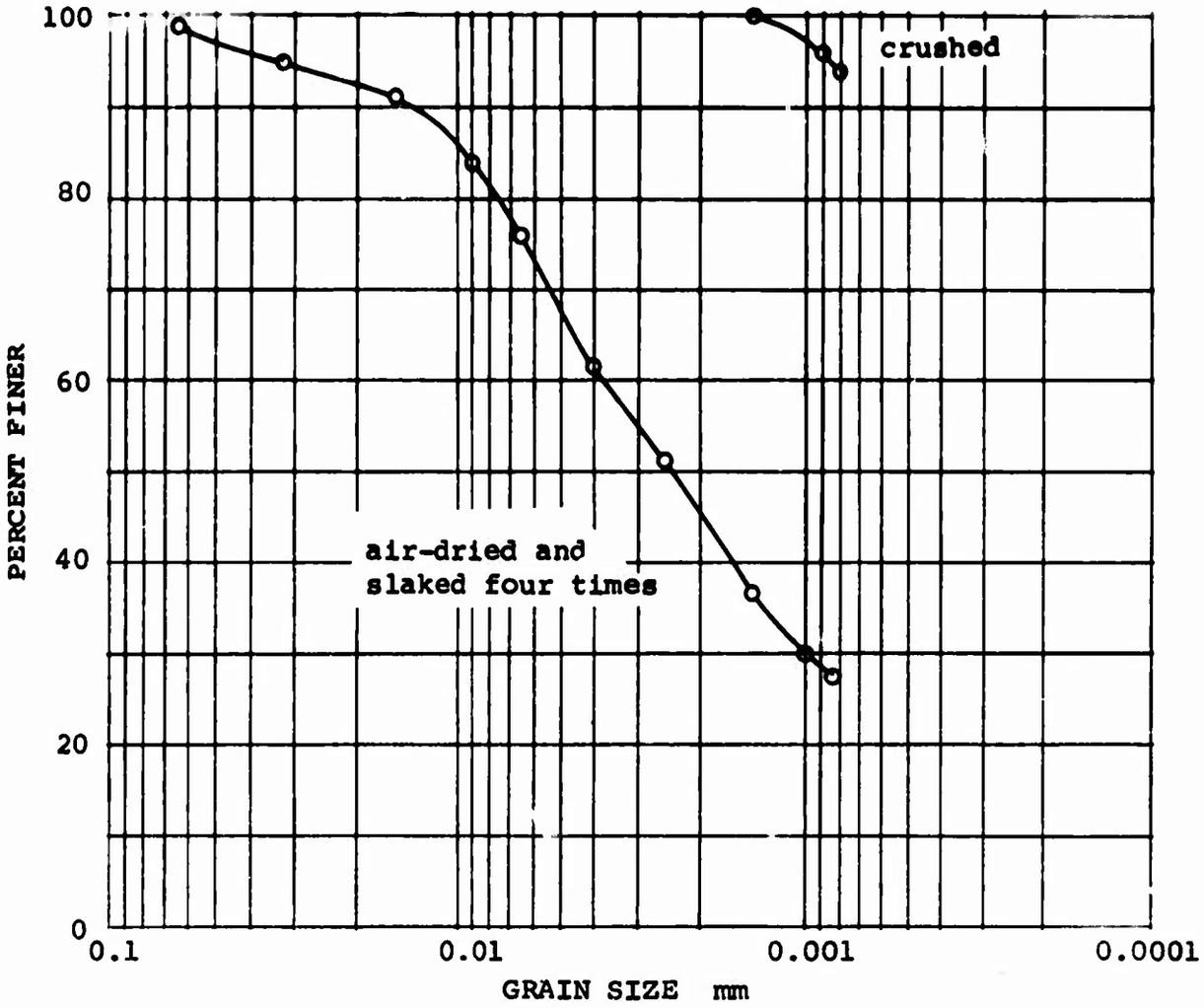

CUCARACHA FORMATION
Hodges Hill, Panama Canal
Boring CRW15 Sample 13

FIG. 8-3

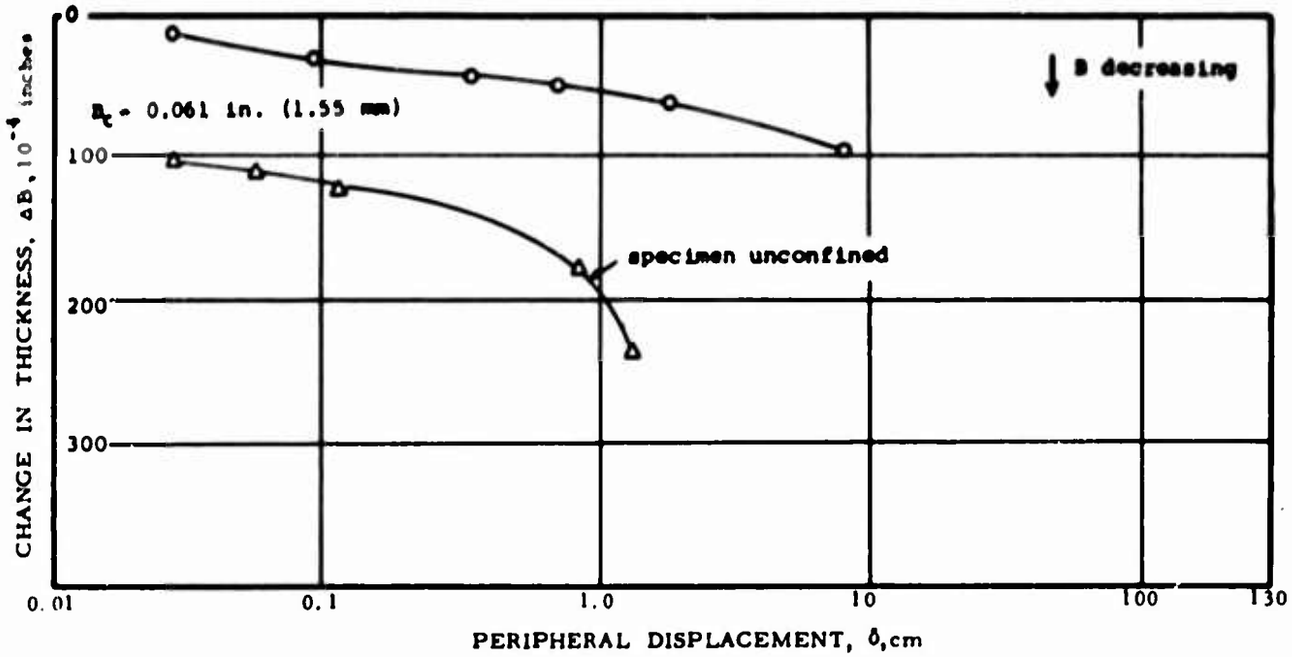
0
100
200
300
CHANGE IN THICKNESS, ΔB, 10^{-4} inches
B_t = 0.061 in. (1.55 mm)
B decreasing
specimen unconfined
0.01
0.1
1.0
10
100
130
PERIPHERAL DISPLACEMENT, δ, cm

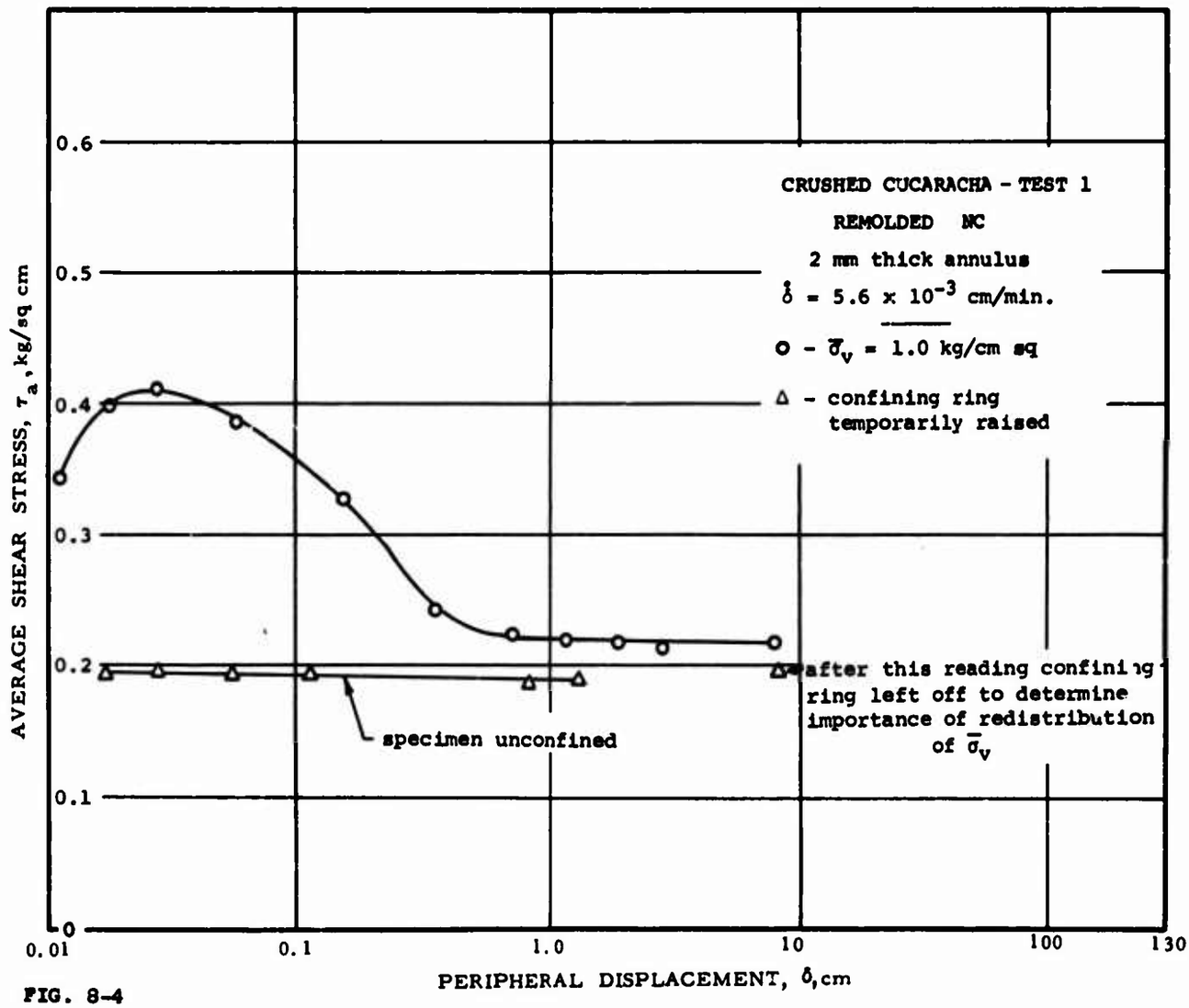
0.6
0.5
0.4
0.3
0.2
0.1
0
AVERAGE SHEAR STRESS, τ_a, kg/sq cm
CRUSHED CUCARACHA - TEST 1
REMOLDED NC
2 mm thick annulus
$\dot{\delta}$ = 5.6 x 10^{-3} cm/min.
o - $\bar{\sigma}_v$ = 1.0 kg/cm sq
Δ - confining ring temporarily raised
after this reading confining ring left off to determine importance of redistribution of $\bar{\sigma}_v$
specimen unconfined
0.01
0.1
1.0
10
100
130
PERIPHERAL DISPLACEMENT, δ, cm

FIG. 8-4

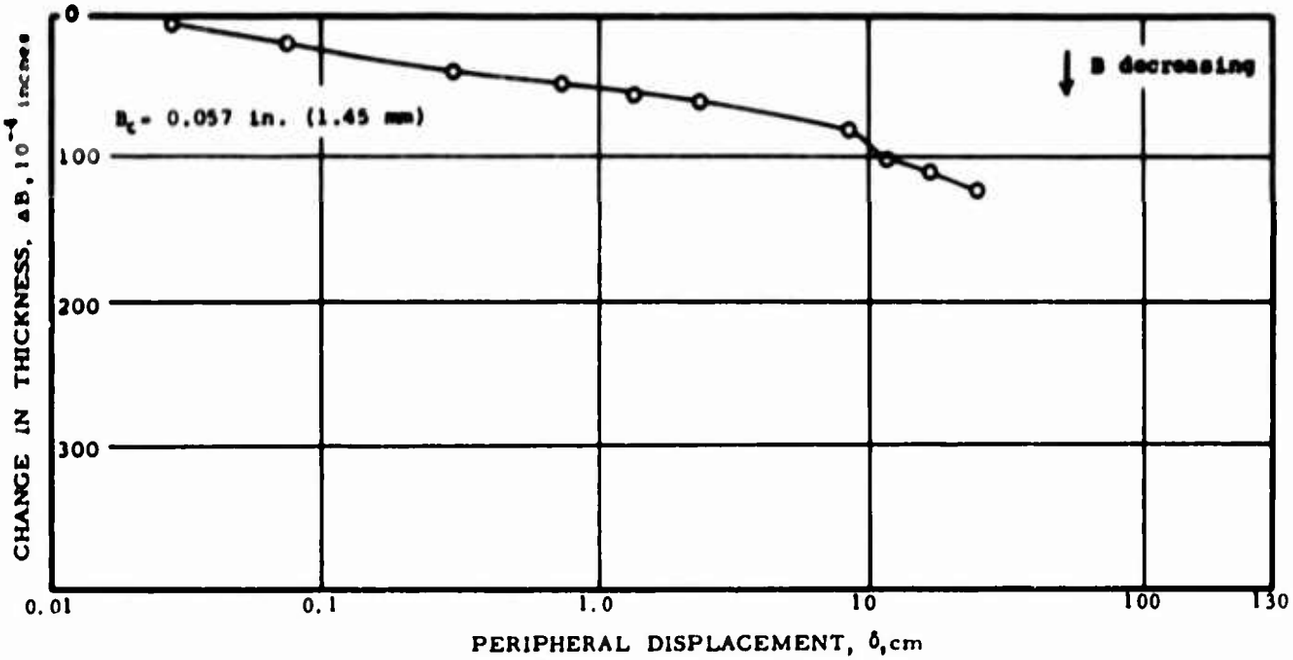
0
100
200
300
B_c = 0.057 in. (1.45 mm)
B decreasing
CHANGE IN THICKNESS, ΔB, 10^{-4} inches
0.01
0.1
1.0
10
100
130
PERIPHERAL DISPLACEMENT, δ, cm

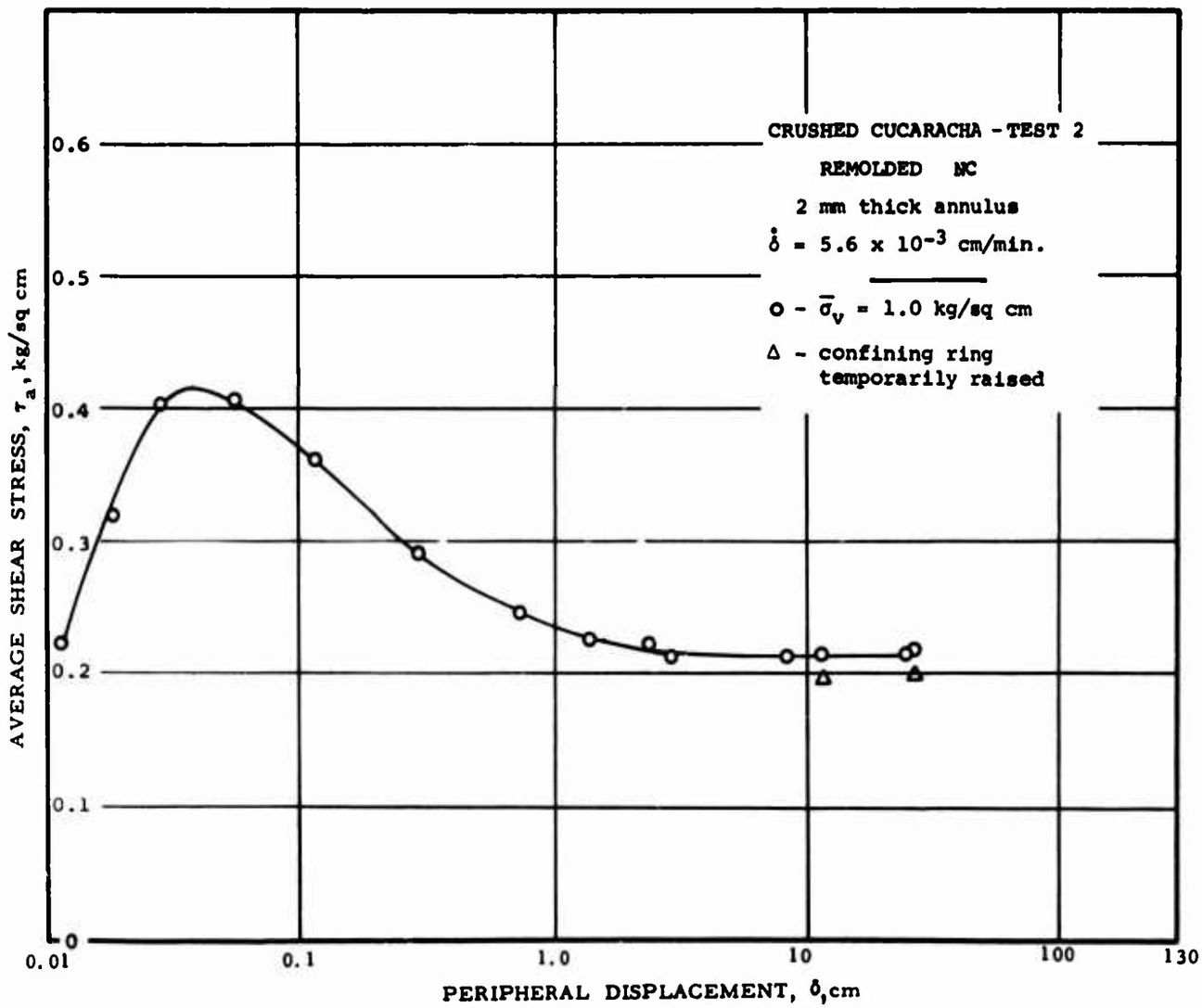
CRUSHED CUCARACHA - TEST 2
REMOLDED NC
2 mm thick annulus
$\dot{\delta}$ = 5.6 x 10^{-3} cm/min.
o - $\bar{\sigma}_v$ = 1.0 kg/sq cm
Δ - confining ring temporarily raised
0.6
0.5
0.4
0.3
0.2
0.1
0
AVERAGE SHEAR STRESS, τ_a, kg/sq cm
0.01
0.1
1.0
10
100
130
PERIPHERAL DISPLACEMENT, δ, cm

FIG. 8-5

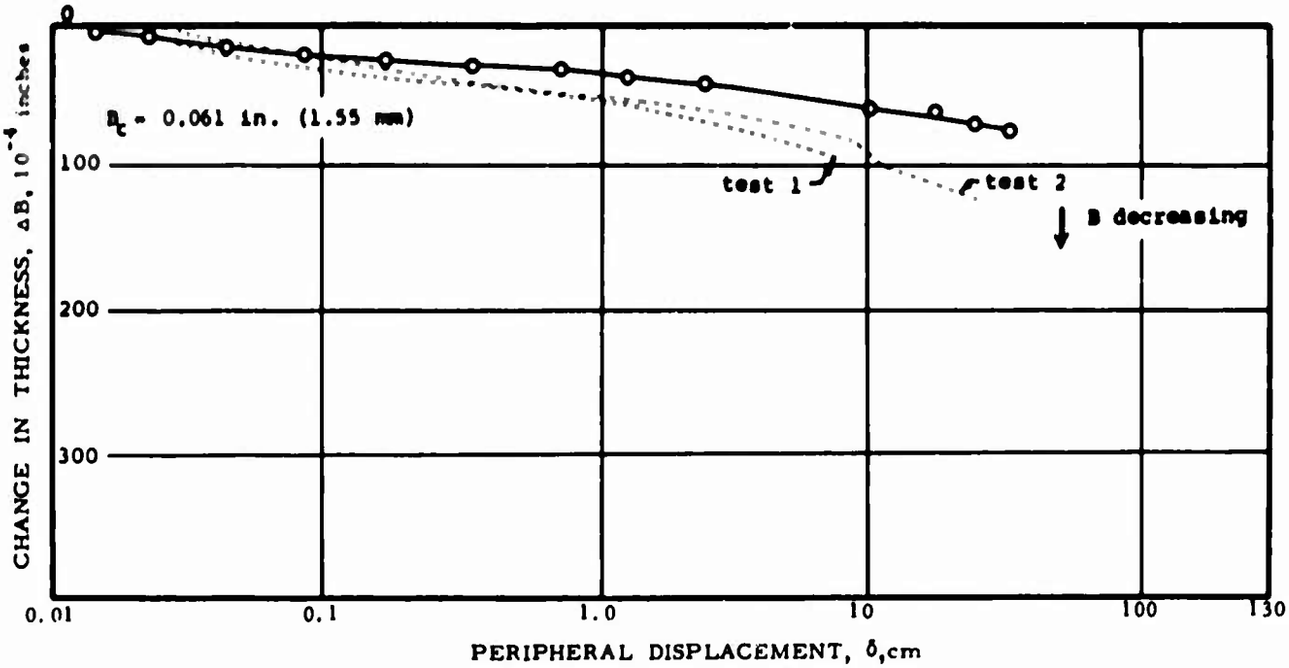
0
100
200
300
R_t = 0.061 in. (1.55 mm)
test 1
test 2
B decreasing
CHANGE IN THICKNESS, ΔB, 10^{-4} inches
0.01
0.1
1.0
10
100
130
PERIPHERAL DISPLACEMENT, δ,cm

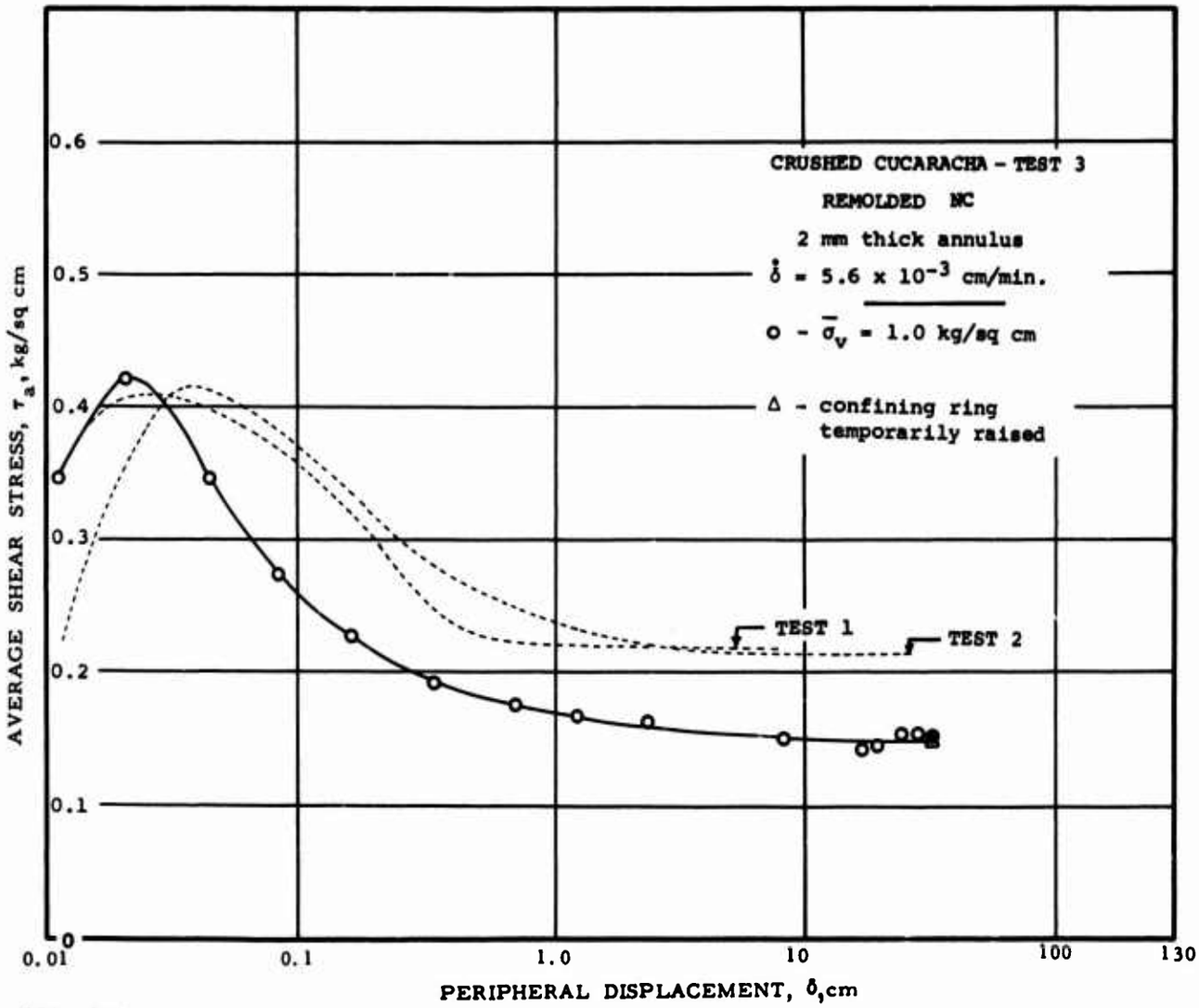
0.6
0.5
0.4
0.3
0.2
0.1
0
CRUSHED CUCARACHA - TEST 3
REMOLDED NC
2 mm thick annulus
$\dot{\delta}$ = 5.6 x 10^{-3} cm/min.
o - $\bar{\sigma}_v$ = 1.0 kg/sq cm
Δ - confining ring temporarily raised
TEST 1
TEST 2
AVERAGE SHEAR STRESS, τ_a, kg/sq cm
0.01
0.1
1.0
10
100
130
PERIPHERAL DISPLACEMENT, δ,cm

FIG. 8-6

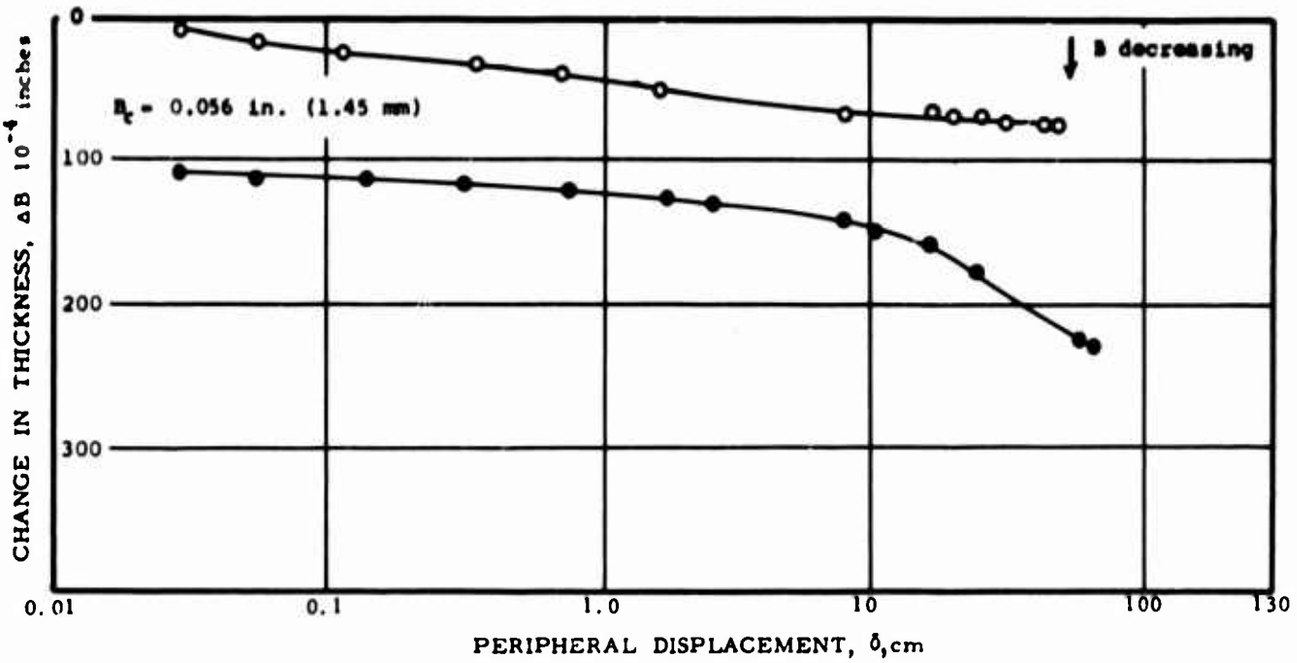
CHANGE IN THICKNESS, ΔB 10^{-4} inches
0
100
200
300
B decreasing
B_c = 0.056 in. (1.45 mm)
0.01
0.1
1.0
10
100
130
PERIPHERAL DISPLACEMENT, δ, cm

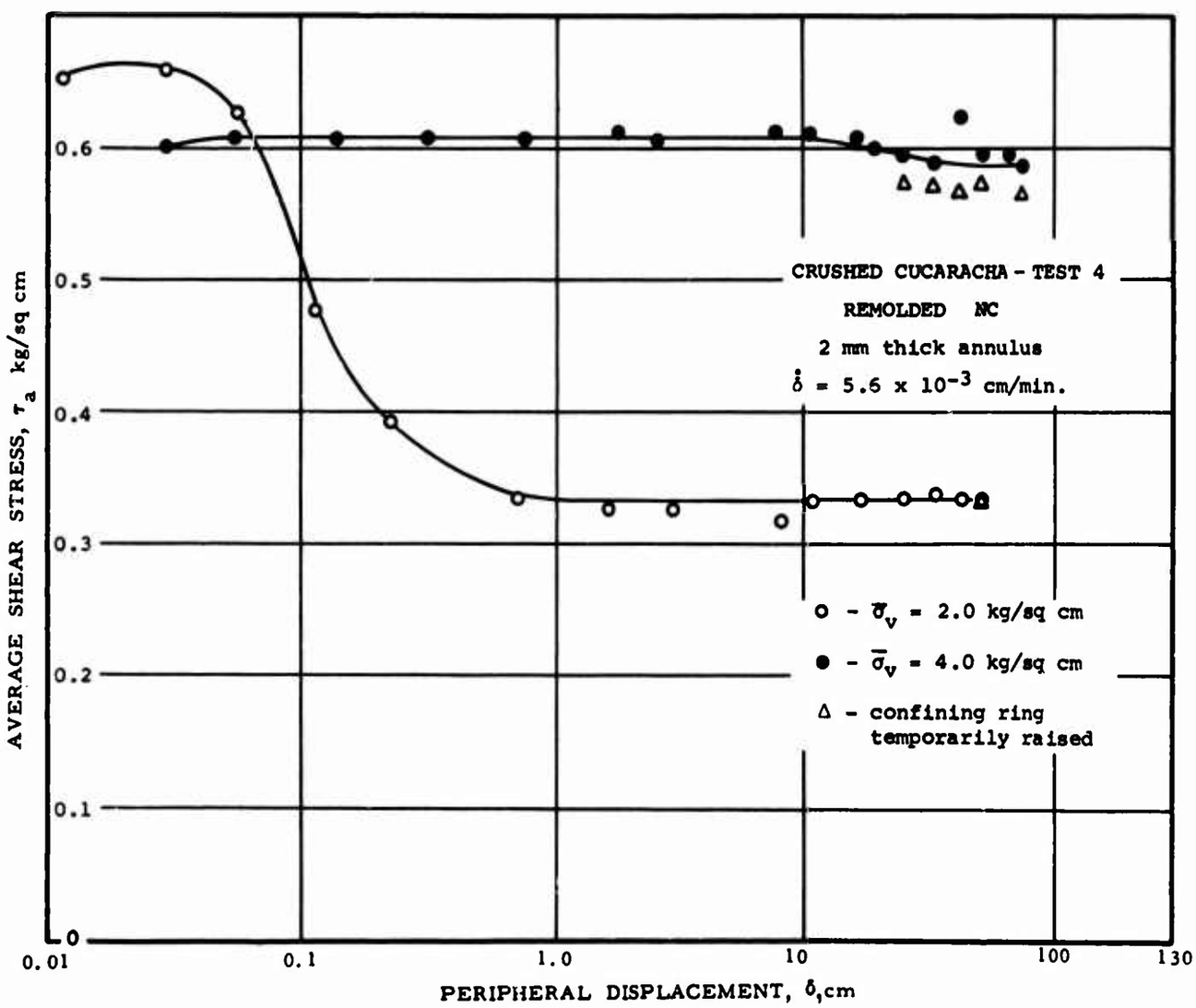
AVERAGE SHEAR STRESS, τ_a kg/sq cm
0.6
0.5
0.4
0.3
0.2
0.1
0
CRUSHED CUCARACHA - TEST 4
REMOLDED NC
2 mm thick annulus
$\dot{\delta}$ = 5.6 x 10^{-3} cm/min.
o - $\bar{\sigma}_v$ = 2.0 kg/sq cm
● - $\bar{\sigma}_v$ = 4.0 kg/sq cm
Δ - confining ring temporarily raised
0.01
0.1
1.0
10
100
130
PERIPHERAL DISPLACEMENT, δ, cm

FIG. 8-7

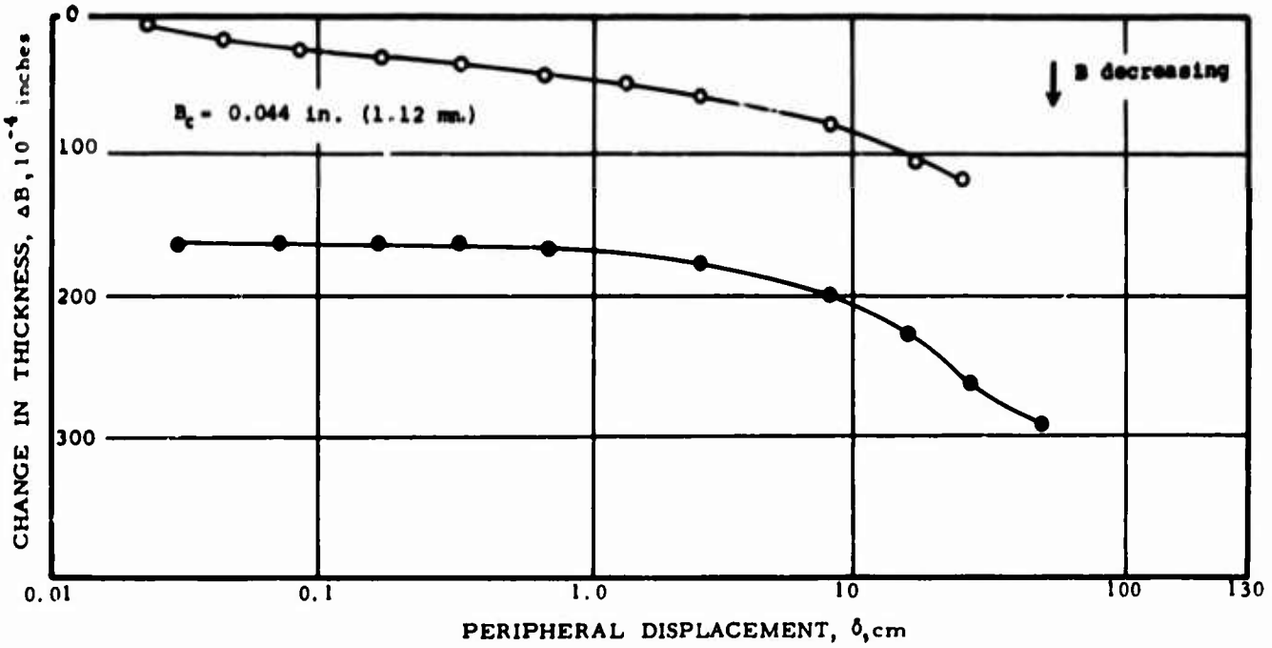
CHANGE IN THICKNESS, ΔB, 10^{-4} inches
0
100
200
300
B_c = 0.044 in. (1.12 mm.)
B decreasing
0.01
0.1
1.0
10
100
130
PERIPHERAL DISPLACEMENT, δ, cm

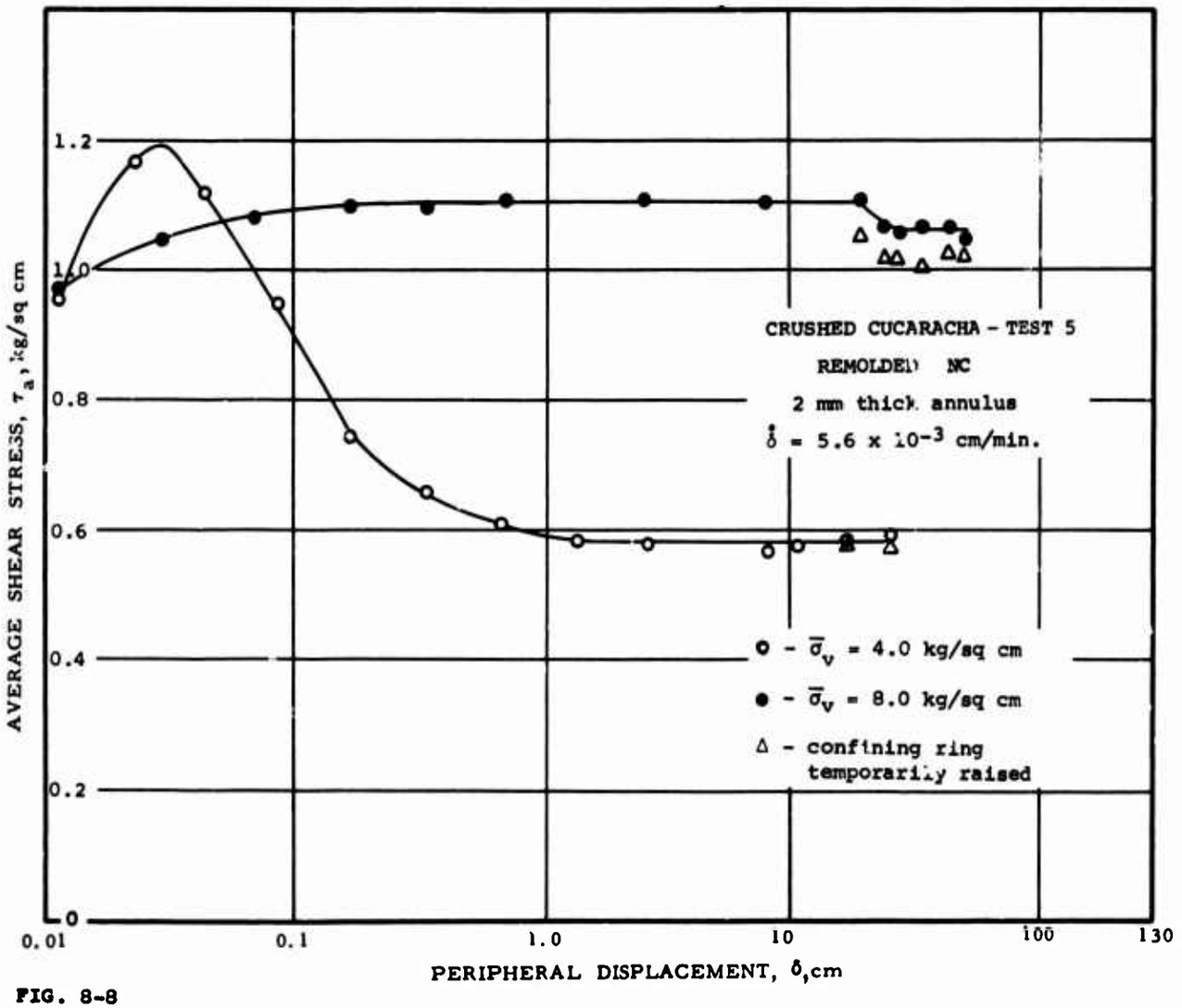
AVERAGE SHEAR STRESS, τ_a, kg/sq cm
1.2
1.0
0.8
0.6
0.4
0.2
0
CRUSHED CUCARACHA - TEST 5
REMOLDED NC
2 mm thick annulus
$\dot{\delta}$ = 5.6 x 10^{-3} cm/min.
○ - $\bar{\sigma}_v$ = 4.0 kg/sq cm
● - $\bar{\sigma}_v$ = 8.0 kg/sq cm
△ - confining ring temporarily raised
0.01
0.1
1.0
10
100
130
PERIPHERAL DISPLACEMENT, δ, cm

FIG. 8-8

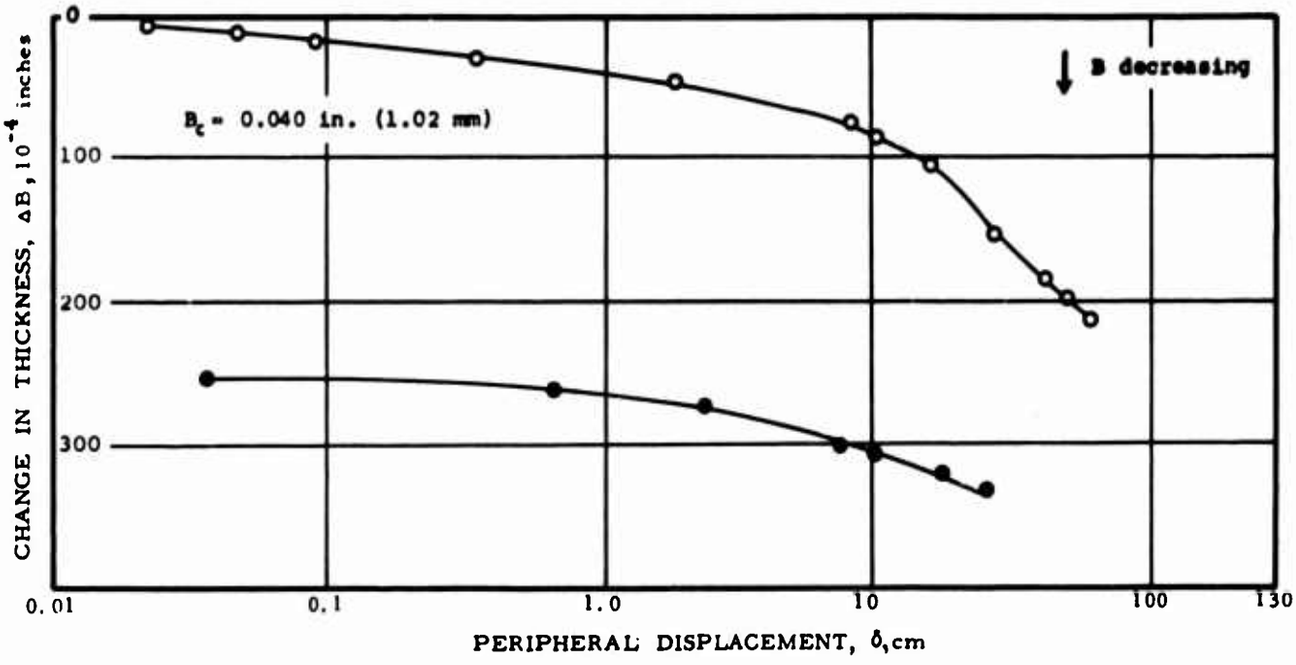
CHANGE IN THICKNESS, ΔB, 10^{-4} inches
0
100
200
300
B_c = 0.040 in. (1.02 mm)
B decreasing
0.01
0.1
1.0
10
100
130
PERIPHERAL DISPLACEMENT, δ, cm

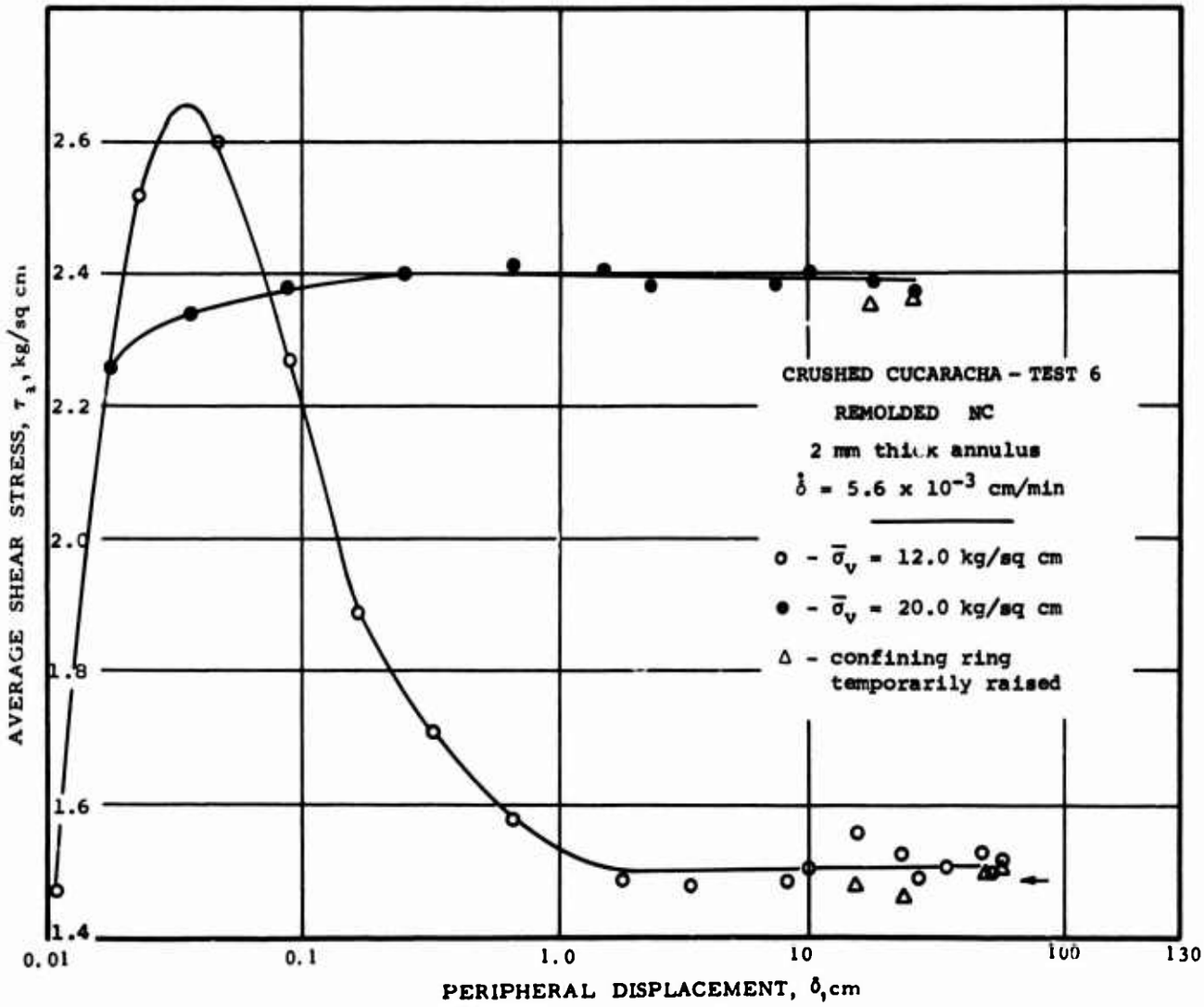
AVERAGE SHEAR STRESS, τ_a, kg/sq cm
2.6
2.4
2.2
2.0
1.8
1.6
1.4
CRUSHED CUCARACHA - TEST 6
REMOLDED NC
2 mm thick annulus
$\dot{\delta}$ = 5.6 x 10^{-3} cm/min
o - $\bar{\sigma}_v$ = 12.0 kg/sq cm
● - $\bar{\sigma}_v$ = 20.0 kg/sq cm
Δ - confining ring temporarily raised
0.01
0.1
1.0
10
100
130
PERIPHERAL DISPLACEMENT, δ, cm

FIG. 8-9

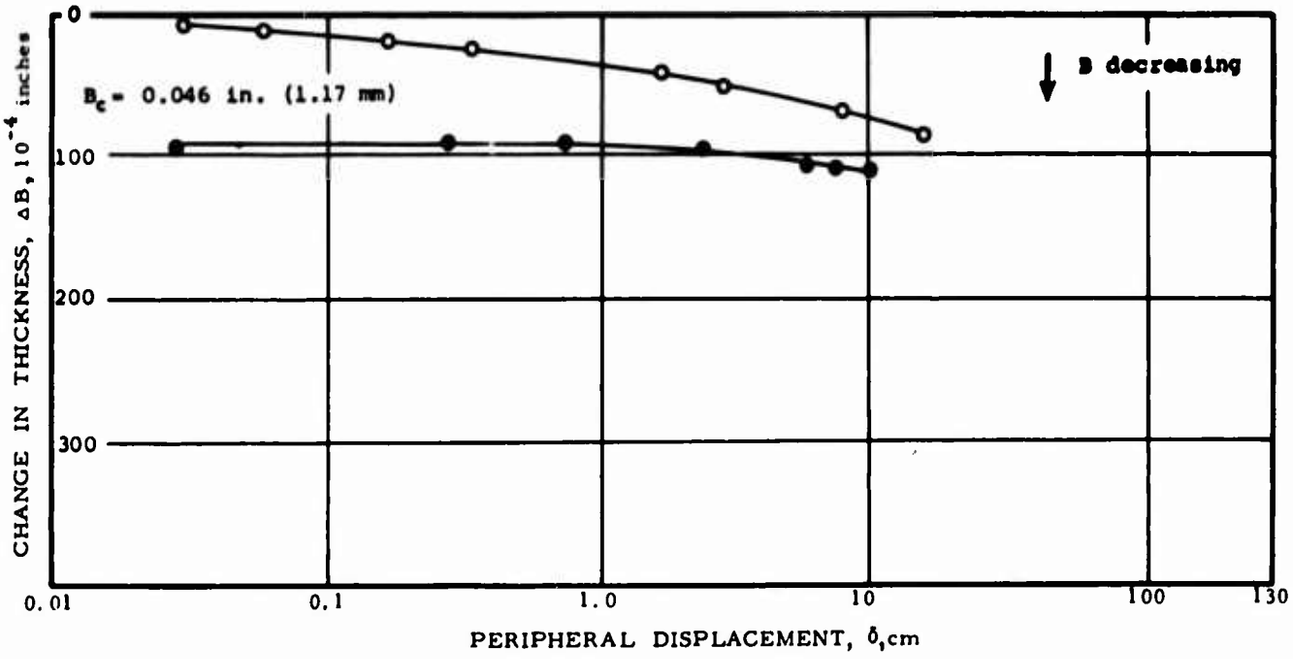
0
100
200
300
B_c = 0.046 in. (1.17 mm)
B decreasing
CHANGE IN THICKNESS, ΔB, 10^{-4} inches
0.01
0.1
1.0
10
100
130
PERIPHERAL DISPLACEMENT, δ, cm

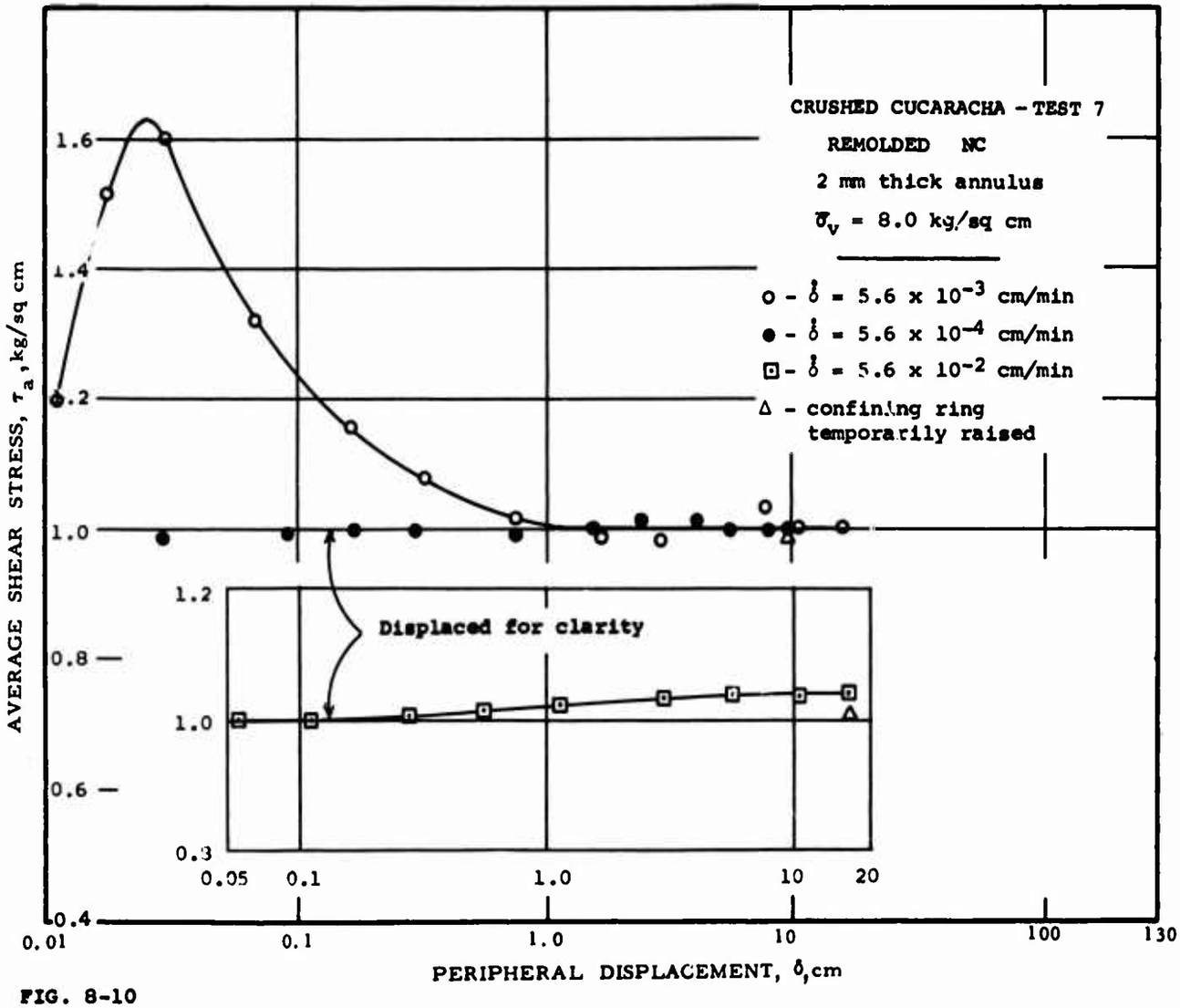
CRUSHED CUCARACHA - TEST 7
REMOLDED NC
2 mm thick annulus
$\bar{\sigma}_v$ = 8.0 kg/sq cm
○ - $\dot{\delta}$ = 5.6 x 10^{-3} cm/min
● - $\dot{\delta}$ = 5.6 x 10^{-4} cm/min
⊡ - $\dot{\delta}$ = 5.6 x 10^{-2} cm/min
Δ - confining ring temporarily raised
Displaced for clarity
1.6
1.4
1.2
1.0
0.8
0.6
0.4
0.3
0.05
20
AVERAGE SHEAR STRESS, τ_a, kg/sq cm
0.01
0.1
1.0
10
100
130
PERIPHERAL DISPLACEMENT, δ, cm

FIG. 8-10

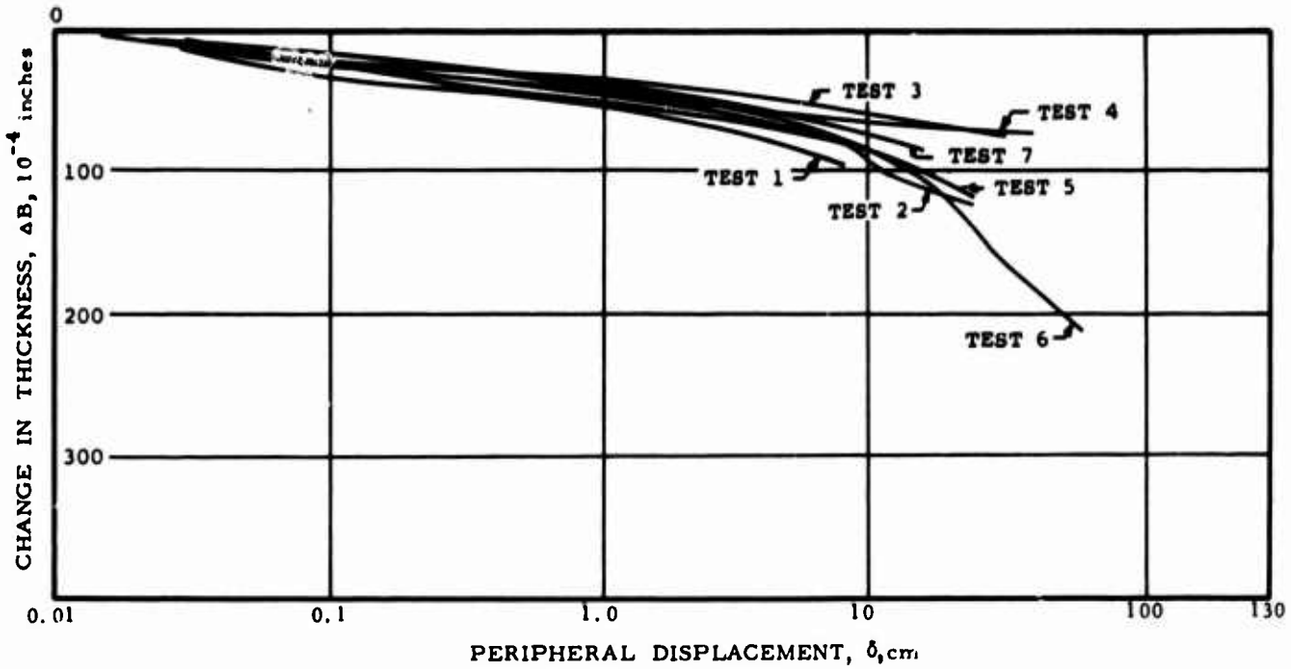
0
100
200
300
CHANGE IN THICKNESS, ΔB, 10^{-4} inches
TEST 3
TEST 4
TEST 7
TEST 1
TEST 5
TEST 2
TEST 6
0.01
0.1
1.0
10
100
130
PERIPHERAL DISPLACEMENT, δ, cm

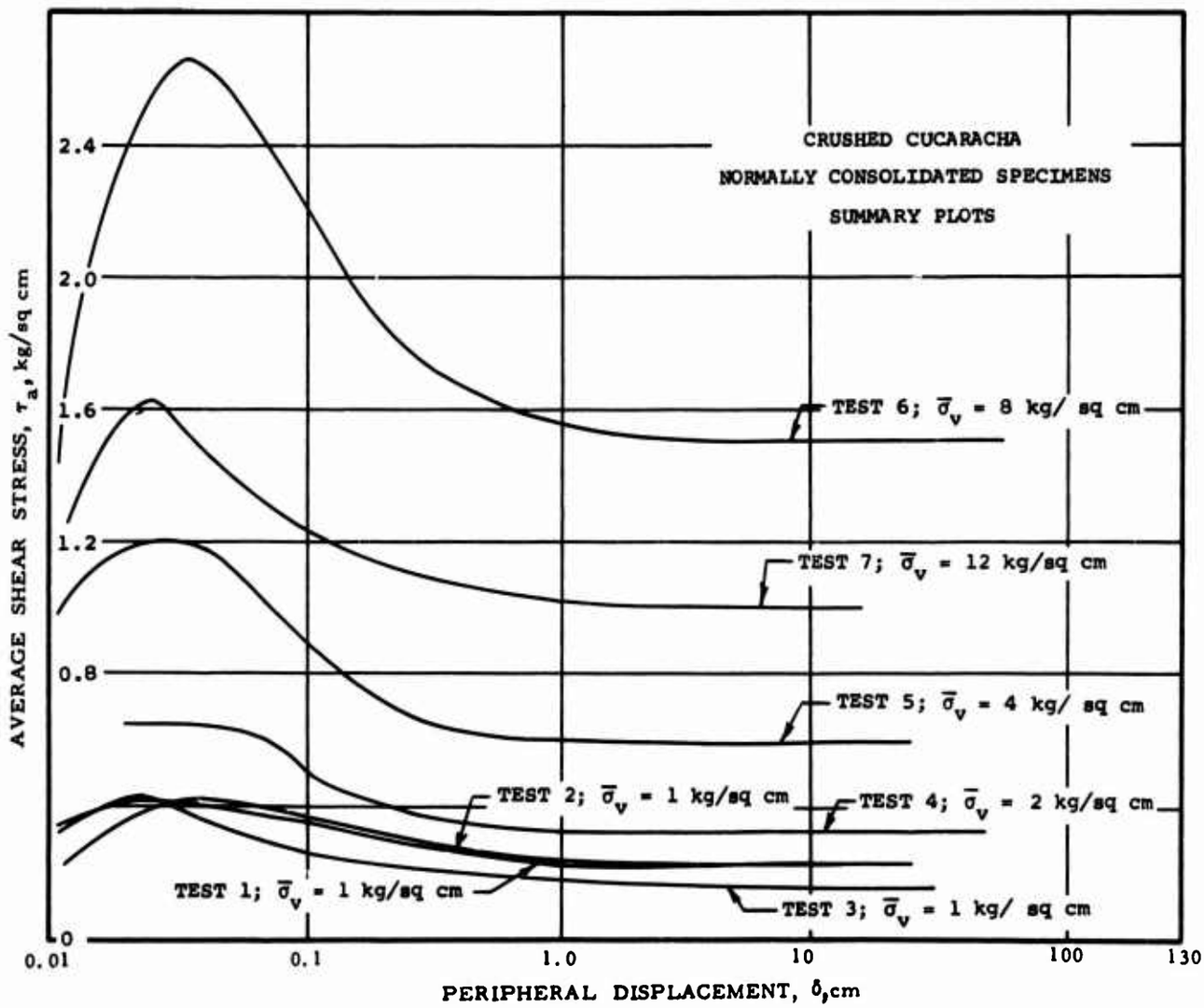
CRUSHED CUCARACHA
NORMALLY CONSOLIDATED SPECIMENS
SUMMARY PLOTS
2.4
2.0
1.6
1.2
0.8
0
AVERAGE SHEAR STRESS, τ_a, kg/sq cm
TEST 6; $\bar{\sigma}_v$ = 8 kg/ sq cm
TEST 7; $\bar{\sigma}_v$ = 12 kg/sq cm
TEST 5; $\bar{\sigma}_v$ = 4 kg/ sq cm
TEST 2; $\bar{\sigma}_v$ = 1 kg/sq cm
TEST 4; $\bar{\sigma}_v$ = 2 kg/sq cm
TEST 1; $\bar{\sigma}_v$ = 1 kg/sq cm
TEST 3; $\bar{\sigma}_v$ = 1 kg/ sq cm
0.01
0.1
1.0
10
100
130
PERIPHERAL DISPLACEMENT, δ, cm

FIG. 8-11

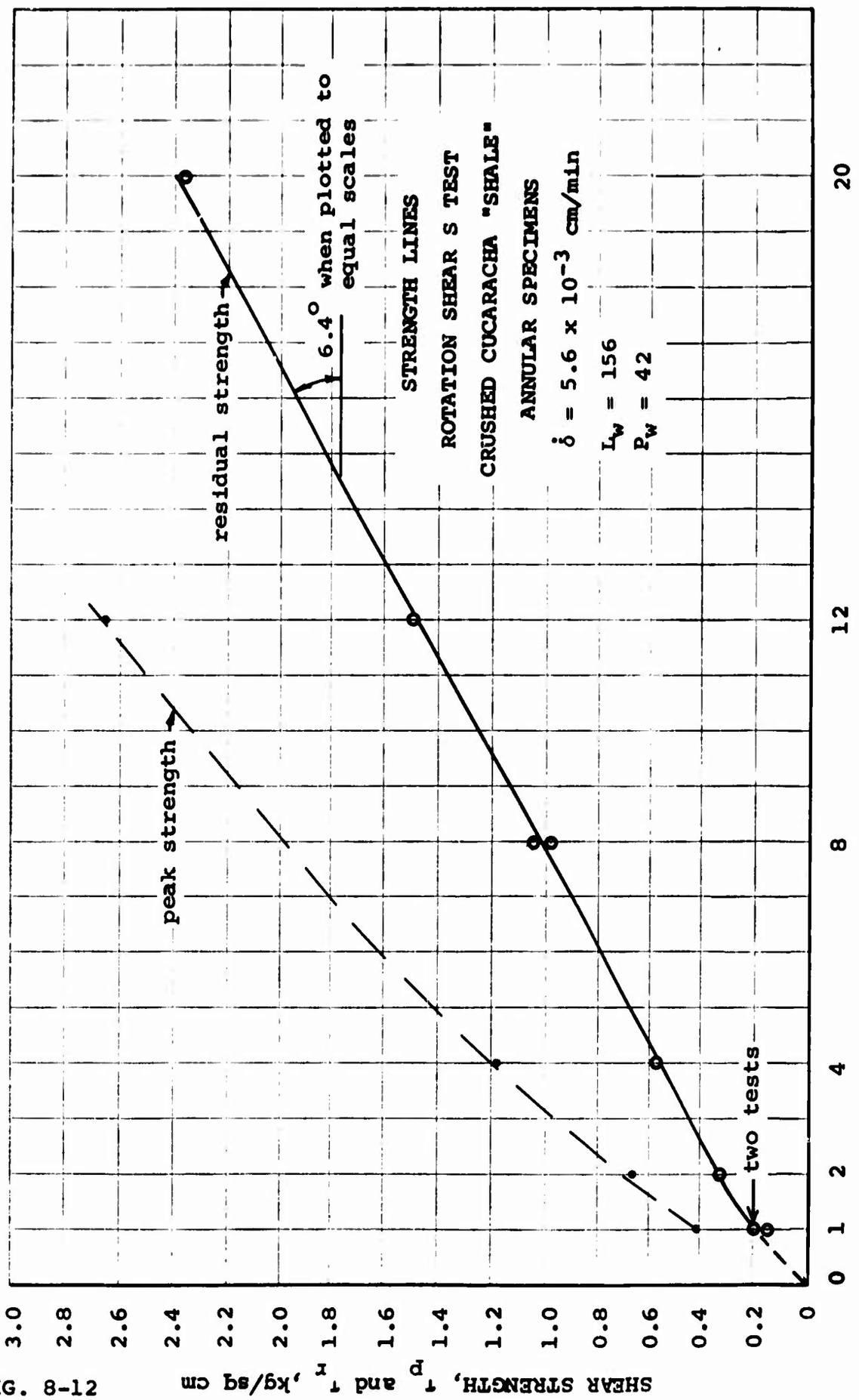
STRENGTH LINES
ROTATION SHEAR S TEST
CRUSHED CUCARACHA "SHALE"
ANNULAR SPECIMENS
$\dot{\delta}$ = 5.6 x 10^{-3} cm/min
L_w = 156
P_w = 42
residual strength
6.4° when plotted to equal scales
peak strength
two tests
SHEAR STRENGTH, τ_p and τ_r, kg/sq cm
EFFECTIVE VERTICAL STRESS, $\bar{\sigma}_v$, kg/sq cm
0
0.2
0.4
0.6
0.8
1.0
1.2
1.4
1.6
1.8
2.0
2.2
2.4
2.6
2.8
3.0
0
1
2
4
8
12
20

FIG. 8-12

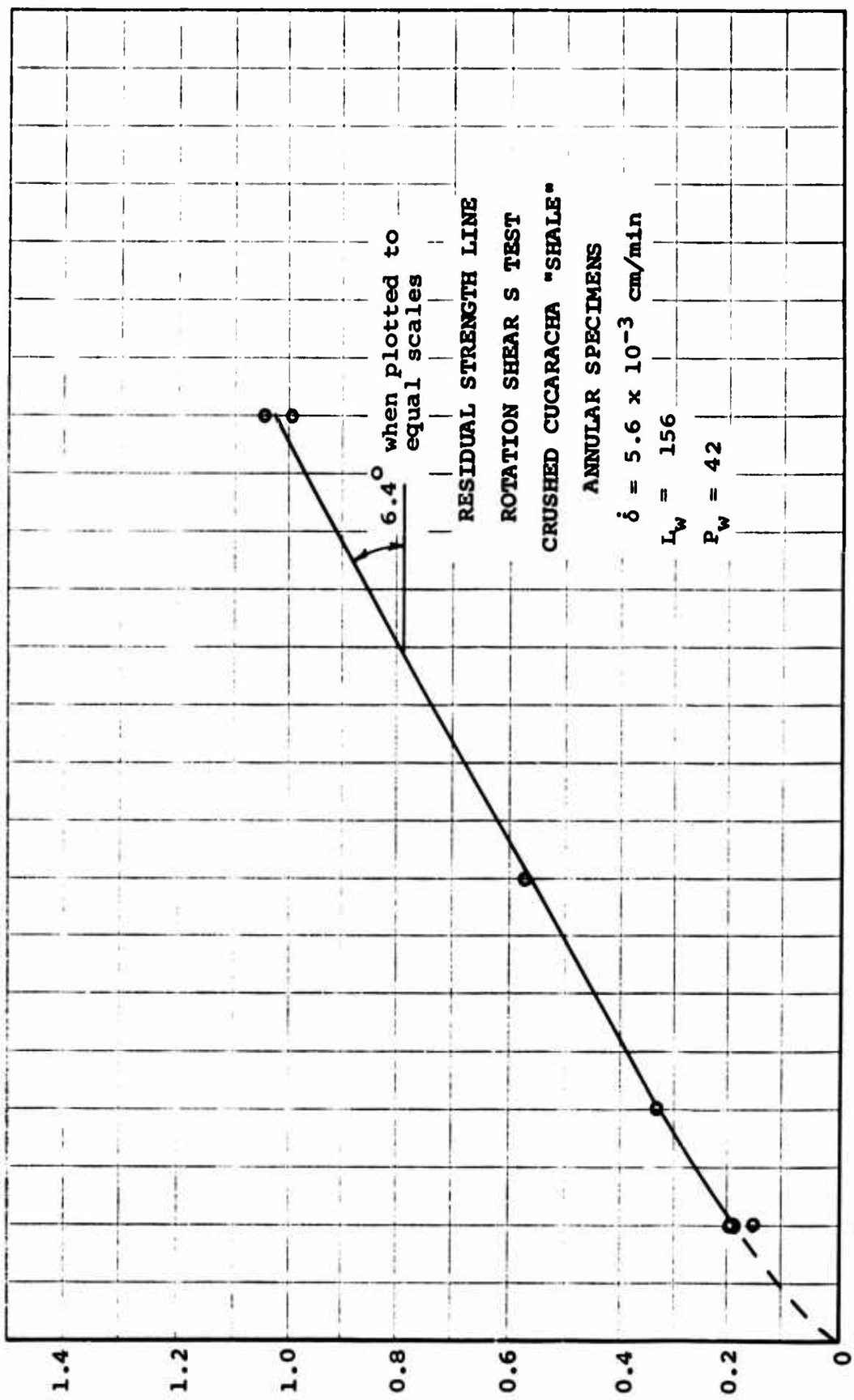
RESIDUAL STRENGTH LINE
ROTATION SHEAR S TEST
CRUSHED CUCARACHA "SHALE"
ANNULAR SPECIMENS
$\dot{\delta}$ = 5.6 x 10^{-3} cm/min
L_w = 156
P_w = 42
6.4° when plotted to equal scales
RESIDUAL SHEAR STRENGTH, τ_r, kg/sq cm
EFFECTIVE VERTICAL STRESS, $\bar{\sigma}_v$, kg/sq cm
0
0.2
0.4
0.6
0.8
1.0
1.2
1.4
0
1
2
3
4
5
6
7
8

FIG. 8-13

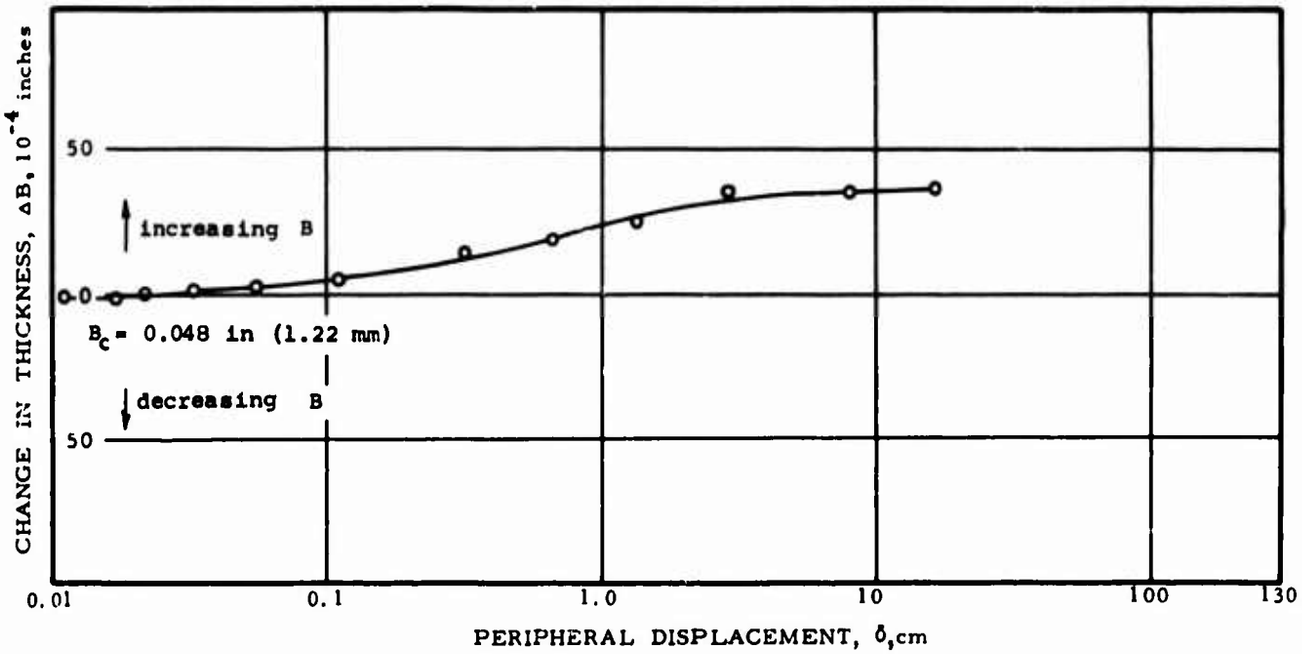
CHANGE IN THICKNESS, ΔB, 10^{-4} inches
50
increasing B
0
B_c = 0.048 in (1.22 mm)
decreasing B
50
0.01
0.1
1.0
10
100
130
PERIPHERAL DISPLACEMENT, δ,cm

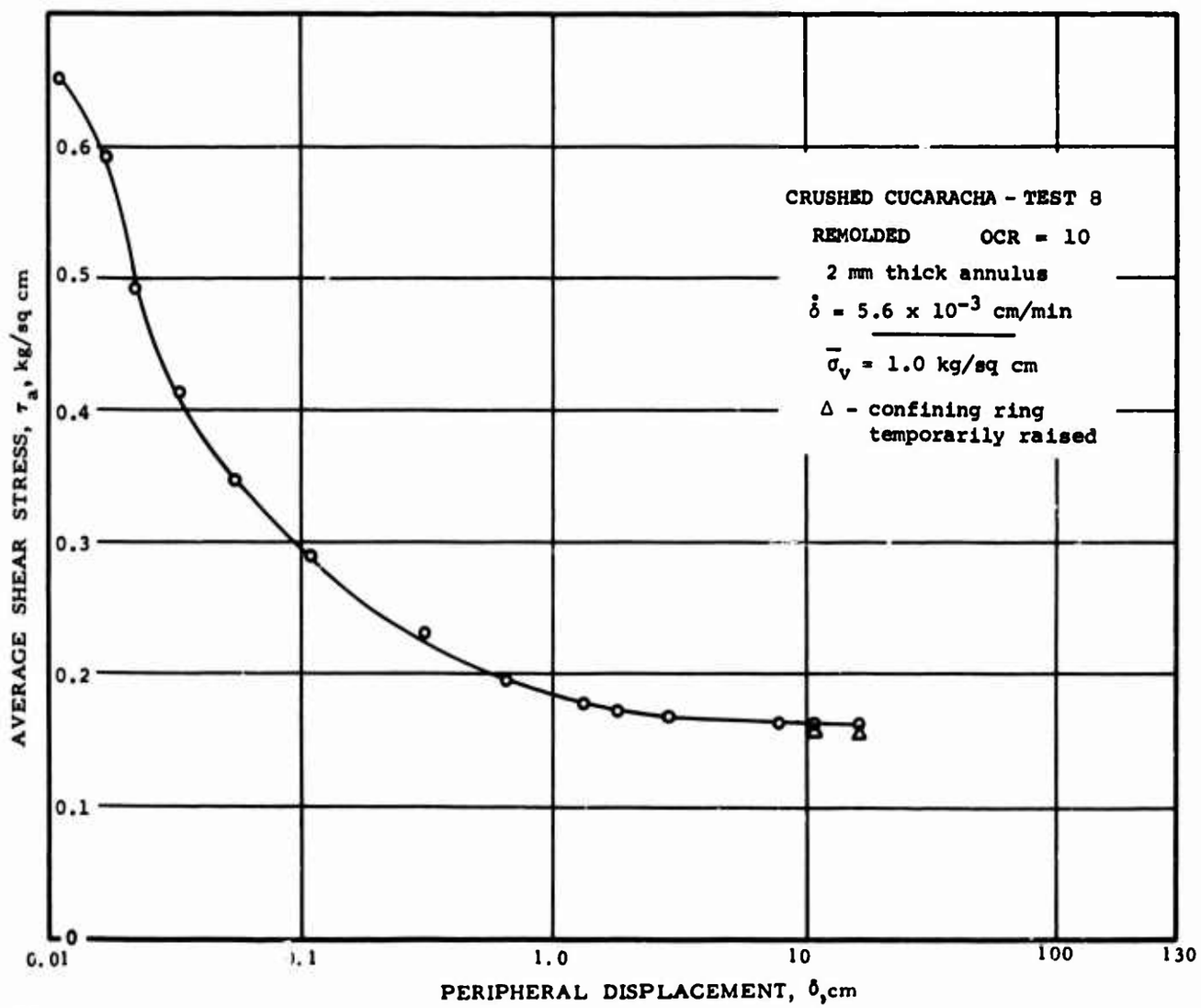
AVERAGE SHEAR STRESS, τ_a, kg/sq cm
0.6
0.5
0.4
0.3
0.2
0.1
0
CRUSHED CUCARACHA - TEST 8
REMOLDED OCR = 10
2 mm thick annulus
$\dot{\delta}$ = 5.6 x 10^{-3} cm/min
$\bar{\sigma}_v$ = 1.0 kg/sq cm
Δ - confining ring temporarily raised
0.01
0.1
1.0
10
100
130
PERIPHERAL DISPLACEMENT, δ,cm

FIG. 8-14

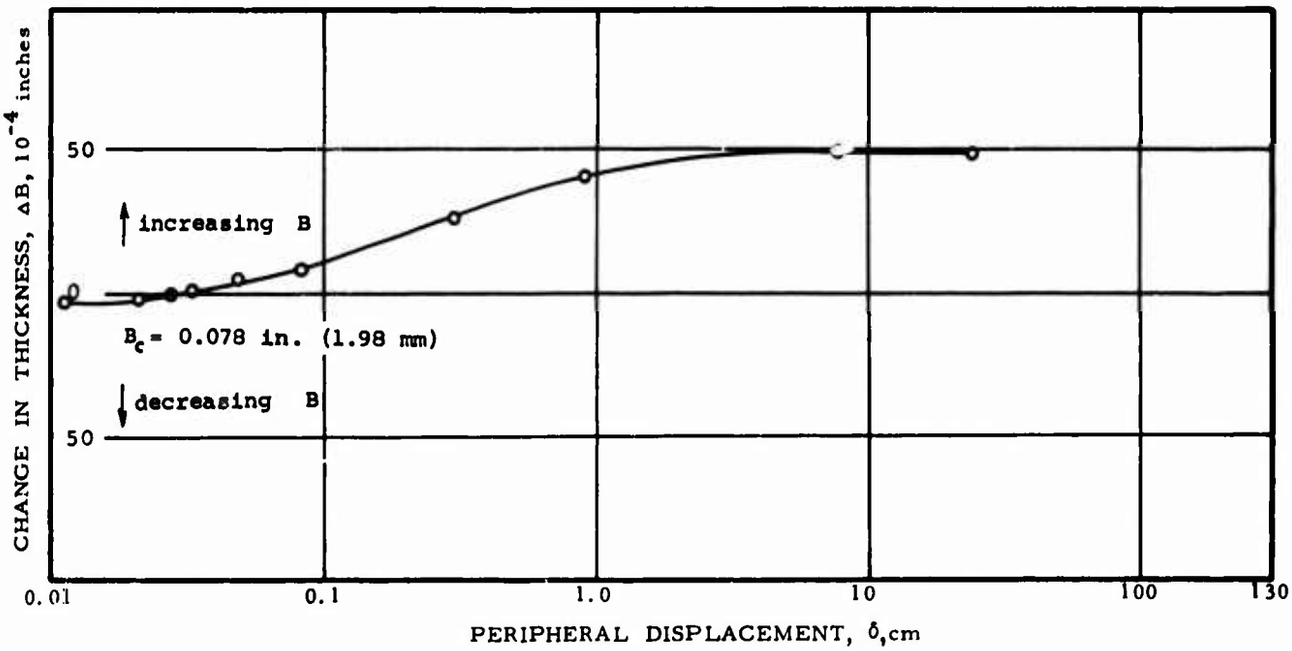
CHANGE IN THICKNESS, ΔB, 10^{-4} inches
50
increasing B
0
B_c = 0.078 in. (1.98 mm)
decreasing B
50
0.01
0.1
1.0
10
100
130
PERIPHERAL DISPLACEMENT, δ,cm

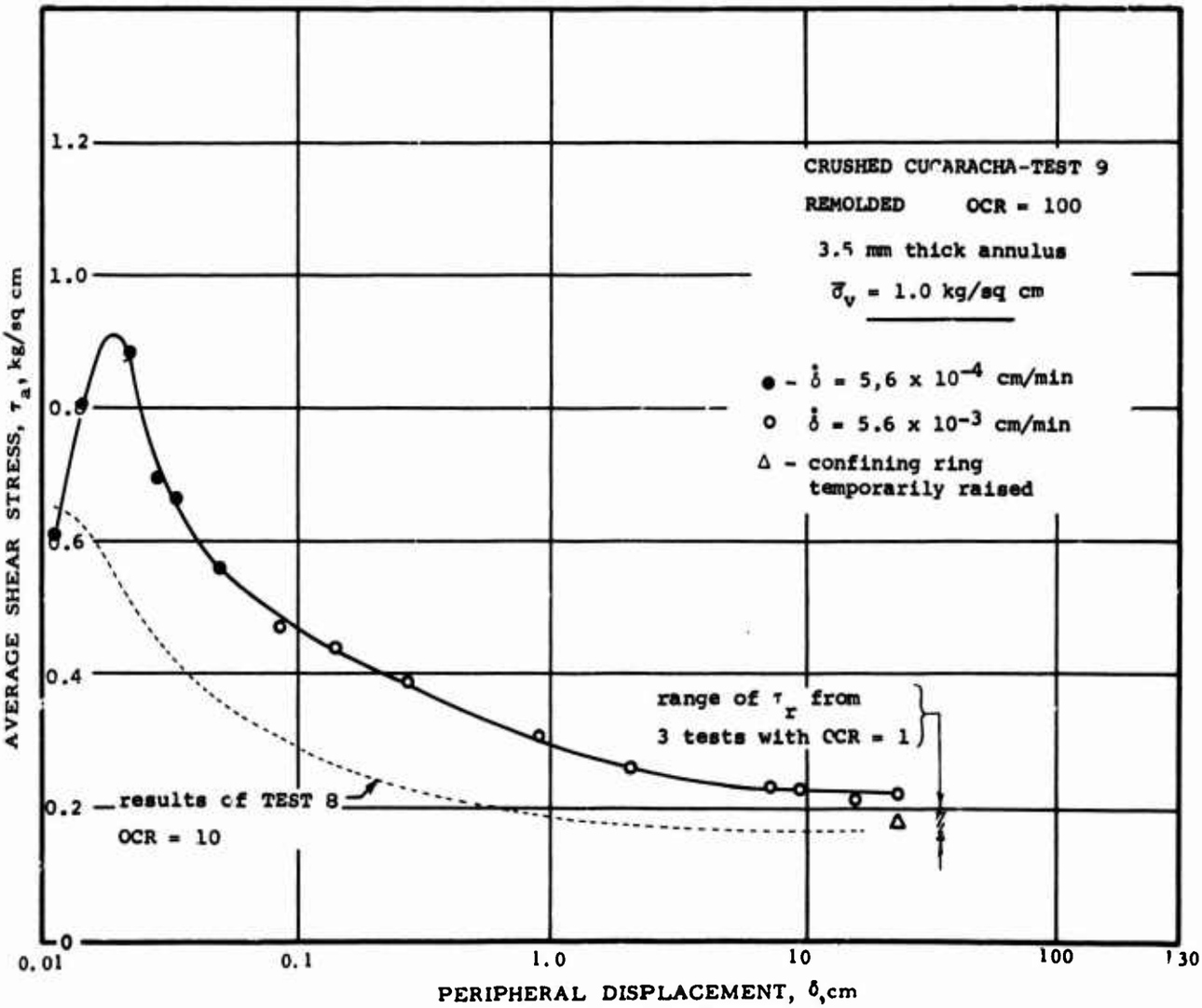
AVERAGE SHEAR STRESS, τ_a, kg/sq cm
1.2
1.0
0.8
0.6
0.4
0.2
0
CRUSHED CUCARACHA-TEST 9
REMOLDED OCR = 100
3.5 mm thick annulus
$\bar{\sigma}_v$ = 1.0 kg/sq cm
● - $\dot{\delta}$ = 5,6 x 10^{-4} cm/min
o $\dot{\delta}$ = 5.6 x 10^{-3} cm/min
Δ - confining ring temporarily raised
range of τ_r from 3 tests with OCR = 1
results of TEST 8
OCR = 10
0.01
0.1
1.0
10
100
130
PERIPHERAL DISPLACEMENT, δ,cm

FIG. 8-15

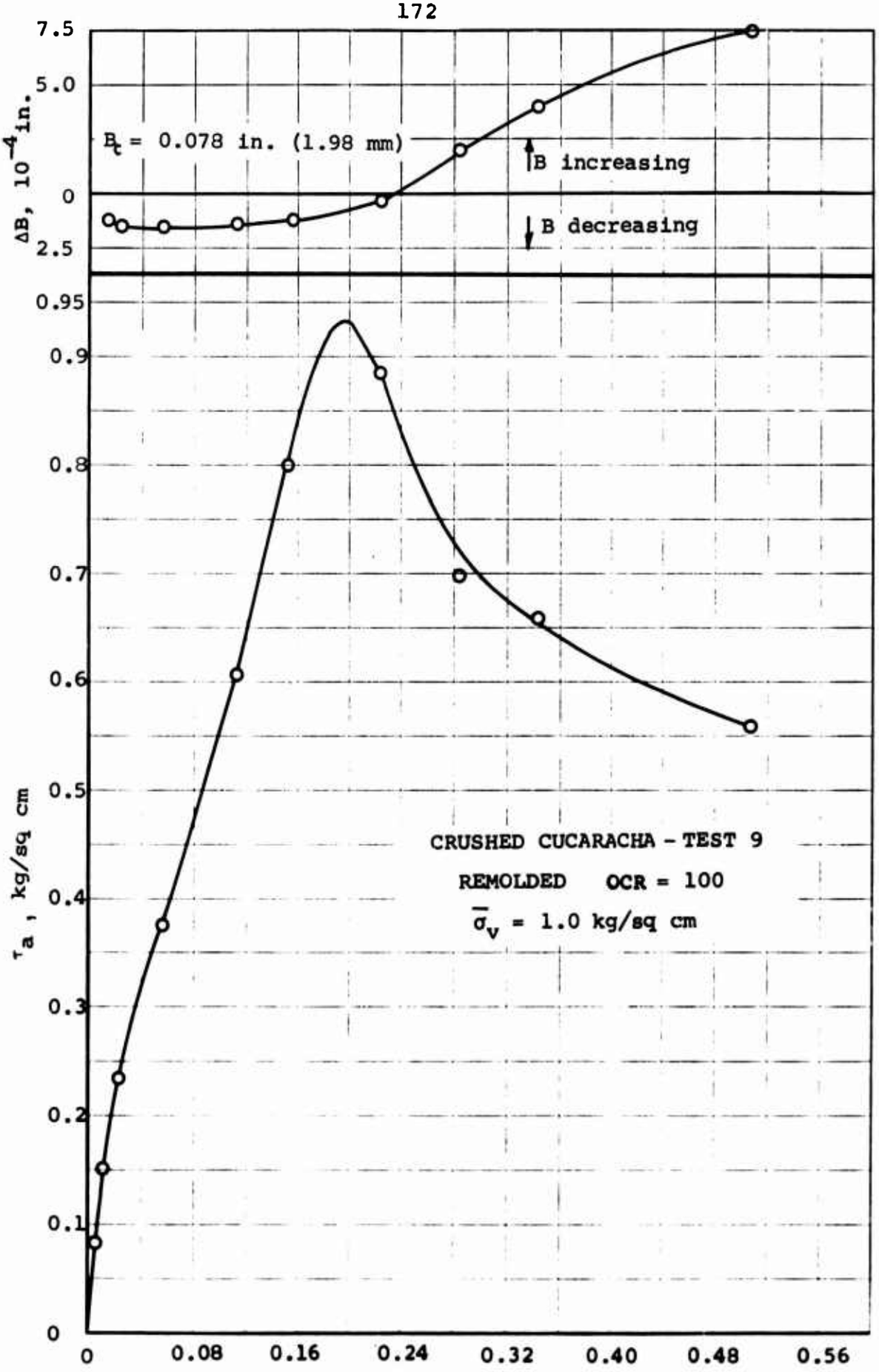
7.5
5.0
0
2.5
ΔB, 10⁻⁴ in.
B_c = 0.078 in. (1.98 mm)
B increasing
B decreasing
0.95
0.9
0.8
0.7
0.6
0.5
0.4
0.3
0.2
0.1
0
τa , kg/sq cm
CRUSHED CUCARACHA - TEST 9
REMOLDED OCR = 100
σ̄v = 1.0 kg/sq cm
0
0.08
0.16
0.24
0.32
0.40
0.48
0.56
δ, mm

FIG. 8-16

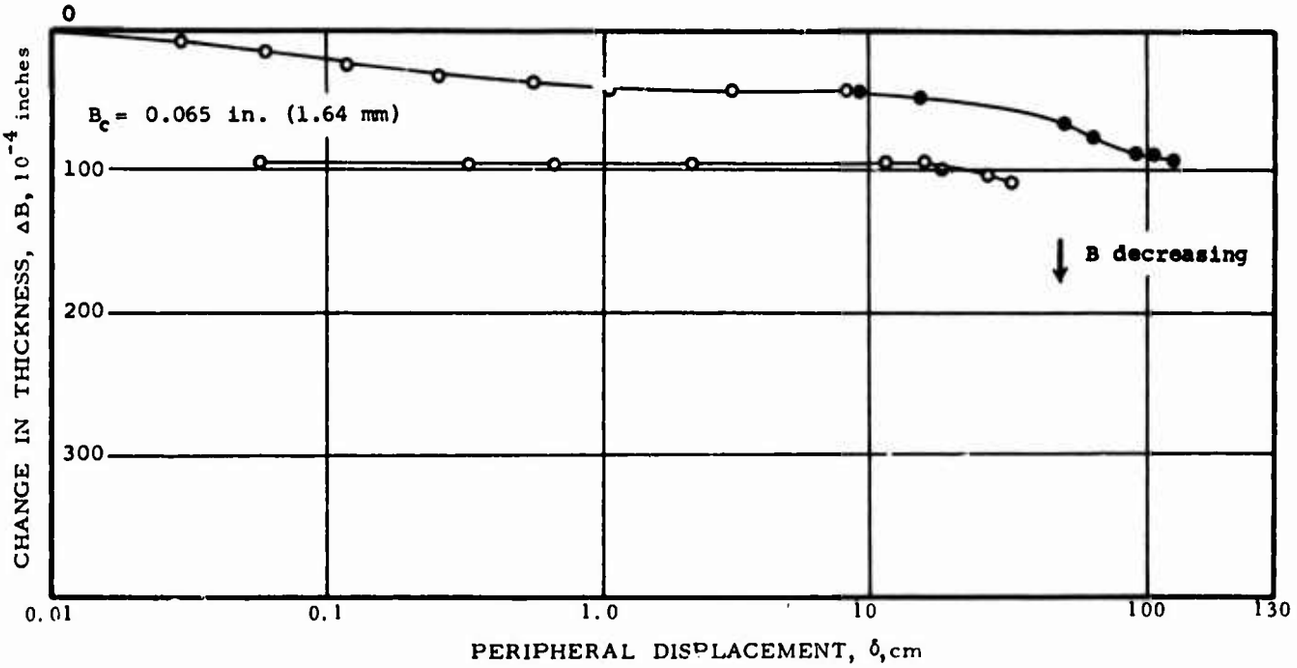
0
100
200
300
B_c = 0.065 in. (1.64 mm)
B decreasing
CHANGE IN THICKNESS, ΔB, 10^{-4} inches
0.01
0.1
1.0
10
100
130
PERIPHERAL DISPLACEMENT, δ, cm

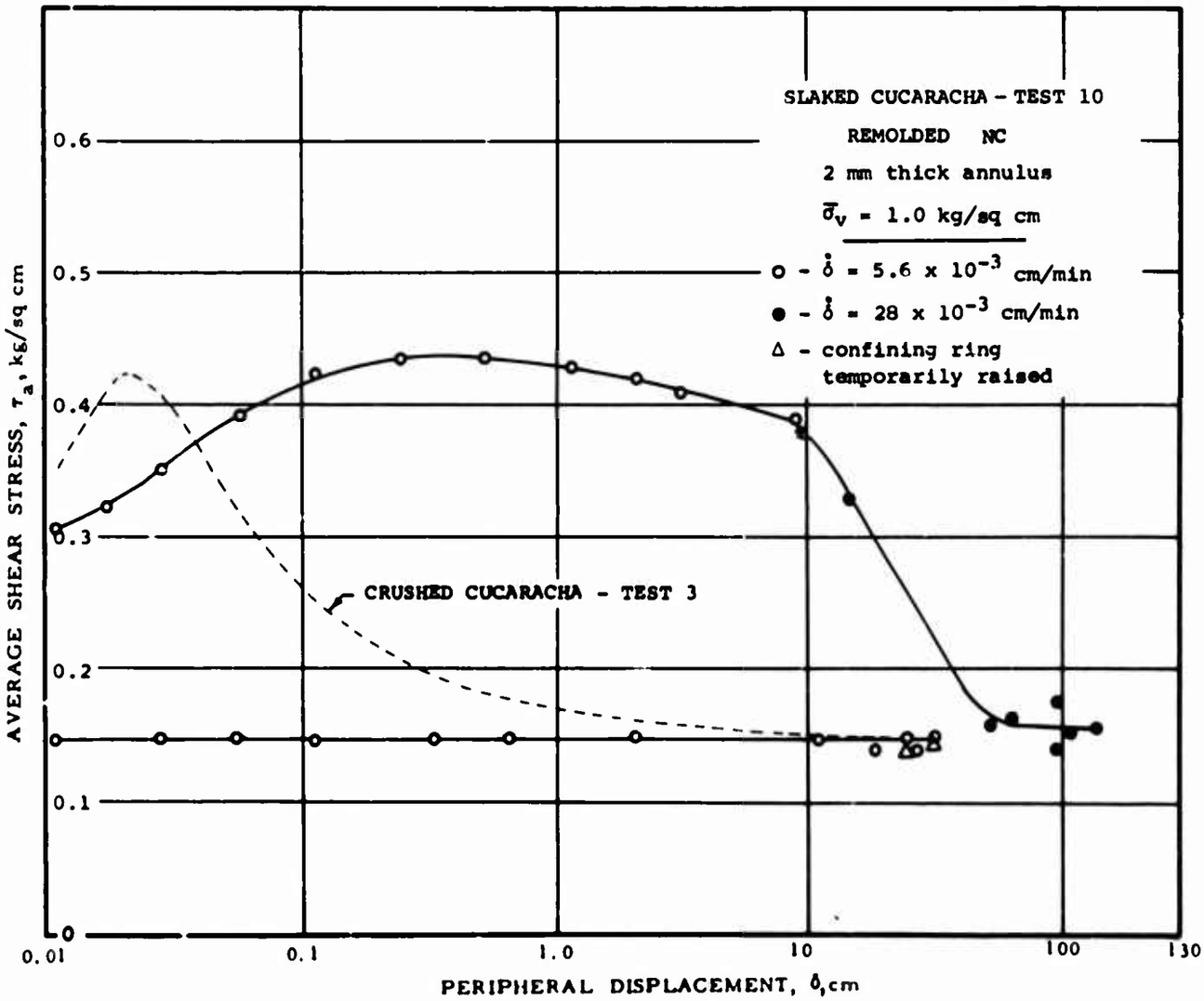
SLAKED CUCARACHA - TEST 10
REMOLDED NC
2 mm thick annulus
$\bar{\sigma}_v$ = 1.0 kg/sq cm
o - $\dot{\delta}$ = 5.6 x 10^{-3} cm/min
● - $\dot{\delta}$ = 28 x 10^{-3} cm/min
Δ - confining ring temporarily raised
CRUSHED CUCARACHA - TEST 3
0.6
0.5
0.4
0.3
0.2
0.1
0
AVERAGE SHEAR STRESS, τ_a, kg/sq cm
0.01
0.1
1.0
10
100
130
PERIPHERAL DISPLACEMENT, δ, cm

FIG. 8-17

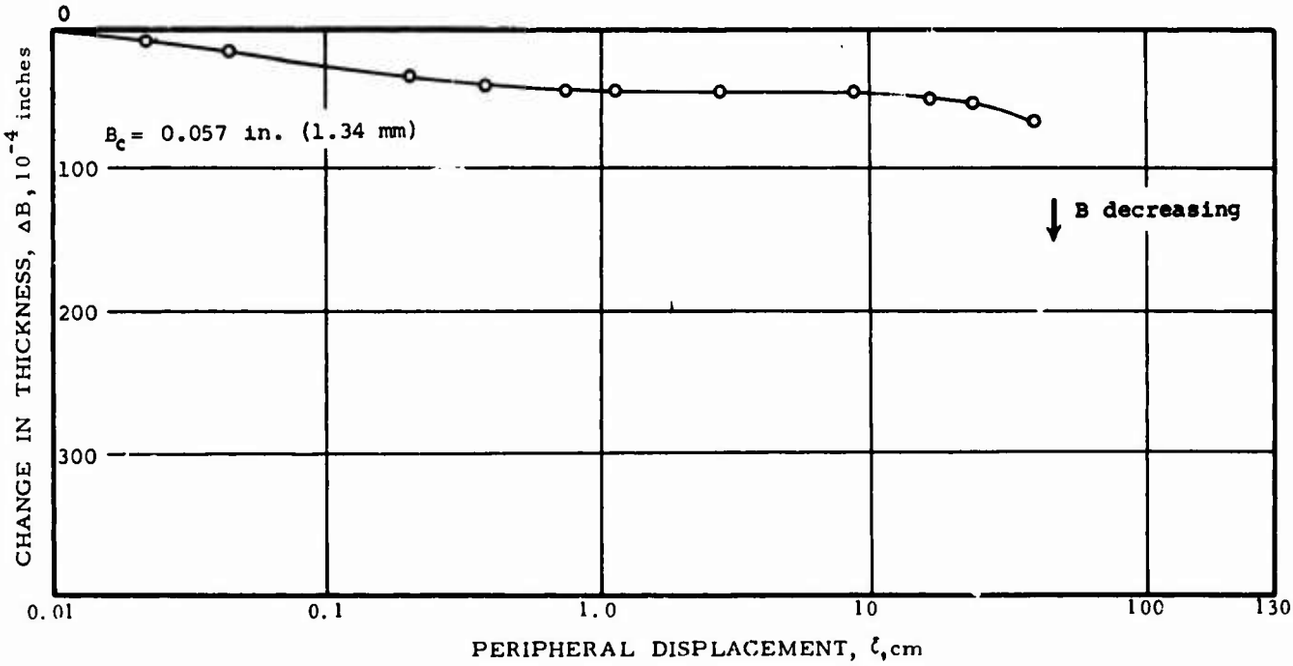
0
100
200
300
B_c = 0.057 in. (1.34 mm)
B decreasing
CHANGE IN THICKNESS, ΔB, 10^{-4} inches
0.01
0.1
1.0
10
100
130
PERIPHERAL DISPLACEMENT, ζ, cm

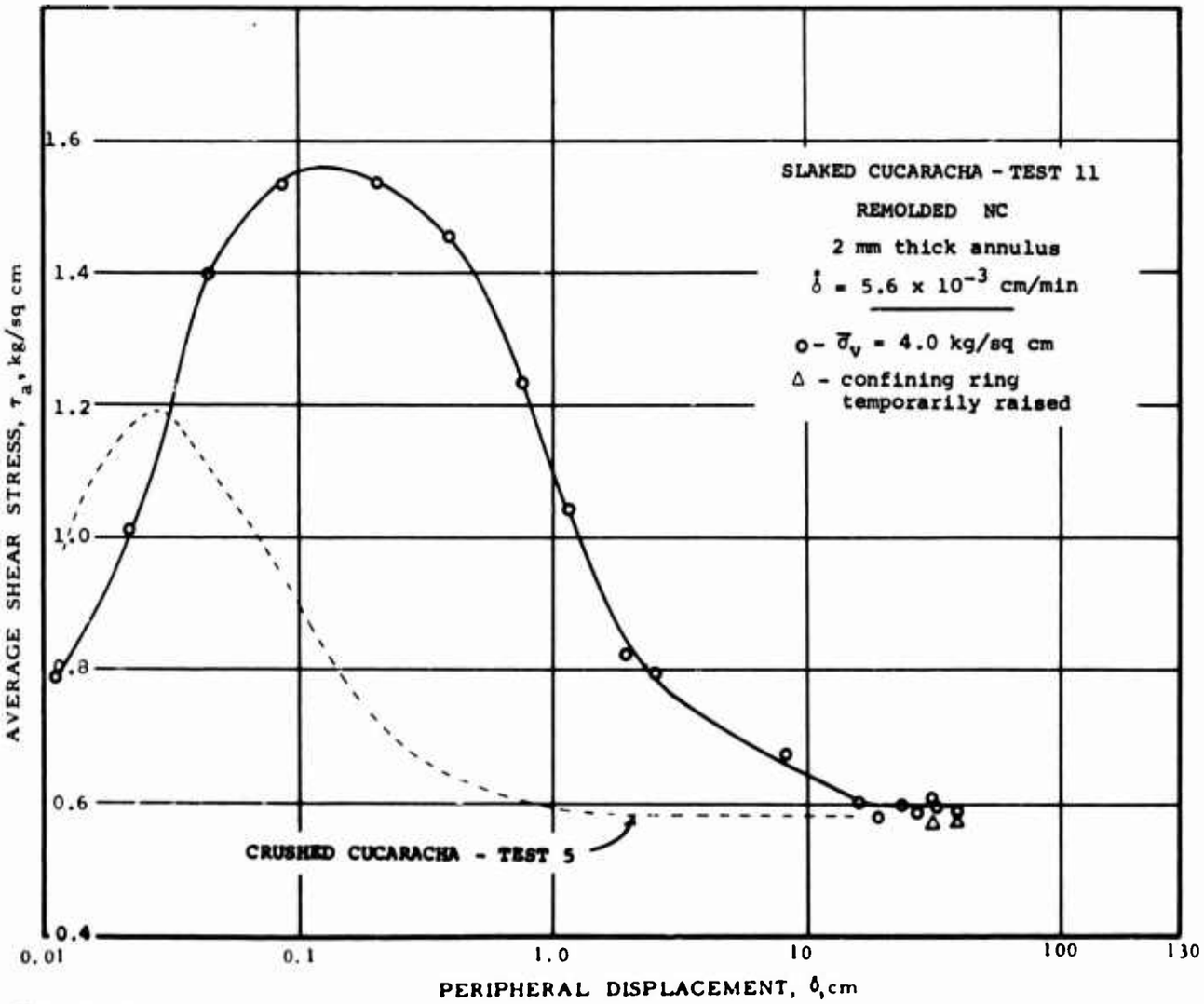
1.6
1.4
1.2
1.0
0.8
0.6
0.4
SLAKED CUCARACHA - TEST 11
REMOLDED NC
2 mm thick annulus
$\dot{\delta}$ = 5.6 x 10^{-3} cm/min
o - $\bar{\sigma}_v$ = 4.0 kg/sq cm
Δ - confining ring temporarily raised
CRUSHED CUCARACHA - TEST 5
AVERAGE SHEAR STRESS, τ_a, kg/sq cm
0.01
0.1
1.0
10
100
130
PERIPHERAL DISPLACEMENT, δ, cm

FIG. 8-18

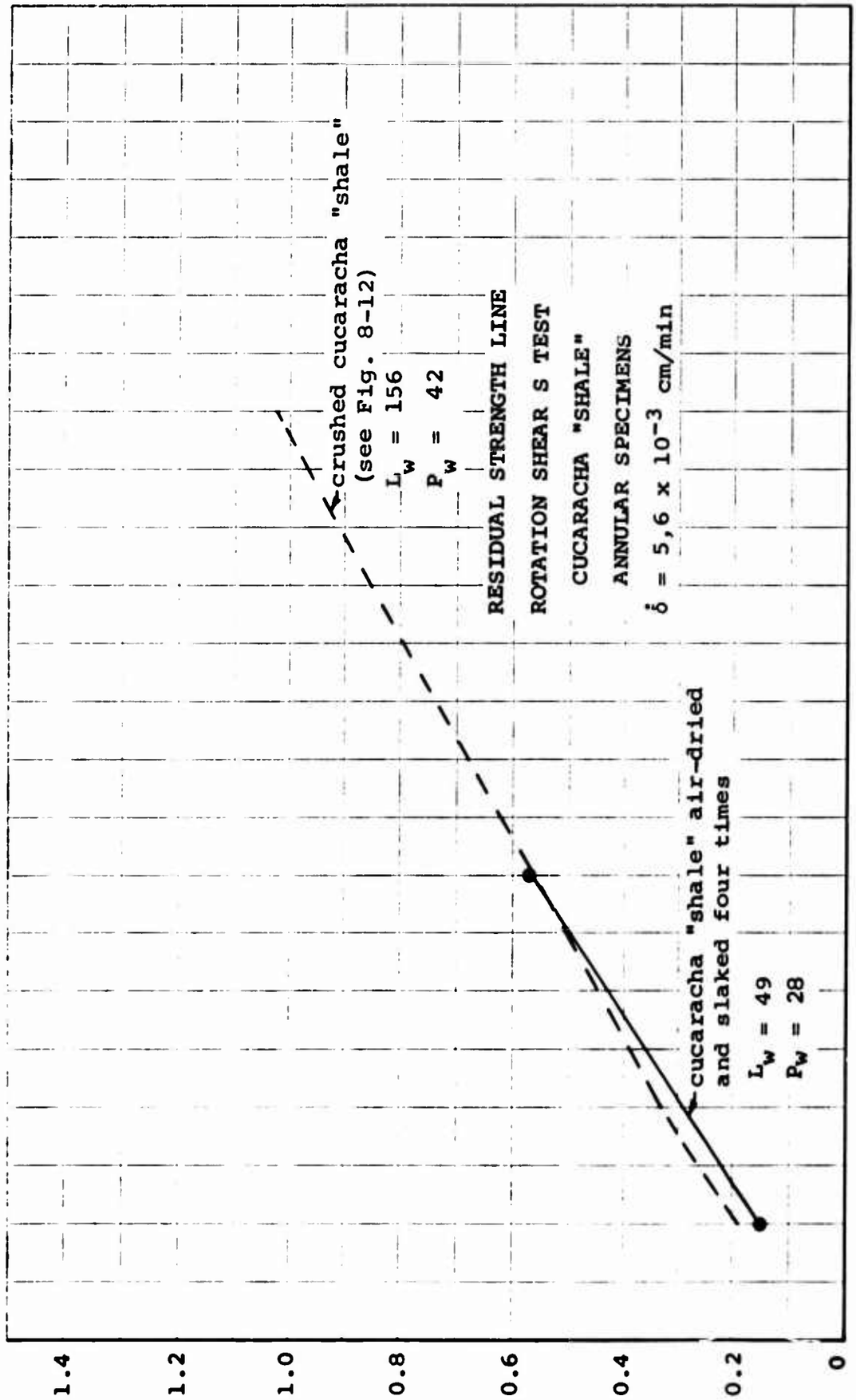
RESIDUAL SHEAR STRENGTH, τ_r, kg/sq cm
EFFECTIVE VERTICAL STRESS, $\bar{\sigma}_v$, kg/sq cm
RESIDUAL STRENGTH LINE
ROTATION SHEAR S TEST
CUCARACHA "SHALE"
ANNULAR SPECIMENS
$\dot{\delta}$ = 5,6 x 10^{-3} cm/min
crushed cucaracha "shale"
(see Fig. 8-12)
L_w = 156
P_w = 42
cucaracha "shale" air-dried
and slaked four times
L_w = 49
P_w = 28

FIG. 8-19

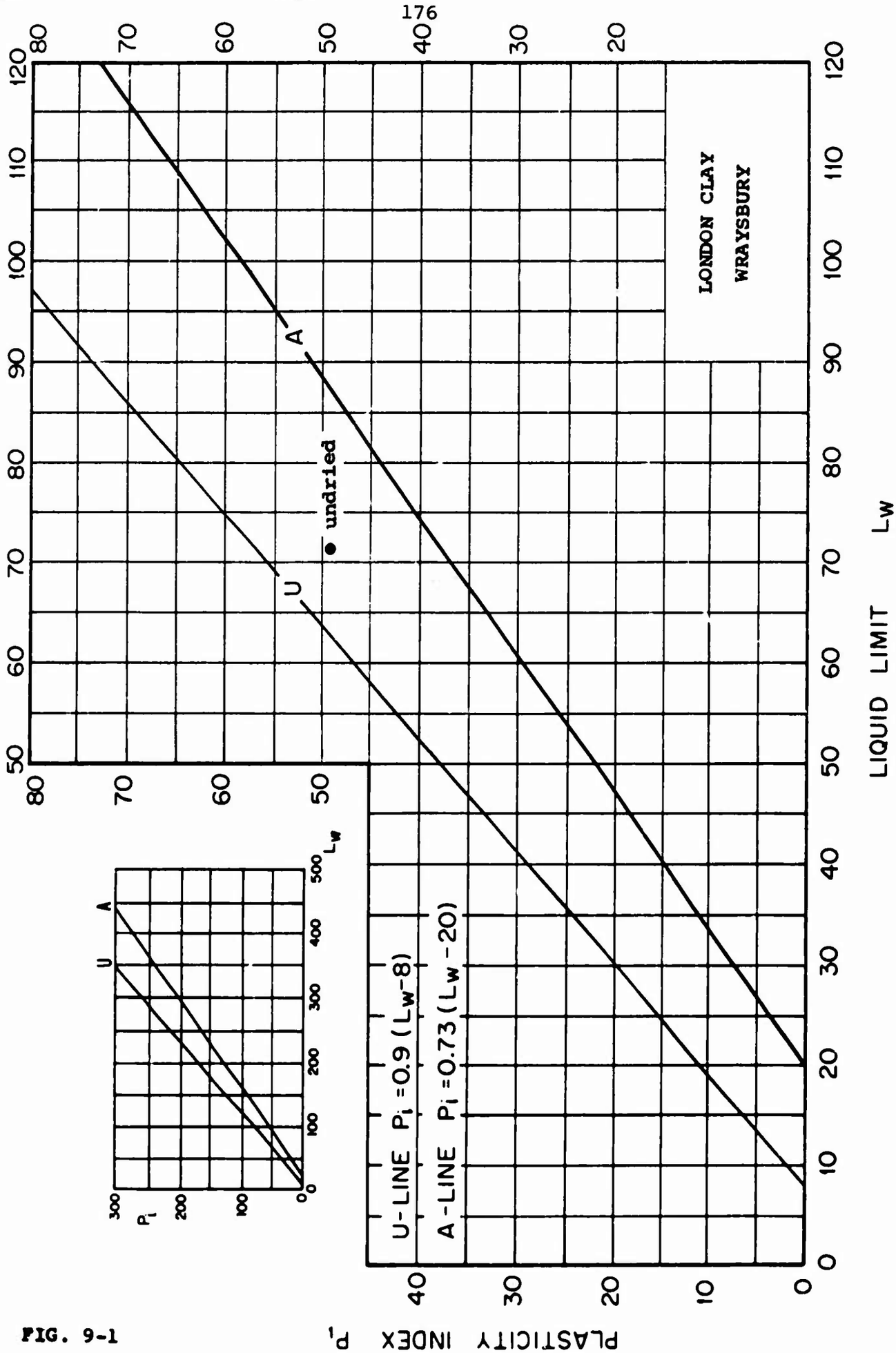
LONDON CLAY
WRAYSBURY
A
U
● undried
U-LINE $P_i = 0.9 (L_w - 8)$
A-LINE $P_i = 0.73 (L_w - 20)$
PLASTICITY INDEX P_I
LIQUID LIMIT L_w
P_i
L_w

FIG. 9-1

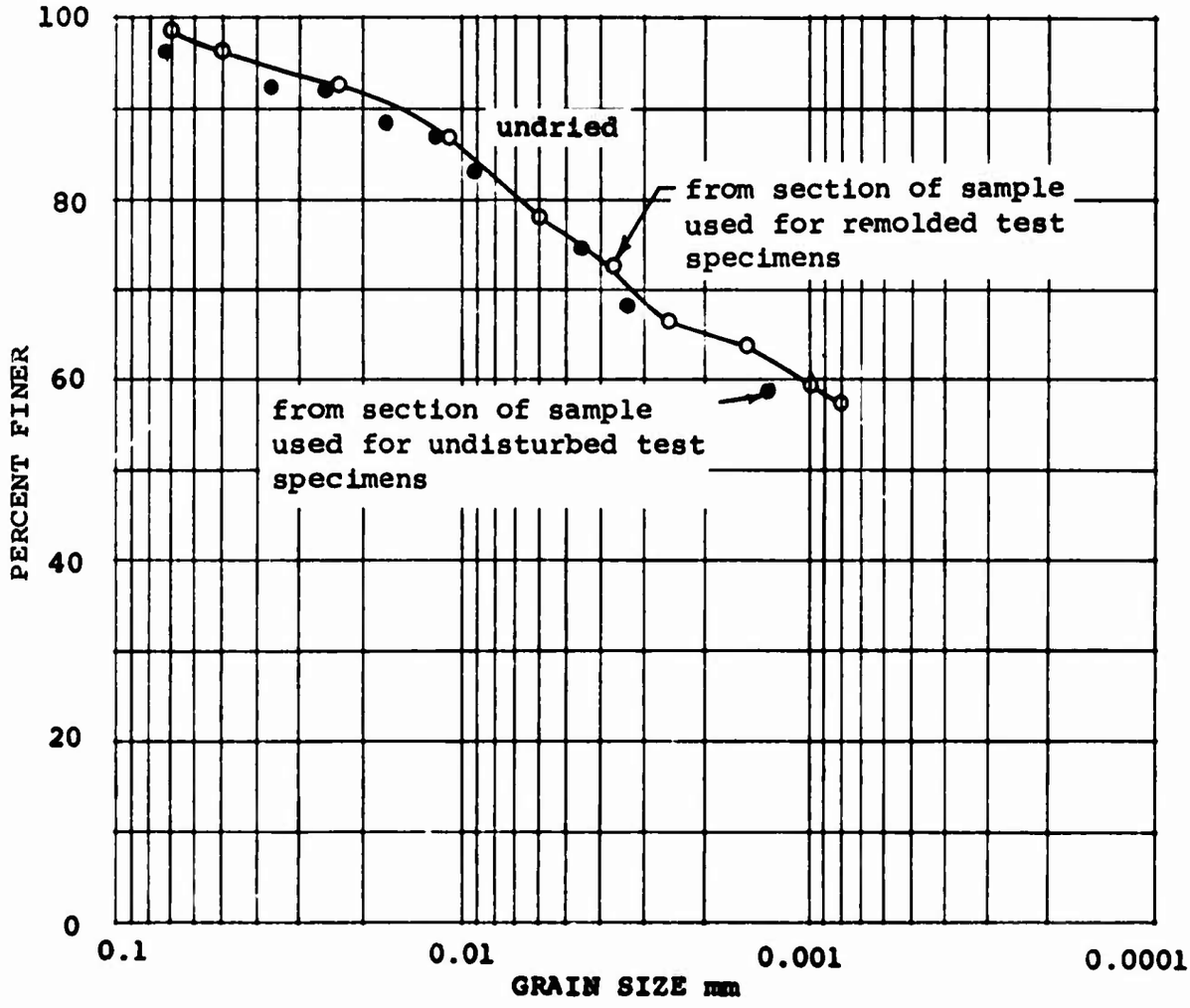

LONDON CLAY

WRAYSBURY

FIG. 9-2

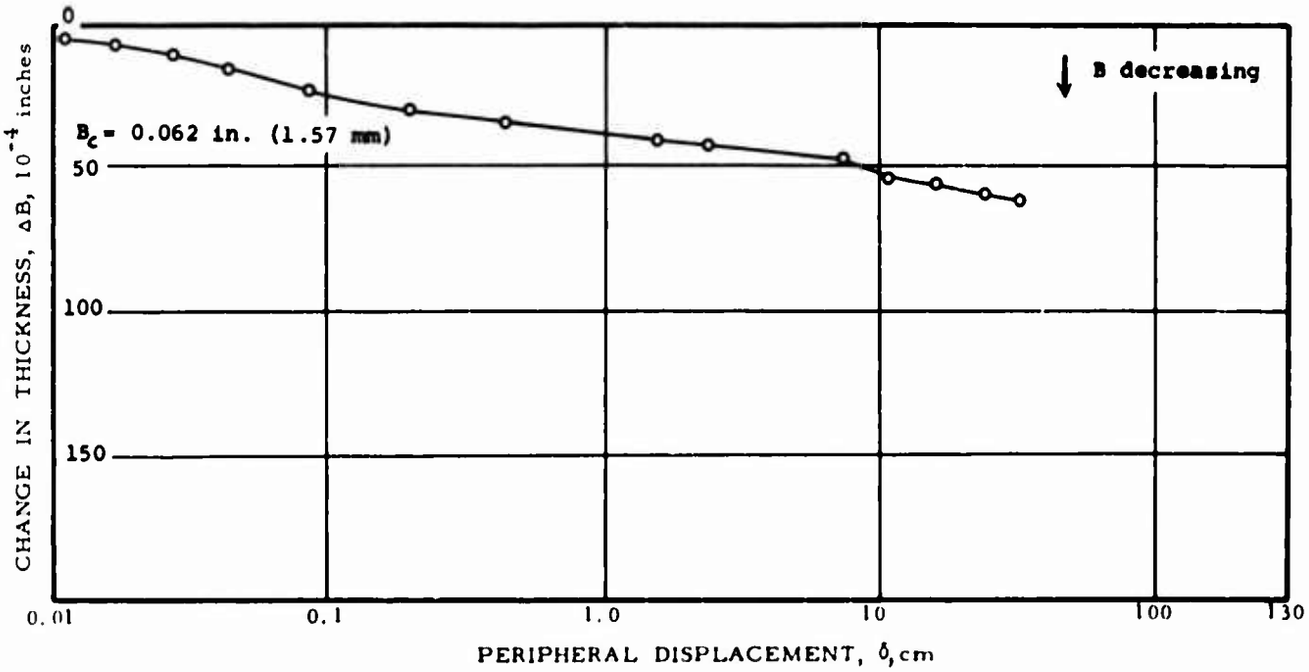
0
50
100
150
B_c = 0.062 in. (1.57 mm)
B decreasing
CHANGE IN THICKNESS, ΔB, 10^{-4} inches
0.01
0.1
1.0
10
100
130
PERIPHERAL DISPLACEMENT, δ, cm

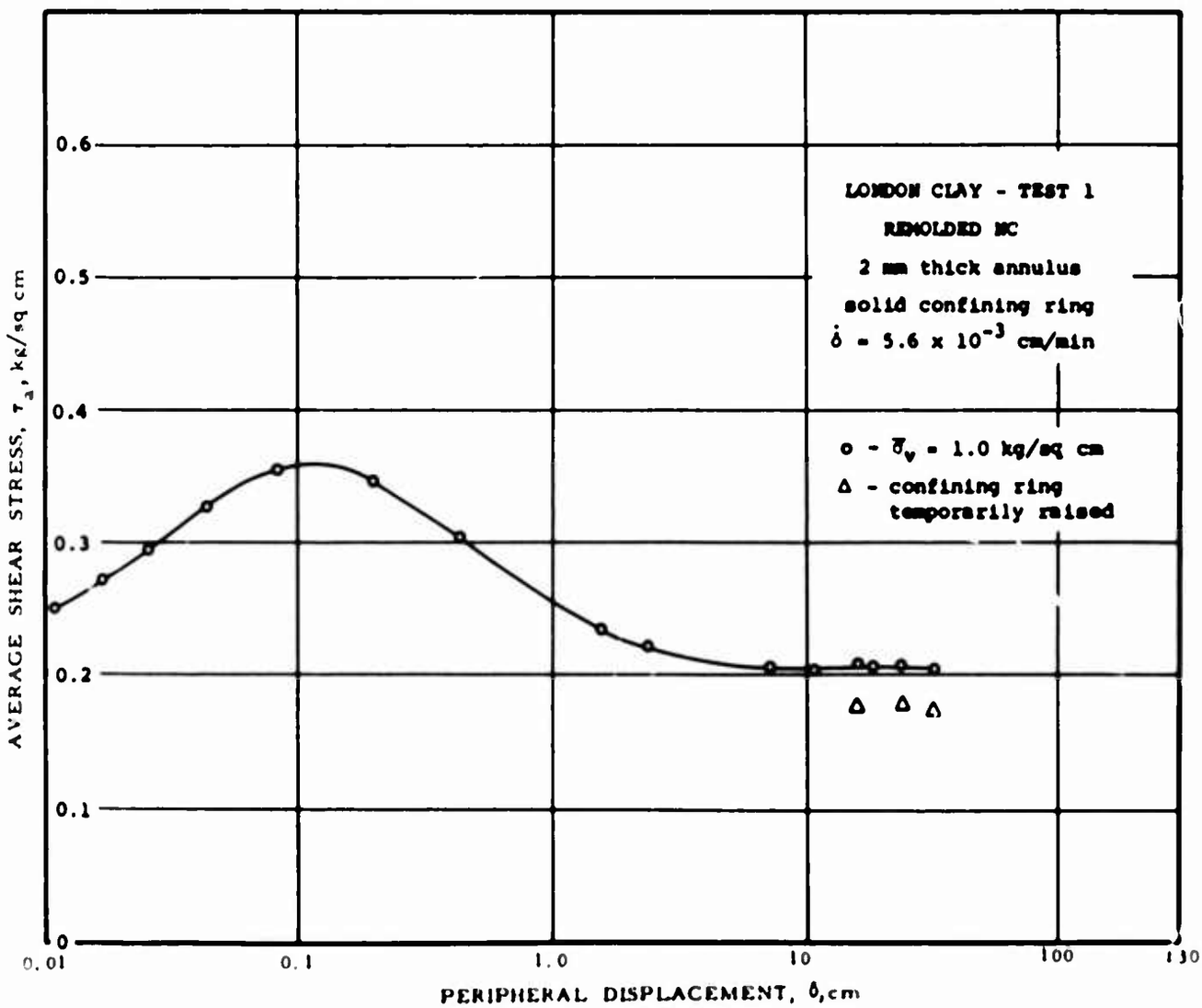
0.6
0.5
0.4
0.3
0.2
0.1
0
LONDON CLAY - TEST 1
REMOLDED MC
2 mm thick annulus
solid confining ring
$\dot{\delta}$ = 5.6 x 10^{-3} cm/min
o - $\bar{\sigma}_v$ = 1.0 kg/sq cm
Δ - confining ring temporarily raised
AVERAGE SHEAR STRESS, τ_a, kg/sq cm
0.01
0.1
1.0
10
100
130
PERIPHERAL DISPLACEMENT, δ, cm

FIG. 9-3

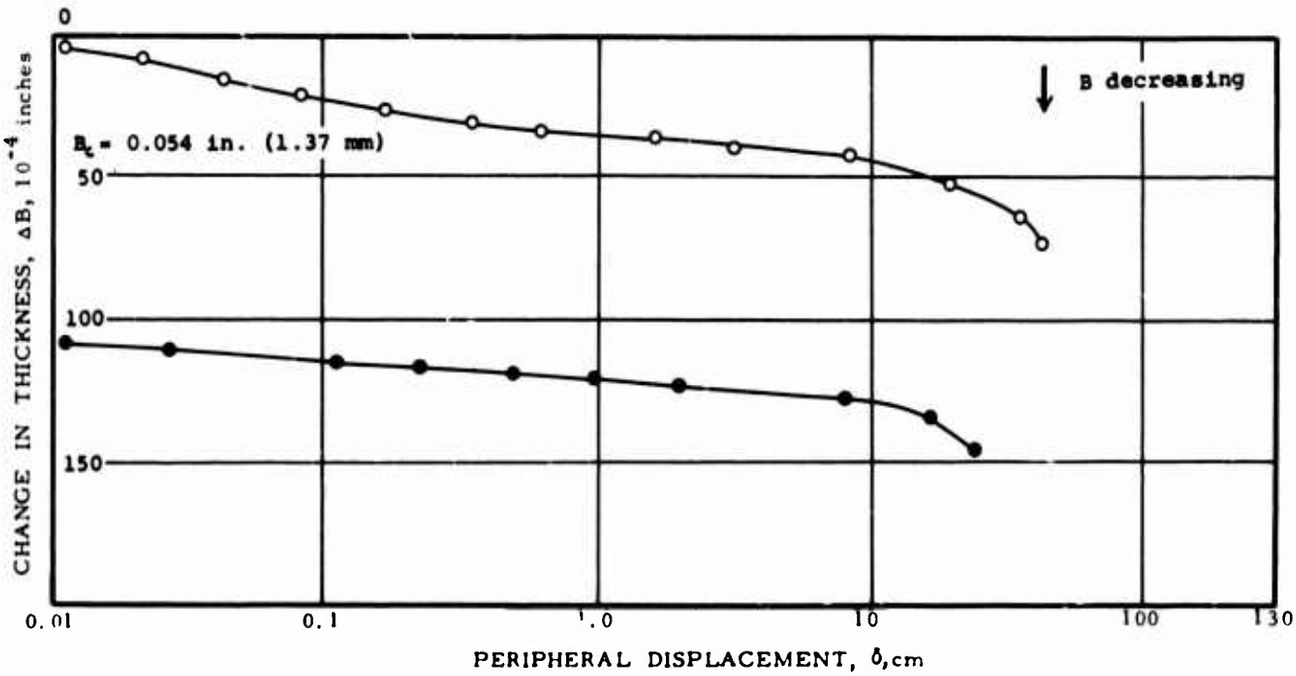
0
50
100
150
B decreasing
B_c = 0.054 in. (1.37 mm)
CHANGE IN THICKNESS, ΔB, 10^{-4} inches
0.01
0.1
1.0
10
100
130
PERIPHERAL DISPLACEMENT, δ, cm

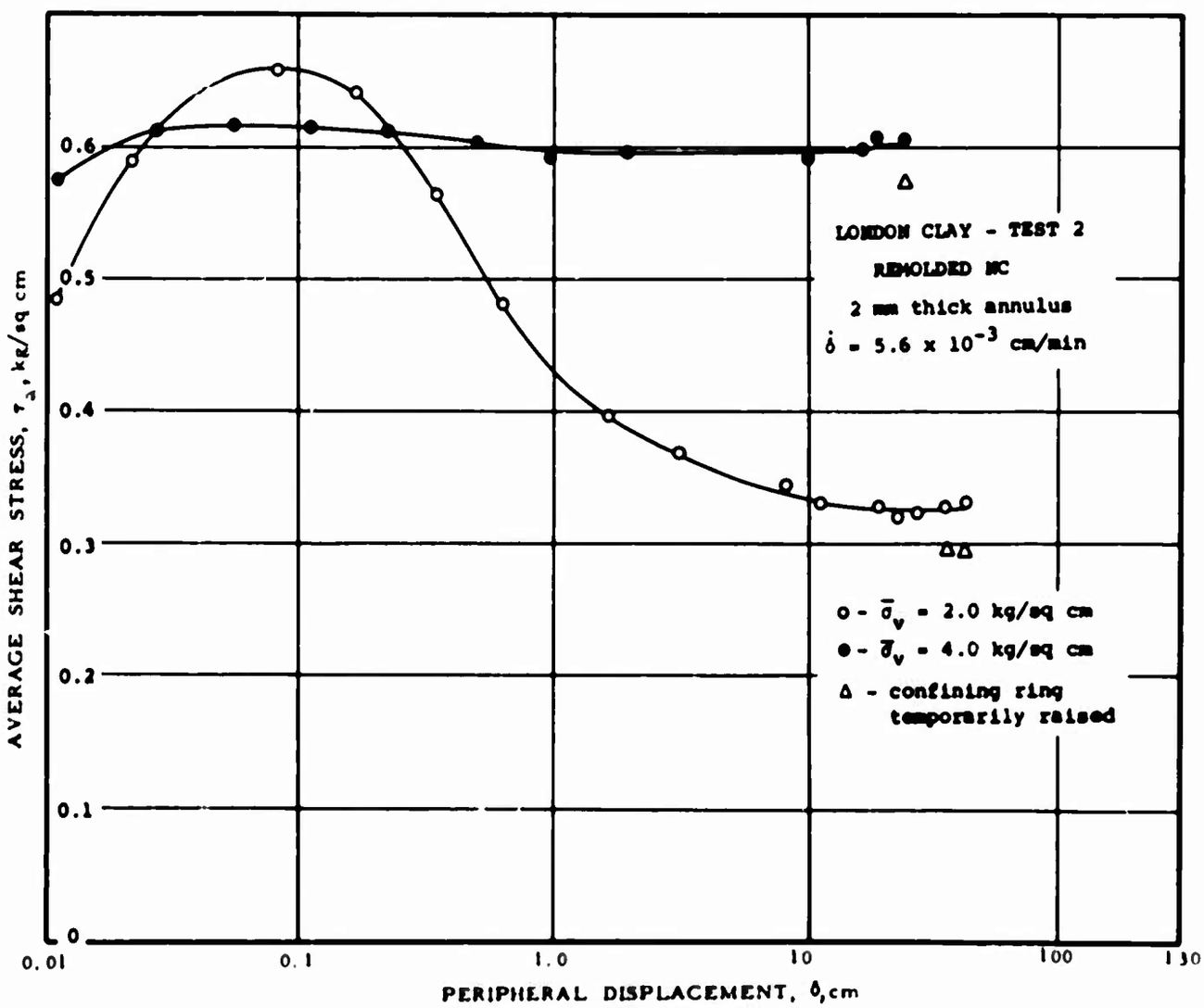
0.6
0.5
0.4
0.3
0.2
0.1
0
LONDON CLAY - TEST 2
REMOLDED NC
2 mm thick annulus
$\dot{\delta}$ = 5.6 x 10^{-3} cm/min
o - $\bar{\sigma}_v$ = 2.0 kg/sq cm
● - $\bar{\sigma}_v$ = 4.0 kg/sq cm
Δ - confining ring temporarily raised
AVERAGE SHEAR STRESS, τ_a, kg/sq cm
0.01
0.1
1.0
10
100
130
PERIPHERAL DISPLACEMENT, δ, cm

FIG. 9-4

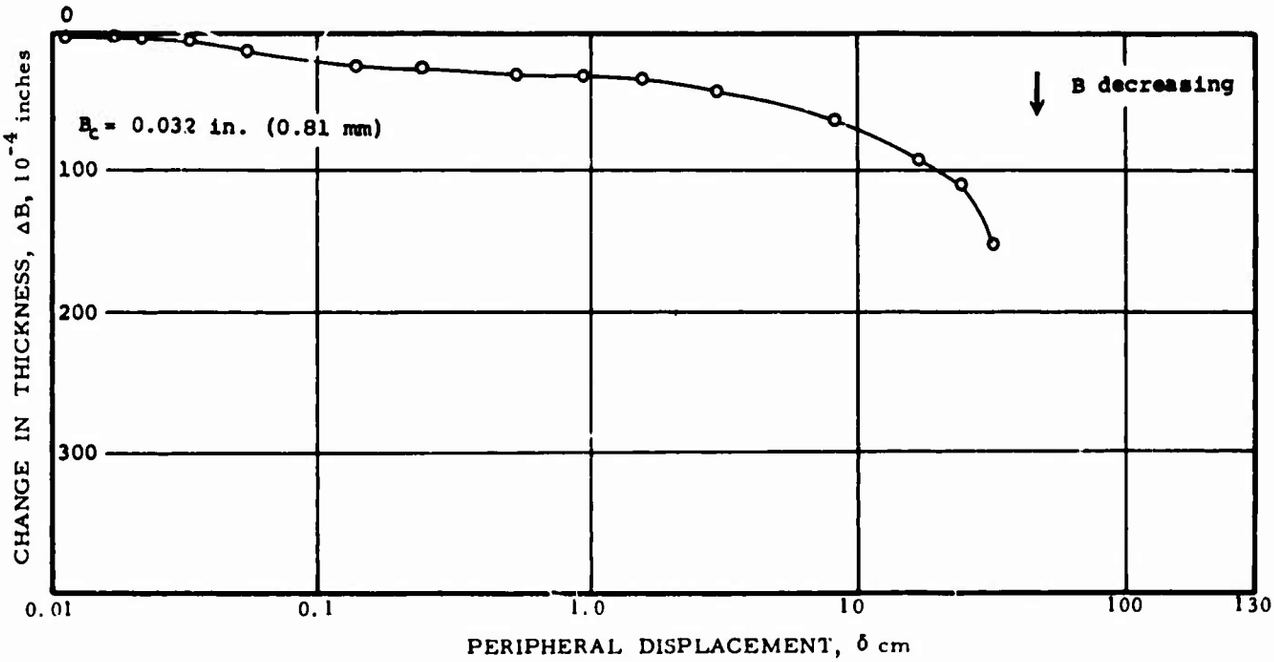
0
100
200
300
B_c = 0.032 in. (0.81 mm)
B decreasing
CHANGE IN THICKNESS, ΔB, 10^{-4} inches
0.01
0.1
1.0
10
100
130
PERIPHERAL DISPLACEMENT, δ cm

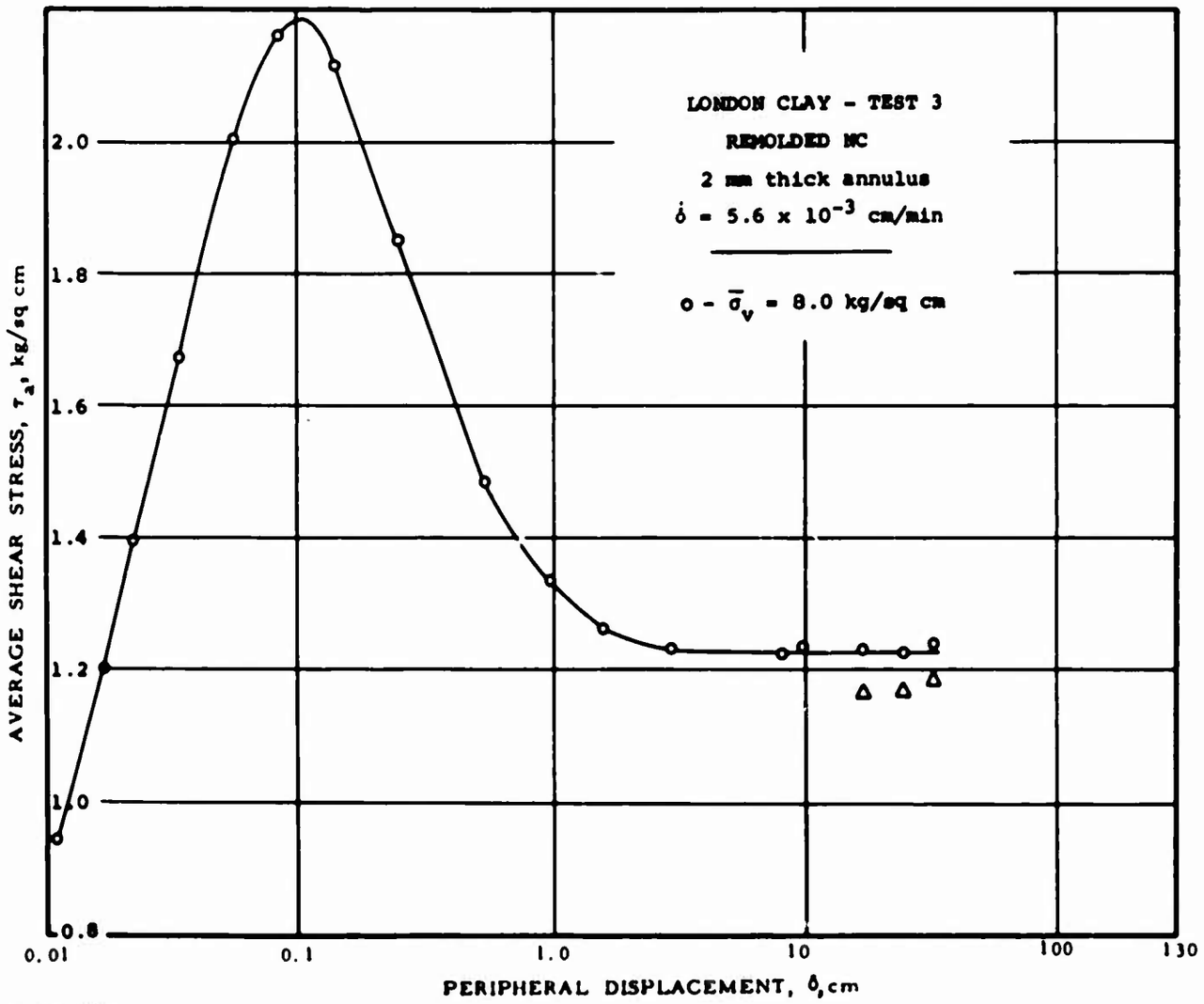
LONDON CLAY - TEST 3
REMOLDED MC
2 mm thick annulus
$\dot{\delta}$ = 5.6 x 10^{-3} cm/min
o - $\bar{\sigma}_v$ = 8.0 kg/sq cm
2.0
1.8
1.6
1.4
1.2
1.0
0.8
AVERAGE SHEAR STRESS, τ_a, kg/sq cm
0.01
0.1
1.0
10
100
130
PERIPHERAL DISPLACEMENT, δ, cm

FIG. 9-5

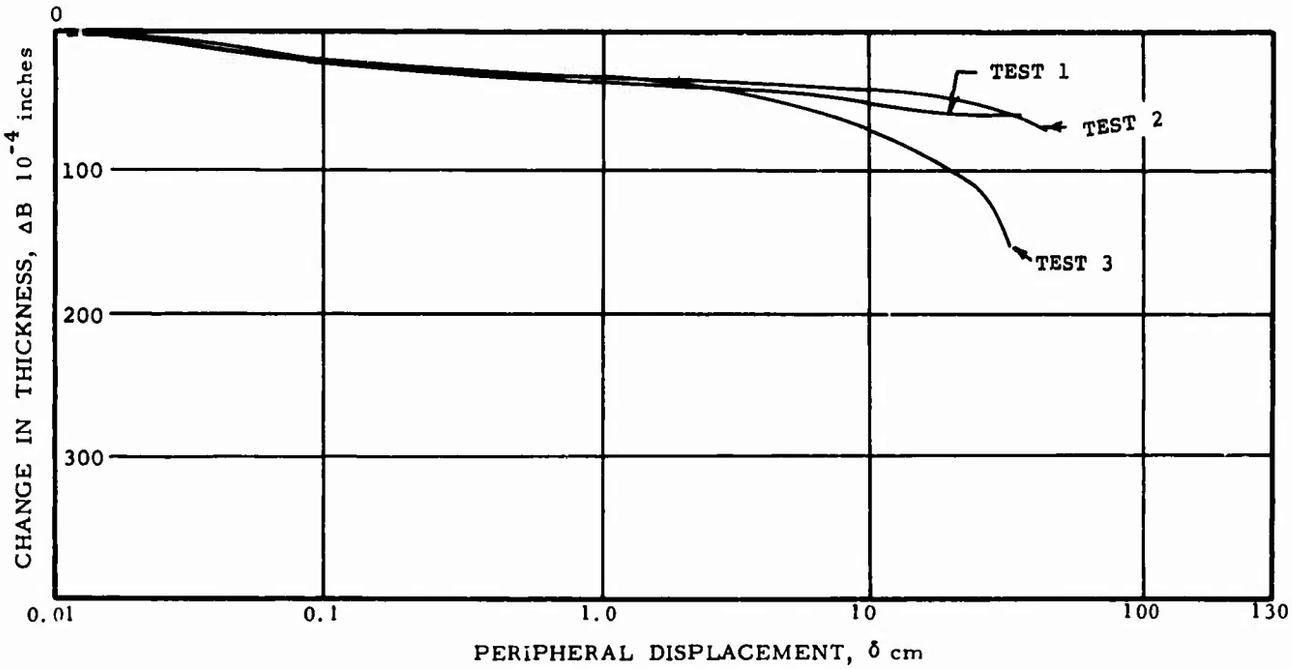
0
100
200
300
CHANGE IN THICKNESS, ΔB 10^{-4} inches
TEST 1
TEST 2
TEST 3
0.01
0.1
1.0
10
100
130
PERIPHERAL DISPLACEMENT, δ cm

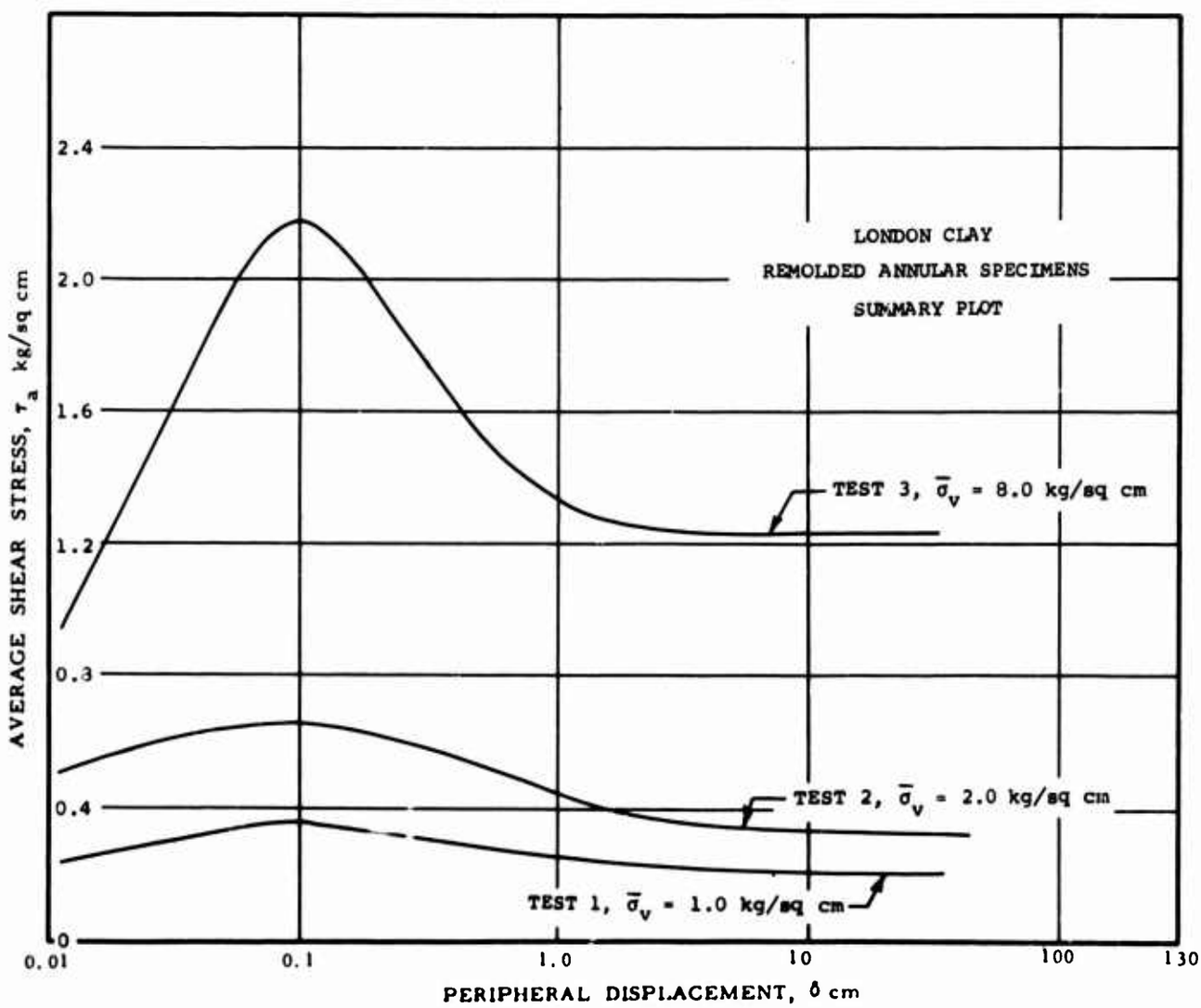
2.4
2.0
1.6
1.2
0.3
0.4
0
AVERAGE SHEAR STRESS, τ_a kg/sq cm
LONDON CLAY
REMOLDED ANNULAR SPECIMENS
SUMMARY PLOT
TEST 3, $\bar{\sigma}_v$ = 8.0 kg/sq cm
TEST 2, $\bar{\sigma}_v$ = 2.0 kg/sq cm
TEST 1, $\bar{\sigma}_v$ = 1.0 kg/sq cm
0.01
0.1
1.0
10
100
130
PERIPHERAL DISPLACEMENT, δ cm

FIG. 9-6

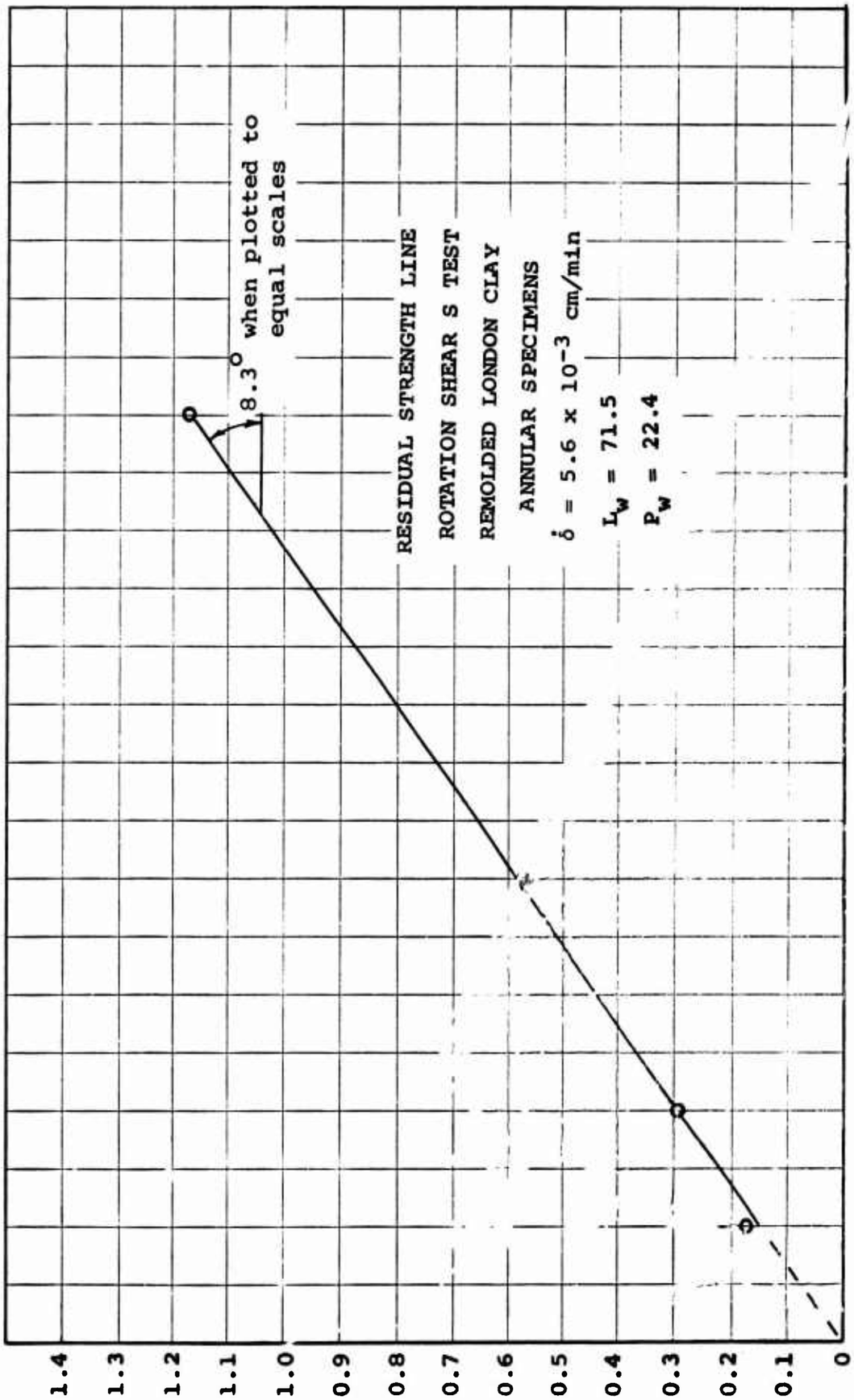
RESIDUAL STRENGTH LINE
ROTATION SHEAR S TEST
REMOLDED LONDON CLAY
ANNULAR SPECIMENS
$\dot{\delta}$ = 5.6 x 10^{-3} cm/min
L_w = 71.5
P_w = 22.4
8.3° when plotted to equal scales
RESIDUAL SHEAR STRENGTH, τ_r, kg/sq cm
EFFECTIVE VERTICAL STRESS, $\bar{\sigma}_v$, kg/sq cm
0
0.1
0.2
0.3
0.4
0.5
0.6
0.7
0.8
0.9
1.0
1.1
1.2
1.3
1.4
1
2
3
4
5
6
7
8

FIG. 9-7

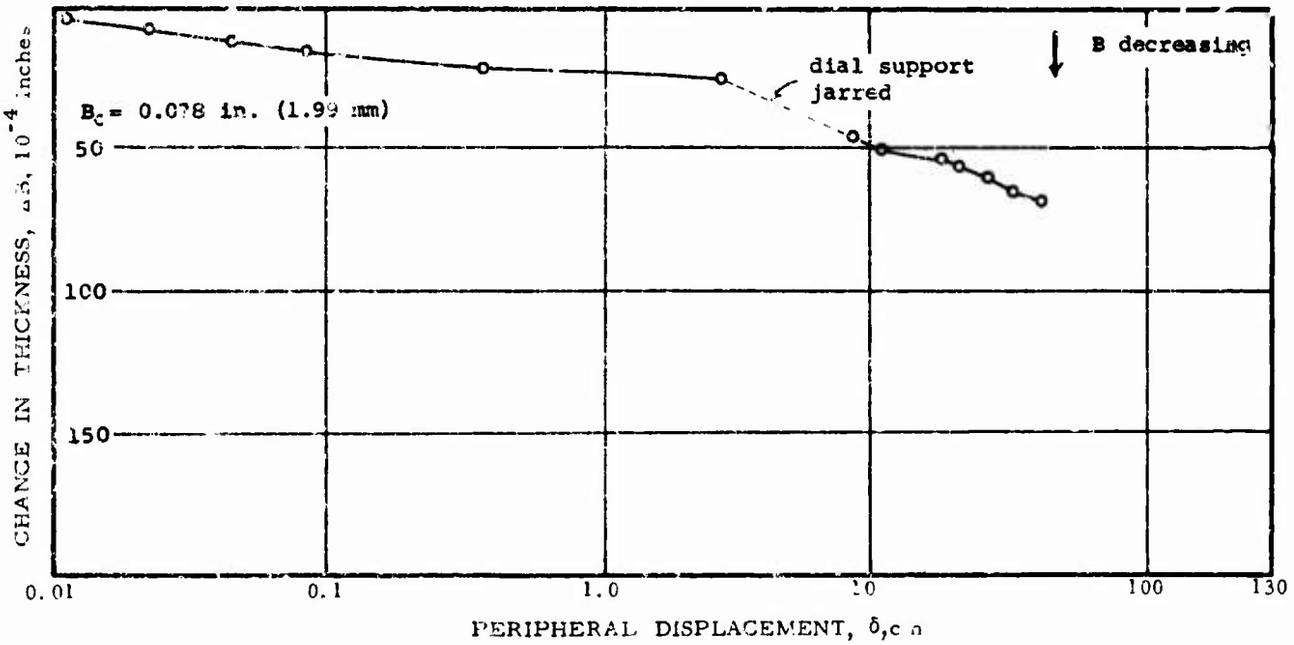
B decreasing
dial support jarred
B_c = 0.078 in. (1.99 mm)
50
100
150
0.01
0.1
1.0
10
100
130
CHANGE IN THICKNESS, 10^{-4} inches
PERIPHERAL DISPLACEMENT, δ,cm

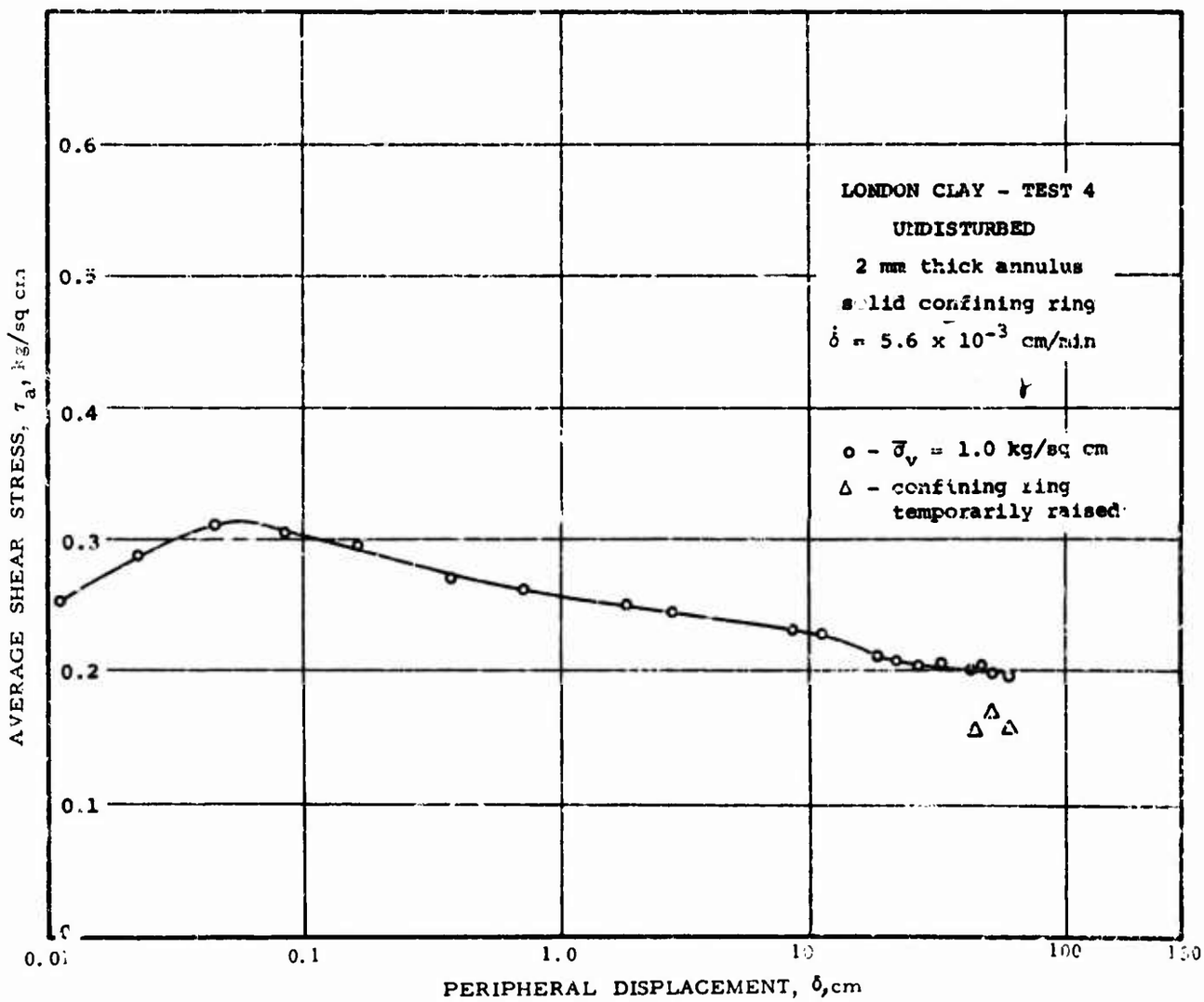
LONDON CLAY - TEST 4
UNDISTURBED
2 mm thick annulus
solid confining ring
$\dot{\delta}$ = 5.6 x 10^{-3} cm/min
o - $\bar{\sigma}_v$ = 1.0 kg/sq cm
Δ - confining ring temporarily raised
0.6
0.5
0.4
0.3
0.2
0.1
0
0.01
0.1
1.0
10
100
130
AVERAGE SHEAR STRESS, τ_a, kg/sq cm
PERIPHERAL DISPLACEMENT, δ,cm

FIG. 9-8

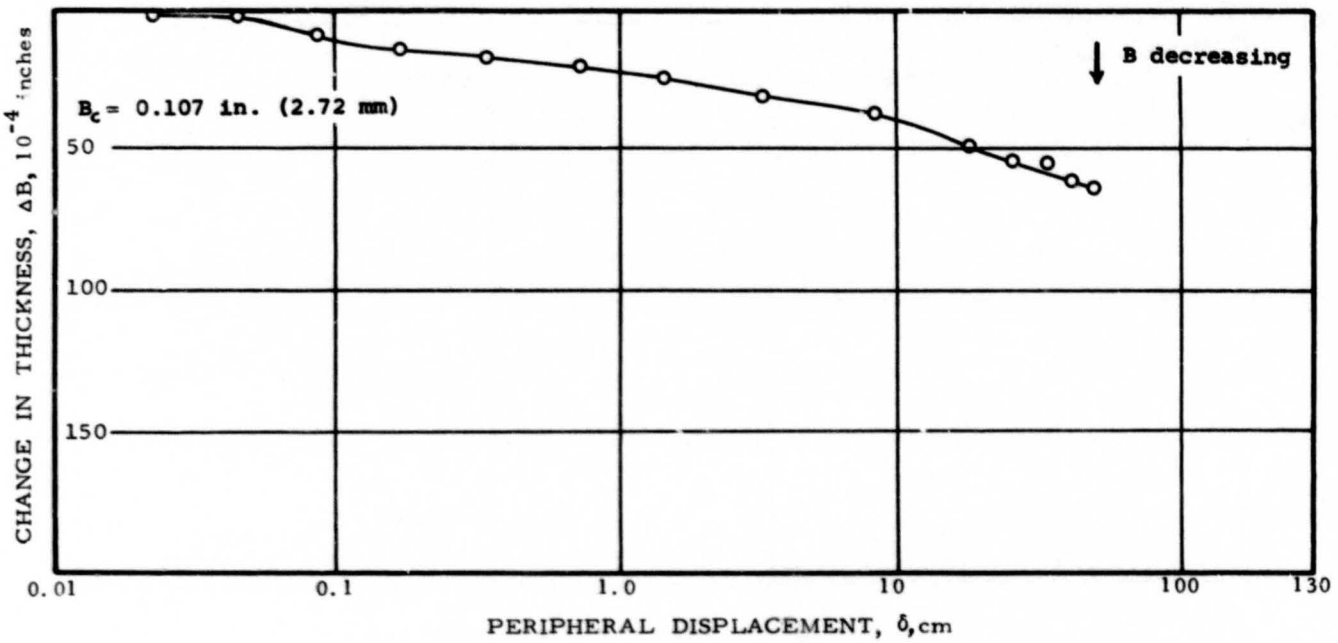
B decreasing
B_c = 0.107 in. (2.72 mm)
CHANGE IN THICKNESS, ΔB, 10^{-4} inches
50
100
150
0.01
0.1
1.0
10
100
130
PERIPHERAL DISPLACEMENT, δ, cm

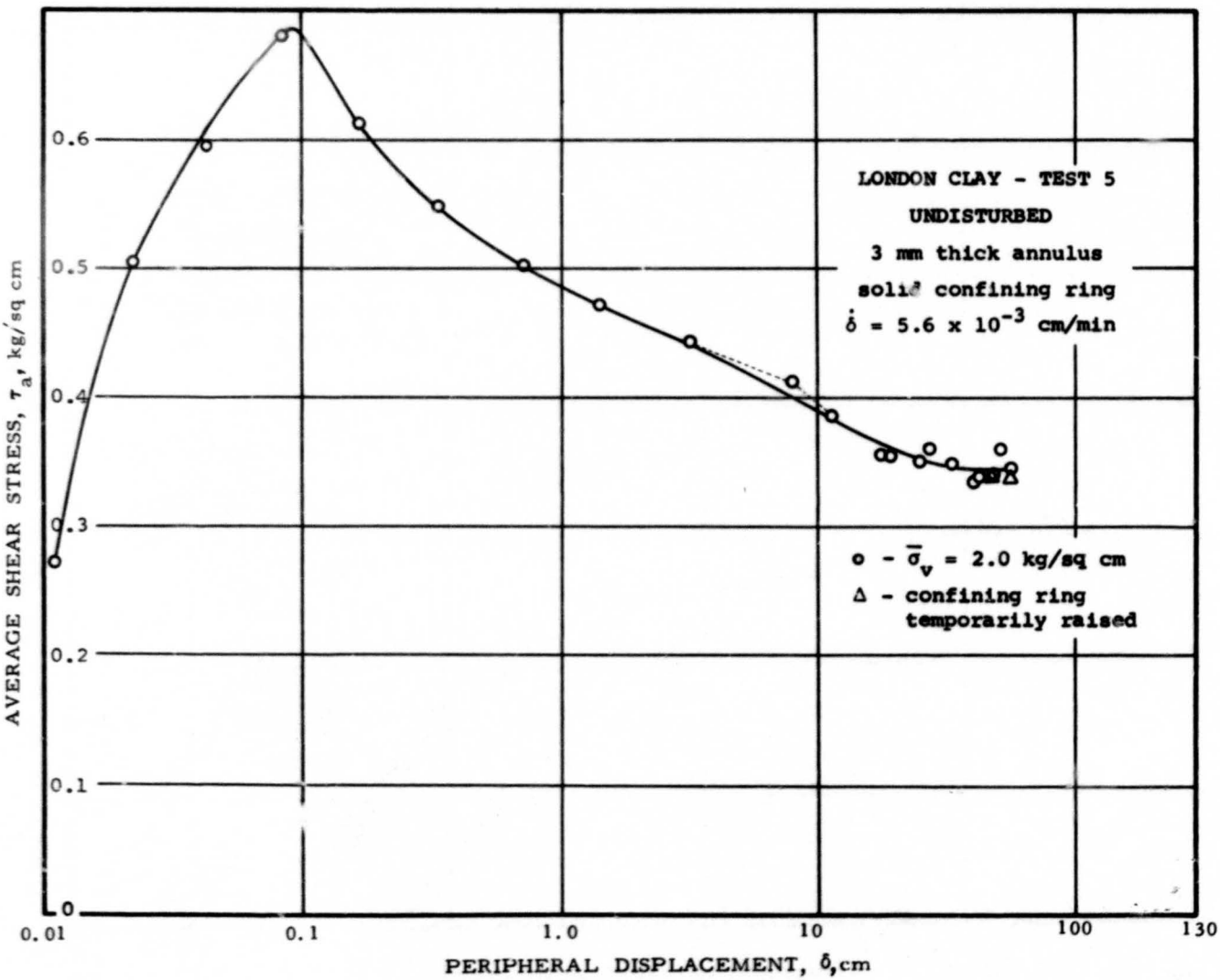
LONDON CLAY - TEST 5
UNDISTURBED
3 mm thick annulus
solid confining ring
$\dot{\delta}$ = 5.6 x 10^{-3} cm/min
o - $\bar{\sigma}_v$ = 2.0 kg/sq cm
Δ - confining ring temporarily raised
AVERAGE SHEAR STRESS, τ_a, kg/sq cm
0
0.1
0.2
0.3
0.4
0.5
0.6
0.01
0.1
1.0
10
100
130
PERIPHERAL DISPLACEMENT, δ, cm

FIG. 9-9

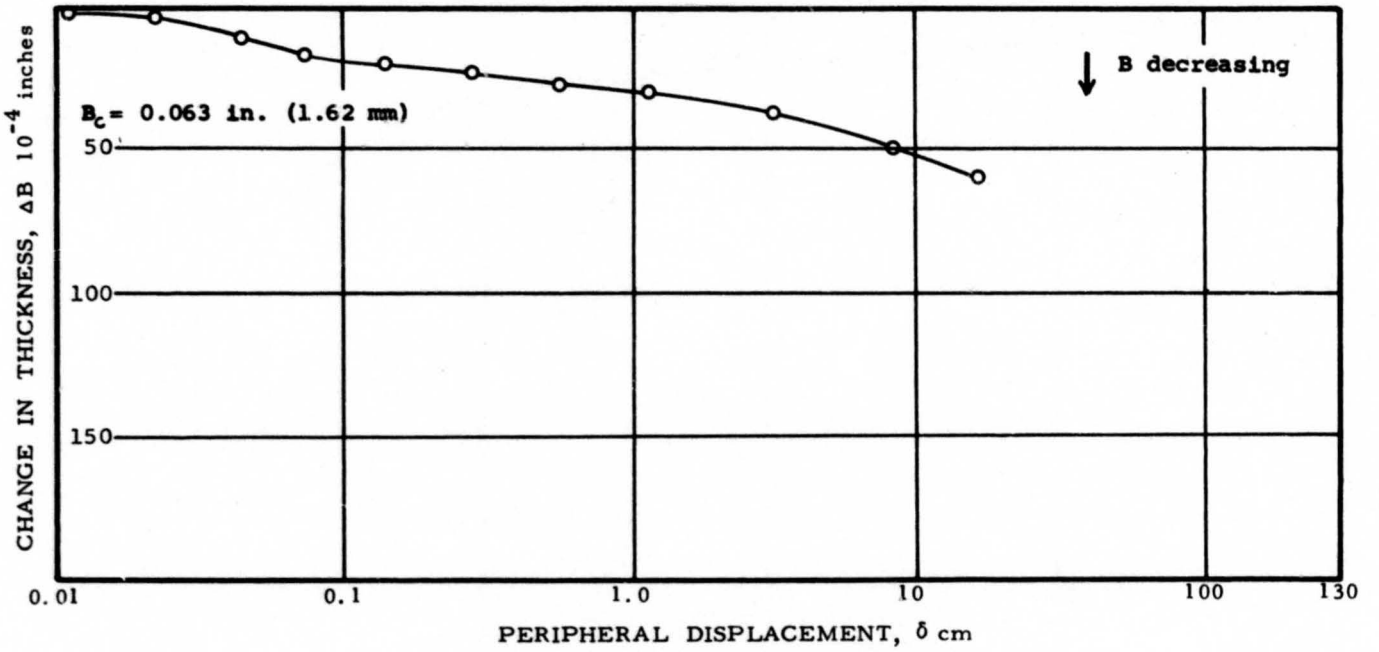
CHANGE IN THICKNESS, ΔB 10^{-4} inches
B_c = 0.063 in. (1.62 mm)
B decreasing
50
100
150
0.01
0.1
1.0
10
100
130
PERIPHERAL DISPLACEMENT, δ cm

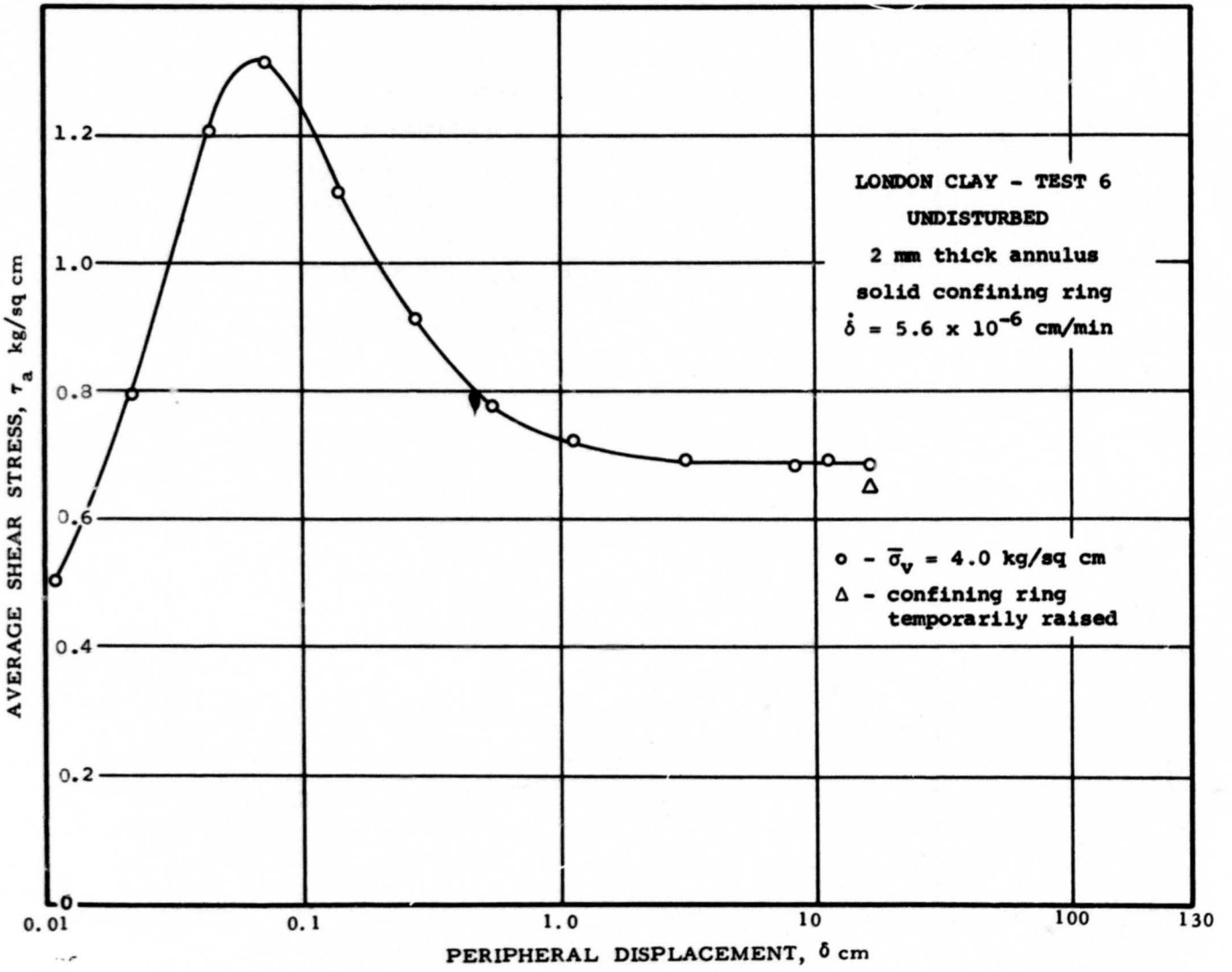
AVERAGE SHEAR STRESS, τ_a kg/sq cm
LONDON CLAY - TEST 6
UNDISTURBED
2 mm thick annulus
solid confining ring
$\dot{\delta}$ = 5.6 x 10^{-6} cm/min
o - $\bar{\sigma}_v$ = 4.0 kg/sq cm
Δ - confining ring temporarily raised
1.2
1.0
0.8
0.6
0.4
0.2
0
0.01
0.1
1.0
10
100
130
PERIPHERAL DISPLACEMENT, δ cm

FIG. 9-10

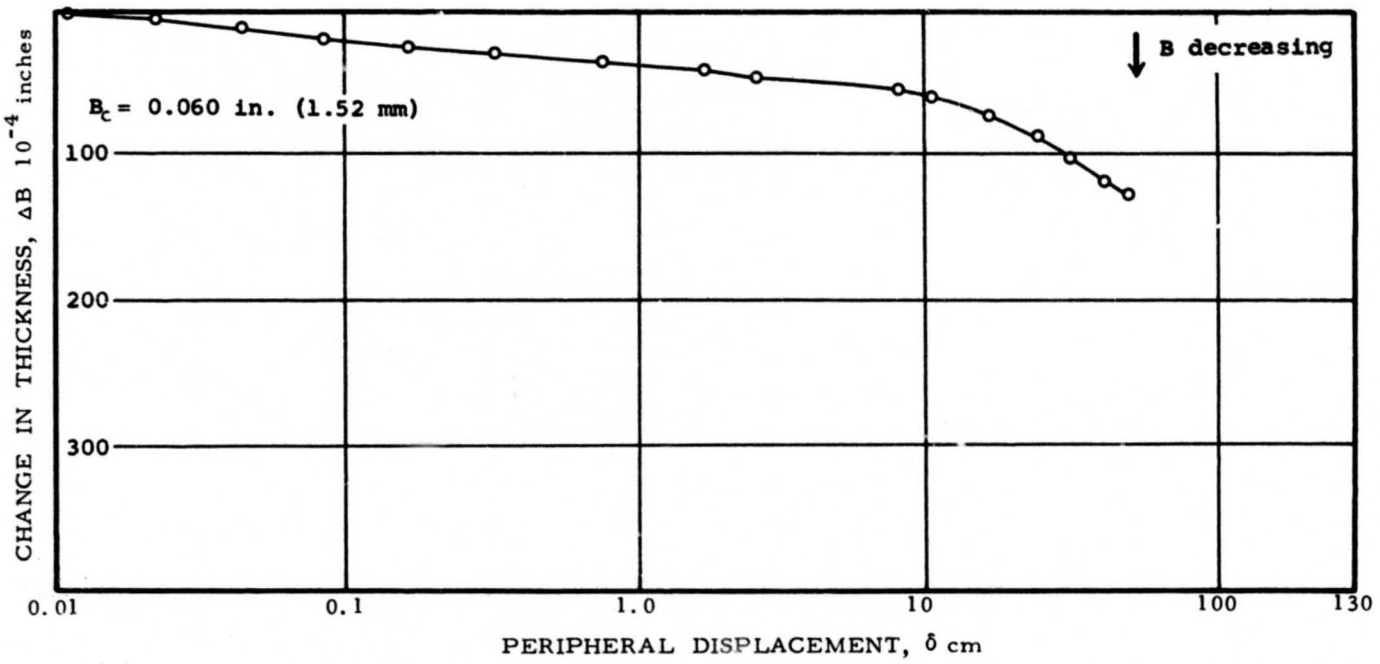
B decreasing
B_c = 0.060 in. (1.52 mm)
CHANGE IN THICKNESS, ΔB 10^{-4} inches
100
200
300
0.01
0.1
1.0
10
100
130
PERIPHERAL DISPLACEMENT, δ cm

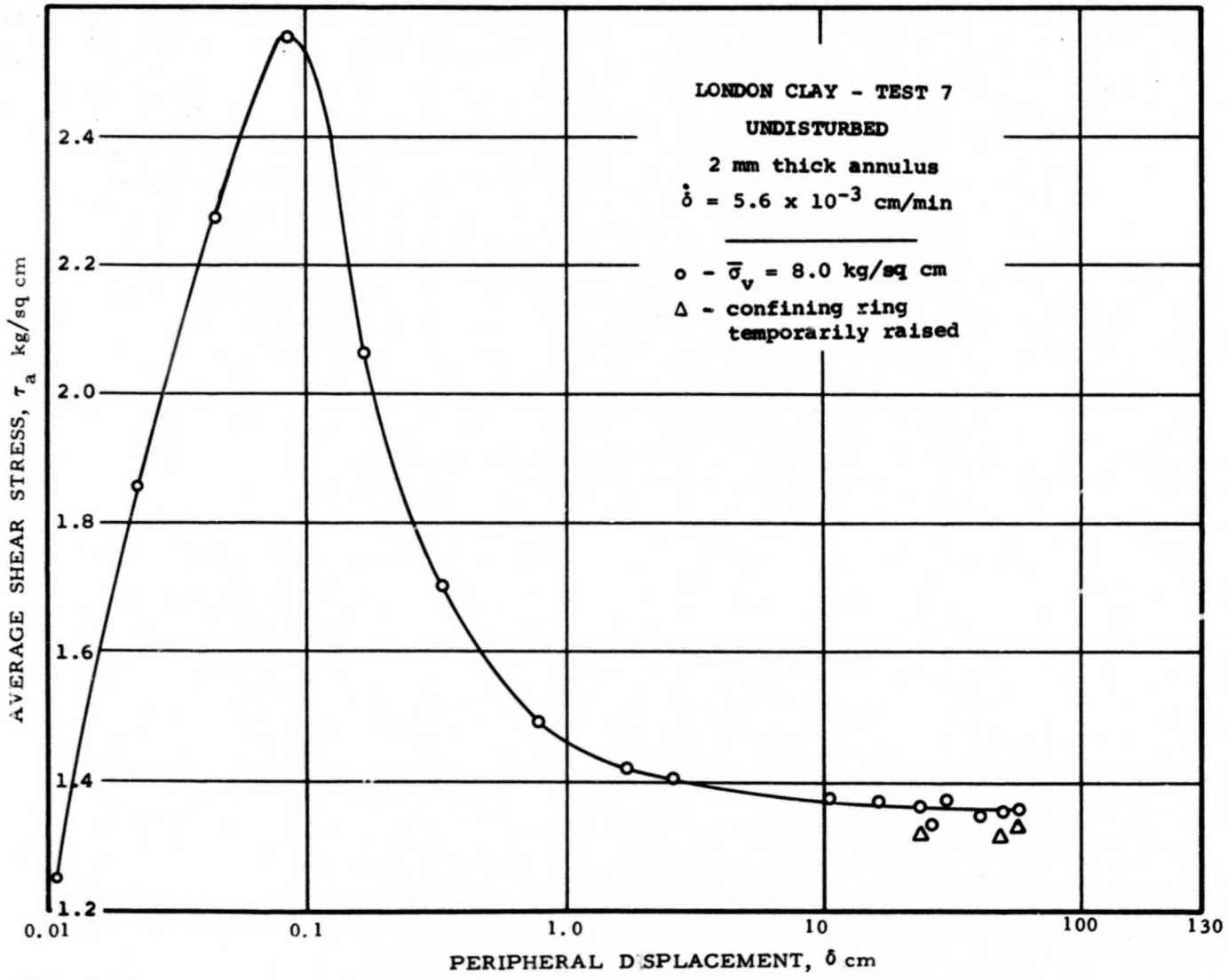
LONDON CLAY - TEST 7
UNDISTURBED
2 mm thick annulus
$\dot{\delta}$ = 5.6 x 10^{-3} cm/min
o - $\overline{\sigma}_v$ = 8.0 kg/sq cm
Δ - confining ring temporarily raised
AVERAGE SHEAR STRESS, τ_a kg/sq cm
2.4
2.2
2.0
1.8
1.6
1.4
1.2
0.01
0.1
1.0
10
100
130
PERIPHERAL DISPLACEMENT, δ cm

FIG. 9-11

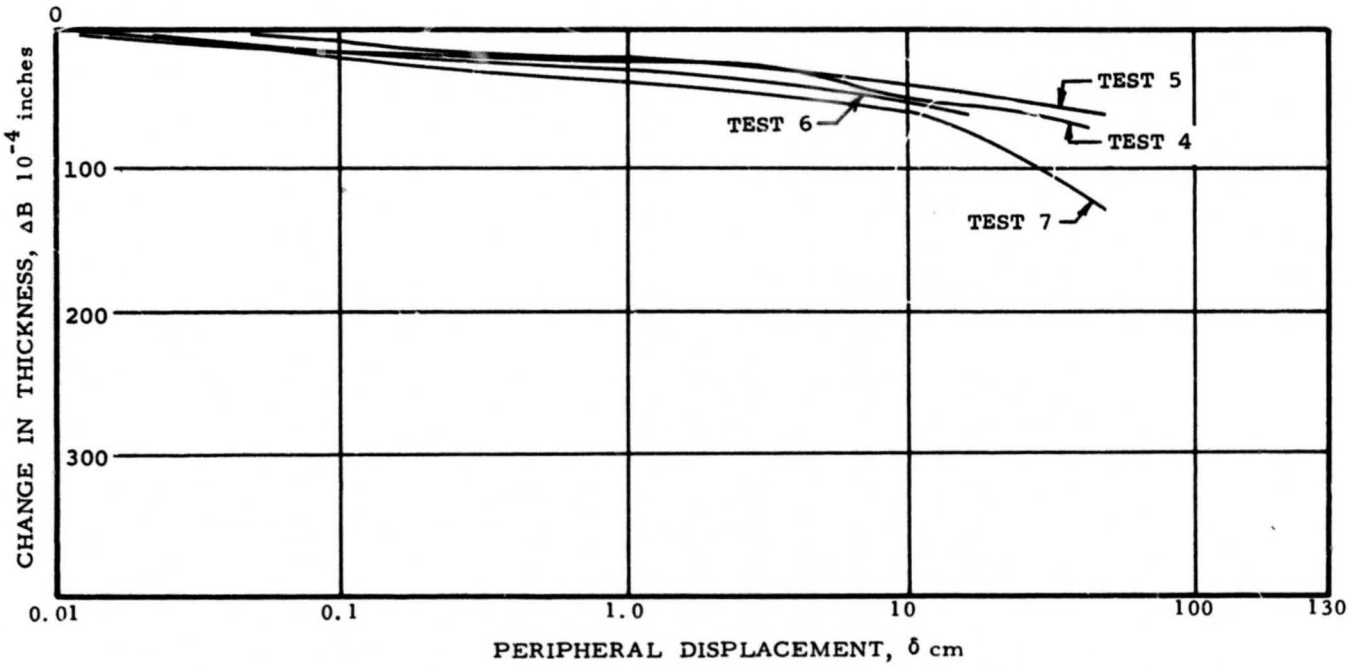
CHANGE IN THICKNESS, ΔB 10^{-4} inches
0
100
200
300
TEST 5
TEST 4
TEST 6
TEST 7
0.01
0.1
1.0
10
100
130
PERIPHERAL DISPLACEMENT, δ cm

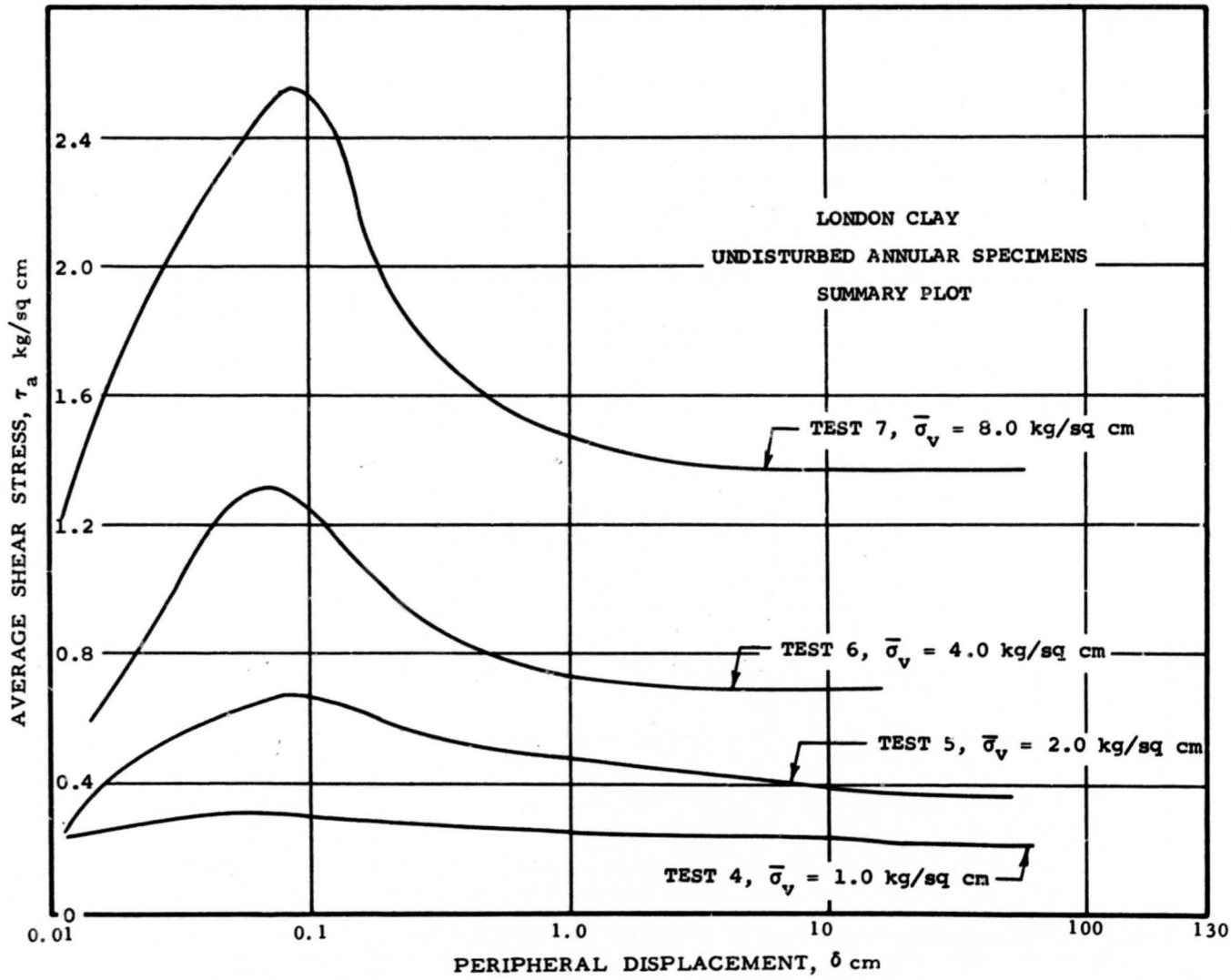
AVERAGE SHEAR STRESS, τ_a kg/sq cm
2.4
2.0
1.6
1.2
0.8
0.4
0
LONDON CLAY
UNDISTURBED ANNULAR SPECIMENS
SUMMARY PLOT
TEST 7, $\bar{\sigma}_v$ = 8.0 kg/sq cm
TEST 6, $\bar{\sigma}_v$ = 4.0 kg/sq cm
TEST 5, $\bar{\sigma}_v$ = 2.0 kg/sq cm
TEST 4, $\bar{\sigma}_v$ = 1.0 kg/sq cm
0.01
0.1
1.0
10
100
130
PERIPHERAL DISPLACEMENT, δ cm

FIG. 9-12

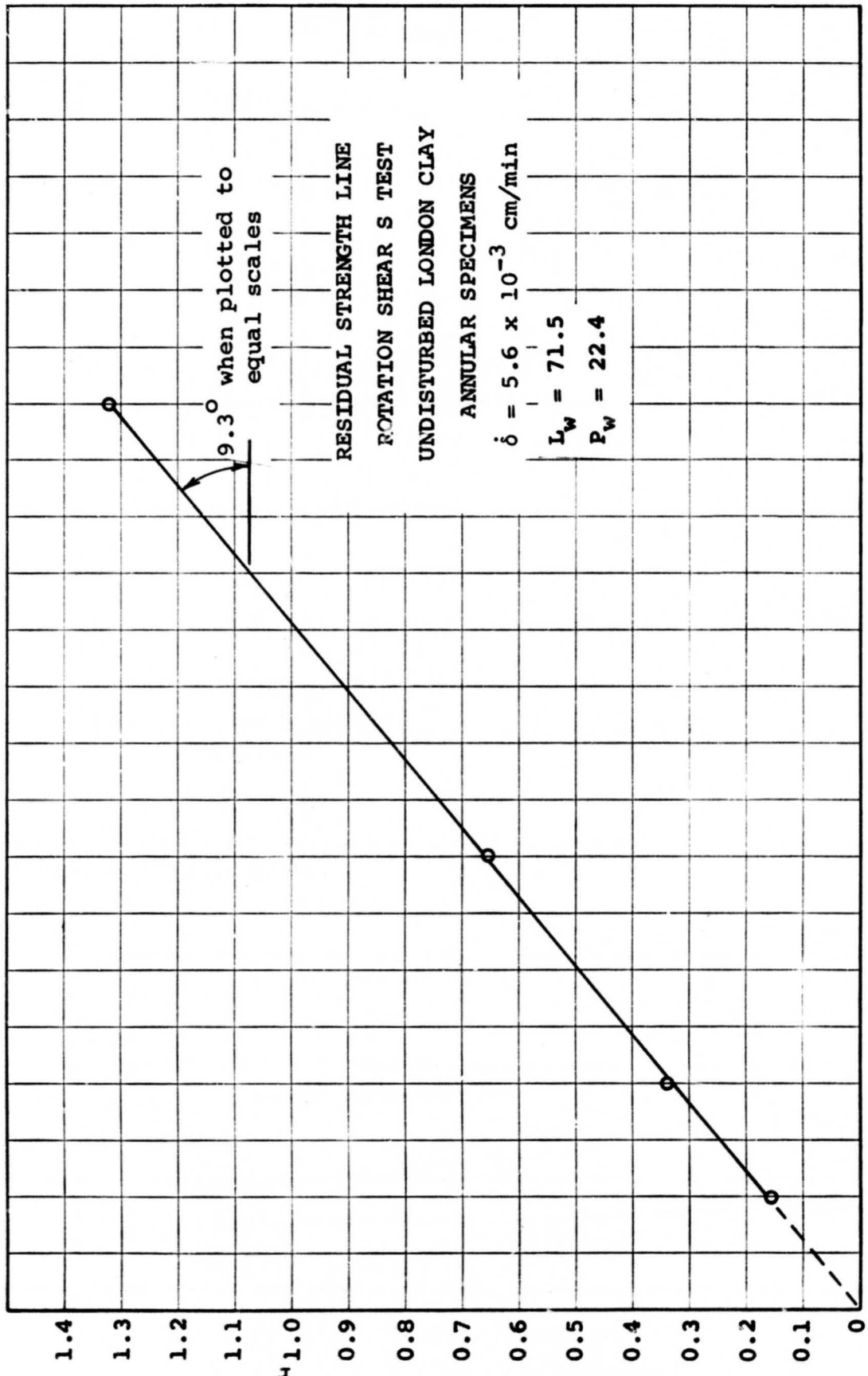
RESIDUAL STRENGTH LINE
ROTATION SHEAR S TEST
UNDISTURBED LONDON CLAY
ANNULAR SPECIMENS
$\dot{\delta}$ = 5.6 x 10^{-3} cm/min
L_w = 71.5
P_w = 22.4
9.3° when plotted to equal scales
RESIDUAL SHEAR STRENGTH, τ_r, kg/sq cm
EFFECTIVE VERTICAL STRESS, $\bar{\sigma}_v$, kg/sq cm
0
0.1
0.2
0.3
0.4
0.5
0.6
0.7
0.8
0.9
1.0
1.1
1.2
1.3
1.4
1
2
3
4
5
6
7
8

FIG. 9-13

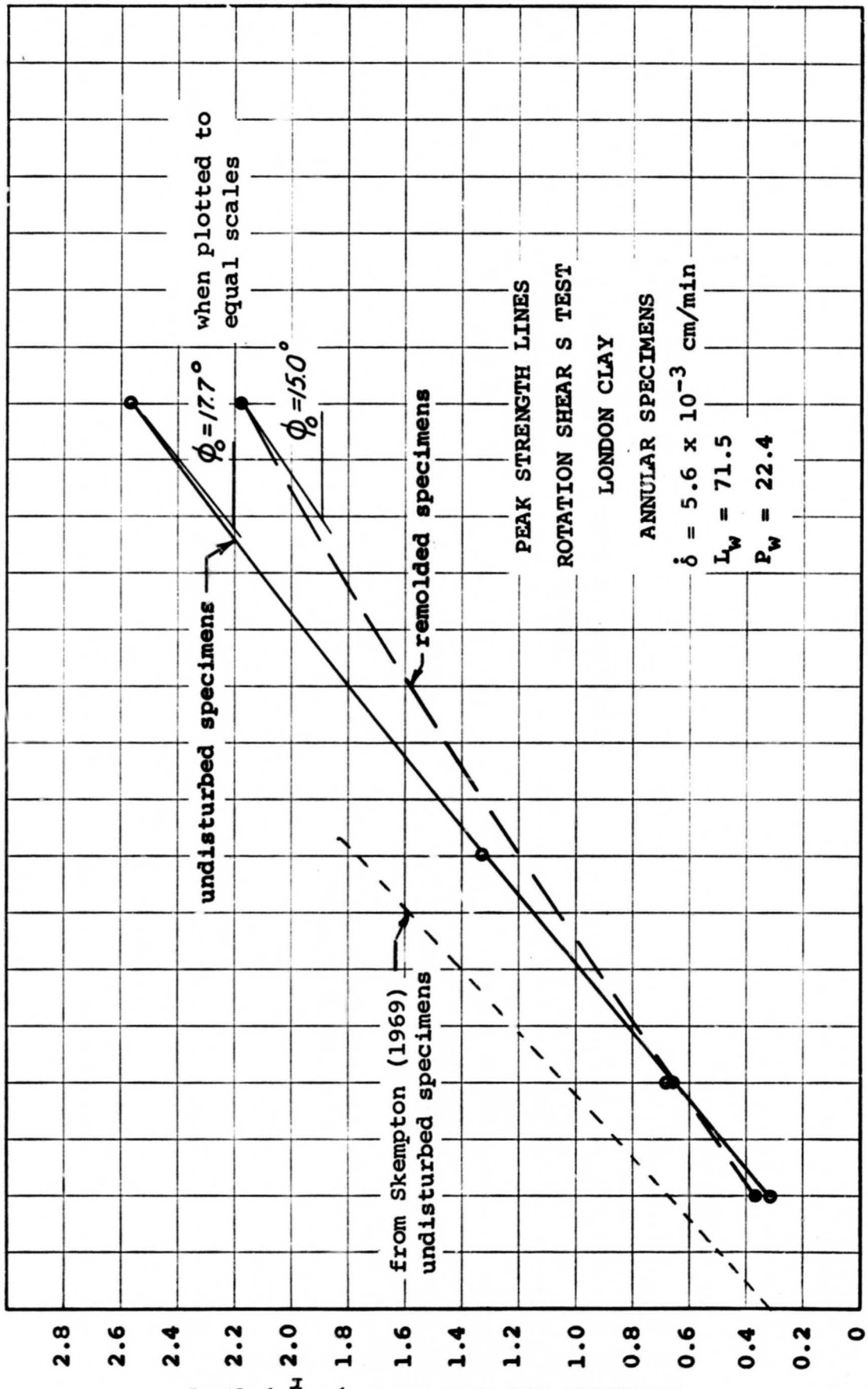
RESIDUAL SHEAR STRENGTH, τ_r, kg/sq cm
EFFECTIVE VERTICAL STRESS, $\bar{\sigma}_v$, kg/sq cm
PEAK STRENGTH LINES
ROTATION SHEAR S TEST
LONDON CLAY
ANNULAR SPECIMENS
$\dot{\delta} = 5.6 \times 10^{-3}$ cm/min
$L_w = 71.5$
$P_w = 22.4$
undisturbed specimens
remolded specimens
$\phi_o = 17.7°$
$\phi_o = 15.0°$
when plotted to equal scales
from Skempton (1969)
undisturbed specimens

FIG. 9-14

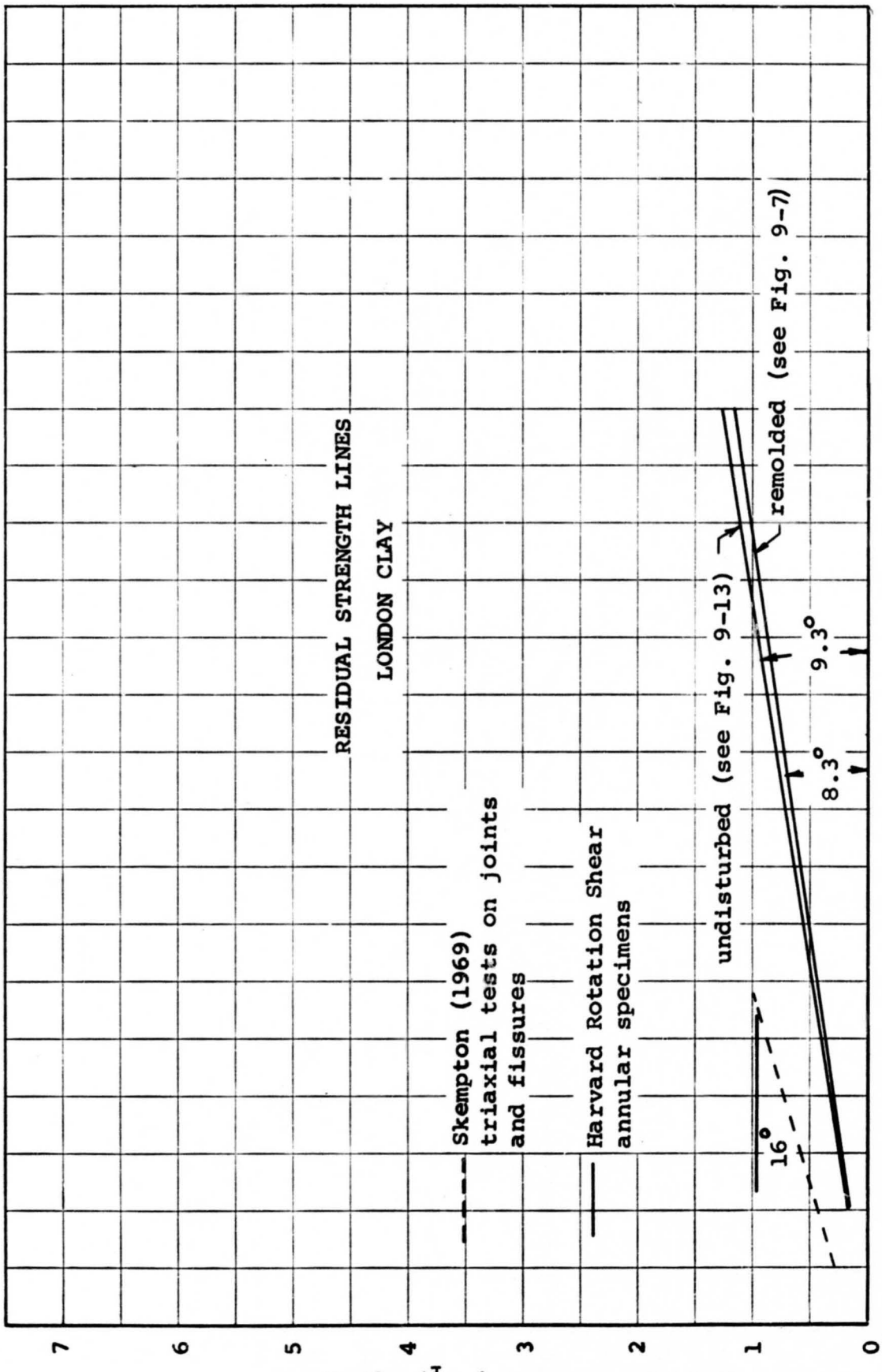
RESIDUAL STRENGTH LINES
LONDON CLAY
Skempton (1969)
triaxial tests on joints
and fissures
Harvard Rotation Shear
annular specimens
undisturbed (see Fig. 9-13)
remolded (see Fig. 9-7)
16°
8.3°
9.3°
RESIDUAL STRENGTH, τ_r, kg/sq cm
EFFECTIVE VERTICAL STRESS, $\bar{\sigma}_v$, kg/sq cm
0
1
2
3
4
5
6
7
8

FIG. 9-15

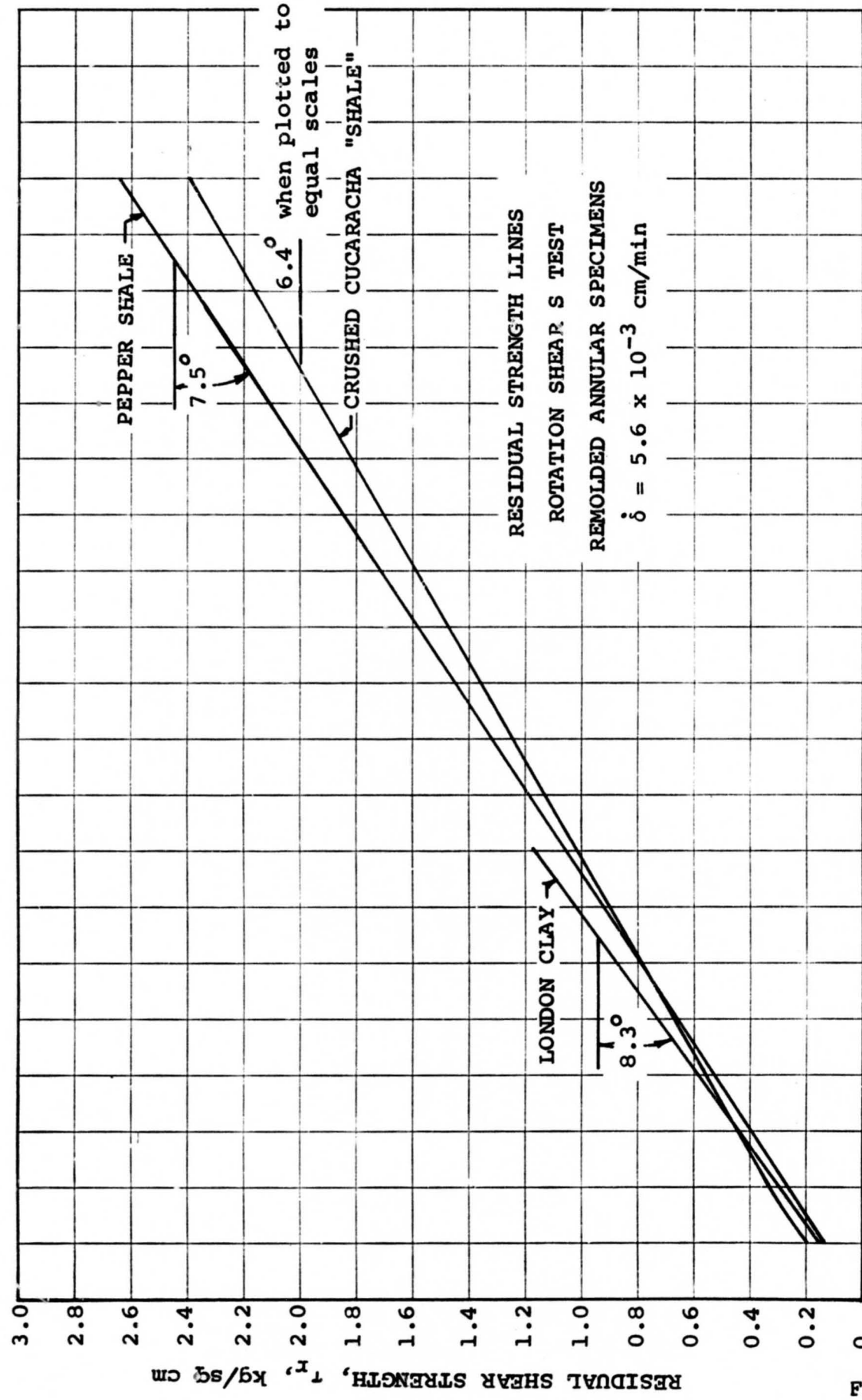
RESIDUAL SHEAR STRENGTH, τ_r, kg/sq cm
EFFECTIVE VERTICAL STRESS, $\bar{\sigma}_v$, kg/sq cm
RESIDUAL STRENGTH LINES
ROTATION SHEAR S TEST
REMOLDED ANNULAR SPECIMENS
$\dot{\delta}$ = 5.6 x 10^{-3} cm/min
PEPPER SHALE
7.5°
6.4° when plotted to equal scales
CRUSHED CUCARACHA "SHALE"
LONDON CLAY
8.3°
0
0.2
0.4
0.6
0.8
1.0
1.2
1.4
1.6
1.8
2.0
2.2
2.4
2.6
2.8
3.0
0
4
8
12
16
20

FIG. 10-1

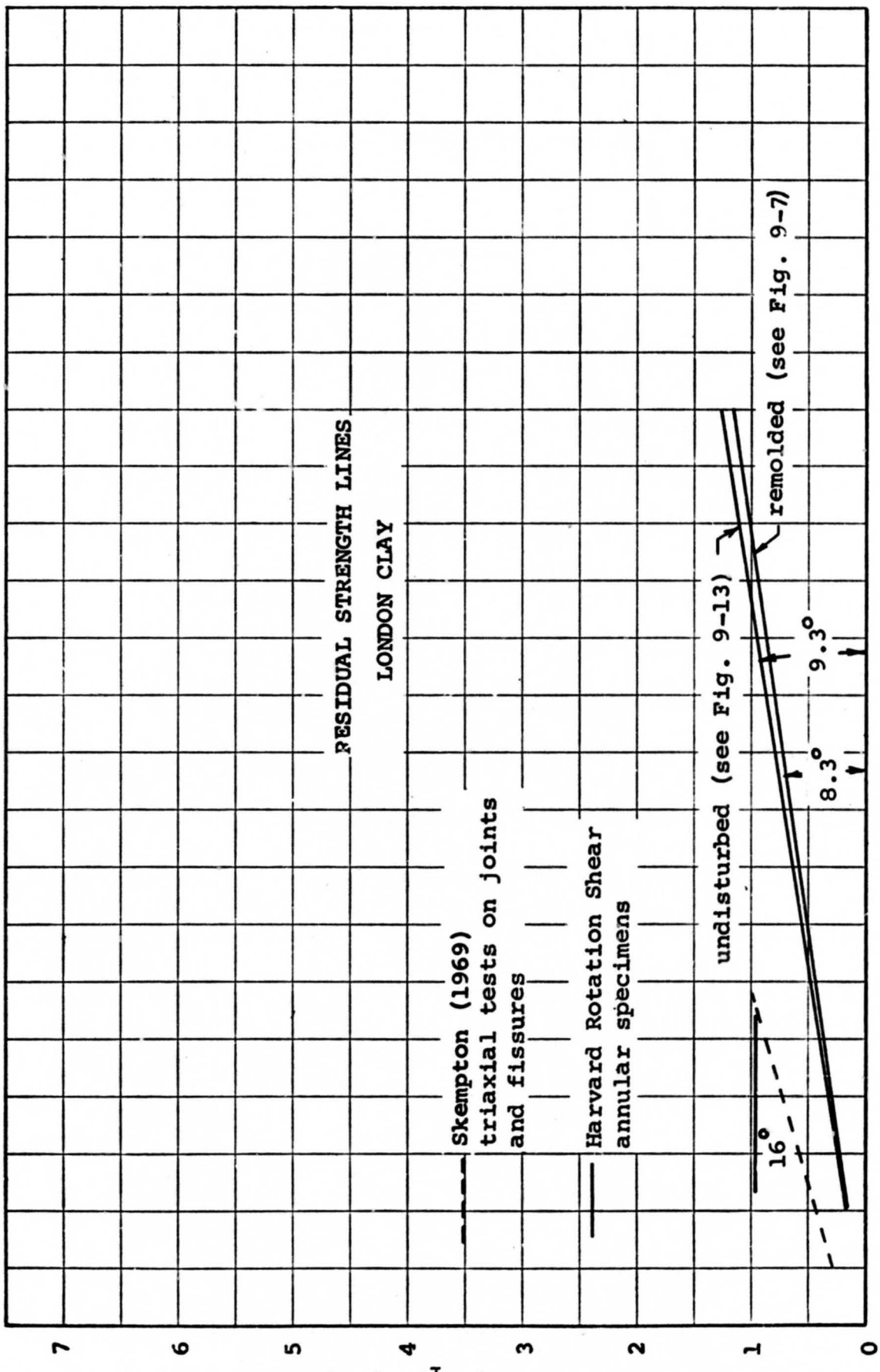
RESIDUAL STRENGTH LINES
LONDON CLAY
Skempton (1969)
triaxial tests on joints
and fissures
Harvard Rotation Shear
annular specimens
undisturbed (see Fig. 9-13)
remolded (see Fig. 9-7)
16°
8.3°
9.3°
RESIDUAL STRENGTH, τ_r, kg/sq·cm
EFFECTIVE VERTICAL STRESS, $\bar{\sigma}_v$, kg/sq cm
0
1
2
3
4
5
6
7
8

FIG. 10-2

APPENDIX A

DISCUSSION OF TEST ERRORS

A.1 ERROR IN VERTICAL STRESS CAUSED BY LEVER SYSTEM

The lever ratios were computed by measuring the distances between knife edges after the levers were installed. These ratios were checked by direct measurement of loads transmitted to a high-tensile steel proving ring that replaced the shearing unit in the machine.* The largest differences between ratios computed using these two techniques occurred when loads smaller than 25 kg were applied to the proving ring by the levers. The maximum difference occurred when using the 40:1 hanger ratio of Machine No. 1 to apply these small loads which gave a computed ratio of 39.62:1 compared with 39.85 computed from measurement of lever distances. The larger difference in ratios at the lower loads is attributed to the poor proving ring repeatability at the lower loads.

The ratios obtained by measuring the distances between knife edges are listed below and were used to compute specimen loads.

Machine Number	Design Ratio	Measured Ratio
1	20:1	19.92:1
1	40:1	39.85:1
2	5:1	4.99:1
2	10:1	9.98:1

The precision of the lever system was determined by a series of load-unload cycles performed with proving rings in place of the shearing unit. The precision was found to be as good as the proving rings themselves, i.e., 0.1% to 0.25%. The lead weights used in these precision tests were weighed on a Mettler balance.

The error in the residual strength, caused by the lever system, is estimated to be no greater than plus or minus 0.1% to 0.25% of any given value.

A.2 ERROR IN VERTICAL STRESS CAUSED BY SIDE FRICTION

Load applied to the horizontal top surface of a specimen confined in a ring is diminished with depth due to side friction. Assuming both the coefficient of side friction and the coefficient of lateral earth pressure are constants, the friction on the boundary between the specimen and the ring will decrease with depth. For simplicity, it will be assumed that the stress due to side friction is constant and equal to:

$$\mu_{st} K \bar{\sigma}_v \qquad \text{where:}$$

*The loads placed on the proving ring during these tests range between 12 kg and 450 kg.

$\bar{\sigma}_v$ = vertical stress applied to the top of the specimen

K = coefficient of lateral earth pressure

μ_{st} = coefficient of friction between soil and Teflon ring

This simplification will exaggerate any change in $\bar{\sigma}_v$ with depth.

The vertical stress on the failure plane of a specimen using a fixed confining ring will be computed with the aid of the following definitions:

h = distance from the top of the specimen to failure plane

P = load applied to top of the specimen

P_c = vertical load in confining ring due to side friction

P_d = vertical load in center disc due to side friction

A_s = area of specimen

$\bar{\sigma}_v$ = vertical stress applied to the top of the specimen

$\bar{\sigma}'_v$ = vertical stress on failure plane

K = coefficient of lateral earth pressure

μ_{st} = coefficient of friction between soil and Teflon ring

For annular specimens, the load in the confining ring, P_c, and the load in the center disc, P_d, will be:

$$P_c = K\bar{\sigma}_v h\pi D_1 \mu_{st}$$

$$P_d = K\bar{\sigma}_v h\pi D_2 \mu_{st}$$

The stress on the failure plane $\bar{\sigma}'_v$ will be:

$$\bar{\sigma}'_v = \bar{\sigma}_v - \left[\frac{P_d}{A_s} + \frac{P_c}{A_s}\right]$$

which becomes:

$$\bar{\sigma}'_v / \bar{\sigma}_v = 1 - 4Kh\mu_{st} \frac{D_1 + D_2}{D_1^2 - D_2^2} \qquad \text{(A-1)}$$

The center disc for an annular specimen in the Harvard rotation shear machine is designed not to take any vertical load.* Equation A-1 simplifies to:

$$\bar{\sigma}'_v / \bar{\sigma}_v = 1 - 4Kh\mu_{st} \frac{D_1}{D_1^2 + D_2^2} \qquad \text{(A-2)}$$

When a disc-shaped specimen is used, D_2 is zero and Equation A-1 reduces:

$$\bar{\sigma}'_v / \bar{\sigma}_v = 1 - \frac{4Kh\mu_{st}}{D_1} \qquad \text{(A-3)}$$

*If the upper platen tilted 8 degrees from the horizontal, the center disc would contact the inside of both the upper and lower platens and further tilting would cause the disc to jam. This amount of tilting has never been observed, nor has the center spacer ever been observed to be jammed into the upper and lower platens at the end of a test.

Equations A-2 and A-3 will be evaluated using the following assumptions:

1. $K = 0.8$
2. $\mu_{st} = 0.1$
3. h = 0.2 cm for split confining rings and 0.5 cm for solid confining rings

The coefficient of friction between soil and Teflon has not been determined, but $\mu_{st} = 0.1$ is probably on the high side. Tests using split confining rings result in a failure plane 0.2 cm below the upper platen when using test specimens that were initially 0.6 cm thick. For tests using a solid confining ring, h is generally 0.05 cm or less. The results of inserting these assumptions into Equations A-2 and A-3 are tabulated below:

h	$\bar{\sigma}_v' / \bar{\sigma}_v$	
cm	Annulus	Disc
0.2	0.982	0.992
0.05	0.995	0.998

Hence, when using a split ring, side friction will cause $\bar{\sigma}_v$ to be about 2% low for annular specimens and 1% low for disc-shaped specimens. When using a solid confining ring, $\bar{\sigma}_v$ will be about 0.5% low for annular specimens and 0.2% low for disc-shaped specimens.

A.3 ERROR IN MEASURED MOMENT CAUSED BY MEASURING SYSTEM

The transducers used to measure the force couple transmitted through the specimen were calibrated by applying load directly on their probes.* They were calibrated for several cycles of loading and unloading and were found to have a repeatability of about 0.1% for the upper 80% of their range and 0.3% for lower 20% when the zero shift was accounted for (Sections 3.6 and B.1).

Excitation voltage for the transducers is obtained from a precision DC power source which has an accuracy of 0.1%. Transducer output voltage is displayed on digital millivoltmeters having an accuracy of 0.1%.

Numerous checks of transducer calibration have been made in the course of the testing program by exchanging sets of transducers during a test. For example, transducers with a maximum force range of 100 lbs may be required to measure the peak strength of a soil in a given test, while 25-lb transducers may be sufficient to measure the residual strength.

Thus, when the residual strength is reached, the 100-lb transducers will be replaced with 25-lb transducers to obtain more precise measurements. This also permits a cross-check of the pairs of transducers, since both sets should measure an identical force couple. Such an exchange of transducers (25-lb for 100-lb and 10-lb for 25-lb) has been done many times and indicates that there has been no change in transducer calibrations.

With the proper selection of transducers, the maximum error in the measured moment due to the electronic measuring system would be plus or minus 0.3%.

---

*Lead weights used for the transducer calibration were weighed on a Mettler balance to determine their actual weight.

A.4 ERROR IN THE MEASURED MOMENT CAUSED BY FRICTION IN THE SPLIT CONFINING RING

Section A.2 pointed out that friction between the soil and the confining ring causes a reduction in the applied stress on the failure plane. When using the split confining rings, vertical load transmitted from the soil to the upper confining ring by side friction will cause friction between the stationary upper ring and the rotating lower ring. This friction is measured as a part of the moment required to maintain the upper half of the shearing unit stationary. The technique of raising the solid ring and separating the confining rings eliminates this error, but it will be useful to estimate this error analytically. This error can be estimated with the aid of the following sketch and definitions:

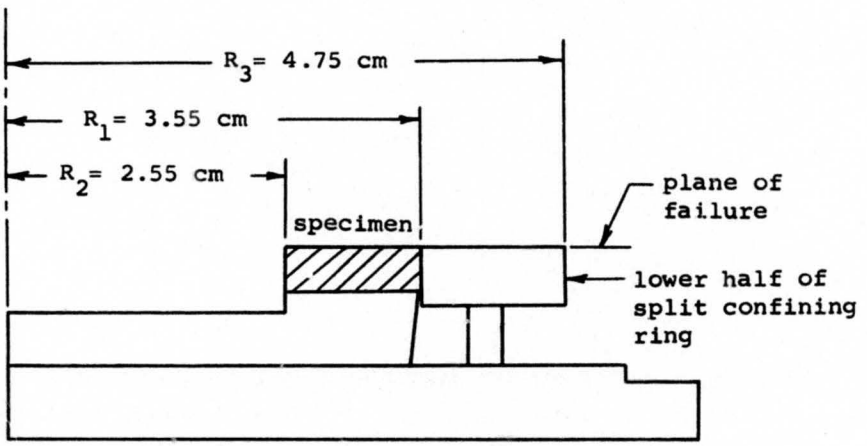

A_s = area of soil specimen

A_c = area of mating surfaces of split confining rings

P = load applied at the top of the specimen

P_c = load transmitted to upper confining ring due to side friction

$\bar{\sigma}_v$ = vertical stress at the top of the specimen

$\bar{\sigma}'_v$ = vertical stress on failure plane

$\bar{\sigma}_{vc}$ = vertical stress on mating surfaces of split confining rings

τ_r = shear stress on failure plane

τ_c = shear stress on mating surfaces of confining ring

μ_{st} = coefficient of friction between soil and Teflon = 0.1

μ_c = coefficient of friction between confining rings

M_r = moment due to shear stress on failure plane

M_c = moment due to friction between confining rings

Assuming τ_r is uniformly distributed on the failure plane, and τ_c is uniformly distributed on the mating surface of the confining rings, the equations for the moments caused by these stresses are:

$$M_r = 2/3\ \pi\ R_1^3 - R_2^3\ \tau_r \qquad \text{(A-4)}$$

$$M_c = 2/3\ \pi\ R_3^3 - R_1^3\ \tau_c \tag{A-5}$$

$$M_c/M_r = \frac{R_1^3 - R_2^3}{R_3^3 - R_1^3}\ \frac{\tau_c}{\tau_r} \tag{A-6}$$

$$\tau_c = \mu_c\ \frac{P_c}{A_c} = \mu_c\ \frac{2\mu_{st} K \bar{\sigma}_v h \pi R_1}{A_c} \tag{A-7}$$

$$\tau_r = \mu_r \bar{\sigma}_v \tag{A-8}$$

$$M_c/M_r = \frac{R_1^3 - R_2^3}{R_3^3 - R_1^3}\ \frac{\mu_c}{\mu_r}\ \frac{2\mu_{st} K h \pi R_1}{A_c}$$

$$M_c/M_r = \frac{R_1^3 - R_2^3}{R_3^3 - R_1^3} \cdot \frac{R_1}{R_1^2 - R_2^2}\ 2h\ \frac{\mu_t \mu_{st} K}{\mu_r}$$

Substituting the values of R_1, R_2, R_3,

$$M_c/M_r = (0.79)\ 2h\ \frac{\mu_c \mu_{st} K}{\mu_r} \tag{A-9}$$

During a test, there is always a thin film of soil between the rings and it is reasonable and conservative to assume

$$\mu_c = \mu_{st} = 0.1$$

If $K = 0.8$, $h = 0.2$, and $\mu_r = 0.01$ ($\phi = 5.7$ degrees),

$$M_c/M_r = 0.025$$

This analysis indicates that the measured moment, hence τ_r, is about 2.5% larger than it would be if there were no friction between the confining rings. The assumptions made to evaluate Equation A-9 are believed to be conservative; in particular, the value of μ_{st} is probably too large.

If the Lucite C-clamps are used to restrict the clearance between the split confining ring (Section 3.7), then the foregoing analysis will not be applicable because the stress on the mating surfaces of the split ring cannot be estimated.

The technique of removing the Lucite C-clamps and temporarily separating the confining ring eliminates friction between the two halves, and hence any error due to this friction is also eliminated.

A.5 ERROR IN MOMENT CAUSED BY FRICTION BETWEEN THE SOLID CONFINING RING, THE STATIONARY PLATEN AND THE STATIONARY PART OF THE SPECIMEN

When a solid confining ring is used, it introduces a moment due to friction between the ring (which rotates) and the stationary portion of the specimen as well as the upper platen, as shown below.

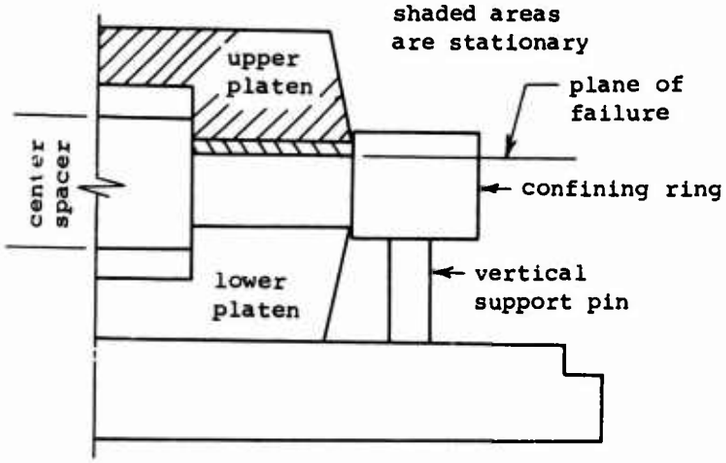

An evaluation of the error introduced by this friction may be made by studying the data available from 34 tests in this research which were performed with solid confining rings. In these tests, the moment was measured with the confining ring in position and again with the ring lifted off the specimen and the shear stress computed for each of these moments.

The shear stress, τ_r, computed with the confining ring lifted and the difference between this shear stress and the stress computed with the ring in position are shown in Tables A-1 to A-3. These data indicate that the additional shear stress due to ring friction is independent of vertical stress and overconsolidation ratio, and varies between 0.010 and 0.030 with an average of 0.020 kg/sq cm for both the Pepper Shale and the soil from the Cucaracha "Shale." The results for the London Clay (Table A-3) indicate that ring friction averages about 0.030 kg/sq cm in this soil. This higher value is probably the result of the higher silt content of the London Clay.

The difference between τ_r measured with the ring in position and with it lifted off is not entirely due to elimination of friction. When side friction is eliminated by lifting the ring, the total stress on the failure plane is increased by an amount equal to the total vertical side friction. It was pointed out in Section A.2 that the ratio $\bar{\sigma}'_v / \bar{\sigma}_v$ is approximately 0.995 for tests using a solid confining ring. The second, and more important, phenomenon that occurs when the ring is lifted is the reduction in the measured moment due to soil extrusion. It was pointed out in Section 6.5.2 and Section 6.5.3 as well as in Section 8.3.1 that the effect of soil extrusion did not occur immediately upon removal of radial confinement. The interaction of these two phenomena when the ring is lifted may be explained with the aid of the following sketch:

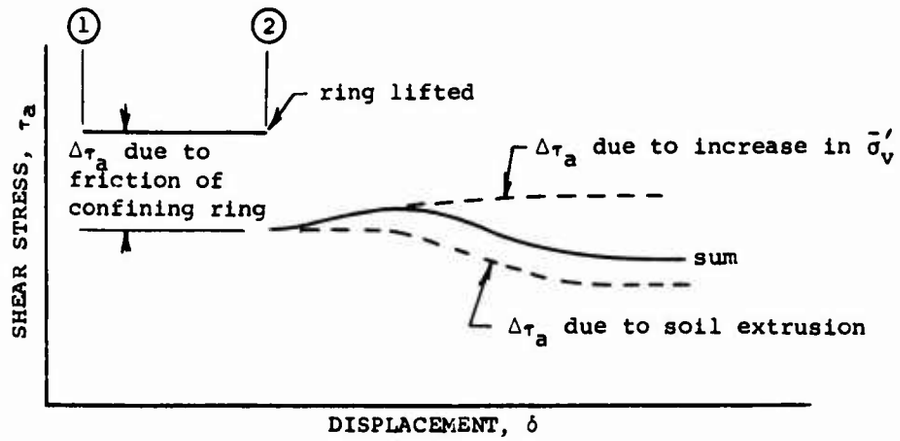

When the residual strength is reached with the confining ring in position, τ_a is constant, as shown between Points 1 and 2. At Point 2 the ring is lifted and there is an immediate reduction in τ_a.* With the ring lifted, the effective vertical stress increases on the failure plane, and τ_a will increase as shown by the line labeled "$\Delta\tau_a$ due to increase in $\bar{\sigma}'_v$." The increase is very small since the change in vertical effective stress is very small. Soil extrusion also affects the shear stresses, as shown by the line labeled "$\Delta\tau_a$ due to soil extrusion." The sum of these two effects, indicated by the heavy black line, is actually observed. In a test, the transducer readings are recorded at one-minute intervals (or less) after the ring is lifted until there is a reduction in the measured force couple, indicating extrusion is becoming dominant. Then the confining ring is replaced. The transducer readings recorded just before the reduction started are used to compute τ_a. In this manner, the effect of friction due to confinement is eliminated and the effect of soil extrusion is minimized. The actual strength may be slightly higher than the strength computed by this technique.

A.6 ERROR IN THE MEASURED MOMENT CAUSED BY FRICTION BETWEEN THE ROTATING CENTER DISC AND THE STATIONARY PART OF THE SPECIMEN

Experience has shown that the center spacer used to form the inner periphery of annular specimens rotates with that part of the specimen below the failure plane.**

The error due to friction between this Teflon disc and the stationary part of the specimen above the failure plane may be estimated as follows:

$$M_d/M_r = \frac{R_2^2}{R_1^3 - R_2^3} \cdot 3h \cdot \frac{K\mu_{st}}{\mu_r} \qquad \text{(A-10)}$$

$$M_d/M_r = (0.23)\, 3hK\, \frac{\mu_{st}}{\mu_r}$$

If h = 0.05 cm and K = 0.8,

$$M_d/M_r = 0.027\, \frac{\mu_{st}}{\mu_r}$$

Rotation of the center disc on the inner periphery of the stationary part of the specimen results in a slickenside on this surface. It would seem reasonable to assume that t coefficient of friction between this slickensided surface and the Teflon center disc is about $0.5\,\mu_r$. Based on this assumption, Equation A-10 becomes:

$$\frac{M_d}{M_r} = 0.014$$

Hence, the computed residual strength will be about 1.4% high due to this error.

---

*The act of lifting the ring generally disturbs the alignment of the top plate very slightly, and the instant the ring is lifted the transducers will not be measuring forces which are truly representative of the test conditions. The transducer readings will change very rapidly; however, after about 15 seconds, the output of the transducers will stop changing rapidly and assume a slow, steady increase. It is this 15-second reading which is used to represent the shear stress due to friction in the above sketch.

**Inferred from the observation of a slickenside on the inner periphery of the stationary part of the specimen.

APPENDIX B

CALIBRATION OF APPARATUS

B.1 CALIBRATION OF FORCE TRANSDUCERS

The transducers used to measure the force couple in the Harvard rotation shear machine are manufactured by Dynisco Division of Microdot, Westwood, Massachusetts. They are factory-calibrated and the combined effect of nonlinearity, hysteresis, and nonrepeatability are advertised as less than 0.75% of their full scale output.

Careful calibration in the Harvard Laboratory practically eliminated the effects of nonlinearity and hysteresis.

Each transducer was calibrated by application of dead weight directly on its probe. Several cycles of loading and unloading are performed over a period of a few days. The transducers were calibrated using the same excitation and signal cables that are used during a rotation shear test.

The output versus load and unload curves for a given transducer were found to have essentially constant shape, but the curves were displaced along the voltage axis because of zero drift. The repeatability of these curves for a given transducer was determined to be less than 0.1% of full scale output when the "no load" voltage was subtracted from the voltage obtained at any given load.

Data for a typical transducer calibration are presented in Tables B-1 and B-2. Table B-1 shows the results of one trial, consisting of three loading and unloading cycles. The no load output voltage before each loading cycle has been subtracted from the output at each load increment, and the no load output voltage at the end of the unloading cycle has been subtracted from the output voltage at each load decrement.

The average output voltage is then taken for each load decrement and recorded in Table B-2 where it may be compared with other similar calibration trials.* For this particular transducer, three trials have been made. The secant slope for each measured point on the calibration shown in Table B-2 indicates the linearity of the calibration curve.

Forces are determined during a rotation shear test by subtracting the zero load reading from the loaded readings.** Entering the calibration table with this difference, the secant slope of the calibration curve is obtained. The difference between loaded and unloaded readings is multiplied by the appropriate secant slope to obtain the force. The small deviation from linearity for the calibration curves has made this more convenient than using a curve of output voltage versus load.

B.2 APPARATUS COMPRESSIBILITY

Measurements of the vertical movement of the upper beam of the loading yoke (Section 3.8) include the compressibility of the shearing unit. The apparatus compressibility was determined for both testing machines by placing a brass disc between the loading platens. Results of these calibrations are shown in Figs. B-1 and B-2 and are practically identical.

---

*Only the unloading cycle is shown because the transducer is being unloaded as the residual strength is being approached.

**During the early part of the test, the zero load readings taken before the test are assumed to apply. As the shear stress versus displacement curve approaches a horizontal asymptote, new zero load readings are taken after each set of loaded readings is recorded.

TABLE A-1

PEPPER SHALE (ϕ_r = 7.5°)

EVALUATION OF FRICTION DUE TO SOLID CONFINING RING

Test No.	$\bar{\sigma}_v$ kg/cm^2	OCR	Residual Strength, τ_r kg/cm^2		$\Delta\tau_r$ kg/cm^2
			With Ring	Ring Temporarily Lifted	
1	1	1	0.143	0.118	0.025
	2		0.275	0.250	0.025
	4		0.540	0.515	0.025
2	4	1	0.510	0.500	0.010
3	8	1	1.060	1.040	0.020
4	12	1	1.553	1.529	0.024
	20		2.695	2.680	0.015
5	1	1	0.125	0.115	0.010
	2		0.240	0.230	0.010
	4		0.505	0.490	0.015
7	1	10	0.166	0.141	0.025
8	1	10	0.168	0.145	0.023
9	2	5	0.285	0.265	0.020
10	4	2.5	0.533	0.508	0.025
11	1	100	0.142	0.122	0.020
12	1	Undis.	0.132	0.122	0.010
13	1	Undis.	0.129	0.119	0.010
14	2	Undis.	0.263	0.253	0.010
15	4	Undis.	0.420	0.400	0.020
16	4	Undis.	0.420	0.400	0.020

TABLE A-2

CUCARACHA "SHALE" (ϕ_r = 6.4°)

EVALUATION OF FRICTION DUE TO SOLID CONFINING RING

Test No.	$\bar{\sigma}_v$ kg/cm^2	OCR	Residual Strength, τ_r kg/cm^2		$\Delta\tau_r$ kg/cm^2
			With Ring	Ring Temporarily Lifted	
1	1	1	0.215	0.195	0.020
2	1	1	0.208	0.190	0.018
3	1	1	0.156	0.151	0.005
4	2	1	0.335	0.335	0
	4		0.590	0.570	0.020
5	4	1	0.580	0.570	0.010
	8		1.040	1.020	0.020
6	12	1	1.520	1.490	0.030
	20		2.388	2.358	0.030
7	8	1	0.990	0.980	0.010
8	1	10	0.170	0.160	0.010
9	1	100	0.200	0.180	0.020
10	1	1	0.155	0.145	0.010
11	4	1	0.580	0.570	0.010

TABLE A-3

LONDON CLAY (ϕ_r = 9.3°)

EVALUATION OF FRICTION DUE TO SOLID CONFINING RING

Test No.	$\bar{\sigma}_v$ kg/cm^2	OCR	Residual Strength, τ_r kg/cm^2		$\Delta\tau_r$ kg/cm^2
			With Ring	Ring Temporarily Lifted	
1	1	1	0.207	0.177	0.030
2	2	1	0.338	0.293	0.035
	4		0.602	0.572	0.030
3	8	1			
4	1	Undis.	0.200	0.160	0.040
5	2	Undis.	0.349	0.339	0.010
6	4	Undis.	0.680	0.650	0.030
7	8	Undis.			

TABLE B-1

RESULTS OF TYPICAL TRANSDUCER CALIBRATION – TRIAL 3

Load kg	Difference Between Loaded and Unloaded Output – mv					
	Loading Cycles			Unloading Cycles		
1.424	3.421	3.428	3.430	3.382	3.340	3.341
2.0	4.766	4.783	4.780	4.665	4.701	4.698
4.0	9.470	9.478	9.479	9.309	9.341	9.363
6.0	14.141	14.156	14.157	14.004	14.010	14.045
8.0	18.747	18.831	18.824	18.618	18.680	18.711
10.0	23.481	23.494	23.490	23.301	23.410	23.421
11.3	26.365	26.538	26.544			

TABLE B-2

SUMMARY OF THREE TRANSDUCER CALIBRATION TRIALS
(UNLOADING CYCLE)

Load kg	Difference Between Loaded and Unloaded Output - mv			Average Output mv	Maximum Deviation from Average %	Secant Slope kg/mv
	Trial 1	Trial 2	Trial 3			
10.0	23.374	23.386	23.377	23.379	0.03	0.4277
8.0	18.6	18.672	18.669	18.670	0.01	0.4284
6.0	13.998	14.010	14.020	14.009	0.07	0.4282
4.0	9.349	9.357	9.337	9.348	0.1	0.4278
2.0	4.683	4.688	4.684	4.684	0.1	0.4269
1.424	3.335	3.337	3.354	3.343	0.3	0.4259

COMPRESSIBILITY
MACHINE NO. 1
loading
unloading
LOAD, kg
0
1000
2000
3000
4000
VERTICAL DEFLECTION, .0001 in.
0
20
100
200
300

Fig. B-1

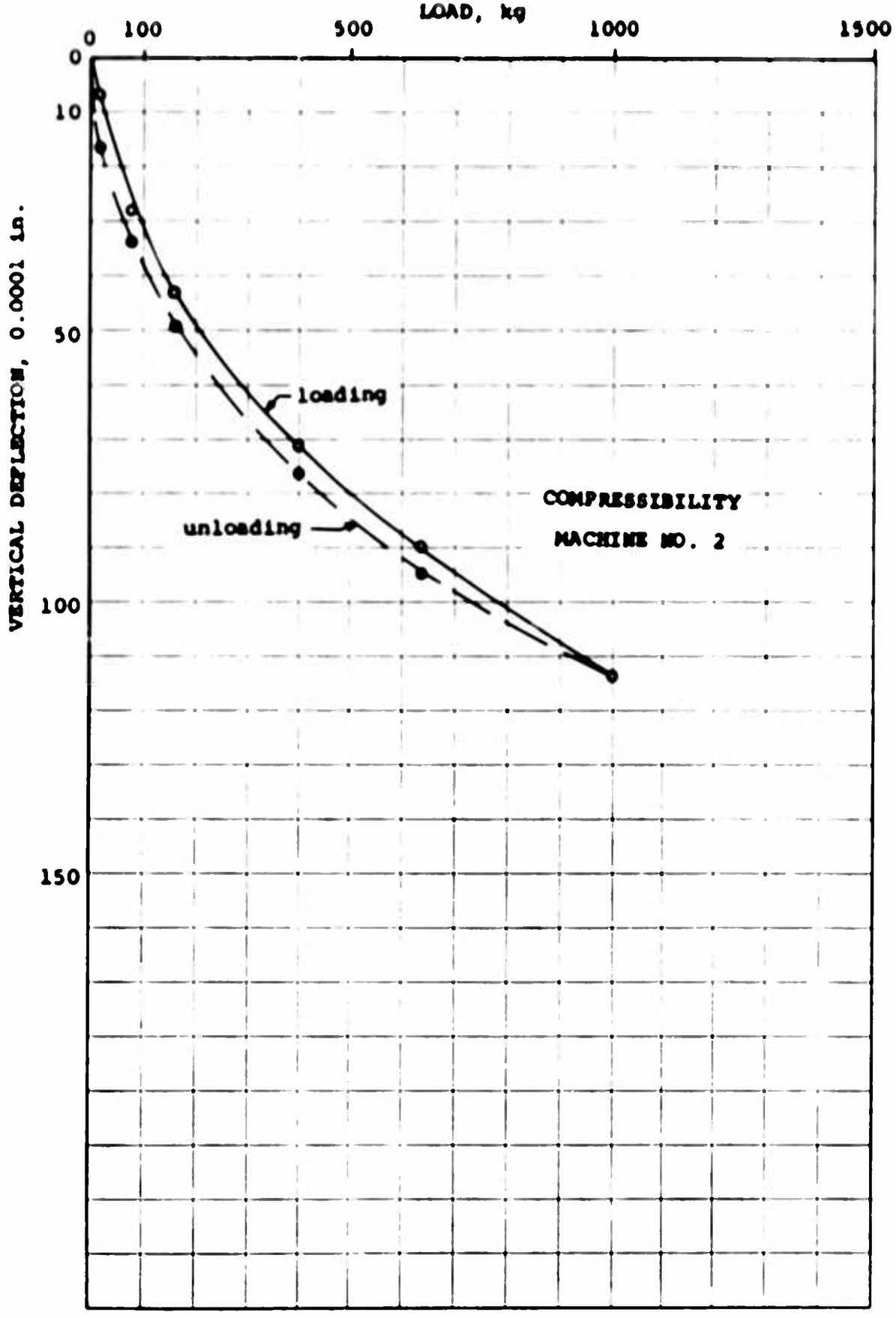
LOAD, kg
0
100
500
1000
1500
0
10
50
100
150
VERTICAL DEFLECTION, 0.0001 in.
loading
unloading
COMPRESSIBILITY
MACHINE NO. 2

Fig. B-2